Marta Isabel Heitor Cerejo

Mestre em Ciências das Zonas Costeiras

Contribution to drug discovery and development for tauopathies using yeast as a model

Dissertação para obtenção do Grau de Doutor em Bioengenharia

Orientador: Prof. Doutora Ana Cristina Carvalho Rego, Professora Auxiliar com Agregação, Faculdade de Medicina e Centro de Neurociências e Biologia Celular, Universidade de Coimbra

Co-orientador: Prof. Doutora Helena Margarida Moreira de Oliveira Vieira, Professora Associada Convidada, Faculdade de Ciências, BioISI – Biosystems & Integrative Sciences Institute, Universidade de Lisboa

Co-orientador: Prof. Doutor Manuel Nunes da Ponte, Professor Catedrático, Faculdade de Ciências e Tecnologia, Universidade Nova de Lisboa

Júri:

Presidente: Prof. Doutora Ana Isabel N. M. A. de Oliveira Ricardo
Arguentes: Prof. Doutor Vítor Manuel Vieira da Costa
Prof. Doutora Cláudia Maria Fragão Pereira

Vogais: Prof. Doutor Tiago Fleming de Oliveira Outeiro
Prof. Doutora Paula Cristina da Costa A. M. Ludovico
..Prof Doutor Christophe François Aimé Roca

FACULDADE DE CIÊNCIAS E TECNOLOGIA
UNIVERSIDADE NOVA DE LISBOA

Setembro 2015

Contribution to drug discovery and development for tauopathies using yeast as a model

Copyright

To my boys Pedro and Lucas

Acknowledgments

No PhD is easy. Mine was a roller-coaster. From the birth of my first child to the insolvency of BIOALVO, Life found a way to push me beyond what I thought my limits were. It was an incredible journey and it wouldn't have been possible without the contribution of amazing people to whom I wish to thank.

To BIOALVO and *Fundação para a Ciência e Tecnologia* for granting me the opportunity and financial support to develop my PhD work.

To Professor Helena Vieira, my CEO/supervisor/mentor/friend/sister, for trusting in my ability to do this work at BIOALVO. Thank you for teaching me about biotech and about how we can bring science closer to people. Thank you for your support, even during the most difficult times of your life.

To Professor Ana Cristina Rego, for your scientific supervision, comprehension, trust and friendship. Thank you for receiving me at your lab in CNC-UC. I have never been received so well in a lab and, although it was a short time, I learned a lot about cell biology and of what science in academia is.

To the MIT-Portugal Doctoral Program that allowed me to learn and experience so many new things, but especially to meet inspiring people, including my teachers and my colleagues. Particularly, to Professor Manuel Nunes da Ponte, my co-supervisor, for all the support provided during the toughest circumstances and to Professor José Silva Lopes, for support, kind words and availability to answer all my questions.

To Professor Tiago Outeiro and Professor Paula Ludovico, advisors of my Thesis Advisory Committee, for listening to all my progress presentations, for helpful scientific discussion, constructive critic and valuable insights.

To BioISI-FCUL team, particularly to Professor Rogério Tenreiro and Cláudia Luís, for scientific discussions and technical tips. Thank you for receiving me in your lab, when everything else was collapsing. Likewise, thank you Sandra Tenreiro and Tiago Mendes from IMM, for your support and for receiving me at your lab. I will never forget that you were there for me.

To my work family at BIOALVO, particularly Ricardo Pinheiro, Ana Almeida, Ana Martins, Maria Antónia Pereira and Gianmario Ciaccioli. To my master student, Maria Fernandes, always willing to help and participate and with a smile to spare. To my friend Cátia Rodrigues, my perfect work partner, always there. To all my colleagues at CNC, particularly Carla Lopes (thank you for being a part of my life so easily and so quickly!), Luana Naia, Ana Oliveira, Sandra Mota, Luísa Ferreira and Isabel Dantas, that made me feel so at home away from home.

To "The Dancerzzzzz", Ilaria Stefani, Joana Cruz and Inês Isidro, who made those crazy days of the first year more fun and rich! To Joaquim Barbosa, for your friendship, your optimism and for always being there. To Veronica Corrales the "super wonder woman with all-mighty access to very incredible scientific papers". All of you have brighten my life with your friendship and I will always carry you in my heart.

To my dearest parents, for their love and comprehension, constant encouragement and unconditional support. To all my (big) family, sisters and nephews, parents-in-law and sisters-in-law, for your support, comprehension and care.

Last but never the least, to Pedro, my love, my best friend, my safe harbour, who once more travelled with me in one of my career journeys. Thank you for your unconditional support and pride in me. Thank you for the joyful boy that we have and for being a father and a mother when I wasn't around.

Resumo

Este trabalho pretendeu contribuir para a descoberta e desenvolvimento de drogas (DDD) para tauopatias, enquanto expandia o conhecimento sobre este grupo de doenças neurodegenerativas, incluindo a doença de Alzheimer (DA). Utilizando a levedura, um modelo reconhecido em estudos de neurodegenerescência, foram produzidos modelos úteis para o estudo da interação entre tau e beta-amilóide ($A\beta_{1-42}$), características de DA. A caracterização destes modelos sugere que estas proteínas co-localizam e que $A\beta_{1-42}$, tóxica para a levedura, está envolvida na fosforilação de tau (Ser396/404), via o ortólogo de GSK-3β de levedura, enquanto tau facilita a oligomerização de $A\beta_{1-42}$. O mapeamento do interactoma de tau, conseguido através de um rastreio da colecção de leveduras de genes *knockout,* constitui uma ferramenta nova, constituída por 31 genes, para identificar novos mecanismos de toxicidade de tau e para identificar novos alvos terapêuticos ou biomarcadores. Este estudo genómico também selecionou a levedura *mir1*Δ-tau40 para o desenvolvimento de um sistema de rastreio de drogas GPSD^{2TM}. Uma biblioteca de 138 extratos únicos de bactérias marinhas, recolhidas nas fontes hidrotermais da Crista Meso-Atlântica, foi rastreada utilizando *mir1*Δ-tau40. Foram identificados 3 extratos supressores da toxicidade de tau, que constituem bons pontos de partida para DDD. A estirpe *mir1*Δ é suscetível à toxicidade de tau, relacionando a patologia de tau com a função mitocondrial. *SLC25A3* é o gene humano homólogo de *MIR1* e codifica a proteína mitocondrial transportadora de fosfato (PiC). Utilizando iRNA, a expressão de *SLC25A3* foi silenciada em células neurais. Este foi o primeiro passo para a construção de um modelo que, futuramente, permitirá estudar a relação entre tau e a mitocôndria e validar PiC como um alvo terapêutico. O conjunto de ferramentas de DDD aqui apresentado contribui para o desenvolvimento de terapias inovadoras e eficazes, urgentemente necessárias para lidar com estas doenças neurodegenerativas, de elevado impacto humano e socioeconómico.

Palavras-chave: tau, beta-amilóide, tauopatias, doença de Alzheimer, *S. cerevisiae*, descoberta e desenvolvimento de drogas

Este trabalho foi suportado por uma Bolsa de Doutoramento em Empresas (SFRH/BDE/51142/2010) co-financiado pela BIOALVO SA e Fundação para a Ciência e Tecnologia.

Abstract

This work aimed to contribute to drug discovery and development (DDD) for tauopathies, while expanding our knowledge on this group of neurodegenerative disorders, including Alzheimer's disease (AD). Using yeast, a recognized model for neurodegeneration studies, useful models were produced for the study of tau interaction with beta-amyloid (Aβ), both AD hallmark proteins. The characterization of these models suggests that these proteins co-localize and that $A\beta_{1-42}$, which is toxic to yeast, is involved in tau40 phosphorylation (Ser396/404) *via* the GSK-3β yeast orthologue, whereas tau seems to facilitate $A\beta_{1-42}$ oligomerization. The mapping of tau's interactome in yeast, achieved with a tau toxicity enhancer screen using the yeast deletion collection, provided a novel framework, composed of 31 genes, to identify new mechanisms associated with tau pathology, as well as to identify new drug targets or biomarkers. This genomic screen also allowed to select the yeast strain *mir1*Δ-tau40 for development of a new GPSD^{2TM} drug discovery screening system. A library of unique 138 marine bacteria extracts, obtained from the Mid-Atlantic Ridge hydrothermal vents, was screened with *mir1*Δ-tau40. Three extracts were identified as suppressors of tau toxicity and constitute good starting points for DDD programs. *mir1*Δ strain was sensitive to tau toxicity, relating tau pathology with mitochondrial function. *SLC25A3,* the human homologue of *MIR1*, codes for the mitochondrial phosphate carrier protein (PiC). Resorting to iRNA, SLC25A3 expression was silenced in human neuroglioma cells, as a first step towards the engineering of a neural model for replicating the results obtained in yeast. This model is essential to understand the mechanisms of tau toxicity at the mitochondrial level and to validate PiC as a relevant drug target. The set of DDD tools here presented will foster the development of innovative and efficacious therapies, urgently needed to cope with tau-related disorders of high human and social-economic impact.

Keywords: tau, beta-amyloid, tauopathies, Alzheimer's disease, *S. cerevisiae*, drug discovery and development

This work was supported by a Doctoral Grant in Companies (SFRH/BDE/51142/2010), co-financed by BIOALVO SA and *Fundação para a Ciência e Tecnologia*.

Contents

List of Figures

List of Tables

List of Equations

Abbreviations

Aβ	Beta-amyloid
$A\beta_{1-42}$	Beta-amyloid peptide residues 1-42
Abl	Tyrosine-protein kinase ABL1
AD	Alzheimer's disease
AD2	Phosphorylation-dependent monoclonal antibody directed against tau proteins found in Alzheimer's disease
ADI	Alzheimer's disease international
ADME	Absorption, Distribution, Metabolism, Excretion
ADMET	Absorption, Distribution, Metabolism, Excretion, Toxicity
ALS	Amyotrophic Lateral Sclerosis
ANOVA	Analysis of Variance
APP	Amyloid precursor protein
ATP	Adenosine triphosphate
ATPAF1	ATP synthase mitochondrial F1 complex assembly factor 1
β-ME	Beta mercaptoethanol
BSA	Bovine serum albumin
$Ca^{2+}i$	Intracellular Ca^{2+}
CAPS	N-cyclohexyl-3-aminopropanesulfonic acid
CDK5	Cyclin-dependent kinase 5
cDNA	Complementary DNA
CHIP-Seq	Chromatin immunoprecipitation sequencing
CIAP	Calf Intestinal Alkaline Phosphatase
CK1	Casein kinase 1
CSNK2B	Casein kinase 2, beta polypeptide
DDD	Drug discovery and development
DMEM	Dulbecco’s modified Eagle’s medium
DMSO	Dimethyl sulfoxide
DNA	Deoxyribonucleic acid
dNTP	Deoxynucleotide
DRP-1	Dynamin 1-like protein
dsDNA	Double stranded DNA
DTT	Dithiothreitol
EDTA	Ethylenediamine tetraacetic acid
eGFP	Enhanced green fluorescent protein
EGTA	Ethylene glycol tetraacetic acid
ETC	Electron transport chain
EV	Empty vector
FAD	Familial Alzheimer's disease
FAP	Familial amyloidotic polyneuropathy
FBS	Foetal bovine serum
FCCP	Carbonyl cyanide-p-trifluoromethoxyphenylhydrazone
FTD	Frontotemporal dementias

FTDP-17	Frontotemporal dementia and parkinsonism linked to chromosome 17
FTLDU	Frontotemporal lobar degeneration with ubiquitin-positive pathology
Fura-2AM	Fura-2 acetoxy-methyl-ester
FUS	Fused in Sarcoma protein
Fyn	Proto-oncogene tyrosine-protein kinase Fyn
G418	Geneticin
GADPH	Glyceraldehyde 3-phosphate dehydrogenase
GAL	Galactose
GAL1	Galactose inducible promoter 1
GAL10	Galactose inducible promoter 10
GCLc	Glutamate-cysteine ligase, catalytic subunit
gDNA	Genomic DNA
GLU	Glucose
GPS D^{2TM}	Global Platform Screening for Drug Discovery
GSK-3β	Glycogen synthase kinase-3 beta subunit
GSPT1	G1 to S phase transition 1 protein
GTO	Granular tau oligomers
h	Hour
HD	Huntington's disease
HEPES	4-(2-hydroxyethyl)-1-piperazineethanesulfonic acid
hERG	Human ether-a-go-go related gene
HIST1H2BB	Histone cluster 1, H2bb
HRP	Horseradish peroxidase
HSP60	Heat shock protein 60
HSP70	Heat shock protein 70
HTS	High-throughput screening
IgG	Immunoglobulin G
IKBKAP	Kinase complex-associated protein
IND	Investigative New Drug
INT	Iodonitrotetrazolium chloride
iRNA	Interference RNA
KanMX	Kanamycin selector module conferring kanamycin resistance in yeast
kb	Kilo nucleotide bases
KD	knockdown
LB	Luria Broth media
LDH	Lactate dehydrogenase
Leu	Leucine
LEU2	Leucine locus
LiAc	Lithium acetate
MAPT	Microtubule associated protein tau gene
MARK	Microtubule affinity-regulating kinase
mCh	mCherry fluorescent protein
MCI	Mild cognitive impairment
min	Minute
MIR1	Mitochondrial phosphate carrier yeast gene
*mir1*Δ	Yeast strain carrying a deletion of *MIR1* ORF

mPTP	Mitochondrial permeability transition pore
mRNA	Messenger ribonucleic acid
MRPL15	Mitochondrial ribosomal protein L15
MRPS2	Mitochondrial ribosomal protein S2
MTBD	Microtubule binding domain
NAD^+/NADH	Nicotinamide adenine dinucleotide
NCE	New chemical entity
NDA	New drug application
NFT	Neurofibrillary tangle
NMDA	*N*-methyl-D-aspartate
NP	Natural product
NRF1	Nuclear respiratory factor-1
OCR	Oxygen consumption rate
OD_{600}	Optical density at 600 nm
ON	Overnight
ORF	Open reading frame
OXPHOS	Oxidative phosphorylation
PARS2	Mitochondrial prolyl-tRNA synthetase 2
PBS	Phosphate buffered saline
PCR	Polymerase chain reaction
PD	Parkinson's disease
PDR5	Plasma membrane ATP-binding cassette (ABC) yeast transporter
PEG	Polyethylene glycol
PFDN6	Prefoldin subunit 6
PGK-1	Phosphoglycerate kinase 1
PHF	Paired helical filaments
Pi	Inorganic phosphate
PiC	Mitochondrial phosphate carrier protein
PIK3R4	Phosphoinositide-3-kinase, regulatory subunit 4
PK/PD	Pharmacokinetics/pharmacodynamics
PMS	N-methylphenazonium methyl sulfate
PP2A	Protein phosphatase 2A
PPP2R4	Protein phosphatase 2A activator, regulatory subunit 4
PSD95	Postsynaptic density protein 95
p-tau	Phosphorylated tau
PVDF	Polyvinylidene difluoride
R&D	Research and development
RAF	Raffinose
RBMX	RNA Binding Motif Protein, X-Linked
RIM11	Yeast gene coding for a protein kinase homologue to human GSK-3β
*rim11*Δ	Yeast strain carrying a deletion of RIM11 ORF
Rim11	Protein kinase homologue to human GSK-3β
RIPA	Radio-immunoprecipitation assay
RNA	Ribonucleic acid
RNase A	Endoribonuclease that specifically degrades single-stranded RNA
ROS	Reactive oxygen species

rpm	Rotations per minute
RT	Room temperature
SAD	Sporadic Alzheimer's disease
SC	Synthetic complete media
SDS	Sodium dodecyl sulfate
SDS-PAGE	Sodium dodecyl sulfate polyacrylamide gel electrophoresis
SEM	Standard error of the mean
Ser	Serine
shRNA	Short harpin RNA
SLC25A3	Solute carrier family 25 member 3 gene
SNQ2	Plasma membrane ATP-binding cassette (ABC) yeast transporter
SOD	Superoxide dismutase
ssDNA	Single stranded DNA
TAE	Tris-acetate-EDTA buffer
tau	Microtubule associated protein tau
tau40	441 amino acid long tau isoform
TBS	Tris buffered saline
TBST	Tris buffered saline supplemented with Tween 20
TCA	Tricarboxylic acid
TDP-43	TAR DNA-binding protein 43
TMRM	Tetramethylrhodamine methyl ester perchlorate
TRIS	Tris(hydroxymethyl)aminomethane
UPS	Ubiquitin-proteasome system
Ura	Uracil
URA3	Uracil locus
UV	Ultraviolet light
VDAC	Voltage-dependent anion channel proteins
VPS18	Vacuole protein sorting 18 homologue
WT	Wild-type
YKO	Yeast knockout collection
YPD	Yeast extract peptone dextrose
ZNF70	Zinc finger protein 70 gene
$\Delta\Psi m$	Mitochondrial membrane potential

Chapter 1.

Introduction

1.1. Proteinopathies

Protein misfolded disorders are triggered by changes in three-dimensional structure of proteins that lead to their self-association and precipitation (Bayer, 2013). Genetic defects, changes in the physical-chemical properties of proteins and/or failure of the protein quality control are processes that influence protein misfolding and formation of small order oligomers that tend to aggregate in higher order structures. These changes in conformation make proteins pathologically active, either by acquiring toxic functions or by losing their physiological functions (Bayer, 2013; Wolfe, 2012).

The aggregation of misfolded proteins may occur in different cells and regions of the body, originating a variety of disorders. When affecting the central nervous system (CNS), proteinopathies are often neurodegenerative disorders, and can be characterized by one or more proteinaceous aggregates (Bayer, 2013). Neurons are quite sensitive to the effects of misfolded proteins due to their post-mitotic nature and structure (Wolfe, 2012). Indeed, the long and narrow axonal projections of neurons can be easily clogged by accumulating proteins or by inefficient transport of nutrients and organelles (Wolfe, 2012). Additionally, accumulated misfolded proteins cannot be diluted through cell division, thereby turning neuron's integrity highly dependent on the protein homeostasis processes that usually start to fail during ageing (Bayer, 2013; Chen *et al.*, 2011; Wolfe, 2012). These processes involve different yet interconnected cellular strategies that aim at refolding, degrading, or sequestering misfolded proteins. A network of molecular chaperones is central to all these processes, being able to recognize misfolded proteins, actively promoting its refolding or, if not possible, promoting their degradation *via* the ubiquitin-proteasome system (UPS) (Chen *et al.*, 2011). Another pathway of misfolded protein degradation is autophagy, namely macroautophagy, a process mediating bulk degradation of long-lived proteins or organelles (Rami, 2009).

Neurodegeneration following intra- or extracellular deposition of misfolded aggregated proteins is a common feature of disorders such as Alzheimer's disease (AD), Parkinson's disease (PD) and Huntington's disease (HD). Despite the diversity of proteins involved in these disorders, all seem to adopt a similar, insoluble structure, consisting in fibrils with crossed β-pleated sheet structures (Skovronsky, Lee & Trojanowski, 2006). These disorders are associated with dementia that either occurs in the beginning of the disease, as in AD, or during its progression, as in PD or HD. These age-dependent syndromes are associated with the loss of neuronal function, ultimately leading to the impairment of several cognitive functions, such as memory, thinking, orientation, comprehension and learning capacity (Prince & Jackson, 2009).

The Alzheimer's disease International (ADI) estimated that, in 2013, 44.4 million people suffered with dementia worldwide (ADI, 2015). This number will increase to about 75.6 million in 2030 and will reach 135.5 million by 2050 (ADI, 2015). The prevalence of dementia is higher in developing countries where the life expectancy continues to increase, as a result of improved healthcare and quality of life (Prince & Jackson, 2009). Dementia disorders have a dramatic social impact, inflicting a personal and social burden to patients, their families and caregivers, and causing huge direct and indirect costs in

healthcare. In 2010, the total worldwide costs of dementia were US$604 billion dollars (Wimo & Prince, 2010). Based on demographics, ADI estimates that by 2030 these costs have increased by 85%, with developing countries bearing the highest share of this economic burden (Wimo & Prince, 2010). For all these reasons, dementia is considered a global health priority (Wortmann, 2012).

A significative progress has been made towards the understanding of the aetiology of many dementias in the last decades, but so far there are no mechanism-based treatments for most disorders. It is therefore imperative that new and better therapeutic solutions are promptly found and made available. Several international cooperative programmes tackle this health threat in several fronts, including (1) raising population awareness and identifying forms of prevention; (2) defining biomarkers to improve early diagnosis and clinical trial assessment; (3) developing drugs and vaccines; and (4) identifying new risk genes and factors that will help define the exact mechanism of disease, essential for the development of effective therapies (Prince & Jackson, 2009).

The most common neurodegenerative disorder is AD, accounting to 50-70% of all cases of dementia. Clinically, AD is characterized by progressive memory loss and cognitive decline due to synapse loss and neuronal cell death (Weintraub, Wicklund & Salmon, 2012). Histopathologically, AD is characterized by two types of *post-mortem* protein deposits: extracellular amyloid plaques composed of beta-amyloid (Aβ), and neurofibrillary tangles (NFTs) composed by hyperphosphorylated microtubule-associated protein tau (tau) (Goedert & Spillantini, 2006; Wolfe, 2012).

1.2. Tauopathies

The presence of NFTs is a unifying characteristic of a group of heterogeneous dementias and movement disorders known as tauopathies, listed in Table 1.1 (Spillantini & Goedert, 2013b).

Table 1.1. Diseases with tau pathology.

• Alzheimer's disease	• Hallervorden-Spatz disease
• Amyotrophic lateral sclerosis/parkinsonism-dementia complex	• Myotonic dystrophy
• Argyrophilic grain disease	• Niemann-Pick disease type C
• Chronic traumatic encephalopathy	• Non-Guamanian motor neuron disease with neurofibrillary tangles
• Corticobasal degeneration (CBD)	• Pantothenate kinase-associated neurodegeneration
• Creutzfeldt-Jakob disease	• Pick's disease
• Dementia pugilistic	• Postencephalitic parkinsonism
• Diffuse neurofibrillary tangles with calcification	• Prion protein cerebral amyloid angiopathy
• Down's syndrome	• Progressive subcortical gliosis
• Familial British dementia	• Progressive supranuclear palsy (PSP)
• Familial Danish dementia	• SLC9A6-related mental retardation
• Frontotemporal dementia and parkinsonism linked to chromosome 17 (FTDP-17)	• Subacute sclerosing panencephalitis
• Gerstmann–Sträussler–Scheinker disease	• Tangle-only dementia
• Guadeloupean parkinsonism	• White matter tauopathy with globular glial inclusions
• Guam parkinsonism dementia complex	

Some of the disorders listed above, such as CBD and PSP, are characterized by hyperphosphorylated misfolded tau and formation of NFTs in the absence of other neuropathological abnormalities, clearly involving tau in neurodegeneration. However, other disorders, such as AD, are called secondary tauopathies, due to the involvement of other aggregating proteins in the pathology (Ballatore, Lee & Trojanowski, 2007; Spillantini & Goedert, 2013b).

1.3. Tau protein – state-of'-the-art

1.3.1. Tau biology

1.3.1.1. Gene structure, transcripts and isoforms of tau

Tau is encoded in the human brain by a single gene (*MAPT*) located over 100kb on the long arm of chromosome 17 at band position 17q21.1 (Figure 1.1, top panel) (Gendron & Petrucelli, 2009; Neve *et al.*, 1986; Spillantini & Goedert, 2013b).Two main haplotypes have been identified (H1 and H2), being H1 the most common and overexpressed in some tauopathies (Ávila *et al.*, 2004; Spillantini & Goedert, 2013b).

The *MAPT* gene is constituted by 16 exons (E), 8 of which are constitutive (1, 4, 5, 7, 9, 11, 12 and 13). After transcription, remaining exons are subjected to mRNA alternative splicing (Figure 1.1, middle-panel) (Spillantini & Goedert, 2013b). E0 is part of the promoter and E14, which is part of the 3' region of tau mRNA, are not translated (Spillantini & Goedert, 2013b). E6 and E8 are not transcribed in the human brain and E4A is only expressed in the peripheral nervous system, originating a larger molecular weight tau isoform, termed big tau (695 amino acids) (Lee, Goedert & Trojanowski, 2001; Spillantini & Goedert, 2013b). Alternative splicing of E2, E3 and E10 results in six tau isoforms expressed in the human CNS, ranging from 352 to 441 amino acids long (Figure 1.1, bottom panel) (Gendron & Petrucelli, 2009; Spillantini & Goedert, 2013b). E2 and E3 encode two inserts of 28 amino acids near the N-terminal portion of tau protein and exons 9-12 encode four microtubule-binding domains (MTBD), located at the C-terminal end of the protein, of 31 or 32 amino acids length. Lack of E2 and E3 originates 0N tau isoforms, whereas inclusion of E2 produces 1N and inclusion of both E2 and E3 results in 2N tau isoforms. Inclusion of exon 10 results in tau with four MTBD repeats (4R tau) and exclusion results in three repeats (3R tau) (Gendron & Petrucelli, 2009; Spillantini & Goedert, 2013b). The abundance of 3R and 4R tau changes with brain development and neuronal differentiation: 3R tau isoforms are more abundant during embryonic stages of development, providing structural and morphological plasticity to developing neurons, while 4R tau isoforms are more important in mature neurons (Crespo-Biel, Theunis & Van Leuven, 2012). In the adult human brain, the molar ratio of 3R and 4R tau isoforms is ~1, and deviations from this ratio are characteristic of neurodegenerative tauopathies (Ballatore *et al.*, 2007). 0N, 1N and 2N tau isoforms comprise ~37, 54, and 9%, respectively, of total tau in the human CNS (Lee *et al.*, 2001).

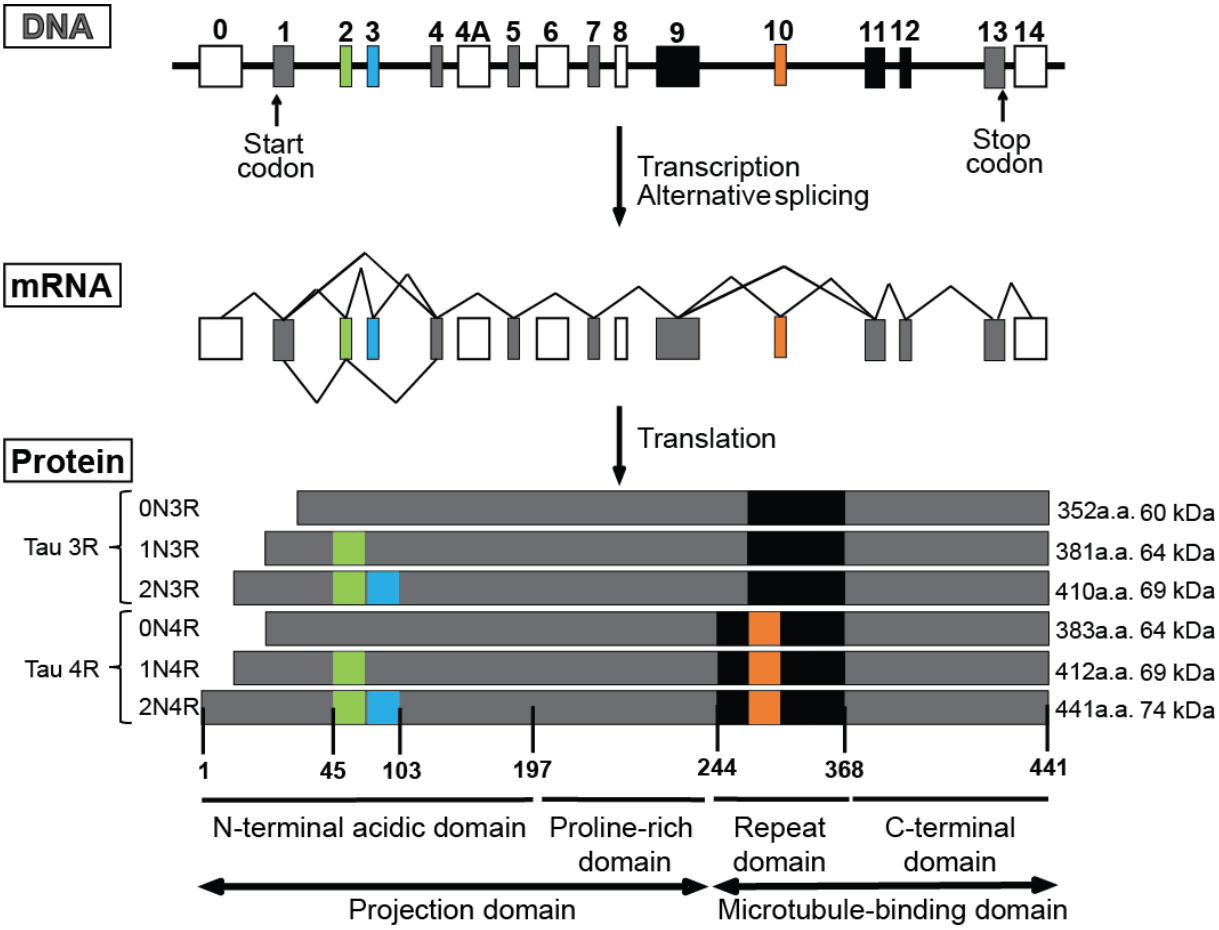

Figure 1.1. Tau gene, mRNA and protein isoforms in the human brain.
Top panel depicts the *MAPT* gene, composed of 16 exons (E). Coloured boxes represent alternative spliced exons, white boxes represent untranslated boxes and black boxes represent the exons coding for the repeat domain. In the middle panel, alternative mRNA splicing of E2, E3 and E10 (in colour), produces 6 tau isoforms that are expressed in the adult human brain. The commonly used terms to designate each tau isoform are listed and schematized in the bottom panel, with the number of amino acids and corresponding molecular weight (adapted from Brunden, Trojanowski & Lee, 2009; Martin, Latypova & Terro, 2011).

1.3.1.2. Tau protein structure, expression and post-translational modifications

Tau proteins were identified in 1975 as microtubule-binding proteins, promoting tubulin polymerization and assembly (Weingarten *et al.*, 1975). Independently of the isoform, tau is divided in several domains (Figure 1.1): (i) the microtubule binding domain, located at the C-terminal half and responsible for the binding to microtubules (Zempel & Mandelkow, 2014); (ii) the projection domain, located at the N-terminal of the protein, responsible for binding with the plasma membrane and other organelles (Morris *et al.*, 2011); and (iii) the proline-rich domain, localized in the middle of the protein (amino acids 150-

240), which contains seven PxxP motifs, an interaction motif for binding proteins with SH3[1] domains (Zempel & Mandelkow, 2014).

Tau is a natively unfolded protein, highly soluble, heat and acid-stable, and therefore, does not precipitate during boiling or acid treatment (Mandelkow *et al.*, 2007). Its high solubility and unfolded nature are explained by an enrichment in polar and charged amino acids, being a highly hydrophilic protein (Mandelkow *et al.*, 2007). Despite these characteristics, in disease, tau forms amyloid-like deposits (paired helical filaments, PHF), due to the existence of short hexapeptide motifs in the MTBD 2 and 3 (275VQIINK280 and 306VQIVYK311). These motifs are hydrophobic and interact *via* a cross-β structure that contributes to the core of PHFs, while the rest of the protein remains highly disordered (Mandelkow *et al.*, 2007).

Tau proteins have been found to be mainly expressed in the central and peripheral nervous systems, but relatively high levels have been detected also in heart, skeletal muscle, kidney, lung and testis and lower levels in adrenal gland, stomach and liver (Morris *et al.*, 2011; Wolfe, 2012). In the CNS, tau is mainly expressed in neurons, but it also occurs in astrocytes and perineuronal glial cells (Gendron & Petrucelli, 2009). In neurons, tau localizes predominantly to axons (Gendron & Petrucelli, 2009), being also found in dendrites (Ittner *et al.*, 2010) and in the nucleus (Shea & Cressman, 1998; Sultan *et al.*, 2011).

Tau proteins are subjected to a high number of post-translational modifications, such as phosphorylation, glycosylation, glycation, prolyl-isomerization, cleavage or truncation, nitration, polyamination, ubiquitination, sumoylation, oxidation and aggregation (reviewed in Martin *et al.*, 2011). The diversity of these modifications suggests that tau biology is highly regulated (Morris *et al.*, 2011).

Phosphorylation is the most common and extensively studied tau post-translational modification, because it is widely accepted that (i) phosphorylation level regulates tau binding to the microtubules and (ii) abnormal phosphorylation of tau occurs before the onset of NFTs (Martin *et al.*, 2011; Noble *et al.*, 2013). Tau isoforms can be phosphorylated in more than 80 serine, threonine and tyrosine residues by a variety of kinases (Noble *et al.*, 2013). Kinases that phosphorylate tau at serine/threonine residues include proline-directed kinases, such as glycogen synthase kinase-3β (GSK-3β) and cyclin-dependent kinase 5 (CDK5), non-proline-directed kinases such as casein kinase 1 (CK1) and microtubule affinity-regulating kinases (MARKs) (Noble *et al.*, 2013). Tau tyrosine kinases include Fyn, Abl and Syk (Noble *et al.*, 2013). A complete list of tau phosphorylation sites can be found at http://cnr.iop.kcl.ac.uk/hangerlab/tautable. The level of tau phosphorylation is also regulated by phosphatases that dephosphorylate tau. Indeed, protein phosphatase A (PP2A), the major cell phosphatase, has been implicated in the regulation of tau phosphorylation level and its activity is decreased by about 50% in AD brains (Martin *et al.*, 2011; Noble *et al.*, 2013). The balance between kinase and phosphatase activity is critical for tau function and dysfunction (Wolfe, 2012).

[1] SH3 domain is a conserved sequence of 60 amino acids found in proteins of signalling pathways regulating the cytoskeleton, the Ras protein, the Src kinase and many other proteins (Mayer, 2001).

1.3.1.3. Tau binding partners and functions

Tau most widely accepted function is the regulation of microtubule assembly and stability (Weingarten *et al.*, 1975). *In vivo*, tau may be more involved in microtubules dynamics, participating in processes such as establishment of neuronal polarity, axonal outgrowth and transport of cellular cargoes along axons and dendrites (Gendron & Petrucelli, 2009; Wolfe, 2012). The interaction of the N-projection domain of tau with the plasma membrane (Brandt, Leger & Lee, 1995) and the actin cytoskeleton (Fulga *et al.*, 2007) suggests that tau serves as a mediator between microtubules and the plasma membrane and the actin network (Morris *et al.*, 2011).

Due to intense study of tau biology in the last decade, many dogmas have been challenged and new functions of tau are being established. Although many studies point to a critical function of tau in cytoskeleton-related processes, four independently generated tau knockout mice strains were shown to be viable, fertile and relatively normal (Ke *et al.*, 2012b). Moreover, knockdown of tau with small interference RNA (siRNA) is not cytotoxic to primary cultured neurons and does not prevent axon formation (Qiang *et al.*, 2006). These results indicate that tau is not essential to neurons or microtubule formation. This can be explained by mechanisms of compensation and/or redundant functions of other microtubule-binding proteins, such as MAP1A and MAP1B (Ke *et al.*, 2012b; Morris *et al.*, 2011; Wolfe, 2012).

Other tau functions have been reported as a result of interactions with other cellular structures and enzymes (Morris *et al.*, 2011). Table 1.2 presents a list (non-exhaustive) of several tau-binding partners, placing the protein in many other cell processes.

Table 1.2. Partial list of tau interactors.

Gene	Protein	Function	References
AATF	apoptosis antagonizing transcription factor	Interacts with MAP3K12/DLK, a protein kinase known to be involved in the induction of cell apoptosis	(Barbato *et al.*, 2003)
AKT1	RAC-alpha serine/threonine-protein kinase	Regulate many processes including metabolism, proliferation, cell survival, growth and angiogenesis	(Sadik *et al.*, 2009)
APOE	apolipoprotein E3	Mediates the binding, internalization, and catabolism of lipoprotein particles	(Huang & Jiang, 2009)
APP	Amyloid beta A4 protein	Cell surface receptor and performs physiological functions on the surface of neurons relevant to neurite growth, neuronal adhesion and axonogenesis	(Guo *et al.*, 2006)
ASYN	alpha-synuclein	May integrate presynaptic signalling and membrane trafficking. Involved in Parkinson's disease	(Kawakami *et al.*, 2011)
BAG1	BCL2-associated athanogene	Binds to BCL2 enhancing its anti-apoptotic effects, representing a link between growth factor receptors and anti-apoptotic mechanisms	(Elliott, Tsvetkov & Ginzburg, 2007)

Gene	Protein	Function	References
BIN1	Myc box-dependent-interacting protein 1	May be involved in regulation of synaptic vesicle endocytosis. May act as a tumour suppressor and inhibits malignant cell transformation	(Chapuis *et al.*, 2013)
CAPN2	calpain 2, (m/II) large subunit	Calcium-activated neutral proteases, are nonlysosomal, intracellular cysteine proteases	(Glading *et al.*, 2004)
CDK5	Cyclin-dependent-like kinase 5	Proline-directed serine/threonine-protein kinase essential for neuronal cell cycle arrest and differentiation and may be involved in apoptotic cell death in neuronal diseases by triggering abortive cell cycle re-entry	(Liu *et al.*, 2002)
DCTN1	dynactin 1	Required for the cytoplasmic dynein-driven retrograde movement of vesicles and organelles along microtubules. Dynein-dynactin interaction is a key component of the mechanism of axonal transport of vesicles and organelles	(Magnani *et al.*, 2007)
DNAAF2	dynein, axonemal, assembly factor 2	Highly conserved protein involved in the preassembly of dynein arm complexes that power cilia	(Scholz & Mandelkow, 2014)
EP300	histone acetyltransferase p300	Regulates transcription via chromatin remodelling and is important in the processes of cell proliferation and differentiation	(Min *et al.*, 2010)
FYN	Tyrosine-protein kinase Fyn	Non-receptor tyrosine-protein kinase that plays a role in many biological processes including regulation of cell growth and survival, cell adhesion, integrin-mediated signalling, cytoskeletal remodelling, cell motility, immune response and axon guidance	(Usardi *et al.*, 2011)
GSK-3b	Glycogen synthase kinase-3 beta	Constitutively active protein kinase involved in many signalling pathways	(Kawakami *et al.*, 2014)
HDAC6	histone deacetylase 6	Plays a critical role in transcriptional regulation, cell cycle progression, and developmental events. Histone acetylation/deacetylation alters chromosome structure and affects transcription factor access to DNA	(Ding, Dolan & Johnson, 2008)
HSP90AB1	Heat shock protein HSP 90-beta	Chaperone that promotes the maturation, structural maintenance and proper regulation of specific target proteins involved, for instance, in cell cycle control and signal transduction	(Karagoz *et al.*, 2014)
HSPA1A	Heat shock 70 kDa protein 1A/1B	Stabilizes existing proteins against aggregation and mediates the folding of newly translated proteins in the cytosol and in organelles. It is also involved in the ubiquitin-proteasome pathway	(Jinwal *et al.*, 2013)
HSPA4	Heat shock 70 kDa protein 4	Chaperone-mediated protein complex assembly; Protein import into mitochondrial outer membrane; response to unfolded protein	(Jinwal *et al.*, 2013)
HSPA8	Heat shock 70kDa protein 8	Chaperone: binds to nascent polypeptides to facilitate correct folding. It also functions as an ATPase in the disassembly of clathrin-coated vesicles during transport of membrane components through the cell	(Elliott *et al.*, 2007)

Gene	Protein	Function	References
LRKK2	Leucine-rich repeat serine/threonine-protein kinase 2	Regulates autophagy, plays a role in retrograde trafficking pathway for recycling proteins, regulates neuronal process morphology in the intact CNS. Involved in Parkinson's disease	(Kawakami *et al.*, 2014)
NUB1	Negative regulator of ubiquitin-like proteins 1	Negative regulator of NEDD8, a ubiquitin-like protein that conjugates with cullin family members in order to regulate vital biological events	(Richet *et al.*, 2012)
PEG10	Embryonal carcinoma differentiation-regulated protein	Reported to have a role in cell proliferation, differentiation and apoptosis	(Gu *et al.*, 2013)
PINCH	LIM and senescent cell antigen-like-containing domain protein 1	Adapter protein in a cytoplasmic complex linking beta-integrins to the actin cytoskeleton, bridges the complex to cell surface receptor tyrosine kinases and growth factor receptors. Involved in the regulation of cell survival, cell proliferation and cell differentiation	(Ozdemir *et al.*, 2013)
PRNP	Major prion protein	May play a role in neuronal development and synaptic plasticity	(Schmitz *et al.*, 2014)
PSEN1	Presenilin 1	Mutations in this gene cause AD. Presenilins are postulated to regulate APP processing through their effects on gamma-secretase, an enzyme that cleaves APP. Also, it is thought that the presenilins are involved in the cleavage of the Notch receptor, such that they either directly regulate gamma-secretase activity or are protease enzymes	(Takashima *et al.*, 1998)
PSMC2	Proteasome 26S subunit, ATPase, 2	Part of multicatalytic proteinase complex; this subunit interacts with several basal transcription factors-; so, in addition to participation in proteasome functions, participates in the regulation of transcription	(Babu, Geetha & Wooten, 2005)
RPS6KB1	Ribosomal protein S6 kinase beta-1	Serine/threonine-protein kinase that acts downstream of mTOR signalling in response to growth factors and nutrients to promote cell proliferation, cell growth and cell cycle progression	(Pei *et al.*, 2006)
S100B	S100 calcium-binding protein, beta (neural)	Ion-binding protein	(Yu & Fraser, 2001)
SIRT1	NAD-dependent deacetylase sirtuin-1	Studies suggest that the human sirtuins may function as intracellular regulatory proteins with mono-ADP-ribosyltransferase activity	(Min *et al.*, 2010)
SLC1A2	Excitatory amino acid transporter 2	Transports L-glutamate and also L- and D-aspartate. Essential for terminating the postsynaptic action of glutamate by rapidly removing released glutamate from the synaptic cleft. Acts as a symport by co-transporting sodium	(Sasaki *et al.*, 2009)
SQSTM1	Sequestosome 1	Multifunctional protein that binds ubiquitin and regulates activation of the nuclear factor kappa-B (NF-kB) signalling pathway	(Babu *et al.*, 2005)
STUB1 (CHIP)	STIP1 homology and U-box containing protein 1	E3 ubiquitin-protein ligase which targets misfolded chaperone substrates towards proteasomal degradation	(Petrucelli *et al.*, 2004)

Gene	Protein	Function	References
STXBP1	Syntaxin binding protein 1	Appears to play a role in release of neurotransmitters via regulation of syntaxin, a transmembrane attachment protein receptor	(Bhaskar *et al.*, 2004)
TRAF6	TNF receptor-associated factor 6	E3 ubiquitin protein ligase, acts as a signalling molecule	(Babu *et al.*, 2005)
TTLL6	Tubulin polyglutamylase TTLL6	Polyglutamylase that preferentially modifies alpha-tubulin, by generating side chains of glycine on the gamma-carboxyl groups of specific glutamate residues	(Zempel *et al.*, 2013)
UBC	Polyubiquitin-C	Ubiquitination has been associated with protein degradation, DNA repair, cell cycle regulation, kinase modification, endocytosis, and regulation of other cell signalling pathways	(Petrucelli *et al.*, 2004)
UBE2D2	Ubiquitin-conjugating enzyme E2D 2	Regulated degradation of misfolded, damaged or short-lived proteins in eukaryotes occurs via the ubiquitin (Ub)-proteasome system (UPS)	(Shimura *et al.*, 2004)
YWHAB	14-3-3-zeta	Adapter protein implicated in the regulation of a large spectrum of both general and specialized signalling pathways	(Luong *et al.*, 2000)
YWHAQ	14-3-3 protein theta	Adapter protein implicated in the regulation of a large spectrum of both general and specialized signalling pathways	(Chun *et al.*, 2004)

Most of tau kinases and phosphatases are not listed.

Tau binding partners include cytoskeletal proteins, as expected, signalling molecules, proteins involved in the heat shock response and protein folding pathways, regulation of cell cycle and apoptosis. Taking into consideration some of these interactors, tau can act as a protein scaffold, regulating many signalling pathways. One of the most studied of such pathways, in neurons, involves tau interaction with the tyrosine kinase Fyn, establishing tau as a post-synaptic protein (Ittner *et al.*, 2010). The authors hypothesize that tau acts as scaffold protein bringing together Fyn and postsynaptic density protein 95 (PSD95), localizing Fyn at synapses, enabling its activation through *N*-methyl-D-aspartate (NMDA) receptors. Indeed, tau is required for phosphorylation of NMDA receptor subunit GluN2B in dendrites and mediates Aβ toxicity at dendrites in a mice model of AD (Ittner *et al.*, 2010). Functional roles for nuclear tau have been also proposed (Sjoberg *et al.*, 2006). Moreover, the high degree of tau post-translational modifications, which significance has not been fully characterized yet, further contributes to the complexity of tau biological and pathological roles (Ballatore *et al.*, 2007).

1.3.2. Tau in disease

As described in the previous section, tau has multiple functions and therefore can be involved in neurodegeneration in a variety of ways. Whereas in AD tau mechanisms of disease appear to be connected with Aβ, in other tauopathies tau mutations are sufficient to cause disease (Ballatore *et al.*, 2007; Spillantini & Goedert, 2013b).

Abnormal tau hyperphosphorylation is common between human tauopathies, reducing its normal association with microtubules and axonal distribution and, eventually, leading to its aggregation in intracellular filamentous deposits (Figure 1.2). The morphology, isoform content and intracellular localization of these deposits differs depending on the tauopathy (Ballatore *et al.*, 2007). How exactly these morphological changes lead to neurodegeneration is still not fully understood and is a matter of intense debate in the field.

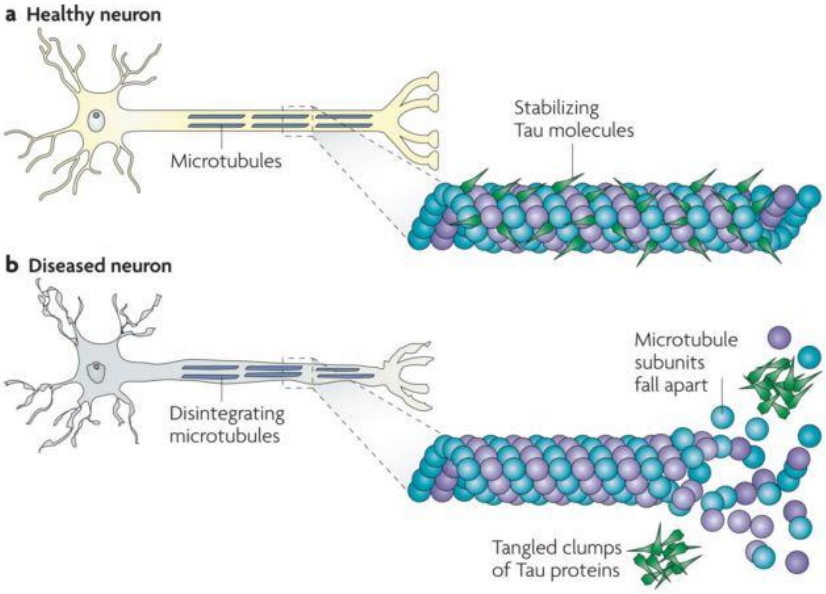

Figure 1.2.Tau in healthy and diseased neurons.
Tau binds and stabilizes microtubules in healthy neurons. In disease, tau becomes hyperphosphorylated, detaching from the microtubules and losing its normal distribution, accumulating in the neuron cytosol (Brunden et al., 2009).

1.3.2.1. Alzheimer's disease

First described in 1907 by Alois Alzheimer, AD is clinically characterized by progressive memory loss and cognitive decline, mood swings, personality changes and loss of independence. The main risk factor for developing AD is age, with prevalence increasing exponentially every 5 years over the age of 65. Early onset is more uncommon and usually suggests a genetic cause (Prince & Jackson, 2009). Death usually occurs 3 or 4 years after diagnosis in people older than 80, or 10 to more years when the disease is diagnosed in younger people.

AD begins in the entorhinal cortex, spreading to the hippocampus and cerebral cortex, leading to loss of brain tissue and brain atrophy (Figure 1.3) (Rodgers, Aging & Health, 2008). Although the course of the disease is not the same in every person, AD progression has been divided in several stages. The Preclinical stage includes changes in the brain that start to occur decades before the clinical onset (Figure 1.3). As the disease progresses, memory and cognitive problems ensue, in a stage designated as Mild Cognitive Impairment (MCI). Not all patients diagnosed with MCI develop AD, but are thought to have a higher probability to do so. As AD continues to spread to the cerebral cortex, cognitive decline accelerates (clinically diagnosed as Mild to Moderate AD), leading to widespread pathology in the brain

(Severe AD). Definitive diagnostic of AD is only obtained at authopsy (Hampel *et al.*, 2011; Rodgers *et al.*, 2008).

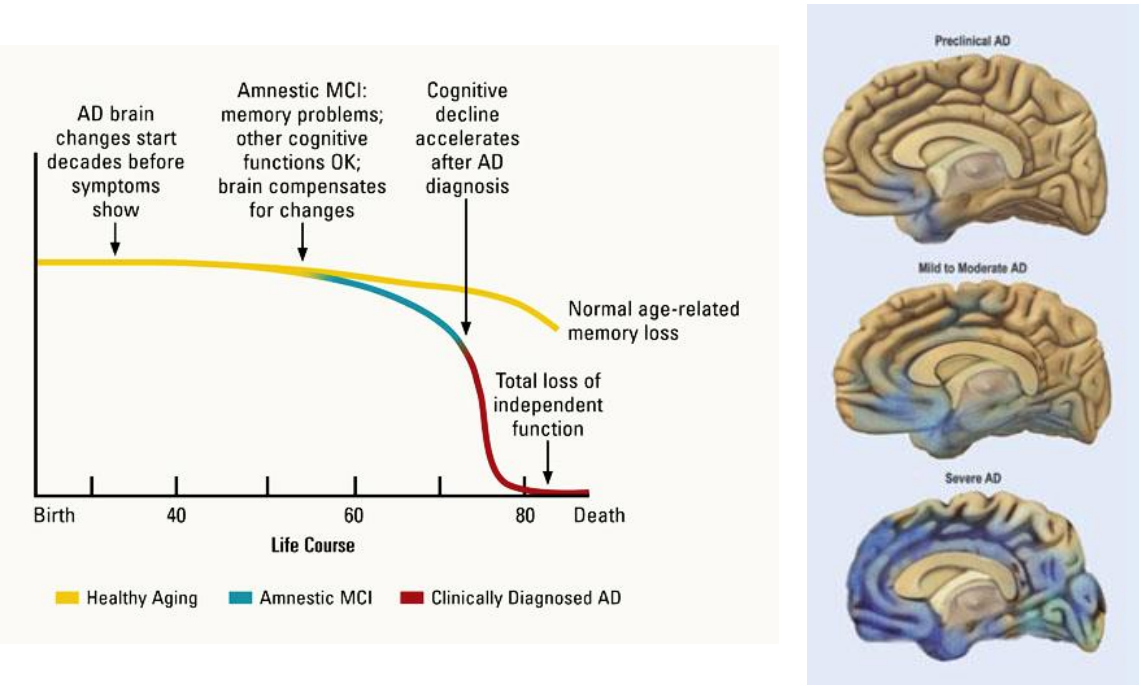

Figure 1.3. Alzheimer's disease predicted progression.
The left panel correlates dementia symptoms between AD and normal age-related memory loss. The right panel, presents a schematics of AD brain morphology, depicting the characteristic brain atrophy (Rodgers *et al.*, 2008).

The most common form of AD is called sporadic AD (SAD) presumed to occur due to a complex combination between genetic and environmental causes. The major risk factor for developing SAD is aging, presence of AD risk genes and other environmental factors, as diabetes and cholesterol (Hampel *et al.*, 2011). The hereditary form of AD, usually of early onset, is designated as familial AD (FAD), accounting for less than 5% of all AD cases. FAD occurrence has been associated with mutations in the gene coding for amyloid precursor protein (*APP*), or its duplication, as occurs in Down Syndrome, and in the presenilin genes (*PSEN1* and *PSEN2*), coding for gamma-secretase subunits, responsible for the cleavage of APP and formation of Aβ. Mutations in the *MAPT* gene, coding for tau proteins, have not been identified in AD (Medina & Avila, 2014).

Despite the progress in AD detection using cerebral spinal fluid biomarkers and brain imaging scans, the definite confirmation of diagnostics occurs only at autopsy, with the histopathological detection of the two hallmark protein aggregates, the extracellular amyloid plaques and intracellular NFTs (Figure 1.4) (Goedert & Spillantini, 2006).

Increasing evidences show that the central dogma of extracellular amyloid and intracellular tau is incomplete, as the accumulation of intraneuronal Aβ is becoming widely demonstrated in human brains with AD, Down syndrome and in transgenic mice and rat models of AD (reviewed in LaFerla, Green & Oddo, 2007).

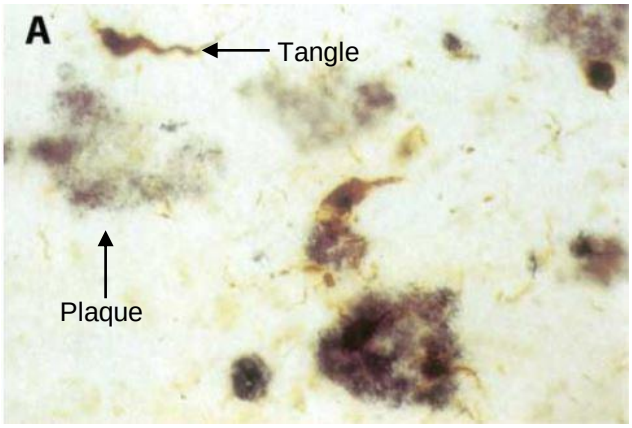

Figure 1.4. Alzheimer's disease hallmark *post-mortem* lesions.
Senile plaques formed by beta-amyloid and neurofibrillary tangles, the latter composed of hyperphosphorylated microtubule-associated protein tau (Goedert & Spillantini, 2006).

Aβ peptides are produced by sequential proteolytic cleavage of APP, by beta- and gamma-secretases. Aβ peptides of 40-42 amino acids (3-4 kDa) are produced at a ratio 10:1, being the peptide $A\beta_{1-42}$ the most amyloidogenic (Goedert & Spillantini, 2006; LaFerla *et al.*, 2007). The source of intraneuronal Aβ is still debatable, since it can be internalized by the cell from the extracellular plaques or, depending on the site of its production, not secreted to the extracellular space and, hence, intracellular. In principle, intraneuronal Aβ can be produced whenever APP and beta- and gamma-secretases co-localize, and this includes the plasma membrane, trans-Golgi network, endoplasmic reticulum, and endosomal, lysosomal and mitochondrial membranes (LaFerla *et al.*, 2007). If Aβ is produced in the plasma membrane or in the secretory pathway it will be extracellular; if it occurs within the cell, then it will be located intracellularly (LaFerla *et al.*, 2007). The high neurotoxicity of intraneuronal Aβ has been demonstrated in *in vitro* and *in vivo* studies (Billings *et al.*, 2005; LaFerla *et al.*, 2007; Oddo *et al.*, 2003) and several reports suggest a direct link between Aβ and tau in causing toxicity in AD (reviewed in Ittner & Gotz, 2011). The mechanism of such interplay, however, is not fully understood and three main modes of interaction have been proposed. Briefly, Aβ may be the trigger of AD, driving tau pathology, probably by activating tau kinases, such as GSK-3β or CDK5; conversely, tau may mediate Aβ toxicity, through its recently established interaction with Fyn kinase; and finally, both proteins may have synergistic toxic effects, as occurs at the level of mitochondria (Ittner & Gotz, 2011).

Other evidences opening new areas of investigation are the reports of the existence of extracellular tau that can induce pathology in surrounding neurons, thus contributing for the spreading of tauopathy throughout the brain (Clavaguera *et al.*, 2009; Guo & Lee, 2011).

1.3.2.2. Frontotemporal dementia

Frontotemporal lobar degeneration (FTLD) is a heterogeneous group of disorders, characterized by frontal and temporal brain atrophy and neuronal loss (Pan & Chen, 2013; Rademakers, Neumann & Mackenzie, 2012). A subset of FTLD disorders arise from fully penetrant, autosomal dominant point mutations in the *MAPT* gene coding for the microtubule associated protein tau (FTLD-tau), such as FTDP-17, associated with P301L mutation (Rademakers *et al.*, 2012). These genetic tauopathies are

accompanied by complex behavioural and cognitive disturbances, including compromised executive function (Pan & Chen, 2013; Rademakers *et al.*, 2012).

Since the discovery of mutations in the *MAPT* gene associated with FTDP-17, in 1998, over 40 mutations have been identified (Figure 1.5) (Goedert, 2005). Many mutations cluster in and around the regions encoding the microtubule binding domain, suggesting that perturbations in the ability of tau to bind microtubules could be involved in neurodegeneration (Wolfe, 2012). The discovery of these mutations associated with disease demonstrated without doubt that tau dysfunction alone is capable of causing disease (Ballatore *et al.*, 2007; Goedert, 2005). There are mainly two classes of mutations: missense mutations within the coding region of the gene that may conduce to decreased ability of tau to bind microtubules or increase the propensity to form insoluble fibrils; and mutations that affect the splicing of exon 10, leading to an increase of 4R isoforms and therefore to a disequilibrium of the molar ratio between 3R and 4R tau isoforms (Brunden *et al.*, 2009; Goedert, 2005).

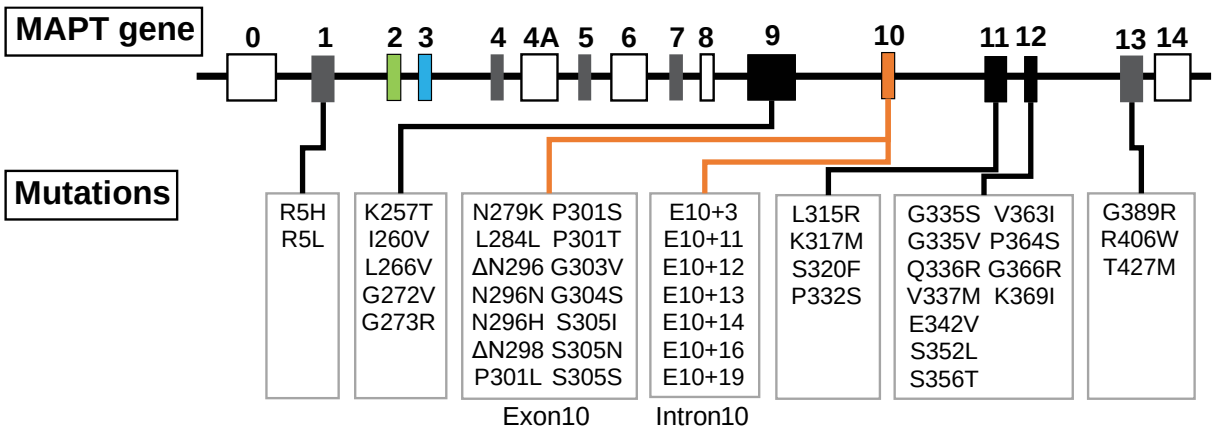

Figure 1.5. *MAPT* gene mutations.
Schematic diagram of tau gene with mutations in the coding region indicated using the numbering of the 441-amino-acid tau isoform (Goedert, 2005).

The clinical and pathological phenotype differs between the different tau mutations (reviewed in Goedert, 2005). Some lead to tau accumulation in both neurons and glial cells, whereas others are exclusive to neurons. Tau filaments also present ultrastructural differences depending on mutations, with some presenting twisted helical filaments; others paired helical filaments (similar to what occurs in AD) and others straight helical filaments (Goedert, 2005).

1.3.3. Loss *vs*. gain of function

As in other proteins associated with different neurodegenerative diseases, tau-induced neurodegeneration is thought to be a consequence of mechanisms of gain of toxic function combined with mechanisms of loss of normal function (Frost, Gotz & Feany, 2015; Medina & Avila, 2014; Noble, Pooler & Hanger, 2011).

1.3.3.1. Loss of normal function of tau protein in disease

Under normal physiological conditions, the binding of tau to microtubules, and consequently its function as a cytoskeleton protein, is regulated by a balance between phosphorylation and dephosphorylation (Noble *et al.*, 2013). In disease, hyperphosphorylation or mutations that decrease tau's ability to bind microtubules lead to tau detachment from microtubules and missorting from the axon to the somatodendritic compartment. This would reduce the functionality of microtubules and disruption of the structure of the neuronal cytoskeleton, interfering with neuronal polarity, synaptic plasticity, transport of nutrients and organelles along the axon to the synapse, leading to synapse dysfunction and neuronal loss. In this sense, tau mechanism of neurodegeneration would be associated with loss of its normal function (Frost *et al.*, 2015; Medina & Avila, 2014; Noble *et al.*, 2011).

1.3.3.2. Toxic gain of function of tau protein in disease

Hyperphosphorylation, misfolding and missorting of tau from the axon to the cytoplasm leads to increased propensity of tau for suffering additional conformational changes that ultimately lead to formation of soluble oligomers, aggregates and fibrils in the cell body and dendrites of neurons (Ballatore *et al.*, 2007; Ittner *et al.*, 2011). The exact mechanism of tau aggregation is still not fully understood, but there are evidences suggesting that hyperphosphorylation and other post-translational modifications, such as proteolysis, precede tau aggregation (Noble *et al.*, 2013). Also, larger tau aggregates appear to evolve from the successive aggregation of smaller tau species, such as monomers, dimers and soluble oligomers (Figure 1.6) (reviewed in Cowan & Mudher, 2013).

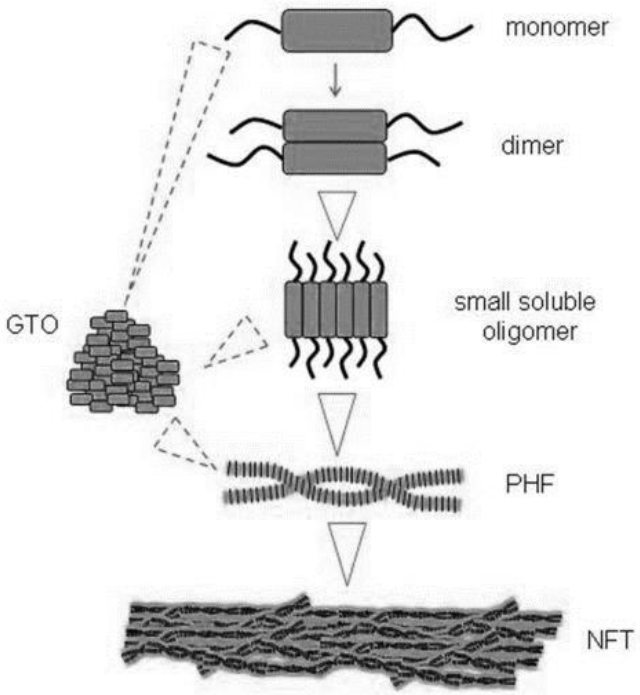

Figure 1.6. Putative sequence of events in tau aggregation into neurofibrillary tangles.
GTO: granular tau oligomers; PHF: paired helical filaments; NFT: neurofibrillary tangle (Cowan & Mudher, 2013).

Tau filaments can originate directly from soluble oligomers or from granular tau oligomers (GTO) and can have three forms, as mentioned in the previous section: paired helical filaments (PHF's), predominant in AD, straight filaments and twisted helical filaments (Cowan & Mudher, 2013; Goedert, 2005). These filaments exhibit β-sheet structure and can be considered amyloid. The bundling of tau filaments originates NFTs that may fill the entire neuron cytosol. The accumulation of tau filaments also in dendrites originates neuropil threads (Cowan & Mudher, 2013). These aberrant species would be, *per se*, the cause of neuronal dysfunction and degeneration, acting in a variety of cellular processes (reviewed in Frost *et al.*, 2015). Increasing evidences demonstrate that small tau oligomers are the most toxic form of tau, since filamentous and fibrillary tau are not necessary or sufficient to cause tau toxicity and may even be considered a neuroprotective strategy, as suggested by studies with other aggregating proteins such as Aβ, huntingtin or alpha-synuclein (Cowan & Mudher, 2013; Wolfe, 2012). With disease progression, larger tau aggregates will physically impair protein homeostasis and disrupt normal cell functioning (Yoshiyama, Lee & Trojanowski, 2013).

Independently of which tau species is the most toxic, tau misfolding and aggregation suggest that tau mechanism of disease would be a result of gain of toxic functions (Frost *et al.*, 2015; Wolfe, 2012). Indeed, studies with tau knockout mice showed that deletion of tau does not cause neurodegeneration, while transgenic overexpression of wild-type or mutated tau in various animals of tauopathy causes progressive neuronal death (Frost *et al.*, 2015; Ke *et al.*, 2012b). Other evidences of gain of toxic functions include increased amount of 4R isoforms in some tauopathies due to mutations in tau gene that could lead to over-stabilization of microtubules, thereby reducing their required plasticity (Noble *et al.*, 2011). Additionally, impaired degradation or clearance of aggregated tau might contribute to a clogging of the cell with obvious consequences in the transport of organelles and nutrients to the axon and dendrites (Noble *et al.*, 2011). Tau missorting to the somatodendritic compartment has been found to trap proteins essential for the kinesin-driven axonal transport and other proteins, such as SFPQ (splicing factor proline/glutamine rich), a transcription regulator (Ittner, Ke & Gotz, 2009; Ke *et al.*, 2012a). Also, tau has been found capable of inducing the formation of actin bundles, causing an over stabilization of actin. This reduces actin turnover and dynamics, with significant consequences for cellular function, such as inhibition of myosin-mediated organelle transport, which is reduced in tauopathies, and oxidative stress that also contributes to neurotoxicity in tauopathies (Frost *et al.*, 2015; Fulga *et al.*, 2007). Moreover, this excess of filamentous actin physically interacts with DRP-1 (dynamin 1-like) in tauopathy, blocking the myosin-based translocation of DRP1 to the mitochondria, compromising mitochondria fission and promoting its elongation (Eckert *et al.*, 2014). Indeed, it has been demonstrated that structural and functional mitochondria abnormalities are caused by tau in several *in vivo* and *in vitro* models of tauopathy, either independently or in synergy with Aβ toxicity (Eckert *et al.*, 2014). Mitochondrial dysfunction has been reported in human brains with AD and FTDP-17 (Eckert *et al.*, 2014; Frost *et al.*, 2015). At the level of synapses, tau mediates Aβ toxicity through its interaction with the Src tyrosine kinase Fyn (Ittner *et al.*, 2010). While Aβ is usually placed upstream of tau in the cascade of such events, *in vivo* studies using transgenic mice showed that reduction of tau levels were actually sufficient to improve the features that characterize mice with Aβ deposition, which include reduced lifespan, memory impairment and increased susceptibility to seizures (Ittner *et al.*, 2010;

Roberson *et al.*, 2007). Other study suggested a feedback mechanism with tau regulating Aβ, since tau removal resulted in reduced plaque load (Leroy *et al.*, 2012). Finally, pathological tau has been found to activate cell cycle re-entry in post mitotic neurons, initiating a cascade of events resulting from tau-induced actin-stabilization, mitochondrial dysfunction, oxidative stress, DNA damage, heterochromatin relaxation and aberrant gene expression that ultimately leads to neuronal cell death (Frost *et al.*, 2015).

1.4. Tau as a drug target

As mentioned in the previous section, some tauopathies are characterized by accumulation of hyperphosphorylated misfolded tau in the absence of deposition of other proteins, clearly demonstrating the role of tau in disease onset and progression. Moreover, the discovery of mutations in tau gene (*MAPT*) in FTDP-17 has proved unequivocally that tau dysfunction is sufficient to cause neurodegeneration and dementia (Ballatore *et al.*, 2007; Goedert, 2005).

Increasing evidences also advocate to a more central role of tau in AD pathogenesis and neurotoxicity, albeit the established amyloid cascade hypothesis that postulates Aβ as the disease trigger (Hardy & Allsop, 1991). One of such evidences is the high correlation between cognitive decline and tau pathology, rather than with extracellular Aβ deposition (Medina & Avila, 2014). Additionally, it is becoming widely accepted that tau interacts with Aβ in causing neurotoxicity in AD, although the mechanism of such interaction is not fully understood (Ittner & Gotz, 2011). Further support of tau causative role in neurodegeneration is given by evidences of tauopathy spreading to neighbouring neurons in AD (Clavaguera *et al.*, 2009). Moreover, drug discovery and development programmes focused on Aβ pathology have shown limited efficacy in late stage clinical studies for AD. For example, active immunisation with Aβ resulted in the clearance of the peptide but did not prevent tau pathology or neurodegeneration (Yoshiyama *et al.*, 2013).

The failure of Aβ-based therapies together with increasing understanding of the role of tau in neuropathogenesis, contributed to the focus on tau as a potential target for therapeutic intervention in a wide-range of neurodegenerative disorders (Davidowitz & Moe, 2012; Medina & Avila, 2014). Tau-based therapeutic strategies have, therefore, become a priority and will benefit from the clarification of tau biology and tau-mediated mechanisms of disease (Davidowitz & Moe, 2012; Noble *et al.*, 2011).

1.4.1. Therapeutic strategies targeting tau

To date, there is no effective disease-modifying therapy for tauopathies. Regarding AD, the 5 marketed drugs used for treating symptoms include: four acetylcholinesterase inhibitors and one NMDA-receptor antagonist (Calcul *et al.*, 2012; Noble *et al.*, 2011).

Increased knowledge on tau function in biology and pathology has contributed to the development of several different therapeutic strategies based on the genetic players involved in the different pathways through which tau mediates neuronal dysfunction and death (mentioned previously). The variety of the

different approaches allows covering all aspects of tau dysfunction at different stages of disease progression (Figure 1.7) (Noble *et al.*, 2011; Yoshiyama *et al.*, 2013).

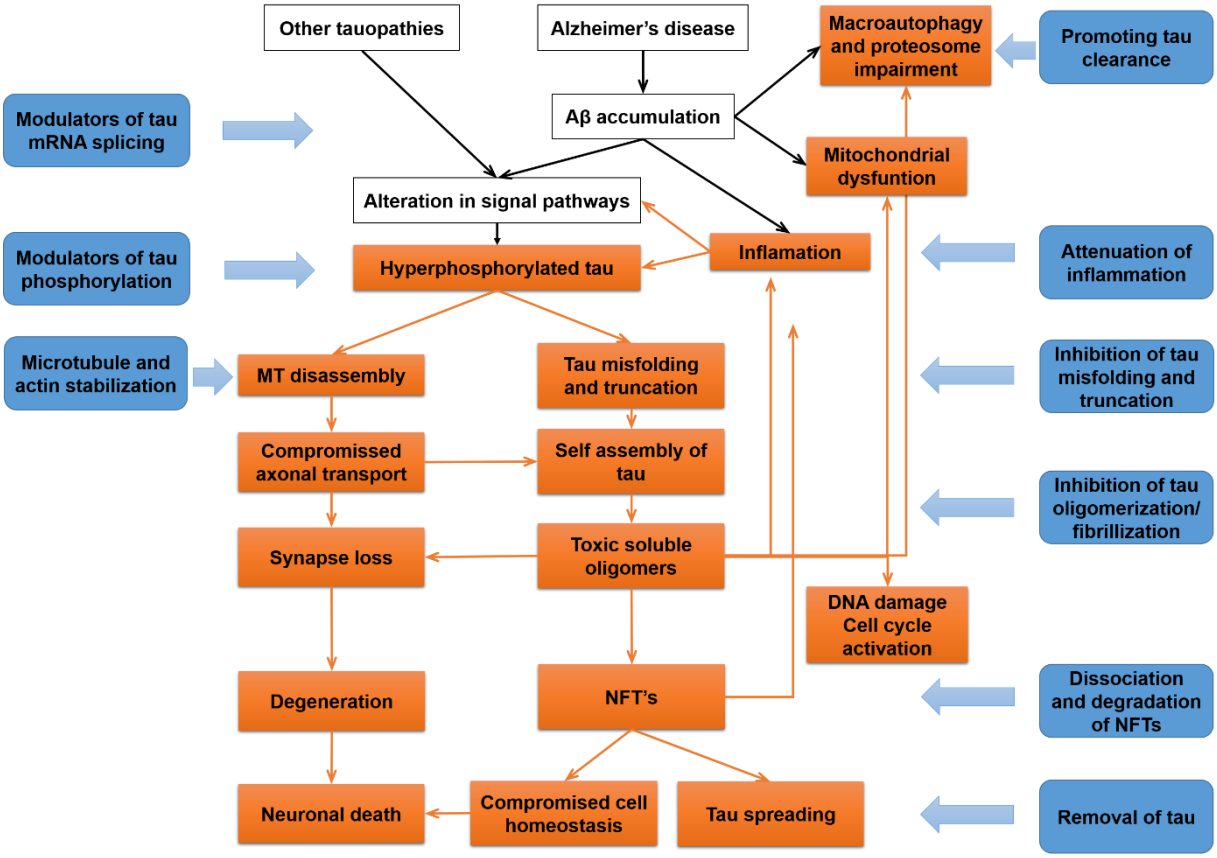

Figure 1.7. Tau-based therapeutic strategies.
Representation of several aspects of tau dysfunction at different stages of disease (orange squares), correlated with the different therapeutic strategies under development (blue squares) (adapted from Yoshiyama *et al.*, 2013).

The therapeutic strategies available include inhibitors of tau phosphorylation and misfolding, aggregation blockers, promoters of tau clearance, tau immunotherapies, inhibitors of tau propagation, attenuation of inflammation and mitochondrial dysfunction and oxidative stress, and approaches targeting the regulation of tau pre-mRNA splicing, cell cycle activation, DNA damage and heterochromatin relaxation. There are also strategies that tackle loss of function of tau, such as microtubule-stabilizing agents (Frost *et al.*, 2015; Medina & Avila, 2014; Noble *et al.*, 2011; Yoshiyama *et al.*, 2013). Most of the studies are still in pre-clinical stage, however several small molecules have reached the early stages of clinical development (Medina & Avila, 2014; Noble *et al.*, 2011). Table 1.3 summarizes the small molecules that have reached the clinical stage of development (based on ALZFORUM therapeutics database available at http://www.alzforum.org/).

The lack of reliable biomarkers and exact knowledge of the mechanism of disease has hampered the development of effective disease-modifying therapeutic strategies for tauopathies, including AD, so urgently needed to overcome the social and economic burden of these disorders. It is therefore imperative that new and innovative therapeutic strategies are developed to fuel the pipeline of drugs in development, thereby increasing the probabilities of success.

Table 1.3. Tau-based therapeutics in development.

Name	Development phase	Sponsor	Mechanism of action	Disease
AADvac-1	Phase I	Axon Neuroscience SE	Immunotherapy (active)	AD
ACI-35	Phase I	Janssen	Immunotherapy (active)	AD
Davunetide (AL-108)	Inactive	Allon Therapeutics Inc., Paladin Labs Inc.	MT stabilizer	MCI, AD
Epothilone D	Discontinued	Bristol-Myers Squibb	MT stabilizer	AD
Rember TM (methylene blue)	Discontinued	TauRx Therapeutics Ltd	aggregation inhibitor	AD
Tideglusib	Discontinued	Zeltia Group	GSK-3β inhibitor	AD, PSP
TPI 287	Phase I	Cortice Biosciences	MT stabilizer	AD, CBD, PSP
TRx0237 (LMTX, methylene blue)	Phase III	TauRx Therapeutics Ltd	aggregation inhibitor	AD, FTD

Source http://www.alzforum.org/therapeutics.

1.5. BIOALVO SA

Aiming to discover innovative drugs against neurological disorders, BIOALVO was founded in 2006 as a biopharmaceutical company. Its platform technology – GPS D^{2TM} (Global Platform Screening for Drug Discovery) was patented and demonstrated true potential to identify active compounds against different targets. In a constant search for innovative molecules and compounds, BIOALVO turned into the sea and natural sources of new bioactives. This powerful combination gave very positive results in identifying new compounds and activities. In 2010, the company started to slowly enter into other pharmaceutical and cosmetics areas through work with its partners/clients. In 2011, BIOALVO made a deep repositioning strategy, focusing on the exploitation of its assets and uniqueness: the combination of unique and proprietary libraries of extracts with its patented GPS D^{2TM} technology to maximize the applications of natural ingredients in all possible industries. BIOALVO became the Biotech for Natural Products, dedicated to providing fully-integrated biotech solutions to maximize natural products market applications.

BIOALVO designed and developed several applications derived from its technology platform, GPS D^{2TM}, aimed at the discovery of new drugs with therapeutic potential for unmet medical needs, including CNS disorders. BIOALVO's robust bioactive discovery assays were based on genetically modified yeast strains, designed to express the desired target (human or not). GPS D^{2TM} used yeast as a model organism due to its easy manipulation and physiological response similar to many human aspects, providing a valuable tool for the testing of biological activities, as further developed in the next section. GPS D^{2TM} assays were highly informative as they provided data on both the efficacy and the toxicity of test compounds and in addition they were highly amenable to high throughput screening (HTS) adaptation, allowing a fast and cost-effective bioactive discovery process. GPS D^{2TM} technology was already adapted to the identification of bioactives for cosmetic, pharmaceutical and other applications, creating a strong portfolio of available assays and technologies (Cerejo et al., 2012; Ciaccioli, Martins, Rodrigues, Vieira, & Calado, 2012; Martins et al., 2013; Rodrigues et al., 2011).

BIOALVO owned a large natural extract library, holding unique extracts derived mostly from a diverse array of microorganisms that could be industrially produced by laboratorial sustainable culturing methods. This collection reached 50.000 extracts, at the end of 2012, produced from phylogenetically diverse and unique microorganisms isolated from exclusive and extreme sources, such as deep sea hydrothermal vents in Azores, where physical extremes of temperature and pressure are present. Also, the deep sub seafloor biosphere is nowadays considered a dynamic environment, providing a diverse range of living conditions that are the host to rich microbial communities. Not that extreme but also unique were Portuguese traditional products such as wine, olive dairy products and cured meats from which derived microorganisms constituting a unique and representative sample of Portuguese microbial diversity that can be industrially explored. BIOALVO's microbial natural extracts libraries were constituted by three libraries: PharmaBUG, LUSOEXTRACT and LUSOMAREXTRACT. These natural extract libraries were validated for applications in neurodegenerative disorders, such as PD with associated tau pathology and familial amyloidotic polyneuropathy (FAP), amongst many other applications that were under development by BIOALVO SA. The collections were also made available to partners through licensing deals that explored the potential of these collections to their chosen field of application.

In addition, BIOALVO offered a simple, customizable, quick and fully integrated cell-based robotized unit designed for screening and evaluating extract bioactivity for partners who wished to take advantage of BIOALVO's one-stop-shop organization to speed up their product development.

The work developed under the scope of this PhD thesis was aligned with the company objectives and integrated into BIOALVO internal R&D drug discovery and development TAU program. This program aimed at generating drug-like molecules with optimal properties in terms of safety and efficacy for the treatment of tau-related diseases, with a particular focus on AD, due to the dramatic clinical relevance and social burden of this pathology.

1.6. Yeast as a model and a screening tool

Saccharomyces cerevisiae, the baker's yeast, is the most well studied eukaryote organism and it is present throughout our daily lives. Its widespread use in biotechnology industries brings to our table bread and beer, helps to take care of our environment (waste recycling and pollution clean-up) and fuels our industries with ethanol. But *S. cerevisiae* has long been used in medicine, since it is a recognized tool for biomedical research. Indeed, yeast has greatly contributed to understand many conserved cellular mechanisms such as cell division, DNA replication, metabolism, protein folding and intracellular transport, and is a recognized model for the study of many human disorders, including neurodegenerative diseases (Khurana & Lindquist, 2010; Tenreiro & Outeiro, 2010).

Two main characteristics make yeast a suitable model: (1) it is a relevant organism for the study of human disease, due to the high degree of conservation of many biological processes from yeast to human (Figure 1.8), and (2) is extremely amenable for analysis and development of high-throughput assays, due to its short generation time, genetic tractability and scalability (Khurana & Lindquist, 2010).

Yeast was the first eukaryotic organism to be fully sequenced and currently around 80% of the 6000 open reading frames (ORFs; protein-coding sequences) have been functionally characterized (Khurana & Lindquist, 2010). At least 60% of yeast genes have a well-characterized human homologue or possess, at least, one conserved domain with human genes (Khurana & Lindquist, 2010). This high degree of genomic homology explains why yeast recapitulate fundamental aspects of eukaryotic biology, including genetic transmission and transcriptional regulation, protein folding and secretion, biogenesis and function of cellular organelles, cytoskeletal dynamics, cell cycle, and regulation of cellular metabolism (Khurana & Lindquist, 2010). Many of these processes are involved in neurodegeneration (Figure 1.8). Moreover, nearly 50% of human genes implicated in heritable diseases have yeast homologues, thereby making yeast a suitable model for understanding conserved mechanisms involved in human diseases (Khurana & Lindquist, 2010; Miller-Fleming, Giorgini & Outeiro, 2008). Indeed, many humanized yeast models, expressing human proteins involved in human neurodegenerative disorders have been constructed and studied, providing invaluable insights into the biology and pathology of such proteins. For example, APP processing, Aβ oligomerization and tau phosphorylation and aggregation have been modelled with success in yeast, establishing it as a valid system for AD studies (reviewed in Bharadwaj, Martins & Macreadie, 2010). Other examples are the yeast models for HD and PD (Outeiro & Giorgini, 2006), amyotrophic lateral sclerosis (ALS) and frontotemporal lobar degeneration with ubiquitin-positive pathology (FTLDU) where protein aggregates of FUS (Fused in Sarcoma) occur (FTD-FUS) (Fushimi *et al.*, 2011) and TDP-43 (TAR DNA-binding protein 43) proteinopathies (FTD-TDP43) (Johnson *et al.*, 2008).

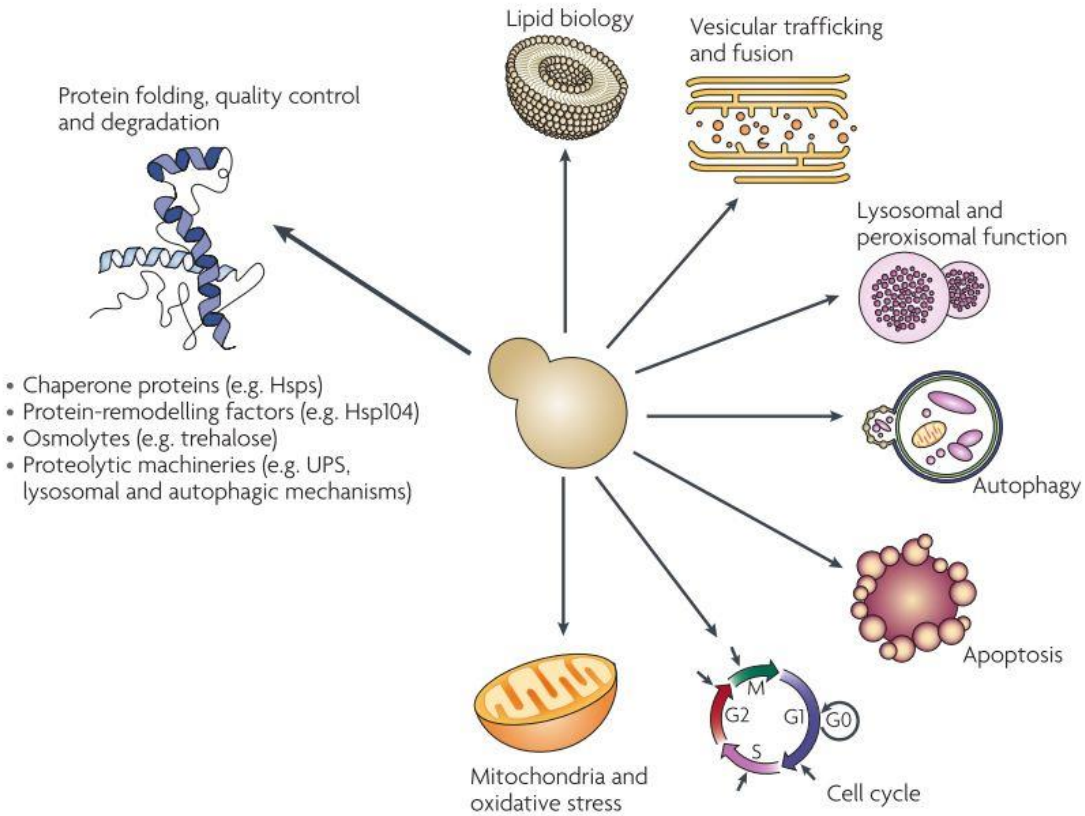

Figure 1.8. Cellular processes conserved in yeast, relevant for neurodegeneration.
Source: Khurana & Lindquist, 2010.

Genetic and biochemical manipulations in yeast are simple, rather quick and inexpensive (Miller-Fleming *et al.*, 2008). Yeast grow in a reproducible and genetically stable way, possessing a short generation time, of around 90 min on rich media, and survive indefinitely in frozen glycerol stocks (Khurana & Lindquist, 2010; Miller-Fleming *et al.*, 2008). Importantly, this organism is also easily transformed and has the ability to integrate genes by homologous recombination (Khurana & Lindquist, 2010; Miller-Fleming *et al.*, 2008). As a unicellular organism, yeast is also scalable and therefore suitable for genetic and chemical HTS assays (Khurana & Lindquist, 2010). A vast array of yeast genetic tools has been developed for all "omics" sciences (Khurana & Lindquist, 2010). Particularly for the field of functional genomics, several genetic screening libraries have been developed by a large and very collaborative yeast community (Tenreiro & Outeiro, 2010). These libraries (Euroscarf yeast knockout collection and yeast genomic collection, for example) allow to investigate the expression and function of genes in yeast and rapid genomic systematic screenings for the identification of genomic interactions (Mager & Winderickx, 2005). The coupling of such libraries with the modelling of neurodegenerative disorders has provided much information about the cellular pathways where the proteins involved in these diseases exert their toxicity. Such functional studies have been performed with success for HD and PD (Willingham *et al.*, 2003), AD (Aβ toxicity) (Treusch *et al.*, 2011) and ALS (Sun *et al.*, 2011), providing relevant frameworks for the identification of new drug targets for therapeutic intervention in human disease (Smith *et al.*, 2010).

Yeast has also emerged as a valuable platform for drug discovery screenings (Barberis *et al.*, 2005; Khurana & Lindquist, 2010). While mammalian cell-based drug discovery assays can be highly informative, they also present many technical challenges for implementing automated systems for HTS, its genetic manipulation is at times problematic and time and cost-consuming, and the readouts of the assay can be redundant and difficult to distinguish from the target-specific effects (Barberis *et al.*, 2005). The use of yeast for drug discovery can overcome these drawbacks of mammalian cells, since, as already mentioned, yeast is easy to grow and genetically manipulate, is scalable and amenable for HTS, and provides a clean readout in a null-background environment for the expression of the human proteins (Barberis *et al.*, 2005). At the same time, the assay is still developed intracellularly, in a eukaryotic and relevant environment that allows to extract high quality information on the drug's efficacy and safety, already at the first stages of drug discovery (Barberis *et al.*, 2005). Additionally, the presence of the yeast cell wall and compound efflux pumps, despite being considered by some as a disadvantage of yeast, allows, in fact, to design highly restrictive assays, since only drugs able to cross these barriers will be able to exert their activity on the target, thereby selecting only the best compounds for proceeding to the next stages of drug discovery (Cerejo *et al.*, 2012). This important advantage, coupled to the information on the cytotoxicity of the compounds, greatly reduces the drug-attrition rates in the following stages of drug development (Cerejo *et al.*, 2012; Kramer, Sagartz & Morris, 2007).

As a unicellular organism, yeast does not allow the study of mechanisms related with the multicellularity of human neurodegeneration considering that many pathways have diversified and specialized in mammalian cells, and thus are usually much more complex than the ones found in yeast. Additionally, yeast is devoid of a nervous system, thereby not recapitulating processes such as axonal transport and synaptic dysfunction, important in the context of neurodegeneration. Therefore, all insights gained in

yeast must be validated in more complex biological systems. Nonetheless, basic mechanisms underlying these processes are present in yeast, making the heterologous expression of human proteins in yeast highly informative, and allowing to study and manipulate such processes without the full complexity of a higher order eukaryotic cell (Khurana & Lindquist, 2010).

1.7. Pharmaceutical drug discovery and development

The identification of a new drug and its development into a final, commercial product is a long, complex, costly and highly risky process that takes, on average, 10-15 years of research and around $1 billion US dollars of investment (Lombardino & Lowe, 2004; Royle, Jimenez del Val & Kontoravdi, 2013).

Classically, the drug discovery and development process is divided into two primary stages: drug discovery and clinical drug development (Figure 1.9) (Royle *et al.*, 2013). The pre-clinical and non-clinical stage is sometimes considered as a third stage, included in drug development (Royle *et al.*, 2013). Drug discovery and development programs are usually driven by an unmet medical need. Traditionally, the process is based on extensive fundamental research data gathered around the biological players involved in cellular processes that lead to disease. This fundamental research is usually carried out by academia and demonstrates that the modulation of such biological players results in a therapeutic effect in a disease. This biological player is designated as drug target (Hughes *et al.*, 2011).

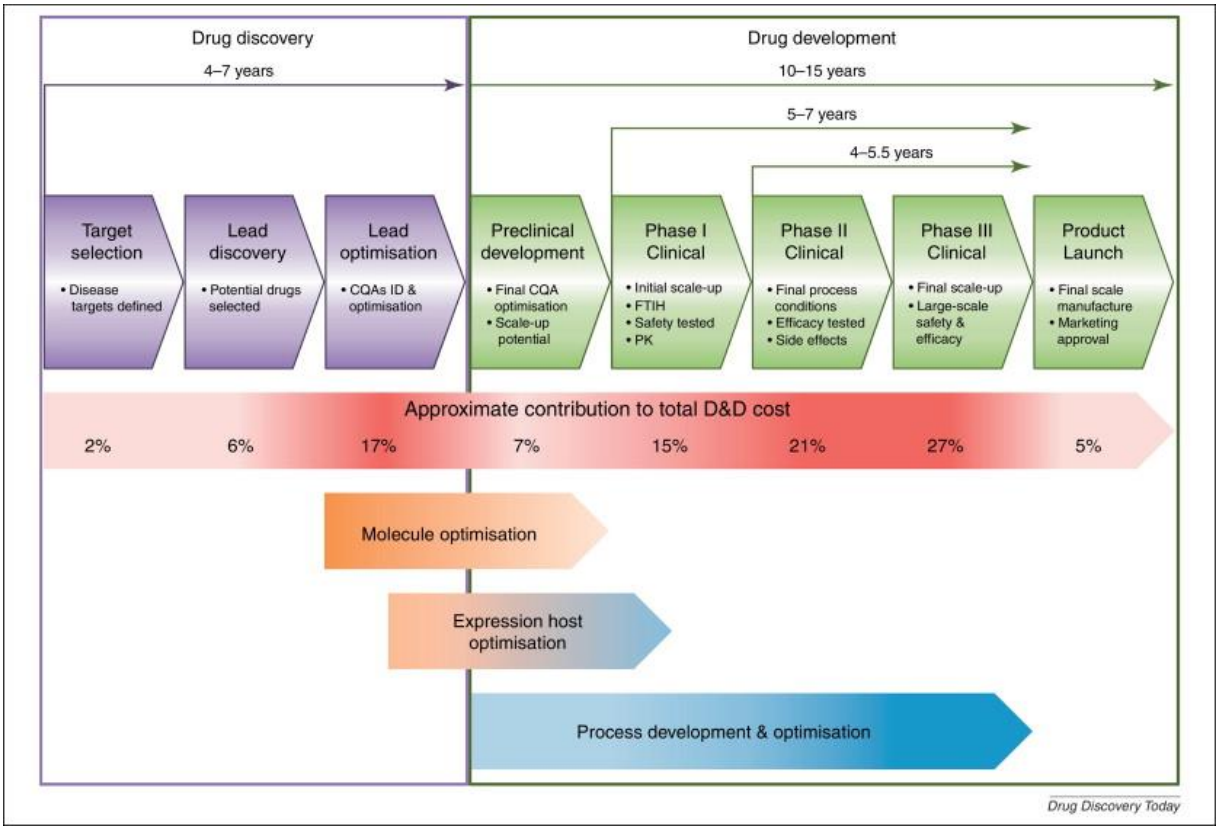

Figure 1.9. Drug discovery and development process phases, with reference to average time and approximate cost of development.
Source: Royle *et al.*, 2013.

A typical drug discovery program for identification of small molecules with therapeutic potential begins with large numbers of compounds and high-throughput assays. The number of compounds decreases as increasingly predictive, but with lower throughput, assays are applied, in order to sort the best candidates for development, those with the most drug-like properties and optimal *in vitro* and *in vivo* efficacy (Hughes *et al.*, 2011). Confirmed hits identified in high-throughput screening (HTS) assays are evaluated for potency, selectivity, ADME (Absorption, Distribution, Metabolism, and Excretion), physical and chemical properties, and activity in relevant cell models of disease (Hughes *et al.*, 2011; Kramer *et al.*, 2007). This strategy leads to molecules that meet the defined criteria, according with the regulatory requirements, and are designated as candidates for formal drug development (Kramer *et al.*, 2007).

In the pre-clinical stage of drug development, only the most promising candidates are tested for therapeutic efficacy and safety in *in vivo* animal models (Brightfocus.org, 2015). Other parameters are also assessed such as delivery to target organ(s) or tissue(s) and formulation (Brightfocus.org, 2015). The research performed at this stage must show that the results obtained in animals can be translated successfully to humans. If the drug candidate mediates a promising treatment and demonstrates a minimal safety profile, an Investigative New Drug (IND) is prepared and submitted for authorization to the regulatory agencies in order to preform clinical trials. The IND contains all the information about the drug candidate, safety profile and treatment, gathered during the drug discovery and pre-clinical stages (Brightfocus.org, 2015).

A clinical drug development process is composed of three main phases, each with its own purpose of ensuring that a treatment is safe and effective for human use. After the completion of each stage, a document with the results is submitted to the regulatory agency, asking permission to proceed to the next clinical phase. Only after the completion of three stages will the regulatory agency consider the market entry of the treatment (Brightfocus.org, 2015). Clinical Phase I tests are usually performed in small groups of healthy volunteers, although some trials may already include patients. Its purpose is to ensure the safety of the treatment in humans, monitoring serious adverse events. In a Phase II clinical trial, the right dosage and effectiveness of the treatment are assessed in a larger number of volunteers who have the disease in order to confirm the therapeutic window for treatment. The phase III clinical trial involves a much larger number of volunteers with the disease and focuses on determining if a treatment is safe and effective in a wider population. Phase II and Phase III trials compare results between control (placebo) and treatment groups. After the completion of Phase III trials and assuming that the treatment is effective and safe and performed better than the existing methods to treat a condition (when these exist), a New Drug Application (NDA) is submitted to the regulatory agency (Brightfocus.org, 2015). An NDA includes all the research performed since the early drug discovery process to the end of the clinical stages of drug development. After approval by the regulatory agency and manufacturing of the drug in a large scale and under controlled manufacturing procedures, the treatment enters in Phase IV clinical trials, meaning that safety continues to be monitored as long as the medicine is on the market (Brightfocus.org, 2015).

Despite technological advancements such as HTS, chemical synthesis, human genome sequencing and increasing investments in R&D, the number of NDAs has been decreasing (Khanna, 2012; Kramer

et al., 2007; Paul *et al.*, 2010). In fact, most of the drug discovery and development projects fail to produce a marketable medicine (Lombardino & Lowe, 2004; Paul *et al.*, 2010). In the drug discovery phase only a fraction of the scientific hypothesis that support a given project actually yield a drug candidate for development (Lombardino & Lowe, 2004). Actually, it is estimated that, for each indication, from 100,000 compounds tested, 1 will become a marketed drug (Han & Wang, 2005). In the drug development phase approximately 1 out 15-25 drug candidates survives the detailed efficacy and safety testing required to become a marketed product (Lombardino & Lowe, 2004). Lack of efficacy and safety issues are the most common reasons for drug attrition (Khanna, 2012; Kramer *et al.*, 2007). Particularly, safety-related attrition is usually detected in the preclinical stages or in Phase II or III, the most time- and cost-expensive stages of drug development. Therefore, the pharmaceutical industry has been progressively incorporating preclinical assessment early in the drug discovery stages. The approach of "failing fast and cheap" facilitates earlier data-driven decisions to discontinue the development of drug candidates before entry into more costly phases of development, with the added advantage of delivering safer leads into development (Kramer *et al.*, 2007; Paul *et al.*, 2010).

1.7.1. The drug discovery phase

The drug discovery phase can be divided into three main steps: target identification and validation, lead discovery and lead optimization (Figure 1.9) (Hughes *et al.*, 2011; Royle *et al.*, 2013).

1.7.1.1. Target identification and validation

As mentioned previously, potential drug targets are usually identified following extensive academic research that determines the involvement of a given molecular entity or pathway in a disease. The term drug target can be applied to a range of biological entities such as proteins, genes and RNA (Brightfocus.org, 2015; Hughes *et al.*, 2011). To be considered a good target, such biological entity must have proven modulatory capacity of the disease outcome; its modulation must show reduced adverse side effects; should meet clinical and commercial needs and, above all, should be "druggable". A druggable target is one that is accessible by potential drugs or larger biologicals and upon binding elicits a measurable biological response (Hughes *et al.*, 2011).

More recently, systems biology[2] approaches have been applied to identify new drug targets (Berg, 2014). In the post-genomic era, many new players in disease have been identified by coupling information regarding DNA copy number, transcriptomics and proteomics into networks to recognise key nodes controlling important disease pathways. However, one of the biggest challenges of this approach is that, often, the identified potential drug targets are not druggable, since they may consist in transcription factors, structural components of the cell or with unknown function. This has prompted the

[2] Systems biology is the "study of a biological system by comprehensive analysis of its components and their interactions, and integration of this information into predictive models" (Berg, 2014). When applied to medicine, its main goal is to understand the physiology and disease across multiple hierarchical levels of organization, since the chemical and molecular interactions, to pathways and pathways networks, at the cell and tissue level, organs system and ultimately, to the functioning of the whole organism (Berg, 2014).

use of systems biology for screening for drug targets and compounds using functional phenotypic assays, renewing the interest in more direct drug discovery approaches (Berg, 2014). In fact, small organisms relevant for the modelling of diseases, including neurodegenerative disorders, are being extensively used to perform functional and phenotypic genome-wide studies to identify the interactome of genes involved in disease (Suter, Auerbach & Stagljar, 2006; van Ham *et al.*, 2009). These studies provide valuable information on the molecular and cellular processes involved in disease, allowing to pin-point potential new drug targets (Suter *et al.*, 2006; van Ham *et al.*, 2009). Importantly, this strategy was followed in the present study.

Whereas in the classical identification of drug targets, extensive research supporting its role in disease already exists, when the drug target is identified by systems biology approaches, a very important work on target validation is necessary prior to advancing in the drug discovery process. There are a multitude of techniques for validating drug targets, including *in vitro* and *in vivo* cell and animal models (Hughes *et al.*, 2011). For example, transgenic animals are an attractive validation tool, since they involve the whole organism and allow observation of phenotypic endpoints to elucidate the functional consequence of drug target modulation (Benson *et al.*, 2006). Additionally, RNA interference (iRNA) approaches for gene silencing, coupled to overexpression of the same target, are increasingly used to validate the role of a potential relevant target in disease ethiopathogenesis (Appasani, 2003; Benson *et al.*, 2006; Hughes *et al.*, 2011). Also, systems biology approaches have been used to facilitate target validation. Chemical genomics assays have been developed to identify chemical tools that modulate the target, evaluating its cellular function prior to full commitment to a screening campaign against the target (Berg, 2014; Hughes *et al.*, 2011).

1.7.1.2. Lead discovery phase

The lead discovery phase is a multidisciplinary stage, and one of the most costly in the whole process, that starts with the screening of a library of compounds or natural products in a biochemical or cell-based assay, to identify molecules capable of eliciting a measurable response involving the drug target (Lombardino & Lowe, 2004). These molecules are then further evaluated in terms of potency, cytotoxicity and selectivity, and improved using combinatorial chemistry, until a lead compound is selected for development (Lombardino & Lowe, 2004). Therefore, a lead is defined as a chemical structure or series of structures that show activity and selectivity in a pharmacological or biochemically relevant screen (Hughes *et al.*, 2011; Lombardino & Lowe, 2004).

The screening of compounds usually involves a quick and automated process where the biological or biochemical activity of a large number of drug-like compounds or natural products is tested. This process is widely used in drug discovery programs and is designated as HTS (Hughes *et al.*, 2011). Libraries of thousands of synthesized compounds have been developed to contain only “drug-like” molecules, i.e. molecules that obey to certain chemical parameters, such as Lipinski Rule of Five (Hughes *et al.*, 2011; Leeson, 2012). This set of rules states that molecules with molecular weights inferior to 500 Da, logP (lipophilicity measure) inferior to 5, hydrogen-bound donors less than 5, and hydrogen-bond acceptors inferior to 10, are more likely to be membrane permeable and easily absorbed by the body, thereby with

higher chances of being developed into a medicine (Lipinski *et al.*, 2001). However, few *de novo* new chemical entities (NCE) have been approved for drug use, which has greatly influenced the shift towards the traditional use of natural products as a source of compounds for drug discovery. Indeed, around 60% of the drugs currently on the market are of natural origin (Martins *et al.*, 2014). A natural product (NP) is a compound chemically produced by a living organism, such as plants, animals and microorganisms, which has a biological activity useful for different applications (Newman & Cragg, 2007). Although not following the Lipinski rule of five, NPs present advantages relative to synthesized molecules such as high chemical diversity, biochemical specificity, binding efficiency and propensity to interact with biological targets, which make them favourable lead structures. Moreover, they might contain novel chemical structures yet undiscovered, contributing to the development of innovative solutions (Harvey, 2008; Kingston, 2011; Martins *et al.*, 2014). Moreover, particularly in what concerns NPs obtained from microorganisms, such as bacteria and fungi, the compounds readily enter the cells, being able to modulate difficult targets. Additionally, microorganisms are prone for sustainable upscaling production processes, which make them an important source of compounds (Martins *et al.*, 2014). However, this is not always the case for other sources of natural products, which may present difficulties in access and supply, decreasing its attractiveness for large pharmaceutical companies. Additionally, the difficulty of isolating the active principle, the more complex natural product chemistry and consequent slowness of working with natural products, as well as concerns about intellectual property rights (since the active compound may be a known compound and therefore not protectable), are also recognized disadvantages of natural products (Harvey, 2008; Kingston, 2011).

Independently of the source of compounds used, the HTS campaigns are designed to identify hit compounds, i.e., molecules that present the desired activity in a computational, biochemical or cell-based assay, in a reproducible way (Hughes *et al.*, 2011). While in computational and biochemical assays the binding of compounds to the drug target is evaluated, the more complex cell-based assays access the modulation of the drug target expression by compounds, which results in a measurable phenotypic effect (Hughes *et al.*, 2011). Although lacking the throughput capability of computational and biochemical *in vitro* assays, cell-based assays have the advantage of providing vital information on the membrane permeability and cytotoxicity of a compound in a single test, while still allowing reasonable cost-effective throughput (Hughes *et al.*, 2011). Whatever the format of assay development, several criteria must be taken into account when designing an HTS assay:

1. Pharmacological relevance: prior to screening campaigns, the assay should be validated, ideally using known ligands with activity at the target under study (Hughes *et al.*, 2011). However, if the drug discovery program aims to identify first-in-class drugs, this validation is not always possible, since no chemical modulators of the target exist;
2. Reproducibility of the assay: the assay must be reproducible across assay plates, screening days and the entire drug discovery program;
3. Assay costs: screening format (96, 384 or 1536-well microplates), reagents and assay volumes should be optimized in order to minimize costs, while maximizing the quality of the information gathered;

4. Assay quality: numerous statistical tools exist to guarantee assay robustness. One of the most used is the Z factor that considers the signal window and the variance that exists around such window. It ranges from 0 to 1, and assays with a Z factor higher than 0.5 are already considered appropriate (Hughes *et al.*, 2011; Zhang, 1999).
5. Effect of compounds: chemical libraries are usually stored in DMSO, which is usually toxic to cells above 1%; therefore, the assay validation must be performed taking into account the solvent of the compounds. Also, the assay must have defined criteria to identify false negative and positive compounds. The later are more important to discontinue, since they imply increased costs in the next stages of development.

The identification of hit molecules is usually made in two steps, since the reproducibility of compound activity is essential to be considered a hit. Two rounds of HTS are usually performed to obtain a list of hits that are then evaluated in secondary screenings of dose-response, that allow to obtain the half maximal inhibitory concentration, used to compare the potency of drug candidates (Hughes *et al.*, 2011). The effort of the screening campaign can be greatly reduced if the reproducibility of compounds is performed at the same time of the dose-response assays. This strategy, applied at BIOALVO's drug discovery programmes, allows to confirm positive compounds and obtain information of their potency and cytotoxicity using a range of concentrations. In two steps, safer and effective compounds are selected and ranked, while cytotoxic and false positives are eliminated. False negative compounds are not picked with this stringiest strategy, ensuring that only the most promising compounds continue in development.

Further hit triage is performed in secondary assays for evaluation of efficacy, specificity and cytotoxicity, usually in more biological relevant organism models. Hit series, i.e., a set of compounds that share common structures are identified and SAR (structure-activity relationship) investigations around the core structure of each series, coupled with a set of secondary assays, are performed systematically in order to produce more potent, selective and less toxic compounds. Prospective ADME/T (Absorption, Distribution, Metabolism, Excretion and Toxicity) assays are usually conducted at this stage, before the first *in vivo* studies, in an attempt to predict development-limiting toxicities (Kramer *et al.*, 2007). These assays include evaluation of acute and chronic general and cell-specific toxicity, genotoxicity, solubility, drug-drug interactions, metabolite-mediated cytotoxicity, among others (Hughes *et al.*, 2011; Kramer *et al.*, 2007).

1.7.1.3. Lead optimization

The goal of this final stage in drug discovery is to maintain the favourable chemical and physical properties of the lead compound or compound series, while improving the less good aspects (Hughes *et al.*, 2011). This is performed by continued coupling of medicinal chemistry with more complex prospective toxicity assays. For example, as the effect of the lead compounds in hERG (human ether-a-go-go related gene) potassium channels, critical in cardiac action potential repolarization, are always analysed and considered eliminatory. Permeability assays, to predict the *in vivo* drug absorption, are also performed using as a model, for example, the Caco-2 cell line, derived from a human colon epithelial

cancer. At this stage, *in vivo* models can be incorporated in order to determine high-dose pharmacology[3], pharmacokinetics[4] (PK) and pharmacodynamics (PDy), dose linearity and repeat dosing PK, looking for drug-induced metabolism. Attention to chemical stability and manufacturing issues and early formulation considerations (depending on drug delivery strategy) should also be included at this stage (Hughes *et al.*, 2011).

When a compound meets all the desired criteria, defined at the beginning of the lead optimization stage and dependent on the drug target and application, it is designated as a formal candidate for pre-clinical lead development.

1.8. Main aim and specific objectives

Considering the increasing prevalence of tauopathies, such as AD, their human and socioeconomic effects and that, to date, there are no effective disease-modifying therapies for these disorders, since the knowledge on the exact mechanism of disease is yet elusive, this PhD thesis aims to contribute to drug discovery and development for tau-based disorders, while, at the same time, expanding our knowledge on the aetiology of tauopathies, with particular emphasis on AD.

Specifically, this works aims to:

(i) Develop new yeast models for the study of tau and beta-amyloid interaction (Chapter 3);
(ii) Identify novel proteins in tau's interactome (Chapter 4);
(iii) Develop new drug screening systems for identification of new modulators of tau toxicity (Chapter 5);
(iv) Identify natural products able to modulate tau toxicity (Chapter 6);
(v) Perform the first steps of construction of a neural model for future validation of a new drug target for tauopathies' therapeutics (Chapter 7).

The elected approach uses yeast as a model, a recognized organism for the study of neurodegenerative disorders, that has greatly contributed to discriminate disease-related protein interactions and new drug targets for neurodegeneration, as described previously in detail (section 1.6). It is expected that the yeast models produced in this study will be useful tools in drug discovery and development for tauopathies. Also, the mapping of tau's interactome in yeast is expected to provide a valuable framework for the identification of novel drug targets and biomarkers for tauopathies, while at the same time, expands our knowledge on tau physiological and pathological roles. Finally, the natural products identified as tau toxicity modulators can be valuable starting points for new drug discovery programmes. Thus, focusing on tau, different opportunities for therapeutic intervention will be highly relevant for a number of life-threatening diseases, including AD.

[3] Pharmacology: sometimes defined as the study of the effects of a drug in the body.
[4] Pharmacokinetics: comprehend the study of the effects of the body on the drug.

Chapter 2.

Material and Methods

2.1. Material

The following sections list the items necessary for performing all experiments in the scope of this work.

2.1.1. Reagents

Concerning molecular biology procedures, the reagents used were acquired to several suppliers. Synthetic oligonucleotides and Platinum® Taq DNA Polymerase High Fidelity or Phusion Hot Start II High-Fidelity DNA Polymerase for polymerase chain reaction (PCR) were obtained from Invitrogen Life Technologies (ThermoFisher Scientific, Waltham, MA, USA). dNTPs mix, endonucleases, CIAP, T4 DNA ligase and ethidium bromide, were supplied by Fermentas (Thermo Fisher Scientific, Waltham, MA, USA) or New England Biolabs (Ipswich, MA, USA). O´Gene Ruler 1 Kb DNA ladder and PageRuler™ Plus Prestained Protein Ladder, were acquired from Fermentas. Klenow was purchased from New England Biolabs. Agarose was acquired to Lonza (Basel, CH). Cyber safe for DNA electrophoresis and NZYColour Protein Marker II were purchased from nzyTech (Lisbon, PT). The plasmid pESC-LEU was acquired to Stratagene (La Jolla, CA, USA). Short harpin RNA (shRNA) constructs in pLKO.1 lentiviral vector were acquired to GE Dharmacon (Lafayette, CO, USA). DNA extraction was performed using QIAprep Spin Miniprep Kit and Qiagen HiSpeed Maxi Prep Kit, both purchased to Qiagen (Venlo, Limburg, NL), and PureLink HiPure Plasmid Maxiprep Kit from Invitrogen Life Technologies (ThermoFisher Scientific, Waltham, MA, USA). Also from Qiagen was the DNeasy® Blood & Tissue Qiagen kit, used for extraction of yeast genomic DNA, QIAquick Gel Extraction Kit, used to purify DNA from agarose and QIAquick PCR Purification Kit, to purify DNA from PCR reactions. DNA quantification was performed by fluorometry using the Qubit® Fluorometer from Invitrogen Life Technologies (ThermoFisher Scientific, Waltham, MA, USA). PhosSTOP® phosphatase inhibitor cocktail (proprietary mixture containing inhibitors of acid phosphatases; alkaline phosphatases; serine/threonine phosphatases; tyrosine phosphatases and dual-specificity phosphatases) was acquired to Roche (Basel, CH). PhosphoBlocker™ blocking reagent was acquired to Cell Biolabs (San Diego, CA, USA).

For microbiology procedures (bacterial and yeast cultures), yeast extract, glucose and agar were purchased from Scharlau (Sentmenat, ES) and bactopeptone from BD biosciences (Franklin Lakes, NJ, USA). Yeast drop-out mix without leucine and uracil was purchased to MP Biomedicals (Santa Ana, CA, USA) and galactose to Applichem (Darmstadt, DE). LB media was prepared in-house or otherwise acquired to Invitrogen™ Life Technologies (ThermoFisher Scientific, Waltham, MA, USA). Yeast nitrogen base without amino-acids, raffinose, leucine, uracil, 1x protease inhibitor cocktail (contains inhibitors of serine, cysteine and metallo-proteases), N-Lauroylsarcosine sodium salt (Sarkosyl), lyticase, lysozyme, G418 antibiotic, DMSO, Ionomycin, penicillin/streptomycin (Pen/Strep), carbenicillin and other common life-sciences reagents were acquired from Sigma-Aldrich (St, Louis, MO, USA), except when otherwise stated.

Mammalian cell procedures used Dulbecco's modified Eagle's media (DMEM) with 4500 mg/l glucose and 4 mM glutamine, foetal bovine serum (FBS), Opti-Mem and trypsin-EDTA, which were purchased from Gibco™ Life Technologies (ThermoFisher Scientific, Waltham, MA, USA). Tissue culture material was acquired from Corning (New York, NY, USA) and Sarstedt AG & Co. (Nümbrecht, GE). FuGENE HD reagent was purchased to Promega (Fitchburg, WI, USA). TMRM probe was acquired to Calbiochem (Merck Millipore, Billerica, MA, USA) and Fura-2AM to Molecular Probes™ Invitrogen (Life Technologies, ThermoFisher Scientific, Waltham, MA, USA).

2.1.2. Cells

2.1.2.1. *Escherichia coli* strains

The supercompetent *E. coli* XL1-Blue (Stratagene, La Jolla, CA, USA) [endA1 gyrA96(nal^R) thi-1 recA1 relA1 lac glnV44 F'[::Tn10 proAB$^+$ lacI^q Δ(lacZ)M15] hsdR17(r_K^- m_K^+)] and the ultracompetent *E.coli* DH5-α [F$^-$ endA1 glnV44 thi-1 recA1 relA1 gyrA96 deoR nupG Φ80d*lacZ*ΔM15 Δ(*lacZYA-argF*)U169, hsdR17(r_K^- m_K^+), λ–] were used for plasmid replication.

2.1.2.2. *Saccharomyces cerevisiae* strains

2.1.2.2.1. Individual yeast strains

The *S. cerevisiae* strain W303-1A (*MAT*a *leu2-3,112 trp1-1 can1-100 ura3-1 ade2-1 his3-11, 15*) (courtesy T. Outeiro, IMM) was used for construction of yeast strains using integrative yeast expression plasmids.

The *S. cerevisiae* strain BY4741 (*MAT*a; *his3Δ1*; *leu2Δ0*; *met15Δ0*; *ura3Δ0*) and the single deletion mutant *rim11*Δ (BY4741 background), obtained from the genome-wide yeast deletion collection YSC1053 (Thermo Scientific, Waltham, MA, USA), were used for the construction of yeast strains using episomal yeast expression plasmids.

2.1.2.2.2. Yeast knockout collection (YKO)

The yeast gene knockout collection (YKO), comprised of 5153 modified haploid yeast BY4741 strains, was acquired from Thermo Scientific, Waltham, MA, USA (Cat. YSC1053, YSC4298, YSC4341, YSC4506). This collection was originally produced by the Saccharomyces Genome Deletion Project (SGDP). Each yeast strain bears one non-essential single gene deletion, performed by a one-step gene replacement with a kanMX4 module. Gene replacement can be confirmed using standard PCR techniques, using the unique 20-bp oligonucleotide sequences inserted with the kanMX4 module in each deletion, serving as unique identifiers of each ORF. This collection was distributed in 55 sealed microplates of 96-wells each and stored in 150 µl of glycerol containing media at -80ºC.

2.1.2.3. H4 neuronal mammalian cells

H4 cells (kind gift T. Outeiro Lab, IMM, Lisbon, PT) are human brain neuroglioma cells, with epithelial morphology, were used to construct the neural model of PiC silencing resorting to iRNA, useful for future validation of PiC as a drug target.

2.1.3. Plasmids

2.1.3.1. Yeast plasmids

Episomal expression of the proteins of interest was accomplished using the yeast high-copy (2µ) bi-directional expression episomal plasmid pESC-LEU (Stratagene, La Jolla, CA, USA) (Figure 2.1).

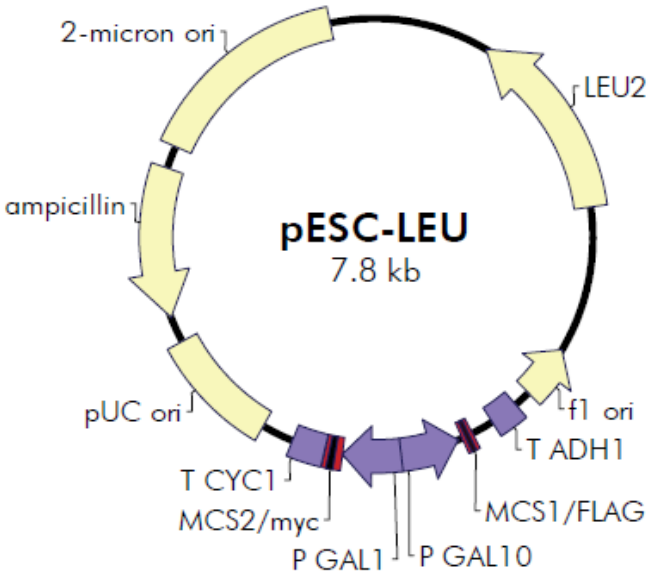

Figure 2.1. pESC-LEU vector map (Stratagene).

This plasmid contains two promoters, *GAL1* and *GAL10*, in opposing directions, and the auxotrophic selection market LEU2. Culture media for yeast strains transformed with this plasmid lacks, therefore, the amino acid leucine.

Yeast strains containing a copy of the DNA of interest integrated into the yeast genome were constructed with the integrative yeast expression plasmid YIp211 (Figure 2.2).The auxotrophic selection marker of YIp211 is URA3, and therefore, yeast strains transformed with this plasmid were cultivated in culture media lacking the amino acid uracil.

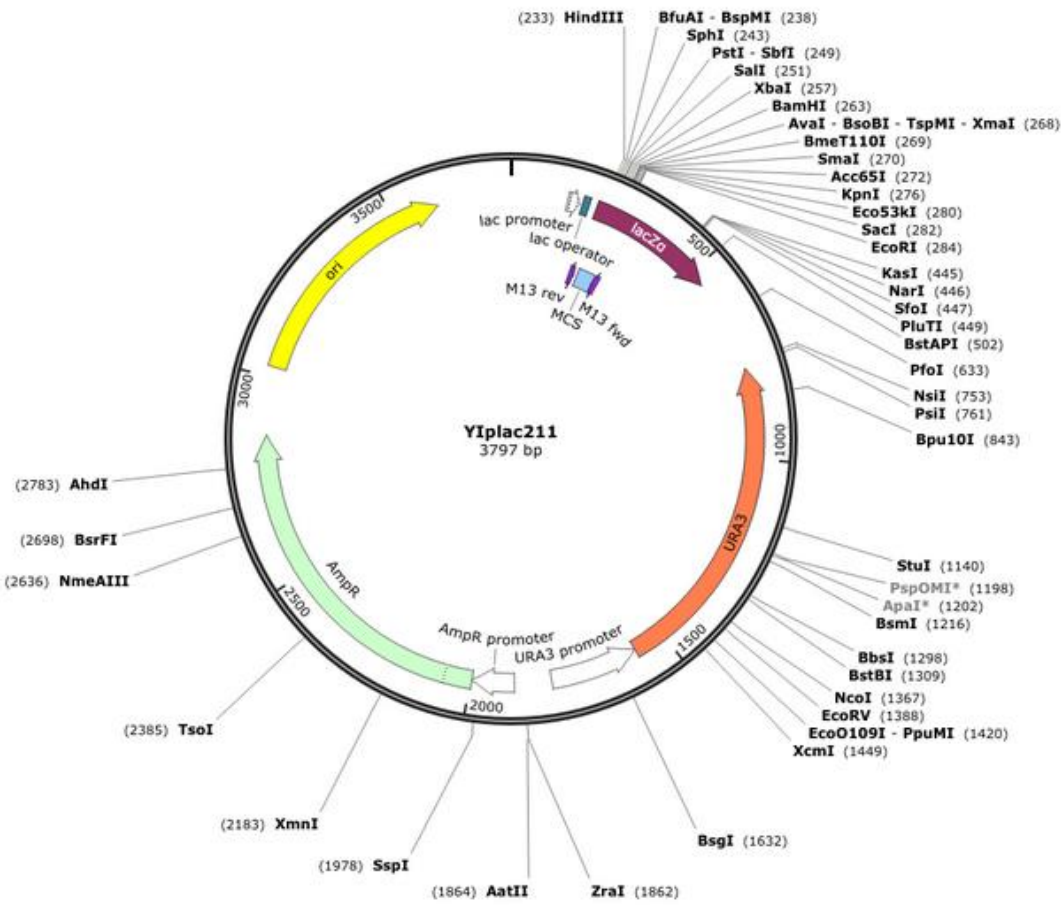

Figure 2.2. YIp211 vector map (http://www.snapgene.com/).

2.1.3.2. Mammalian cell plasmids

The plasmid pCDNA3-eGFP (BIOALVO) was used to optimize H4 cells transient transfection (Figure 2.3).

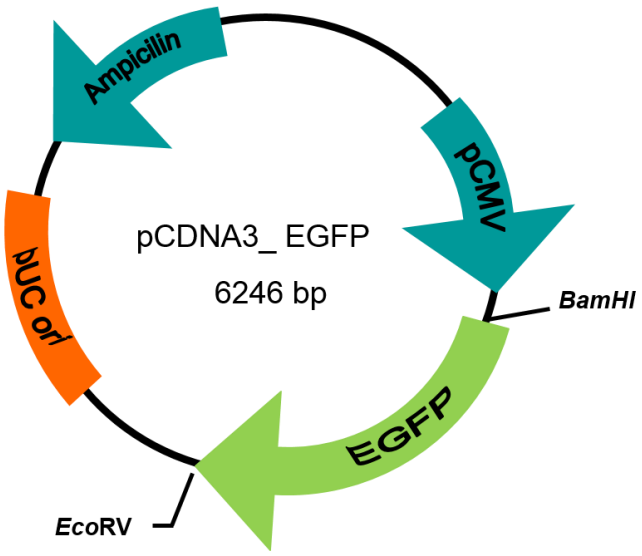

Figure 2.3. pCDNA3_eGFP vector map.

The mature antisense shRNA sequences used to knockdown *SLC25A3* gene: (shRNA 1) AACAGTACGTTCAAAGCAGGC, (shRNA 2) AATGTCAGCAAAGAATTCAGC and (shRNA 3) AAGTCTGAAGTAGACCTTCAC were provided by the manufacturer inserted into pLKO.1 HIV-based lentiviral vector (Figure 2.4). This vector allows for transient and stable transfection of shRNA and also the production of viral particles using lentiviral packaging systems. The antibiotic resistance marker is puromycin.

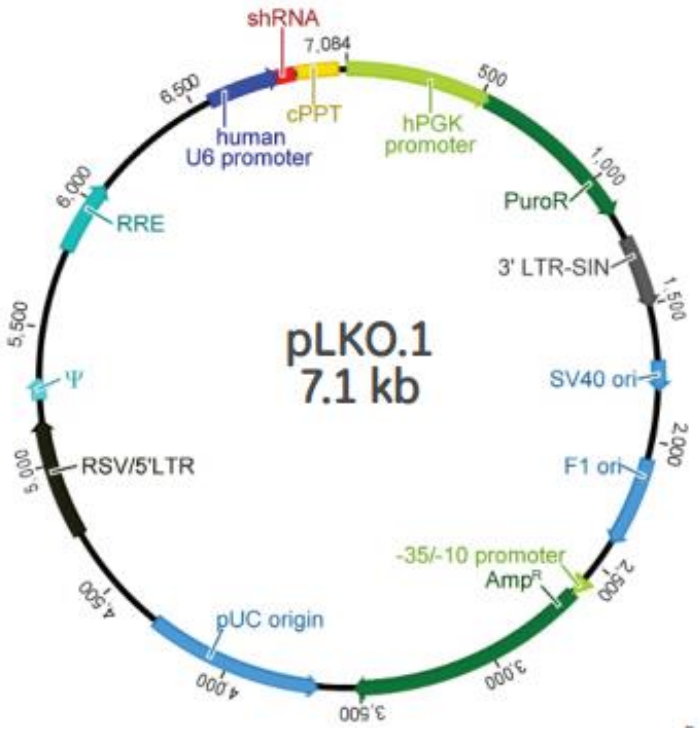

Figure 2.4. Map of the pLKO.1 vector.

2.2. Methods

The following sections describe the methods performed in the scope of this work.

2.2.1. Cells media, growth and storage

2.2.1.1. *Escherichia coli* media and growth

Bacterial cells were cultured in Luria-Broth (LB) media (10 g/l Bacto-peptone, 5 g/l yeast extract, 10 g/l sodium chloride), supplemented with the antibiotic ampicillin (100 µg/ml), carbenicillin (100 µg/ml) or kanamycin (50 µg/ml), depending on the plasmid, as required for selection and maintenance of transformed cells.

Bacterial cells were routinely cultivated at the optimal growth temperature of 37ºC for 16-18h (overnight, ON). For liquid cultures, agitation at 200 rpm was used. For growth in solid media, agar was added to

the media (15 g/l). For long-term storage, bacterial strains were cryopreserved with glycerol (50% final concentration) and kept at -80ºC.

2.2.1.2. Yeast media and growth

Yeast strains were cultivated in complex media yeast peptone dextrose (YPD: 2% glucose, 2% bactopeptone, 1% yeast extract). For YKO collection strains, YPD media was supplemented with 200 $\mu g.ml^{-1}$ G418 antibiotic. When auxotrophic selection and maintenance of colonies was required, yeast strains were cultivated in synthetic complete media (SC: 0.67% yeast nitrogen base without amino acids, 0.067% yeast drop-out mix without leucine and uracil, 2% (w/v) carbon source) supplemented with the required amino acids, leucine (Leu) and/or uracil (Ura). The carbon sources used were raffinose (RAF) and glucose (GLU), for non-protein expression conditions, and galactose (GAL), for induction of protein expression. For solid media cultures, 2% agar was added. Yeast were cultivated at the optimal growth temperature of 30ºC for routine growth and at 37ºC, depending on experiments, with 200 rpm agitation. When cultures were performed in test tubes, yeast were incubated in an incubator hood TH 30 combined with an orbital shaker (Edmund Bühler GmbH, Tübingen, DE) and yeast growth was monitored by measuring optical density at 600 nm (OD_{600}) using an Evolution™ 300 UV-Vis Spectrophotometer (Thermo Scientific, Waltham, MA, USA). When cultivation was performed in 96-well microplates, yeast were incubated in an incubator Storex series STX40, LiCONiC Instruments (Woburn, MA, USA) and yeast growth was monitored also by measuring OD_{600} with an Infinite M200 multiplate reader (Tecan, Männedorf, CH). Starter cultures (pre-inoculums) were performed to acclimatize cells to liquid media and to ensure that experiments were carried out using yeast cultures at the same growth phase. For long term storage, liquid (500 µl) or solid (10 µl loop) yeast cultures were cryopreserved with 15% glycerol (final concentration) and kept at -80ºC. Reactivation of yeast strains was always performed in non-inducing protein expression conditions in agar SC media supplemented with GLU (SC+GLU).

2.2.1.3. H4 neuronal mammalian cells

H4 cells were grown in DMEM 4500 mg/l glucose and 4 mM glutamine, supplemented with 1 mM pyruvate, 1.5 g/l sodium bicarbonate, 10% FBS (Foetal Bovine Serum) and 1% antibiotics (penicillin and streptomycin). Cells were maintained at 80 to 90% confluence at 37ºC and in a humidified atmosphere with 5% CO_2.

A batch of stocks of H4 cells was prepared at the same passage number, in 10% DMSO in FBS, and stored at -80ºC. Cell spread was performed in T25 flasks with fresh culture media acclimatized to 37ºC. After 6h incubation at 37ºC, 5% CO_2, the media was replaced to completely remove DMSO, and cells were returned to the incubator.

Cells were passaged twice weekly with trypsin-EDTA, to a maximum of 8 passages, using T75 flasks at 1:10 or 1:20 sub-cultivation ratio.

2.2.2. Molecular biology methods

2.2.2.1. DNA extraction

2.2.2.1.1. Plasmid DNA extraction by boiling from *E.coli*

The boiling method for plasmid DNA preparations used 1 ml of a 5 ml ON culture of *E. coli* grown at 37ºC, 200 rpm agitation, in selective LB media. Cell lysis was accomplished by resuspending the cell pellet with 160 µl of Lysis buffer (50 mM Tris-HCl pH 8.0, 50 mM EDTA pH 8.0, 8% Glucose, 0.5% Triton X-100) containing 1 mg/ml of lysozyme, added fresh. Cells were vortexed vigorously, incubated in boiling water (> 95ºC) for 2 min and centrifuged for 15 min at 12000 rpm, at 4ºC. The cell pellet was removed with a sterile toothpick and 160 µl of ice-cold isopropanol was added to allow precipitation of DNA (samples were incubated at -20ºC for no more than 10 min). Samples were centrifuged at 12000 rpm for 15 min at 4ºC and the supernatant was removed completely. The DNA pellet was resuspended in 50 µl of sterile MilliQ H_2O.

2.2.2.1.2. Small scale high quality and purified plasmid DNA preparations from *E.coli*

For small scale preparation of plasmid DNA, 5 ml ON cultures of *E. coli* were grown at 37ºC with 200 rpm agitation in LB media supplemented with the appropriate antibiotic. High quality and purified plasmid DNA preparations were obtained using the QIAprep Spin Miniprep Kit, following manufacturer's instructions. Purified DNA was eluted from columns with sterile H_2O and used immediately or stored at -20ºC until required. These DNA preparations were used for cloning and sequencing.

2.2.2.1.3. Large scale high quality and purified plasmid DNA preparations from *E.coli*

Larger quantities of plasmid DNA preparations were obtained using the Qiagen HiSpeed Maxi Prep Kit, following manufacturer instructions. Bacteria cells were grown in 5 ml LB media supplemented with the required antibiotic, for 8 h, 37ºC, 200 rpm. This culture was then inoculated in 250 ml of media and allowed to grow until saturation for 16 h, 37ºC, 200 rpm. DNA was twice eluted with 1 ml elution buffer, and used immediately or stored at -20ºC until required.

2.2.2.2. Quantification of DNA concentration

Quantification of DNA concentration was performed by fluorometry using the Qubit® Fluorometer (Life Technologies, ThermoFisher Scientific, Waltham, MA, USA). The quantification assay Qubit® dsDNA BR Assay was used to quantify small and large scale DNA preparations. This assay allowed the quantification of double-stranded DNA (dsDNA) within the range of concentrations 100 pg/µl – 1000 ng/µl. An aliquot of 1 µl of DNA sample was usually used for quantification following manufacturer instructions. For the purpose of mammalian cell transfection, quantification of DNA was performed with

the Nanodrop 2000 (Thermo Fisher Scientific, Waltham, MA, USA), using 1 µl of DNA sample, following manufacturer instructions.

2.2.2.3. Agarose gel electrophoresis and DNA gel extraction and purification

Routine analysis of DNA was performed using agarose gels (0.8% - 1.5% w/v, depending on application) cast with 1x TAE (Tris-acetate-EDTA) buffer and ethidium bromide (0.2 µg/ml). Electrophoresis was performed using mini or medium EasyCast horizontal apparatus (OWL Separation system, Thermo Fisher Scientific, Waltham, MA, USA) at a constant voltage of 80 V-120 V (depending on the gel concentration and size of the gel) until the desired separation was achieved. DNA fragments size was estimated by including in each DNA electrophoresis 5 µl of O´Gene Ruler 1 Kb DNA ladder. DNA was visualised using the Mini Bis Pro imaging system (DNR Bio-imaging systems, Jerusalem, Israel). Excision of DNA fragments was performed on an UVIvue transilluminator (UVItec Cambridge, Cambridge, UK). DNA extraction and purification from low-melt agarose gels in 1x TAE was performed with QIAquick Gel Extraction Kit, following manufacturer instructions.

2.2.2.4. Polymerase chain reaction (PCR)

PCR was used for amplification of DNA for construction of plasmids and for verification of positive clones.

For cloning, proof-reading high fidelity polymerases were used (Platinum® Taq DNA Polymerase High Fidelity, Phusion Hot Start II High-Fidelity DNA Polymerase). For routine use, Taq DNA polymerase or MyTaq were used. Synthetic oligonucleotides (primers) were resuspended in sterile MilliQ H_2O at the final concentration of 50 µM. The stock solution was kept at -80ºC whereas a working solution was kept at -20ºC and used without further purification. Typical PCR reactions contained 50-100 µg of template DNA or 1 yeast colony), 0.2 mM of each dNTP, 0.5 µM of each primer, 1x PCR reaction buffer (as supplied by the manufacturer) and 1.25 units of polymerase per 20 µl reaction. When the reaction buffer did not contain magnesium chloride, it was added usually to a final concentration of 1.5 mM. A negative control (PCR reaction without DNA) was routinely performed for each PCR mix.

Reactions were performed using a Whatman Biometra Thermocycler T300 combi (Biometra GmbH, Gottingen, DE). Typical cycling conditions consisted of 94ºC denaturation step for 10 min, followed by 35 cycles of denaturation at 94ºC for 30 sec, annealing for 40 sec, with temperatures depending on the pair of primers melting temperature, and extension at 68ºC for high fidelity polymerases or 72ºC, for routine use polymerase, for 60-90 sec (depending on the size of the amplicon). A final extension step of 72ºC for 10 min was included. Successful amplification was confirmed *via* agarose DNA electrophoresis. When the amplicon was used for cloning, a purification step before restriction digestion was included using the QIAquick™ PCR Purification Kit, following manufacturer instructions.

2.2.2.5. Restriction digestion

Single and multiple restriction digestions reactions were performed according with the manufacturer instructions. Particularly for restriction digestion with multiple enzymes, a step of heat inactivation or purification of DNA using the Qiagen QIAquick™ PCR purification kit was performed, when necessary, between endonucleases digestion. Double digested plasmids were dephosphorylated using the enzyme CIAP. When there was no compatible enzymes for cloning and no availability of primers with restriction enzymes, blunt-end cloning was performed by treating both insert and plasmid with DNA Polymerase I (Klenow), following manufacturer instructions. This polymerase allows the fill-in of 5´ overhangs and removal of 3´ overhangs. Successful digestion of DNA was confirmed *via* agarose DNA electrophoresis relative to undigested DNA. For cloning, when vectors were digested with two endonucleases, controls of single endonuclease digestion were performed. DNA fragments excised from agarose were purified using the QIAquick™ Gel Extraction Kit. When performing restriction digestions for selection of positive clones, DNA plasmid preparations by boiling were used and the reaction's mix included the addition of RNase A.

2.2.2.6. DNA ligation

DNA ligation reactions were performed using T4 DNA ligase. Plasmid and insert DNA fragments were analysed in a DNA agarose electrophoresis to estimate relative concentrations and size ratio, to calculate the proportions of plasmid/insert in the ligation reaction. Ligation of single digested plasmid and double digested plasmid without insert were also performed as controls.

The ligation reaction was typically performed using 5 units of T4 DNA ligase in a 1x concentration of T4 ligase buffer (containing adenosine triphosphate, ATP), as supplied by the manufacturer. For ligation of blunt-end DNA fragments, 50% PEG 4000 solution was added to the reaction (5% final concentration). Reactions were incubated for 2 h at 24ºC, or ON at 16ºC for ligation of blunt-ended DNA fragments, before transformation into *E. coli*.

2.2.2.7. Competent *E. coli*

Chemically competent *E. coli* were generated by treatment with calcium chloride. An ON 10 ml starter culture of cells was grown in LB media at 37ºC, 180 rpm agitation. A 200 ml LB culture was inoculated from the starter culture (5 ml) and grown at 37ºC, 180 rpm agitation, until it reached an optical density at 600 nm (OD_{600}) of 0.6. Cells were cooled on ice for 30 min and pelleted at 4000 rpm for 15 min at 4ºC. The supernatant was removed and the pellet gently resuspended in 50 ml of ice-cooled Solution A (22 mM KCH_3COO, 37 mM $MnCl_2$, 7.5 mM $CaCl_2$, 75 mM KCl, 10 % v/v glycerol). Cells were pelleted by centrifugation at 4000 rpm for 8 min at 4ºC and gently resuspended in 10 ml of ice-cold Solution B (8 mM NaMOPS pH 7.5, 60 mM $CaCl_2$, 8 mM KCl, 10% v/v glycerol). Aliquots of 200 µl were dispensed into pre-chilled microcentrifuge tubes and snap-frozen in liquid nitrogen prior to storage at -80ºC.

2.2.2.8. Introduction of plasmid DNA into *E. coli*

For transformation of *E.coli*, frozen 200 µl aliquots of competent *E. coli* were thawed on ice. 10 µl of DNA solution (ligation of plasmid DNA preparations diluted 1:10) was added to 100 µl of competent *E. coli* cells in ice-cold microcentrifuge tubes, and cells were incubated on ice for 30 min. Cells were heat shocked at 42ºC for 50 sec and then cooled on ice for 2 min. Cells were recovered by incubation in 900 µl of LB media, at 37ºC, 200 rpm, for 1 h. Cells were pelleted by centrifugation at 840 rpm for 3 min, resuspended in 100 µl of the supernatant and plated onto selective LB media plates. Positive colonies were observed after ON incubation at 37ºC. When cloning, single and double digested plasmid ligation reactions without insert were also transformed and plated, as controls of restriction digestion efficiency.

2.2.2.9. Selection of positive clones and DNA sequencing

Selection of positive clones was performed by restriction analysis after extraction of DNA by the boiling method, as described in 2.2.2.1.1. Restriction digestion was performed with one or two endonucleases, making sure that both insert and plasmid were digested. The resulting pattern of restriction, visualised in an agarose electrophoresis, was analysed in terms of size, verifying the presence of insert and its correct direction relative to the promoter (in case of blunt-end DNA ligation). In certain cases, selection of positive clones was performed by PCR, using insert-specific primers. Independently of the screening method for selection of positive clones, one positive colony was then selected and small scale DNA extraction was performed using the QIAprep Spin Miniprep Kit. DNA plasmid sequences were sent to Stab Vida (Lisbon, PT) for sequencing. Oligonucleotides used for sequencing were designed by the user.

2.2.3. Genetically engineered yeast strains to express human proteins

2.2.3.1. Yeast episomal plasmids for Aβ_{1-42} and tau40 expression

For the construction of the episomal model of Aβ_{1-42} and tau40 co-expression (Chapter 3), standard PCR reactions (section 2.2.2.4) were used to amplify the coding sequences of interest, using primers with appropriate restriction enzymes (Table 2.1).

After digestion with the corresponding endonucleases (section 2.2.2.5) and confirmation of size and purification of the DNA (section 2.2.2.3), these sequences were inserted in the yeast high-copy (2µ) bi-directional expression episomal plasmid pESC-LEU (Figure 2.1), cut with appropriate enzymes. Aβ_{1-42}, mCherry (mCh) and Aβ_{1-42}-mCh coding sequences were inserted into the multiple cloning site II (MCSII), under the control of *GAL1* promoter, whereas tau40 and tau40-eGFP sequences were inserted in MCSI, under the control of *GAL10* promoter. Ligation reactions (section 2.2.2.6) were transformed into XL1-Blue *E.coli* cells (section 2.2.2.8) and transformed colonies were selected in LB agar plates containing

ampicillin, and incubated ON at 37ºC (section 2.2.2.9). Several transformants were selected for extraction of plasmid DNA by boiling (section 2.2.2.1.1). Confirmation of positive clones was performed by double restriction analysis of plasmid DNA, with one endonuclease cutting in the backbone and the other cutting the inserted sequence. In some cases, a prior selection of positive clones was performed by colony PCR (section 2.2.2.4). The integrity of the inserted sequence was confirmed by sequencing (outsourced to Stab Vida, Lisbon, PT) prior to transformation in yeast. The plasmids pESC-LEU_Gal10-tau40 and pESC-LEU_Gal1-mCh were also used in Chapters 4 and 5.

Table 2.1. Coding sequences used for construction of yeast episomal plasmids, with template sources, restriction sites, and oligonucleotides sequences used for PCR amplification.

Coding sequence	Source	Restriction sites (5', 3')	Primers (5' - 3')
$A\beta_{1-42}$	pVAX_$A\beta_{1-42}$ (BIOALVO)	*Bam*HI, *Xho*I	CGCGGATCCATGGATGCAGAATTCCGACATG CCGCTCGAGTTACGCTATGACAACACCGCCC
mCherry	pCAGGS_mCherry (A. C. Rego, CNC)	*Bam*HI, *Xho*I	CGCGGATCCATGGTGAGCAAGGGCGAGGAGG CCGCTCGAGTTACTTGTACAGCTCGTCCATG
$A\beta_{1-42}$-mCherry	pVAX_$A\beta_{1-42}$ (BIOALVO)	*Bam*HI, *Hind*III	CGCGGATCCATGGTGAGCAAGGGCGAGGAGG CCCAAGCTTCGCTATGACAACACCGCCCAC
	pCAGGS_mCherry (A. C. Rego, CNC)	*Hind*III, *Xho*I	CCCAAGCTTATGGTGAGCAAGGGCGAGGAGG CCGCTCGAGTTACTTGTACAGCTCGTCCATG
tau40	pBLV_TAU-2N4Rwt-EGFP (BIOALVO)	*Not*I, *Bam*H1/*Bgl*II (compatible ends)	ATAAGAATGCGGCCGCATGGCTGAGCCCCGCCAGGAG CGCGGATCCTCACAAACCCTGCTTGGCCAG
eGFP	pEGFP-N1 (BIOALVO)	*Not*I, *Bgl*II	ATAAGAATGCGGCCGCATGGTGAGCAAGGGCGAGGAG GAAGATCTTTACTTGTACAGCTCGTCCATGCC
tau40-eGFP	pBLV_TAU-2N4Rwt-EGFP (BIOALVO)	*Not*I, *Bgl*II	ATAAGAATGCGGCCGCATGGCTGAGCCCCGCCAGGAG GAAGATCTTTACTTGTACAGCTCGTCCATGCC

2.2.3.2. Yeast integrative plasmids for $A\beta_{1-42}$ and tau40 expression

For the construction of the integrative model of $A\beta_{1-42}$ and tau40 co-expression (Chapter 3), an integrative yeast expression plasmid containing *GAL1/10* divergent promoter's cassette was first engineered. Restriction digestion of pESC-LEU with *Pvu*II (blunt-end) allowed to cut the entire *GAL1/10* cassette which was then inserted into YIp211 (Figure 2.2), open with *Sma*I (blunt-end). This expression plasmid was named YIp211_GAL (Figure 2.5).

The directionality of the insert was determined by double restriction analysis, using one enzyme cutting in the vector backbone and the other cutting in the insert. The coding sequences of mCh and $A\beta_{1-42}$-mCh were cut from pESC-LEU_*GAL1*-mCh and pESC-LEU_*GAL1*-$A\beta_{1-42}$-mCh, respectively, with *Bam*H1/blunt ended at the N-terminal and *Xho*I at the C-terminal, and inserted into YIp211_GAL, digested with *Sma*I at de N-terminal and *Xho*I at C-terminal.

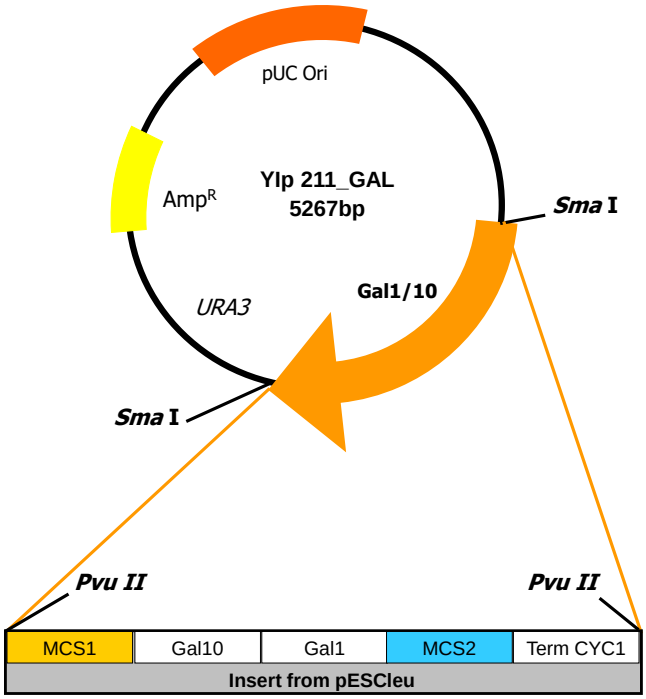

Figure 2.5. Schematic diagram of YIp211_GAL (BIOALVO).

Ligation reactions (section 2.2.2.6) were transformed into XL1-Blue *E.coli* cells (section 2.2.2.8) and transformed colonies were selected in LB agar plates containing ampicillin, with incubation ON at 37ºC. Confirmation of positive clones was performed by double restriction analysis of plasmid DNA extracted by the boiling method (section 2.2.2.1.1), with one endonuclease cutting in the backbone and the other cutting the inserted sequence. The integrity of the inserted sequence was confirmed by sequencing (outsourced to Stab Vida, Lisbon, PT). Prior to transformation in yeast, the integrative plasmids were linearized with *Eco*RV for target integration into the yeast genome. Correct integration of mCh and $A\beta_{1-42}$-mCh plasmids in yeast was confirmed with the primer Fw_TTGCGAGGCATATTTATGGTG (genomic sequence) and Rv_CGCGGATCCATGGTGAGCAAGGGCGAGGAGG for strains containing mCh sequence or Rv_CGCGGATCCATGGATGCAGAATTCCGACATG for strains containing $A\beta_{1-42}$-mCh sequence.

2.2.3.3. Yeast transformation

Two protocols of yeast transformation were used, based on the lithium acetate/PEG protocol.

2.2.3.3.1. One-step yeast transformation protocol

For introduction of episomal expression plasmids in yeast, the protocol One-step yeast transformation was used (Chen, Yang & Kuo, 1992). A generous loop of stationary phase *S. cerevisiae* cells was scraped from a media plate (stored at 4ºC up to 1 month), resuspended in sterile MilliQ H_2O and distributed in 100 µl aliquots in microcentrifuge tubes. Cells were pelleted and resuspended in One-Step Buffer (0.2 M LiAc, 40% w/v PEG 4000, 100 mM DTT, kept in aliquots at -20ºC), and 1 µg of plasmid DNA and 20 µg of ssDNA (previously boiled) was added. This cell suspension was vigorously vortexed

prior to heat shock at 45ºC for 30 min. After this incubation, cells were washed with 1 ml of sterile MilliQ H_2O and spun for 10 sec at maximum speed. The supernatant was discarded and cells were resuspended in 100 µl of sterile MilliQ H_2O and transformants were selected in agar SC+GLU lacking leucine (SC+GLU-Leu). Several colonies (usually 3) were selected and isolated in a new media plate and again incubated for 2 additional days at 30ºC.

2.2.3.3.2. High-efficiency yeast transformation protocol

For introduction of integrative expression plasmids in yeast, the high-efficiency yeast transformation protocol was performed, using mid-exponential phase yeast cultures (Woods & Gietz, 2001). Starter ON yeast cultures grown at 30ºC, 200 rpm, in SC+GLU media lacking leucine or leucine and uracil (double integration strains), were used to inoculate a 50 ml culture at the starting OD_{600} 0.2. This culture was incubated at 30ºC, 200 rpm agitation until OD_{600} 0.8-1. Cells were collected by centrifugation (6000 rpm, 5 min), washed once with sterile MilliQ H_2O and then with 1 ml of 100 mM LiAc. After centrifugation and removal of supernatant, cells were resuspended in 500 µl of 100 mM LiAc. Aliquots of 50 µl of yeast cells prepared this way were used for each transformation. The cells were pelleted, the supernatant removed and the transformation mix was added (PEG 4000 33% v/v, 100 mM LiAc, 100 µg of freshly boiled ssDNA). Finally, 1 µg of linearized plasmid DNA was added, the solution vortexed vigorously and incubated at 30ºC for 30 min. The heat shock was performed by incubating cells at 42ºC for 20 min. Cells were washed once with sterile MilliQ H_2O before recovery incubation for 2 h, at 30ºC, 200 rpm agitation, in culture media. After this incubation cells were pelleted by centrifugation (13000 rpm, 10 sec), resuspended in 100 µl of supernatant and plated onto selective media plates. Integration of mCh and $A\beta_{1-42}$-mCh plasmids in W303-1A yeast was performed in the URA3 locus and, therefore, transformants were selected in agar SC+GLU lacking uracil (SC+GLU-Ura). The integration of these plasmids in W303-1A-tau40 required the selection of transformants in media lacking leucine (to maintain tau40 integration) and uracil. 16 colonies of each transformation were selected and isolated in new media plates and incubated for two additional days at 30ºC, before confirmation of the correct integration of the plasmids, by standard colony PCR reactions (section 2.2.2.4).

2.2.4. Characterization of yeast strains

2.2.4.1. Yeast growth analysis

2.2.4.1.1. Dot spot analysis

Yeast strains were pre-inoculated on liquid SC+RAF media, lacking the required amino acids, depending on the plasmid auxotrophic marker (lacking leucine or leucine and uracil). Cultures were incubated at 30ºC with agitation (200 rpm). After ON growth, yeast OD_{600} was monitored using an Evolution™ 300 UV-Vis Spectrophotometer and cultures were inoculated on the same media at a starting OD_{600} 0.2 and again incubated at 30ºC until reaching mid exponential phase (OD_{600} 0.8-1.2). Equal amounts of each yeast strain were then collected, 10 or 5-fold serially diluted using sterile MilliQ H_2O and 10 µl of each

cell suspension were spotted on selective agar SC-GLU (non-inducing media) or SC-GAL (inducing media). Plates were incubated at 30ºC and 37ºC for 3 to 6 days and yeast growth was monitored every 24 h. Images of plates were acquired with Mini Bis Pro imaging system (DNR Bio-imaging systems, Jerusalem, IL).

2.2.4.1.2. Yeast growth analysis in liquid media

Episomal yeast strains growth was evaluated immediately after transformation or after cryopreservation. In the first case, one transformant of each strain was tested (6 technical replicates) after colony isolation from the transformation plate. When cryopreserved, yeast were inoculated from the glycerol stocks in selective SC+GLU media, and incubated at 30ºC for 3 days. Independently of the source, yeast were pre-inoculated on selective liquid SC+RAF and incubated at 30ºC with 200 rpm agitation. After ON growth, yeasts were inoculated at a starting OD_{600} 0.1 in selective SC+GLU media (non-inducing media) or SC+GAL (inducing media) and incubated at 30 ºC or 37ºC in 96-well plates (200 µl final volume). Yeast cells were grown in a LiCONiC STX40 Automated Incubator (Perkin Elmer, Waltham, MA, USA) and growth was automatically monitorized by measuring OD_{600} using a Victor 3V microplate reader (Perkin Elmer, Waltham, MA, USA) using a liquid handling system Janus Automated Workstation (Perkin Elmer, Waltham, MA, USA).

2.2.4.2. Protein expression analysis

2.2.4.2.1. Extraction of total yeast protein, in denaturing conditions

Yeast cells were pre-inoculated in selective liquid SC+RAF media, lacking the required amino acids, depending on the auxotrophic marker (lacking leucine or leucine and uracil). Cultures were inoculated at 30ºC with 200 rpm agitation. After ON growth, yeast were inoculated in liquid selective SC+GAL media, to induce protein expression, at a starting OD_{600} 0.2, and incubated at 30ºC and 37ºC. After 18h growth (OD_{600} ~ 1-3) equal amounts of yeast were collected by centrifugation, washed with sterile water and pellets resuspended in 100 µl of 1x SDS sample buffer (60 mM Tris-HCl pH 6.8, 10% glycerol, 2% SDS, 70 mM βME, 1% bromophenol blue supplemented with 1x protease inhibitor cocktail and 1x PhosSTOP® phosphatase inhibitor cocktail). After resuspension, cells were lyzed by boiling for 5 min. A final centrifugation was performed to eliminate cell debris. Protein samples were stored at -20ºC until use.

2.2.4.2.2. Western Blotting

Equal amounts of each protein sample were loaded in 12% SDS-PAGE and blotted onto a nitrocellulose or PVDF membrane by semi-dry transference using a Trans-Blot® Turbo™ Transfer System (Bio-Rad, Hercules, CA, USA). Membrane blocking was performed using 5% solutions of milk, BSA or PhosphoBlocker™ blocking reagent in Tris-buffered saline with Tween20 1x (TBST1x). Immunodetection was performed using the following antibodies: total tau (polyclonal rabbit anti-human tau, Dako Agilent Technologies, Glostrup, DK) diluted 1:10000, phospho-tau in Ser396/404 (mouse AD2

anti-tau protein monoclonal, Bio-Rad) diluted 1:3000, $A\beta_{1-42}$ (monoclonal mouse Amyloid β, clone W0-2, Merck Millipore, Billerica, MA, USA) diluted 1:1000, GSK-3β (11B9) (mouse monoclonal antibody, Santa Cruz Biotechnology, Dallas, TX, USA) diluted 1:500 and PGK-1 (monoclonal yeast phosphoglycerate kinase antibody, Invitrogen Molecular Probes, Carlsbad, CA, USA), used as loading control, diluted 1:10000, all in TBST1x containing 1% of the blocking solution. Membrane-bound proteins were detected by chemiluminescence using the secondary antibodies: goat anti-mouse IgG (H+L)-HRP conjugate (Bio-Rad, Hercules, CA, USA) diluted 1:8000 and goat anti-rabbit IgG (H+L), horseradish peroxidase conjugate (Invitrogen Molecular Probes, Carlsbad, CA, USA) diluted 1:10000, all in TBST1x containing 1% blocking solution. The Immobilon Western Chemiluminescent HRP Substrate (Millipore) was used and digital images acquired with Alliance 4.7 (UVitec Cambridge, Cambridge, UK).

2.2.4.3. Sarkosyl protein fractionation

Protein fractionation using the Sarkosyl detergent was performed as described in Fushimi *et al.*, 2011 with some modifications. Yeast cells were pre-inoculated at 30ºC with 200 rpm agitation in selective SC+RAF media. After ON growth, yeast were inoculated at OD_{600} 0.2 in 50 ml of selective SC+GAL media and protein expression was induced for 24h at 37ºC, 200 rpm agitation. Mid-exponential stage yeast cells (OD_{600} 2-5) were collected by centrifugation, washed in sterile ice-cold phosphate-buffered saline 1x (PBS 1x) and resuspended in 500 μl of Extraction Buffer (100 mM Tris-HCl pH 7.9, 250 mM ammonium sulphate, 1 mM EDTA, 10% glycerol, 0.5 mM DTT supplemented with 1x protease inhibitor cocktail and 1x PhosSTOP® phosphatase inhibitor cocktail). Crude protein extraction was performed by vortex with glass beads for 10 min at 4ºC and glass beads and cell debris were eliminated by centrifugation (10000 rpm, 15 min, 4ºC). Protein concentration was measured by the Bradford dye-binding assay. 1 µl of protein sample was diluted 1:10 and 3 µl of this dilution was used for quantification. Bovine serum albumin (BSA) was used as a standard. Absorbance was determined using a Thermo Scientific Spectrophotometer (Thermo Fisher Scientific, Waltham, MA, USA). Protein concentration was adjusted at 1 mg/mL with Extraction Buffer (input samples). Sarkosyl was added to the protein lysates to a final concentration of 1% and samples were incubated at room temperature for 5 min. Sarkosyl-soluble and insoluble protein fractions were separated by centrifugation at 35000 g for 1 h at 4ºC. Pellets were washed once with ice-cold extraction buffer and centrifuged at 35000 g for 30 min to eliminate residual soluble protein. Pellets were recovered with 5 μl of 1X SDS sample buffer and boiled for 5 min, and then 5 μl of 10 M urea was added before loading into a 10% SDS-PAGE gel. Equal amounts of input and Sarkosyl soluble protein fraction (10 μl) were collected and protein denaturing was performed by adding 2x SDS sample buffer and boiling for 5 min, before loading into a 10% SDS-PAGE gel. Immunodetection of $A\beta_{1-42}$ in input, Sarkosyl-soluble and insoluble samples was performed as previously described. GAPDH (mouse monoclonal anti-GAPDH, Ambion Life Technologies, Carlsbad, CA, USA) was used as loading control, diluted 1:3000.

2.2.4.4. Fluorescence microscopy and counting of cells with protein inclusions

Episomal model yeast strains were pre-inoculated on selective liquid SC+RAF media, at 30ºC, 200 rpm agitation. After ON growth, yeast were inoculated in selective SC+GAL media, at a starting OD_{600} 0.2, to induce protein expression, at 37ºC. After ON incubation, equal amounts of yeast were collected and fixed with formaldehyde (10% final concentration). After 1 h incubation at 37ºC, cells were collected by centrifugation (3000 rpm) and the supernatant discarded. Yeast were washed once with KPO_4/Sorbitol solution (0.6% 2 M sorbitol, 10% 1 M potassium phosphate, pH 7.5), and resuspended in 200 µl of the same solution. Yeast suspensions were stained with Hoechst 33342 (final concentration 10 µg/ml).

Microscopic observation was performed using the laser scanning confocal microscope Zeiss LSM 710 and image acquisition and treatment was performed using the software Zen 2012. eGFP proteins were observed using a Argon/2 488 nm, 45 mW laser, whereas mCh proteins were observed using a DPSS 561-10, 15 mW laser. Hoechst 33342 labelling was observed using the Diode 405-30, 30 mW. Z-stack images were acquired using a Plan-Apochromat 63x/1.4 objective and then processed as a maximum intensity projection using the Image J.

Counting of yeast cells with protein inclusions was performed in a 10 µl aliquot of yeast suspension, using mCh fluorescent signal. At least 200 cells expressing mCh were counted in all samples and the percentage of cells containing protein inclusions was calculated. Counting was performed using a Zeiss Observer D1 epifluorescent microscope with a Plan-Neofluar 40x/0.6 objective. eGFP constructs were observed using band pass excitation filter 470 nm and emission band pass 525 nm filter, whereas mCh constructs were observed using the band pass 596 nm excitation filter and emission long pass 590 nm.

2.2.4.5. Statistical analysis

2.2.4.5.1. Counting of cells with protein inclusions

Data of the number of cells with protein inclusions corresponds to the average of 3 independent experiments. Statistical significance was determined using Graph Pad Prism software, by performing one-way ANOVA followed by Tukey’s multiple comparison test.

2.2.4.5.2. Immunoblot quantification analysis

Data for immunoblot quantification analysis corresponds to the average of 3 independent experiments. Quantification was performed using Image J (Schneider, Rasband & Eliceiri, 2012) and statistical significance was determined using Graph Pad Prism software, by performing one-way ANOVA. Multiple comparison test of samples towards one control sample was performed using Dunnett’s test. For comparison of all samples with one another, the Tuckey’s multiple comparison test was used. For comparison between 2 groups of samples, the standard Student’s t-test was performed.

2.2.5. Screen for gene enhancers of tau40 toxicity with the YKO collection

2.2.5.1. Preparations of high quality and purified pESC-Leu_*Gal10*-tau40 plasmid

Plasmid DNA extraction was performed as described in section 2.2.2.1.3 using the Qiagen HiSpeed Maxi Prep Kit. After extraction, all maxipreps were merged and quantified as described in 2.2.2.2 , using the Qubit® Fluorometer.

2.2.5.2. YKO collection replication

Prior to the screening, the YKO collection was replicated to maintain the integrity of the original collection plates. The YKO strains were inoculated in 100 µl of YPD supplemented with 200 $\mu g.ml^{-1}$ G418, using a 96 pin replica plater, into 96-well round-bottom microplates. After 2 days incubation at 30ºC with agitation (200 rpm, Storex series STX40, LiCONiC Instruments, Woburn, MA, USA), sterile glycerol was added to each well at a final concentration of 15%. Plates were sealed, labelled with a unique bar code, and stored at -80ºC until use.

2.2.5.3. Transformation of YKO strains

The YKO collection replica plates were transformed with the plasmid pESC-LEU_*GAL10*-tau40 in several rounds. In each round, 4 microplates of the YKO collection were transformed. In each round, wild-type BY4741 was transformed with pESC-LEU_*GAL10*-tau40 as a positive control of transformation. Also, a negative control of transformation (transformation mix without plasmid DNA) was performed in each round to rule-out contaminations.

2.2.5.3.1. Transformation in 96-well format

Yeast transformation was performed using the LiAc/Carrier DNA/PEG method applied to a 96-well plate format (Gietz & Schiestl, 2007). Yeast cells were grown for 24 h at 30ºC, 200 rpm (Storex series STX40, LiCONiC Instruments, Woburn, MA, USA) in 100 µl of YPD until OD_{600} 0.2-1.2 (absorbance readings performed with VICTOR™ X3 Multilabel Plate Reader (Perkin Elmer, Waltham, MA, USA), centrifuged at 2500 g for 5 min, room temperature (Allegra 25R Centrifuge, Beckman Coulter, Brea, CA, USA) and the supernatant discarded. Using a 8x 300 multichannel pipette (HTL, Labmate), cells were resuspended in 50 µl of transformation mix (per well: 0.7 µg of plasmid DNA, 100 mM LiAc and 40 µg ss carrier DNA, freshly boiled) and after mixing by pipetting, 100 µl of PEG 4000 50% (w/v) was added to each well. Mixing was performed at 250 rpm, for 5 min (Heidolph™ Titramax Vibrating Platform Shaker). Following the heat shock for 1 h at 42ºC, cells were centrifuged (1500 g, 10 min, RT), resuspended in 50 µl of sterile MilliQ H_2O. Microplates were agitated at 250 rpm until plating.

2.2.5.3.2. Transformation of individual YKO strains

Transformation of individual yeast strains followed the protocol described in the previous section, based on the LiAc/Carrier DNA/PEG method, with some modifications. YKO strains were reactivated from glycerol stocks (original YKO 96-well plates) in agar YPD supplemented with 200 µg.ml^{-1} and incubated for 2-3 days at 30ºC. For transformation, a loop of yeast cells was inoculated in 3 ml of YPD and incubated at 30ºC with 200 rpm agitation, so that yeast cells would be fitter prior to transformation. Before adding the transformation mix, yeast cells were washed twice with sterile MilliQ H_2O (centrifugation 6000 rpm, 1 min) to eliminate residual culture media. The remaining protocol was performed as already described. The entire transformation mix of each strain was plated in agar SC+GLU media lacking leucine, for selection of transformants for 3-6 days incubation at 30ºC. One or more colonies of each transformed YKO strain were selected and isolated in a new agar plate, and incubated for 2 additional days at 30ºC. 15% glycerol stocks of each mutant strain were prepared and stored at -80ºC. Reactivation of yeast stocks was performed in agar SC+GLU-Leu media for 2-3 days incubation at 30ºC.

2.2.5.4. Screening yeast gene deletions enhancers of tau40 toxicity

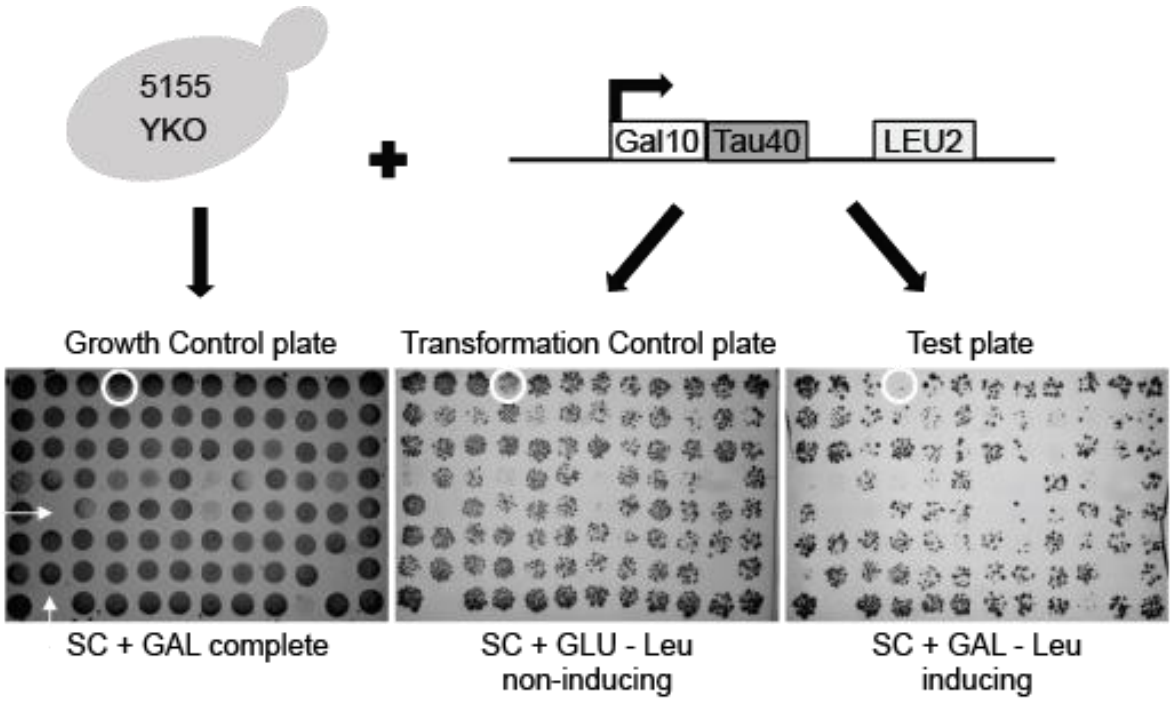

Figure 2.6. Example of a screening plate set.
5155 yeast knockout mutants (YKO) were spotted into complete SC media supplemented with 2% galactose (growth control plate) prior to transformation, to evaluate yeast growth fitness in galactose. This collection was transformed with a construct for tau40 expression regulated by the promoter *GAL10* and 10 µl of each transformation were spotted into selective non-inducing media plates containing glucose (transformation control plate) and in inducing media plates containing galactose (test plate). Arrow-highlighted areas of the plate indicate empty wells. Circle-highlighted areas indicate a yeast mutant strain hit.

In the day prior to the screening, 5 µl of each yeast strain were inoculated in 200 µl of YPD, in round-bottom transparent microplates (BD Bioscience, San Jose, CA, USA). Yeast cells were incubated for 24 h, at 30ºC, 200 rpm, until OD_{600} was monitored at the end of the incubation using a VICTOR™ X3 Multilabel Plate Reader (Perkin Elmer, Waltham, MA, USA). From each well, a 10 µl aliquot of yeast culture was spotted into SC+GAL media plates supplemented with uracil and leucine (SC+GAL complete), to evaluate the effect of galactose on yeast mutant growth. The remaining yeast culture was used for transformation with the plasmid pESC-LEU_*GAL10*-tau40. After transformation, 10 µl aliquots of yeast were spotted in SC+GLU-Leu non-inducing media plates, as a transformation control, and in SC+GAL-Leu inducing media plates (Figure 2.6).

The transformation control plate allowed to identify yeast strains that incorporated the plasmid and thus were able to grow in media lacking leucine. In the test plate (inducing media), only mutant yeast not affected by galactose, successfully transformed and expressing tau40 were able to grow. Plates were incubated at 30ºC for 6 days, as the read-out of the experiment was growth/no growth, this way decreasing the probability of slow growers being picked as hits. After this period of incubation, plates were analysed for yeast growth. Image acquisition was performed with a Mini Bis Pro imaging system (DNR Bio-imaging systems, Jerusalem, IL).

At the end of each round, YKO strains were classified as hits, incongruences, doubts and negative results (Table 2.2). To be considered a hit, a yeast mutant strain should (1) not be affected by galactose, (2) be able to grow in selective non-inducing media after transformation and (3) unable to grow in selective inducing-media.

Table 2.2. Classification of yeast knockout strains after transformation with pESC-Leu_GAL10-tau40.

Classification	Inoculum (YPD)	Growth Plate (SC+GAL complete)	Transformation plate (SC+GLU-LEU)	Test Plate (SC+GAL-LEU)
Hits	+	+	+	-
Incongruences	+	+	-	+
Doubts	+	-	-	-
	+	+	-	-
	+	-	+	-
Negative	+	+	+	+

Legend: “+” growth; “-“no growth

The percentage of yeast mutant strains transformed was calculated using the total number of strains that were successfully recovered in YPD (tested strains). The mutant yeast strains that displayed reduced or no growth in the presence of galactose (growth control plate) were excluded from the analysis. Also excluded from the analysis were yeast mutant yeast strains that did not grow in the transformation plate but did so in the test plate, indicating technical issues. Yeast strains not grown both in transformation and test plates were also excluded from the analysis and probably reflect strains sensitive to the transformation protocol.

To eliminate false positives, the putative hits identified in the first screening were again transformed with tau40 expression plasmid and the resulting growth phenotype evaluated (secondary screening). Only strains depicting a reproducible outcome were considered as hits. The Yeast Genome Database

(www.yeastgenome.org/) was used to identify the function or genetic role of the picked yeast ORFs. Yeast genes with human homologues were identified using the Yeast Genome Database automatic search tools, and were also confirmed by using the Protein Basic Local Search Tool at NCBI (Blastp, http://blast.ncbi.nlm.nih.gov/). The yeast protein sequence was blast with the non-redundant human protein database and results yielding the smallest E score were considered as the human homologues of the yeast gene. A functional analysis of the human homologue gene hits was performed using the annotations of the Proteome Database (http://www.biobase-international.com/). Yeast ORFs with human homologues were selected for further target-narrowing studies. These strains were transformed a third time with tau40 expression plasmid and the resulting yeast growth was evaluated by spotting assays, in comparison with wild-type strain BY4741 (section **Error! Reference source not found.**.). east strains which were confirmed as sensitive to tau40 toxicity were transformed with the control protein mCherry, to evaluate the specificity of the phenotype towards tau.

2.2.5.5. Confirmation of yeast ORF deletion

2.2.5.5.1. Yeast genomic DNA extraction

Yeast mutant strains and control wild-type BY4741 were inoculated in 5 ml YPD and incubated at 30ºC, 200 rpm agitation. After ON growth, yeast were collected by centrifugation (6000 rpm, 5 min) and treated to form spheroplasts (2 h, at 30ºC, with gentle agitation in K_2HPO_4 50 mM, KH_2PO_4 50 mM, $MgCl_2$ 0.5 mM, sorbitol 1.2 M, β-ME 70 mM, lyticase 50 mg/ml, pH 6,8). After this treatment, genomic DNA extraction was performed using the DNeasy® Blood & Tissue Qiagen kit, following manufacturer instructions. Genomic DNA was eluted twice in the same volume of elution buffer (100 µl) for maximum DNA yield. Genomic DNA (gDNA) samples were used immediately or stored at 4ºC until use.

2.2.5.5.2. PCR for confirmation of yeast ORF deletion

Prior to confirmation of the ORF deletion, the quality of the gDNA was evaluated by DNA electrophoresis and by PCR amplification of the internal control gene *NPT1*. Confirmation of the deletion strains was performed using primers for the specific bar codes of each yeast deletion strains using standard PCR techniques, as described in section 2.2.2.4, following the recommendations and the oligonucleotide sequences provided by the Yeast Deletion Project (http://www-sequence.stanford.edu/group/yeast_deletion_project/deletions3.html). For each pair of primers a PCR negative control gDNA was performed, as well as a PCR mix containing wild-type BY4741 gDNA for control of amplification specificity.

2.2.6. Identification of bacterial natural extracts suppressors of tau toxicity in yeast

The screening for identification of bacterial natural products with activity in suppressing tau40 toxicity was performed using the yeast strain BY4741 *mir1*Δ transformed with pESC-Leu_*Gal10*-tau40, as described in section 2.2.3.3.2, hereinafter designated as *mir1*Δ-tau40.

2.2.6.1. Validation of the platform *mir1*Δ-tau40

Prior to the screening, a liquid growth evaluation assay was performed to confirm the phenotype of the yeast strain *mir1*Δ and to choose the best starting OD_{600} to perform future drug discovery screenings. The growth of *mir1*Δ-tau40 yeast strain *versus* the control strain (*mir1*Δ-pESC), was evaluated in culture media containing glucose (non-inducing conditions) or galactose (protein inducing conditions) and supplemented with DMSO, solvent of the solutions of natural extracts (Martins *et al.*, 2013b).

Yeast were pre-inoculated in liquid SC+RAF-Leu media, at 30ºC with 200 rpm agitation. After ON growth, yeast OD_{600} was measured using an Evolution™ 300 UV-Vis Spectrophotometer (Thermo Scientific, Waltham, MA, USA) and cultures were diluted to a starting OD_{600} of 0.05, 0.1 and 0.2 in SC+GAL-Leu media. Then, 196 µl of cell suspension was dispensed into wells of 96-well round-bottom microplates. DMSO was added to the cell suspension to a final concentration of 2%. The experimental design included 6 replicates per test condition. Controls added included *mir1*Δ strains inoculated in non-inducing SC+RAF-Leu media and the wild-type strain BY4741 carrying tau40 plasmid or empty plasmid inoculated in inducing SC+GAL-Leu media, both at a starting OD_{600} 0.2. Cells were incubated in an Incubator hood TH 30 combined with an orbital shaker (Edmund Bühler GmbH, Tübingen, GE) with 200 rpm agitation. Growth monitoring was performed by measuring OD_{600} with an Infinite M200 multiplate reader (Tecan, Männedorf, CH), every 2 h during labour-time, for approximately 70 h.

The data obtained was used to calculate the average (A) and standard deviation (SD) of the control strain *mir1*Δ-pESC (maximum signal) and test strain *mir1*Δ-tau40 (minimum signal), at each time-point, for the three different starting OD_{600}, using Microsoft Excel. The assay signal dynamic range was calculated by subtracting the average maximum signal by the average minimum signal. The choice of the starting OD_{600} was based on the extent of the lag phase of yeast growth and on the assay dynamic range.

The evaluation of the overall quality of the assay for HTS was performed using the Z-prime factor (Z'-factor), a dimensionless parameter that takes into account the assay signal dynamic range and the data variation associated with samples, without intervention of test compounds (Zhang, 1999) (Equation 2.1). Larger the Z' factor the higher confidence on the data obtained in a HTS assay (Zhang, 1999). Z' values equal to 1 correspond to the ideal assays, with high signal dynamic range and low variation of references measurements. Z' values below 1 and superior or equal to 0.5 are considered excellent assays. Below Z' values of 0.5, some assays can still be used with care and negative values classify assays as unsuitable for HTS (Zhang, 1999).

$$Z' = 1 - (\frac{(3 \times SD\ Maximum\ signal) + (3 \times SD\ Minimum\ signal)}{|A\ Maximum\ signal - A\ Minimum\ signal|}$$

Equation 2.1. Z-prime factor (Z') equation applied to *mir1*Δ-tau40 drug discovery platform.
Z prime is a parameter used to evaluate the quality of HTS assays. Larger the Z' the higher the data quality of the assay for HTS (Z'=1 ideal assay, Z'≥0.5 excellent assay and Z'<0.5 use with caution assay). The maximum signal corresponds to the OD_{600} of *mir1*Δ-pESC control strain and the minimum signal corresponds to the OD_{600} of *mir1*Δ-tau40 strain.

Statistical difference between the growth curves of *mir1*Δ-pESC and *mir*Δ-tau40 with and without DMSO was determined by a two-way ANOVA, followed by Tukey's multiple comparison test, using the GraphPad Prism software. The multiple comparison test compared the OD_{600} average of each strain with every other strain, with and without DMSO, at each time-point.

2.2.6.2. SEAVENTbugs marine prokaryotic collection

The SEAVENTbugs collection is composed of 246 marine prokaryotic strains, property of Faculdade de Ciências da Universidade de Lisboa. These marine bacteria were isolated from 36 samples of water, sediments, small animals, rocks and chimney samples, collected in five MAR sites along the Azores archipelago (Menez Gwen, Lucky Strike, Mount Saldanha, Rainbow and Menez Hom), during the Portuguese research mission SEAHMA-I. Deep-sea sampling was performed using the submersible VICTOR 6000 that, alongside sampling, also recorded the physicochemical parameters of each sampling site. Already on board, samples were processed in sterile environments and put to grow on several sea salts based culture solid and liquid media. The culture conditions applied tried to mimic the original setting of the samples, such as temperature (10-85ºC), metals composition, and presence or absence of oxygen. After the campaign, the firstly isolated microorganisms were sent to TEC LABS – Centro de Inovação for further isolation in the Microbiology and Biotechnology Laboratory. Bacteria isolates were grown in a commercial culturing media (0.5% peptone (w/v), 0.3% meat extract (w/v)) supplemented with 3% sea salts.

A sub-set of this collection, composed of 138 psychrotolerant[5], anaerobic or facultative anaerobic bacteria, was selected for commercial exploitation by a technology transfer agreement with BIOALVO (Martins *et al.*, 2013b). The bacteria selected were adapted to controlled laboratory growth conditions and both aqueous and organic extracts were obtained using standard protocols (Sarker, Latif & Gray, 2006). Regarding aqueous extracts, used in this work, 20 ml of pure water were added to each 3 to 5 g of wet biomass. Cells were then broken using a high pressure homogenizer and the produced aqueous extracts were lyophilized and re-suspended in DMSO at a concentration of 25 mg/ml (Martins *et al.*, 2013b). The natural products (NPs) were distributed in 96-well microplates, sealed and maintained at -80ºC.

[5] Psychrotolerant: an organism that grows best at a low temperature (0-32°C), with optimal growth occurring at 15-20°C.

2.2.6.3. Screening of 138 natural aqueous extracts from the SEAVENTbugs marine prokaryotic collection

The yeast strain *mir1*Δ-tau40 was used as a screening system for the identification of molecules with activity in suppression of tau40 toxicity. The screening was designed to search for natural products (NPs) that restored the growth of *mir1*Δ-tau40 yeast strain closer to the levels of the control strain *mir1*Δ-pESC. The NPs library screened was obtained from a sub-set of the SEAVENTbugs marine bacteria collection, property of the Faculty of Sciences of the University of Lisbon, described in the previous section.

2.2.6.3.1. Primary screening with the platform *mir1*Δ-tau40

The yeast strains *mir1*Δ-tau40 and *mir1*Δ-pESC were pre-inoculated in 5 ml of liquid SC+RAF-Leu media, at 30ºC with 200 rpm agitation. After ON growth, in the day of the screening, cultures were diluted at OD_{600} 0.2 in SC+GAL-Leu media, for induction of protein expression, in a volume sufficient to add 196 µl of culture per well. NPs were added to *mir1*Δ-tau40 to a final concentration of 5 mg/ml (4 µl per well). Controls included *mir1*Δ-tau40 and *mir1*Δ-pESC with DMSO only (21 wells each). Plates were incubated at 30ºC in an Incubator hood TH 30 combined with an orbital shaker (Edmund Bühler GmbH, Tübingen, GE), for approximately 60 h and OD_{600} was monitored with an Infinite M200 microplate reader (Tecan, Männedorf, CH) every 4 h during labour-time. Microplates were maintained in a humidified atmosphere to avoid sample evaporation.

Results obtained were analysed with Microsoft Excel. A data correction was applied to the OD_{600} measured in NP-containing wells to take into account the colour of the NPs. Therefore, the OD_{600} at time-point zero (T0) was subtracted to the OD_{600} measured at the following time-points, for each NP tested. The parameters average (A), standard deviation (SD), maximum value (M) and Z' factor (Equation 2.1) were calculated for the OD_{600} of strains growing without NPs (control strains).

To be considered a hit, a NP had to rescue the growth of *mir1*Δ-tau40 above a certain threshold OD_{600}. This threshold was calculated taking into consideration the parameters above mentioned and the OD_{600} distribution of all samples (i.e. *mir1*Δ-tau40 with NPs), compared with the OD_{600} distribution of controls (*mir1*Δ-tau40 and *mir1*Δ-pESC without NP). This way, the minimal threshold applied was (A+SD) *mir1*Δ-tau40 OD_{600}. To increase the stringency of the assay, the maximal OD_{600} was considered instead of the average: (M+SD) *mir1*Δ-tau40 OD_{600}. Considering the maximal growth of the control strain *mir1*Δ-pESC, the NPs considered hits would have to rescue *mir1*Δ-tau40 growth to OD_{600} values within the signal dynamic range of (M+SD)*mir1*Δ-pESC - (M+SD)*mir1*Δ-tau40.

$$Threshold = (M + SD)mir1\Delta tau40 + \frac{[(M + SD)mir1\Delta pESC - (M + SD)mir1\Delta tau40]}{4}$$

Equation 2.2. Equation used to calculate the minimal threshold (OD_{600}) for determination of NP hits in the drug discovery assay using *mir1*Δ-tau40 yeast strain.

The sample distribution analysis allowed to further increase stringency by removing NPs which rescued *mir1*Δ-tau40 to OD_{600} values falling within the first quarter of this range. So, to be considered a hit, a NP must have rescued OD_{600} to values higher than (M+SD) *mir1*Δ-tau40 plus 25% of the signal dynamic range (M+SD) *mir1Δ*-pESC - (M+SD) *mir1Δ*-tau40 (Equation 2.2).

To identify hits, the threshold was compared with the OD_{600} of *mir1*Δ-tau40 treated with NP at the time-point when the signal dynamic range was larger, with highly significative difference between the growth of *mir1*Δ-tau40 and *mir1*Δ-pESC. The NPs identified as hits were then ranked according with their potency. Hits able to rescue the growth of *mir1*Δ-tau40 to higher OD_{600} values were the most potent hits. A ratio between the threshold OD_{600} and the measured OD_{600} was calculated for each hit, at the defined time-point, as a measure of hit potency. Additionally, the recovery rate of *mir1*Δ-tau40 treated with NP was calculated relative to the control strain for each hit NP. This allowed to rank hits according to their potency: higher percentage of recovery indicate the most potent hits (Equation 2.3):

$$Recovery\ rate = 100 \times \frac{(NP\ OD600 - M\ mir1\Delta tau40\ OD600)}{(M\ mir1\Delta pESC\ OD600 - M\ mir1\Delta tau40\ OD600)}\ (\%)$$

Equation 2.3. Formula to calculate the recovery rate, i.e., the percentage of growth recovery induced by a NP to *mir1*Δ-tau40 yeast strain, relative to the growth of the control strain (*mir1*Δ-pESC).

After hit selection, the primary hit rate was calculated, which corresponds to the ratio of the number of hits identified in the primary screening campaign to the total number of NPs tested, expressed in percentage (Ilouga & Hesterkamp, 2012).

2.2.6.3.2. Dose-response screening: Hit confirmation

The hits identified in the primary screening were confirmed in a dose-response assay, where each NP was tested in four concentrations: 0.125, 0.25, 0.5 and 0.75 mg/ml. The control strain *mir1*Δ-pESC was also used for testing the NPs at the highest concentration (0.75 mg/ml) to identify potential cytotoxic or false positives NPs. Additionally, *mir1*Δ-tau40 and *mir1*Δ-pESC strains were incubated with DMSO, in the corresponding volume of NP at the different concentrations (1, 2, 4, 6 µl). Plates were incubated at 30ºC in an Incubator hood TH 30 combined with an orbital shaker (Edmund Bühler GmbH, Tübingen, GE), for approximately 60 h and OD_{600} was monitored with an Infinite M200 microplate reader (Tecan, Männedorf, CH) every 4 h during labour-time. Microplates were maintained in a humidified atmosphere to avoid sample evaporation.

The results obtained were used to calculate the same parameters as described in section 3.4.2. (average, maximal, standard deviation OD_{600}, threshold and recovery rate), in the time-point where the difference between the OD_{600} of the control strain *mir1*Δ-pESC and *mir1*Δ-tau40 untreated was higher. Data was treated independently for each test concentration.

Hits were ranked according with activity by counting the number of concentrations for which the OD_{600} of *mir1*Δ-tau40 treated was higher than the threshold and by the recovery rate (the highest recovery rate

with the lowest extract concentration identified the most potent hit). The established ranking criteria are depicted in Table 2.3.

Table 2.3. Hit ranking of *mir1*Δ-tau40 drug discovery screening.

Ranking	
4 concentrations	Excellent
3 concentrations	Very good
2 concentrations	Good
1 concentration	Weak

Additionally, the hit confirmation rate and the false-positive rate were also calculated (Ilouga & Hesterkamp, 2012). The former is defined as the ratio between the number of confirmed hits and the total number of hits identified in the primary screening. The false-positive rate corresponds to the ratio of the number of primary hits not confirmed to the total number of NPs that have been tested in the primary screening, expressed in percentage (Ilouga & Hesterkamp, 2012). A final hit rate, correspondent to the ratio between confirmed hits and the total number of NPs tested was calculated as well.

2.2.7. Genetically engineered PiC knockdown (KD) H4 cells

PiC, the mitochondrial phosphate carrier, is encoded by the gene *SLC25A3*, the human homologue of *MIR1*. The next sections describe the protocols performed for knockdown of *SLC25A3* gene and subsequent characterization of resulting phenotype.

2.2.7.1. H4 cells transient transfection

Optimization of H4 cells transient transfection was performed using the plasmid pCDNA3-EGFP (BIOALVO) (Figure 2.3). Prior to the day of transfection, cells were seeded onto tissue culture treated 6-multiwell plates at different densities, depending on the time of transfection incubation (24, 48 and 72 h). Transfection of H4 cells was carried out with 1:2.5, 1:3 and 1:4 ratios (µg DNA:µl FuGENE), using the lipofection reagent FuGENE® HD, following manufacturer instructions. Complexes DNA:FuGENE were prepared in Opti-Mem, incubated for 10 min at room temperature and added to the cells. After 6 h incubation, the culture media was replaced with fresh culture media, and left to incubate at 37ºC for 24, 48 and 72 h. Transfection efficiency was visually evaluated by fluorescence microscopy, using a Zeiss Observer D1 epifluorescent microscope with a Plan-Neofluar 40x/0.6 objective an A-Plan10x Ph 1 objective and a band pass excitation 470 nm filter and emission band pass 525 nm filter.

2.2.7.2. PiC knockdown in H4 cells

Optimization of PiC KD was performed in tissue culture treated 6-multiwell plates. H4 cells were seeded in the day prior to transfection at different cell densities, depending on the time of transfection: 2.25 x 10^5 cells/well for 24 h, 1.6 x 10^5 cells/well for 48 h and 1.1 x 10^5 cells/well for 72 h. Transfection of H4 cells with *SLC25A3* shRNAs and pLKO.1 empty vector (*vide* section 2.2.7.1) was carried out using

FuGENE® HD, at an 1:3 ratio (µg DNA: µl FuGENE). The transfection mixture was incubated in a final volume of 150 µl for 10 min and then added to H4 cells, cultured in a final volume of 2 ml. Cells were incubated at 37ºC, 5% CO_2 and after 6 h of transfection the culture media containing transfection complexes was replaced with fresh media. After incubation for 24 h, 48 h and 72 h, cells were harvested for subsequent analysis.

2.2.8. Characterization of PiC KD H4 cells

2.2.8.1. Cell viability analysis: LDH assay

Cell viability was assessed by measuring the activity of lactate dehydrogenase (LDH) in the culture media by using a colorimetric assay presented by Chan & co-workers, with some modifications (Chan, Moriwaki & De Rosa, 2013). Cells were seeded into 96-well plates (5.6 x 10^3 cells/well) in a final in-well volume of 100 µl. After 72 h of transfection, 50 µl of culture media were collected to a new 96-well plate and stored at -20ºC until processing. Fifty µl of 2x LDH sample buffer (100 mM Tris, 37 mM lactate, 0.45 mM iodonitrotetrazolium chloride [INT], 0.2 mM N-methylphenazonium methyl sulfate [PMS], 0.4 mM β-nicotinamide adenine dinucleotide sodium salt [NAD]; aliquots of 5 ml were kept protected from light, at -20ºC for no longer than 1 month) were added to each well. LDH activity was measured for 30 min by measuring absorbance at 490 nm with background subtraction at 690 nm.

2.2.8.2. Protein expression analysis

2.2.8.2.1. Total cell protein

For normal Western Blotting, H4 cells were seeded in 6-multiwell plates. Cells were washed twice with ice-cold PBS 1x solution. Cells were then harvested directly in RIPA buffer (150 mM NaCl, 50 mM Tris-HCl pH 7.4, 5 mM EGTA, 1% TritonX-100, 0.5 % sodium deoxycholate, 0.1% SDS) supplemented at the time of cell collection with 1 mM DTT, 1x protease inhibitor cocktail, 1x PhosSTOP® phosphatase inhibitor cocktail. The lysates were left on ice for 30 min, vortexed every 10 min, and then centrifuged (14000 rpm for 10 min) to remove cell debris. The supernatants were collected, assayed for protein content using the Bio-Rad reagent, following manufacturer instructions. The protein concentration of a sample was derived by reference to a BSA standard curve. Samples were stored at -20ºC.

2.2.8.2.2. Mitochondrial fraction

For collection of the mitochondrial fraction, H4 cells were cultivated in T75 flasks until 90% confluence. Cells were washed twice with sucrose media (250 mM sucrose, 20 mM HEPES, 10 mM KCl, 1.5 mM $MgCl_2$, 1 mM EGTA and 1 mM EDTA, pH 7.4) and resuspended in ice-cold sucrose buffer supplemented with 1x protease inhibitor cocktail and 1x PhosSTOP® phosphatase inhibitor cocktail. Lysates were homogenized in a potter and centrifuged for 12 min at 2300 rpm, 4ºC, to pellet the nuclei and cell debris. The supernatant was collected and centrifuged for 20 min at 10600 rpm, 4ºC. The resulting pellet,

corresponding to the mitochondrial protein fraction, was resuspended in supplemented sucrose buffer containing protease and phosphatase inhibitors. The cytosolic fraction (supernatant) was discarded. Protein concentration was determined using the Bio-Rad protein assay, following manufacturer instructions. The protein concentration of a sample was derived by reference to a BSA standard curve. Samples were stored at -20ºC.

2.2.8.2.3. Western blotting

Protein samples were denatured with 6x concentrated denaturing buffer (300 mM Tris-HCl pH 6.8, 12% SDS, 30% Glycerol, 0.06% bromophenol blue and 600 mM DTT) at 95ºC for 5 min. Equivalent amounts of protein were separated in a 12% SDS-PAGE gel electrophoresis and electroblotted onto PVDF membranes in 10% CAPS/methanol at 0.75 A (Trans-Blot® Cell, BioRAD, Hercules, CA, USA). Membrane blocking was performed with 5% BSA in TBST1x (Tris-buffered saline supplemented with 1% Tween 20), for 60 min at room temperature. Immunodetection was performed using the following antibodies: total tau (polyclonal rabbit anti-human tau, Dako Agilent Technologies, Glostrup, DK) diluted 1:10000, phospho-tau (monoclonal mouse anti-human AT8-tau, Pierce Biotechnology, Thermo Scientific, Rockford, IL, USA) diluted 1:1000, HSP60 (Chemicon, Merck Millipore, Billerica, MA, USA) diluted 1:1000 and beta-actin (mouse monoclonal beta-actin, Sigma-Aldrich, St. Louis, MO, USA) diluted 1:5000, all in TBST1x containing 1% BSA. Membrane-bound proteins were detected by chemifluorescence using the ECF™ Western Blotting Reagent Pack (GE Healthcare, Little Chalfont, Buckinghamshire, UK). Secondary antibodies conjugated with alkaline phosphatase were used at a dilution of 1:20000 in TBST1x containing 1% BSA. Digital images were detected with the VersaDoc 3000 Imaging System (Bio-Rad, Hercules, CA, USA), using the Quantity One 1-D Analysis Software (Bio-Rad, Hercules, CA, USA).

2.2.8.3. Assessment of mitochondrial function

2.2.8.3.1. Determination of mitochondrial membrane potential (ΔΨm) and intracellular Ca^{2+} (Ca^{2+}i) in cell population

The mitochondrial membrane potential (ΔΨm) is one of the two components of the proton circuit that occurs across the inner mitochondrial membrane, being the second component the pH gradient (ΔpH). The proton circuit is central for mitochondrial bioenergetics (Brand & Nicholls, 2011). ΔΨm is the difference in electrical potential between the intermembrane space and the mitochondrial matrix and is indicative of mitochondrial function. ΔΨm was determined using the cell-permeant, cationic, red-orange fluorescent probe Tetramethylrhodamine methyl ester perchlorate ($TMRM^+$). This probe is a positively charged molecule that accumulates predominantly in polarized mitochondria in inverse proportion to ΔΨm (Brand & Nicholls, 2011). When evaluating changes in ΔΨm in quench mode, healthier cells, with more polarized mitochondria, will accumulate more cationic dye, whereas depolarized mitochondria accumulate less dye. When inhibitors of different components of the ETC are added to cells, causing mitochondrial depolarization, the dye is released from the mitochondria and the fluorescence level

measured is proportional to the amount of dye accumulated and therefore indicative of mitochondria polarization state.

Intracellular Ca^{2+} was measured using the Fura-2 acetoxy-methyl-ester (Fura-2AM) fluorescent probe. Once inside the cells, the probe Fura-2AM acetoxymethyl groups are removed by cytosolic esterases, originating Fura-2, a pentacarboxylate calcium indicator. Measurement of Ca^{2+}-induced fluorescence at both 340 nm (free calcium) and 380 nm (complexed calcium) allows to determine the intracellular calcium levels based on 340/380 ratios.

Mitochondrial function was modulated using known inhibitors of specific components of the ETC. Oligomycin inhibits ATP synthesis by blocking ATP synthase (or complex V) (Brand & Nicholls, 2011). FCCP is an uncoupling agent because it disrupts ATP synthesis by transporting hydrogen ions (Brand & Nicholls, 2011). When used together, these reagents conduce to maximal mitochondrial membrane depolarization. The Ca^{2+} present within the mitochondria is then released to the cytosol where it is free to bind to Fura-2, changing the fluorescence level.

H4 cells were cultured in 96-multiwell plates at a density proportional to the optimized for 6-multiwell plates for 72 h incubation post-transfection. Then, cells were washed twice in acclimatized (37ºC) sodium and incubated at 37ºC, 5% CO_2 for 1 h with 300 nM $TMRM^+$ (quench mode) and 5 µM Fura-2 acetoxy-methyl-ester (Fura-2AM) solution, prepared in sodium media. After incubation, cells were washed with acclimatized sodium media (140 mM NaCl, 5 mM KCl, 1 mM $CaCl_2$, 1 mM $MgCl_2$, 10 mM Glucose, 10 mM Hepes, pH 7.4/NaOH) and 100 µl of 300 nM TMRM solution were added to each well, to prevent probe release by the mitochondria. Bottom-read fluorescence levels of TMRM were measured at λ_{EXC} 540/ λ_{EM} 590 (cut-off at 570 nm) whilst Fura-2 fluorescence was monitored at λ_{EXC} 340 and λ_{EXC} 380 with fixed λ_{EM} 510 (no cut-off), using a Gemini EM Microplate reader (Molecular Devices, Sunnyvale, CA, USA). Basal fluorescence levels were measured every 15 sec for 3 min. Oligomycin (2.5 µg/ml) and p-trifluoromethoxy carbonyl cyanide phenyl hydrazone (FCCP) (2.5 µM), were then added to cells and the resulting fluorescence monitored every 15 sec for 3 min. Working solution of this reagent was prepared in sodium media containing 10% DMSO, so that the final concentration of DMSO in each well was 0.5%. Cells were also challenged with 2 µM ionomycin, a Ca^{2+} ionophore, which increases its cellular levels, thereby serving as an internal control.

For $\Delta\Psi m$, results were expressed as the difference between $TMRM^+$ fluorescence at the basal level and the maximal fluorescence obtained after addition of oligomycin/FCCP. For $Ca^{2+}i$ levels, the ratio 340 nm/380 nm was calculated and, as before, the difference between the fluorescence at the basal level and after addition of oligomycin/FCCP was calculated.

2.2.8.3.2. Measurement of O_2 consumption and mitochondrial bioenergetics using the Seahorse XF24-extracellular flux analyser

Bioenergetic function of PiC KD H4 cells vs. controls (untransfected and transfected with empty pLKO.1 vector) was monitored using the XF24 Cell Mito Stress Test Kit and the XF24 Extracellular Flux Analyser (Seahorse Bioscience, North Billerica, MA, USA). H4 cells were seeded onto Seahorse Bioscience XF24

cell culture plates to a density proportional to the optimized in 6-multiwell plates, in 250 µl of culture media, and allowed to adhere and grow for 24 h in a 37ºC humidified incubator with 5% CO_2. The cells were then transfected with PiC shRNA 2 and empty pLKO.1, as previously described (section 2.2.7.2). Seventy-two h post-transfection, 1 ml of XF Calibrant Solution was dispensed into each well of the sensor hydration microplate and the sensor cartridge placed onto the microplate. The plate was incubated ON with immersed sensors in a non-CO_2 incubator at 37°C. 50 ml of XF assay media were supplemented with 4500 mg/l glucose, 4 mM glutamine, 1 mM pyruvate and 1.5 g/l sodium bicarbonate, the pH adjusted to 7.4 with 0.1 N NaOH and filter sterilized. The culture media was discarded by gentle aspiration and each well was washed with 0.5 ml of XF assay media before incubation in a non-CO_2 incubator at 37 °C for 1 h, with 450 µl of XF assay media. The final concentrations of the respiration modulators added into injection ports A, B or C were 1 µM oligomycin (injection 1), 2 µM FCCP (injection 2), 0.5 µM rotenone and 0.5 µM antimycin (injection 3). Data were normalized to total protein content per well to control for variation in cell number (Hill *et al.*, 2012). On completion of the XF assay, cells were lysed with 20 µl of RIPA buffer and protein concentration determined using the Bio-Rad protein assay. The oxygen consumption rate (OCR) data were expressed as pmol/min/µg protein.

The mitochondrial function of PiC KD cells was compared with untransfected cells and cells transfected with empty pLKO.1 vector (EV cells). The bioenergetic profile of each sample was obtained by sequentially adding modulators of respiration that target different components of the ETC (Brand & Nicholls, 2011; SeaHorseBioscience, 2015). Figure 2.7 presents a typical bioenergetic profile.

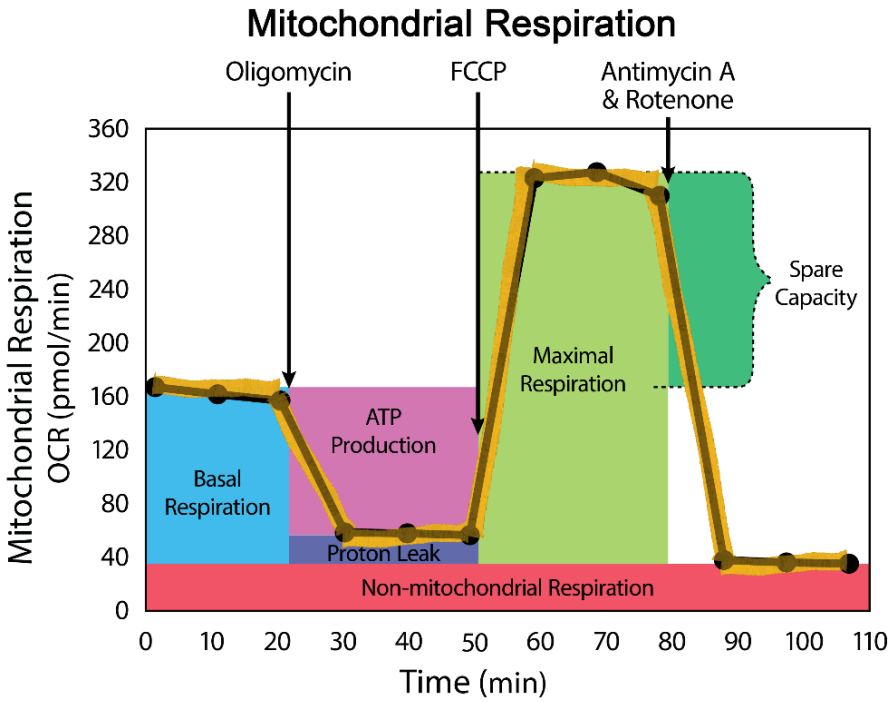

Figure 2.7. Representative OCR profile obtained with the XF Cell Mito Stress test.
Sequential injections of inhibitors of different components of the electron transport chain (ETC) allow to measure basal respiration, ATP production, proton leak, maximal respiration, spare respiratory capacity and non-mitochondrial respiration (SeaHorseBioscience, 2015).

Oligomycin was the first modulator to be injected, an inhibitor of ATP synthase, causing a decrease in OCR that correlates with the mitochondrial respiration associated with cellular ATP production. The second injection used FCCP, which interferes with the proton gradient, thereby disrupting the mitochondrial membrane potential. Consequently, electron flow through the ETC is uninhibited and oxygen is maximally consumed leading to an increase in the OCR. A combination of rotenone which inhibits complex I, and antimycin A, inhibitor of complex III, completely shuts down mitochondrial respiration, enabling the calculation of non-mitochondrial respiration, used to baseline the components of mitochondrial respiration (Brand & Nicholls, 2011; Hill *et al.*, 2012; SeaHorseBioscience, 2015).

From the bioenergetic profile, six parameters of mitochondrial function were calculated: basal OCR, ATP-linked OCR, proton leak OCR, maximal OCR, spare capacity and non-mitochondrial OCR. The equations used to calculate these parameters are shown in Table 2.4. These parameters were then used to derive the percentage of coupling efficiency i.e., the proportion of the O_2 consumed to drive ATP synthesis compared with that driving proton leak.

Table 2.4. Mitochondrial function parameters measured by the XF24 Extracellular Flux Analyser.

Parameter	Rate measurement equation
Non-mitochondrial OCR	$miminum\ OCR\ after\ rotenone/antimycinA$
Basal OCR	$(last\ OCR\ before\ oligomycin) - (non\ mitochondrial\ respiration\ rate)$
Maximal OCR	$(Max\ OCR\ after\ FCCP) - (non\ mitochondrial\ respiration)$
Proton (H^+) Leak OCR	$(Min\ OCR\ after\ oligomycin) - (non\ mitochondrial\ respiration)$
ATP-linked OCR	$(last\ OCR\ before\ oligomycin) - (Min\ OCR\ after\ oligomycin)$
Spare respiratory capacity	$Max\ respiration - Basal\ respiration$
Coupling Efficiency (%)	$\frac{ATP\ production}{Basal\ respiration} \times 100$

2.2.8.3.3. Statistical analysis

Data were expressed as the mean ± SEM of the number of experiments indicated in the figure legends. Comparisons between samples were performed by one-way analysis of variance (one-way ANOVA) followed by Tuckey's post-hoc test. $P<0.05$ was considered significant. Data were analysed using GraphPad Prism v6.0 software (GraphPad Software, San Diego, CA, USA).

Chapter 3.

A yeast model for studying tau and beta-amyloid interaction[6]

[6] Work submitted to *Yeast*.

3.1. Summary

Beta-amyloid (Aβ) and tau deposits are hallmarks of Alzheimer's disease (AD). Increasing evidences suggest a direct link between tau and intraneuronal Aβ in causing cytotoxicity in AD through mechanisms not fully understood. This study aimed to develop yeast-based models of $A\beta_{1-42}$ and tau40 co-expression to analyse the interaction of these proteins and resulting toxicity. Integrative and episomal yeast strains expressing native and fluorescent versions of $A\beta_{1-42}$ and tau40 were developed and characterized in terms of growth, protein expression, tau phosphorylation, presence of protein inclusions and sub-cellular localization. Reduced yeast growth was found following co-expression of $A\beta_{1-42}$ and tau40, an effect mediated by $A\beta_{1-42}$. Expression of $A\beta_{1-42}$ in the yeast cytoplasm formed amorphous structures. Cells containing protein inclusions were more frequent in yeast co-expressing tau40 and $A\beta_{1-42}$-mCh, and observation of tau40-eGFP localization demonstrated co-localization with $A\beta_{1-42}$-mCh, suggesting a direct interaction. Tau40 was phosphorylated at pathological epitopes (Ser396/404) by Rim11, the yeast GSK-3β orthologue. Tau40 phosphorylation levels increased when $A\beta_{1-42}$-mCh was co-expressed. The recapitulation of essential pathological features of $A\beta_{1-42}$ and tau pathologies renders this model a useful test tube to understand $A\beta_{1-42}$ and tau40 interaction and, potentially, a useful tool for drug discovery and development in AD.

Keywords: *S. cerevisiae*, cytotoxicity, tau, beta-amyloid, GSK-3β, yeast, Alzheimer disease

3.2. Introduction

Alzheimer's disease (AD) is the most prevalent age-related neurodegenerative disorder with 35.6 million cases reported worldwide in 2009, a number estimated to double every 20 years (Prince & Jackson, 2009). Clinically, AD is characterized by progressive memory loss and cognitive decline due to synapse loss and selective neuronal cell death (Weintraub *et al.*, 2012). Histopathologically, the disease is characterized by intracellular neurofibrillary tangles (NFTs) composed of hyperphosphorylated tau and extracellular accumulation of beta-amyloid peptide (Aβ) forming the senile plaques. This peptide also accumulates intraneuronally in smaller order oligomers (LaFerla *et al.*, 2007). Both proteins have been extensively studied with regard to their separate mechanisms of toxicity, but increasing evidences suggest a direct link between tau and Aβ, particularly the intraneuronal form, in causing cytotoxicity in AD (Ittner & Gotz, 2011).

Considerable controversy regarding the mechanism of interaction between tau and Aβ still exists. According with the modified amyloid cascade hypothesis, the accumulation of intraneuronal Aβ is the driver for AD pathology (Wirths et al., 2004, Ittner & Gotz, 2011). Three possible modes of interaction have been proposed, the first indicating Aβ as the trigger of tau pathology, leading to its hyperphosphorylation, mislocalization and aggregation, probably via activation of tau kinases such as GSK-3β and CDK5 (Terwel et al., 2008, Iijima et al., 2010, Sofola et al., 2010, Hurtado et al., 2012). Other hypothesis places tau simply as a mediator of Aβ toxicity (Ittner & Gotz, 2011), a hypothesis that has been challenged by the fact that tau-/- neurons are protected from Aβ toxicity and reduction of tau levels also prevents Aβ-induced pathology (Rapoport et al., 2002, Roberson et al., 2007, Ittner et al., 2010, Vossel et al., 2010). Other studies suggest that both proteins have synergistic toxic effects, particularly at mitochondria (Rhein et al., 2009, Eckert et al., 2014). According with the tau hypothesis, this protein is suggested to have a more central role in the disease, particularly in the dendritic compartment, since postsynaptic Aβ toxicity is tau-dependent (Ittner & Gotz, 2011, Shipton et al., 2011). Finally, alternative studies point to a dual pathway hypothesis, where Aβ and tau are linked by separate mechanisms of toxicity driven by a common upstream factor, which seems particularly relevant in late-onset AD (Small & Duff, 2008). Taking this into account, modulating the interaction between Aβ and tau could be a valuable therapeutic strategy for this devastating disease (Shipton et al., 2011). The elucidation of the mechanism of interaction between these proteins is thus relevant for the development of a possible therapy.

Yeast is a validated organism model for the study of neurodegenerative disorders (Miller-Fleming *et al.*, 2008; Summers & Cyr, 2011) with wide application in the field of drug discovery (Barberis *et al.*, 2005; Outeiro & Giorgini, 2006) and in functional genomic and proteomic studies (Suter *et al.*, 2006; Treusch *et al.*, 2011). In fact, the separate mechanisms of toxicity of Aβ and tau have already been explored in yeast (Bharadwaj *et al.*, 2010). Expression of wild-type or mutated tau is non-toxic for yeast growth, but yeast recapitulates several features of pathological tau, such as tau phosphorylation in disease-related epitopes and accumulation in insoluble aggregates (Ciaccioli *et al.*, 2013; De Vos *et al.*, 2011; Vandebroek *et al.*, 2006; Vandebroek *et al.*, 2005b). Also, several models of Aβ expression have been developed in yeast. Most of them use $A\beta_{1-42}$ peptide, which is more prone to aggregate. This peptide

accumulates in punctate structures in the cytoplasm, resulting in minor toxicity for yeast growth (Bagriantsev & Liebman, 2006; Caine *et al.*, 2007; Morell *et al.*, 2011). In the secretory pathway several features of Aβ pathology are replicated with visible toxicity to yeast growth (D'Angelo *et al.*, 2013; Treusch *et al.*, 2011).

This study aimed at designing a yeast-based model of $A\beta_{1-42}$ and tau co-expression to evaluate the mechanism of toxicity of both AD hallmark proteins in a simple, yet biologically relevant organism model, since major biological pathways known to be involved in neurodegeneration are conserved from yeast to humans (Tenreiro & Outeiro, 2010). Such a model would be useful not only as a disease model to study the mechanism of action of drug candidates in development but also as a drug discovery platform for the identification of modulatory compounds of $A\beta_{1-42}$ and tau interaction. Likewise, it could be used as a platform to identify genes able to modulate $A\beta_{1-42}$ and tau interaction, and thus define relevant new targets for the development of therapeutic strategies for AD and related disorders.

Accordingly, we developed four different yeast models of co-expression of native and fluorescent versions of $A\beta_{1-42}$ peptide and wild-type longest tau isoform (tau40), resorting to integrative and episomal expression plasmids. The resulting phenotype was evaluated in terms of growth in solid selective media and protein expression. Sub-cellular localization of $A\beta_{1-42}$ and tau40 fluorescent proteins, presence of $A\beta_{1-42}$ cytoplasmic inclusions and tau phosphorylation levels were also evaluated. The yeast episomal model of $A\beta_{1-42}$ C-terminal fusion to mCherry and untagged tau40 co-expression shows co-localization between these proteins and the recapitulation of important features of their pathology. The results obtained here suggest that yeast is a relevant model to study tau and beta-amyloid interaction and that further proof-of-concept studies should be conducted in order to establish such model as a useful tool for drug discovery and development in AD, while contributing to better understand the mechanisms of toxicity of AD hallmark proteins.

3.3. Results

3.3.1. Yeast strains produced in this study

Table 3.1 summarizes the yeast strains produced in this study, as described in Chapter II, sections 2.2.3.1 (episomal strains, in yeast BY4741 background) and 2.2.3.2 (integrative strains, in yeast W303-1A background).

Table 3.1. Episomal and integrative yeast strains engineered for the model of Aβ_{1-42} and tau40 co-expression.

Expression	Episomal		Integrative
Background yeast	BY4741 WT	BY4741 *rim11*Δ	W303-1A
Plasmid	Empty vector (EV) *GAL1*-mCherry (mCh) *GAL1*-Aβ_{1-42} *GAL1*-Aβ_{1-42}-mCh *GAL10*-tau40 *GAL1*-mCh *GAL10*-tau40 *GAL1*-Aβ_{1-42}-mCh *GAL10*-tau40 *GAL10*-eGFP *GAL10*-tau40-eGFP *GAL1*-mCh *GAL10*-eGFP *GAL1*-Aβ_{1-42}-mCh *GAL10*-tau40-eGFP	Empty vector (EV) *GAL1*-mCherry (mCh) *GAL1*-Aβ_{1-42}-mCh *GAL10*-tau40 *GAL1*-mCh *GAL10*-tau40 *GAL1*-Aβ_{1-42}-mCh *GAL10*-tau40	Empty vector (EV) *GAL1*-mCherry (mCh) *GAL1*-Aβ_{1-42}-mCh *GAL1*-tau40 (G. Ciaccioli) *GAL1*-mCh *GAL1*-tau40 *GAL1*-Aβ_{1-42}-mCh *GAL1*-tau40

3.3.2. Single copy beta-amyloid and tau40 integrated into W303-1A genome did not cause toxicity to yeast growth

The expression of Aβ_{1-42} and tau40 in yeast was directed towards the cytoplasm, since tau is mainly a cytosolic protein and intraneuronal Aβ_{1-42} can also be found in the neuron cytoplasm, mainly through internalization by endocytosis, although in lower amounts than in the secretory pathway (Wirths, Multhaup & Bayer, 2004). Aβ_{1-42} c-terminal fusion to mCherry (mCh) was used as the untagged peptide was not detected in yeast protein extracts (Figure 3.1.A) and exerted no effect on yeast growth in glucose or galactose media (Figure 3.1.B), as previously reported by others (Caine *et al.*, 2007).

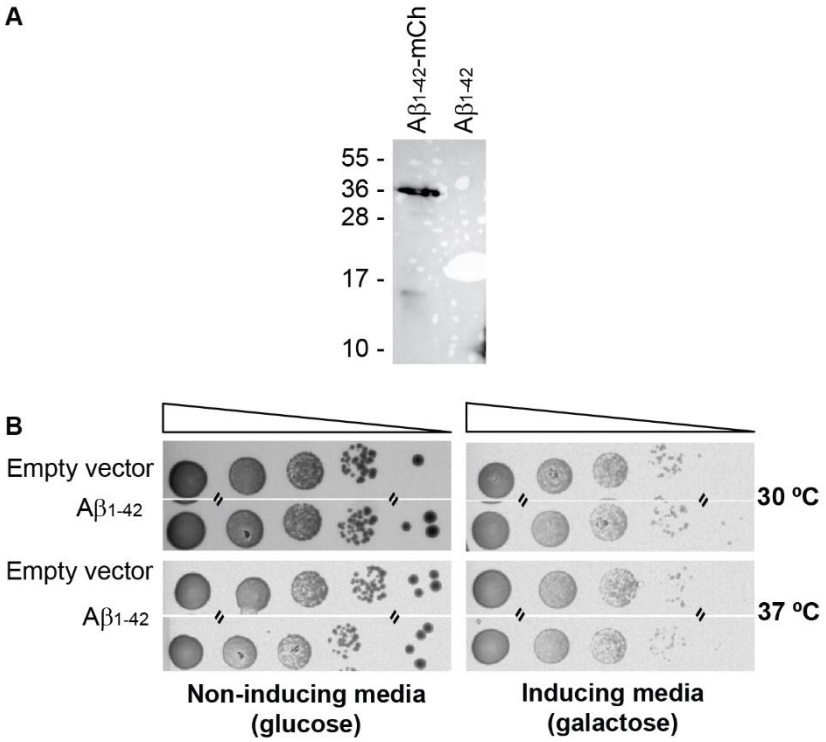

Figure 3.1 Expression of untagged Aβ$_{1-42}$ in the cytoplasm of *S. cerevisiae* BY4741.
(A) Immunoblot analysis using anti-Aβ Antibody, clone W0-2, did not detect untagged Aβ$_{1-42}$. **(B)** Dot spot assays in solid media did not detect differences between the growth of yeast expressing Aβ$_{1-42}$, under the control of the *GAL1* promoter, and yeast carrying the empty high copy expression plasmid (Empty vector). Equal amounts of cells collected in mid-exponential phase (OD_{600} 0.8 – 1.2) were 10-fold serially diluted and spotted on SC+GLU-Leu (non-inducing media) or SC+GAL-Leu (inducing media) and incubated at 30 and 37ºC degrees for 3 days.

We first explored the effects of Aβ$_{1-42}$-mCh and tau40 when integrated into the yeast genome, using the *S. cerevisiae* strain W303-1A. One copy of mCh and Aβ$_{1-42}$-mCh were integrated into the uracil locus of a yeast strain already containing one copy of tau40 integrated in the leucine locus (kind gift by G. Ciaccioli, BIOALVO, (Ciaccioli *et al.*, 2013)) and in wild-type yeast. The expression of both transgenes was controlled by *GAL1* promoter and therefore induced by the addition of galactose to the culture media. After proper confirmation of mCh and Aβ$_{1-42}$-mCh integration into the yeast genome by PCR, the resulting strains were evaluated in terms of protein expression (37ºC) and cell growth at 30ºC and 37ºC. Analysis of yeast growth at 37ºC allowed to evaluate the toxicity of the heterologous proteins in a sub-optimal context for yeast, where several key cellular processes are affected, including altered expression and/or activity of proteins involved in protein quality control and unfolded protein response, such as chaperones and heat shock proteins (Verghese *et al.*, 2012).

Western blot analysis of yeast total extracts prepared in denaturing conditions showed that Aβ$_{1-42}$-mCh migrates as a single band of around 35 kDa and tau40 migrates as a double band between 50-70 kDa, at 37ºC (Figure 3.2.A). The higher molecular weight band of tau40 corresponds to phosphorylated tau (p-tau), as previously designated in (Vandebroek *et al.*, 2005b). Dot spot assays (Figure 3.2.B) show equal growth of strains expressing Aβ$_{1-42}$-mCh and tau40, alone or in combination, when compared with W303-1A transformed with just empty vector, after 3 days incubation at 30 and 37ºC. This indicates that the expression of Aβ$_{1-42}$-mCh and tau40 transgenes, present in a single copy in the yeast genome, does not cause toxicity to W303-1A yeast growth.

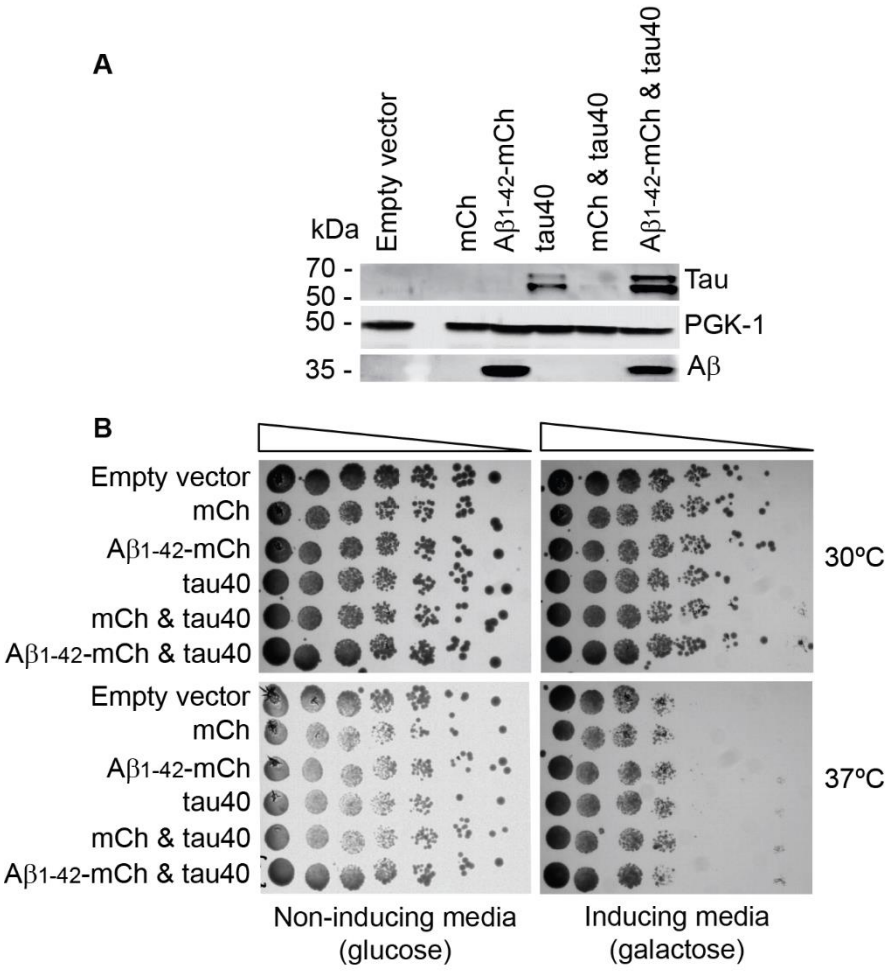

Figure 3.2. Integrative model of co-expression of Aβ$_{1-42}$-mCh and tau40 in the cytoplasm of *S. cerevisiae* W303-1A.
(A) Immunoblot analysis detected Aβ$_{1-42}$-mCh as a 35 kDa band and tau40 as a double band between 50 and 70 kDa, at 37ºC. **(B)** Expression of one integrated copy of tau40 and Aβ$_{1-42}$-mCh is not toxic to yeast at 30 ºC and 37ºC. Equal amounts of strains carrying the plasmids were collected in mid-exponential phase (OD_{600} 0.8 – 1.2), 5-fold serially diluted and spotted on SC+GLU-Leu-Ura (non-inducing media) or SC+GAL-Leu-Ura media (inducing media) and incubated at 30 and 37ºC for 3 days. Results are representative of at least 3 independent experiments.

3.3.3. Beta-amyloid mCherry fusion protein was toxic to yeast growth at 37ºC

Other studies modelling Aβ$_{1-42}$ toxicity in yeast secretory pathway indicated that its toxicity to yeast growth was dependent on protein concentration (Treusch *et al.*, 2011). Therefore, we explored the effects of the co-expression of Aβ$_{1-42}$ and tau40 in yeast by increasing the protein levels using the high-copy number (2µ) yeast episomal expression plasmid pESC-LEU. This vector contains *GAL1*/*GAL10* divergent promoters allowing co-expression of two transgenes in the same number of copies in the same host cell. This plasmid was used in the attempt to obtain similar transgene protein levels. The wild-type yeast strain BY4741 was transformed with constructs for Aβ$_{1-42}$-mCh expression alone or in combination with tau40. Constructs for expression of mCh expression, alone or in combination with tau40, were also included in the experiments to rule out any interference of the fluorescent protein. Protein expression and yeast growth were evaluated at 30ºC and 37ºC.

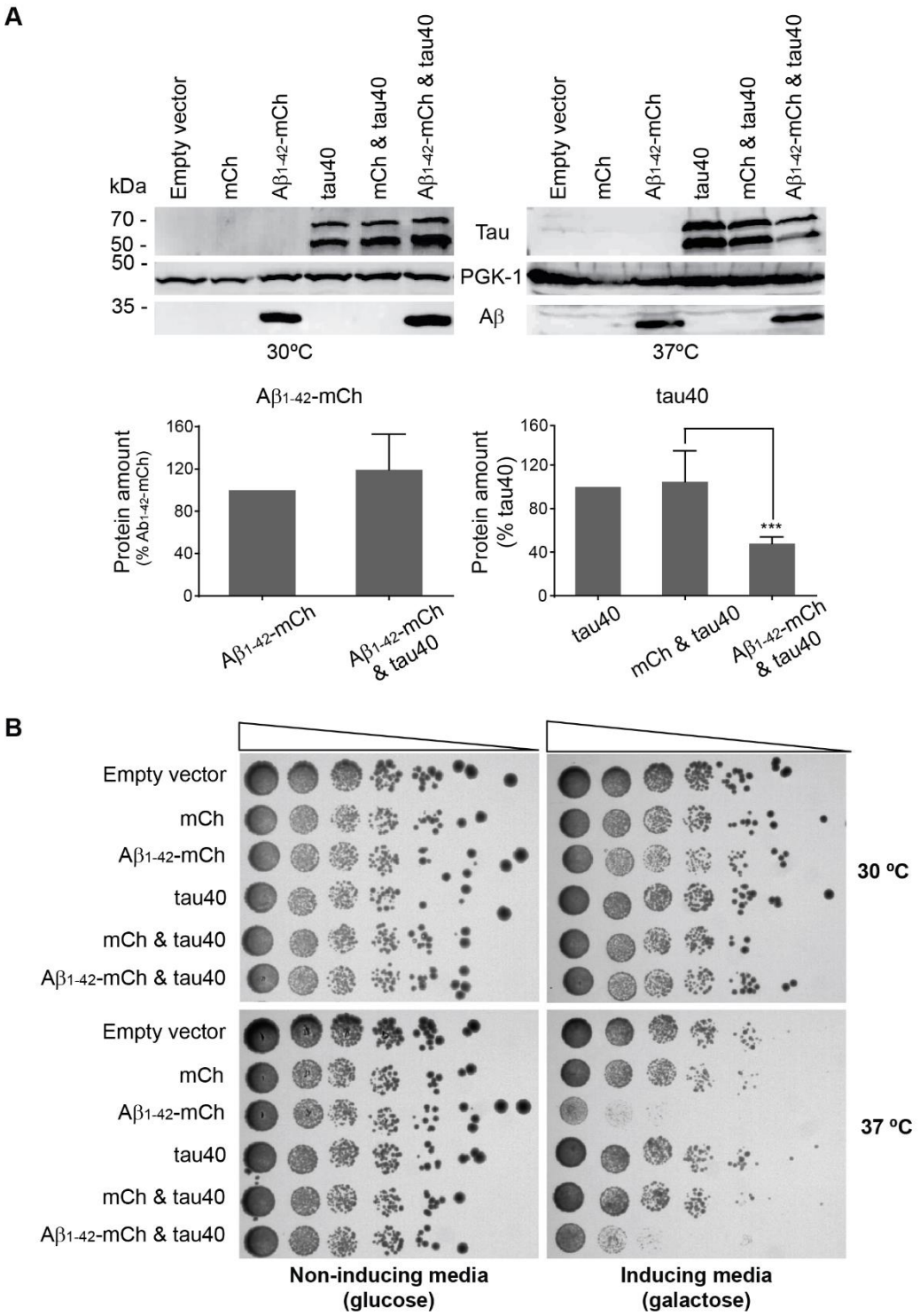

Figure 3.3. Episomal model of co-expression of Aβ$_{1-42}$-mCh and tau40 in the cytoplasm of *S. cerevisiae* BY4741.

(A) Immunoblot analysis detected Aβ$_{1-42}$-mCh at similar levels when expressed alone or in combination with tau40, at 30ºC and 37ºC whereas tau40 levels were found to decrease when co-expressed with Aβ$_{1-42}$-mCh (p= 0.0001), but not with mCh. Results represent mean values of 3 independent experiments, first normalized to the loading control PGK-1 and then to control of Aβ$_{1-42}$-mCh or tau40 expressed alone. Error bars represent standard deviations. **(B)** Aβ$_{1-42}$-mCh is toxic to yeast at 37ºC whereas tau40 is not. Toxicity to yeast upon co-expression of both proteins is driven by Aβ$_{1-42}$-mCh. Expression of mCh and Aβ$_{1-42}$-mCh was driven by *GAL1* promoter whereas tau40 expression was driven by *GAL10* promoter. Equal amounts of strains carrying the plasmids were collected in mid-exponential phase (OD_{600} 0.8 – 1.2), 5-fold serially diluted and spotted on SC+GLU-Leu (non-inducing media) or SC+GAL-Leu (inducing media) and incubated at 30 and 37ºC for 5 days. Results are representative of at least 3 independent experiments.

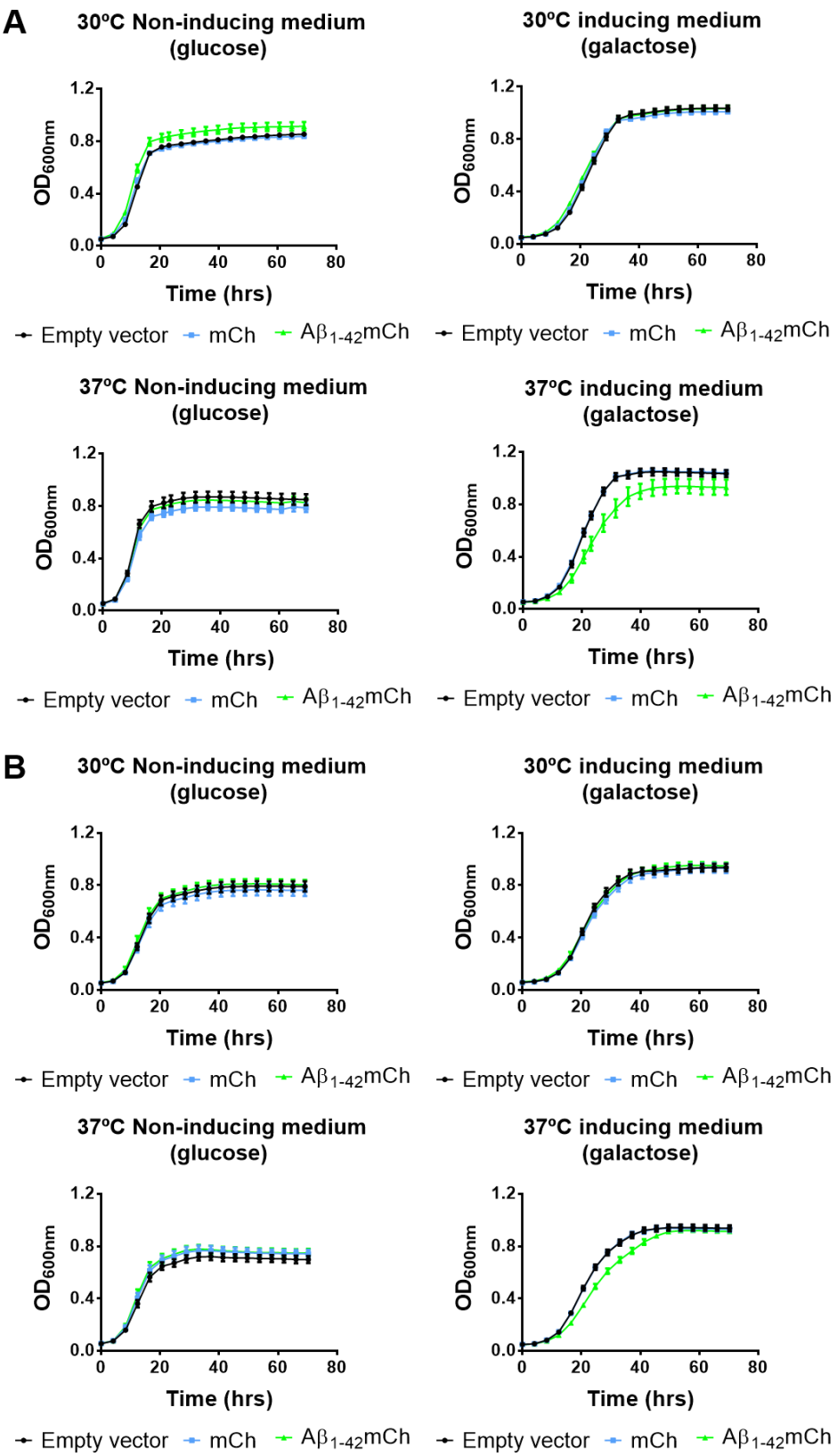

Figure 3.4. Overexpression of Aβ$_{1-42}$-mCh in *S. cerevisiae* (BY4741) induces growth delay at 37ºC
(A) in yeast freshly transformed and **(B)** reactivated from glycerol stocks when compared to yeast expressing just the fluorescent protein (mCh) or transformed with the empty vector (vector pESC-Leu). Expression of mCh and Aβ$_{1-42}$-mCh was driven by *GAL1* promoter. Stationary phase yeast incubated ON in SC+RAF media were re-inoculated at a starting OD_{600} of 0.1, in SC+GLU-Leu (non-inducing media) or SC+GAL-Leu (inducing media). Yeast growth was automatically monitored every 4 h.

Western blot analysis showed that $A\beta_{1-42}$-mCh migrated as a single band of around 35 kDa and tau40 migrated as a double band between 50-70 kDa (Figure 3.3.A). Quantification of protein levels, normalized to the loading control PGK-1, resulted in equal levels of $A\beta_{1-42}$-mCh when expressed alone or in combination with tau40 at 37ºC (Figure 3.3.A). However, tau40 protein levels decreased significantly when co-expressed with $A\beta_{1-42}$-mCh ($p= 0.014$), but not with mCh ($p= 0.918$).

Dot spot assays in selective solid media were performed to examine the effect of $A\beta_{1-42}$-mCh and tau40 co-expression in wild-type yeast BY4741 (Figure 3.3.B). $A\beta_{1-42}$-mCh was found to induce a growth delay when compared to the control strain mCh, at 37ºC, during 5 days incubation. Induction of tau40 expression did not cause any effect on yeast growth, when compared to the control strain empty vector. Moreover, co-expression of both proteins maintained the same levels of growth as observed following expression of $A\beta_{1-42}$-mCh alone. The innocuous effect of mCh in this model was reinforced by the results of the control strains expressing mCh alone or in combination with tau40, which did not present decreased growth, when compared to the empty vector strain. Taken together, these data strongly suggest that the cytotoxic effect observed upon co-expression of $A\beta_{1-42}$-mCh and tau40 is mediated by $A\beta_{1-42}$-mCh. Nevertheless, the reduction of tau40 expression levels in the presence of $A\beta_{1-42}$-mCh may hinder the observation of a synergistic toxic effect in yeast growth.

Pilot tests were also performed to evaluate $A\beta_{1-42}$-mCh toxicity to yeast growth in liquid selective media. These tests intended to determine if the yeast strain expressing $A\beta_{1-42}$-mCh had the potential of being a drug discovery platform for identification of Aβ toxicity modulators. The growth of the strain was evaluated with cells freshly transformed and with cells reactivated from glycerol stocks (Figure 3.4). $A\beta_{1-42}$-mCh is toxic to yeast growth at 37ºC, when compared with yeast expressing mCh alone or transformed with empty vector, confirming the results obtained in solid media. However, this difference is reduced when the strain is tested after cryopreservation.

3.3.4. Yeast presenting protein cytoplasmic inclusions were more abundant when co-expressing beta-amyloid and tau40 and tau40 co-localized with beta-amyloid inclusions

It has been previously demonstrated that fluorescent versions of $A\beta_{1-42}$ accumulate in small inclusions in yeast (Bagriantsev & Liebman, 2006; Caine *et al.*, 2007; Morell *et al.*, 2011). Also, although tau40 has been extensively studied in yeast, so far, only one study reports its subcellular localization in this model organism (Timmers *et al.*, 2002). Therefore, a C-terminal eGFP fluorescent version of tau40 was engineered, cloned into pESC-LEU under the control of *GAL10* promoter, and transformed in BY4741. After inducing protein expression in galactose containing SC media, cells were observed by laser confocal microscopy (Figure 3.5).

$A\beta_{1-42}$-mCh was found in the yeast cytoplasm, excluding the vacuole and in certain cells to accumulate in amorphous inclusions, whereas mCh alone was found distributed in the cytoplasm, also excluding

the vacuole. The fluorescent protein tau40-eGFP was found distributed in the yeast cytoplasm, excluding the vacuole, similarly to eGFP alone. No evidences of visible aggregates were found.

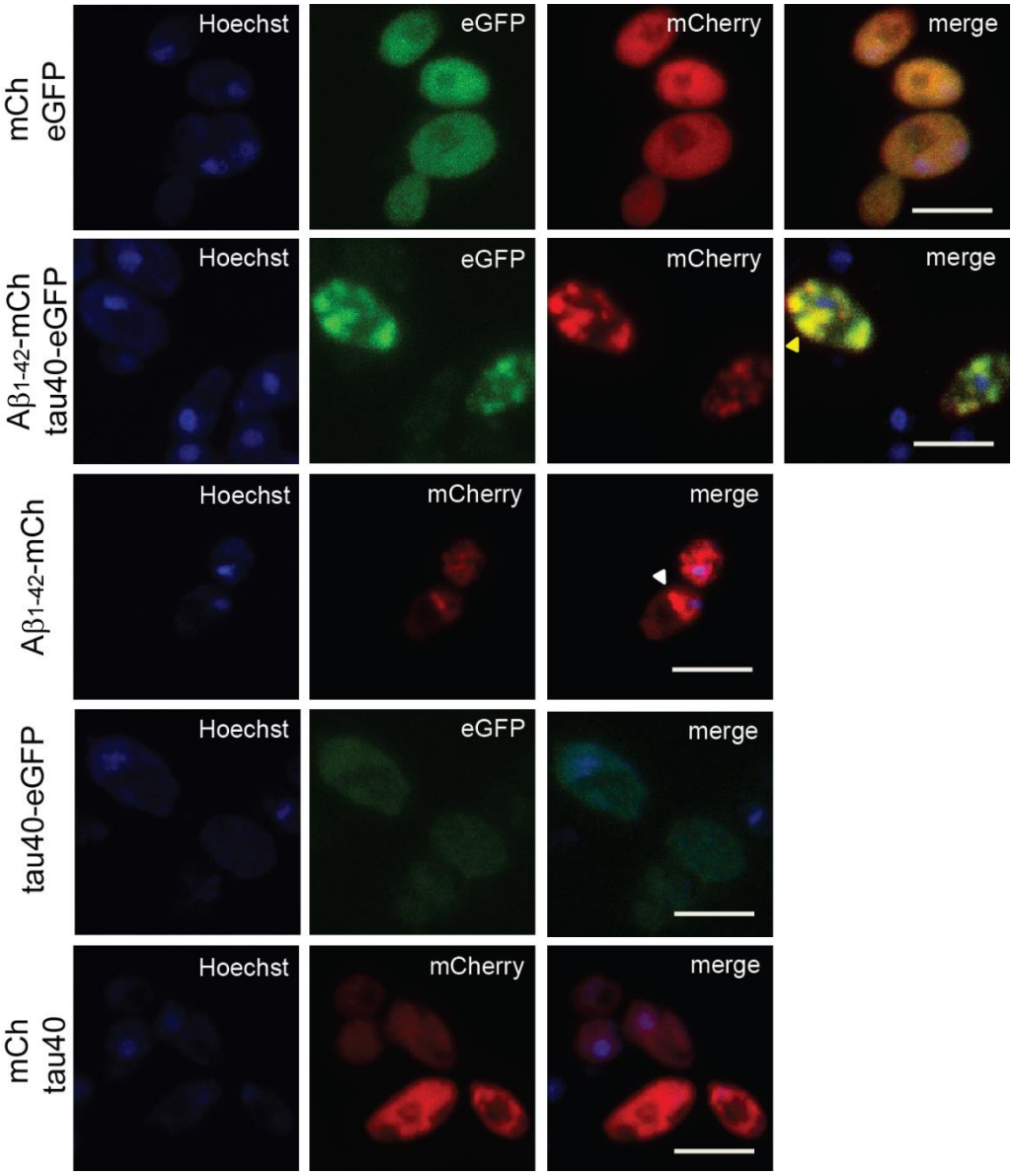

Figure 3.5. Expression of Aβ$_{1-42}$-mCh and tau40 fluorescent proteins in the cytoplasm of *S. cerevisiae* BY4741.
The fluorescent proteins mCh and eGFP distribute uniformly in the yeast cytoplasm as the proteins Aβ$_{1-42}$-mCh and tau40eGFP. Aβ$_{1-42}$-mCh accumulates in amorphous inclusions in some yeast cells and tau40 -eGFP co-localizes with such inclusions in the yeast strain expressing both proteins. When expressed alone, tau40-eGFP does not form visible aggregates. Protein expression was induced at 37ºC for 24h. Equal amounts of yeast carrying the plasmids were collected and fixed with formaldehyde and stained with Hoechst 33342. Microscopic observation was performed using a laser scanning confocal microscope Zeiss LSM 710. Bar dimension: 5 µm. Images shown are composites of maximum intensity of Z-stack images.

Interestingly, in the yeast strain co-expressing Aβ$_{1-42}$-mCh and tau40-eGFP, tau40-eGFP was found to co-localize with Aβ$_{1-42}$-mCh inclusions. Since no aggregation was observed in the controls expressing tau40-eGFP alone, mCh together with eGFP and mCh together with untagged tau, these results suggest that Aβ$_{1-42}$-mCh is sequestering tau40-eGFP and promoting its aggregation. The eGFP fluorescent signal in yeast expressing tau40-eGFP was low and not all yeast cells expressed tau40-eGFP at the

same intensity. Therefore, the number of cells presenting $A\beta_{1-42}$-mCh inclusions was determined in the yeast strains expressing $A\beta_{1-42}$-mCh alone or in combination with untagged tau40 and in control strains expressing mCh alone or in combination with untagged tau40 (Figure 3.6.A).

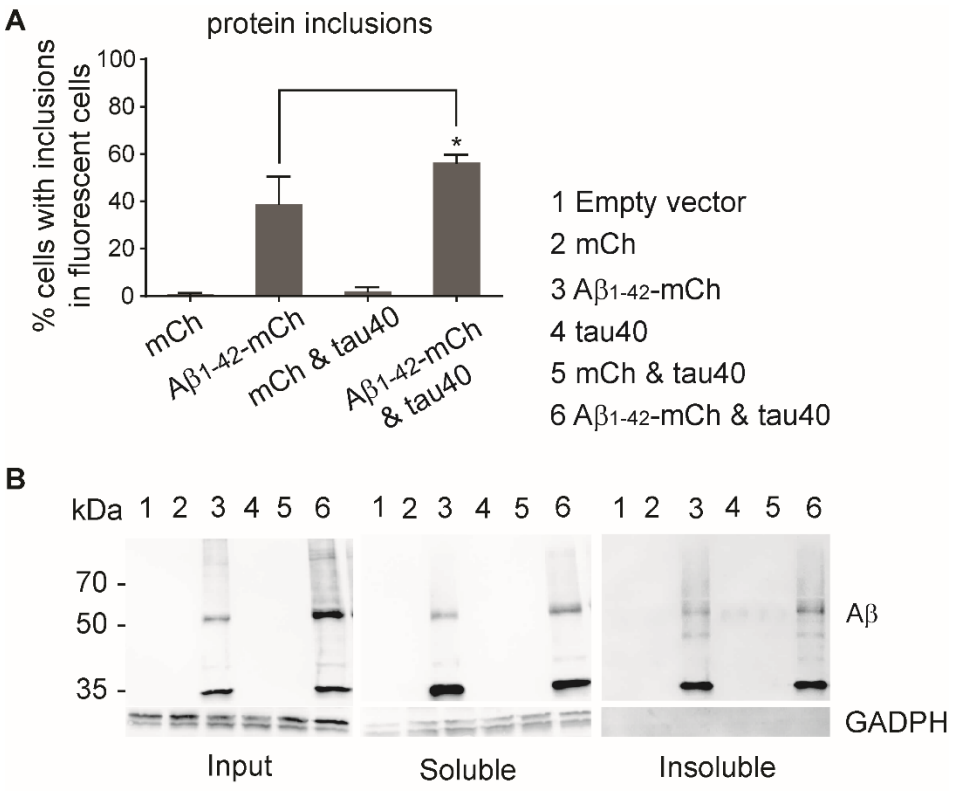

Figure 3.6. Accumulation of $A\beta_{1-42}$-mCh in *S. cerevisiae* BY4741.
(A) The percentage of cells with inclusions in the total number of mCh-expressing cells is significantly more abundant in the strain co-expressing $A\beta_{1-42}$-mCh and tau40 ($p = 0.033$), when compared to yeast expressing $A\beta_{1-42}$-mCh alone. No statistical difference was obtained between cells expressing mCh alone or in combination with tau40. Results are the average of 3 independent experiments where at least 200 expressing cells were counted in each sample. Error bars indicate standard deviations. **(B)** Presence $A\beta_{1-42}$-mCh in Sarkosyl insoluble protein fraction. There is no difference in the amount of insoluble $A\beta_{1-42}$-mCh when expressed alone or in combination with tau40. The antibody specific for Aβ (clone W02) detects oligomers of $A\beta_{1-42}$-mCh.

The percentage of cells presenting protein inclusions was calculated relatively to the total number of cells expressing the fluorescent protein. The percentage of cells presenting protein inclusions increased significantly when tau40 and $A\beta_{1-42}$-mCh were co-expressed ($p= 0.033$), when compared with the strain expressing $A\beta_{1-42}$-mCh alone (Figure 3.6.A). Analysis of the Sarkosyl soluble and insoluble protein fraction of yeast expressing $A\beta_{1-42}$-mCh alone or together with tau shows that $A\beta_{1-42}$-mCh forms small order oligomers that are resistant to SDS and that are present both in the Sarkosyl-soluble and -insoluble protein fractions (Figure 3.6.B). However, the amount of insoluble $A\beta_{1-42}$-mCh did not increase when tau40 was co-expressed, suggesting that the accumulations of $A\beta_{1-42}$-mCh and tau40 are constituted by soluble $A\beta_{1-42}$-mCh oligomers. The sarkosyl protein fractionation protocol was also performed for tau but inconsistent results between the replicates performed did not allow concluding with certainty about the state of tau oligomerization in this model.

3.3.5. Tau phosphorylation at Ser396/404 residues increased when beta-amyloid and tau were co-expressed

Previous reports show that tau is phosphorylated by GSK-3β yeast orthologue (Rim11) at the AD-related phospho-epitopes Ser396 and Ser404 (Ciaccioli *et al.*, 2013; Vandebroek *et al.*, 2005b). Moreover, several studies in other organism models indicate that beta-amyloid is able to drive such phosphorylation by activating GSK-3β (LaFerla, 2010; Shipton *et al.*, 2011; Terwel *et al.*, 2008). Therefore, tau phosphorylation status was analysed in this yeast model using the AD2 antibody, which recognizes phosphorylated tau at Ser396/404. These phosphorylation sites appear to be crucial for the formation of tau fibrils (Kremer *et al.*, 2011; Lei *et al.*, 2011; Noble *et al.*, 2013) and are characteristic of PHFs in AD (Buée-Scherrer *et al.*, 1996). Analysis of AD2 immunoreactivity *versus* total tau protein levels resulted in a significant increase in Ser396/404 phosphorylated tau40 when co-expressed with $A\beta_{1-42}$-mCh (p= 0.02), and compared with tau40 phosphorylation levels expressed alone or in combination with mCh, which occurred despite decreased total tau levels (Figure 3.7).

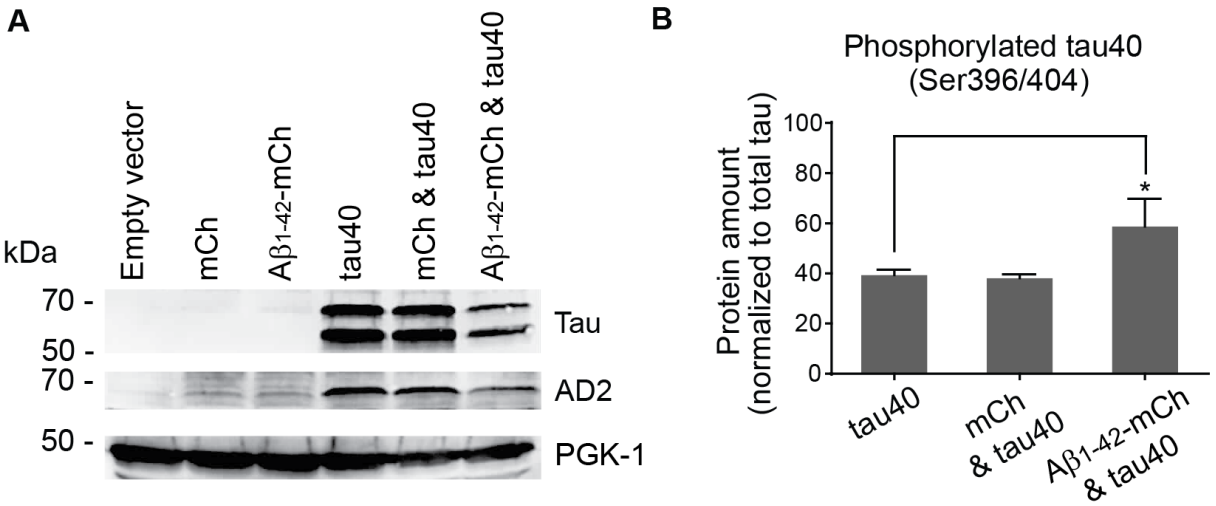

Figure 3.7. Increase in tau phosphorylation at AD-related epitopes (Ser396/404) when co-expressed with $A\beta_{1-42}$-mCh.
(A) Immunoblot analysis detected tau phosphorylated at Ser396/404 epitopes, as detected by the AD2 antibody. **(B)** The percentage of phosphorylated tau, increases significantly when tau40 is co-expressed with $A\beta_{1-42}$-mCh, when comparing with expression on tau40 together with mCh (* p = 0.02). Data corresponds to the average of three independent experiments and error bars indicate standard deviations.

To evaluate if phosphorylation of tau40 at the epitopes Ser396/404 was due to the activity of the yeast GSK-3β orthologue, Rim11, as described in (Ciaccioli *et al.*, 2013), the expression plasmids were transformed in a yeast strain lacking *RIM11* (BY4741 *rim11*Δ). Resulting strains were analysed for protein expression and growth by dot spot analysis (Figure 3.8).

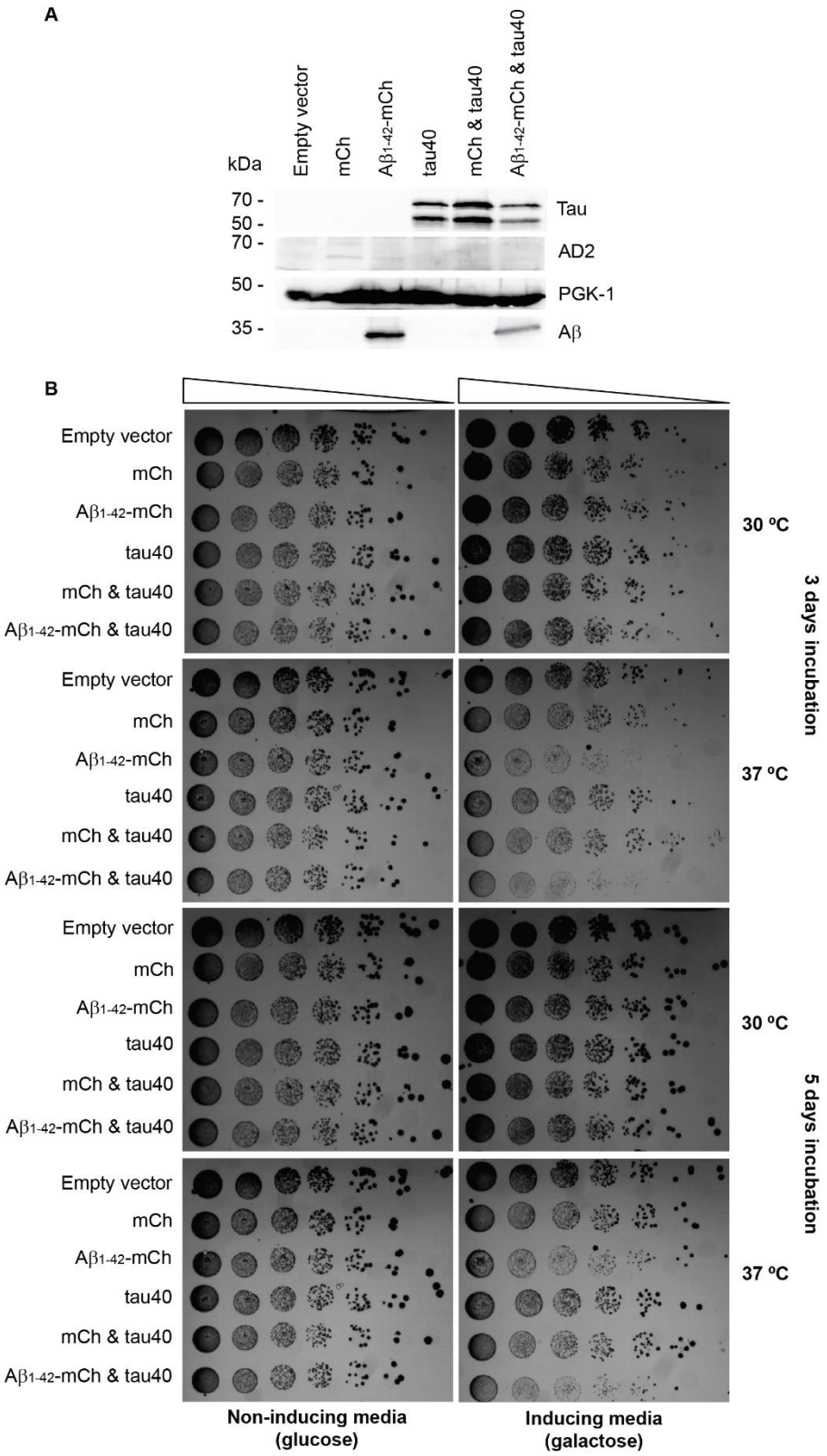

Figure 3.8. Tau40 phosphorylation at the AD-related epitopes S396/404 by Rim11, the GSK-3β yeast orthologue.

(A) Immunoblot analysis did not detected tau40 phosphorylated at the epitopes Ser396/404, as expected in yeast lacking *RIM11*. **(B)** $A\beta_{1-42}$-mCh expression alone or in combination with tau40 in BY4741 *rim11*Δ at 37ºC caused growth delay to yeast growth after 3 days incubation, which recovered after 5 days. Expression of mCh and $A\beta_{1-42}$-mCh was driven by *GAL1* promoter whereas tau40 expression was driven by *GAL10* promoter. Equal amounts of strains carrying the plasmids were collected in mid-exponential phase (OD_{600} 0.8 – 1.2), 5-fold serially diluted and spotted on SC+GLU-Leu media (non-inducing media) or SC+GAL-Leu media (inducing media) and incubated at 30 and 37ºC for 5 days. Results are representative of at least 3 independent experiments.

Phosphorylated tau40 was detected using the total tau antibody (higher molecular weight band) and, as expected, tau40 phosphorylated at sites Ser396/404 was no longer detected (Figure 3.8.A), when compared to data shown in Figure 3.7, suggesting that Rim11 is phosphorylating tau at the epitopes Ser396/404. Regarding yeast growth, $A\beta_{1-42}$-mCh expression alone or in combination with tau40 caused a growth delay after 3 days incubation but yeast recovered after 5 days incubation, which does not occur in the wild-type BY4741 strains (Figure 3.3.B). These results suggest that GSK-3β yeast orthologue may be involved in the toxicity of $A\beta_{1-42}$-mCh for yeast cell growth, and therefore implicated both with intracellular $A\beta_{1-42}$-mCh and tau40 pathologic events.

3.4. Discussion

In this work, different models of $A\beta_{1-42}$ and tau40 co-expression in yeast were produced and characterized. Expression of a single copy of each transgene integrated into W303-1A genome did not cause toxicity to yeast growth. However, increased levels of transgene proteins co-expressed in the BY4741 episomal model were cytotoxic to yeast, at 37ºC, an effect mediated by $A\beta_{1-42}$-mCh. Tau40 expression was not toxic to yeast and, intriguingly, its protein levels were reduced when co-expressed with $A\beta_{1-42}$-mCh. Tau40 was found to be hyperphosphorylated, in the AD-related epitopes Ser396/404 by Rim11, the main GSK-3β yeast orthologue. $A\beta_{1-42}$-mCh accumulated into cytoplasmic inclusions, constituted by soluble and insoluble Aβ oligomers. When co-expressed, $A\beta_{1-42}$-mCh and tau40 co-localized, suggesting a direct interaction between these two AD-related proteins. In fact, the number of cells presenting protein inclusions increased in the yeast strain co-expressing tau40 and $A\beta_{1-42}$-mCh, and the level of tau40 phosphorylation at Ser396/404 also increased with $A\beta_{1-42}$-mCh co-expression. When both proteins were expressed in a yeast strain lacking *RIM11*, not only the level of tau40 phosphorylation decreased, but also the toxicity of $A\beta_{1-42}$-mCh to yeast growth decreased. These results implicate GSK-3β in the mechanisms of Aβ and tau toxicity and confirm the interplay between these proteins in yeast. As this model replicates important pathologic features of AD-hallmark proteins, further characterization will be necessary, not only to add further insights to tau and Aβ interaction, but also to establish a useful tool for drug discovery and development for AD.

The expression of human $A\beta_{1-42}$ and tau40 transgenes in yeast was promoted using galactose inducible expression vectors. Expression of $A\beta_{1-42}$ was immunodetected only when in fusion with the fluorescent protein mCh, as reported elsewhere (Caine *et al.*, 2007). Tau40 protein migrated as a double band, consistent with previous reports of tau expression in yeast (Ciaccioli *et al.*, 2013; Vandebroek *et al.*, 2005b). Vandebroek and co-workers (Vandebroek *et al.*, 2005b) showed a higher number of tau40 phospho-isoforms than the ones detected in this work. This difference may be due to the different expression systems used, since the authors used a strong constitutive promoter for tau40 expression, whereas in this study, tau40 expression was induced only when galactose was added to the culture media, which resulted in no exogenous protein accumulation prior to experiments. Despite these differences, a higher molecular weight band of tau40 was detected, similarly to the one described in Ciaccioli *et al.*, 2013 and Vandebroek *et al.*, 2005b, and designated as hyperphosphorylated tau, a pathologic feature of this protein in AD.

Previous studies directing $A\beta_{1-42}$-GFP and $A\beta_{1-42}$-Sup35 fusion proteins expression towards the yeast cytoplasm described only mild consequences for yeast growth (Caine *et al.*, 2007; von der Haar *et al.*, 2007). These experiments were performed in different yeast background strains and also at the standard temperature of 30ºC (Summers & Cyr, 2011). In the present study, $A\beta_{1-42}$-mCh fusion protein did not pronouncedly affect yeast growth at 30ºC, in accordance with these previous studies. At 37ºC, $A\beta_{1-42}$-mCh expression induced yeast growth delay on solid media, when compared to the control strain expressing just mCh. This phenotype was also reported in liquid media. As mentioned before, the temperature of 37ºC increases stress to yeast growth, since the expression levels and/or activity of many proteins involved in cellular processes related with neurodegeneration are affected, such as protein folding and heat shock response processes. This increased stress emphasizes the phenotype caused by the heterologous protein expression, while allowing the modelling of the disease at the physiological temperature of the human proteins Aβ and tau. Moreover, high temperatures reinforce hydrophobic interactions among polypeptides, promoting *in vivo* and *in vitro* protein aggregation, further mimicking the conditions that these proteins are subjected in human cells (Morell *et al.*, 2011). A higher toxicity caused by $A\beta_{1-42}$ expression in BY4741 yeast growth at 37ºC was also achieved in the work of Morell and co-workers (Morell *et al.*, 2011). When integrating one copy of $A\beta_{1-42}$-mCh into the yeast W303-1A genome the growth arrest phenotype was not observed. This suggests that the toxicity of $A\beta_{1-42}$-mCh may be dependent on protein concentration, as occurs in AD (Treusch *et al.*, 2011). Regarding tau40, the expression of this protein in yeast *per se* did not cause any effect on yeast growth at 30ºC or 37ºC, as previously reported by different authors, using different yeast backgrounds and different systems of expression (Vandebroek *et al.*, 2006; Vandebroek *et al.*, 2005b; Vanhelmont *et al.*, 2010). The co-expression of $A\beta_{1-42}$-mCh and tau40 resulted in a growth arrest phenotype similar to that observed when $A\beta_{1-42}$-mCh was expressed alone, indicating that there is no synergistic toxic effect on yeast growth following expression of both proteins. Such synergistic effect may be masked by the reduced levels of tau40 protein when co-expressed with $A\beta_{1-42}$-mCh, which did not occur when tau40 was co-expressed with mCh (control). This reduction also seems to occur with other neurodegeneration-linked proteins, since tau40 expression levels were found to be reduced when co-expressed with α-synuclein, using pESC-LEU (Ciaccioli *et al.*, 2013). Additionally, the use of *GAL1-GAL10* divergent promoters and subsequent downstream processes may also contribute to differences in protein expression efficiencies. On the other hand, protein levels of the considerably smaller transcript of $A\beta_{1-42}$-mCh (and of α-synuclein in the episomal model described by Outeiro and co-workers (Outeiro & Giorgini, 2006)), when compared to tau40 transcript, were not affected by co-expression of a second transgene. Therefore, the size of the transgene may also affect the efficiency of protein expression.

The yeast episomal model, expressing fluorescent versions of $A\beta_{1-42}$ and tau40, allowed the determination of the subcellular localization of both proteins. As expected, $A\beta_{1-42}$-mCh was present in the cytoplasm excluding the vacuoles, and accumulated in amorphous inclusions, in contrast with mCh uniform distribution in the cytoplasm. When whole cell protein extracts were prepared in the absence of reducing agents, such as β-mercaptoethanol, SDS-resistant oligomers of $A\beta_{1-42}$-mCh were detected in the western blot analysis, which are a characteristic hallmark of oligomeric Aβ assemblies (Haass & Selkoe, 2007). Increasing evidences suggest that such soluble assembly forms are better candidates

for inducing neuronal and synaptic dysfunction in AD, since its levels correlate much better with the presence and degree of cognitive decline (Haass & Selkoe, 2007). In this study, the fact that the $A\beta_{1-42}$ oligomers were present both in the Sarkosyl soluble and insoluble fractions indicates that the amorphous structures observed are composed of soluble and insoluble $A\beta_{1-42}$ oligomers.

Tau40-eGFP appeared distributed in the cytoplasm, excluding vacuoles, and the same for eGFP alone. Interestingly, tau40-eGFP was present in the yeast nucleus, as revealed by the Z-stack analysis. This is in agreement with the findings that detect tau in the nuclei of neuronal and non-neuronal cells (Liu & Gotz, 2013; Shea & Cressman, 1998). When tau40-eGFP was expressed alone no evidence of protein accumulation was observed, as described previously (Timmers *et al.*, 2002). However, when co-expressed with $A\beta_{1-42}$-mCh, tau40-eGFP clearly co-localized with $A\beta_{1-42}$-mCh inclusions, which is in agreement with studies that report co-localization between Aβ and tau deposits in the same intracellular structures in the AD brain (Haass & Selkoe, 2007). These results suggest that $A\beta_{1-42}$-mCh and tau40-eGFP directly interact in this model system. Despite the information that the fluorescent tagged version of tau40 could provide, the eGFP signal was low and not all yeast cells expressed tau40-eGFP at the same intensity. This could be due to low translation efficiencies of the tau40-eGFP transcript, improper GFP folding, post-translational modification or a combination of both. Therefore, subsequent microscopy and aggregation studies were performed using the more physiologically relevant native form of tau40. The number of cells with protein inclusions significantly increased when tau40 and $A\beta_{1-42}$-mCh were co-expressed, suggesting that tau40 may be facilitating the accumulation of $A\beta_{1-42}$-mCh in yeast while at the same time, is being sequestered into those accumulations. This increase in the number of cells presenting protein inclusions did not result, however, in an increase of protein levels in the Sarkosyl insoluble $A\beta_{1-42}$-mCh protein fraction and in a measurable synergistic effect on yeast growth. Moreover, the quantification of tau insoluble fraction in the presence or absence of $A\beta_{1-42}$-mCh will be necessary to confirm this hypothesis.

Results also show that there is an increase in the amount of phosphorylated tau40 at Ser396/404, as detected by the specific antibody AD2 (Buée-Scherrer *et al.*, 1996), when $A\beta_{1-42}$-mCh and tau are co-expressed. This suggests that the expression of $A\beta_{1-42}$-mCh facilitates tau phosphorylation in pathology-related epitopes, which is in agreement with *in vitro* studies (Guo *et al.*, 2006) and studies made in a *Drosophila* model expressing $A\beta_{1-42}$ and tau (Iijima, Gatt & Iijima-Ando, 2010).

Previous studies have reported a link between $A\beta_{1-42}$ and the tau kinase GSK-3β (Hurtado *et al.*, 2012; LaFerla, 2010; Sofola *et al.*, 2010; Terwel *et al.*, 2008). Hence, both proteins were expressed in the absence of the GSK-3β yeast orthologue, Rim11. As expected, phosphorylation of tau at Ser396/404 epitopes was no longer detected and, interestingly the phenotype of growth arrest upon expression of $A\beta_{1-42}$-mCh was less evident, as observed also in Hurtado *et al.*, 2012 and Sofola *et al.*, 2010. Decreased levels of tau phosphorylation and decreased toxicity of $A\beta_{1-42}$-mCh to yeast growth in the absence of the main GSK-3β yeast orthologue, implicate GSK-3β in the pathological cascade of both intracellular Aβ and tau, supporting GSK-3β activity modulation as a relevant target for therapeutic intervention in AD.

Taken together, the results obtained in this work suggest that $A\beta_{1-42}$-mCh and tau40 directly interact, since they co-localize when co-expressed in the same subcellular compartment. Aβ expression appears

to be involved in the induction of tau40 phosphorylation in pathological epitopes, via GSK-3β, although we cannot exclude the involvement of other kinases. On the other hand, tau seems to facilitate Aβ oligomerization. However, these occurrences do not manifest as an increased synergistic toxic effect to yeast growth. Importantly, this model recapitulates essential features of $A\beta_{1-42}$ and tau40 pathologies and therefore constitutes a biologically relevant test tube to understand the interaction between AD hallmark proteins and other relevant players in neurodegeneration. Indeed, major biological processes involved in neurodegeneration, such as mitochondrial dysfunction, transcriptional dysregulation, trafficking defects and proteasomal impairment, are highly conserved between yeast and human (Miller-Fleming *et al.*, 2008; Tenreiro & Outeiro, 2010). Also, yeast has been instrumental for the current understanding of these conserved cellular mechanisms, and as such the techniques necessary to study these processes have already been developed (Fields & Johnston, 2005). Notably, the results obtained in modelling other neurodegenerative disorders in yeast were confirmed in other *in vitro* and *in vivo* models (Tenreiro & Outeiro, 2010). Further characterization of the episomal model here described in terms of the cellular processes affected by Aβ and tau will build a framework of tests useful as a first platform to evaluate the modes of action of drug candidates. Moreover, given the relative easiness of manipulating yeast genetics and the high degree of biologic resources developed by an active and cooperative yeast research community (Tenreiro & Outeiro, 2010), the interplay between Aβ and tau and other AD risk genes will be also relatively simple to study. Since $A\beta_{1-42}$-mCh and tau40 pathological events here described do not conduce to a measurable synergistic toxic effect on yeast growth, a drug discovery program using this model would have to include an extra step to evaluate whether the compounds capable of rescuing the growth of $A\beta_{1-42}$-mCh and tau40 yeast expressing strain intervene in $A\beta_{1-42}$-mCh or tau40 pathology separately, or in pathways where both proteins are involved. The yeast strain expressing $A\beta_{1-42}$-mCh, however, may prove to be a suitable drug discovery platform for the identification of compounds capable of modulating intracellular $A\beta_{1-42}$ toxicity. Although variability and reproducibility assays still must be performed in order to validate this strain as a drug screening platform, the preliminary results here performed show that only freshly transformed strains should be used for screening compounds, since cryopreservation greatly decreases the growth delay phenotype in liquid media.

Concluding, yeast recapitulates essential features of $A\beta_{1-42}$ and tau40 pathologies and further characterization of this model will provide a valuable tool for understanding the interaction of these proteins and their combined mechanism of toxicity and for drug discovery and development in AD, thus contributing to the advance of new therapeutic strategies for this devastating neurodegenerative disease.

Chapter 4.

A genome-wide screening to identify yeast gene deletions that enhance tau toxicity

4.1. Summary

Therapies based on tau mechanisms of disease have become a priority in drug discovery for Alzheimer's disease (AD). The development of effective therapies depends on the complete knowledge of the molecular cascade of neurodegenerative events, which still remains elusive. The aim of this study was to identify genes that modulate tau toxicity in yeast and that may constitute new relevant players in tau biological and pathological roles. Important features of tau pathology are recapitulated in yeast, such as hyperphosphorylation in pathology-related epitopes (Ser396/404) by the GSK-3β yeast orthologue, but tau expression is non-toxic to yeast growth. Therefore, a loss-of-function tau toxicity enhancer genomic screen was performed by conditionally expressing the longest wild-type human tau isoform (tau40) in the yeast gene deletion collection. This screen identified 31 yeast gene deletions enhancers of tau toxicity, 20 of which have well characterized human orthologues, placing tau in biological processes relevant for neurodegeneration, such as mitochondrial function, vesicular-mediated transport, macroautophagy and protein folding. This study also aimed to prioritize one yeast deletion strain for the development of a novel drug discovery screening system, following a high throughput strategy. The yeast strain *mir1*Δ was selected as suitable for the development of such system, since it presented a reproducible and specific synthetic lethal phenotype with tau40 expression. This work provides a novel framework for the identification of new drug targets and/or biomarkers for therapeutic intervention in tauopathies, including AD, while expanding our knowledge on the aetiology of this group of diseases.

Keywords: *S. cerevisiae*, loss-of-function genomic screen, tau, drug target, drug discovery, tauopathies

4.2. Introduction

Therapeutic strategies based on microtubule-associated protein tau (tau) mechanisms of disease have become a priority in drug discovery and development for tauopathies, including Alzheimer's disease (AD) (Wolfe, 2012). While it is known, since 1998, that mutations in tau gene (*MAPT*) are sufficient to cause neurodegeneration (Spillantini & Goedert, 2013b), only more recently has tau become widely accepted as playing a central role in AD onset and progression (Ittner & Gotz, 2011; Small & Duff, 2008). This, together with the recent failures in β-amyloid-based therapies for AD in late stages of development, have contributed to the emergence of tau as a drug target for AD (Yoshiyama *et al.*, 2013).

The development of effective disease-modifying therapeutic strategies depends on the deep understanding of tau biology and mechanisms of toxicity, which still remains largely incomplete (Spillantini & Goedert, 2013a). While the most well described biological function of tau is the stabilization of the cytoskeleton and regulation of axonal transport (Spillantini & Goedert, 2013b), novel putative functions are emerging due to the identification of new tau protein interactions (Table 1.2) (Lee & Leugers, 2012). This implicates tau in many other vital cellular processes, such as signalling pathways, cell cycle and apoptosis (as described in detail in Chapter 1, section 1.3.1.3) and emphasises the high complexity of tau biological and pathological role (Morris *et al.*, 2011; Wolfe, 2012).

Tau binding partners include cytoskeletal proteins, as expected, signalling molecules, proteins involved in the heat shock response and protein folding pathways, regulation of cell cycle and apoptosis. Taking into consideration some of these interactors, tau can act as a protein scaffold, regulating many signalling pathways. One of the most studied of such pathways, in neurons, involves tau interaction with the tyrosine kinase Fyn, establishing tau as a post-synaptic protein (Ittner *et al.*, 2010). The authors hypothesize that tau acts as scaffold protein bringing together Fyn and postsynaptic density protein 95 (PSD95), localizing Fyn at synapses, enabling its activation through *N*-methyl-D-aspartate (NMDA) receptors. Indeed, tau is required for phosphorylation of NMDA receptor subunit GluN2B in dendrites and mediates Aβ toxicity at dendrites in a mice model of AD (Ittner *et al.*, 2010). Functional roles for nuclear tau have been also proposed (Sjoberg *et al.*, 2006). Moreover, the high degree of tau post-translational modifications, which significance has not been fully characterized yet, further contributes to the complexity of tau biological and pathological roles (Ballatore *et al.*, 2007).

Under the hypothesis that there are still unravelled participants on tau mechanism of disease, the aim of this study was to identify genes that interact with tau, providing a novel framework for the identification of new drug targets and/or biomarkers, which may contribute for the development of innovative therapies for tauopathies.

In the post-genomic era, the molecular role of disease-related genes in the context of their genetic and physical interaction networks has been investigated resorting to genetic and proteomic studies in small model organisms (Miller-Fleming *et al.*, 2008; van Ham *et al.*, 2009). One of such organisms is yeast *Saccharomyces cerevisiae*, often described as a recognized living test tube to study the molecular basis of neurodegeneration (Braun *et al.*, 2010; Tenreiro & Outeiro, 2010). Neurodegenerative disorders such as AD (Morell *et al.*, 2011), PD, HD (Outeiro & Giorgini, 2006), FTD-FUS (Ju *et al.*, 2011) and FTD-

TDP43 (Armakola, Hart & Gitler, 2011) have been studied with success in yeast, and subsequent genetic studies have identified new targets for therapeutic intervention (Sun *et al.*, 2011; Treusch *et al.*, 2011; Willingham *et al.*, 2003).

When human tau is expressed in yeast, it becomes hyperphosphorylated and accumulates in insoluble aggregates, recapitulating important features of tau pathology and suggesting a strong conservation of pathways between yeast and human (Ciaccioli *et al.*, 2013; De Vos *et al.*, 2011; Vandebroek *et al.*, 2005a; Vanhelmont *et al.*, 2010). Based on this and on the success of previous studies for other neurodegenerative proteins, we reasoned yeast might prove to be a powerful genetic model for the identification of relevant genes involved in tau biology and pathology. Since tau expression is non-toxic to yeast (Vandebroek *et al.*, 2005a) and (Chapter 3), a typical loss-of-function genomic screen using the yeast gene deletion collection would allow to identify gene deletions that enhance tau toxicity. The genes identified code for proteins that are possibly involved in pathways that suppress tau toxicity (Miller-Fleming *et al.*, 2008), thereby constituting potential relevant drug targets for the development of new neuroprotective therapeutic strategies.

In this work, a high-copy plasmid (2µ) carrying the longest wild-type human tau isoform (tau40), was conditionally expressed in the yeast gene deletion collection, composed of 5155 yeast strains each bearing one single non-essential gene deletion. The resulting phenotype was then subsequently analysed, resulting in the identification of 31 yeast gene deletions, from which 20 have a well characterized human orthologue. The identified genes have placed tau in diverse biological processes relevant for neurodegeneration such as mitochondrial function, vesicular-mediated transport, macroautophagy and protein folding. A bottom-up high throughput strategy was followed aiming to prioritize one yeast gene deletion for the development of a novel drug discovery screening system for the identification of bioactive compounds capable of suppressing tau cytotoxicity. This strategy consisted in a trimming down of the gene targets in study by combining defined selection criteria, such as the existence of well-defined human homologues, reproducibility of phenotype and specificity towards tau. The selected yeast deletion strain lacks the gene *MIR1*, that codes for the mitochondria phosphate carrier (PiC), critical for ATP production and hence, for cell energy requirements (Palmieri, 2013).

The knowledge of tau interactome in yeast constitutes a relevant basis for the identification of new drug targets and/or biomarkers for tauopathies, while expanding the knowledge on the mechanisms and pathways involved in these disorders. Together with the identified yeast-based drug discovery screening system, this information will hopefully foster the development of innovative therapeutic interventions for such a devastating group of disorders.

4.3. Results

4.3.1. Human tau40 expression was phosphorylated by Rim11, the yeast orthologue of GSK-3β

As described in detail in the previous chapter (Chapter 3), the expression of the longest wild-type human tau isoform (tau40), controlled by the galactose inducible promoter *GAL10*, in a high-copy plasmid (2μ) is non-toxic to yeast (De Vos *et al.*, 2011) (Figure 4.1.A).

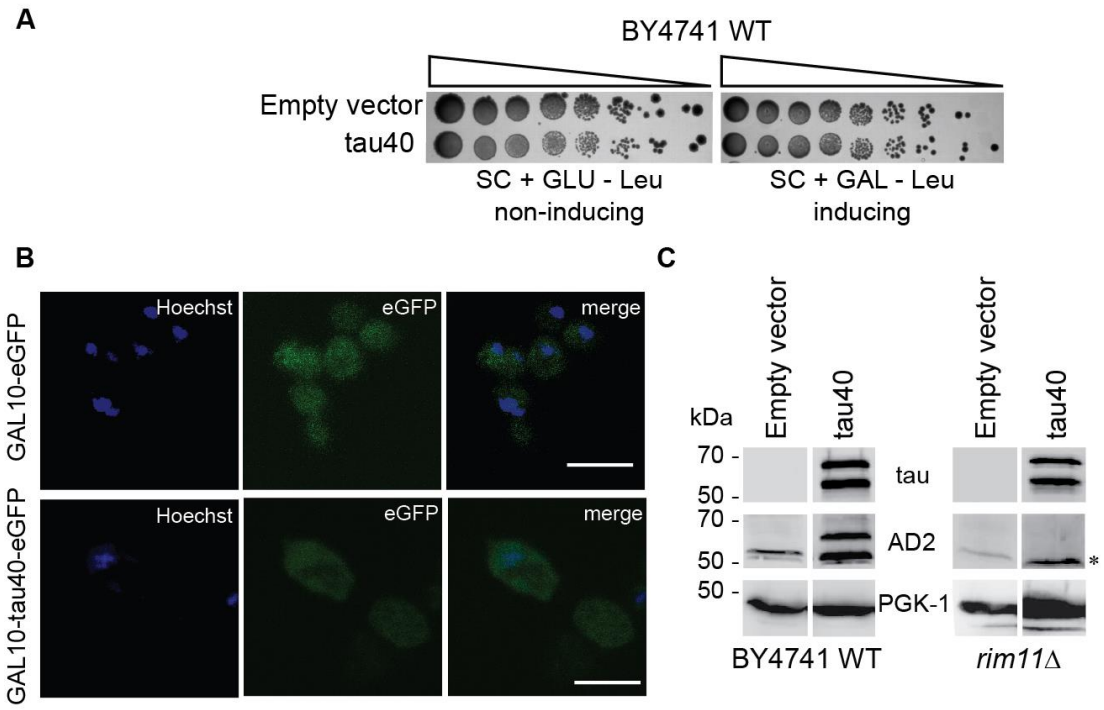

Figure 4.1. Tau40 expression in the cytoplasm of *Saccharomyces cerevisiae* is non-toxic to yeast. Tau40 is phosphorylated in the pathology-related epitopes Ser396/404.
(A) Growth of yeast cells expressing tau40 is similar to that of yeast carrying the empty plasmid in inducing media. Equal amounts of cells carrying human tau40 expression plasmid under the control of *GAL10* promoter, and cells carrying the empty high copy expression plasmid pESC-Leu (vector) were collected in mid-exponential phase (OD_{600} 0.8 – 1.2), 5-fold serially diluted and spotted on SC+GLU-Leu (non-inducing media) and SC+GAL-Leu (inducing media) and incubated at 30 ºC for 3 days. **(B)** tau40-eGFP localizes to yeast cytoplasm and nucleus, excluding the vacuoles, and does not form visible aggregates. Protein expression was induced at 30ºC for 24 h. Equal amounts of yeast carrying the plasmids were collected and fixed with formaldehyde and stained with Hoechst 33342. Microscopic observation was performed using a laser scanning confocal microscope Zeiss LSM 710 equipped with a Plan-Apochromat 63x/1.4 objective. Images shown are composites of maximum intensity of Z-stack images. Bar dimension: 5 μm. **(C)** Western blotting shows that tau40 migrates as a double band between 50-70 kDa as detected by a pan-tau polyclonal antibody. The upper band corresponds to phosphorylated tau, and it is phosphorylated at the AD-related epitopes Ser396/404 as detected by the AD2 antibody, specific for GSK-3β phosphorylated residues (*unspecific band). The yeast strain *rim11*Δ, the orthologue of GSK-3β, lacks phosphorylated tau in these residues. PGK-1 was used as loading control.

Confocal images of yeast expressing tau40-eGFP show that this fusion protein appears distributed in the cytoplasm, excluding vacuoles, similarly to eGFP alone. Interestingly, tau40-eGFP was present in the yeast nucleus, as revealed by the Z-stack analysis. No evidences of visible protein aggregation were

observed (Figure 4.1.B). Western blotting analysis of yeast total extracts prepared in denaturing conditions showed that tau40 migrates as a double band between 50-70 kDa, at 30ºC. The higher molecular weight band of tau40 corresponds to phosphorylated tau (p-tau), as previously observed by others (Vandebroek *et al.*, 2005b).

Tau40 is phosphorylated in pathology-related epitopes (Ser396/404) in yeast as detected by the phospho-tau antibody AD2 (Figure 4.1.C) (Ciaccioli *et al.*, 2013; Vandebroek *et al.*, 2005a). When tau is expressed in yeast lacking *RIM11*, the main GSK-3β yeast orthologue, tau40 phosphorylation at Ser396/404 is no longer detected, indicating that this kinase is able to phosphorylate tau40 in yeast (Figure 4.1.C). These results suggest strong conservation of pathways involved in tau pathology between yeast and humans. Based on this, we reasoned yeast might prove as a powerful genetic model for the identification of relevant genes involved in tau biology and pathology.

4.3.2. Tau40 toxicity enhancer screen

The screening for tau40 toxicity enhancer yeast ORF deletions followed a high-throughput strategy, encompassing four stages: primary and secondary screening, dot spot assays and specificity evaluation (Figure 4.2).

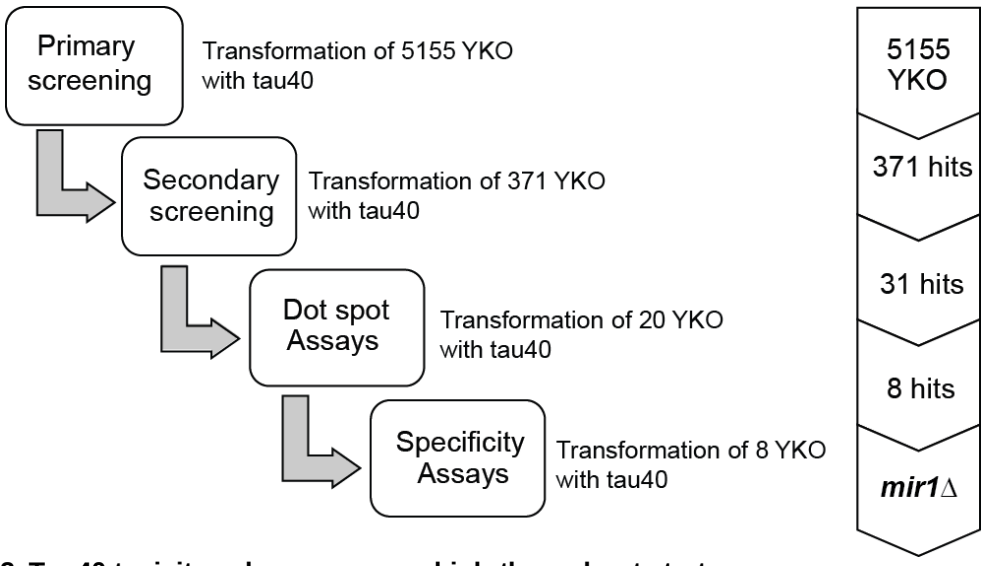

Figure 4.2. Tau40 toxicity enhancer screen high-throughput strategy.

The classification of the YKO strains after the primary screening is shown in Appendix I. 5155 YKO strains were reactivated from glycerol stocks into liquid rich media (YPD). 5083 yeast strains were able to recover and classified as tested strains. The remaining 72 YKO strains did not recover, and therefore were not considered in the data analysis. From the tested strains, 94.2% (4789/5083) were successfully transformed with tau40 construct, confirmed by the ability to grow in the transformation control plate (selective non-inducing media). From the transformed strains tested, 7.8% (399/5083) were affected by growth in galactose (complete GAL media) and were excluded from the analysis. From the remaining strains, 2.1% (100/4684) were unable to grow in the transformation and test (selective inducing media) plates and considered as sensitive to the transformation protocol. 2.6% (123/4684) were considered as

incongruences, since no growth was detected in the transformation plate but colonies were present in the test plate. Maintaining the high-throughput approach, these strains were not included in the analysis, but its identity was saved for potential future re-test.

Concluding, 95.2% (4461/4684) of the tested yeast strains unaffected by galactose were able to grow in the transformation plate. In the primary screening, 371 YKO strains were found sensitive to tau40 toxicity as no growth was detected in the test plate and therefore designated as Hits. Also, 4090 strains were considered negative results, since yeast were able to grow in all culture conditions and therefore not sensitive to tau40 expression. To eliminate false positives, the 371 candidate hit strains were re-tested in a secondary screening that confirmed 31 YKO strains as sensitive to tau40 expression, representing 0.7% of the YKO strains transformed and unaffected by galactose (31/4684). Table 4.1 displays the list of 31 tau40-sensitive yeast mutants which function or genetic role has been determined experimentally or can be predicted using the Yeast Genome Database (www.yeastgenome.org/). The human homologues of the deleted yeast gene are also shown and represent 67.7% (21/31) of the list tau40-sensitive yeast strains.

Table 4.1. Yeast mutant strains sensitive to tau40.

Strain	Yeast gene name	Brief description	Human gene Homologue	Protein name
aft1Δ	Activator of Ferrous Transport	Transcription factor involved in iron utilization and homeostasis	--	
aim10Δ	Altered Inheritance rate of Mitochondria	Protein with similarity to tRNA synthetases	*PARS2*	Prolyl-tRNA synthetase 2, mitochondrial (putative)
aim21Δ	Altered Inheritance rate of Mitochondria	Protein of unknown function	--	
atp11Δ	ATP synthase	Mitochondrial molecular chaperone	*ATPAF1*	ATP synthase mitochondrial F1 complex assembly factor 1
atp23Δ		Putative metalloprotease of the mitochondrial inner membrane	*XRCC6BP1*	XRCC6 binding protein 1
atp4Δ	ATP synthase	Subunit b of the stator stalk of mitochondrial F1F0 ATP synthase	*ATP5F1*	ATP synthase, H+ transporting, mitochondrial Fo complex, subunit B1
ckb1Δ	Casein Kinase Beta subunit	Beta regulatory subunit of casein kinase 2 (CK2); a Ser/Thr protein kinase	*CSNK2B*	casein kinase 2, beta polypeptide
coq9Δ	Coenzyme Q	Protein required for ubiquinone (coenzyme Q) biosynthesis and respiratory growth	*COQ9*	coenzyme Q9
cox20Δ	Cytochrome c Oxidase	Mitochondrial inner membrane protein	*COX20*	COX20 cytochrome C oxidase assembly factor
cox7Δ	Cytochrome c Oxidase	Subunit VII of cytochrome c oxidase	--	
etr1Δ	2-Enoyl Thioester Reductase	Mitochondrial 2-enoyl thioester reductase	*MECR*	mitochondrial trans-2-enoyl-CoA reductase
gsh1Δ	glutathione (GSH)	Gamma glutamylcysteine synthetase	*GCLC*	glutamate-cysteine ligase, catalytic subunit
htb2Δ	Histone h Two B	Histone H2B, core histone protein required for	*HIST1H2BB*	histone cluster 1, H2bb

Strain	Yeast gene name	Brief description	Human gene Homologue	Protein name
		chromatin assembly and chromosome function		
iki3Δ	Insensitive to KIller toxin	Subunit of Elongator complex	*IKBKAP*	kinase complex-associated protein
mdm12Δ	Mitochondrial Distribution and Morphology	Mitochondrial outer membrane protein, ERMES complex subunit	--	
mir1Δ		Mitochondrial phosphate carrier also known as PTP	*SLC25A3*	mitochondrial phosphate carrier family 25, member 3
mrp1Δ	Mitochondrial Ribosomal Protein	Mitochondrial ribosomal protein of the small subunit involved in mitochondrial translation	--	
mrp4Δ	Mitochondrial Ribosomal Protein	Mitochondrial ribosomal protein of the small subunit involved in mitochondrial translation	*MRPS2*	mitochondrial ribosomal protein S2
mrpl10Δ	Mitochondrial Ribosomal Protein, Large subunit	Mitochondrial ribosomal protein of the large subunit involved in mitochondrial translation	*MRPL15*	Mitochondrial ribosomal protein L15
pep3Δ	carboxyPEPtidase Y-deficient	vacuolar peripheral membrane protein that promotes vesicular docking/fusion reactions	*VPS18*	vacuolar protein sorting 18
pes4Δ	Polymerase Epsilon Suppressor	Poly(A) binding protein, suppressor of DNA polymerase epsilon mutation	*RBMX*	Heterogeneous Nuclear Ribonucleoprotein G
pet100Δ	PETite colonies	Chaperone that facilitates the assembly of cytochrome c oxidase	--	
pho88Δ	PHOsphate metabolism	Probable membrane protein involved in phosphate transport	--	
rrd1Δ	Resistant to Rapamycin Deletion	Peptidyl-prolyl cis/trans-isomerase, activator of the phosphotyrosyl phosphatase activity of PP2A	*PPP2R4*	protein phosphatase 2A activator, regulatory subunit 4
rsm26Δ	Ribosomal Small subunit of Mitochondria	Mitochondrial ribosomal protein of the small subunit involved in mitochondrial translation	--	
ski7Δ	SuperKIller	Coupling protein for the Ski complex and cytoplasmic exosome	*GSPT1*	G1 to S phase transition 1
vps15Δ	Vacuolar Protein Sorting	Serine/threonine protein kinase involved in vacuolar protein sorting	*PIK3R4*	phosphoinositide-3-kinase, regulatory subunit 4
yke2Δ	Yeast ortholog of mouse KE2	Subunit of the heterohexameric Gim/prefoldin protein complex	*PFDN6*	prefoldin subunit 6
zap1Δ	Zinc-responsive Activator Protein	Zinc-regulated transcription factor	*ZNF70 /ZNF648*	zinc finger protein 70 and zinc finger protein 648

Human homologues of yeast genes are indicated.

Based on the annotations of the Proteome Database (http://www.biobase-international.com/) a functional analysis of the human homologue gene hits was performed. The genes were classified according with their gene onthology (GO) attributes (Table 4.2).

Table 4.2. Classification of the human homologue gene hits by GO term*

GO TERM		Quantity	Human Gene name
Cellular component	Mitochondria	38% (8/21)	ATPSF1, COQ9, IKBKAP, MECR, PARS2, SLC25A3, MRPS2, MRPL15
Molecular function	Phosphorylation	21% (4/21)	CSNK2B, PIK3R4, IKBKAP, PPP2R4
	RNA-binding activity and protein biosynthesis	14.3% (3/21)	MRPL15, MRPS2, PARS2

*GO Term: Gene onthology term, bioinformatics designation that allows to classify gene and gene products attributes across species.

Remaining genes code for proteins with diverse molecular function. No evident cluster of genes in functionally related categories was identified. A network analysis resulted in the identification of one network of proteins connecting *HIST1H2BB*, *CSNK2B*, *ZNF70*, *IKBKAP* and *GCLC* protein products to Src tyrosine kinase.

Putative tau40-sensitive yeast mutants which deleted gene has a human homologue and the corresponding human protein has a characterized function (20/31) were confirmed by re-transforming yeast with the tau40 construct.

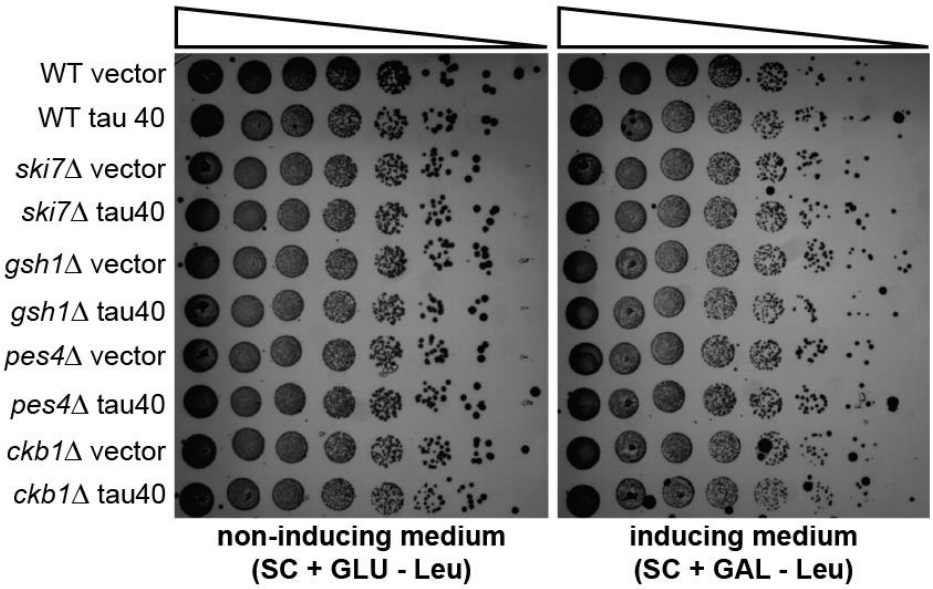

Figure 4.3. Dot spot assays of yeast knockout strains *ski7*Δ, *gsh1*Δ, *pes4*Δ and *ckb1*Δ after induction of tau40 expression for 3 days incubation at 30ºC.
The growth of these mutant yeast strains is similar to that of BY4741 wild-type strain when carrying the empty plasmid or expressing human tau40 and therefore these strains are not sensitive to tau40 toxicity in these culture conditions. Equal amounts of cells carrying human tau40 expression plasmid under the control of *GAL10* promoter, and cells carrying the empty high copy expression plasmid pESC-Leu (vector) were collected in mid-exponential phase (OD_{600} 0.8 – 1.2), 5-fold serially diluted and spotted on SC+GLU-Leu media (non-inducing media) and SC+GAL-Leu media (inducing media) and incubated at 30 ºC for 3 days.

Dot spot assays were performed with transformed yeast isolated in new selective media plates for 2-3 additional days. Cell growth was evaluated by comparing the effects of tau40 expression in the mutant

versus wild-type parental strain (BY4741). These assays allowed confirming the synthetic lethal effect of the gene deletion and overexpression of tau in fittest yeast cells.

Figure 4.3 shows the spotting assays performed for *ski7*Δ, *gsh1*Δ, *pes4*Δ and *ckb1*Δ. The growth of these strains was similar to that of the wild-type strain after 3 days of incubation at 30ºC, indicating that tau40 expression was not toxic to yeast growth. For other strains, conclusive results on their growth phenotype were obtained only after 6 days incubation at 30ºC (Figure 4.4 and Figure 4.5).

The growth of the yeast strains *atp23*Δ, *atp4*Δ, *etr1*Δ and *iki3*Δ transformed with tau40, in inducing media, is similar to the growth of these strains carrying the empty plasmid (Figure 4.4). Therefore, these strains are not sensitive to tau40 toxicity in these culture conditions. Additionally, the yeast strain *atp4*Δ grows very poorly in galactose, since after 6 days of incubation only the first dilution of cells (~1.8 x10^7 cells) grew in the inducing media plate. This number of cells is equivalent to the number of cells plated in the growth plate in the primary and secondary screenings, indicating that this strain was correctly included in the list of putative tau40-sensitive hits, despite the slow growth in galactose, since it complied with the defined criteria.

The strains *atp11*Δ, *rrd1*Δ, *vps15*Δ and *aim10*Δ were also not confirmed as sensitive to tau40 toxicity by dot spot assays (Figure 4.5), since growth of yeast expressing tau40 is similar to the growth of yeast carrying the empty plasmid, in inducing-media.

As tau40 was inserted in an episomal expression plasmid, different yeast cells may uptake different number of plasmid copies, which affects the concentration of protein level. As the pathology of tau may be dependent on the protein concentration, the absence of the phenotype in yeast may be due to the yeast clone isolated and tested. Therefore, due to the relevance of the human homologue gene for tau biology, more colonies of *atp11*Δ, *rrd1*Δ, *vps15*Δ, *etr1*Δ, *pep3*Δ and *zap1*Δ yeast strains transformed with tau40 plasmid were tested by dotspot (results not shown). However, no different outcome was observed. Since these results did not reproduce the ones obtained in the primary and secondary screenings, the set of strains presented in Figure 4.3, Figure 4.4 and Figure 4.5 were not further studied.

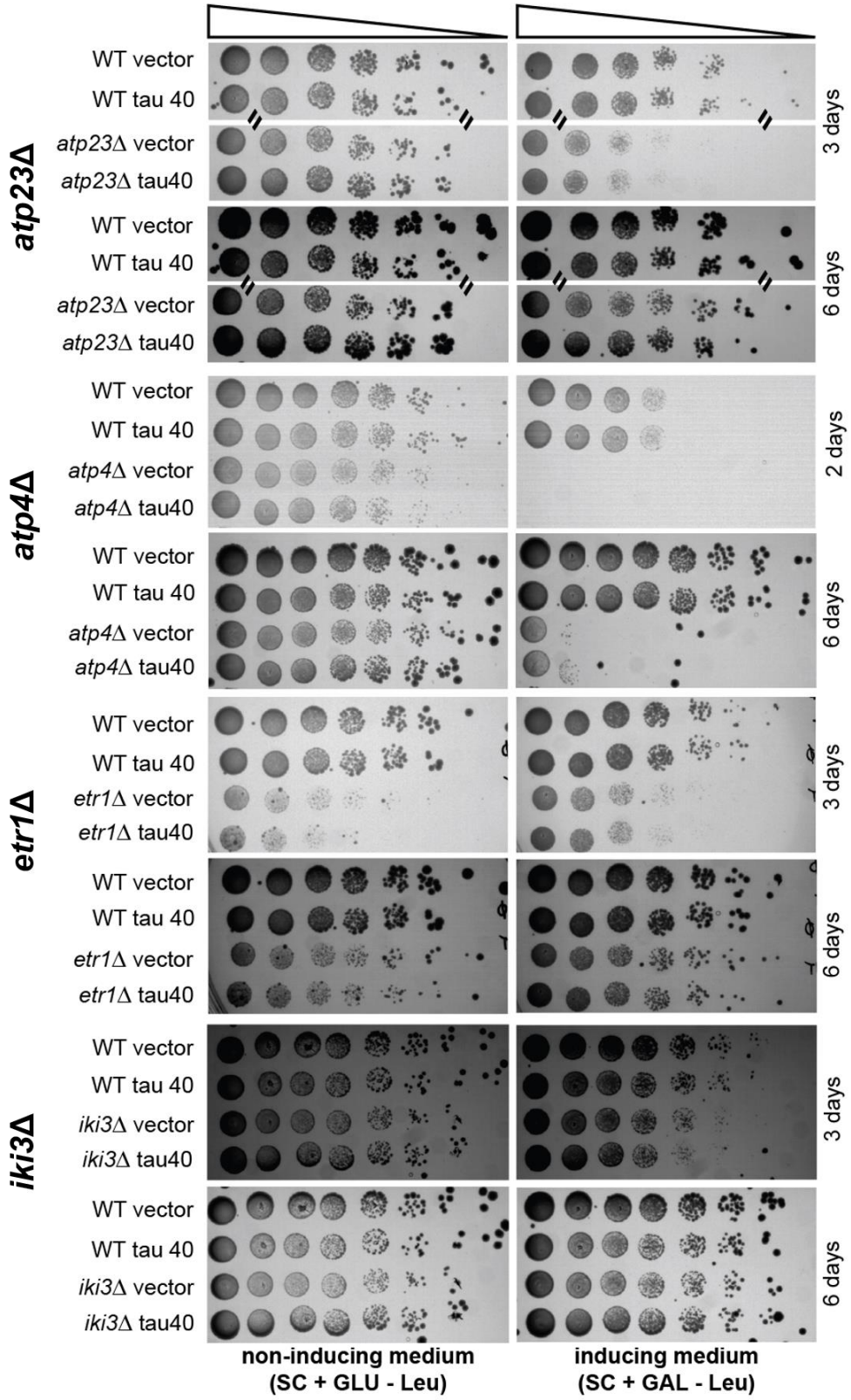

Figure 4.4. Dot spot assays of yeast knockout strains *atp23*Δ, *atp4*Δ, *etr1*Δ and *iki3*Δ after induction of tau40 expression for 2-3 and 6 days incubation at 30ºC.
The growth of these mutant yeast strains when expressing tau40 is similar to that of strains carrying the empty plasmid. Therefore, they are not sensitive to tau40 toxicity in these culture conditions. Equal amounts of cells carrying human tau40 expression plasmid under the control of *GAL10* promoter, and cells carrying the empty high copy expression plasmid pESC-LEU (vector) were collected in mid-exponential phase (OD_{600} 0.8 – 1.2), 5-fold serially diluted and spotted on SC+GLU-Leu media (non-inducing media) and SC+GAL-Leu media (inducing media) and incubated at 30 ºC for 2-6 days.

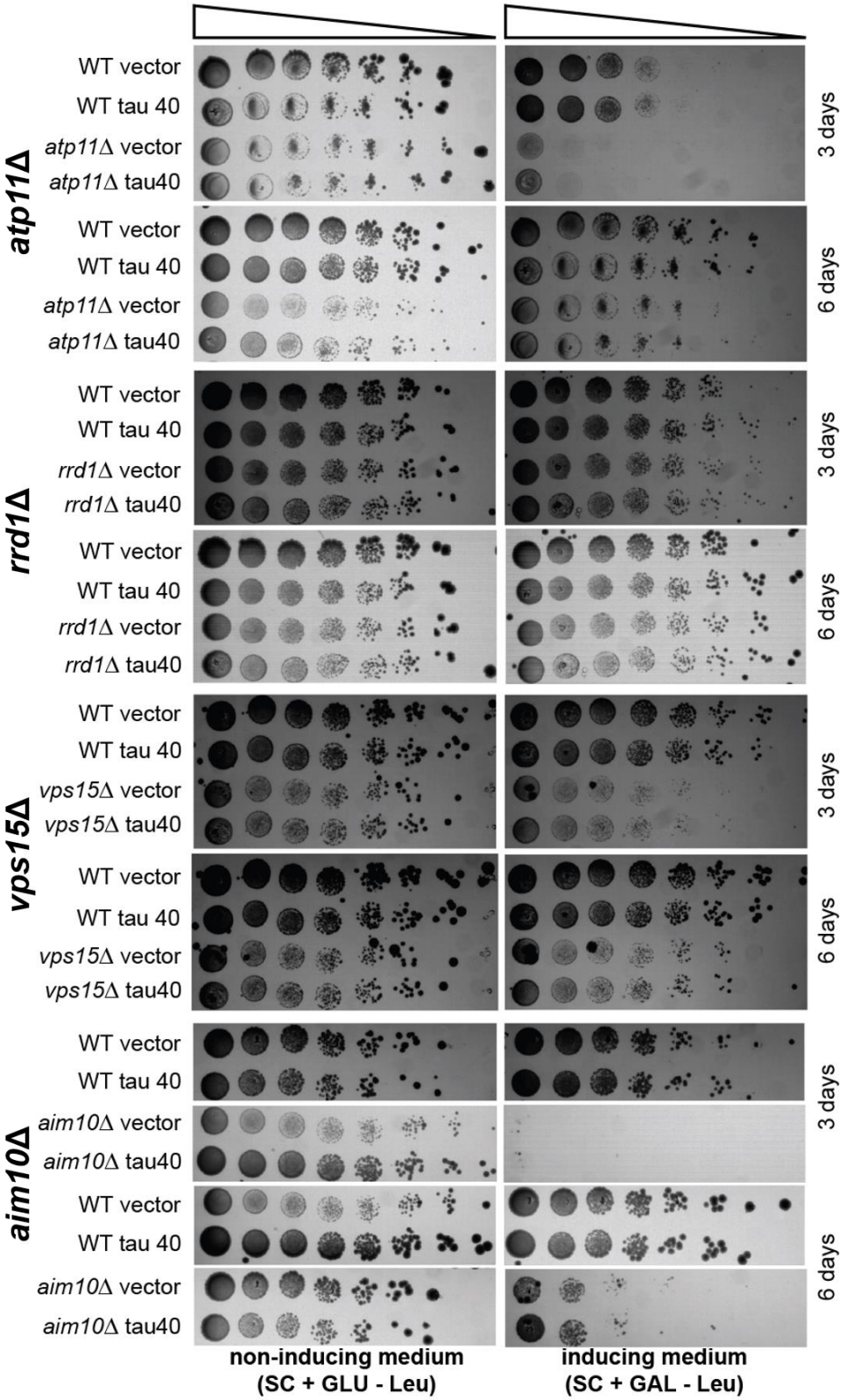

Figure 4.5. Dot spot assays of yeast knockout strains *atp11*Δ, *rrd1*Δ, *vps15*Δ and *aim10*Δ after induction of tau40 expression for 2-3 and 6 days incubation at 30ºC.

The growth of these mutant yeast strains when expressing tau40 is similar to that of strains carrying the empty plasmid. Therefore, they are not sensitive to tau40 toxicity in these culture conditions. Equal amounts of cells carrying human tau40 expression plasmid under the control of *GAL10* promoter, and cells carrying the empty high copy expression plasmid pESC-LEU (vector) were collected in mid-exponential phase (OD_{600} 0.8 – 1.2), 5-fold serially diluted and spotted on SC+GLU-Leu media (non-inducing media) and SC+GAL-Leu media (inducing media) and incubated at 30 ºC for 3 to 6 days.

Figure 4.6, Figure 4.7 and Figure 4.8 depict YKO strains that were confirmed as sensitive to tau toxicity by dot spot assays. For these strains, the expression of tau40 was evaluated by western blotting, confirming that all were expressing human tau at the expected molecular weight (50-70 kDa) and that in all strains, tau appeared phosphorylated (higher molecular weight band).

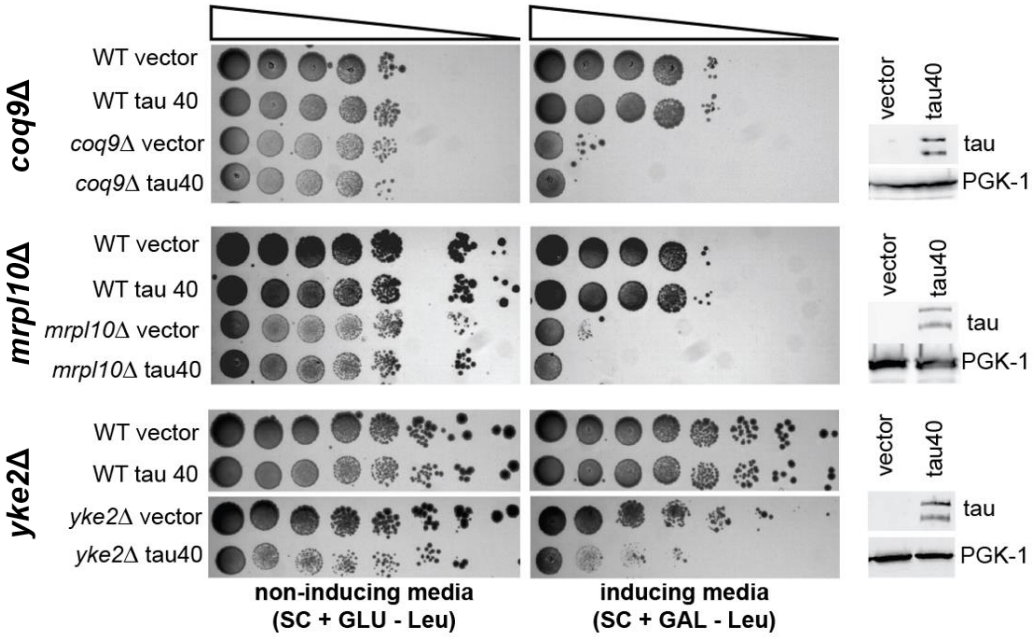

Figure 4.6. Dot spot assays of yeast knockout strains *coq9*Δ, *mrpl10*Δ and *yke2*Δ after induction of tau40 expression for 6 days incubation at 30ºC.
The growth of these mutant yeast strains when expressing tau40 is reduced when compared to the growth of the same strain carrying the empty plasmid, thereby confirming these yeast mutant strains as sensitive to tau40 toxicity. Equal amounts of cells carrying human tau40 expression plasmid under the control of *GAL10* promoter, and cells carrying the empty high copy expression plasmid pESC-LEU (vector) were collected in mid-exponential phase (OD_{600} 0.8 – 1.2), 5-fold serially diluted and spotted on SC+GLU-Leu media (non-inducing media) and SC+GAL-Leu media (inducing media) and incubated at 30 ºC for 6 days.

The yeast strains *coq9*Δ, *mrpl10*Δ, *yke2*Δ (Figure 4.6) and *pep3*Δ and *zap1*Δ (Figure 4.7) presented a sub-lethal effect in growth, as the more concentrated dilutions of cells were still able to survive upon tau40 expression. In the case of *pep3*Δ and *zap1*Δ (Figure 4.7), the growth delay observed upon tau expression recovered after 6 days incubation.

The yeast strains *htb2*Δ, *mrp4*Δ and *mir1*Δ (Figure 4.8) presented a lethal phenotype when expression of tau40 was induced in the presence of galactose, since no growth was detected in inducing media plates.

Despite the control performed to rule-out strains affected by galactose, the strains *htb2*Δ, *mrp4Δ*, *coq9*Δ and *mrpl10*Δ grew very poorly in galactose. The number of cells plated in the first dilution was equivalent to the number of cells plated in the growth plate of the primary and secondary screenings. The fact that growth was observed in this first spot confirms the results of the screening and that these strains were correctly included in the list of tau sensitive yeast strains. Despite this low growth rate, the strains growth when expressing tau40 was reduced when compared to the control strains, thereby confirming these strains as sensitive to tau toxicity.

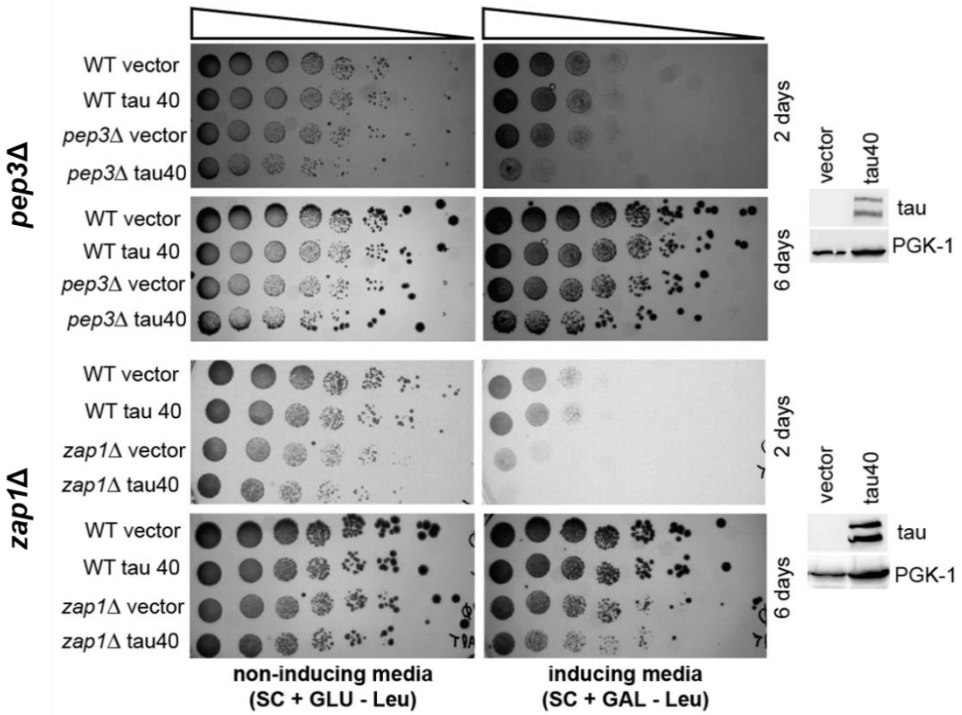

Figure 4.7. Dot spot assays of yeast knockout strains *pep3*Δ and *zap1*Δ after induction of tau40 expression for 6 days incubation at 30ºC.
The growth of these mutant yeast strains when expressing tau40 is reduced when compared to the growth of the same strain carrying the empty plasmid after 2 days incubation at 30ºC. However, after 6 days incubation, the growth of these strains recovers to levels equal to the empty plasmid carrying yeast. Equal amounts of cells carrying human tau40 expression plasmid under the control of *GAL10* promoter, and cells carrying the empty high copy expression plasmid pESC-LEU (vector) were collected in mid-exponential phase (OD_{600} 0.8 – 1.2), 5-fold serially diluted and spotted on SC+GLU-Leu media (non-inducing media) and SC+GAL-Leu media (inducing media) and incubated at 30 ºC for 6 days.

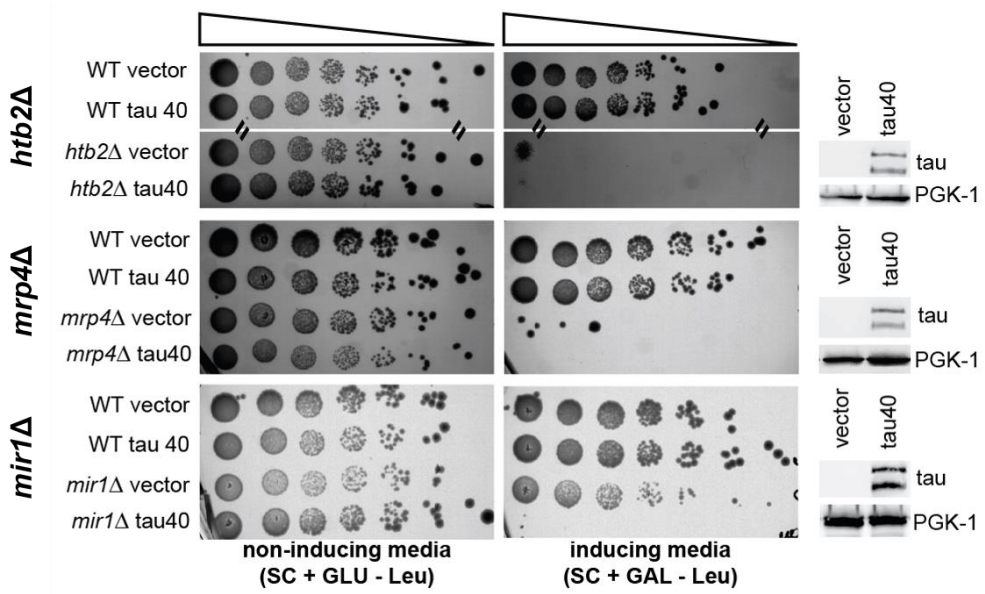

Figure 4.8. Dot spot assays of yeast knockout strains *htb2*Δ, *mrp4*Δ and *mir1*Δ after induction of tau40 expression for 6 days incubation at 30ºC.
These strains are unable to grow when tau40 expression is induced in presence of galactose, when compared to the control strain, carrying the empty plasmid, and therefore present a lethal phenotype upon tau40 expression. Equal amounts of cells carrying human tau40 expression plasmid under the control of *GAL10* promoter, and cells carrying the empty high copy expression plasmid pESC-LEU (vector) were collected in mid-exponential phase (OD_{600} 0.8 – 1.2), 5-fold serially diluted and spotted on SC+GLU-Leu media (non-inducing media) and SC+GAL-Leu media (inducing media) and incubated at 30 ºC for 6 days.

The ORF deletions of the strains identified as sensitive to tau40 toxicity by spotting assays (8/21) were confirmed by standard PCR using primers specific for the barcodes that identify each strain (Figure 4.9).

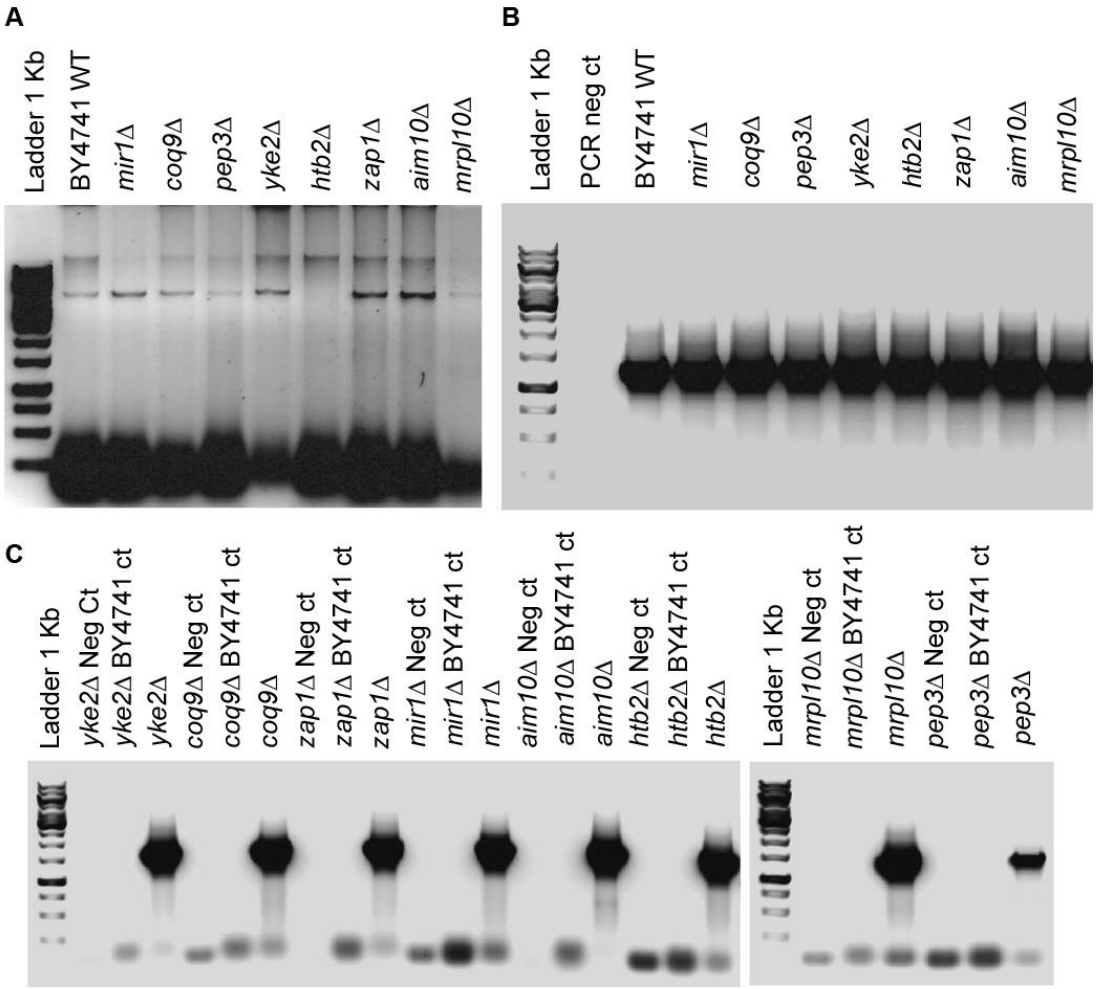

Figure 4.9. ORF deletion confirmation of yeast strains identified as sensitive to tau40 toxicity by dot spot assays.
(A) Genomic DNA was extracted from yeast and analysed by DNA electrophoresis. **(B)** Quality of genomic DNA was analysed by performing a PCR to amplify the internal control gene NPT1. **(C)** Standard PCR results using primers specific for the barcode of each yeast strain. For each pair of primers a negative control (without DNA) and a positive control (genomic DNA from BY4741 WT) was included.

The next step consisted in evaluating if the phenotype observed was specific for tau40 overexpression. Therefore, the strains confirmed as sensitive to tau40 toxicity were transformed with the control protein mCh and the resulting phenotype of yeast growth was evaluated by dot spot assays (Figure 4.10). These selectivity assays identified *coq9*Δ sub-lethal and *mir1*Δ lethal growth effect observed as specific for tau40 toxicity.

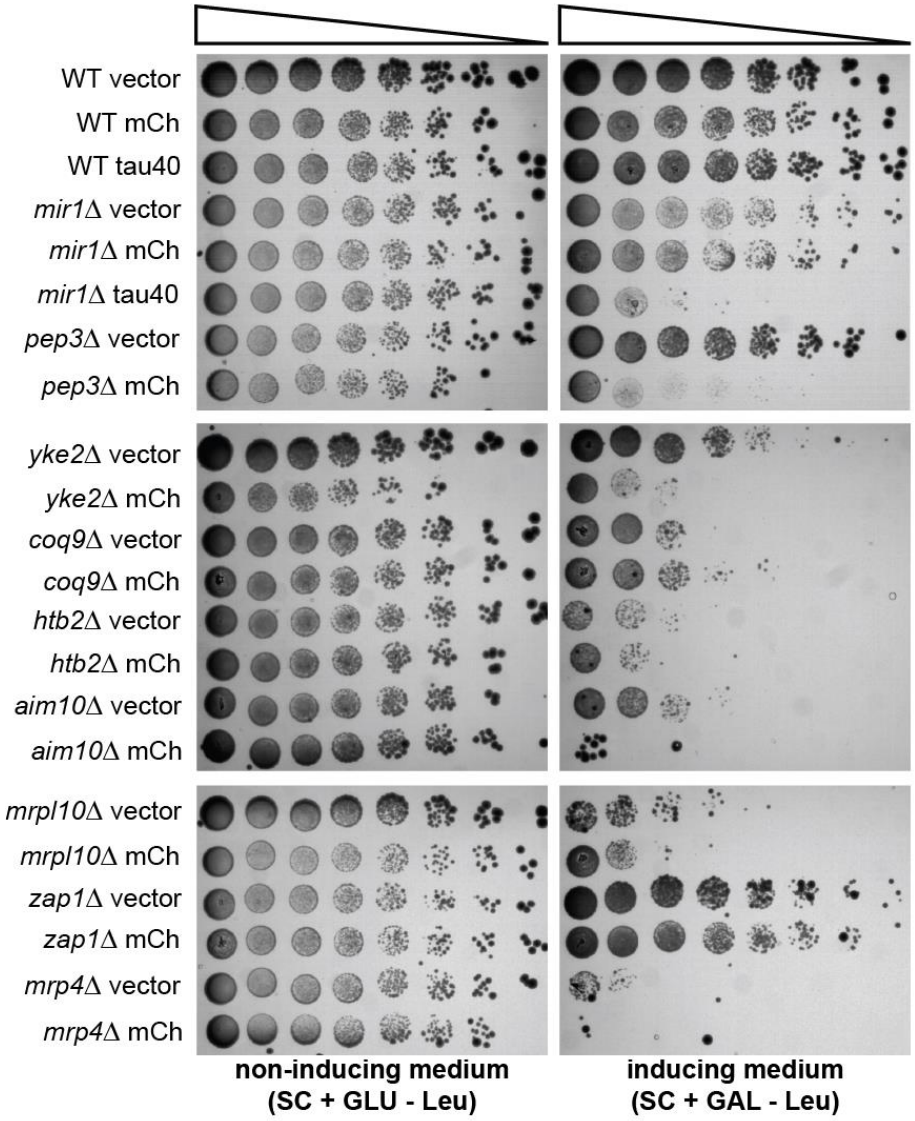

Figure 4.10. Dot spot assays of yeast knockout strains *mir1*Δ, *pep3*Δ, *yke2*Δ, *coq9*Δ, *htb2*Δ, *aim10*Δ, *mrpl10*Δ, *zap1*Δ and *mrp4*Δ after induction of mCherry expression for 6 days incubation at 30ºC.

The growth of strain *mir*Δ after induction of tau40 expression was again evaluated and it the phenotype observed is specific for tau40, since the growth of the strain expressing mCh is similar to that of *mir1*Δ carrying the empty plasmid. The strain coq9Δ growth is also not affected by mCh expression induction. The growth of remaining strains are affected by mCh expression induction and therefore the phenotype of decreased cell growth is not specific to tau40. Equal amounts of cells carrying human mCh expression plasmid under the control of *GAL1* promoter, and cells carrying the empty high copy expression plasmid pESC-LEU (vector) were collected in mid-exponential phase (OD_{600} 0.8 – 1.2), 5-fold serially diluted and spotted on SC+GLU-Leu media (non-inducing media) and SC+GAL-Leu media (inducing media) and incubated at 30 ºC for 6 days.

4.4. Discussion

In this work, a loss-of-function genomic screen was performed to map tau40's interactome in yeast, providing a framework of 31 yeast genes for further studies in the identification of potential new relevant drugs targets and/or biomarkers for tauopathies therapeutics. The human homologues of some of these genes are involved in biological processes pertinent in the context of neurodegeneration, such as mitochondrial function, vesicular-mediated transport, macroautophagy and protein folding. The high

throughput strategy applied identified the most promising yeast mutant strain for the development of a drug discovery screening system aiming to identify bioactives modulators of tau toxicity. Indeed, the yeast strain *mir1*Δ presented a reproducible and specific synthetic lethal phenotype with tau40 expression, involving tau in mitochondrial function.

Yeast models of tau expression reproduce important features of tau pathology (Ciaccioli *et al.*, 2013; Vandebroek *et al.*, 2005a; and this work Chapter 3). Therefore, a loss-of-function genome-wide screen was performed by conditionally expressing tau40 in the yeast knockout collection. Since tau40 is non-toxic to yeast growth, this screen has identified 31 gene deletions enhancers of tau toxicity (Miller-Fleming *et al.*, 2008). These genes possibly function in pathways that suppress tau40 toxicity, since when functionally expressed in the wild-type strain there is no loss of viability after induction of tau40 expression (Miller-Fleming *et al.*, 2008).

A significant percentage of the genes identified as putative tau40 toxicity suppressors have a well-defined and characterized human homologue (67.7%). This suggests a high degree of conservation of pathways involved in neurodegeneration between yeast and human, further supporting the use of yeast in modelling human diseases. No enrichment in a particular functional category was detected in the functional analysis performed, but most of the gene target hits are involved in biological processes relevant for neurodegenerative disorders, including tauopathies. Many of these functional categories have also been identified in other functional genomic studies using *Drosophila melanogaster* as the model organism (Ambegaokar & Jackson, 2011; Karsten *et al.*, 2006; Shulman & Feany, 2003; Shulman *et al.*, 2014). Indeed, one of these studies has also identified *GSPT1*, coding for G1 to S phase transition 1 protein, as a suppressor of tau toxicity (Ambegaokar & Jackson, 2011). The present functional screen has identified genes involved in vesicular-mediated transport and macroautophagy (*PIK3R4* (Yan *et al.*, 2009), VPS18 (Peng *et al.*, 2012) and *GSPT1* (Ambegaokar & Jackson, 2011)) and protein folding (*ATPAF1* (Ackerman, 2002) and *PFDN6* (Petrucelli *et al.*, 2004; Sorgjerd *et al.*, 2013)). Some of the identified genes suggest tau involvement in processes such as transcription (*HIST1H2BB*, *RBMX* and *ZNF70/ZNF648*) and translation (*PARS2*, *MRPS2* and *MRPL15*). Also, *CSNK2B*, *GSPT1* and *PPP2R4* are involved in the mitotic G1 phase, placing tau in the cell cycle process, in accordance with previous studies (Gotz *et al.*, 2008). The identified gene network connected to Src tyrosine kinase further supports this last result. This network involves tau in processes related with cell cycle control, neurite outgrowth, and signal transduction (Lee, 2005; Minami *et al.*, 2012). Src kinases such as Fyn and Lck have been found to phosphorylate tau and have a critical role in mediating synaptic toxicity and neuronal loss in response to β-amyloid (Aβ) in models of AD (Minami *et al.*, 2012; Scales *et al.*, 2011; Usardi *et al.*, 2011). Increasing evidences show that these pathways may have a role in tau-mediated neurodegeneration and are thus relevant for therapeutic intervention.

A significant number of gene hits occur at the mitochondria, suggesting that the correct function of this organelle is important for yeast cells to cope with tau40 overexpression. The role of mitochondrial dysfunction in neuropathogenesis is still under debate, since some suggest that it is the cause of neurodegeneration rather than a consequence. This hypothesis is supported by the connection between aging and increased mitochondrial malfunction (Swerdlow, Burns & Khan, 2010). Mitochondrial

dysfunction has been described in Alzheimer's, Parkinson's and Huntington's diseases and tau has been associated with some of the pathologic events that occur in mitochondria in neurodegeneration. For example, tau impairs mitochondrial fission and complex I (NADH dehydrogenase) and also inhibits axonal anterograde transport, as described with more detail in Chapter 6 (Ferrer, 2009; Johri & Beal, 2012).

Four of the identified ORF deletions that enhance yeast sensitiveness to tau toxicity have kinase or phosphatase activity, highlighting the importance of phosphorylation in tau toxicity mechanisms (Noble *et al.*, 2013). Particularly, casein kinase 2, which beta subunit is coded by the gene hit CSNK2B, has already been associated with another neurodegenerative disease (PD), since its product is usually detected in Lewy Bodies (Waxman & Giasson, 2008).

The high throughput strategy followed in this screening allowed to narrow-down the number of genes that may be subject of future validation studies in organism models of higher biological relevance. The 4 stages of the screening (primary and secondary screening, dot spot assays and specificity evaluation) allowed increased confidence in the picked gene target hits as relevant potential suppressors of tau40 toxicity. It has also eliminated a high number of false positives between the primary and secondary screenings attributed to the inherent variability of the whole HTS screening concept and in particular to the transformation protocol: the death of a strain could be due not to its sensitivity to tau40 toxicity, but to the culture conditions (liquid or solid media, carbon source) or heat shock temperature. Also, the inclusion of dot spot assays, using yeast cells, allowed to recover after the transformation and before induction of tau40 expression, permitted to identify yeast strains that, even in fitter conditions, were still sensitive to tau40 toxicity. These strains constitute the best candidates for development of drug discovery screening systems for identification of bioactive modulators of tau toxicity. The screen design was also different from typical loss-of-function genomic studies in yeast, which usually are directed to proteins toxic to yeast growth and use yeast survival as read-out. Nonetheless, important genes and potential new roles for tau in the cell were identified and still the final number of yeast mutant strains picked is in alignment with the results presented by those other studies (Giorgini *et al.*, 2005; Giorgini & Muchowski, 2006; Sun *et al.*, 2011; Treusch *et al.*, 2011; Willingham *et al.*, 2003).

The selectivity evaluation studies asserted *MIR1* as a potential specific suppressor of tau40 toxicity, although it will be necessary to replicate and validate such results in models of higher biological relevance. The human homologue of this yeast gene is *SLC25A3*, a gene that encodes for the mitochondrial phosphate carrier (also known as PiC) that catalyses the transport of phosphate into the mitochondrial matrix, either by proton co-transport or in exchange for hydroxyl ions, a process essential for the oxidative phosphorylation of ADP to ATP (Palmieri, 2013). *SLC25A3* function was investigated in Chapter 6, during the preliminary tests for development of a mammalian cell model able to replicate the yeast results, and its involvement with mitochondria function was verified. One CHIP-Seq study identified *SLC25A3* as a target of the transcription factor NRF1, which appears to play an important role in neurodegenerative diseases (Satoh, Kawana & Yamamoto, 2013). This transcription factor is required for normal expression of genes essential for mitochondrial biogenesis and function and proteasome genes (Satoh *et al.*, 2013). In addition, mutations in *SLC25A3* gene are the cause of PiC oxidative

phosphorylation disorder, which is fatal in the first year of life (Mayr *et al.*, 2007). Given the relevance of *SLC25A3* human gene in mitochondrial dysfunction and the results of this study, showing a reproducible and specific synthetic lethal effect of its yeast orthologue (*MIR1*) deletion with tau40 overexpression, the yeast mutant strain *mir1*Δ has great potential to be used as a drug discovery screening system to identify modulators of tau toxicity.

Importantly, the other genes picked up in the dot spot assays, and found unspecific for tau40 toxicity, still hold great promise as drug targets for therapeutic intervention in neurodegeneration in general. *COQ9*, for example, is a protein required for ubiquinone (coenzyme Q) biosynthesis and respiratory growth found to be downregulated in brains of FTD and Pick's disease patients and it has been used in the treatment of mitochondrial disorders (Bronner *et al.*, 2009). The gene *PFDN6* that codes for prefoldin, is also a relevant drug-target, since it is a chaperone found to prevent aggregation of misfolded proteins, co-chaperone of heat shock protein 70 (*HSP70*), up-regulated in AD brains (Broer *et al.*, 2011) and considered to be a regulator of tau ubiquitination, degradation and aggregation (Petrucelli *et al.*, 2004). In addition, *VPS18*, a vacuole protein sorting protein which ablation leads to neurodegeneration (Peng *et al.*, 2012), is also considered a relevant drug target.

The identification of tau40's interactome in yeast has provided a relevant framework for identification of potential new drug targets and/or biomarkers for therapeutic intervention in tauopathies. The gene target hits identified place tau40 in biological processes worthy of further study, in order to increase our understanding on tau biology and pathology, critical for the development of mechanistic-based therapies so urgently needed. Additionally, the strain *mir1*Δ was identified as a suitable drug discovery screening system for identification of bioactive modulators of tau toxicity. Taken together, these results greatly contribute to the main goal of this work, which is to accelerate drug discovery and development for tauopathies such as FTD and AD.

Chapter 5.

Bacterial natural extracts suppressors of tau toxicity in yeast

5.1. Abstract

Tau protein has become an attractive drug target for the development of therapeutic strategies useful for a group of neurodegenerative disorders, called tauopathies, including Alzheimer's disease, the most prevalent dementia worldwide. Several therapeutic strategies based on tau-mechanism of disease have been developed but more innovative solutions are needed to fuel the pipeline of drugs in development. Taking advantage of the mapping of tau's interactome in yeast, this work aims to go one step further in accelerating drug discovery for tauopathies by coupling an innovative drug discovery technology – GPS D^{2TM} – with new sources of natural compounds, for the development of new therapeutic strategies for tauopathies. One yeast deletion strain identified in a loss-of-function tau toxicity enhancer genomic screen, demonstrated a reproducible and specific synthetic lethal phenotype after induction of tau expression. The yeast gene deleted in this strain – *MIR1* - codes for the mitochondrial phosphate carrier protein (PiC), a phosphate transporter essential for ATP production. The phenotype of growth delay upon tau expression was verified in liquid media and the robustness of the yeast strain was evaluated for high throughput drug screenings. This screening system was used to scan a small library of 138 unique natural extracts obtained from the SEAVENTbugs bacteria collection, which identified 3 natural extracts with activity in suppressing tau's toxicity in a mitochondria-compromised cellular environment. These extracts constitute excellent starting points for the discovery of new safe and effective biological entities for the development of innovative therapies for tauopathies.

Keywords: yeast-based assay, tau protein, natural products, tau toxicity suppressors, drug discovery;

5.2. Introduction

The microtubule-associated protein tau (tau) has become an attractive target for the development of therapeutic strategies for a range of neurodegenerative disorders, called tauopathies, including Alzheimer's disease (AD), the most prevalent type of dementia worldwide (Prince & Jackson, 2009). In tauopathies, tau is hyperphosphorylated and aggregated, affecting several cellular processes that ultimately lead to synaptic and neuronal loss (*vide* Chapter 1). The lack of reliable biomarkers and exact knowledge of the mechanism of disease has hampered the development of effective disease-modifying therapeutic strategies for tauopathies, including AD (Davidowitz & Moe, 2012; Noble *et al.*, 2011; Prince, Bryce & Ferri, 2011). Increasing evidences suggest a central role for tau in AD onset and progression, which, together with recent failures in the development of Aβ-based therapies, in phase III clinical trials, contributed to prioritize tau-based drug discovery strategies (Davidowitz & Moe, 2012; Noble *et al.*, 2011). Indeed, several different therapeutic strategies have been developed, covering all aspects of tau dysfunction in different times of disease progression (*vide* Chapter 1) (Noble *et al.*, 2011; Yoshiyama *et al.*, 2013). Most of these studies are still in pre-clinical stage, with only 4 molecules reaching the clinical development (Chapter 1, Table 1.3), reflecting the early-stage of this trend.

More innovative solutions are therefore needed to fuel the pipeline of tau-based therapies, so urgently needed to overcome the social and economic burden of these disorders. Novel functions of tau are still being elucidated and future drug discovery programs may focus on these alternative functions of tau and will benefit from novel biomarkers and tau's interactome deeper knowledge (Noble *et al.*, 2011). Therefore, taking advantage of the data generated by a loss-of-function tau toxicity enhancer genomic screen (*vide* Chapter 4), the goal of the present work was to foster drug discovery for tauopathies by coupling an innovative drug discovery technology – GPS D^{2TM} – with new sources of natural compounds, for the development of new therapeutic strategies for tau-related disorders. With the mapping of tau's interactome in yeast, novel tau interactors have been identified, with the potential to become new drug targets/biomarkers for tauopathies. Also, one yeast ORF deletion mutant – *mir1*Δ - was successfully prioritized for the development of a yeast-based drug discovery platform for identification of tau toxicity modulators. In the current work, a screening platform based on such yeast strain was developed for identification of modulators of tau toxicity.

Yeast is a recognized organism model for the study of human neurodegenerative disorders (Tenreiro & Outeiro, 2010) and it is also widely used as a screening platform for drug discovery (Barberis *et al.*, 2005). Yeast-based GPS D^{2TM} assays are highly informative as they provide data on both the efficacy and the toxicity of test compounds and in addition they are highly amenable to HTS adaptation, allowing a fast and cost-effective bioactive discovery process. GPS D^{2TM} technology has been adapted to the identification of bioactives for several applications, including the pharmaceutical (Cerejo *et al.*, 2012; Ciaccioli *et al.*, 2013; Martins *et al.*, 2013a; Martins *et al.*, 2013b).

The yeast strain *mir1*Δ has a compromised mitochondrial function, due to the deletion of the gene *MIR1*. This gene codes for the mitochondrial phosphate carrier protein (also known as PiC), that catalysis the transport of phosphate to the mitochondrial matrix, thereby being essential to the production of ATP

(Baseler *et al.*, 2012). The survival of this strain is decreased by inducing the overexpression of the longest wild-type human tau isoform (tau40), placing tau in the biological processes involved with mitochondrial function (*vide* Chapter 4). Indeed, tau has been associated with some of the pathologic events that occur in mitochondria in neurodegeneration, including impaired mitochondrial fission and complex I (NADH dehydrogenase) and inhibition of anterograde transport (Eckert *et al.*, 2014). Mitochondrial dysfunction has been described in several neurodegenerative disorders, including AD and other tauopathies (Moreira, Santos & Oliveira, 2007; Schon & Przedborski, 2011). Although the relationship between the aggregating pathologic proteins and mitochondrial dysfunction is not completely understood, it is clear that impaired oxidative phosphorylation or mitochondrial dynamics influence neuronal death (Schon & Przedborski, 2011). Mitochondrial dysfunction may well have a significative role in disease progression in the sporadic forms of neurodegenerative disorders and is considered as another pathway for therapeutic intervention, particularly at later stages of disease (Schon & Przedborski, 2011).

The screening system presented in this work - *mir1*Δ-tau40 platform - was used to screen a small library of 138 aqueous natural extracts obtained from the SEAVENTbugs marine prokaryotic collection (Martins *et al.*, 2013b), as a proof-of-concept on the use of this system for HTS tau-based drug discovery programmes.

Natural products (NP) extracted from a variety of organisms represent an excellent source of new chemical entities for drug discovery and development (Bauer & Bronstrup, 2014; Martins *et al.*, 2014). Indeed, over 60% of the drugs currently on the market are of natural origin (Martins *et al.*, 2014). NPs have higher chemical diversity, biochemical specificity, binding efficiency and propensity to interact with biological targets, characteristics that render them more advantageous for drug development than non-natural compounds (Martins *et al.*, 2014). Several NPs from different biological sources have been found active in many tau-related screens, such as curcumin, a polyphenol isolated from *Curcuma longa* extract; paclitaxel, isolated from the Pacific Yew *Taxus brevifolia*, and compounds with bacterial origin (*Streptomyces peucetius*) such as anthraquinones (reviewed in Calcul *et al.*, 2012).

The SEAVENTbugs marine bacteria collection was obtained during the Portuguese mission SEAHMA-1 (Seafloor and Sub-Seafloor Hydrothermal Modelling in the Azores Sea), in the extreme environment of deep-sea hydrothermal vents near the Mid-Atlantic Ridge (MAR) (Menez Gwen, Menez Hom, Rainbow, Lucky Strike and Mount Saldanha) (Martins *et al.*, 2013b; Rodrigues *et al.*, 2011). These very dynamic environments are characterized by physical extremes of temperature (4 to 400 ºC) and pressure, complete absence of light and abrupt chemical, pH and temperature gradients and are populated with a diverse array of microorganisms that were forced to adapt to these harsh environmental conditions (Martins *et al.*, 2013b). This adaptation is thought to occur through the production of secondary metabolites that might possess unexplored bioactivities for a range of different applications, including the pharmaceutical (Martins *et al.*, 2013b; Rodrigues *et al.*, 2011). In fact, the aqueous extracts obtained from a sub-set of the SEAVENTbugs collection, composed of 138 psychrotolerant anaerobic or facultative anaerobic bacteria, have already been validated for applications in neurodegenerative disorders, such as Parkinson's disease with associated tau pathology (Ciaccioli *et al.*, 2013) and familial

amyloidotic polyneuropathy (unpublished data), amongst other applications developed at BIOALVO (Martins *et al.*, 2013a; Martins *et al.*, 2013b). From these, anti-infectious, anti-UV and antioxidant activities have been identified (Martins *et al.*, 2014).

The stringent screening system here presented, coupled to a unique marine bacterial extracts library, allowed the identification of 3 safe and effective modulators of tau toxicity in a mitochondrial-compromised environment, that constitute good candidates for drug development for therapeutic intervention in tau-related disorders.

5.3. Results

5.3.1. The yeast strain *mir1*Δ-tau40 was suitable for drug discovery screenings

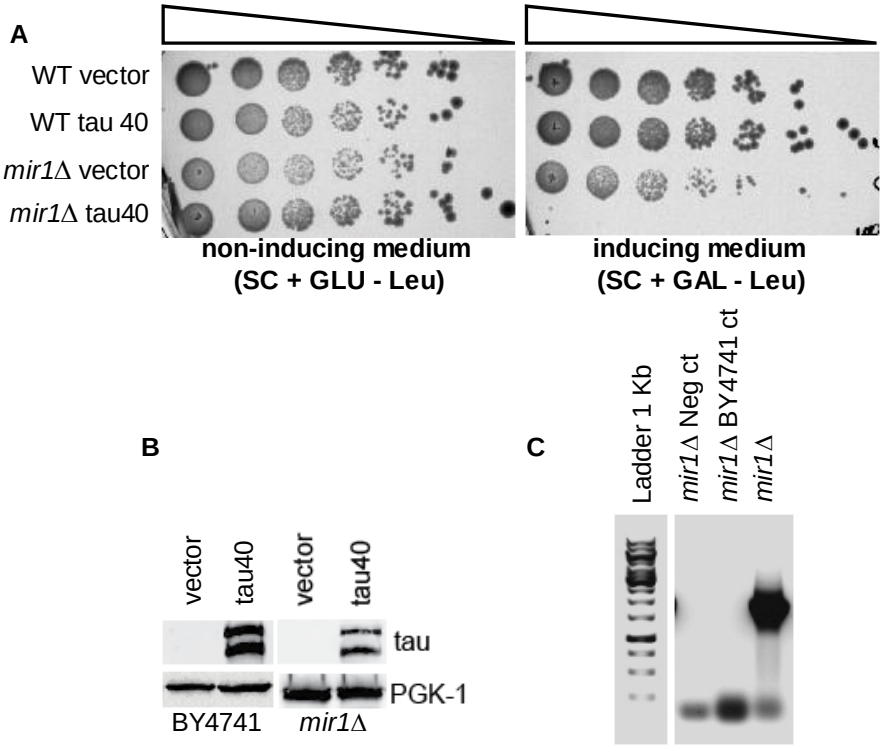

Figure 5.1. Yeast strain *mir1*Δ-tau40.
(A) Expression of tau40 in *mir1*Δ is toxic to yeast growth, when comparing with the same strain carrying the empty plasmid. Equal amounts of yeast cells of BY4741 WT and *mir1*Δ, carrying human tau40 expression plasmid under the control of *GAL10* promoter, or carrying the empty high copy expression plasmid pESC-LEU (vector) were collected in mid-exponential phase (OD_{600} 0.8 – 1.2), 5-fold serially diluted and spotted on SC media lacking leucine and supplemented with glucose (SC + GLU - Leu; non-inducing media) and galactose (SC + GAL - Leu; inducing media) and incubated at 30 ºC for 3 days. **(B)** Western blotting analysis shows that tau40 migrates as a double band between 50-70 kDa as detected by a pan-tau polyclonal antibody in BY4741 wild-type and *mir1*Δ yeast strains. The upper band corresponds to phosphorylated tau. PGK-1 was used as loading control. **(C)** the substitution of *MIR1* ORF with the KanMX cassette was verified by standard PCR, using primers specific for *MIR1* deletion barcode (*mir1*Δ).Controls include PCR mix without DNA (*mir*1Δ Neg Ct) and PCR mix with genomic DNA from wild-type BY4741 (*mir*1Δ BY4741 Ct).

As described in the previous chapter, induction of tau40 expression in the yeast strain *mir1*Δ is lethal to yeast, since its growth is reduced in inducing media, when comparing with the empty vector strain and strain expressing a control protein, as depicted in the dotspot of Figure 4.10. The expression of tau was evaluated by western blotting, confirming that *mir1*Δ-tau40 expressed human tau40 at the expected molecular weight (50-70 kDa) and that the band corresponding to phosphorylated tau was also detected (higher molecular weight band) (Figure 5.2.B). The substitution of *MIR1* ORF with the KanMX cassette was verified by standard PCR, using primers specific for *MIR1* deletion barcode (Figure 5.1.C).

The liquid growth evaluation assay (Figure 5.2) confirmed the phenotype of toxicity of tau40 expression to the growth of *mir1*Δ yeast strain, for all starting OD_{600} tested (0.5, 01 and 0.2), in presence or absence of the vehicle DMSO.

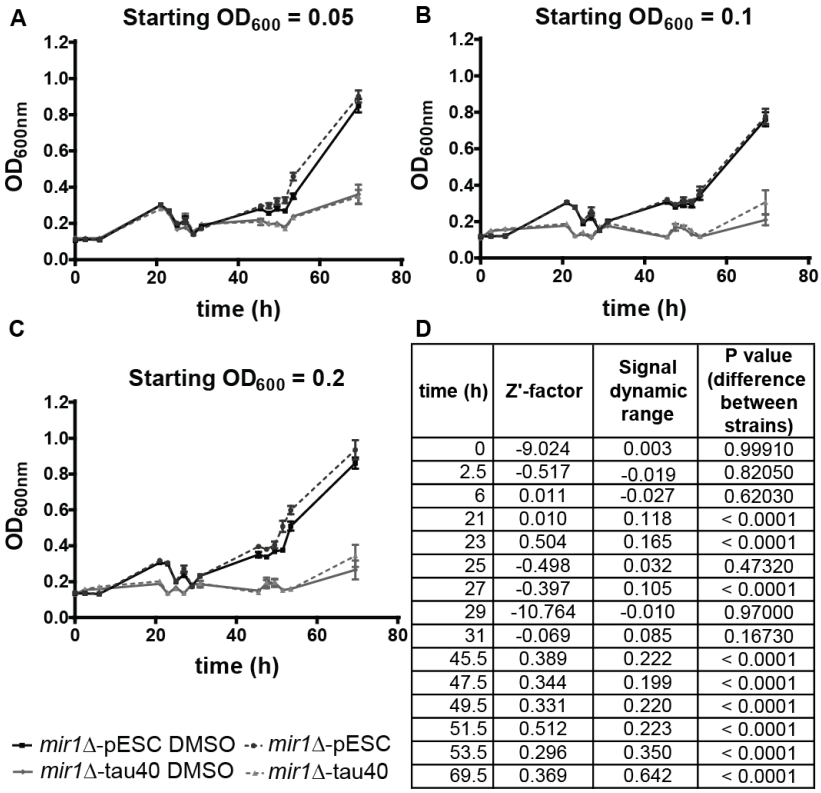

D

time (h)	Z'-factor	Signal dynamic range	P value (difference between strains)
0	-9.024	0.003	0.99910
2.5	-0.517	-0.019	0.82050
6	0.011	-0.027	0.62030
21	0.010	0.118	< 0.0001
23	0.504	0.165	< 0.0001
25	-0.498	0.032	0.47320
27	-0.397	0.105	< 0.0001
29	-10.764	-0.010	0.97000
31	-0.069	0.085	0.16730
45.5	0.389	0.222	< 0.0001
47.5	0.344	0.199	< 0.0001
49.5	0.331	0.220	< 0.0001
51.5	0.512	0.223	< 0.0001
53.5	0.296	0.350	< 0.0001
69.5	0.369	0.642	< 0.0001

Figure 5.2. Validation of the *mir1*Δ-tau40 drug discovery platform.
(A-C) The strain *mir1*Δ-tau40, expressing human tau40, presents a growth delay when compared with the control strain *mir1*Δ-pESC, when inoculated at different starting OD_{600} (0.05, 0.1 and 0.2). Yeast strains were inoculated at different OD_{600} and incubated at 30ºC. Growth monitoring was made by measuring the OD_{600} every 2 h during labour-time. **(D)** Z'-factor, signal dynamic range and P value of the difference between *mir1*Δ-pESC and *mir1*Δ-tau40 growth, at each time point. After the time-point 45.5h there is a consistent very significant difference between the growth of *mir1*Δ-tau40 and the control strain, as well as increasing signal dynamic range. An excellent Z'-factor is obtained at time-point 51.5h.

The results of a 2-way ANOVA followed by Tukey's multiple comparison test (Appendix II), show that there are very significative differences ($p<0.0001$) between the growth curves of *mir1*Δ-pESC and *mir1*Δ-tau40, in presence of DMSO. For the strains inoculated at the starting OD_{600} 0.05, the lag growth phase is longer, resulting in a longer time to reach such significative differences (51.5 h incubation), when compared to strains incubated at the starting OD_{600} 0.1 and 0.2 (41.5 h incubation). Considering the average dynamic range signal parameter (calculated for each time-point and starting OD_{600}), it is higher for the growth curves obtained with a yeast inoculum at 0.2 OD_{600} (Figure 5.2C). Taken together,

these results indicate that yeast strains should be inoculated at an OD_{600} 0.2, to ensure a higher signal dynamic range and increased statistical significance between the growth curves of *mir1*Δ-tau40 and control strain.

The Z'-factor was also calculated at each time point for the growth curve of yeast inoculated at 0.2 OD_{600} (Figure 5.2D). Negative values of Z'-factor were obtained during the lag growth phase, since there was no difference between the growth of *mir1*Δ-tau40 and the control strain, indicating that data obtained at these time-points cannot be considered. However, after 45.5h incubation, the control strain enters in the exponential growth phase and a consistent and very significant statistical difference is calculated relative to *mir1*Δ-tau40 ($p < 0.0001$). This originates a higher signal dynamic range that elicits good values of Z'-factor at the time-point 51.5h (0.512), indicating that at this time point the data obtained in the HTS is reliable. The Z'-factor decreases when *mir1*Δ-tau40 also enters in the exponential growth phase, which decreases the signal dynamic range. Therefore, at each screening campaign, the Z'-factor and signal dynamic range must be taken into account for selection of the assay time-point at which the results can be trusted and analysed.

5.3.2. Eleven natural extracts were able to rescue *mir1*Δ-tau40 yeast growth in the primary screening

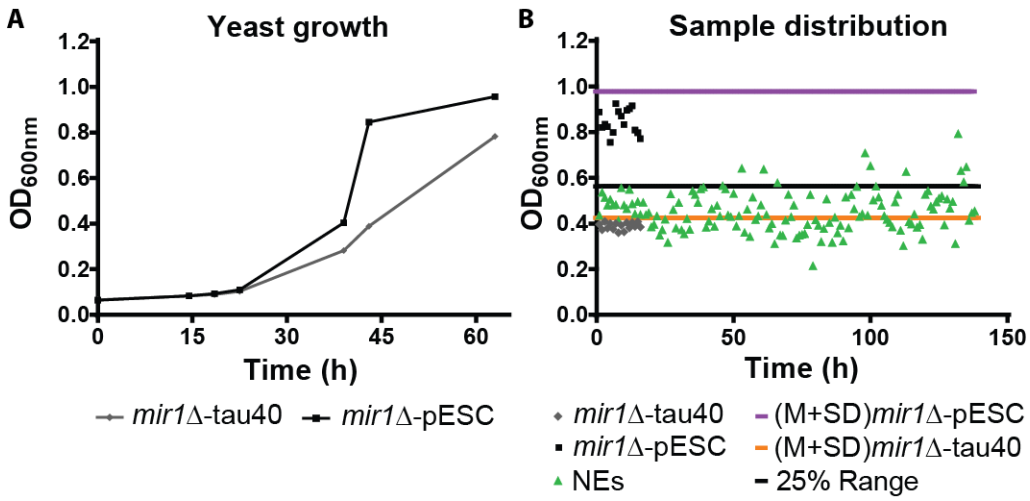

Figure 5.3. *mir*1Δ-tau40 primary screening.
(A) Yeast growth curves: the strain *mir1*Δ-tau40 presents a growth delay when compared with the control strain *mir1*Δ-pESC. Yeast strains were inoculated at OD_{600} 0.2 in inducing media (with galactose), containing DMSO (final concentration 2%) or 5 mg/ml natural extracts (NP) and incubated at 30ºC. Growth monitoring was made by measuring the OD_{600} every 4 h during labour-time. (B) Sample (*mir1*Δ-tau40 + NP) and reference (*mir1*Δ-pESC and *mir1*Δ-tau40 with DMSO) OD_{600} distribution, relative to the dynamic signal range ((M+SD) *mir1*Δ-pESC – (M+SD) *mir1*Δ-tau40). Most of the OD_{600} of *mir1*Δ-tau40 treated with NP fall within the first quarter (25% range) of the dynamic signal range.

The growth of *mir1*Δ-tau40 yeast strain in liquid selective media relative to that of the control strain is presented in Figure 5.3.A. The results obtained were plotted in a sample distribution chart (Figure 5.3.B) and used to calculate the parameters shown in Table 5.1 These values were used to determine the

adequate threshold OD_{600} for hit selection and also the robustness of the HTS assay at time-point 43h, where the highest dynamic signal range was obtained in this campaign.

Table 5.1. Parameters used for hit determination in the primary screening with *mir1*Δ-tau40 drug discovery platform.

	Strains	
Parameters (T=43h)	***mir1*Δ-tau40**	***mir1*Δ-pESC**
(A) Average OD_{600}	0.388	0.846
(M) MAX OD_{600}	0.409	0.925
(SD) STDEV OD_{600}	0.016	0.053
Threshold	0.563	
Z' factor	0.550	

The Z' factor calculated was 0.550, classifying the HTS assay as excellent (Zhang, 1999) and indicating that the results obtained can be trusted. The NPs able to rescue the growth of *mir1*Δ-tau40 yeast strain to OD_{600} values equal or superior to the threshold 0.563 were classified as hits, following the reasoning described in section 2.2.6.3.1 of Chapter 2.

A total of 11 out of 138 NP tested were selected as hits (Table 5.2), representing a primary hit rate of 7.9%. Also presented in this table are the marine bacterial strains from which the NP was extracted. The hits were ranked according with their potency, depending of the ratio between the threshold and the OD_{600} obtained at the time-point 43h for each NP and of the percentage of recovery of *mir1*Δ-tau40 strain.

Table 5.2. Ranking of hits identified in the primary screening with *mir1*Δ-tau40 drug discovery platform.

Ranking	Hit ID	Marine strain	OD_{600} (T43h)	OD_{600} ratio	Recovery (%)
1	AEWC066	LSBA066	0.7943	1.411	66.8
2	AEWC037	RBRS037	0.7093	1.260	51.4
3	AEWC045	RBPS045	0.6532	1.160	41.3
4	AEWC074	LSWA074	0.6486	1.152	40.5
5	AEWC080	LSWA080	0.6420	1.140	39.3
6	AEWC138	LSBA138O2	0.6382	1.134	38.6
7	AEWC073	LSWA073	0.6315	1.122	37.4
8	AEWC024	MGSC024	0.6276	1.115	36.7
9	AEWC061	RBBA061	0.5830	1.036	28.6
10	AEWC184	MGCR184O2	0.5793	1.029	28.0
11	AEWC070	LSWA070	0.5657	1.005	25.5

In the next figure, one example of a hit (*mir1*Δ-tau40 with NP AEWC066), compared with the controls *mir1*Δ-tau40 and *mir1*Δ-pESC (with DMSO) average is shown (Figure 5.4). As it is possible to see, the addition of the NP AEWC066 was able to rescue the growth of *mir1*Δ-tau40 to the OD_{600} levels of the control strain, at the time-point of analysis (T=43 h).

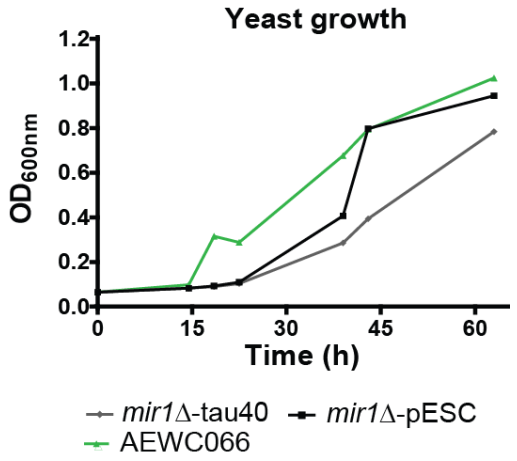

Figure 5.4. Hit example of the primary screening with *mir1*Δ-tau40 drug discovery platform. The growth curve of *mir1*Δ-tau40 treated with 5 mg/ml of the natural extract AEWC066 is compared with the average OD_{600} of the controls *mir1*Δ-tau40 and *mir1*Δ-pESC treated with vehicle (DMSO) only. At the time-point of analysis (T=43h), AEWC066 rescued the growth of *mir1*Δ-tau40 to the levels of the control strain.

5.3.3. Three natural extracts were classified as good candidates for future development in the dose-response confirmation assay

The hits identified in the primary screening were subjected to a confirmatory dose-response secondary screening aiming to eliminate false positives and to define which hits were the best candidates for development of potential drugs for suppressing tau40 toxicity, since it allowed to classify hits according with their potency.

Table 5.3. Parameters for hit determination in the secondary dose-response screening with *mir1*Δ-tau40.

Strains	[NP] (mg/ml)	0.125	0.25	0.5	0.75
***mir1*Δ-pESC**	(A) Average OD_{600}	0.520	0.495	0.447	0.444
	(M) MAX OD_{600}	0.539	0.510	0.518	0.464
	(SD) STDEV OD_{600}	0.013	0.013	0.036	0.009
***mir1*Δ-tau40**	(A) Average OD_{600}	0.269	0.271	0.253	0.215
	(M) MAX OD_{600}	0.321	0.304	0.293	0.240
	(SD) STDEV OD_{600}	0.035	0.024	0.023	0.013
	Threshold	**0.405**	**0.377**	**0.375**	**0.308**

The results obtained were used to calculate the same parameters as in the primary screening. Since 4 concentrations of extract were tested (0.125, 0.25, 0.5 and 0.75 mg/ml) the threshold was calculated for each concentration (Table 5.3). Hit determination was performed per concentration by comparing the threshold with the OD_{600} of *mir*Δ-tau40 strains treated with NP. Hits were ranked according with the classification on Table 2.3 depending on the number of concentrations at which there was a recovery of *mir1*Δ-tau40 yeast growth. The final ranking of NPs, obtained after the secondary dose-response screening, is presented in Table 5.4.

Table 5.4. Ranking of hits obtained after the secondary dose-response screening with *mir1*Δ-tau40.

Hit ID	Initial ranking	Recovery (%)				Ranking
		0.125	0.25	0.5	0.75	
AEWC037	2			73.9	151.0	good
AEWC066	1			39.8	84.5	good
AEWC080	5			27.0	62.0	good
AEWC138	6				84.3	weak
AEWC045	3				71.7	weak
AEWC061	9				55.6	weak
AEWC184	10				39.7	weak
AEWC074	4				33.6	weak
AEWC073	7					false positive
AEWC024	8					false positive
AEWC070	11					false positive

This screening has identified 3 bacterial crude extracts as good candidates for development of drugs, suppressors of tau40 toxicity. Other 5 extracts were positive but weak modulators, representing a hit confirmation rate of 72.7%. Three extracts were considered as false positives, representing a false-positive rate of 2.1%. Overall, this pilot campaign presented a final hit rate of 5.7%.

Next table presents the bacterial strains from which the aqueous extracts were obtained, selected as hits in this screening campaign (Table 5.5).

Table 5.5. Marine bacterial strains information.

Hit ID	Marine strain	Hydrothermal vent	Type of original sample
AEWC037	RBRS037	Rainbow	Rimicardis sp
AEWC066	LSBA066	Lucky Strike	Bathymordiolus azoricus
AEWC080	LSWA080	Lucky Strike	Water
AEWC138	LSBA138O2	Lucky Strike	Bathymordiolus azoricus
AEWC045	RBPS045	Rainbow	Pachichara sp
AEWC061	RBBA061	Rainbow	Bathymordiolus azoricus
AEWC184	MGCR184O2	Menez Gwen	Crab
AEWC074	LSWA074	Lucky Strike	Water

5.4. Discussion

Drug discovery programs focused on tau mechanism of disease are gaining *momentum* and will open new possibilities for therapeutic development for a wide-range of neurodegenerative disorders, including AD. To foster drug discovery for tauopathies, a new GPS D^{2TM} yeast-based drug screening system was developed and coupled with a unique library of marine bacteria extracts allowing the identification of 3 natural products capable of modulating tau toxicity in a mitochondrial-compromised environment.

One of the specific goals of this doctoral work was to develop a robust yeast-based platform for the identification of new bioactives as potential suppressors of tau toxicity. Although many important features of tau pathology are replicated in yeast, tau expression is non-toxic to yeast growth (Chapter 3) (Vandebroek *et al.*, 2005a). Therefore, the data generated by the loss-of-function tau toxicity enhancer genomic screen performed in Chapter 4 was used to prioritize one yeast deletion strain sensitive to tau toxicity, eliciting a phenotype that could be used as a read-out in a screening system. Following a bottom-up high throughput strategy, the list of yeast deletion strains considered as hits was trimmed down until the yeast strain *mir1*Δ was selected as suitable for the development of such screening platform. The deleted ORF, *MIR1*, codes for the mitochondrial phosphate carrier, essential for ATP production by the mitochondria (Palmieri, 2013). Therefore, the lack of expression of this gene might compromise the mitochondrial function of the cell (*vide* Chapter 6 for preliminary results of the study of this gene in mammalian cells).

In solid media, the yeast strain *mir1*Δ-tau40 demonstrated a reproducible and specific synthetic lethal phenotype after induction of tau40 expression (Chapter 4). In the present work, validation tests were performed to evaluate the viability of using *mir1*Δ-tau40 as a screening system. After verification of the ORF deletion and confirmation of tau expression and phosphorylation, this phenotype was verified in liquid media, with the yeast strain *mir1*Δ-tau40 presenting a very significative growth delay when compared to the control strain (*mir1*Δ-pESC-Leu, the empty vector). The best conditions for yeast culture were determined, identifying the starting OD_{600} of 0.2 as the most appropriate to perform the screen, since the signal dynamic range was higher and the yeast lag growth phase was smaller, allowing for reduced time-length screening campaigns. Indeed, very significative differences between the growth of *mir1*Δ-tau40 and the control strain were consistently observed after 45.5h incubation. The overall quality of this screening system as an HTS assay was assessed using a variation of the screening window coefficient (denoted Z'-factor), that takes into account the assay signal dynamic range and the data variation of the controls (standard deviation [SD] of untreated *mir1*Δ-pESC and *mir1Δ*-tau40 strains) without the need of a positive control compound, i.e. a molecule previously known capable of suppressing tau toxicity (Zhang, 1999). The Z' was calculated for each time-point of yeast growth monitoring during the validation assay and found to be 0.512, at 51.5 h incubation, classifying this platform as robust for HTS assays, specifically at this time point. Before this time-point, the Z' values were negative, and therefore the results could not be considered. Above this time-point the Z' value was inferior to 0.4, and hence, results were less reliable, particularly due to increased data variation. This sort of analysis helped determining the best time-point to evaluate the screening results.

With the confirmation that this screening system was robust to perform reliable HTS assays, a proof-of-concept screen was performed using a small, but unique, library of 138 natural extracts obtained from bacteria collected at the extreme environments of the Portuguese hydrothermal vents of the Mid-Atlantic Ridge (Menez Gwen, Lucky Strike, Rainbow and Monte Saldanha) (Martins *et al.*, 2013b; Rodrigues *et al.*, 2011). The screening system was designed to select molecules capable of rescuing the growth of the platform strain to the levels of the control strain, above a strictly defined threshold. The primary screening, classified with a Z' factor of 0.505 at 43 h incubation, resulted in the identification of 11 hits. A secondary dose-response assay confirmed 3 NPs as good suppressors of tau toxicity and another 5

NPs as weak suppressors of tau toxicity, in a cellular environment with compromised mitochondria function. This corresponds to a final hit rate of 5.7 %, which is above the expected hit rate (around 2%). This may be due to the small number of starting samples.

It is widely recognized that yeast is a suitable organism model for HTS drug discovery programs for human diseases, due to the high degree of conservation of biological processes and its extreme amenability for genetic manipulation, short generation times, genetic tractability and scalability (Khurana & Lindquist, 2010). Also, yeast-based screening systems are extremely informative and are cost-competitive, allowing short time frames for hit identification. The GPS D^{2TM} technology further maximizes yeast usefulness by refining the screening criteria to develop stringent screening tools that potentially reduce attrition rates in subsequent phases of drug discovery. This was accomplished by leaving unaltered the two major yeast efflux pumps, *PDR5* and *SNQ2*, usually deleted in other yeast-based screening systems to increase yeast sensitiveness to drugs (Cerejo *et al.*, 2012; Kaur & Bachhawat, 1999; Kolaczkowski *et al.*, 1998). Keeping these transporters intact allows to detect only compounds with high specificity and efficacy. This strategy deliberately loses potential hits, but ensures that only the most potent candidates are selected (Cerejo *et al.*, 2012; Kramer *et al.*, 2007; Paul *et al.*, 2010). This yeast system also addresses key features of a candidate bioactive, such as membrane permeability, toxicity and biological stability, increasing the predictability of the assay and allowing data-driven decisions for candidate selection (Cerejo *et al.*, 2012).

The use of NPs has been increasingly brought back for drug discovery and development, particularly products derived from bacteria, following the failure of automated chemical synthesis in delivering new drugs in the market (Lawrence, 2015). The rationale is that "*nature has had billions of years to perfect widely diverse molecules*" designed to target proteins in order to elicit a biological response. Its use as drugs would then be dependent on their modification to effectively target human proteins (Lawrence, 2015). Particularly, the collection used in this work is very appealing for the search of new industrially relevant bioactives, since the phenotypic analysis of the bacteria strains that compose the collection indicates that almost half of the collection is constituted by new prokaryotic species and, hence, in principle, higher the probability of identifying new biological entities (Martins *et al.*, 2013b; Rodrigues *et al.*, 2011). However, while NPs constitute a rich source of new biological entities, they also introduce additional challenges to the drug discovery and development programmes (Bauer & Bronstrup, 2014; Martins *et al.*, 2014). These challenges are approached in detail by Martins and colleagues in their review of NP exploration for pharmaceutical and cosmeceutical industries (Martins *et al.*, 2014).

Regarding the three NPs selected in this work as good starting points for drug discovery and development programs aiming to identify bioactives suppressors of tau toxicity, AEWC037 was extracted from a marine bacteria classified in the genus *Pseudoalteromonas sp.*, probably being a new species as preliminary whole genome sequencing seems to suggest (Martins *et al,* data not published), collected near 2300 m depth from the Rainbow hydrothermal vent (Martins *et al.*, 2013a; Martins *et al.*, 2013b). Remarkably, this extract has been selected as hit in other GPSD^{2TM} screening systems designed for other applications for the pharmaceutical and cosmeceutical industries. AEWC066 and AEWC080 were extracted from LSBA066 and LSWA080, respectively, both collected at Lucky Strike

vent, near 1700 m depth. To date, there is no conclusive information of the final taxonomy of these marine bacteria. Although these aqueous extracts were obtained from marine bacteria able to grow on nutrient broth supplemented with 3% sea salts at 22ºC for 72 h (Martins *et al.*, 2013b), and therefore already adapted to grow in laboratory conditions, the definitive identification of the microorganism and the technical challenges of supply and mass production, following good manufacturing practices, would have to be addressed as early as possible in a drug discovery and development program based on one of these extracts, in order to ensure a sustainable bioactive (Kingston, 2011; Martins *et al.*, 2014). Therefore, aspects such as the isolation and cultivation method of the microorganism, understanding and exploration of the biosynthesis pathway for optimization of the bioactive bioprocessing should be taken into account (Martins *et al.*, 2014).

Preferably, this work should be addressed in parallel with the identification of the bioactive and its structure elucidation, which is absolutely indispensable for the pharmaceutical industry. This task is usually challenging, since it is traditionally performed by a bioassay-guided fractionation of the crude extract, until the active principle – the lead molecule – is identified (Sarker *et al.*, 2006). The crude extracts would be separated into various discrete fractions containing compounds of similar polarities or molecular sizes, which would then have to be re-tested for potency with the screening system *mir1*Δ-tau40. This is a labour intensive process and not always a guarantee of success, particularly due to the complex nature of crude extracts (Martins *et al.*, 2014). Different molecules exist in a crude extract and a given activity may be a result of a synergistic interaction of two or more molecules that may disappear when sub-fractions are evaluated for efficacy. Moreover, false negative readouts may also occur more often, either because the active principle is present at low concentrations or because other constituents of the extract inhibit its activity (Martins *et al.*, 2014). Indeed, the use of crude extracts in discovery programs has been recently discouraged (Kingston, 2011). However, considering the costs of pre-fractionating a crude extracts library, particularly stressful for a small biotech company, BIOALVO continued to include the use of crude extracts libraries in its business model. The company followed a *develop-on-demand* strategy, meaning that only extracts found to be active in a given application would be fractionated, while at the same time worked internally to fractionate its proprietary libraries.

Considering the NPs used in this work, they were obtained by water aqueous extraction of the bacterial biomass, followed by freeze drying and powder collection (Martins *et al.*, 2013b). This method of extraction results in a complex mixture containing a large amount of inorganic salts and highly polar macromolecules, mostly proteins (Sarker *et al.*, 2006). Usually, organic extracts contain less polar compounds, which are usually secondary metabolites of lower size and with more drug-like features, thereby being preferred for drug discovery and development programs (Sarker *et al.*, 2006). However, peptides and proteins therapeutics are rising in prominence (Hu, 2011; Leader, Baca & Golan, 2008; Ratnaparkhi, Chaudhari & Pandya, 2011). This is because protein therapeutics present several advantages over small-molecule drugs, namely, higher specificity and potency, lower incidence of toxicity and, for diseases in which a gene is mutated or deleted, protein therapeutics can provide effective replacement treatment without the need of gene therapy (Hu, 2011; Leader *et al.*, 2008). From a financial perspective, protein therapeutics clinical development and FDA approval time may be faster than that of small molecules and because proteins are unique, far-reaching patent protection can be

obtained by companies (Leader *et al.*, 2008). Indeed, the market and technology research firm Frost & Sullivan has reported that over 40 peptide-based drugs have been approved and that approximately 800 are being developed to treat allergies and cancer as well as AD, HD and PD (Leader *et al.*, 2008).

The knowledge on the mechanism of disease and mode of action of the bioactive is also a strong requirement in drug discovery in general but with NPs in particular (Martins *et al.*, 2014). This is because any medicinal chemistry programme applied in the lead development phase, already more challenging due the high complexity of the biological molecules, has to take into account the mode of action of the compound so that a NP can be structurally changed to enhance potency and optimize pharmacodynamics, pharmacokinetic and safety properties (Bauer & Bronstrup, 2014; Martins *et al.*, 2014). In the specific case of the present work, the drug discovery plan must include the understanding of the mechanisms of tau toxicity in the absence of PiC, so that the mechanism of action of the bioactive can be explained and explored. Also, due to the incipient characteristic of the data used to produce this screening system, PiC is not yet a fully validated target for therapeutic intervention in neurodegeneration. A successful drug discovery program depends on this validation (*vide* Chapter 1, 1.7.1.1) (Hughes *et al.*, 2011).

The development of a secondary screening platform, using a more relevant biological organism model, such as neural mammalian cells, will be necessary in order to confirm the bioactive efficacy obtained in the yeast-based screening system. Depending on the nature of the identified bioactive, specificity assays should also be performed, using models with other neurodegenerative disease-related proteins, or even a simple fluorescent protein overexpression, to address if the compound is specific to the drug target in question (tau) or if it acts in the general protein quality control processes of the cell.

Considering that most investigational new drugs fail in preclinical and clinical phases of development because of inadequate absorption, distribution, metabolism, excretion and/or toxicity (ADMET), *in vitro* screening methods should be applied earlier in the drug discovery process to decrease this attrition rate (Passeleu-Le Bourdonnec *et al.*, 2013; Tsaioun & Kates, 2011). One of the issues that should be addressed at the hit-to-lead process is the bioactive toxicity, using, for example, *in vitro* hepatotoxicity assays in cells, measuring hepatocytes viability after bioactive treatment, simulating acute (2 h) and chronic (24 h) administration (Cerejo *et al.*, 2012). Other aspect to be addressed early in the program, particularly important since the target are CNS disorders, is the permeation of the blood brain barrier (BBB) to the bioactive (Passeleu-Le Bourdonnec *et al.*, 2013). The BBB is a highly selective barrier that regulates the passage of molecules from the blood to the brain, which is very important for the uptake of essential nutrients or active CNS drugs and protects the brain from undesirable compounds (Passeleu-Le Bourdonnec *et al.*, 2013). With many drugs targeting the CNS failing because of inefficient crossing of the BBB, this issue will be even more challenging in the current drug development plan, since there is a high probability that the bioactive is a peptide or protein, with large molecular weight. This implicates that an effective formulation and innovative drug delivery system should be developed and tested in conjunction with BBB permeation in *in vitro* assays (Leader *et al.*, 2008). The solubility and metabolic stability of the bioactive must also be evaluated to ensure proper bioavailability of the molecule. Coupling the information of efficacy, safety, specificity, stability and solubility of the bioactive

early in the programme will allow the medicinal chemists to further refine the molecules in development, eliminating weak candidates, and eliciting data-driven decisions towards the identification of the lead molecule, as well as the second *best-in-class* molecule (Tsaioun & Kates, 2011).

Finally, the development plan should also include an early assessment of the market requirements towards the bioactive, such as market space, best-fit and competition segment, intellectual property space, price tag per kilogram and supply volume necessary for the chosen market, as well as regulatory requirements for bioactive approval (Martins *et al.*, 2014).

Despite all the challenges that the use of NP pose to a drug discovery programme, the marine bacteria crude extracts identified in this work constitute excellent starting points for the discovery of new safe and effective biological entities for the development of innovative therapies for a wide-range of tau-related disorders, such as AD.

.

Chapter 6.

Initial characterization of a mammalian cell model of PiC silencing

6.1. Abstract

Results in yeast indicate that concomitant deletion of *MIR1* and overexpression of tau is lethal to yeast growth. *MIR1* human homologue is *SLC25A3* which codes for the mitochondrial phosphate carrier (PiC). PiC catalyses the transport of inorganic phosphate to the mitochondrial matrix and is essential for ATP production and O_2 consumption. Previous data obtained in yeast suggest that tau is involved in mitochondrial dysfunction and that PiC may have an important role in mitochondrial dysfunction in tauopathies. The current work presents the first steps towards the creation of a mammalian cell model aimed to replicate and validate in future studies the results obtained in yeast. Thus, PiC expression was knockdown in human brain neuroglioma H4 cells using shRNA and the resulting phenotype was evaluated in terms of cell viability and mitochondrial function. PiC knockdown was achieved after 72h, with about 65% efficiency, and was not cytotoxic. This knockdown efficiency was insufficient to alter calcium uptake by mitochondria or mitochondrial membrane potential, but cells presented a reduced bioenergetic profile due to decreased ATP production. The future steps of completion of this cell model are also discussed. A model in which tau overexpression is associated with PiC knockdown would be useful not only to understand tau mechanisms of toxicity involving the mitochondria, but also to evaluate PiC as a drug target for tauopathies, potentially constituting a valuable secondary screening system for analysis of the efficacy of drugs in development, which are potential suppressors of tau toxicity.

Keywords: H4 cells, mitochondria, PiC knockdown, oxygen consumption, mitochondrial bioenergetics, ATP production, cytotoxicity

6.2. Introduction

The loss-of-function tau toxicity enhancer genomic screen performed in yeast (described in Chapter 4) provided a framework for the identification of novel drug targets and/or biomarkers for therapeutic intervention in tauopathies. The high-throughput strategy allowed to prioritize one yeast gene – *MIR1* – which deletion increases yeast sensitiveness to tau toxicity. The human homologue of *MIR1* is the gene *SLC25A3* that codes for the mitochondrial phosphate carrier protein (PiC), essential for ATP production and O_2 consumption, since it catalyses the transport of inorganic phosphate (Pi) to the mitochondrial matrix (Palmieri, 2013). Interestingly, mutations in *SLC25A3* cause an oxidative phosphorylation disorder, fatal within the first year of life (Mayr *et al.*, 2007). Additionally, PiC plays a role in the regulation of the mitochondrial permeability transition pore (mPTP), important in the regulation of apoptosis (Varanyuwatana & Halestrap, 2012). The reproducible and specific lethal phenotype observed upon induction of tau expression in the yeast mutant *mir1*Δ suggests that tau is involved in mitochondrial dysfunction, considering the high degree of conservation of basic cellular processes and homology of genes involved in human diseases between yeast and humans (Khurana & Lindquist, 2010; Tenreiro & Outeiro, 2010). It also suggests that PiC has a potential relevant function in mitochondrial dysfunction in the context of tau-related disorders.

Increasing evidences place mitochondrial dysfunction in several neurodegenerative disorders, from which AD and other tauopathies are no exception (Schon & Przedborski, 2011). Mitochondria are the powerhouses of the cell with a critical role in cell survival since they regulate energy metabolism and apoptotic pathways (Brand & Nicholls, 2011; Eckert *et al.*, 2014; Moreira *et al.*, 2007). Particularly for neurons, the maintenance of mitochondria dynamics, homeostasis and bioenergetics is even more important, since these cells greatly depend on mitochondrial-derived ATP (Eckert *et al.*, 2014; Moreira *et al.*, 2007; Schon & Przedborski, 2011). Mitochondria produce ATP through the combined action of the tricarboxylic acid (TCA) cycle and the oxidative phosphorylation (OXPHOS) system of the electron transport chain (ETC). The ETC is composed by four protein complexes I, II, III and IV, as well as two electron carriers, ubiquinone/coenzyme Q and cytochrome C, which are localized to the inner mitochondrial membrane and in the intermembrane space, respectively (Eckert *et al.*, 2014; Moreira *et al.*, 2007; Schon & Przedborski, 2011). Through the oxidation of substrates obtained from nutrients, the ETC generates a proton gradient across the inner membrane to drive ATP synthesis *via* ATP synthase. At the same time, electrons are transferred to oxygen to produce water. The production of energy by the OXPHOS is also accompanied by the formation of reactive oxygen species (ROS) (Moreira *et al.*, 2007; Schon & Przedborski, 2011). Increased ROS production associated with antioxidant imbalance leads to oxidative stress, which may cause neuronal damage (Moreira *et al.*, 2007). Dysfunction of the OXPHOS system and related oxidative stress have been described in several neurodegenerative disorders (Schon & Przedborski, 2011). Regarding AD, three modes of involvement of mitochondrial dysfunction in neuropathology can be envisaged: (i) intrinsic dysfunctional mitochondria may cause increased ROS production, leading to oxidative stress and neurodegeneration; (ii) mitochondrial dysfunction may be a downstream consequence of other pathological processes, such as toxicity caused by Aβ and tau and/or (iii) mitochondrial dysfunction might synergistically act with tau and/or Aβ

toxicity, exacerbating protein's toxicity (Eckert *et al.*, 2014; Schon & Przedborski, 2011). Moreover, defects in mitochondrial dynamics have been recently proposed to be relevant in the progression of late-onset neurodegeneration (Schon & Przedborski, 2011).

Regarding tau, several studies performed in tau transgenic mouse models point towards a pathological role involving mitochondria (reviewed in detail by Eckert *et al.*, 2014). Increased levels of hyperphosphorylated tau disrupt mitochondrial dynamics by impairing fission, leading to elongated mitochondria, which may affect mitophagy, a process of mitochondria quality control (Eckert *et al.*, 2014). Additionally, phosphorylated tau also impairs anterograde transport of mitochondria, and insufficient transport of mitochondria to synapses leads to synaptic degeneration (Eckert *et al.*, 2014). Moreover, tau has been found to impair the activity of NADH dehydrogenase (complex I of the ETC), which leads to increased production of ROS and decreased ATP production (Eckert *et al.*, 2014). Tau also reduces the activities of detoxifying enzymes such as superoxide dismutase (SOD) and through its interaction with voltage-dependent anion channel proteins (VDAC), located at the outer mitochondrial membrane, it may block the formation of mitochondrial permeability transition pore (Eckert *et al.*, 2014; Manczak & Reddy, 2012).

No correlation between PiC and tau physiological and pathological functions has been described yet. One CHIP-Seq-based study has identified *SLC25A3* as a target of the nuclear respiratory factor-1 (NRF1), a transcription factor that activates the expression of nuclear genes essential for mitochondrial biogenesis and function, including mitochondrial respiratory complex subunits and regulatory factors involved in the replication and transcription of mitochondrial DNA (Satoh *et al.*, 2013). The authors of this study based their hypothesis on the fact that NRF1 may be relevant in neurodegeneration, since the disruption of its orthologue in *Drosophila* caused a severe neurological defect (Satoh *et al.*, 2013). Apart from this, no further evidences of involvement of *SLC25A3* in neurodegeneration have been found in the literature.

Despite the recognized advantages of yeast for the study of neurodegeneration and for systems biology studies, yeast is unicellular and devoid of a nervous system (Khurana & Lindquist, 2010; Miller-Fleming *et al.*, 2008). Therefore, the findings obtained in yeast (described in Chapter 4) should be validated in models of higher biological relevance. By using a mammalian cell line, this work aims to perform the first steps towards the validation of PiC as a novel drug target for tauopathies. Hence, PiC knockdown was optimized in the human brain neuroglioma H4 cell line using shRNA. The resulting phenotype was then evaluated in terms of cell viability and mitochondrial function. Taking into consideration the results obtained, a set of suggestions are given to complete this model, which might constitute a useful tool for validation of PiC as a drug target; a potential secondary screening system to evaluate the efficacy and safety of drug candidates; and as a disease model to further understand tau pathology at the mitochondria level.

6.3. Results

6.3.1. PiC knockdown apparently was not toxic to cells

Prior to any experiment, PiC protein levels were determined in H4 total cell extracts. The mitochondria subcellular fraction was used as a positive control, since PiC is localized at the inner mitochondrial membrane (Varanyuwatana & Halestrap, 2012). Increasing amounts of total protein extracts were analysed (using 25, 50 and 75 µg) in order to determine the minimal amount of loading protein that would enable the visualization of PiC protein levels using a mouse polyclonal anti-human *SLC25A3* antibody (Abcam, Cambridge, UK). HSP60 and beta-actin were used as mitochondria and total protein loading controls, respectively (Figure 6.1).

In the total protein extracts, PiC was detected as a double band appearing slightly below the 35 kDa control band (estimated molecular weight was 40 kDa). The minimal amount of protein loading that elicited the detection of PiC in total cellular extracts was 50 µg. In the mitochondrial fraction a second band of around 25 kDa of "undetermined nature" as referred by the antibody supplier, was also detected.

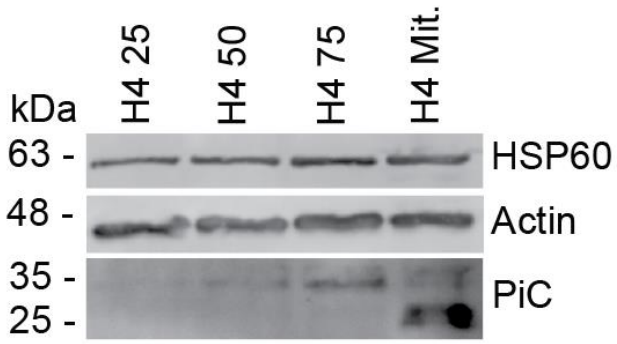

Figure 6.1. Optimization of immunoblot for detection of the mitochondrial phosphate carrier (PiC).
PiC was detected when 50 µg of total cell extracts were used. H4 total cell protein lysates (lanes 1-3) were loaded in increasing amounts of protein in a 12% SDS-PAGE together with a mitochondrial fraction of H4 cells (lane 4, H4 Mit.). Membrane bound PiC was detected with a mouse polyclonal anti-human antibody *SLC25A3*. Protein loading was controlled using antibodies against HSP60 and actin, respectively, a mitochondrial and cytoskeleton protein, the later for analysis of total cell extract.

The next step consisted in determining which shRNA transcript could conduce to a more efficient knockdown of PiC. For that purpose, a preliminary optimization of H4 transfection was performed using the lipofection reagent FuGENE and the plasmid pCDNA3-EGFP (Figure 2.3) to identify the most efficient DNA:FuGENE ratio and cell density, at 24h, 48h and 72h post-transfection. Transfection efficiency was evaluated by visually estimating the number of cells expressing eGFP by fluorescence microscopy. The most efficient DNA:FuGENE ratio was 1:3 and the cell densities that conduced to lower cell death, whilst still presenting a good transfection efficiency were: 2.2 x 10^5 cells/well for 24h, 1.6 x 10^5 cells/well for 48h and 1.1 x 10^5 cells/well for 72h.

After extraction and purification of shRNA plasmids and confirmation of the integrity of the DNA molecule by double restriction analysis, each shRNA construct was transfected into H4 cells following the pre-

determined experimental settings. Analysis of protein expression by Western blotting after 24h, 48h and 72h transfection, demonstrated that the shRNA 2 (mature antisense sequence: AATGTCAGCAAAGAATTCAGC) caused the silencing of *SLC25A3* after 72h transfection (Figure 6.2. A) with and efficiency of around 65% (Figure 6.2.B).

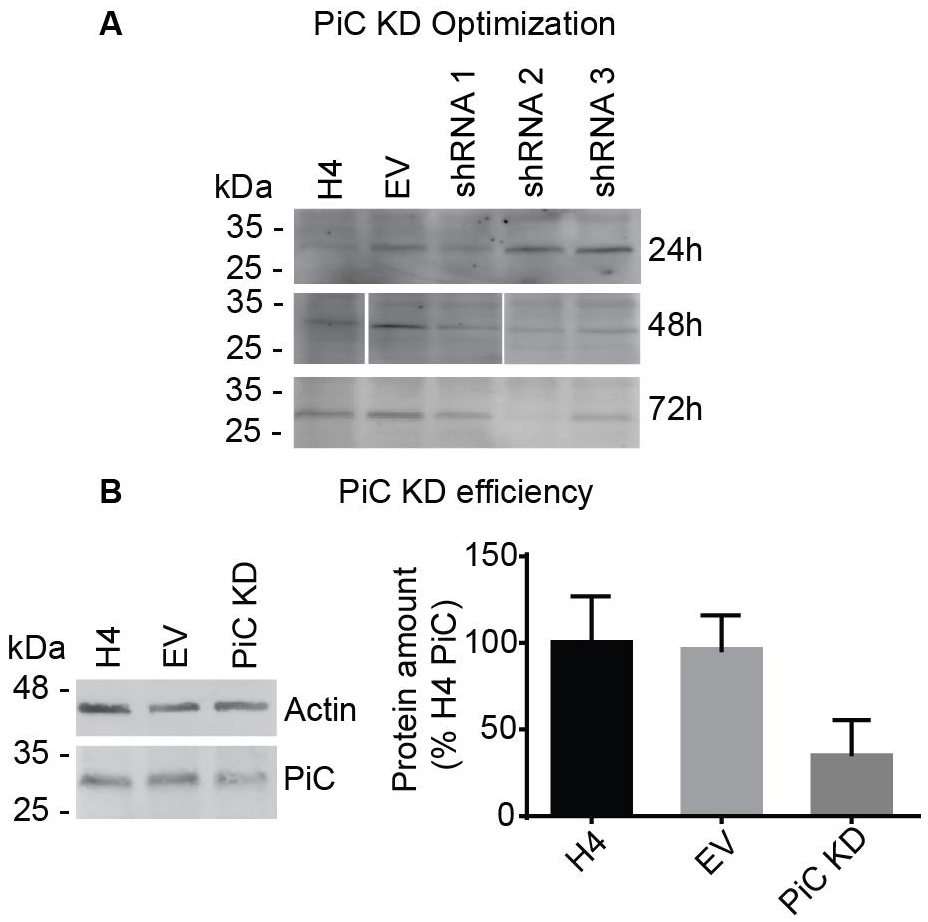

Figure 6.2. Knockdown of *SLC25A3* in H4 cells.
(A) The shRNA transcript that elicited an efficient knockdown of *SLC25A3* was shRNA2, 72h post-transfection. H4 cells were transfected with three shRNAs for knockdown of *SLC25A3*. After 24h, 48h and 72h post-transfection, total protein extracts were collected and 50 µg of protein were applied in 12% SDS-PAGE. PiC expression level was evaluated in comparison with untransfected cells (H4) and cells transfected with empty vector (EV). Note: empty spaces in the 48h membrane are empty wells removed from the picture. **(B)** PiC knockdown was achieved with an average efficiency of about 65% using shRNA2 transcript. Untransfected H4 cells (H4) and transfected with empty vector (EV) and with the plasmid carrying the selected PiC shRNA (PiC KD) were collected 72h post-transfection for extraction of total protein. Protein levels were quantified using Image J and normalized to actin. The percentage of PiC protein levels was calculated relative to H4 untransfected cells. A representative blot of three independent experiments is shown.

The effect of PiC knockdown on cell viability was also evaluated, now using only the selected shRNA transcript (shRNA2) (Figure 6.3). Cell viability was assessed by indirectly measuring the activity of lactate dehydrogenase (LDH) in the culture media after 72h of transfection (Figure 6.3). Knockdown of PiC did not significantly increase H4 cell death, probably due to low number of replicates and high variability of knockdown efficiency between replicates. Many transfected cells were detached from the tissue culture vessel after 72h of incubation. Therefore, after removal of the culture media for analysis of extracellular LDH release, which was followed by a wash with PBS, many cells were lost before the lysis of the cell monolayer necessary for estimation of intracellular LDH. Hence, intracellular LDH activity

was not considered because it would be underestimated and accordingly, the % of LDH release could not be determined.

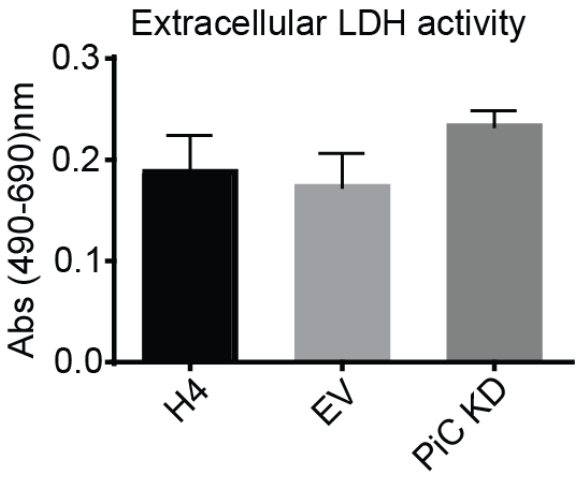

Figure 6.3. PiC knockdown effect on cell viability.
PiC knockdown (PiC KD) apparently did not influence cell death, as indicated by unaltered activity of lactate dehydrogenase (LDH) in the extracellular medium. Results correspond to average ± SEM of 3 independent experiments performed in duplicates to quadruplicates.

6.3.2. Tau phosphorylation at Ser202/Thr205 was not altered by PiC knockdown

Tau phosphorylation at Serine 202 and Threonine 205 (Ser202/Thr205) was evaluated in H4 cells subjected to PiC KD, using the phospho-tau AT8 antibody. Hyperphosphorylation of tau in these epitopes has been shown to be toxic, preventing the interaction of tau with neuronal membranes and inducing apoptosis, and is predominant in neurofibrillary tangles (Avila *et al.*, 2012; Gotz *et al.*, 2010).

Total tau was detected as a triple protein band migrating between 48 and 63 kDa, probably due to the inherent phosphorylation status of this protein (Figure 6.4.A). Phosphorylated tau at the pathology-related epitopes Ser202/Thr205 (AT8-tau) was detected at 50 kDa. When protein levels were normalized to actin (Figure 6.4.B, left side graph), total tau levels did not vary significantly between samples. For phosphorylated tau (AT8-tau) there was a tendency (although not statistically significant) for increased phosphorylated tau between untransfected and PiC knockdown cells (Figure 6.4. B, left side graph). When phosphorylated tau levels (AT8-tau) were normalized to total tau protein levels, no differences between phosphorylated AT8-tau were detected (Figure 6.4. B right side graph). However, an increased phosphorylated tau/total tau was also observed when comparing untransfected with EV-transfected cells, suggesting that the transfection protocol might have affected the pathways that influenced tau phosphorylation.

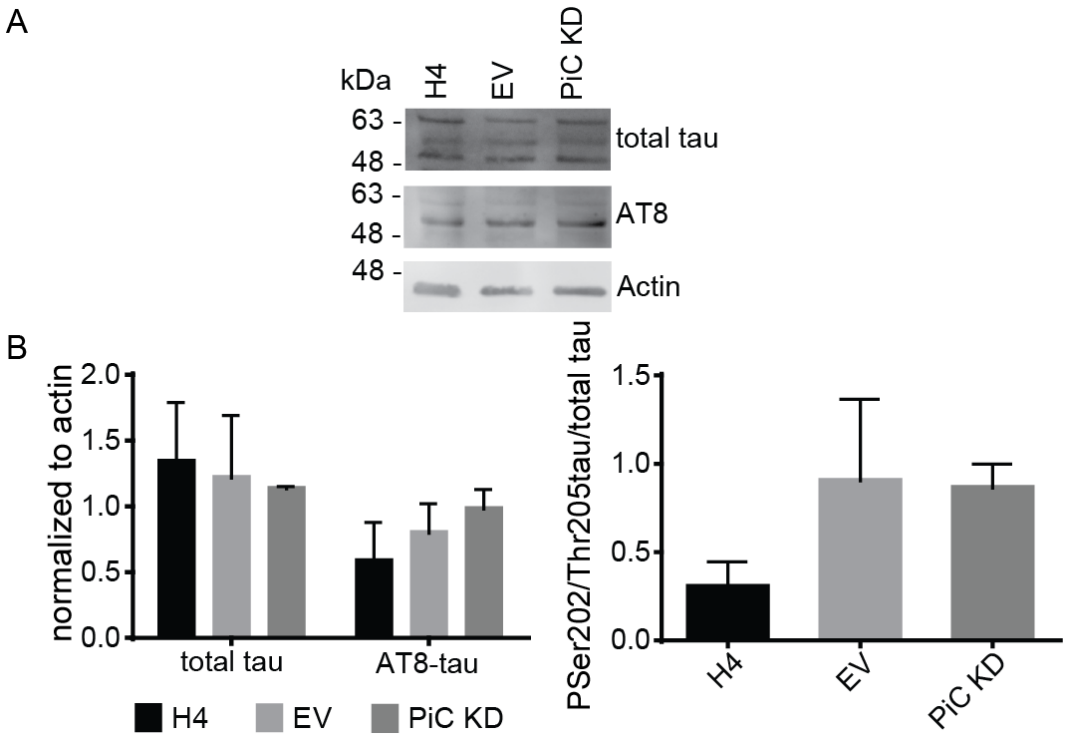

Figure 6.4. Levels of tau phosphorylation at Ser202/Thr205 (AT8-tau).
(A) Representative immunoblot for detection of total tau and phosphorylated tau with the antibody phospho-tau AT8. Actin was used as loading control. Total tau was detected as a triple band between 48-63 kDa. Phosphorylated tau at the epitopes Ser202/Thr205 (AT8-tau) was detected around 50 kDa. **(B)** Total and phosphorylated tau levels. Total tau levels normalized to actin (left bar chart) did not significantly change between samples. There was a tendency for increased phosphorylated tau when comparing the expression of the vector carrying PiC shRNA (PiC KD) with untransfected H4 cells (H4). However, this tendency was not visible when tau phosphorylation levels were normalized to total tau (right bar chart). There was a tendency for increased (although not statistically significant) phosphorylated tau in transfected *versus* untransfected cells (right bar chart). Total protein extracts were collected after 72h transfection. Results correspond to average ± SEM of 3 independent experiments.

6.3.3. PiC knockdown cells presented apparent compromised mitochondrial function

Different methodologies were used to characterize mitochondrial function in PiC knockdown cells. Indeed, the combination of measurements of mitochondrial respiration rate, mitochondrial membrane potential and variation in mitochondrial Ca^{2+} is more informative than the use of either technique alone (Brand & Nicholls, 2011).

6.3.3.1. PiC knockdown did not affect intracellular calcium levels or mitochondrial membrane potential

Changes in mitochondrial membrane potential ($\Delta\Psi_m$) and intracellular calcium levels ($Ca^{2+}i$) were evaluated using two different probes, $TMRM^+$ and Fura-2AM, respectively, after silencing PiC expression for 72h (Figure 6.5).

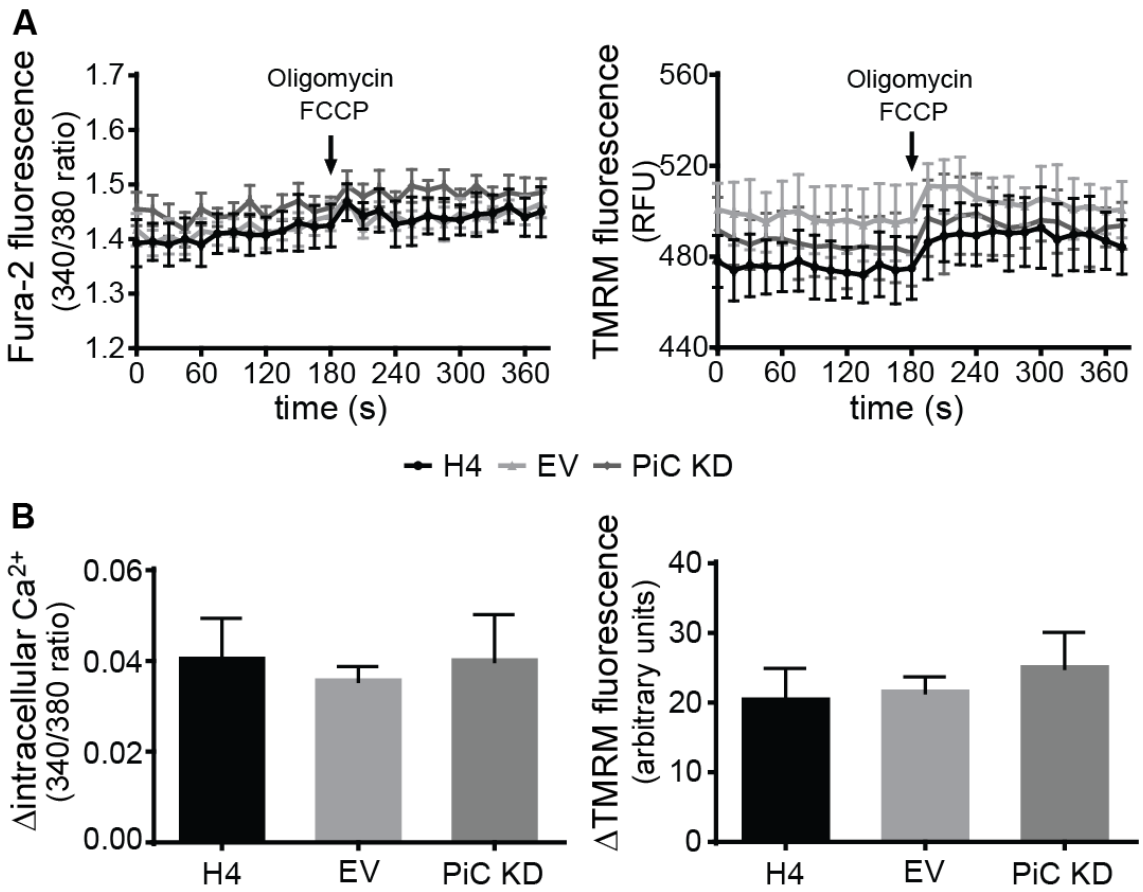

Figure 6.5. Variation of intracellular Ca^{2+} and mitochondrial membrane potential ($\Delta\Psi_m$) in PiC knockdown H4 cells.
(A) Representative tracings of Fura-2 fluorescence 340nm/380nm ratio (left chart) and $TMRM^+$ fluorescence (right chart). **(B)** Difference between the maximal fluorescence values achieved after addition of oligomycin plus FCCP and the basal fluorescence level. There were no differences in intracellular Ca2+ levels (left bar chart) or in $\Delta\Psi_m$ between samples. H4 cells were incubated with $TMRM^+$ and Fura-2AM 72h post-transfection. Bottom-read fluorescence levels of TMRM were measured at λ_{EXC} 540nm/ λ_{EM} 590nm (cut-off at 570 nm) whilst Fura-2 fluorescence was monitored at λ_{EXC} 340nm and λ_{EXC} 380nm with fixed λ_{EM} 510. Results correspond to average ± SEM of 3 independent experiments performed in duplicates to quadruplicates.

No significative differences in basal Ca^{2+}i or mitochondrial accumulated Ca^{2+} (detected following the addition of oligomycin and FCCP) were detected in PiC KD cells, when compared to controls. This suggests that Ca^{2+} homeostasis was not affected by PiC silencing. The $\Delta\Psi_m$ of PiC knockdown cells did not differ from $\Delta\Psi_m$ of controls (untransfected H4 cells or transfected with empty vector), as evaluated through similar retention of $TMRM^+$ in mitochondria.

6.3.3.2. Apparent reduced mitochondrial respiration rate and ATP production in PiC knockdown H4 cells

The OCR of PiC KD cells was apparently lower than the OCR of H4 untransfected cells and cells transfected with empty pLKO.1 plasmid (Figure 6.6.A). No statistical difference was obtained possibly due to the low number of replicates and high variability. Nonetheless, the different components of the bioenergetic profile were analysed. All parameters of mitochondrial function obtained from the bioenergetic profile were decreased in PiC KD cells, in particular the basal respiration, ATP production,

maximal respiration and the spare respiratory capacity, which decreased by about 75% when compared to EV-transfected cells (Figure 6.6). These results suggest that PiC KD cells have compromised mitochondrial function.

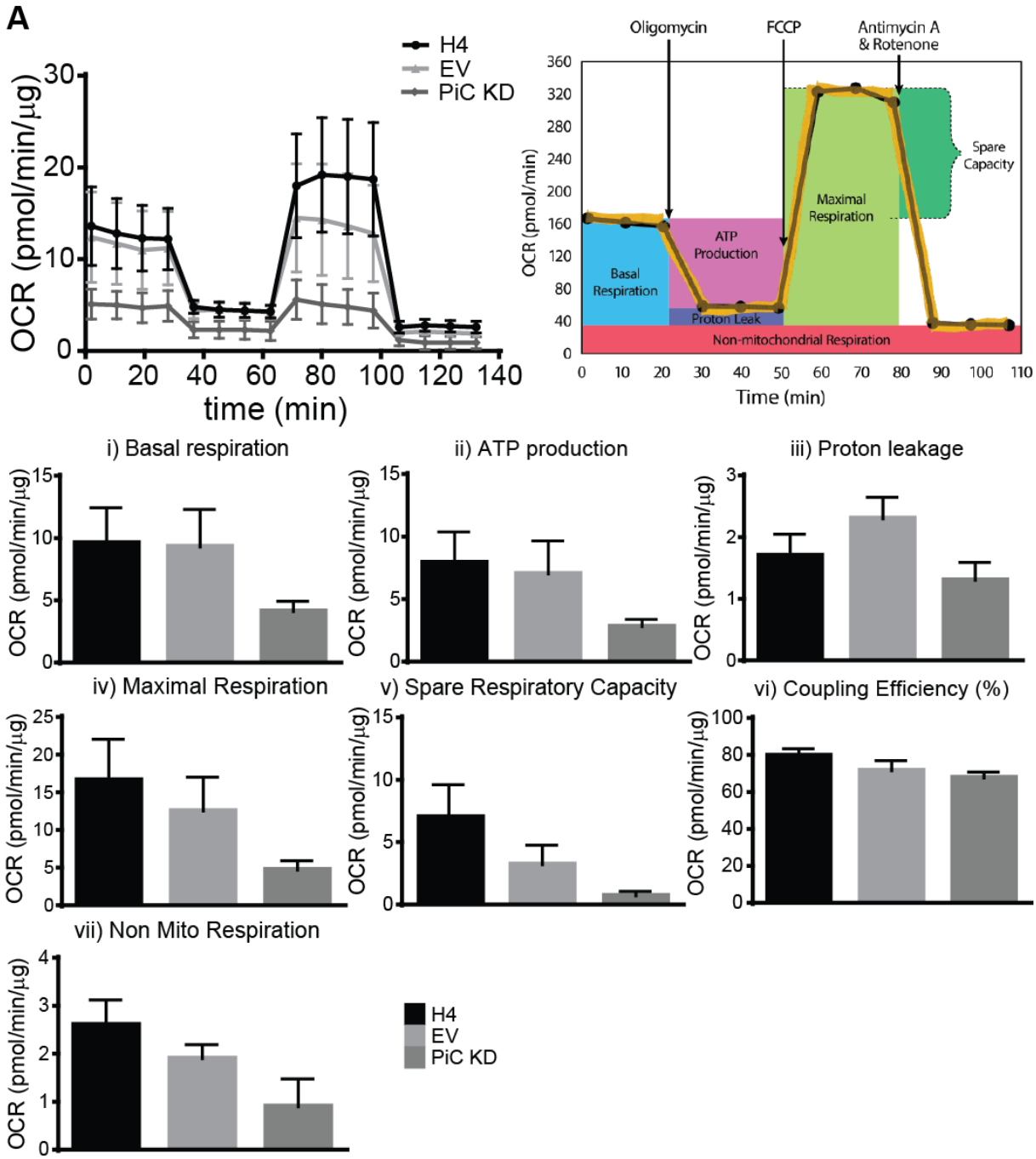

Figure 6.6. Oxygen consumption rate (OCR) of PiC knockdown cells.
(A) Mitochondrial respiration and its components (i-vi) plus the non-mitochondrial respiration rate (vii) in untransfected (H4) and both EV- and PiC shRNA (PiC KD) transfected H4 cells. PiC knockdown cells exhibited reduced mitochondrial respiration, visible in all components of the OCR. Non-mitochondrial respiration rate was also reduced. Bioenergetic function of PiC KD H4 cells *versus*. controls (untransfected and transfected with empty pLKO.1 vector) was monitored using the XF24 Cell Mito Stress Test Kit and the XF24 Extracellular Flux Analyser following manufacturer instructions, 72h post transfection. Results were normalized to total protein content and correspond to average ± SEM of 3 independent experiments.

6.4. Discussion

Results obtained in yeast show that concomitant deletion of *MIR1* (the yeast orthologue of *SLC25A3*) with overexpression of tau is lethal to yeast growth (v*ide* Chapter 4). Since *SLC25A3* codes for the mitochondrial phosphate carrier (PiC), localized at the inner mitochondrial membrane and essential for ATP production, these data suggested that tau is involved in mitochondrial dysfunction, as corroborated by several *in vivo* studies (Eckert *et al.*, 2014). The data obtained in yeast also suggested that PiC function might be important in maintaining mitochondrial function in the context of tau neurodegeneration. If this is proven true, PiC may constitute a relevant novel target for therapeutic intervention in tauopathies.

This work presents the first steps towards the creation of a model of higher physiological relevance to replicate and validate the results obtained in yeast. Knockdown of PiC was performed in human brain neuroglioma H4 cells that express tau endogenously (Dickey *et al.*, 2006), which is present at different phosphorylation states. PiC silencing was optimized by transient transfection of different shRNA sequences. Transient transfection was selected over stable transfection because it would allow selecting the most efficient PiC shRNA in a shorter time frame and in less demanding technical conditions. The resulting phenotype after PiC silencing was evaluated in terms of cell viability and mitochondrial function. PiC knockdown was achieved after 72h, with average 65% efficiency, and apparently was not toxic to cells. This efficiency was not sufficient to impair either mitochondrial calcium uptake or mitochondrial membrane potential, as previously described by Varanyuwatana and colleagues (Varanyuwatana & Halestrap, 2012), that also silenced PiC expression in HeLa cells. Nevertheless, H4 cells subjected to PiC KD apparently exhibited a compromised bioenergetic profile, with a generalized decrease in the OCR when compared to controls. These data were expected since PiC catalyses the transport of inorganic phosphate (Pi) to the mitochondrial matrix, which is essential for the production of ATP and correlates with decreased OCR (Brand & Nicholls, 2011).

Analysing the different components of the OCR, modulated by specific inhibitors of different components of the ETC, allowed a detailed characterization of the bioenergetic profile of PiC KD cells. The basal respiration of PiC KD cells was smaller than the basal respiration of controls. Basal respiration corresponds to the oxygen consumption used to meet cellular ATP demand and resulting from mitochondrial proton leak and is an indicator of the baseline energetic demand (Brand & Nicholls, 2011). Therefore, lower basal respiration is indicative of reduced ATP demand, reduced proton leak, inhibition of ATP synthase or ETC or decreased supply of energetic substrates (e.g. Hill *et al.*, 2012). Although ATP synthase is not directly inhibited in PiC KD cells, lack of Pi transport to the mitochondrial matrix reduces the amount of ATP produced, mimicking such conditions. Indeed, ATP production rate appears to be reduced in PiC KD cells. Moreover, when analysing the bioenergetic profile after addition of oligomycin, an inhibitor of ATP synthase, the OCR linked to ATP production decreased severely in untransfected and EV cells, while for PiC KD cells, this decrease was much less pronounced. This is indicative that PiC KD cells were already producing less ATP at the beginning of the experiment. The maximal oxygen consumption rate was accomplished after adding the uncoupler FCCP, which stimulates the respiratory chain to work at maximum capacity, causing rapid oxidation of substrates

(sugars, fatty acids, amino acids) to meet this metabolic challenge (Brand & Nicholls, 2011). PiC KD cells were unable to attain maximal OCR levels following addition of FCCP, when compared with untransfected cells, maintaining the OCR at the basal level. This implies that, at basal levels, PiC KD cells were operating closer to the maximal OCR capacity, which is also reduced. In this situation, any increase in the OCR would not be possible, resulting in a lower spare capacity. A decrease in spare respiratory capacity is a strong indicator of mitochondrial dysfunction (Brand & Nicholls, 2011). Noteworthy, H4 cells transfected with the empty plasmid, also exhibited a tendency for reduced spare respiratory capacity, suggesting that transfection alone might compromise mitochondrial function. The coupling efficiency is a respiratory flux control ratio that allows to accurately compare PiC KD cells and controls, since it is internally normalised and independent on the number of cells (Hill *et al.*, 2012). No differences were found for the coupling efficiency of PiC KD cells, although there was a tendency for a decrease, suggesting that PiC KD cells have reduced mitochondrial respiration efficiency (Hill *et al.*, 2012).

PiC silencing was performed using short hairpin RNA (shRNA), a double stranded RNA molecule, delivered to the cell as a DNA construct (Rao *et al.*, 2009). shRNA molecules are more stable and the replication of the plasmid inside the cell allows for prolonged effects (Rao *et al.*, 2009). Additionally, the desired effect is achieved using smaller dosages, which makes these molecules more appropriate for the study of chronic, life-threatening disorders (Rao *et al.*, 2009). PiC KD did not induce increased LDH activity in the extracellular culture media. LDH is a cytoplasmic enzyme that is released to the extracellular media upon cell membrane damage caused by the expression of exogenous proteins or treatment with cytotoxic compounds, being an indication of cell death by necrosis (Chan *et al.*, 2013). Considering that LDH release was not presented as a percentage of total LDH (extra- plus intracellular LDH), which might have led to an underestimation of cell death, the protocol should be re-evaluated in future studies to account for the inclusion of cells that have been detached and evaluate LDH release. Moreover, complementary viability tests should be used, such as Alamar blue (rezasurin) assay, fluorescence cell imaging of Hoechst 33342 plus propidium iodide staining to detect DNA fragmentation/condensation *versus* necrosis, and/or caspases activity to accurately estimate cell viability after PiC silencing.

H4 cells endogenously express tau (Dickey *et al.*, 2006) and western blot analysis revealed that tau is phosphorylated at epitopes usually correlated with the formation of neurofibrillary tangles (Avila *et al.*, 2012; Gotz *et al.*, 2010). Tau is a naturally phosphorylated protein, with 85 potential serine, threonine, and tyrosine phosphorylation sites (Noble *et al.*, 2013). Under pathological conditions tau phosphorylation increases almost 3-fold relatively to normal phosphorylation levels (Alonso *et al.*, 2010). In the present study, no changes in tau phosphorylation were detected in PiC KD cells, at the epitopes analysed, and there is no indication that PiC could interfere with the pathways that regulate tau phosphorylation or dephosphorylation.

The results obtained in this work require confirmation by increasing the number of experimental replicates. Also, they do not allow inferring about the relevance of PiC as a drug target for tauopathies. However, they provide valuable information that should be considered when improving the design of the

model of tau pathology in mammalian cells lacking PiC expression. For example, an aspect that contributed to the lack of statistical significance was the high variability of the transient transfection efficiency of the DNA plasmid carrying the shRNA sequence between replicates. Despite the advantages of transient transfection for selecting the most efficient PiC shRNA, for construction of the definitive model, it might be advisable to work with a stable knockdown PiC cell line to decrease variability, thereby increasing the reproducibility and confidence of the results obtained. Care should be taken, however, when deciding if PiC knockdown should be constitutive or inducible. Indeed, longer periods of PiC silencing can significantly decrease cell viability, therefore hindering the use of a stable constitutive knockdown of PiC. In previous studies, knockdown times longer than 72h were found to cause cell death in HeLa cells (Varanyuwatana & Halestrap, 2012).

Several strategies can be followed to induce tau pathology which could also be used in future studies. Overexpression of wild-type and mutated forms of tau has been extensively used for *in vitro* and *in vivo* modelling of tauopathies (DeTure *et al.*, 2002; Khlistunova *et al.*, 2006; Oddo *et al.*, 2003). Different tau mutations have been engineered at BIOALVO and are therefore available to insert in the desired mammalian expression plasmids. Additionally, producing fluorescent-tagged versions of these cDNAs would distinguish exogenous from endogenous tau and allow the study of its subcellular localization by immunocytochemistry. As discussed previously for PiC KD, a stable cell line of tau overexpression should be considered, since it would reduce result's variability. However, the engineering of a double stable cell line would be rather time-consuming. Currently there are RNAi-based lentivirus systems that allow for concomitant stable inducible expression of shRNA and cDNA (Meerbrey *et al.*, 2011; Shin *et al.*, 2006). These systems are powerful tools for the functional analysis of gene expression or knockdown. Addition of enhancers of tau fibrillization, such as Congo red (Bandyopadhyay *et al.*, 2007), okadaic acid (Del Barrio *et al.*, 2011; Kamat, Rai & Nath, 2013; Zhang & Simpkins, 2010) or beta-amyloid, which is particularly relevant for modelling AD, are also frequently used techniques to induce tau pathology in cellular models (Ferrari *et al.*, 2003; Ittner & Gotz, 2011). Independently of the strategy followed, the resulting phenotype should be carefully characterized in terms of tau hyperphosphorylation in pathology-related epitopes, protein subcellular localization and formation of insoluble oligomers. Together with cell viability assays, this battery of tests will allow to monitor changes in tau pathology caused by the silencing of PiC.

The construction of a model of tau pathology in mammalian cells lacking PiC would be an initial, and necessary, step towards the validation of PiC as a drug target for tauopathies. This model would be a useful tool to further understand the mechanisms of tau toxicity at the level of mitochondria and a valuable secondary screening system for evaluating the efficacy of new drugs potential suppressors of tau neurotoxicity.

Chapter 7.

Conclusions

7.1. Conclusions

With an estimated number of 44.4 million people suffering from dementia worldwide, a number that can reach 135.5 million by 2050 and will keep increasing due to the ageing population, individuals, families and society are facing one of the most challenging global health problems. Many countries have launched programmes to tackle this threat in several fronts, and importantly, international scientific cooperative efforts are contributing for the development of better preventive, diagnostics and treatment strategies. Despite the variety of mechanisms to be targeted therapeutically, there are no mechanism-based treatments for the majority of dementia disorders. It is, therefore, imperative that new and better therapeutic solutions are promptly found and made available.

Alzheimer's disease (AD) and Frontotemporal Dementias (FTD) are the first and second most frequent cause of dementia, respectively. AD and some FTDs are part of a heterogeneous group of disorders, called tauopathies, characterized by the accumulation of misfolded hyperphosphorylated microtubule-associated protein tau into soluble oligomers that eventually lead to the formation of intraneuronal neurofibrillary tangles. Accumulation of misfolded tau become pathologically active, either by mechanism of loss of function or gain of toxic function, ultimately leading to the death of neurons. With the exception of AD, sometimes called as a "secondary" tauopathy due to the obligatory combination with Aβ pathology, mutations in the gene encoding tau (*MAPT*) are sufficient to cause neurodegeneration. Tau most well understood biologic function is the regulation and stabilization of microtubules assembly. Hence, tau is involved in many vital cellular processes, such as establishment of neuronal polarity, axonal growth and transport of cellular cargoes. However, novel functions of tau are still being elucidated, as new tau interactions are reported, implicating tau in many other biological processes.

Although still incomplete, the increased knowledge on the role of tau in disease onset and progression, together with the recent failures of Aβ-based therapies, has contributed to increase the focus on tau, and its network of interactions, as potential targets for therapeutic intervention in a wide-range of neurodegenerative disorders. Tau-based therapeutic strategies have, therefore, become a priority and will benefit from further clarification of tau biology and tau-mediated mechanisms of disease. Indeed, following this trend, several therapeutic strategies based on tau have been developed, but more innovative solutions are needed to fuel the pipeline of drugs in development.

With this in mind, the aim of this work was to foster drug discovery and development for tauopathies while, at the same time, expand our knowledge on the aetiology of tau-related diseases. To this goal, *Saccharomyces cerevisiae*, the baker's yeast, was used as model organism. Yeast is a recognized model for the study of neurodegenerative disorders and has greatly contributed to discriminate disease-related protein interactions and new drug targets for several neurodegenerative disorders, such as PD, HD, ALS, FTD-FUS, FTD-TDP43, among others. The success of these approaches, together with previous reports that yeast recapitulated many important molecular features of tau pathology, has led us to use yeast as a test tube to identify new tau protein interactors, to study tau interaction with its most

relevant player – Aβ – and to develop innovative drug screening systems that allowed to identify bioactives modulators of tau toxicity.

To study tau interaction with Aβ, in Chapter 3, different integrative and episomal yeast strains models, expressing native and fluorescent versions of $A\beta_{1-42}$ and tau40, were developed and characterized in terms of growth, protein expression, tau phosphorylation, presence of protein inclusions and sub-cellular localization. Reduced yeast growth was found following co-expression of $A\beta_{1-42}$ and tau40, an effect apparently mediated by $A\beta_{1-42}$. Expression of $A\beta_{1-42}$ in the yeast cytoplasm formed amorphous structures, partially resistant to 1% Sarkosyl that were more abundant in the yeast strain co-expressing tau40. These inclusions co-localized with tau40-eGFP, which does not form visible aggregates when expressed alone. Tau40 was phosphorylated at pathological epitopes (Ser396/404) by Rim11, the GSK-3β yeast orthologue. Furthermore, tau40 phosphorylation levels increased when $A\beta_{1-42}$ was co-expressed. These results suggest that $A\beta_{1-42}$-mCh and tau40 directly interact and $A\beta_{1-42}$ appears to be involved in the induction of tau40 phosphorylation, whereas tau seems to facilitate $A\beta_{1-42}$-mCh oligomerization. The recapitulation of essential pathological features of $A\beta_{1-42}$ and tau40 pathologies makes this model a potential useful tool to study $A\beta_{1-42}$ and tau40 interaction. Also, further understanding of the mechanisms of interaction will allow using this model as a tool to investigate the interaction of other relevant proteins with tau and Aβ, as well as, to investigate the mode of action of drug candidates in development.

Since tau co-expression with Aβ did not result in a measurable toxic effect to yeast, the use of this model as a drug screening system to identify modulators of tau and Aβ interaction would always have to include an extra step to determine whether the bioactives were acting on tau and Aβ co-dependent mechanisms of toxicity or on separate pathways. Yeast cost-effective advantages for use in drug discovery would then be decreased. Nevertheless, the yeast strain expressing $A\beta_{1-42}$-mCh may prove to be a suitable drug discovery platform for the identification of compounds capable of modulating intracellular $A\beta_{1-42}$ toxicity, provided that validation studies are performed and successful.

The fact that tau expression is non-toxic to yeast offers the opportunity of identifying yeast gene deletions that enhance tau toxicity. Therefore, in Chapter 4, a loss-of-function tau toxicity enhancer genomic screen was performed by conditionally expressing the longest wild-type human tau isoform (tau40) in the yeast gene deletion collection (YKO). This screen identified 31 yeast gene deletions enhancers of tau toxicity, 21 of which have well characterized human orthologues, placing tau in biological processes relevant for neurodegeneration, such as mitochondrial function, vesicular-mediated transport, macroautophagy and protein folding. This list of genes constitutes a relevant framework for the identification of novel drug targets and/or biomarkers for tauopathy therapies. Noteworthy, the genes which were found to be unspecific for tau accumulation (since the lethal phenotype was also observed with the control protein) are also worth exploring for therapies focusing on proteinopathies in general. These genes may play relevant roles in pathways essential for the survival of cells under pathological conditions. Following a high throughput strategy this study prioritized one yeast deletion strain for the development of a novel drug discovery screening system. The yeast strain *mir1*Δ was selected as

suitable for the development of such system, since it presented a reproducible and specific synthetic lethal phenotype after tau40 expression.

Chapter 5 presents the validation of such strain as a GPS D^{2TM} system and a screening campaign of a small, but very unique, library of 138 unique natural extracts obtained from the SEAVENTbugs bacteria collection. This campaign identified 8 natural products with activity in suppressing tau's toxicity in a mitochondria-compromised cellular environment, of which 3 were classified as good candidates for the discovery of new safe and effective biological entities for the development of innovative therapies for tauopathies. The drug discovery and development programme based on the natural products identified will have to be designed taking into consideration that (i) the bioactive principle is not known and must be first identified and its structure elucidated; (ii) the bioprocessing of the bioactive must be understood in order to optimize its mass production; (iii) there is a high probability that the bioactive principle is a protein, due to the extraction technique used, thereby posing additional challenges regarding formulation and drug delivery of the bioactive; and (iv) the bioactive targets the CNS and for that it must be able to cross the BBB. Early *in vitro* ADMET assays information coupled with a strong medicinal chemistry program will be decisive in the hit-to-lead phase, in order to select the most promising lead molecule for further development.

Yeast biggest advantages are also its biggest caveat, since this organism lacks the complexity of mammalian eukaryotic cells and, particularly, does not reproduce all the pathways important for neuronal function. Therefore, all findings in yeast must be validated in model organisms of higher physiological relevance, preferentially neural cells. The results in yeast indicated that concomitant deletion of *MIR1* with overexpression of tau was lethal to yeast growth. *MIR1* human homologue is *SLC25A3*, which codes for the mitochondrial phosphate carrier (PiC). PiC catalyses the transport of inorganic phosphate to the mitochondrial matrix and is essential for ATP production and O_2 consumption. Prior data suggested that tau is involved in mitochondrial dysfunction and that PiC may have an important function in mitochondrial dysfunction in tauopathies. The verification of this hypothesis would validate PiC as a relevant drug target for the development of new therapies for tauopathies. Chapter 6 presents the first steps towards this validation by characterizing a model of higher physiological relevance based on PiC expression knockdown in human brain neuroglioma H4 cells using shRNA. PiC silencing was not toxic to cells and insufficient to alter calcium uptake by mitochondria or mitochondrial membrane potential. Nonetheless, these cells presented a reduced bioenergetic profile, possibly due to decreased ATP production. The future steps of engineering of this model were also discussed and included, in one approach, the stable conditional knockdown of PiC with concomitant stable inducible expression of tau40 in H4 cells. Such a model is expected to be useful, not only to understand tau mechanisms involving mitochondria, but also to evaluate PiC as a drug target for tauopathies. Additionally, it might also constitute a valuable secondary screening system for evaluating the efficacy of drugs in development, potential suppressors of tau toxicity.

The work here presented fully integrated with BIOALVO's TAU Program, one of the main internal R&D drug discovery and development programs of the company. This program aimed at generating drug-like molecules with optimal properties in terms of safety and efficacy for the treatment of tau-related

diseases, with a particular focus on AD, due to the dramatic clinical relevance and social burden of this pathology. This work contributed to the TAU program by providing additional targets on tau protein pathway, identifying unique natural products, good starting points for identifying novel modulators of tau toxicity, and giving the first steps for the creation of additional models of disease that could later be used as secondary drug screening tools.

Moreover, the collaboration with the CNC (Center for Neuroscience and Cell Biology, University of Coimbra), and specifically with the group of Professor Ana Cristina Rego, who works in cell and animal models relevant to AD, particularly in what concerns the mitochondrial dysfunction mechanisms involved in neurodegeneration, allowed the exchange of knowledge, expertise and access to mammalian cells for validation of the work developed in the company by the PhD candidate. Together, these interconnections were a great example of how industry and academia can collaborate, contributing to the strengthening of results achieved and going one step further in the development of therapies that can, one day, be a solution for the millions of patients worldwide that suffer from these neuropathies.

Overall, the results obtained in this PhD thesis highlight how useful yeast can be for drug discovery and development. Several tools were developed in this study, which have the potential to foster drug discovery and development for tauopathies. Although still far from having a safe and effective therapy for tauopathies (which would be the ultimate goal), we believe that every small discovery adds up to understand the underlying causes of tau-based neurodegeneration paving the way for innovative therapeutic solutions.

7.2. Go-to-market strategy

The global neurodegenerative diseases market is expected to grow moderately from $8.8 billion in 2012 to $11 billion in 2018, at a Compound Annual Growth Rate (CAGR) of 1.8% from 2012-2015 and at a higher CAGR of 5.9% from 2015-2018. PD and AD therapeutics account for the majority of the global neurodegenerative diseases market, due to their increased prevalence (Wood, 2014). Despite this, the AD market in particular is expected to counteract this tendency as its value is estimated to decrease from $4.2 billion in 2012 to approximately $3.8 billion in 2018 (Gerald & Ockert, 2013). This does not mean that the need for better diagnostics and therapeutics is decreasing. Far from it, an increasingly elderly population, the need for earlier and improved diagnostics and the introduction of new therapeutic classes are the drivers of the AD market. This decrease is mostly due to the fact that the AD market has not seen any recent major breakthroughs and patents of several major products will expiry in this period (Gerald & Ockert, 2013; Wood, 2014).

The work here presented is expected to impact the segment of disease modifying therapies, since it has provided a framework for identification of potential novel drug targets to tackle, within the tau interactome in yeast. Additionally it has provided very unique natural products that constitute excellent starting points for the development of new drug discovery programs for the identification of innovative chemical structures for novel modulators of tau toxicity. Furthermore, the information gathered in this work might pave the way for the identification of new diagnostic and biomarker tools, alongside with drug discovery

tools for faster development, further strengthening the potential of this work to address a portion of this market.

As measurable outcomes of this project, the following translational steps and marketable products and services are highlighted:

1. A yeast model of beta-amyloid and tau co-expression, a test tube for the study of AD hallmark proteins interaction and a potentially useful tool for drug discovery and development for tauopathies;
2. A list of 21 novel potential drug targets and/or biomarkers for tauopathies;
3. A new DDD tool - *mir1*Δ-tau, a yeast-based screening system, amenable for HTS, for identification of new drug candidates for tauopathies;
4. Three bacterial natural extracts, with activity in suppressing tau toxicity, good candidates for the development of new drug discovery programs for tauopathies;
5. Five bacterial natural extracts with potential activity in suppressing tau toxicity if further manipulated and modified, could work as backup samples for a DDD program for tauopathies.

Any of these outcomes has interest *per se* for a variety of end users, mostly biotech companies similar to BIOALVO (HTS platform), Pharma (novel targets and natural extracts hits) and Diagnosis and R&D suppliers (lists of putative targets and biomarkers).

In order to more efficiently translate these outputs to a commercial viable solution, some constrains may arise from publication decisions made. Additionally, most of the assets here developed need more work and a summary of these concerns and steps are described next.

Regarding the yeast model of Aβ and tau co-expression, further characterization of the mechanisms involved in tau and beta-amyloid interaction in yeast will be necessary to fully explore the potential of this model for DDD. For example, pilot studies using drugs already in development for tauopathies could be performed in order to validate this model as a *first-in-line* platform for evaluation of drug candidate's modes of action. The development of these studies will benefit from collaborations with other laboratories with expertise in yeast biology and knowledge of the early stages of drug development.

The list of novel potential drug targets for tauopathies obtained from tau' yeast interactome screening is relevant for pharmaceutical and biotech companies that wish to pursue the development of new models and screening platforms. It can also be useful as a framework to identify novel biomarkers for diagnostics and R&D, and will be open to the whole scientific community, since it will be submitted for publication in a *peer-reviewed* journal.

Regarding the yeast-based screening system (*mir1*Δ-tau40) for modulators of tau toxicity, the publication of this technological platform details in this thesis and in *peer-reviewed* journals hinders its patenting process, due to the loss of the novelty requisite, and may diminish its commercial interest. Additionally, SLC25A3 the human homologue of MIR1, is still not validated as a relevant drug target in tauopathies. Great efforts should be undertaken to perform this validation, increasing the relevance of this screening system and of the therapies that it elicits. However, the platform can already be of use to FCT-UNL and FCUL, and most probably other academic labs interested in the field, as a tool to identify

potential modulators of tau toxicity that can then be further developed and commercialized. Additionally, this screening system can be also made available as part of the services provided by FCUL, through its Center BioISI, to partners or other entities, rendering it a positive outcome to the partners involved in this work.

Finally, and concerning the natural products with positive activity in suppressing tau toxicity identified in this thesis, these may also be subjected to patenting and future licensing to biopharmaceutical companies working in the first stages of drug discovery, with particular emphasis for companies with expertise in natural product development. The preparation of technology transfer packs of information regarding each of these potential hits could be made by the technology transfer offices of FCUL and FCT-UNL and presented to potential end users stakeholders.

Alternatively to all the presented solutions, a spin-off company could be created based on this work to exploit and explore the potentialities of the created tools, acting both as a service provider in drug discovery and in the development of drug discovery programs using the hits identified in this study.

Chapter 8.

References

8.1. References

Ackerman, S. H. (2002). Atp11p and Atp12p are chaperones for F1-ATPase biogenesis in mitochondria. *Biochim Biophys Acta, 1555*(2002), 101-105.

ADI. (2015). Dementia statistics. Retrieved 26/03/2015, 2015, from http://www.alz.co.uk/research/statistics.

Alonso, A. D., Di Clerico, J., Li, B., Corbo, C. P., Alaniz, M. E., Grundke-Iqbal, I., & Iqbal, K. (2010). Phosphorylation of tau at Thr212, Thr231, and Ser262 combined causes neurodegeneration. *J Biol Chem, 285*(40), 30851-30860. doi: 10.1074/jbc.M110.110957.

Ambegaokar, S. S., & Jackson, G. R. (2011). Functional genomic screen and network analysis reveal novel modifiers of tauopathy dissociated from tau phosphorylation. *Hum Mol Genet, 20*(24), 4947-4977. doi: 10.1093/hmg/ddr432.

Appasani, K. (2003). RNA interference a technology platform for target validation, drug discovery and therapeutic development. *Drug Discovery World, Summer 2003,* 61-68.

Armakola, M., Hart, M. P., & Gitler, A. D. (2011). TDP-43 toxicity in yeast. *Methods 53*, 238-245.

Avila, J., Leon-Espinosa, G., Garcia, E., Garcia-Escudero, V., Hernandez, F., & Defelipe, J. (2012). Tau Phosphorylation by GSK3 in Different Conditions. *Int J Alzheimers Dis, 2012*, 578373. doi: 10.1155/2012/578373.

Ávila, J., Lucas, J. J., Pérez, M., & Hernandez, F. (2004). Role of tau protein in both physiological and pathological conditions. *Physiol Rev, 84*, 361-384.

Babu, J. R., Geetha, T., & Wooten, M. W. (2005). Sequestosome 1/p62 shuttles polyubiquitinated tau for proteasomal degradation. *J Neurochem, 94*(1), 192-203. doi: 10.1111/j.1471-4159.2005.03181.x.

Bagriantsev, S., & Liebman, S. (2006). Modulation of Abeta42 low-n oligomerization using a novel yeast reporter system. *BMC Biol, 4*, 32. doi: 10.1186/1741-7007-4-32.

Ballatore, C., Lee, V. M., & Trojanowski, J. Q. (2007). Tau-mediated neurodegeneration in Alzheimer's disease and related disorders. *Nat Rev Neurosci, 8*(9), 663-672. doi: 10.1038/nrn2194.

Bandyopadhyay, B., Li, G., Yin, H., & Kuret, J. (2007). Tau aggregation and toxicity in a cell culture model of tauopathy. *J Biol Chem, 282*(22), 16454-16464. doi: 10.1074/jbc.M700192200.

Barbato, C., Corbi, N., Canu, N., Fanciulli, M., Serafino, A., Ciotti, M., Libri, V., Bruno, T., Amadoro, G., De Angelis, R., Calissano, P., & Passananti, C. (2003). Rb binding protein Che-1 interacts with Tau in cerebellar granule neurons. Modulation during neuronal apoptosis. *Mol Cell Neurosci, 24*(4), 1038-1050.

Barberis, A., Gunde, T., Berset, C., Audetat, S., & Luthi, U. (2005). Yeast as a screening tool. *Drug Discov Today Technol, 2*(2), 187-192. doi: 10.1016/j.ddtec.2005.05.022.

Baseler, W. A., Thapa, D., Jagannathan, R., Dabkowski, E. R., Croston, T. L., & Hollander, J. M. (2012). miR-141 as a regulator of the mitochondrial phosphate carrier (Slc25a3) in the type 1 diabetic heart. *Am J Physiol Cell Physiol, 303*(12), C1244-1251. doi: 10.1152/ajpcell.00137.2012.

Bauer, A., & Bronstrup, M. (2014). Industrial natural product chemistry for drug discovery and development. *Nat Prod Rep, 31*(1), 35-60. doi: 10.1039/c3np70058e.

Bayer, T. A. (2013). Proteinopathies, a core concept for understanding and ultimately treating degenerative disorders? *Eur Neuropsychopharmacol, 25*(5), 713-724. doi: 10.1016/j.euroneuro.2013.03.007.

Benson, J. D., Chen, Y. N., Cornell-Kennon, S. A., Dorsch, M., Kim, S., Leszczyniecka, M., Sellers, W. R., & Lengauer, C. (2006). Validating cancer drug targets. *Nature, 441*(7092), 451-456. doi: 10.1038/nature04873.

Berg, E. L. (2014). Systems biology in drug discovery and development. *Drug Discov Today, 19*(2), 113-125. doi: 10.1016/j.drudis.2013.10.003.

Bharadwaj, P., Martins, R., & Macreadie, I. (2010). Yeast as a model for studying Alzheimer's disease. *FEMS Yeast Res, 10*(8), 961-969. doi: 10.1111/j.1567-1364.2010.00658.x.

Bhaskar, K., Shareef, M. M., Sharma, V. M., Shetty, A. P., Ramamohan, Y., Pant, H. C., Raju, T. R., & Shetty, K. T. (2004). Co-purification and localization of Munc18-1 (p67) and Cdk5 with neuronal cytoskeletal proteins. *Neurochem Int, 44*(1), 35-44.

Billings, L. M., Oddo, S., Green, K. N., McGaugh, J. L., & LaFerla, F. M. (2005). Intraneuronal Abeta causes the onset of early Alzheimer's disease-related cognitive deficits in transgenic mice. *Neuron, 45*(5), 675-688. doi: 10.1016/j.neuron.2005.01.040.

Brand, M. D., & Nicholls, D. G. (2011). Assessing mitochondrial dysfunction in cells. *Biochem J, 435*(2), 297-312. doi: 10.1042/BJ20110162.

Brandt, R., Leger, J., & Lee, G. (1995). Interaction of tau with the neural plasma membrane mediated by tau's amino-terminal projection domain. *J Cell Biol, 131*(5), 1327-1340.

Braun, R. J., Buttner, S., Ring, J., Kroemer, G., & Madeo, F. (2010). Nervous yeast: modeling neurotoxic cell death. *Trends Biochem Sci, 35*(3), 135-144. doi: 10.1016/j.tibs.2009.10.005.

Brightfocus.org. (2015). Understanding Clinical Trials: Details of the Drug Discovery and Approval Process. Retrieved 5 Feb., 2015, from http://www.brightfocus.org/details-of-the-drug-discovery-and-approval-process.html#basic.

Broer, L., Ikram, M. A., Schuur, M., DeStefano, A. L., Bis, J. C., Liu, F., Rivadeneira, F., Uitterlinden, A. G., Beiser, A. S., Longstreth, W. T., Hofman, A., Aulchenko, Y., Seshadri, S., Fitzpatrick, A. L., Oostra, B. A., Breteler, M. M., & van Duijn, C. M. (2011). Association of HSP70 and its co-chaperones with Alzheimer's disease. *J Alzheimers Dis, 25*(1), 93-102. doi: 10.3233/JAD-2011-101560.

Bronner, I. F., Bochdanovits, Z., Rizzu, P., Kamphorst, W., Ravid, R., van Swieten, J. C., & Heutink, P. (2009). Comprehensive mRNA expression profiling distinguishes tauopathies and identifies shared molecular pathways. *PLoS One, 4*(8), e6826. doi: 10.1371/journal.pone.0006826.

Brunden, K. R., Trojanowski, J. Q., & Lee, V. M. (2009). Advances in tau-focused drug discovery for Alzheimer's disease and related tauopathies. *Nat Rev Drug Discov, 8*(10), 783-793. doi: 10.1038/nrd2959.

Buée-Scherrer, V., Condamines, O., Mourton-Gilles, C., Jakes, R., Goedert, M., Pau, B., & Delacourte, A. (1996). AD2, a phosphorylation-dependent monoclonal antibody directed against tau proteins found in Alzheimer' s disease. *Molecular Brain Research, 39*, 79-88.

Caine, J., Sankovich, S., Antony, H., Waddington, L., Macreadie, P., Varghese, J., & Macreadie, I. (2007). Alzheimer's Abeta fused to green fluorescent protein induces growth stress and a heat shock response. *FEMS Yeast Res, 7*(8), 1230-1236. doi: 10.1111/j.1567-1364.2007.00285.x.

Calcul, L., Zhang, B., Jinwal, U. K., Dickey, C. A., & Baker, B. J. (2012). Natural products as a rich source of tau-targeting drugs for Alzheimer's disease. *Future Med Chem, 4*(13), 1751-1761. doi: 10.4155/fmc.12.124.

Cerejo, M., Andrade, G., Roca, C., Sousa, J., Rodrigues, C., Pinheiro, R., Chatterjee, S., Vieira, H., & Calado, P. (2012). A powerful yeast-based screening assay for the identification of inhibitors of indoleamine 2,3-dioxygenase. *J Biomol Screen, 17*(10), 1362-1371. doi: 10.1177/1087057112452595.

Chan, F. K., Moriwaki, K., & De Rosa, M. J. (2013). Detection of necrosis by release of lactate dehydrogenase activity. *Methods Mol Biol, 979*, 65-70. doi: 10.1007/978-1-62703-290-2_7.

Chapuis, J., Hansmannel, F., Gistelinck, M., Mounier, A., Van Cauwenberghe, C., Kolen, K. V., Geller, F., Sottejeau, Y., Harold, D., Dourlen, P., Grenier-Boley, B., Kamatani, Y., Delepine, B., Demiautte, F., Zelenika, D., Zommer, N., Hamdane, M., Bellenguez, C., Dartigues, J. F., Hauw, J. J., Letronne, F., Ayral, A. M., Sleegers, K., Schellens, A., Broeck, L. V., Engelborghs, S., De Deyn, P. P., Vandenberghe, R., O'Donovan, M., Owen, M., Epelbaum, J., Mercken, M., Karran, E., Bantscheff, M., Drewes, G., Joberty, G., Campion, D., Octave, J. N., Berr, C., Lathrop, M., Callaerts, P., Mann, D., Williams, J., Buee, L., Dewachter, I., Van Broeckhoven, C., Amouyel, P., Moechars, D., Dermaut, B., Lambert, J. C., & consortium, G. (2013). Increased expression of BIN1 mediates Alzheimer genetic risk by modulating tau pathology. *Mol Psychiatry, 18*(11), 1225-1234. doi: 10.1038/mp.2013.1.

Chen, B., Retzlaff, M., Roos, T., & Frydman, J. (2011). Cellular strategies of protein quality control. *Cold Spring Harb Perspect Biol, 3*(8), a004374. doi: 10.1101/cshperspect.a004374.

Chen, D. C., Yang, B. C., & Kuo, T. T. (1992). One-step transformation of yeast in stationary phase. *Curr Genet, 21*(1), 83-84.

Chun, J., Kwon, T., Lee, E. J., Kim, C. H., Han, Y. S., Hong, S. K., Hyun, S., & Kang, S. S. (2004). 14-3-3 Protein mediates phosphorylation of microtubule-associated protein tau by serum- and glucocorticoid-induced protein kinase 1. *Mol Cells, 18*(3), 360-368.

Ciaccioli, G., Martins, A., Rodrigues, C., Vieira, H., & Calado, P. (2013). A powerful yeast model to investigate the synergistic interaction of alpha-synuclein and tau in neurodegeneration. *PLoS One, 8*(2), e55848. doi: 10.1371/journal.pone.0055848.

Clavaguera, F., Bolmont, T., Crowther, R. A., Abramowski, D., Frank, S., Probst, A., Fraser, G., Stalder, A. K., Beibel, M., Staufenbiel, M., Jucker, M., Goedert, M., & Tolnay, M. (2009). Transmission and spreading of tauopathy in transgenic mouse brain. *Nat Cell Biol, 11*(7), 909-913. doi: 10.1038/ncb1901.

Cowan, C. M., & Mudher, A. (2013). Are tau aggregates toxic or protective in tauopathies? *Front Neurol, 4*, 114. doi: 10.3389/fneur.2013.00114.

Crespo-Biel, N., Theunis, C., & Van Leuven, F. (2012). Protein tau: prime cause of synaptic and neuronal degeneration in Alzheimer's disease. *Int J Alzheimers Dis, 2012*, 251426. doi: 10.1155/2012/251426.

D'Angelo, F., Vignaud, H., Di Martino, J., Salin, B., Devin, A., Cullin, C., & Marchal, C. (2013). A yeast model for amyloid-beta aggregation exemplifies the role of membrane trafficking and PICALM in cytotoxicity. *Dis Model Mech, 6*(1), 206-216. doi: 10.1242/dmm.010108.

Davidowitz, E. J., & Moe, J. G. (2012). Targeting tau for Alzheimer’s disease and related neurodegenerative disorders. *Drug Discovery World, Fall 2012*, 16-21.

De Vos, A., Anandhakumar, J., Van den Brande, J., Verduyckt, M., Franssens, V., Winderickx, J., & Swinnen, E. (2011). Yeast as a model system to study tau biology. *Int J Alzheimers Dis, 2011*, 428970. doi: 10.4061/2011/428970.

Del Barrio, L., Martin-de-Saavedra, M. D., Romero, A., Parada, E., Egea, J., Avila, J., McIntosh, J. M., Wonnacott, S., & Lopez, M. G. (2011). Neurotoxicity induced by okadaic acid in the human neuroblastoma SH-SY5Y line can be differentially prevented by alpha7 and beta2* nicotinic stimulation. *Toxicol Sci, 123*(1), 193-205. doi: 10.1093/toxsci/kfr163.

DeTure, M., Ko, L. W., Easson, C., & Yen, S. H. (2002). Tau assembly in inducible transfectants expressing wild-type or FTDP-17 tau. *Am J Pathol, 161*(5), 1711-1722. doi: 10.1016/S0002-9440(10)64448-3.

Dickey, C. A., Ash, P., Klosak, N., Lee, W. C., Petrucelli, L., Hutton, M., & Eckman, C. B. (2006). Pharmacologic reductions of total tau levels; implications for the role of microtubule dynamics in regulating tau expression. *Mol Neurodegener, 1*, 6. doi: 10.1186/1750-1326-1-6.

Ding, H., Dolan, P. J., & Johnson, G. V. (2008). Histone deacetylase 6 interacts with the microtubule-associated protein tau. *J Neurochem, 106*(5), 2119-2130. doi: 10.1111/j.1471-4159.2008.05564.x.

Eckert, A., Nisbet, R., Grimm, A., & Gotz, J. (2014). March separate, strike together--role of phosphorylated TAU in mitochondrial dysfunction in Alzheimer's disease. *Biochim Biophys Acta, 1842*(8), 1258-1266. doi: 10.1016/j.bbadis.2013.08.013.

Elliott, E., Tsvetkov, P., & Ginzburg, I. (2007). BAG-1 associates with Hsc70.Tau complex and regulates the proteasomal degradation of Tau protein. *J Biol Chem, 282*(51), 37276-37284. doi: 10.1074/jbc.M706379200.

Ferrari, A., Hoerndli, F., Baechi, T., Nitsch, R. M., & Gotz, J. (2003). beta-Amyloid induces paired helical filament-like tau filaments in tissue culture. *J Biol Chem, 278*(41), 40162-40168. doi: 10.1074/jbc.M308243200.

Ferrer, I. (2009). Altered mitochondria, energy metabolism, voltage-dependent anion channel, and lipid rafts converge to exhaust neurons in Alzheimer's disease. *J Bioenerg Biomembr, 41*(5), 425-431. doi: 10.1007/s10863-009-9243-5.

Fields, S., & Johnston, M. (2005). Cell biology. Whither model organism research? *Science, 307*(5717), 1885-1886. doi: 10.1126/science.1108872.

Frost, B., Gotz, J., & Feany, M. B. (2015). Connecting the dots between tau dysfunction and neurodegeneration. *Trends Cell Biol, 25*(1), 46-53. doi: 10.1016/j.tcb.2014.07.005.

Fulga, T. A., Elson-Schwab, I., Khurana, V., Steinhilb, M. L., Spires, T. L., Hyman, B. T., & Feany, M. B. (2007). Abnormal bundling and accumulation of F-actin mediates tau-induced neuronal degeneration in vivo. *Nat Cell Biol, 9*(2), 139-148. doi: 10.1038/ncb1528.

Fushimi, K., Long, C., Jayaram, N., Chen, X., Li, L., & Wu, J. Y. (2011). Expression of human FUS/TLS in yeast leads to protein aggregation and cytotoxicity, recapitulating key features of FUS proteinopathy. *Protein Cell, 2*(2), 141-149. doi: 10.1007/s13238-011-1014-5.

Gendron, T. F., & Petrucelli, L. (2009). The role of tau in neurodegeneration. *Mol Neurodegener, 4*, 13. doi: 10.1186/1750-1326-4-13.

Gerald, Z., & Ockert, W. (2013). Alzheimer's disease market: hope deferred. *Nat Rev Drug Discov, 12*(1), 19-20. doi: 10.1038/nrd3922.

Gietz, R. D., & Schiestl, R. H. (2007). Microtiter plate transformation using the LiAc/SS carrier DNA/PEG method. *Nat Protoc, 2*(1), 5-8. doi: 10.1038/nprot.2007.16.

Giorgini, F., Guidetti, P., Nguyen, Q., Bennett, S. C., & Muchowski, P. J. (2005). A genomic screen in yeast implicates kynurenine 3-monooxygenase as a therapeutic target for Huntington's disease. *Nat Genet, 37*(5), 526-531.

Giorgini, F., & Muchowski, P. J. (2006). Screening for genetic modifiers of amyloid toxicity in yeast. *Methods Enzymol, 412*, 201-222. doi: 10.1016/S0076-6879(06)12013-3.

Glading, A., Bodnar, R. J., Reynolds, I. J., Shiraha, H., Satish, L., Potter, D. A., Blair, H. C., & Wells, A. (2004). Epidermal Growth Factor Activates m-Calpain (Calpain II), at Least in Part, by Extracellular Signal-Regulated Kinase-Mediated Phosphorylation. *Mol Cell Biol, 24*(6), 2499-2512. doi: 10.1128/mcb.24.6.2499-2512.2004.

Goedert, M. (2005). Tau gene mutations and their effects. *Mov Disord, 20 Suppl 12*, S45-52. doi: 10.1002/mds.20539.

Goedert, M., & Spillantini, M. G. (2006). A century of Alzheimer's disease. *Science, 314*(5800), 777-781. doi: 10.1126/science.1132814.

Gotz, J., David, D., Hoerndli, F., Ke, Y. D., Schonrock, N., Wiesner, A., Fath, T., Bokhari, L., Lim, Y. A., Deters, N., & Ittner, L. M. (2008). Functional genomics dissects pathomechanisms in tauopathies: mitosis failure and unfolded protein response. *Neurodegener Dis, 5*(3-4), 179-181. doi: 10.1159/000113696.

Gotz, J., Gladbach, A., Pennanen, L., van Eersel, J., Schild, A., David, D., & Ittner, L. M. (2010). Animal models reveal role for tau phosphorylation in human disease. *Biochim Biophys Acta, 1802*(10), 860-871. doi: 10.1016/j.bbadis.2009.09.008.

Gu, G. J., Lund, H., Wu, D., Blokzijl, A., Classon, C., von Euler, G., Landegren, U., Sunnemark, D., & Kamali-Moghaddam, M. (2013). Role of individual MARK isoforms in phosphorylation of tau at Ser(2)(6)(2) in Alzheimer's disease. *Neuromolecular Med, 15*(3), 458-469. doi: 10.1007/s12017-013-8232-3.

Guo, J. L., & Lee, V. M. (2011). Seeding of normal Tau by pathological Tau conformers drives pathogenesis of Alzheimer-like tangles. *J Biol Chem, 286*(17), 15317-15331. doi: 10.1074/jbc.M110.209296.

Guo, J. P., Arai, T., Miklossy, J., & McGeer, P. L. (2006). Abeta and tau form soluble complexes that may promote self aggregation of both into the insoluble forms observed in Alzheimer's disease. *Proc Natl Acad Sci U S A, 103*(6), 1953-1958. doi: 10.1073/pnas.0509386103.

Haass, C., & Selkoe, D. J. (2007). Soluble protein oligomers in neurodegeneration: lessons from the Alzheimer's amyloid beta-peptide. *Nat Rev Mol Cell Biol, 8*(2), 101-112. doi: 10.1038/nrm2101.

Hampel, H., Prvulovic, D., Teipel, S., Jessen, F., Luckhaus, C., Frolich, L., Riepe, M. W., Dodel, R., Leyhe, T., Bertram, L., Hoffmann, W., Faltraco, F., & German Task Force on Alzheimer's, D.

(2011). The future of Alzheimer's disease: the next 10 years. *Prog Neurobiol, 95*(4), 718-728. doi: 10.1016/j.pneurobio.2011.11.008.

Han, C., & Wang, B. (2005). Factors That Impact the Developability of Drug Candidates: An Overview *Drug Delivery* (pp. 1-14): John Wiley & Sons, Inc.

Hardy, J., & Allsop, D. (1991). Amyloid deposition as the central event in the aetiology of Alzheimer's disease. *Trends Pharmacol Sci, 12*(10), 383-388.

Harvey, A. L. (2008). Natural products in drug discovery. *Drug Discov Today, 13*(19-20), 894-901. doi: 10.1016/j.drudis.2008.07.004.

Hill, B. G., Benavides, G. A., Lancaster, J. R., Jr., Ballinger, S., Dell'Italia, L., Jianhua, Z., & Darley-Usmar, V. M. (2012). Integration of cellular bioenergetics with mitochondrial quality control and autophagy. *Biol Chem, 393*(12), 1485-1512. doi: 10.1515/hsz-2012-0198.

Hu, G. (2011). Understanding the fundamentals of peptides and proteins. *BioProcess J, 10*(1), 12-14. doi: http://dx.doi.org/10.12665/J101.Hu.

Huang, H. C., & Jiang, Z. F. (2009). Accumulated amyloid-beta peptide and hyperphosphorylated tau protein: relationship and links in Alzheimer's disease. *J Alzheimers Dis, 16*(1), 15-27. doi: 10.3233/JAD-2009-0960.

Hughes, J. P., Rees, S., Kalindjian, S. B., & Philpott, K. L. (2011). Principles of early drug discovery. *Br J Pharmacol, 162*(6), 1239-1249. doi: 10.1111/j.1476-5381.2010.01127.x.

Hurtado, D. E., Molina-Porcel, L., Carroll, J. C., Macdonald, C., Aboagye, A. K., Trojanowski, J. Q., & Lee, V. M. (2012). Selectively silencing GSK-3 isoforms reduces plaques and tangles in mouse models of Alzheimer's disease. *J Neurosci, 32*(21), 7392-7402. doi: 10.1523/JNEUROSCI.0889-12.2012.

Iijima, K., Gatt, A., & Iijima-Ando, K. (2010). Tau Ser262 phosphorylation is critical for Abeta42-induced tau toxicity in a transgenic Drosophila model of Alzheimer's disease. *Hum Mol Genet, 19*(15), 2947-2957. doi: 10.1093/hmg/ddq200.

Ilouga, P. E., & Hesterkamp, T. (2012). On the prediction of statistical parameters in high-throughput screening using resampling techniques. *J Biomol Screen, 17*(6), 705-712. doi: 10.1177/1087057112441623.

Ittner, A., Ke, Y. D., van Eersel, J., Gladbach, A., Gotz, J., & Ittner, L. M. (2011). Brief update on different roles of tau in neurodegeneration. *IUBMB Life, 63*(7), 495-502. doi: 10.1002/iub.467.

Ittner, L. M., & Gotz, J. (2011). Amyloid-beta and tau--a toxic pas de deux in Alzheimer's disease. *Nat Rev Neurosci, 12*(2), 65-72. doi: 10.1038/nrn2967.

Ittner, L. M., Ke, Y. D., Delerue, F., Bi, M., Gladbach, A., van Eersel, J., Wolfing, H., Chieng, B. C., Christie, M. J., Napier, I. A., Eckert, A., Staufenbiel, M., Hardeman, E., & Gotz, J. (2010). Dendritic function of tau mediates amyloid-beta toxicity in Alzheimer's disease mouse models. *Cell, 142*(3), 387-397. doi: 10.1016/j.cell.2010.06.036.

Ittner, L. M., Ke, Y. D., & Gotz, J. (2009). Phosphorylated Tau interacts with c-Jun N-terminal kinase-interacting protein 1 (JIP1) in Alzheimer disease. *J Biol Chem, 284*(31), 20909-20916. doi: 10.1074/jbc.M109.014472.

Jinwal, U. K., Akoury, E., Abisambra, J. F., O'Leary, J. C., 3rd, Thompson, A. D., Blair, L. J., Jin, Y., Bacon, J., Nordhues, B. A., Cockman, M., Zhang, J., Li, P., Zhang, B., Borysov, S., Uversky, V. N., Biernat, J., Mandelkow, E., Gestwicki, J. E., Zweckstetter, M., & Dickey, C. A. (2013). Imbalance of Hsp70 family variants fosters tau accumulation. *FASEB J, 27*(4), 1450-1459. doi: 10.1096/fj.12-220889.

Johnson, B. S., McCaffery, J. M., Lindquist, S., & Gitler, A. D. (2008). A yeast TDP-43 proteinopathy model: Exploring the molecular determinants of TDP-43 aggregation and cellular toxicity. *Proc Natl Acad Sci U S A, 105*(17), 6439-6444. doi: 10.1073/pnas.0802082105.

Johri, A., & Beal, M. F. (2012). Mitochondrial dysfunction in neurodegenerative diseases. *J Pharmacol Exp Ther, 342*(3), 619-630. doi: 10.1124/jpet.112.192138.

Ju, S., Tardiff, D. F., Han, H., Divya, K., Zhong, Q., Maquat, L. E., Bosco, D. A., Hayward, L. J., Brown, R. H., Jr., Lindquist, S., Ringe, D., & Petsko, G. A. (2011). A yeast model of FUS/TLS-dependent cytotoxicity. *PLoS Biol, 9*(4), e1001052. doi: 10.1371/journal.pbio.1001052.

Kamat, P. K., Rai, S., & Nath, C. (2013). Okadaic acid induced neurotoxicity: an emerging tool to study Alzheimer's disease pathology. *Neurotoxicology, 37*, 163-172. doi: 10.1016/j.neuro.2013.05.002.

Karagoz, G. E., Duarte, A. M., Akoury, E., Ippel, H., Biernat, J., Moran Luengo, T., Radli, M., Didenko, T., Nordhues, B. A., Veprintsev, D. B., Dickey, C. A., Mandelkow, E., Zweckstetter, M., Boelens, R., Madl, T., & Rudiger, S. G. (2014). Hsp90-Tau complex reveals molecular basis for specificity in chaperone action. *Cell, 156*(5), 963-974. doi: 10.1016/j.cell.2014.01.037.

Karsten, S. L., Sang, T. K., Gehman, L. T., Chatterjee, S., Liu, J., Lawless, G. M., Sengupta, S., Berry, R. W., Pomakian, J., Oh, H. S., Schulz, C., Hui, K. S., Wiedau-Pazos, M., Vinters, H. V., Binder, L. I., Geschwind, D. H., & Jackson, G. R. (2006). A genomic screen for modifiers of tauopathy identifies puromycin-sensitive aminopeptidase as an inhibitor of tau-induced neurodegeneration. *Neuron, 51*(5), 549-560. doi: 10.1016/j.neuron.2006.07.019.

Kaur, R., & Bachhawat, A. K. (1999). The yeast multidrug resistance pump, Pdr5p, confers reduced drug resistance in erg mutants of Saccharomyces cerevisiae. *Microbiology, 145 (Pt 4)*(1350-0872 (Print)), 809-818.

Kawakami, F., Shimada, N., Ohta, E., Kagiya, G., Kawashima, R., Maekawa, T., Maruyama, H., & Ichikawa, T. (2014). Leucine-rich repeat kinase 2 regulates tau phosphorylation through direct activation of glycogen synthase kinase-3beta. *FEBS J, 281*(1), 3-13. doi: 10.1111/febs.12579.

Kawakami, F., Suzuki, M., Shimada, N., Kagiya, G., Ohta, E., Tamura, K., Maruyama, H., & Ichikawa, T. (2011). Stimulatory effect of alpha-synuclein on the tau-phosphorylation by GSK-3beta. *FEBS J, 278*(24), 4895-4904. doi: 10.1111/j.1742-4658.2011.08389.x.

Ke, Y. D., Dramiga, J., Schutz, U., Kril, J. J., Ittner, L. M., Schroder, H., & Gotz, J. (2012a). Tau-mediated nuclear depletion and cytoplasmic accumulation of SFPQ in Alzheimer's and Pick's disease. *PLoS One, 7*(4), e35678. doi: 10.1371/journal.pone.0035678.

Ke, Y. D., Suchowerska, A. K., van der Hoven, J., De Silva, D. M., Wu, C. W., van Eersel, J., Ittner, A., & Ittner, L. M. (2012b). Lessons from tau-deficient mice. *Int J Alzheimers Dis, 2012*, 873270. doi: 10.1155/2012/873270.

Khanna, I. (2012). Drug discovery in pharmaceutical industry: productivity challenges and trends. *Drug Discov Today, 17*(19-20), 1088-1102. doi: 10.1016/j.drudis.2012.05.007.

Khlistunova, I., Biernat, J., Wang, Y., Pickhardt, M., von Bergen, M., Gazova, Z., Mandelkow, E., & Mandelkow, E. M. (2006). Inducible expression of Tau repeat domain in cell models of tauopathy: aggregation is toxic to cells but can be reversed by inhibitor drugs. *J Biol Chem, 281*(2), 1205-1214. doi: 10.1074/jbc.M507753200.

Khurana, V., & Lindquist, S. (2010). Modelling neurodegeneration in Saccharomyces cerevisiae: why cook with baker's yeast? *Nat Rev Neurosci, 11*(6), 436-449. doi: 10.1038/nrn2809.

Kingston, D. G. (2011). Modern natural products drug discovery and its relevance to biodiversity conservation. *J Nat Prod, 74*(3), 496-511. doi: 10.1021/np100550t.

Kolaczkowski, M., Kolaczowska, A., Luczynski, J., Witek, S., & Goffeau, A. (1998). In vivo characterization of the drug resistance profile of the major ABC transporters and other components of the yeast pleiotropic drug resistance network. *Microb Drug Resist, 4*(3), 143-158.

Kramer, J. A., Sagartz, J. E., & Morris, D. L. (2007). The application of discovery toxicology and pathology towards the design of safer pharmaceutical lead candidates. *Nat Rev Drug Discov, 6*(8), 636-649. doi: 10.1038/nrd2378.

Kremer, A., Louis, J. V., Jaworski, T., & Van Leuven, F. (2011). GSK3 and Alzheimer's Disease: Facts and Fiction. *Front Mol Neurosci, 4*, 17. doi: 10.3389/fnmol.2011.00017.

LaFerla, F. M. (2010). Pathways linking Abeta and tau pathologies. *Biochem Soc Trans, 38*(4), 993-995. doi: 10.1042/BST0380993.

LaFerla, F. M., Green, K. N., & Oddo, S. (2007). Intracellular amyloid-beta in Alzheimer's disease. *Nat Rev Neurosci, 8*(7), 499-509. doi: 10.1038/nrn2168.

Lawrence, J. (2015). Drug discovery returns to the wild. *The Pharmaceutical Journal, 294*(7849, online).

Leader, B., Baca, Q. J., & Golan, D. E. (2008). Protein therapeutics: a summary and pharmacological classification. *Nat Rev Drug Discov, 7*(1), 21-39. doi: 10.1038/nrd2399.

Lee, G. (2005). Tau and src family tyrosine kinases. *Biochim Biophys Acta, 1739*(2-3), 323-330. doi: 10.1016/j.bbadis.2004.09.002.

Lee, G., & Leugers, C. J. (2012). Tau and tauopathies. *Prog Mol Biol Transl Sci, 107*, 263-293. doi: 10.1016/B978-0-12-385883-2.00004-7.

Lee, V. M., Goedert, M., & Trojanowski, J. Q. (2001). Neurodegenerative tauopathies. *Annu Rev Neurosci, 24*, 1121-1159. doi: 10.1146/annurev.neuro.24.1.1121.

Leeson, P. (2012). Drug discovery: Chemical beauty contest. *Nature, 481*(7382), 455-456. doi: 10.1038/481455a.

Lei, P., Ayton, S., Bush, A. I., & Adlard, P. A. (2011). GSK-3 in Neurodegenerative Diseases. *Int J Alzheimers Dis, 2011*, 189246. doi: 10.4061/2011/189246.

Leroy, K., Ando, K., Laporte, V., Dedecker, R., Suain, V., Authelet, M., Heraud, C., Pierrot, N., Yilmaz, Z., Octave, J. N., & Brion, J. P. (2012). Lack of tau proteins rescues neuronal cell death and decreases amyloidogenic processing of APP in APP/PS1 mice. *Am J Pathol, 181*(6), 1928-1940. doi: 10.1016/j.ajpath.2012.08.012.

Lipinski, C. A., Lombardo, F., Dominy, B. W., & Feeney, P. J. (2001). Experimental and computational approaches to estimate solubility and permeability in drug discovery and development settings. *Adv Drug Deliv Rev, 46*(1-3), 3-26.

Liu, C., & Gotz, J. (2013). Profiling murine tau with 0N, 1N and 2N isoform-specific antibodies in brain and peripheral organs reveals distinct subcellular localization, with the 1N isoform being enriched in the nucleus. *PLoS One, 8*(12), e84849. doi: 10.1371/journal.pone.0084849.

Liu, F., Iqbal, K., Grundke-Iqbal, I., & Gong, C. X. (2002). Involvement of aberrant glycosylation in phosphorylation of tau by cdk5 and GSK-3beta. *FEBS Lett, 530*(1-3), 209-214.

Lombardino, J. G., & Lowe, J. A., 3rd. (2004). The role of the medicinal chemist in drug discovery--then and now. *Nat Rev Drug Discov, 3*(10), 853-862. doi: 10.1038/nrd1523.

Luong, A., Hannah, V. C., Brown, M. S., & Goldstein, J. L. (2000). Molecular characterization of human acetyl-CoA synthetase, an enzyme regulated by sterol regulatory element-binding proteins. *J Biol Chem, 275*(34), 26458-26466. doi: 10.1074/jbc.M004160200.

Mager, W. H., & Winderickx, J. (2005). Yeast as a model for medical and medicinal research. *Trends Pharmacol Sci, 26*(5), 265-273. doi: 10.1016/j.tips.2005.03.004.

Magnani, E., Fan, J., Gasparini, L., Golding, M., Williams, M., Schiavo, G., Goedert, M., Amos, L. A., & Spillantini, M. G. (2007). Interaction of tau protein with the dynactin complex. *EMBO J, 26*(21), 4546-4554. doi: 10.1038/sj.emboj.7601878.

Manczak, M., & Reddy, P. H. (2012). Abnormal interaction of VDAC1 with amyloid beta and phosphorylated tau causes mitochondrial dysfunction in Alzheimer's disease. *Hum Mol Genet, 21*(23), 5131-5146. doi: 10.1093/hmg/dds360.

Mandelkow, E., von Bergen, M., Biernat, J., & Mandelkow, E. M. (2007). Structural principles of tau and the paired helical filaments of Alzheimer's disease. *Brain Pathol, 17*(1), 83-90. doi: 10.1111/j.1750-3639.2007.00053.x.

Martin, L., Latypova, X., & Terro, F. (2011). Post-translational modifications of tau protein: implications for Alzheimer's disease. *Neurochem Int, 58*(4), 458-471. doi: 10.1016/j.neuint.2010.12.023.

Martins, A., Andrade, G., Rodrigues, C., Almeida, A., & Vieira, H. (2013a). Anti-Tuberculosis Activity Present in a Unique Marine Bacteria Collection from Portuguese Deep Sea Hydrothermal Vents. *Journal of Marine Biology & Oceanography, 02*(03). doi: 10.4172/2324-8661.1000113.

Martins, A., Tenreiro, T., Andrade, G., Gadanho, M., Chaves, S., Abrantes, M., Calado, P., Tenreiro, R., & Vieira, H. (2013b). Photoprotective bioactivity present in a unique marine bacteria collection

from Portuguese deep sea hydrothermal vents. *Mar Drugs, 11*(5), 1506-1523. doi: 10.3390/md11051506.

Martins, A., Vieira, H., Gaspar, H., & Santos, S. (2014). Marketed marine natural products in the pharmaceutical and cosmeceutical industries: tips for success. *Mar Drugs, 12*(2), 1066-1101. doi: 10.3390/md12021066.

Mayer, B. J. (2001). SH3 domains: complexity in moderation. *J Cell Sci, 114*(Pt 7), 1253-1263.

Mayr, J. A., Merkel, O., Kohlwein, S. D., Gebhardt, B. R., Bohles, H., Fotschl, U., Koch, J., Jaksch, M., Lochmuller, H., Horvath, R., Freisinger, P., & Sperl, W. (2007). Mitochondrial phosphate-carrier deficiency: a novel disorder of oxidative phosphorylation. *Am J Hum Genet, 80*(3), 478-484. doi: 10.1086/511788.

Medina, M., & Avila, J. (2014). New perspectives on the role of tau in Alzheimer's disease. Implications for therapy. *Biochem Pharmacol, 88*(4), 540-547. doi: 10.1016/j.bcp.2014.01.013.

Meerbrey, K. L., Hu, G., Kessler, J. D., Roarty, K., Li, M. Z., Fang, J. E., Herschkowitz, J. I., Burrows, A. E., Ciccia, A., Sun, T., Schmitt, E. M., Bernardi, R. J., Fu, X., Bland, C. S., Cooper, T. A., Schiff, R., Rosen, J. M., Westbrook, T. F., & Elledge, S. J. (2011). The pINDUCER lentiviral toolkit for inducible RNA interference in vitro and in vivo. *Proc Natl Acad Sci U S A, 108*(9), 3665-3670. doi: 10.1073/pnas.1019736108.

Miller-Fleming, L., Giorgini, F., & Outeiro, T. F. (2008). Yeast as a model for studying human neurodegenerative disorders. *Biotechnol J, 3*(3), 325-338. doi: 10.1002/biot.200700217.

Min, S. W., Cho, S. H., Zhou, Y., Schroeder, S., Haroutunian, V., Seeley, W. W., Huang, E. J., Shen, Y., Masliah, E., Mukherjee, C., Meyers, D., Cole, P. A., Ott, M., & Gan, L. (2010). Acetylation of tau inhibits its degradation and contributes to tauopathy. *Neuron, 67*(6), 953-966. doi: 10.1016/j.neuron.2010.08.044.

Minami, S. S., Clifford, T. G., Hoe, H. S., Matsuoka, Y., & Rebeck, G. W. (2012). Fyn knock-down increases Abeta, decreases phospho-tau, and worsens spatial learning in 3xTg-AD mice. *Neurobiol Aging, 33*(4), 825 e815-824. doi: 10.1016/j.neurobiolaging.2011.05.014.

Moreira, P. I., Santos, M. S., & Oliveira, C. R. (2007). Alzheimer's disease: a lesson from mitochondrial dysfunction. *Antioxid Redox Signal, 9*(10), 1621-1630. doi: 10.1089/ars.2007.1703.

Morell, M., de Groot, N. S., Vendrell, J., Aviles, F. X., & Ventura, S. (2011). Linking amyloid protein aggregation and yeast survival. *Mol Biosyst, 7*(4), 1121-1128. doi: 10.1039/c0mb00297f.

Morris, M., Maeda, S., Vossel, K., & Mucke, L. (2011). The many faces of tau. *Neuron, 70*(3), 410-426. doi: 10.1016/j.neuron.2011.04.009.

Neve, R. L., Harris, P., Kosik, K. S., Kurnit, D. M., & Donlon, T. A. (1986). Identification of cDNA clones for the human microtubule-associated protein tau and chromosomal localization of the genes for tau and microtubule-associated protein 2. *Brain Res, 387*(3), 271-280.

Newman, D. J., & Cragg, G. M. (2007). Natural Products as Sources of New Drugs over the Last 25 Years. *J. Nat. Prod., 70*, 461-477.

Noble, W., Hanger, D. P., Miller, C. C., & Lovestone, S. (2013). The importance of tau phosphorylation for neurodegenerative diseases. *Front Neurol, 4*, 83. doi: 10.3389/fneur.2013.00083.

Noble, W., Pooler, A. M., & Hanger, D. P. (2011). Advances in tau-based drug discovery. *Expert Opin Drug Discov, 6*(8), 797-810. doi: 10.1517/17460441.2011.586690.

Oddo, S., Caccamo, A., Shepherd, J. D., Murphy, M. P., Golde, T. E., Kayed, R., Metherate, R., Mattson, M. P., Akbari, Y., & LaFerla, F. M. (2003). Triple-transgenic model of Alzheimer's disease with plaques and tangles: intracellular Abeta and synaptic dysfunction. *Neuron, 39*(3), 409-421. doi: 10.1016/s0896-6273(03)00434-3.

Outeiro, T. F., & Giorgini, F. (2006). Yeast as a drug discovery platform in Huntington's and Parkinson's diseases. *Biotechnol J, 1*(3), 258-269. doi: 10.1002/biot.200500043.

Ozdemir, A. Y., Rom, I., Kovalevich, J., Yen, W., Adiga, R., Dave, R. S., & Langford, D. (2013). PINCH in the cellular stress response to tau-hyperphosphorylation. *PLoS One, 8*(3), e58232. doi: 10.1371/journal.pone.0058232.

Palmieri, F. (2013). The mitochondrial transporter family SLC25: identification, properties and physiopathology. *Mol Aspects Med, 34*(2-3), 465-484. doi: 10.1016/j.mam.2012.05.005.

Pan, X. D., & Chen, X. C. (2013). Clinic, neuropathology and molecular genetics of frontotemporal dementia: a mini-review. *Transl Neurodegener, 2*(1), 8. doi: 10.1186/2047-9158-2-8.

Passeleu-Le Bourdonnec, C., Carrupt, P. A., Scherrmann, J. M., & Martel, S. (2013). Methodologies to assess drug permeation through the blood-brain barrier for pharmaceutical research. *Pharm Res, 30*(11), 2729-2756. doi: 10.1007/s11095-013-1119-z.

Paul, S. M., Mytelka, D. S., Dunwiddie, C. T., Persinger, C. C., Munos, B. H., Lindborg, S. R., & Schacht, A. L. (2010). How to improve R&D productivity: the pharmaceutical industry's grand challenge. *Nat Rev Drug Discov, 9*(3), 203-214. doi: 10.1038/nrd3078.

Pei, J. J., An, W. L., Zhou, X. W., Nishimura, T., Norberg, J., Benedikz, E., Gotz, J., & Winblad, B. (2006). P70 S6 kinase mediates tau phosphorylation and synthesis. *FEBS Lett, 580*(1), 107-114. doi: 10.1016/j.febslet.2005.11.059.

Peng, C., Ye, J., Yan, S., Kong, S., Shen, Y., Li, C., Li, Q., Zheng, Y., Deng, K., Xu, T., & Tao, W. (2012). Ablation of vacuole protein sorting 18 (Vps18) gene leads to neurodegeneration and impaired neuronal migration by disrupting multiple vesicle transport pathways to lysosomes. *J Biol Chem, 287*(39), 32861-32873. doi: 10.1074/jbc.M112.384305.

Petrucelli, L., Dickson, D., Kehoe, K., Taylor, J., Snyder, H., Grover, A., De Lucia, M., McGowan, E., Lewis, J., Prihar, G., Kim, J., Dillmann, W. H., Browne, S. E., Hall, A., Voellmy, R., Tsuboi, Y., Dawson, T. M., Wolozin, B., Hardy, J., & Hutton, M. (2004). CHIP and Hsp70 regulate tau ubiquitination, degradation and aggregation. *Hum Mol Genet, 13*(7), 703-714. doi: 10.1093/hmg/ddh083.

Prince, M., Bryce, R., & Ferri, C. (2011). World Alzheimer Report Alzheimer's Disease International.

Prince, M., & Jackson, J. (2009). World Alzheimer report 2009. Retrieved June, 2014, from http://www.alz.co.uk/research/files/WorldAlzheimerReport.pdf.

Qiang, L., Yu, W., Andreadis, A., Luo, M., & Baas, P. W. (2006). Tau protects microtubules in the axon from severing by katanin. *J Neurosci, 26*(12), 3120-3129. doi: 10.1523/JNEUROSCI.5392-05.2006.

Rademakers, R., Neumann, M., & Mackenzie, I. R. (2012). Advances in understanding the molecular basis of frontotemporal dementia. *Nat Rev Neurol, 8*(8), 423-434. doi: 10.1038/nrneurol.2012.117.

Rami, A. (2009). Review: autophagy in neurodegeneration: firefighter and/or incendiarist? *Neuropathol Appl Neurobiol, 35*(5), 449-461. doi: 10.1111/j.1365-2990.2009.01034.x.

Rao, D. D., Vorhies, J. S., Senzer, N., & Nemunaitis, J. (2009). siRNA vs. shRNA: similarities and differences. *Adv Drug Deliv Rev, 61*(9), 746-759. doi: 10.1016/j.addr.2009.04.004.

Ratnaparkhi, M. P., Chaudhari, S. P., & Pandya, V. A. (2011). Peptides and proteins in pharmaceuticals. *Int J Curr Pharm Res, 3*(2), 1-9.

Richet, E., Pooler, A. M., Rodriguez, T., Novoselov, S. S., Schmidtke, G., Groettrup, M., Hanger, D. P., Cheetham, M. E., & van der Spuy, J. (2012). NUB1 modulation of GSK3beta reduces tau aggregation. *Hum Mol Genet, 21*(24), 5254-5267. doi: 10.1093/hmg/dds376.

Roberson, E. D., Scearce-Levie, K., Palop, J. J., Yan, F., Cheng, I. H., Wu, T., Gerstein, H., Yu, G. Q., & Mucke, L. (2007). Reducing endogenous tau ameliorates amyloid beta-induced deficits in an Alzheimer's disease mouse model. *Science, 316*(5825), 750-754. doi: 10.1126/science.1141736.

Rodgers, A. B., Aging, N. I. o., & Health, N. I. o. (2008). *Alzheimer's Disease: Unraveling the Mystery*: National Institutes of Health.

Rodrigues, C., Martins, A. R., Andrade, G., Cerejo, M., Pinheiro, R., Calado, P., & Vieira, H. (2011). Exploring the industrial value of the portuguese deep sea microorganisms. *Spatial and Organizational Dynamics, 8*, 107-114.

Royle, K. E., Jimenez del Val, I., & Kontoravdi, C. (2013). Integration of models and experimentation to optimise the production of potential biotherapeutics. *Drug Discov Today, 18*(23-24), 1250-1255. doi: 10.1016/j.drudis.2013.07.002.

Sadik, G., Tanaka, T., Kato, K., Yamamori, H., Nessa, B. N., Morihara, T., & Takeda, M. (2009). Phosphorylation of tau at Ser214 mediates its interaction with 14-3-3 protein: implications for the mechanism of tau aggregation. *J Neurochem, 108*(1), 33-43. doi: 10.1111/j.1471-4159.2008.05716.x.

Sarker, S. D., Latif, Z., & Gray, A. I. (2006). An Introduction to Natural Products Isolation. In S. D. Sarker, Z. Latif & A. I. Gray (Eds.), *Natural Products Isolation* (2nd Ed. ed., Vol. 864, pp. 1-25). Totowa, New Jersey: Humana Press.

Sasaki, K., Shimura, H., Itaya, M., Tanaka, R., Mori, H., Mizuno, Y., Kosik, K. S., Tanaka, S., & Hattori, N. (2009). Excitatory amino acid transporter 2 associates with phosphorylated tau and is localized in neurofibrillary tangles of tauopathic brains. *FEBS Lett, 583*(13), 2194-2200. doi: 10.1016/j.febslet.2009.06.015.

Satoh, J., Kawana, N., & Yamamoto, Y. (2013). Pathway Analysis of ChIP-Seq-Based NRF1 Target Genes Suggests a Logical Hypothesis of their Involvement in the Pathogenesis of Neurodegenerative Diseases. *Gene Regul Syst Bio, 7*, 139-152. doi: 10.4137/GRSB.S13204.

Scales, T. M., Derkinderen, P., Leung, K. Y., Byers, H. L., Ward, M. A., Price, C., Bird, I. N., Perera, T., Kellie, S., Williamson, R., Anderton, B. H., & Reynolds, C. H. (2011). Tyrosine phosphorylation of tau by the SRC family kinases lck and fyn. *Mol Neurodegener, 6*, 12. doi: 10.1186/1750-1326-6-12.

Schmitz, M., Wulf, K., Signore, S. C., Schulz-Schaeffer, W. J., Kermer, P., Bahr, M., Wouters, F. S., Zafar, S., & Zerr, I. (2014). Impact of the cellular prion protein on amyloid-beta and 3PO-tau processing. *J Alzheimers Dis, 38*(3), 551-565. doi: 10.3233/JAD-130566.

Schneider, C. A., Rasband, W. S., & Eliceiri, K. W. (2012). NIH Image to ImageJ: 25 years of image analysis. *Nat Methods, 9*(7), 671-675.

Scholz, T., & Mandelkow, E. (2014). Transport and diffusion of Tau protein in neurons. *Cell Mol Life Sci, 71*(16), 3139-3150. doi: 10.1007/s00018-014-1610-7.

Schon, E. A., & Przedborski, S. (2011). Mitochondria: the next (neurode)generation. *Neuron, 70*(6), 1033-1053. doi: 10.1016/j.neuron.2011.06.003.

SeaHorseBioscience. (2015). XF Cell Mito Stress Test Kit User Guide. In S. Bioscience (Ed.), (pp. 1-9): SeaHorse Biosciense.

Shea, T., & Cressman, C. (1998). A 26-30 kDA developmentally regulated tau isoform localized within nuclei of mitotic human neuroblastoma cells. *Int J Devl Neuroscience, 16*(1), 41-48.

Shimura, H., Schwartz, D., Gygi, S. P., & Kosik, K. S. (2004). CHIP-Hsc70 complex ubiquitinates phosphorylated tau and enhances cell survival. *J Biol Chem, 279*(6), 4869-4876. doi: 10.1074/jbc.M305838200.

Shin, K. J., Wall, E. A., Zavzavadjian, J. R., Santat, L. A., Liu, J., Hwang, J. I., Rebres, R., Roach, T., Seaman, W., Simon, M. I., & Fraser, I. D. (2006). A single lentiviral vector platform for microRNA-based conditional RNA interference and coordinated transgene expression. *Proc Natl Acad Sci U S A, 103*(37), 13759-13764. doi: 10.1073/pnas.0606179103.

Shipton, O. A., Leitz, J. R., Dworzak, J., Acton, C. E., Tunbridge, E. M., Denk, F., Dawson, H. N., Vitek, M. P., Wade-Martins, R., Paulsen, O., & Vargas-Caballero, M. (2011). Tau protein is required for amyloid {beta}-induced impairment of hippocampal long-term potentiation. *J Neurosci, 31*(5), 1688-1692. doi: 10.1523/JNEUROSCI.2610-10.2011.

Shulman, J. M., & Feany, M. B. (2003). Genetic modifiers of tauopathy in Drosophila. *Genetics, 165*(3), 1233-1242.

Shulman, J. M., Imboywa, S., Giagtzoglou, N., Powers, M. P., Hu, Y., Devenport, D., Chipendo, P., Chibnik, L. B., Diamond, A., Perrimon, N., Brown, N. H., De Jager, P. L., & Feany, M. B. (2014). Functional screening in Drosophila identifies Alzheimer's disease susceptibility genes and implicates Tau-mediated mechanisms. *Hum Mol Genet, 23*(4), 870-877. doi: 10.1093/hmg/ddt478.

Sjoberg, M. K., Shestakova, E., Mansuroglu, Z., Maccioni, R. B., & Bonnefoy, E. (2006). Tau protein binds to pericentromeric DNA: a putative role for nuclear tau in nucleolar organization. *J Cell Sci, 119*(Pt 10), 2025-2034. doi: 10.1242/jcs.02907.

Skovronsky, D. M., Lee, V. M.-Y., & Trojanowski, J. K. (2006). Neurodegenerative Diseases: New Concepts of Pathogenesis and Their Therapeutic Implications. *Annu. Rev. Pathol. Mech. Dis., 1*, 151–170. doi: 10.1146/.

Small, S. A., & Duff, K. (2008). Linking Abeta and tau in late-onset Alzheimer's disease: a dual pathway hypothesis. *Neuron, 60*(4), 534-542. doi: 10.1016/j.neuron.2008.11.007.

Smith, A. M., Ammar, R., Nislow, C., & Giaever, G. (2010). A survey of yeast genomic assays for drug and target discovery. *Pharmacol Ther, 127*(2), 156-164. doi: 10.1016/j.pharmthera.2010.04.012.

Sofola, O., Kerr, F., Rogers, I., Killick, R., Augustin, H., Gandy, C., Allen, M. J., Hardy, J., Lovestone, S., & Partridge, L. (2010). Inhibition of GSK-3 ameliorates Abeta pathology in an adult-onset Drosophila model of Alzheimer's disease. *PLoS Genet, 6*(9), e1001087. doi: 10.1371/journal.pgen.1001087.

Sorgjerd, K. M., Zako, T., Sakono, M., Stirling, P. C., Leroux, M. R., Saito, T., Nilsson, P., Sekimoto, M., Saido, T. C., & Maeda, M. (2013). Human prefoldin inhibits amyloid-beta (Abeta) fibrillation and contributes to formation of nontoxic Abeta aggregates. *Biochemistry, 52*(20), 3532-3542. doi: 10.1021/bi301705c.

Spillantini, M. G., & Goedert, M. (2013a). Tau pathology and neurodegeneration. *Lancet Neurol, 12*, 609-622.

Spillantini, M. G., & Goedert, M. (2013b). Tau pathology and neurodegeneration. *Lancet Neurol, 12*(6), 609-622. doi: 10.1016/S1474-4422(13)70090-5.

Sultan, A., Nesslany, F., Violet, M., Begard, S., Loyens, A., Talahari, S., Mansuroglu, Z., Marzin, D., Sergeant, N., Humez, S., Colin, M., Bonnefoy, E., Buee, L., & Galas, M. C. (2011). Nuclear tau, a key player in neuronal DNA protection. *J Biol Chem, 286*(6), 4566-4575. doi: 10.1074/jbc.M110.199976.

Summers, D. W., & Cyr, D. M. (2011). Use of yeast as a system to study amyloid toxicity. *Methods, 53*(3), 226-231. doi: 10.1016/j.ymeth.2010.11.007.

Sun, Z., Diaz, Z., Fang, X., Hart, M. P., Chesi, A., Shorter, J., & Gitler, A. D. (2011). Molecular determinants and genetic modifiers of aggregation and toxicity for the ALS disease protein FUS/TLS. *PLoS Biol, 9*(4), e1000614. doi: 10.1371/journal.pbio.1000614.

Suter, B., Auerbach, D., & Stagljar, I. (2006). Yeast-based functional genomics and proteomics technologies: the first 15 years and beyond. *BioTechniques, 40*(5), 625-644. doi: 10.2144/000112151.

Swerdlow, R. H., Burns, J. M., & Khan, S. M. (2010). The Alzheimer's disease mitochondrial cascade hypothesis. *J Alzheimers Dis, 20 Suppl 2*, S265-279. doi: 10.3233/JAD-2010-100339.

Takashima, A., Murayama, M., Murayama, O., Kohno, T., Honda, T., Yasutake, K., Nihonmatsu, N., Mercken, M., Yamaguchi, H., Sugihara, S., & Wolozin, B. (1998). Presenilin 1 associates with glycogen synthase kinase-3beta and its substrate tau. *Proc Natl Acad Sci U S A, 95*(16), 9637-9641.

Tenreiro, S., & Outeiro, T. F. (2010). Simple is good: yeast models of neurodegeneration. *FEMS Yeast Res, 10*(8), 970-979. doi: 10.1111/j.1567-1364.2010.00649.x.

Terwel, D., Muyllaert, D., Dewachter, I., Borghgraef, P., Croes, S., Devijver, H., & Van Leuven, F. (2008). Amyloid activates GSK-3beta to aggravate neuronal tauopathy in bigenic mice. *Am J Pathol, 172*(3), 786-798. doi: 10.2353/ajpath.2008.070904.

Timmers, A. C., Niebel, A., Balague, C., & Dagkesamanskaya, A. (2002). Differential localisation of GFP fusions to cytoskeleton-binding proteins in animal, plant, and yeast cells. Green-fluorescent protein. *Protoplasma, 220*(1-2), 69-78. doi: 10.1007/s00709-002-0026-7.

Treusch, S., Hamamichi, S., Goodman, J. L., Matlack, K. E. S., Chung, C. Y., Baru, V., Shulman, J. M., Parrado, A., Bevis, B. J., Valastyan, J. S., Han, H., Lindhagen-Persson, M., Reiman, E. M., Evans, D. A., Bennett, D. A., Olofsson, A., DeJager, P. L., Tanzi, R. E., Caldwell, K. A., Caldwell,

G. A., & Lindquist, S. (2011). Functional Links Between Aβ Toxicity, Endocytic Trafficking and Alzheimer's Disease Risk Factors in Yeast. *Science, 334*(6060), 1241–1245.

Tsaioun, K., & Kates, S. A. (2011). De-risking drug discovery programmes early with ADMET. In I. M. Kapetanovic (Ed.), Drug Discovery and Development - Present and Future: InTech. Retrieved from http://www.intechopen.com/books/drug-discovery-and-development-present-and-future/de-risking-drug-discovery-programmes-early-with-admet. doi: 10.5772/1179.

Usardi, A., Pooler, A. M., Seereeram, A., Reynolds, C. H., Derkinderen, P., Anderton, B., Hanger, D. P., Noble, W., & Williamson, R. (2011). Tyrosine phosphorylation of tau regulates its interactions with Fyn SH2 domains, but not SH3 domains, altering the cellular localization of tau. *FEBS J, 278*(16), 2927-2937. doi: 10.1111/j.1742-4658.2011.08218.x.

van Ham, T. J., Breitling, R., Swertz, M. A., & Nollen, E. A. (2009). Neurodegenerative diseases: Lessons from genome-wide screens in small model organisms. *EMBO Mol Med, 1*(8-9), 360-370. doi: 10.1002/emmm.200900051.

Vandebroek, T., Terwel, D., Van Helmont, T., Winderickx, J., & Van Leuven, F. (2005a). *Phosphorylation and Aggregation of Protein Tau in Humanized Yeast Cells and in Transgenic Mouse Brain*. Paper presented at the 7th International Conference on Alzheimer's and Parkinson's Disease.

Vandebroek, T., Terwel, D., Vanhelmont, T., Gysemans, M., Van Haesendonck, C., Engelborghs, Y., Winderickx, J., & Van Leuven, F. (2006). Microtubule binding and clustering of human Tau-4R and Tau-P301L proteins isolated from yeast deficient in orthologues of glycogen synthase kinase-3beta or cdk5. *J Biol Chem, 281*(35), 25388-25397. doi: 10.1074/jbc.M602792200.

Vandebroek, T., Vanhelmont, T., Terwel, D., Borghgraef, P., Lemaire, K., Snauwaert, J., Wera, S., Van Leuven, F., & Winderickx, J. (2005b). Identification and isolation of a hyperphosphorylated, conformationally changed intermediate of human protein tau expressed in yeast. *Biochemistry, 44*(34), 11466-11475. doi: 10.1021/bi0506775.

Vanhelmont, T., Vandebroek, T., De Vos, A., Terwel, D., Lemaire, K., Anandhakumar, J., Franssens, V., Swinnen, E., Van Leuven, F., & Winderickx, J. (2010). Serine-409 phosphorylation and oxidative damage define aggregation of human protein tau in yeast. *FEMS Yeast Res, 10*(8), 992-1005. doi: 10.1111/j.1567-1364.2010.00662.x.

Varanyuwatana, P., & Halestrap, A. P. (2012). The roles of phosphate and the phosphate carrier in the mitochondrial permeability transition pore. *Mitochondrion, 12*(1), 120-125. doi: 10.1016/j.mito.2011.04.006.

Verghese, J., Abrams, J., Wang, Y., & Morano, K. A. (2012). Biology of the heat shock response and protein chaperones: budding yeast (Saccharomyces cerevisiae) as a model system. *Microbiol Mol Biol Rev, 76*(2), 115-158. doi: 10.1128/MMBR.05018-11.

von der Haar, T., Josse, L., Wright, P., Zenthon, J., & Tuite, M. F. (2007). Development of a novel yeast cell-based system for studying the aggregation of Alzheimer's disease-associated Abeta peptides in vivo. *Neurodegener Dis, 4*(2-3), 136-147. doi: 10.1159/000101838.

Waxman, E. A., & Giasson, B. I. (2008). Specificity and Regulation of Casein Kinase-Mediated Phosphorylation of α-Synuclein. *Journal of Neuropathology and Experimental Neurology, 67*(5), 402-416. doi: 10.1097/NEN.0b013e3186fc995.

Weingarten, M. D., Lockwood, A. H., Hwo, S. Y., & Kirschner, M. W. (1975). A protein factor essential for microtubule assembly. *Proc Natl Acad Sci U S A, 72*(5), 1858-1862. doi: 10.1073/pnas.72.5.1858.

Weintraub, S., Wicklund, A. H., & Salmon, D. P. (2012). The neuropsychological profile of Alzheimer disease. *Cold Spring Harb Perspect Med, 2*(4), a006171. doi: 10.1101/cshperspect.a006171.

Willingham, S., Outeiro, T. F., DeVit, M. J., Lindquist, S. L., & Muchowski, P. J. (2003). Yeast genes that enhance the toxicity of a mutant huntingtin fragment or alpha-synuclein. *Science, 302*(5651), 1769-1772. doi: 10.1126/science.1090389.

Wimo, A., & Prince, M. (2010). World Alzheimer Report 2010: The Global Economic Impact of Dementia: Alzheimer's Disease International.

Wirths, O., Multhaup, G., & Bayer, T. A. (2004). A modified beta-amyloid hypothesis: intraneuronal accumulation of the beta-amyloid peptide--the first step of a fatal cascade. *J Neurochem, 91*(3), 513-520. doi: 10.1111/j.1471-4159.2004.02737.x.

Wolfe, M. S. (2012). The role of tau in neurodegenerative diseases and its potential as a therapeutic target. *Scientifica (Cairo), 2012*, 796024. doi: 10.6064/2012/796024.

Wood, L. (2014). Research and Markets: Neurodegenerative diseases market to 2018: New entries in niche and broader parkinson's disease treatment will boost market despite patent cliff [Press release]. Retrieved from http://www.reuters.com/article/2014/03/07/research-and-markets-idUSnBw075558a+100+BSW20140307.

Woods, R. A., & Gietz, R. D. (2001). High-efficiency transformation of plasmid DNA into yeast. *Methods Mol Biol, 177*, 85-97.

Wortmann, M. (2012). Dementia: a global health priority - highlights from an ADI and World Health Organization report. *Alzheimers Res Ther, 4*(5), 40. doi: 10.1186/alzrt143.

Yan, Y., Flinn, R. J., Wu, H., Schnur, R. S., & Backer, J. M. (2009). hVps15, but not Ca2+/CaM, is required for the activity and regulation of hVps34 in mammalian cells. *Biochem J, 417*(3), 747-755. doi: 10.1042/BJ20081865.

Yoshiyama, Y., Lee, V. M., & Trojanowski, J. Q. (2013). Therapeutic strategies for tau mediated neurodegeneration. *J Neurol Neurosurg Psychiatry, 84*(7), 784-795. doi: 10.1136/jnnp-2012-303144.

Yu, W. H., & Fraser, P. E. (2001). S100b interaction with tau is promoted by zinc and inhibited by hyperphosphorylation in alzheimer's disease. *The Journal of Neuroscience, 21*(7), 2240-2246.

Zempel, H., Luedtke, J., Kumar, Y., Biernat, J., Dawson, H., Mandelkow, E., & Mandelkow, E. M. (2013). Amyloid-beta oligomers induce synaptic damage via Tau-dependent microtubule severing by TTLL6 and spastin. *EMBO J, 32*(22), 2920-2937. doi: 10.1038/emboj.2013.207.

Zempel, H., & Mandelkow, E. (2014). Lost after translation: missorting of Tau protein and consequences for Alzheimer disease. *Trends Neurosci, 37*(12), 721-732. doi: 10.1016/j.tins.2014.08.004.

Zhang, J. H. (1999). A Simple Statistical Parameter for Use in Evaluation and Validation of High Throughput Screening Assays. *J Biomol Screen, 4*(2), 67-73. doi: 10.1177/108705719900400206.

Zhang, Z., & Simpkins, J. W. (2010). An okadaic acid-induced model of tauopathy and cognitive deficiency. *Brain Res, 1359*, 233-246. doi: 10.1016/j.brainres.2010.08.077.

Appendices

Appendix I

Table I.1. Loss-of-function tau toxicity enhancer screen results.

Euroscarf Information						Replica plate Information			Tau Toxicity Enhancer Primary Screen Results			
record no.	ORF name	Plate	Row	Col	Comment	Replica plate	Well	YPD (OD600nm)	Growth plate (SC+GAL comp.)	Transformation control plate (SC+GLU-Leu)	TEST Plate (SC+GAL-Leu)	Classification
--	empty	1	A	1	empty	YKO_0801	A01	empty	empty	empty	empty	empty
338	YAL068C	1	A	2		YKO_0801	A02	0.905	+	+	+	
339	YAL067C	1	A	3		YKO_0801	A03	0.9	+	+	+	
340	YAL066W	1	A	4		YKO_0801	A04	0.951	+	+	+	
341	YAL065C	1	A	5		YKO_0801	A05	0.961	+	+	+	
345	YAL062W	1	A	6		YKO_0801	A06	0.92	+	+	+	
346	YAL061W	1	A	7		YKO_0801	A07	0.794	+	+	+	
347	YAL060W	1	A	8		YKO_0801	A08	0.879	+	+	+	
348	YAL059W	1	A	9		YKO_0801	A09	0.864	+	+	+	
349	YAL058W	1	A	10		YKO_0801	A10	0.844	+	+	+	
351	YAL056W	1	A	11		YKO_0801	A11	0.693	+	+	+	
352	YAL055W	1	A	12		YKO_0801	A12	0.787	+	+	+	
354	YAL053W	1	B	1		YKO_0801	B01	0.754	+	+	+	
355	YAL051W	1	B	2		YKO_0801	B02	0.862	+	+	+	
356	YAL049C	1	B	3		YKO_0801	B03	0.976	+	+	+	
357	YAL048C	1	B	4		YKO_0801	B04	0.898	-	+	-	Doubt
359	YAL046C	1	B	5		YKO_0801	B05	0.994	+	+	+	
360	YAL045C	1	B	6		YKO_0801	B06	0.955	+	+	+	
361	YAL044C	1	B	7		YKO_0801	B07	0.916	slow	-	-	Doubt
363	YAL042W	1	B	8		YKO_0801	B08	0.882	+	+	+	
364	YAL043C-a	1	B	9		YKO_0801	B09	0.893	+	+	+	
366	YAL040C	1	B	10		YKO_0801	B10	0.965	+	+	+	
367	YAL039C	1	B	11		YKO_0801	B11	0.833	+	+	+	
369	YAL037W	1	B	12		YKO_0801	B12	0.849	+	+	+	
370	YAL036C	1	C	1		YKO_0801	C01	0.882	+	+	+	
371	YAL035W	1	C	2		YKO_0801	C02	0.951	+	+	+	
374	YAL034C	1	C	3		YKO_0801	C03	1.033	+	+	+	
377	YAL031C	1	C	4		YKO_0801	C04	1.02	+	+	+	
378	YAL030W	1	C	5		YKO_0801	C05	1.004	+	+	+	
379	YAL029C	1	C	6		YKO_0801	C06	0.957	+	+	+	
380	YAL028W	1	C	7		YKO_0801	C07	0.862	+	+	+	
381	YAL027W	1	C	8		YKO_0801	C08	0.76	+	+	+	
382	YAL026C	1	C	9		YKO_0801	C09	0.91	+	+	+	
385	YAL023C	1	C	10		YKO_0801	C10	0.815	+	+	-	HIT
386	YAL022C	1	C	11		YKO_0801	C11	0.867	+	+	+	
387	YAL021C	1	C	12		YKO_0801	C12	0.787	+	+	+	
388	YAL020C	1	D	1		YKO_0801	D01	0.883	+	+	+	
389	YAL019W	1	D	2		YKO_0801	D02	0.997	+	+	+	
390	YAL018C	1	D	3		YKO_0801	D03	1.023	+	+	+	
391	YAL017W	1	D	4		YKO_0801	D04	0.982	+	-	-	Doubt
393	YAL015C	1	D	5		YKO_0801	D05	0.956	+	+	+	
394	YAL014C	1	D	6		YKO_0801	D06	0.948	+	+	+	
395	YAL013W	1	D	7		YKO_0801	D07	0.205	slow	+	-	Doubt
397	YAL011W	1	D	8		YKO_0801	D08	0.545	+	+	+	
398	YAL010C	1	D	9		YKO_0801	D09	0.792	+	+	+	
399	YAL009W	1	D	10		YKO_0801	D10	0.761	+	+	+	
400	YAL008W	1	D	11		YKO_0801	D11	0.769	+	+	+	
401	YAL007C	1	D	12		YKO_0801	D12	0.762	+	+	+	
402	YAL004W	1	E	1		YKO_0801	E01	0.89	+	+	+	
403	YAL005C	1	E	2		YKO_0801	E02	0.978	+	+	+	
405	YAL002W	1	E	3		YKO_0801	E03	0.931	+	+	+	
407	YAR002W	1	E	4		YKO_0801	E04	0.823	+	+	+	
408	YAR003W	1	E	5		YKO_0801	E05	0.574	+	+	+	
413	YAR014C	1	E	6		YKO_0801	E06	0.841	+	+	+	
414	YAR015W	1	E	7		YKO_0801	E07	0.956	+	+	+	
415	YAR018C	1	E	8		YKO_0801	E08	0.727	+	+	+	
417	YAR020C	1	E	9		YKO_0801	E09	0.853	+	+	+	
418	YAR023C	1	E	10		YKO_0801	E10	0.802	+	+	+	
419	YAR027W	1	E	11		YKO_0801	E11	0.888	+	+	-	HIT
420	YAR028W	1	E	12		YKO_0801	E12	0.734	+	+	+	
421	YAR029W	1	F	1		YKO_0801	F01	0.844	+	+	+	
422	YAR031W	1	F	2		YKO_0801	F02	0.906	+	+	+	
423	YAR030C	1	F	3		YKO_0801	F03	0.943	+	+	+	
425	YAR035W	1	F	4		YKO_0801	F04	0.863	+	-	+	Incongruence
426	YAR037W	1	F	5		YKO_0801	F05	0.981	+	+	+	
427	YAR040C	1	F	6		YKO_0801	F06	0.787	+	+	+	
428	YAR042W	1	F	7		YKO_0801	F07	0.839	+	+	+	
429	YAR043C	1	F	8		YKO_0801	F08	0.773	+	+	+	
430	YAR044W	1	F	9		YKO_0801	F09	0.835	+	+	+	

Euroscarf Information						Replica plate Information			Tau Toxicity Enhancer Primary Screen Results			
record no.	ORF name	Plate	Row	Col	Comment	Replica plate	Well	YPD (OD600nm)	Growth plate (SC+GAL comp.)	Transformation control plate (SC+GLU-Leu)	TEST Plate (SC+GAL-Leu)	Classification
431	YAR047C	1	F	10		YKO_0801	F10	0.72	+	+	+	
1489	YLL001W	1	F	11		YKO_0801	F11	0.805	+	+	+	
1490	YLL002W	1	F	12		YKO_0801	F12	0.339	+	+	+	
1493	YLL005C	1	G	1		YKO_0801	G01	0.919	+	+	+	
1494	YLL006W	1	G	2		YKO_0801	G02	0.949	slow	-	-	Doubt
1497	YLL009C	1	G	3		YKO_0801	G03	0.848	+	+	+	
1498	YLL010C	1	G	4		YKO_0801	G04	0.782	+	-	-	Doubt
1500	YLL012W	1	G	5		YKO_0801	G05	0.87	+	+	+	
1501	YLL013C	1	G	6		YKO_0801	G06	0.775	+	+	+	
1502	YLL014W	1	G	7		YKO_0801	G07	0.797	+	+	+	
1503	YLL015W	1	G	8		YKO_0801	G08	0.671	+	+	+	
1504	YLL016W	1	G	9		YKO_0801	G09	0.716	+	+	+	
1505	YLL017W	1	G	10		YKO_0801	G10	0.646	+	+	+	
1507	YLL019C	1	G	11		YKO_0801	G11	0.686	+	+	+	
1508	YLL020C	1	G	12		YKO_0801	G12	0.79	+	+	+	
1509	YLL021W	1	H	1		YKO_0801	H01	0.875	+	+	+	
--	--	1	H	2	empty	YKO_0801	H02	empty	empty	empty	empty	empty
1511	YLL023C	1	H	3		YKO_0801	H03	0.94	+	+	+	
1512	YLL024C	1	H	4		YKO_0801	H04	0.971	+	+	+	
1513	YLL025W	1	H	5		YKO_0801	H05	0.97	+	+	+	
1514	YLL026W	1	H	6		YKO_0801	H06	0.905	+	+	+	
1516	YLL028W	1	H	7		YKO_0801	H07	0.695	+	+	+	
1517	YLL029W	1	H	8		YKO_0801	H08	0.792	+	+	-	HIT
1520	YLL032C	1	H	9		YKO_0801	H09	0.896	+	+	-	HIT
1521	YLL033W	1	H	10		YKO_0801	H10	0.729	+	-	+	Incongruence
1526	YLL038C	1	H	11		YKO_0801	H11	0.821	+	-	+	Incongruence
1527	YLL039C	1	H	12		YKO_0801	H12	0.804	+	-	+	Incongruence
1528	YLL040C	2	A	1		YKO_0802	A01	0.8277	+	+	+	
--	empty	2	A	2	empty	YKO_0802	A02	empty	empty	empty	empty	empty
1529	YLL041C	2	A	3		YKO_0802	A03	0.8249	+	+	+	
1530	YLL042C	2	A	4		YKO_0802	A04	0.8095	+	+	+	
1531	YLL043W	2	A	5		YKO_0802	A05	0.8231	+	+	+	
1533	YLL045C	2	A	6		YKO_0802	A06	0.8072	+	+	-	HIT
1534	YLL046C	2	A	7		YKO_0802	A07	0.7823	+	+	+	
1535	YLL047W	2	A	8		YKO_0802	A08	0.7833	+	+	+	
1539	YLL051C	2	A	9		YKO_0802	A09	0.8179	+	+	+	
1540	YLL052C	2	A	10		YKO_0802	A10	0.7803	+	+	+	
1541	YLL053C	2	A	11		YKO_0802	A11	not grown	-	-	-	Not grown
1542	YLL054C	2	A	12		YKO_0802	A12	0.7858	+	+	+	
1543	YLL055W	2	B	1		YKO_0802	B01	0.7876	+	+	+	
1544	YLL056C	2	B	2		YKO_0802	B02	0.7966	+	+	+	
1545	YLL057C	2	B	3		YKO_0802	B03	0.843	+	+	+	
1546	YLL058W	2	B	4		YKO_0802	B04	0.8467	+	+	+	
1548	YLL060C	2	B	5		YKO_0802	B05	0.8532	+	+	+	
1549	YLL061W	2	B	6		YKO_0802	B06	0.7953	+	+	+	
1550	YLL062C	2	B	7		YKO_0802	B07	0.7546	+	+	+	
1551	YLL063C	2	B	8		YKO_0802	B08	0.7645	+	+	+	
1556	YLR001C	2	B	9		YKO_0802	B09	0.8081	+	+	+	
1558	YLR003C	2	B	10		YKO_0802	B10	0.8063	+	+	+	
1559	YLR004C	2	B	11		YKO_0802	B11	0.7443	+	+	+	
1566	YLR011W	2	B	12		YKO_0802	B12	0.8089	+	+	-	HIT
1567	YLR012C	2	C	1		YKO_0802	C01	0.7954	+	+	+	
1568	YLR013W	2	C	2		YKO_0802	C02	0.787	+	+	+	
1569	YLR014C	2	C	3		YKO_0802	C03	0.8102	+	+	+	
1570	YLR015W	2	C	4		YKO_0802	C04	0.729	+	+	+	
1571	YLR016C	2	C	5		YKO_0802	C05	0.7874	+	+	+	
1572	YLR017W	2	C	6		YKO_0802	C06	0.7642	+	+	+	
1573	YLR018C	2	C	7		YKO_0802	C07	0.7458	+	+	+	
1574	YLR019W	2	C	8		YKO_0802	C08	0.7736	+	+	+	
1575	YLR020C	2	C	9		YKO_0802	C09	0.7738	+	+	+	
1576	YLR021W	2	C	10		YKO_0802	C10	0.7615	+	+	+	
1578	YLR023C	2	C	11		YKO_0802	C11	0.7532	+	+	+	
1579	YLR024C	2	C	12	Incorrect	YKO_0802	C12	not grown	-	-	-	Not grown
1580	YLR025W	2	D	1		YKO_0802	D01	0.785	+	+	+	
1582	YLR027C	2	D	2		YKO_0802	D02	0.7663	+	+	+	
1583	YLR028C	2	D	3		YKO_0802	D03	0.7916	+	+	+	
2653	YLR042C	2	D	4		YKO_0802	D04	0.75	+	+	+	
2654	YLR043C	2	D	5		YKO_0802	D05	0.8188	+	+	+	
2655	YLR044C	2	D	6		YKO_0802	D06	0.7408	+	+	+	
2657	YLR046C	2	D	7		YKO_0802	D07	0.7924	+	+	+	
2658	YLR047C	2	D	8		YKO_0802	D08	0.7796	+	+	+	
2659	YLR048W	2	D	9		YKO_0802	D09	0.3771	slow	+	+	
2660	YLR049C	2	D	10		YKO_0802	D10	0.8017	+	+	+	
2664	YLR053C	2	D	11		YKO_0802	D11	0.8678	+	+	+	
2665	YLR054C	2	D	12		YKO_0802	D12	0.8163	+	+	+	
2666	YLR055C	2	E	1		YKO_0802	E01	0.7284	+	+	+	
2667	YLR056W	2	E	2		YKO_0802	E02	not grown	-	-	-	Not grown
2668	YLR057W	2	E	3		YKO_0802	E03	0.7881	+	+	+	
2669	YLR058C	2	E	4		YKO_0802	E04	0.7503	+	+	+	
2670	YLR059C	2	E	5		YKO_0802	E05	0.765	+	+	+	
2672	YLR061W	2	E	6		YKO_0802	E06	not grown	-	-	-	Not grown
2673	YLR062C	2	E	7		YKO_0802	E07	0.3157	slow	+	-	Doubt
2674	YLR063W	2	E	8		YKO_0802	E08	0.7641	+	+	+	
2675	YLR064W	2	E	9		YKO_0802	E09	0.8109	+	+	+	

	Euroscarf Information					Replica plate Information			Tau Toxicity Enhancer Primary Screen Results			
record no.	ORF name	Plate	Row	Col	Comment	Replica plate	Well	YPD (OD600nm)	Growth plate (SC+GAL comp.)	Transformation control plate (SC+GLU-Leu)	TEST Plate (SC+GAL-Leu)	Classification
2676	YLR065C	2	E	10		YKO_0802	E10	0.7969	+	+	+	
2678	YLR067C	2	E	11		YKO_0802	E11	0.7633	slow	+	-	Doubt
2679	YLR068W	2	E	12		YKO_0802	E12	0.787	+	+	+	
2680	YLR069C	2	F	1		YKO_0802	F01	0.7117	slow	+	-	Doubt
2681	YLR070C	2	F	2		YKO_0802	F02	0.7507	+	+	+	
2683	YLR072W	2	F	3		YKO_0802	F03	0.7694	+	+	+	
2684	YLR073C	2	F	4		YKO_0802	F04	0.7619	+	+	+	
2685	YLR074C	2	F	5		YKO_0802	F05	0.6976	+	+	+	
2688	YLR077W	2	F	6		YKO_0802	F06	0.7274	+	+	+	
2690	YLR079W	2	F	7		YKO_0802	F07	0.715	+	+	-	HIT
2691	YLR080W	2	F	8		YKO_0802	F08	0.7697	+	+	+	
2692	YLR081W	2	F	9		YKO_0802	F09	0.8067	slow	+	+	
2693	YLR082C	2	F	10		YKO_0802	F10	0.7967	+	+	+	
2694	YLR083C	2	F	11		YKO_0802	F11	0.8718	+	+	+	
2695	YLR084C	2	F	12		YKO_0802	F12	0.8055	+	+	+	
2696	YLR085C	2	G	1		YKO_0802	G01	0.7549	+	+	+	
2698	YLR087C	2	G	2		YKO_0802	G02	0.7271	+	+	+	
2700	YLR089C	2	G	3		YKO_0802	G03	0.7604	slow	+	+	
2701	YLR090W	2	G	4		YKO_0802	G04	0.7709	+	+	+	
2702	YLR091W	2	G	5		YKO_0802	G05	0.6783	slow	-	-	Doubt
2703	YLR092W	2	G	6		YKO_0802	G06	0.721	+	+	+	
2704	YLR093C	2	G	7		YKO_0802	G07	0.7491	+	+	+	
2705	YLR094C	2	G	8		YKO_0802	G08	0.7768	+	+	+	
2706	YLR095C	2	G	9		YKO_0802	G09	0.7732	+	+	-	HIT
2707	YLR096W	2	G	10		YKO_0802	G10	0.8138	+	+	+	
2708	YLR097C	2	G	11		YKO_0802	G11	0.7969	+	+	+	
2709	YLR098C	2	G	12		YKO_0802	G12	0.7657	+	+	+	
2710	YLR099C	2	H	1		YKO_0802	H01	0.7872	+	+	+	
--		2	H	2	empty	YKO_0802	H02	empty	empty	empty	empty	empty
2713	YLR102C	2	H	3		YKO_0802	H03	0.8276	+	+	+	
2715	YLR104W	2	H	4		YKO_0802	H04	0.8166	+	+	-	HIT
2718	YLR107W	2	H	5		YKO_0802	H05	0.8345	+	-	+	Doubt
2719	YLR108C	2	H	6		YKO_0802	H06	0.8021	+	+	+	
2720	YLR109W	2	H	7		YKO_0802	H07	0.8069	+	+	+	
2722	YLR111W	2	H	8		YKO_0802	H08	0.7741	+	+	+	
2723	YLR112W	2	H	9		YKO_0802	H09	0.76	+	+	+	
2724	YLR113W	2	H	10		YKO_0802	H10	0.7727	+	+	+	
2725	YLR114C	2	H	11		YKO_0802	H11	0.7042	slow	-	-	Doubt
2729	YLR118C	2	H	12		YKO_0802	H12	0.7791	+	-	-	Doubt
2730	YLR119W	3	A	1		YKO_0803	A01	0.701	+	+	+	
2731	YLR120C	3	A	2		YKO_0803	A02	0.734	+	+	+	
--	empty	3	A	3	empty	YKO_0803	A03	empty	empty	empty	empty	empty
2732	YLR121C	3	A	4		YKO_0803	A04	0.93	+	+	+	
2733	YLR122C	3	A	5		YKO_0803	A05	0.906	+	+	+	
2734	YLR123C	3	A	6		YKO_0803	A06	0.949	+	+	+	
2735	YLR124W	3	A	7		YKO_0803	A07	0.948	+	+	+	
2736	YLR125W	3	A	8	Incorrect	YKO_0803	A08	0.82	+	+	+	
481	YML089C	3	A	9		YKO_0803	A09	0.932	+	-	+	Incongruence
482	YML088W	3	A	10		YKO_0803	A10	0.94	slow	+	-	Doubt
483	YML087C	3	A	11		YKO_0803	A11	0.937	+	+	+	
484	YML086C	3	A	12		YKO_0803	A12	0.749	+	+	+	
486	YML084W	3	B	1		YKO_0803	B01	0.943	+	+	+	
487	YML083C	3	B	2		YKO_0803	B02	0.935	+	+	+	
488	YML082W	3	B	3		YKO_0803	B03	0.929	+	+	+	
489	YML081W	3	B	4		YKO_0803	B04	1.031	+	+	+	
490	YML080W	3	B	5		YKO_0803	B05	0.872	+	+	+	
491	YML079W	3	B	6		YKO_0803	B06	0.946	+	+	+	
492	YML078W	3	B	7		YKO_0803	B07	0.932	+	+	-	HIT
507	YML063W	3	B	8		YKO_0803	B08	0.859	+	-	-	Doubt
508	YML062C	3	B	9		YKO_0803	B09	0.812	+	+	+	
509	YML061C	3	B	10		YKO_0803	B10	0.937	+	+	-	HIT
510	YML060W	3	B	11		YKO_0803	B11	0.865	+	+	+	
511	YML059C	3	B	12		YKO_0803	B12	0.965	+	+	-	HIT
512	YML058W	3	C	1		YKO_0803	C01	0.941	+	+	+	
513	YML057W	3	C	2		YKO_0803	C02	1.006	+	+	+	
514	YML058C-A	3	C	3		YKO_0803	C03	1.016	+	+	+	
515	YML056C	3	C	4		YKO_0803	C04	0.937	+	+	+	
516	YML055W	3	C	5		YKO_0803	C05	0.993	+	+	+	
517	YML054C	3	C	6		YKO_0803	C06	0.973	+	+	+	
518	YML053C	3	C	7		YKO_0803	C07	0.967	+	+	+	
519	YML052W	3	C	8		YKO_0803	C08	0.705	+	+	+	
520	YML051W	3	C	9		YKO_0803	C09	1.031	+	+	+	
521	YML050W	3	C	10		YKO_0803	C10	0.928	+	+	+	
523	YML048W	3	C	11		YKO_0803	C11	0.986	+	+	+	
524	YML048W-A	3	C	12		YKO_0803	C12	0.998	+	+	+	
534	YML037C	3	D	1		YKO_0803	D01	0.956	+	+	+	
536	YML035C	3	D	2		YKO_0803	D02	0.988	+	+	-	HIT
537	YML034W	3	D	3		YKO_0803	D03	0.991	+	+	+	
538	YML035C-A	3	D	4		YKO_0803	D04	0.944	+	+	+	
539	YML033W	3	D	5		YKO_0803	D05	1.008	+	+	+	
540	YML032C	3	D	6		YKO_0803	D06	0.713	+	+	+	
543	YML030W	3	D	7		YKO_0803	D07	0.994	+	+	-	HIT
544	YML029W	3	D	8		YKO_0803	D08	0.907	+	+	+	
545	YML028W	3	D	9		YKO_0803	D09	0.891	+	+	+	

	Euroscarf Information					Replica plate Information			Tau Toxicity Enhancer Primary Screen Results			
record no.	ORF name	Plate	Row	Col	Comment	Replica plate	Well	YPD (OD600nm)	Growth plate (SC+GAL comp.)	Transformation control plate (SC+GLU-Leu)	TEST Plate (SC+GAL-Leu)	Classification
547	YML026C	3	D	10		YKO_0803	D10	0.84	+	+	+	
549	YML024W	3	D	11		YKO_0803	D11	0.547	+	+	+	
553	YML020W	3	D	12		YKO_0803	D12	0.84	+	+	+	
554	YML019W	3	E	1		YKO_0803	E01	0.888	+	+	+	
555	YML018C	3	E	2		YKO_0803	E02	0.986	+	+	+	
556	YML017W	3	E	3		YKO_0803	E03	0.919	+	+	+	
557	YML016C	3	E	4		YKO_0803	E04	0.767	+	-	+	Incongruence
559	YML014W	3	E	5		YKO_0803	E05	0.929	+	+	+	
560	YML013W	3	E	6		YKO_0803	E06	0.892	+	+	+	
561	YML013C-A	3	E	7		YKO_0803	E07	0.834	+	-	-	Doubt
562	YML012W	3	E	8		YKO_0803	E08	0.892	+	+	+	
563	YML011C	3	E	9		YKO_0803	E09	0.93	+	+	+	
567	YML009c	3	E	10		YKO_0803	E10	0.948	+	-	-	Doubt
568	YML008C	3	E	11		YKO_0803	E11	0.897	slow	+	-	Doubt
569	YML007W	3	E	12		YKO_0803	E12	0.905	+	+	+	
570	YML006C	3	F	1		YKO_0803	F01	0.866	+	+	+	
571	YML005W	3	F	2		YKO_0803	F02	0.943	+	+	+	
572	YML004C	3	F	3		YKO_0803	F03	0.789	+	+	+	
573	YML003W	3	F	4		YKO_0803	F04	0.825	+	+	+	
574	YML002W	3	F	5		YKO_0803	F05	1.005	+	+	+	
575	YML001W	3	F	6		YKO_0803	F06	not grow n	-	-	-	Not grow n
577	YMR002W	3	F	7		YKO_0803	F07	0.905	+	-	-	Doubt
578	YMR003W	3	F	8		YKO_0803	F08	0.794	+	-	+	Incongruence
581	YMR006C	3	F	9		YKO_0803	F09	0.932	+	+	+	
582	YMR007W	3	F	10		YKO_0803	F10	0.95	+	-	+	Incongruence
583	YMR008C	3	F	11		YKO_0803	F11	0.799	+	+	+	
584	YMR009W	3	F	12		YKO_0803	F12	0.982	+	+	+	
585	YMR010W	3	G	1		YKO_0803	G01	0.935	+	+	-	HIT
586	YMR011W	3	G	2		YKO_0803	G02	0.963	+	+	+	
587	YMR012W	3	G	3		YKO_0803	G03	0.947	+	+	-	HIT
589	YMR014W	3	G	4		YKO_0803	G04	0.93	+	+	+	
590	YMR015C	3	G	5		YKO_0803	G05	0.72	+	+	-	HIT
591	YMR016C	3	G	6		YKO_0803	G06	0.949	+	+	+	
592	YMR017W	3	G	7		YKO_0803	G07	0.981	+	+	+	
593	YMR018W	3	G	8		YKO_0803	G08	0.912	+	+	+	
594	YMR019W	3	G	9		YKO_0803	G09	0.886	+	+	+	
595	YMR020W	3	G	10		YKO_0803	G10	0.834	+	+	+	
596	YMR021C	3	G	11		YKO_0803	G11	0.889	-	-	-	Doubt
597	YMR022W	3	G	12		YKO_0803	G12	0.824	+	+	+	
598	YMR023C	3	H	1		YKO_0803	H01	1.008	+	+	+	
--		3	H	2	empty	YKO_0803	H02	empty	empty	empty	empty	empty
599	YMR024W	3	H	3		YKO_0803	H03	0.957	+	+	+	
600	YMR025W	3	H	4		YKO_0803	H04	0.996	+	-	+	Incongruence
601	YMR026C	3	H	5		YKO_0803	H05	1.012	+	+	-	HIT
602	YMR027W	3	H	6		YKO_0803	H06	0.993	+	-	-	Doubt
604	YMR029C	3	H	7		YKO_0803	H07	0.888	+	+	+	
605	YMR030W	3	H	8		YKO_0803	H08	0.723	+	+	+	
606	YMR031W-A	3	H	9		YKO_0803	H09	0.511	+	+	+	
607	YMR031C	3	H	10		YKO_0803	H10	1.048	+	+	+	
608	YMR032W	3	H	11		YKO_0803	H11	0.77	+	+	-	HIT
610	YMR034C	3	H	12		YKO_0803	H12	1.016	+	+	+	
611	YMR035W	4	A	1		YKO_0804	A01	0.6498	slow	-	-	Doubt
612	YMR036C	4	A	2		YKO_0804	A02	0.7334	+	-	+	Incongruence
615	YMR039C	4	A	3		YKO_0804	A03	0.7003	+	+	-	HIT
--		4	A	4	empty	YKO_0804	A04	empty	empty	empty	empty	empty
616	YMR040W	4	A	5		YKO_0804	A05	0.7428	+	+	+	
617	YMR041C	4	A	6		YKO_0804	A06	0.7666	+	+	+	
618	YMR042W	4	A	7		YKO_0804	A07	0.7438	+	+	+	
620	YMR044W	4	A	8		YKO_0804	A08	0.7481	+	-	-	Doubt
721	YMR140W	4	A	9		YKO_0804	A09	0.719	+	+	+	
722	YMR141C	4	A	10		YKO_0804	A10	0.7184	+	+	+	
724	YMR143W	4	A	11		YKO_0804	A11	0.678	+	+	+	
725	YMR144W	4	A	12		YKO_0804	A12	0.7324	+	+	-	HIT
726	YMR145C	4	B	1		YKO_0804	B01	0.6864	+	+	+	
728	YMR147W	4	B	2		YKO_0804	B02	0.7788	+	+	+	
729	YMR148W	4	B	3		YKO_0804	B03	0.7404	+	+	+	
731	YMR151W	4	B	4		YKO_0804	B04	0.7248	+	+	+	
732	YMR150C	4	B	5		YKO_0804	B05	0.6902	slow	+	-	Doubt
733	YMR152W	4	B	6		YKO_0804	B06	0.7042	+	+	+	
734	YMR153W	4	B	7		YKO_0804	B07	0.708	+	+	+	
735	YMR153C-A	4	B	8		YKO_0804	B08	0.6853	+	+	+	
737	YMR155W	4	B	9		YKO_0804	B09	0.7119	+	+	+	
738	YMR156C	4	B	10		YKO_0804	B10	0.7112	+	+	+	
739	YMR157C	4	B	11		YKO_0804	B11	0.7517	+	+	-	HIT
741	YMR158W-A	4	B	12		YKO_0804	B12	0.7384	+	-	-	Doubt
742	YMR159C	4	C	1		YKO_0804	C01	0.7542	+	+	+	
744	YMR161W	4	C	2		YKO_0804	C02	0.7732	+	+	+	
745	YMR162C	4	C	3		YKO_0804	C03	0.762	+	+	+	
746	YMR163C	4	C	4		YKO_0804	C04	0.7457	+	+	+	
747	YMR164C	4	C	5		YKO_0804	C05	0.6922	+	+	+	
749	YMR166C	4	C	6		YKO_0804	C06	0.6563	+	+	+	
750	YMR167W	4	C	7		YKO_0804	C07	0.6505	+	+	+	
752	YMR169C	4	C	8		YKO_0804	C08	0.7222	+	+	+	
753	YMR170C	4	C	9		YKO_0804	C09	0.736	+	+	-	HIT

	Euroscarf Information					Replica plate Information			Tau Toxicity Enhancer Primary Screen Results			
record no.	ORF name	Plate	Row	Col	Comment	Replica plate	Well	YPD (OD600nm)	Growth plate (SC+GAL comp.)	Transformation control plate (SC+GLU-Leu)	TEST Plate (SC+GAL-Leu)	Classification
756	YMR172C-A	4	C	10		YKO_0804	C10	0.7489	+	+	-	HIT
758	YMR173W-A	4	C	11		YKO_0804	C11	0.7381	+	+	+	
759	YMR174C	4	C	12		YKO_0804	C12	0.731	+	+	+	
760	YMR175W	4	D	1		YKO_0804	D01	0.7397	+	+	+	
761	YMR176W	4	D	2		YKO_0804	D02	0.7225	+	+	+	
762	YMR177W	4	D	3		YKO_0804	D03	0.7306	+	+	+	
763	YMR178W	4	D	4		YKO_0804	D04	0.7658	+	+	+	
764	YMR179W	4	D	5		YKO_0804	D05	0.702	+	+	+	
765	YMR180C	4	D	6		YKO_0804	D06	0.7718	+	-	-	Doubt
767	YMR182C	4	D	7		YKO_0804	D07	0.7411	+	-	-	Doubt
768	YMR183C	4	D	8		YKO_0804	D08	0.7106	+	+	+	
769	YMR184W	4	D	9		YKO_0804	D09	0.6833	slow	+	-	Doubt
771	YMR186W	4	D	10		YKO_0804	D10	0.7002	+	+	+	
772	YMR187C	4	D	11		YKO_0804	D11	0.755	+	+	+	
773	YMR188C	4	D	12		YKO_0804	D12	0.7313	+	+	+	
774	YMR189W	4	E	1		YKO_0804	E01	0.7075	+	+	+	
775	YMR190C	4	E	2		YKO_0804	E02	0.7186	+	-	-	Doubt
776	YMR191W	4	E	3		YKO_0804	E03	0.7242	+	+	+	
777	YMR192W	4	E	4		YKO_0804	E04	0.7098	+	-	+	Incongruence
778	YMR193W	4	E	5		YKO_0804	E05	0.7237	+	+	+	
779	YMR194W	4	E	6		YKO_0804	E06	0.6868	+	+	+	
780	YMR193C-A	4	E	7		YKO_0804	E07	0.6928	+	+	+	
781	YMR195W	4	E	8		YKO_0804	E08	0.7269	+	+	+	
782	YMR196W	4	E	9		YKO_0804	E09	0.7296	+	+	+	
784	YMR198W	4	E	10		YKO_0804	E10	0.6731	+	-	-	Doubt
785	YMR199W	4	E	11		YKO_0804	E11	0.6832	+	+	+	
787	YMR201C	4	E	12		YKO_0804	E12	0.728	+	+	+	
788	YMR202W	4	F	1		YKO_0804	F01	0.7189	+	+	+	
790	YMR204C	4	F	2		YKO_0804	F02	0.6996	+	+	+	
791	YMR205C	4	F	3		YKO_0804	F03	0.6954	+	+	+	
792	YMR206W	4	F	4		YKO_0804	F04	0.7033	+	+	+	
793	YMR207C	4	F	5		YKO_0804	F05	0.6351	+	+	-	HIT
796	YMR210W	4	F	6		YKO_0804	F06	0.691	+	+	-	HIT
800	YMR214W	4	F	7		YKO_0804	F07	0.7173	+	+	+	
801	YMR215W	4	F	8		YKO_0804	F08	0.7102	+	+	+	
802	YMR216C	4	F	9		YKO_0804	F09	0.7197	+	+	+	
805	YMR219W	4	F	10		YKO_0804	F10	0.7398	+	-	+	Incongruence
807	YMR221C	4	F	11		YKO_0804	F11	0.7568	+	+	+	
808	YMR222C	4	F	12		YKO_0804	F12	0.7202	+	-	-	Doubt
809	YMR223W	4	G	1		YKO_0804	G01	0.6826	+	+	-	HIT
810	YMR224C	4	G	2		YKO_0804	G02	not grow n	-	-	-	Not grow n
811	YMR225C	4	G	3		YKO_0804	G03	0.7267	+	+	-	HIT
812	YMR226C	4	G	4		YKO_0804	G04	0.7274	+	+	+	
814	YMR228W	4	G	5		YKO_0804	G05	0.6634	slow	+	-	Doubt
816	YMR230W	4	G	6		YKO_0804	G06	0.6899	+	+	+	
817	YMR231W	4	G	7		YKO_0804	G07	0.7119	+	+	+	
818	YMR232W	4	G	8		YKO_0804	G08	0.7107	+	+	+	
819	YMR233W	4	G	9		YKO_0804	G09	0.7354	+	+	+	
820	YMR234W	4	G	10		YKO_0804	G10	0.7253	+	+	+	
823	YMR237W	4	G	11		YKO_0804	G11	0.7385	+	+	+	
824	YMR238W	4	G	12		YKO_0804	G12	0.7199	+	+	-	HIT
827	YMR241W	4	H	1		YKO_0804	H01	0.7375	+	+	-	HIT
--		4	H	2	empty	YKO_0804	H02	empty	empty	empty	empty	empty
828	YMR242C	4	H	3		YKO_0804	H03	0.6831	+	+	-	HIT
829	YMR243C	4	H	4		YKO_0804	H04	0.6746	+	+	+	
830	YMR244W	4	H	5		YKO_0804	H05	0.6953	+	+	+	
831	YMR245W	4	H	6		YKO_0804	H06	0.6814	+	+	+	
832	YMR244C-A	4	H	7		YKO_0804	H07	0.7224	+	-	-	Doubt
833	YMR246W	4	H	8		YKO_0804	H08	0.7103	+	+	+	
834	YMR247C	4	H	9		YKO_0804	H09	0.7085	+	+	-	HIT
835	YMR250W	4	H	10		YKO_0804	H10	0.6765	+	+	+	
836	YMR251W	4	H	11		YKO_0804	H11	0.6962	+	+	+	
837	YMR251W-A	4	H	12		YKO_0804	H12	0.7127	+	+	-	HIT
838	YMR252C	5	A	1		YKO_0805	A01	0.873	+	+	+	
839	YMR253C	5	A	2		YKO_0805	A02	0.78	+	+	+	
840	YMR254C	5	A	3		YKO_0805	A03	0.845	+	+	+	
841	YMR255W	5	A	4		YKO_0805	A04	0.905	+	+	+	
--		5	A	5	empty	YKO_0805	A05	empty	empty	empty	empty	empty
842	YMR256C	5	A	6		YKO_0805	A06	0.832	+	+	-	HIT
843	YMR257C	5	A	7		YKO_0805	A07	0.763	slow	+	-	Doubt
844	YMR258C	5	A	8		YKO_0805	A08	0.772	+	+	+	
845	YMR259C	5	A	9		YKO_0805	A09	0.694	+	+	+	
847	YMR261C	5	A	10		YKO_0805	A10	0.726	+	+	+	
848	YMR262W	5	A	11		YKO_0805	A11	0.63	+	+	+	
7372	YNL047C	5	A	12		YKO_0805	A12	0.613	+	+	+	
850	YMR264W	5	B	1		YKO_0805	B01	0.908	+	+	+	
851	YMR265C	5	B	2		YKO_0805	B02	0.995	+	+	+	
852	YMR266W	5	B	3		YKO_0805	B03	0.834	+	+	+	
853	YMR267W	5	B	4		YKO_0805	B04	0.983	-	+	-	Doubt
855	YMR269W	5	B	5		YKO_0805	B05	1.021	+	+	+	
858	YMR272C	5	B	6		YKO_0805	B06	0.758	+	+	+	
859	YMR273C	5	B	7		YKO_0805	B07	0.836	+	+	+	
860	YMR274C	5	B	8		YKO_0805	B08	0.925	+	+	+	
861	YMR275C	5	B	9		YKO_0805	B09	0.694	+	+	+	

	Euroscarf Information					Replica plate Information			Tau Toxicity Enhancer Primary Screen Results			
record no.	ORF name	Plate	Row	Col	Comment	Replica plate	Well	YPD (OD600nm)	Growth plate (SC+GAL comp.)	Transformation control plate (SC+GLU-Leu)	TEST Plate (SC+GAL-Leu)	Classification
862	YMR276W	5	B	10		YKO_0805	B10	0.695	+	+	+	
864	YMR278W	5	B	11		YKO_0805	B11	0.883	+	+	+	
866	YMR280C	5	B	12		YKO_0805	B12	0.6	+	+	+	
868	YMR282C	5	C	1		YKO_0805	C01	0.78	+	+	+	
869	YMR283C	5	C	2		YKO_0805	C02	0.998	+	+	+	
870	YMR284W	5	C	3		YKO_0805	C03	0.888	+	-	+	Incongruence
871	YMR285C	5	C	4		YKO_0805	C04	1.047	+	+	+	
872	YMR286W	5	C	5		YKO_0805	C05	0.971	-	+	-	Doubt
873	YMR287C	5	C	6		YKO_0805	C06	0.965	-	+	-	Doubt
875	YMR289W	5	C	7		YKO_0805	C07	0.92	+	+	+	
878	YMR291W	5	C	8		YKO_0805	C08	0.737	+	+	+	
879	YMR292W	5	C	9		YKO_0805	C09	0.696	+	+	+	
880	YMR293C	5	C	10		YKO_0805	C10	0.888	-	+	-	Doubt
881	YMR294W	5	C	11		YKO_0805	C11	0.897	+	+	+	
882	YMR294W-A	5	C	12		YKO_0805	C12	0.79	+	+	+	
883	YMR295C	5	D	1		YKO_0805	D01	0.841	+	+	+	
885	YMR297W	5	D	2		YKO_0805	D02	0.905	+	+	+	
887	YMR299C	5	D	3		YKO_0805	D03	0.979	+	+	+	
888	YMR300C	5	D	4		YKO_0805	D04	0.904	+	+	+	
890	YMR302C	5	D	5		YKO_0805	D05	0.972	+	+	+	
891	YMR303C	5	D	6		YKO_0805	D06	0.781	+	+	+	
892	YMR304W	5	D	7		YKO_0805	D07	0.813	+	-	+	Incongruence
893	YMR304C-A	5	D	8		YKO_0805	D08	0.677	+	+	+	
894	YMR305C	5	D	9		YKO_0805	D09	0.789	+	+	+	
896	YMR306C-A	5	D	10		YKO_0805	D10	0.746	+	-	+	Incongruence
897	YMR307W	5	D	11		YKO_0805	D11	0.694	+	+	+	
900	YMR310C	5	D	12		YKO_0805	D12	0.596	+	+	+	
1105	YNL339C	5	E	1		YKO_0805	E01	0.822	+	+	+	
1106	YNL338W	5	E	2		YKO_0805	E02	0.863	+	+	+	
1108	YNL336W	5	E	3		YKO_0805	E03	0.878	+	+	+	
1109	YNL335W	5	E	4		YKO_0805	E04	0.928	+	+	-	HIT
1110	YNL334C	5	E	5		YKO_0805	E05	0.96	+	+	+	
1111	YNL333W	5	E	6		YKO_0805	E06	0.935	+	+	+	
1112	YNL332W	5	E	7		YKO_0805	E07	0.816	+	+	+	
1114	YNL330C	5	E	8		YKO_0805	E08	0.758	+	+	+	
1115	YNL329C	5	E	9		YKO_0805	E09	0.872	slow	+	-	Doubt
1116	YNL328C	5	E	10		YKO_0805	E10	0.633	+	-	+	Incongruence
1117	YNL327W	5	E	11		YKO_0805	E11	0.671	+	+	+	
1118	YNL326C	5	E	12		YKO_0805	E12	0.64	+	+	+	
1119	YNL324W	5	F	1		YKO_0805	F01	0.83	+	+	+	
1120	YNL325C	5	F	2		YKO_0805	F02	0.775	+	+	+	
1121	YNL323W	5	F	3		YKO_0805	F03	0.76	+	+	+	
1122	YNL322C	5	F	4		YKO_0805	F04	0.938	+	+	+	
1123	YNL321W	5	F	5		YKO_0805	F05	0.767	+	+	+	
1124	YNL320W	5	F	6		YKO_0805	F06	0.789	+	+	+	
1125	YNL319W	5	F	7		YKO_0805	F07	0.833	+	+	+	
1126	YNL318C	5	F	8		YKO_0805	F08	0.704	+	+	+	
1130	YNL314W	5	F	9		YKO_0805	F09	0.64	+	-	-	Doubt
1133	YNL311C	5	F	10		YKO_0805	F10	0.655	+	+	+	
1135	YNL309W	5	F	11		YKO_0805	F11	0.862	+	+	+	
7373	YNL053W	5	F	12		YKO_0805	F12	0.576	+	+	+	
1139	YNL305C	5	G	1		YKO_0805	G01	0.861	+	+	+	
1140	YNL304W	5	G	2		YKO_0805	G02	0.838	+	+	+	
1141	YNL303W	5	G	3		YKO_0805	G03	0.811	+	+	+	
1142	YNL302C	5	G	4		YKO_0805	G04	0.623	+	+	+	
1143	YNL301C	5	G	5		YKO_0805	G05	0.929	+	+	+	
1145	YNL299W	5	G	6		YKO_0805	G06	0.778	+	+	+	
1146	YNL298W	5	G	7		YKO_0805	G07	0.629	+	-	-	Doubt
7377	YNL086W	5	G	8		YKO_0805	G08	0.893	+	+	+	
1148	YNL297C	5	G	9		YKO_0805	G09	0.812	+	-	-	Doubt
1149	YNL295W	5	G	10		YKO_0805	G10	0.615	+	-	-	Doubt
1150	YNL294C	5	G	11		YKO_0805	G11	0.899	+	+	+	
1151	YNL293W	5	G	12		YKO_0805	G12	0.593	+	+	+	
7378	YNL089C	5	H	1		YKO_0805	H01	0.85	+	+	+	
--		5	H	2	empty	YKO_0805	H02	empty	empty	empty	empty	empty
1153	YNL291C	5	H	3		YKO_0805	H03	0.807	+	+	+	
1155	YNL289W	5	H	4		YKO_0805	H04	0.788	+	+	+	
1156	YNL288W	5	H	5		YKO_0805	H05	0.859	+	+	+	
1158	YNL286W	5	H	6		YKO_0805	H06	0.724	+	+	+	
1159	YNL285W	5	H	7		YKO_0805	H07	0.857	+	+	+	
1161	YNL283C	5	H	8		YKO_0805	H08	0.677	+	-	+	Incongruence
1163	YNL281W	5	H	9		YKO_0805	H09	0.704	+	+	+	
1164	YNL280C	5	H	10		YKO_0805	H10	0.619	+	-	-	Doubt
1166	YNL278W	5	H	11		YKO_0805	H11	0.797	+	+	+	
7379	YNL096C	5	H	12		YKO_0805	H12	0.601	+	+	+	
1168	YNL276C	6	A	1		YKO_0806	A01	0.7278	+	+	+	
1169	YNL275W	6	A	2		YKO_0806	A02	0.7605	+	+	+	
1171	YNL273W	6	A	3		YKO_0806	A03	0.7248	+	+	+	
1173	YNL271C	6	A	4		YKO_0806	A04	0.7295	+	+	+	
1174	YNL270C	6	A	5		YKO_0806	A05	0.7632	+	+	+	
--		6	A	6	empty	YKO_0806	A06	empty	empty	empty	empty	empty
1175	YNL269W	6	A	7		YKO_0806	A07	0.7529	+	+	-	HIT
1176	YNL268W	6	A	8		YKO_0806	A08	0.7659	+	+	+	
1178	YNL266W	6	A	9		YKO_0806	A09	0.7195	+	+	+	

	Euroscarf Information					Replica plate Information			Tau Toxicity Enhancer Primary Screen Results			
record no.	ORF name	Plate	Row	Col	Comment	Replica plate	Well	YPD (OD600nm)	Growth plate (SC+GAL comp.)	Transformation control plate (SC+GLU-Leu)	TEST Plate (SC+GAL-Leu)	Classification
1179	YNL265C	6	A	10		YKO_0806	A10	0.7235	+	+	+	
1180	YNL264C	6	A	11	Similar to SEC14p -- growth on -met, growth on -lys	YKO_0806	A11	0.7139	+	+	+	
1185	YNL259C	6	A	12		YKO_0806	A12	0.7576	+	+	+	
1187	YNL257C	6	B	1		YKO_0806	B01	0.7091	+	+	+	
1189	YNL255C	6	B	2		YKO_0806	B02	0.7813	+	+	+	
1190	YNL254C	6	B	3		YKO_0806	B03	0.7705	+	+	+	
1191	YNL253W	6	B	4		YKO_0806	B04	0.7457	+	+	+	
1195	YNL249C	6	B	5		YKO_0806	B05	0.7733	+	+	+	
1196	YNL248C	6	B	6		YKO_0806	B06	0.7725	+	-	-	Doubt
1198	YNL246W	6	B	7		YKO_0806	B07	0.9001	+	-	-	Doubt
1777	YOR001W	6	B	8		YKO_0806	B08	0.7443	+	+	+	
1778	YOR002W	6	B	9		YKO_0806	B09	0.7492	+	+	+	
1779	YOR003W	6	B	10		YKO_0806	B10	0.7844	+	+	+	
1781	YOR005C	6	B	11		YKO_0806	B11	0.7616	+	+	+	
1782	YOR006C	6	B	12		YKO_0806	B12	0.7638	+	+	+	
1783	YOR007C	6	C	1		YKO_0806	C01	0.7614	+	+	+	
1784	YOR008C	6	C	2		YKO_0806	C02	0.7609	+	+	+	
1785	YOR009W	6	C	3		YKO_0806	C03	0.754	+	+	+	
1786	YOR010C	6	C	4		YKO_0806	C04	0.7466	+	+	+	
1787	YOR011W	6	C	5		YKO_0806	C05	0.7778	+	+	+	
1788	YOR012W	6	C	6		YKO_0806	C06	0.7401	+	+	+	
1789	YOR013W	6	C	7		YKO_0806	C07	0.9434	+	+	+	
1790	YOR014W	6	C	8		YKO_0806	C08	0.6274	slow	+	+	
1791	YOR015W	6	C	9		YKO_0806	C09	0.8019	+	+	+	
1792	YOR016C	6	C	10		YKO_0806	C10	0.7357	+	+	+	
1793	YOR017W	6	C	11		YKO_0806	C11	0.7729	+	+	+	
1794	YOR018W	6	C	12		YKO_0806	C12	0.7451	+	+	+	
1795	YOR019W	6	D	1		YKO_0806	D01	0.7237	+	+	+	
1797	YOR021C	6	D	2		YKO_0806	D02	0.7508	+	+	+	
1798	YOR022C	6	D	3		YKO_0806	D03	0.7717	+	+	+	
1799	YOR023C	6	D	4		YKO_0806	D04	0.7563	+	+	+	
1800	YOR024W	6	D	5		YKO_0806	D05	0.7318	+	+	+	
1801	YOR025W	6	D	6		YKO_0806	D06	0.7162	+	+	+	
1802	YOR026W	6	D	7		YKO_0806	D07	0.7237	slow	+	+	
1803	YOR027W	6	D	8		YKO_0806	D08	0.8289	+	+	-	HIT
1804	YOR028C	6	D	9		YKO_0806	D09	0.7945	+	+	+	
1805	YOR029W	6	D	10		YKO_0806	D10	0.7734	+	+	+	
1806	YOR030W	6	D	11		YKO_0806	D11	0.7874	+	+	+	
1807	YOR031W	6	D	12		YKO_0806	D12	0.7448	+	-	-	Doubt
1808	YOR032C	6	E	1		YKO_0806	E01	0.7376	+	+	+	
1809	YOR033C	6	E	2		YKO_0806	E02	0.7359	+	+	+	
1810	YOR034C	6	E	3		YKO_0806	E03	0.7437	+	+	+	
1811	YOR035C	6	E	4		YKO_0806	E04	0.6978	+	+	+	
1812	YOR036W	6	E	5		YKO_0806	E05	0.7241	+	+	+	
1813	YOR037W	6	E	6		YKO_0806	E06	0.6749	+	-	+	Incongruence
1814	YOR038C	6	E	7		YKO_0806	E07	0.674	+	+	+	
1815	YOR039W	6	E	8		YKO_0806	E08	0.6707	slow	+	+	
1816	YOR040W	6	E	9		YKO_0806	E09	0.7288	+	+	+	
1817	YOR041C	6	E	10		YKO_0806	E10	0.7615	+	+	+	
1818	YOR042W	6	E	11		YKO_0806	E11	0.7201	+	+	+	
1819	YOR043W	6	E	12		YKO_0806	E12	0.6798	+	+	+	
1820	YOR044W	6	F	1		YKO_0806	F01	0.7512	+	-	-	Doubt
1821	YOR045W	6	F	2		YKO_0806	F02	0.7186	+	-	+	Incongruence
1823	YOR047C	6	F	3		YKO_0806	F03	0.7419	+	+	+	
1825	YOR049C	6	F	4		YKO_0806	F04	0.726	+	+	+	
1826	YOR050C	6	F	5		YKO_0806	F05	0.9827	+	+	+	
1827	YOR051C	6	F	6		YKO_0806	F06	0.7068	slow	+	+	
1828	YOR052C	6	F	7		YKO_0806	F07	0.9412	+	-	-	Doubt
1829	YOR053W	6	F	8		YKO_0806	F08	0.737	+	+	+	
1830	YOR054C	6	F	9		YKO_0806	F09	0.7293	+	+	+	
1831	YOR055W	6	F	10		YKO_0806	F10	0.7048	+	+	+	
1834	YOR058C	6	F	11		YKO_0806	F11	0.7061	+	+	+	
1835	YOR059C	6	F	12		YKO_0806	F12	0.7285	+	+	+	
1837	YOR061W	6	G	1		YKO_0806	G01	0.6046	+	+	+	
1838	YOR062C	6	G	2		YKO_0806	G02	0.7415	+	+	+	
1840	YOR064C	6	G	3		YKO_0806	G03	0.7565	+	+	+	
1841	YOR065W	6	G	4		YKO_0806	G04	0.6986	-	-	-	Doubt
1842	YOR066W	6	G	5		YKO_0806	G05	0.7358	+	+	+	
1843	YOR067C	6	G	6		YKO_0806	G06	0.67	+	+	+	
1844	YOR068C	6	G	7		YKO_0806	G07	0.9641	+	+	+	
1845	YOR069W	6	G	8		YKO_0806	G08	0.7375	+	+	+	
1846	YOR070C	6	G	9		YKO_0806	G09	0.7615	+	+	+	
1847	YOR071C	6	G	10		YKO_0806	G10	0.7666	+	+	+	
1848	YOR072W	6	G	11		YKO_0806	G11	1.0192	+	+	+	
1849	YOR073W	6	G	12		YKO_0806	G12	0.721	+	+	+	
1852	YOR076C	6	H	1		YKO_0806	H01	0.7545	+	+	-	HIT
--		6	H	2	empty	YKO_0806	H02	empty	empty	empty	empty	empty
1854	YOR078W	6	H	3		YKO_0806	H03	0.7032	+	+	+	
1855	YOR079C	6	H	4		YKO_0806	H04	0.6968	+	+	+	
1856	YOR080W	6	H	5		YKO_0806	H05	0.665	+	+	+	
1857	YOR081C	6	H	6		YKO_0806	H06	0.6636	+	+	+	
1858	YOR082C	6	H	7		YKO_0806	H07	0.728	+	+	-	HIT
1859	YOR083W	6	H	8		YKO_0806	H08	1.0447	+	+	+	
1860	YOR084W	6	H	9		YKO_0806	H09	0.7705	+	+	+	

	Euroscarf Information					Replica plate Information			Tau Toxicity Enhancer Primary Screen Results			
record no.	ORF name	Plate	Row	Col	Comment	Replica plate	Well	YPD (OD600nm)	Growth plate (SC+GAL comp.)	Transformation control plate (SC+GLU-Leu)	TEST Plate (SC+GAL-Leu)	Classification
1861	YOR085W	6	H	10		YKO_0806	H10	0.7387	+	+	+	
1862	YOR086C	6	H	11		YKO_0806	H11	0.7475	+	+	+	
1863	YOR087W	6	H	12		YKO_0806	H12	0.7304	+	+	+	
1864	YOR088W	7	A	1		YKO_0807	A01	0.855	+	+	+	
1865	YOR089C	7	A	2		YKO_0807	A02	0.7724	+	+	+	
1866	YOR090C	7	A	3		YKO_0807	A03	0.7986	+	+	+	
1867	YOR091W	7	A	4		YKO_0807	A04	0.7995	+	+	+	
1868	YOR092W	7	A	5		YKO_0807	A05	0.7903	+	+	+	
1869	YOR093C	7	A	6		YKO_0807	A06	0.7969	+	+	+	
--		7	A	7	empty	YKO_0807	A07	empty	empty	empty	empty	empty
1870	YOR094W	7	A	8		YKO_0807	A08	0.7926	+	+	+	
1585	YOR289W	7	A	9		YKO_0807	A09	0.7762	+	+	+	
1586	YOR290C	7	A	10		YKO_0807	A10	0.6939	+	+	+	
1587	YOR291W	7	A	11		YKO_0807	A11	0.7776	+	+	+	
1588	YOR292C	7	A	12		YKO_0807	A12	0.7803	+	+	+	
1589	YOR293W	7	B	1		YKO_0807	B01	0.7047	+	+	+	
1591	YOR295W	7	B	2		YKO_0807	B02	0.7327	+	+	+	
1592	YOR296W	7	B	3		YKO_0807	B03	0.7654	+	+	+	
1593	YOR297C	7	B	4		YKO_0807	B04	0.7601	+	+	-	HIT
1594	YOR298W	7	B	5		YKO_0807	B05	0.7495	+	+	+	
1595	YOR299W	7	B	6		YKO_0807	B06	0.7347	+	+	+	
1597	YOR301W	7	B	7		YKO_0807	B07	0.7101	+	+	+	
1598	YOR302W	7	B	8		YKO_0807	B08	0.7848	+	+	+	
1599	YOR303W	7	B	9		YKO_0807	B09	0.7617	+	+	-	HIT
1600	YOR304C-A	7	B	10		YKO_0807	B10	0.7603	+	+	+	
1601	YOR304W	7	B	11		YKO_0807	B11	0.7614	+	+	+	
1602	YOR305W	7	B	12		YKO_0807	B12	0.6573	-	+	-	Doubt
1604	YOR307C	7	C	1		YKO_0807	C01	0.7665	+	+	+	
1605	YOR308C	7	C	2		YKO_0807	C02	0.782	+	+	+	
1608	YOR311C	7	C	3		YKO_0807	C03	0.8065	+	+	+	
1609	YOR312C	7	C	4		YKO_0807	C04	0.6622	+	+	+	
1610	YOR313C	7	C	5		YKO_0807	C05	0.7646	+	+	+	
1611	YOR314W	7	C	6		YKO_0807	C06	0.7392	+	+	+	
1612	YOR315W	7	C	7		YKO_0807	C07	0.7401	+	+	+	
1613	YOR316C	7	C	8		YKO_0807	C08	0.7626	+	+	+	
1615	YOR318C	7	C	9		YKO_0807	C09	0.7498	+	+	+	
1617	YOR320C	7	C	10		YKO_0807	C10	0.772	+	+	+	
1618	YOR321W	7	C	11		YKO_0807	C11	0.7588	+	+	+	
1619	YOR322C	7	C	12		YKO_0807	C12	0.7435	+	+	+	
1620	YOR323C	7	D	1		YKO_0807	D01	0.6389	+	+	+	
1621	YOR324C	7	D	2		YKO_0807	D02	0.7879	+	+	+	
1624	YOR327C	7	D	3		YKO_0807	D03	0.7616	+	+	+	
1625	YOR328W	7	D	4		YKO_0807	D04	0.68	+	+	+	
1627	YOR330C	7	D	5		YKO_0807	D05	0.6575	-	-	-	Doubt
1629	YOR332W	7	D	6		YKO_0807	D06	0.7118	+	+	+	
1631	YOR334W	7	D	7		YKO_0807	D07	0.7415	slow	-	+	Incongruence
1634	YOR337W	7	D	8		YKO_0807	D08	0.7647	+	+	+	
1635	YOR338W	7	D	9		YKO_0807	D09	0.7329	+	+	+	
1636	YOR339C	7	D	10		YKO_0807	D10	0.7322	+	+	+	
1639	YOR342C	7	D	11		YKO_0807	D11	0.7543	+	+	+	
1640	YOR343C	7	D	12		YKO_0807	D12	0.7512	+	+	+	
1641	YOR344C	7	E	1		YKO_0807	E01	0.7292	+	+	+	
1643	YOR346W	7	E	2		YKO_0807	E02	0.7335	+	+	+	
1644	YOR347C	7	E	3		YKO_0807	E03	0.7418	+	+	+	
1645	YOR348C	7	E	4		YKO_0807	E04	0.7505	+	+	+	
1646	YOR349W	7	E	5		YKO_0807	E05	0.7575	+	+	+	
1647	YOR350C	7	E	6		YKO_0807	E06	0.6703	-	+	-	Doubt
1648	YOR351C	7	E	7		YKO_0807	E07	0.7422	+	+	+	
1649	YOR352W	7	E	8		YKO_0807	E08	0.6993	+	+	+	
1651	YOR354C	7	E	9		YKO_0807	E09	0.7293	+	+	-	HIT
1652	YOR355W	7	E	10		YKO_0807	E10	0.7257	+	+	+	
1653	YOR356W	7	E	11		YKO_0807	E11	0.7535	+	-	+	Incongruence
1654	YOR357C	7	E	12		YKO_0807	E12	0.7408	+	+	-	HIT
1655	YOR358W	7	F	1		YKO_0807	F01	0.7198	+	+	+	
1656	YOR359W	7	F	2		YKO_0807	F02	0.6844	+	+	+	
1657	YOR360C	7	F	3		YKO_0807	F03	0.6521	+	+	+	
1660	YOR363C	7	F	4		YKO_0807	F04	0.722	+	+	+	
1662	YOR365C	7	F	5		YKO_0807	F05	0.7264	+	+	+	
1664	YOR367W	7	F	6		YKO_0807	F06	0.7222	+	+	+	
1665	YOR368W	7	F	7		YKO_0807	F07	0.7274	+	+	+	
1668	YOR371C	7	F	8		YKO_0807	F08	0.6691	+	+	+	
1671	YOR374W	7	F	9		YKO_0807	F09	0.7397	+	-	+	Incongruence
1672	YOR375C	7	F	10		YKO_0807	F10	0.7637	+	-	+	Incongruence
1673	YOR376W	7	F	11		YKO_0807	F11	0.7415	+	+	+	
1674	YOR377W	7	F	12		YKO_0807	F12	0.7415	+	-	-	Doubt
1675	YOR378W	7	G	1		YKO_0807	G01	0.7314	+	+	+	
1677	YOR380W	7	G	2		YKO_0807	G02	0.7401	+	+	+	
1678	YOR381W	7	G	3		YKO_0807	G03	0.6976	+	+	+	
1679	YOR382W	7	G	4		YKO_0807	G04	0.7025	+	-	-	Doubt
1680	YOR383C	7	G	5		YKO_0807	G05	0.7248	+	+	+	
1681	YOR384W	7	G	6		YKO_0807	G06	0.7462	+	+	+	
1682	YOR385W	7	G	7		YKO_0807	G07	0.7276	+	+	+	
1683	YOR386W	7	G	8		YKO_0807	G08	0.716	+	+	+	
1692	YOL001W	7	G	9		YKO_0807	G09	0.6789	slow	+	+	

	Euroscarf Information					Replica plate Information			Tau Toxicity Enhancer Primary Screen Results			
record no.	ORF name	Plate	Row	Col	Comment	Replica plate	Well	YPD (OD600nm)	Growth plate (SC+GAL comp.)	Transformation control plate (SC+GLU-Leu)	TEST Plate (SC+GAL-Leu)	Classification
1693	YOL002C	7	G	10		YKO_0807	G10	0.737	+	+	+	
1694	YOL003C	7	G	11		YKO_0807	G11	0.7282	+	+	+	
1695	YOL004W	7	G	12		YKO_0807	G12	0.6007	+	+	-	HIT
1697	YOL006C	7	H	1		YKO_0807	H01	0.4586	+	+	+	
--		7	H	2	empty	YKO_0807	H02	empty	empty	empty	empty	empty
1698	YOL007C	7	H	3		YKO_0807	H03	0.7442	+	+	+	
1699	YOL008W	7	H	4		YKO_0807	H04	0.7027	+	+	+	
1700	YOL009C	7	H	5		YKO_0807	H05	0.6978	+	+	-	HIT
1702	YOL011W	7	H	6		YKO_0807	H06	0.7344	+	+	+	
1703	YOL012C	7	H	7		YKO_0807	H07	0.6954	+	+	+	
1704	YOL013C	7	H	8		YKO_0807	H08	0.7443	+	+	+	
1705	YOL014W	7	H	9		YKO_0807	H09	0.7275	+	+	-	HIT
1706	YOL015W	7	H	10		YKO_0807	H10	0.7588	+	+	+	
1708	YOL017W	7	H	11		YKO_0807	H11	0.733	+	-	+	Incongruence
1709	YOL018C	7	H	12		YKO_0807	H12	0.7534	+	-	-	Doubt
1710	YOL019W	8	A	1		YKO_0808	A01	0.6222	+	+	+	
1711	YOL020W	8	A	2		YKO_0808	A02	1.1435	+	+	+	
1714	YOL023W	8	A	3		YKO_0808	A03	0.6056	+	+	+	
1715	YOL024W	8	A	4		YKO_0808	A04	1.1788	+	+	+	
1716	YOL025W	8	A	5		YKO_0808	A05	0.6763	+	+	+	
1718	YOL027C	8	A	6		YKO_0808	A06	1.0086	+	+	+	
1719	YOL028C	8	A	7		YKO_0808	A07	0.6199	+	+	+	
--		8	A	8	empty	YKO_0808	A08	empty	empty	empty	empty	empty
1720	YOL029C	8	A	9		YKO_0808	A09	0.6761	+	+	+	
1721	YOL030W	8	A	10		YKO_0808	A10	0.642	+	+	+	
1722	YOL031C	8	A	11		YKO_0808	A11	1.1086	+	+	+	
1723	YOL032W	8	A	12		YKO_0808	A12	0.6299	+	+	+	
1724	YOL033W	8	B	1		YKO_0808	B01	1.0644	slow	+	-	Doubt
1726	YOL035C	8	B	2		YKO_0808	B02	1.085	+	+	+	
1727	YOL036W	8	B	3		YKO_0808	B03	1.0759	+	+	+	
1728	YOL037C	8	B	4		YKO_0808	B04	0.9976	+	+	+	
1730	YOL039W	8	B	5		YKO_0808	B05	1.0143	+	+	+	
1732	YOL041C	8	B	6		YKO_0808	B06	1.0739	+	+	+	
1733	YOL042W	8	B	7		YKO_0808	B07	1.0217	+	+	+	
1734	YOL043C	8	B	8		YKO_0808	B08	1.0686	+	+	+	
1735	YOL044W	8	B	9		YKO_0808	B09	1.0642	+	+	+	
1736	YOL045W	8	B	10		YKO_0808	B10	1.0276	+	+	+	
1737	YOL046C	8	B	11		YKO_0808	B11	1.0711	+	+	+	
1738	YOL047C	8	B	12		YKO_0808	B12	1.0924	+	+	+	
1739	YOL048C	8	C	1		YKO_0808	C01	1.1392	+	+	+	
1740	YOL049W	8	C	2		YKO_0808	C02	1.0551	+	+	+	
1741	YOL050C	8	C	3		YKO_0808	C03	0.9688	+	+	+	
1742	YOL051W	8	C	4		YKO_0808	C04	1.0844	+	+	+	
1743	YOL052C	8	C	5		YKO_0808	C05	1.102	+	+	+	
1744	YOL053C-A	8	C	6		YKO_0808	C06	1.0347	+	+	+	
1745	YOL053W	8	C	7		YKO_0808	C07	1.0355	slow	+	+	
1746	YOL054W	8	C	8		YKO_0808	C08	1.0439	slow	+	+	
1747	YOL055C	8	C	9		YKO_0808	C09	1.1071	slow	+	+	
1748	YOL056W	8	C	10		YKO_0808	C10	1.0662	+	+	+	
1749	YOL057W	8	C	11		YKO_0808	C11	1.0906	+	+	+	
1750	YOL058W	8	C	12		YKO_0808	C12	0.9579	+	+	+	
1751	YOL059W	8	D	1		YKO_0808	D01	1.1165	+	+	+	
1752	YOL060C	8	D	2		YKO_0808	D02	1.1469	+	+	+	
1753	YOL061W	8	D	3		YKO_0808	D03	1.1012	+	+	+	
1754	YOL062C	8	D	4		YKO_0808	D04	1.101	+	+	+	
1755	YOL063C	8	D	5		YKO_0808	D05	1.0643	+	+	+	
1756	YOL064C	8	D	6		YKO_0808	D06	1.0007	slow	+	+	
1757	YOL065C	8	D	7		YKO_0808	D07	1.0394	slow	+	+	
1759	YOL067C	8	D	8		YKO_0808	D08	1.0875	slow	-	+	Incongruence
1760	YOL068C	8	D	9		YKO_0808	D09	1.0261	slow	+	+	
1762	YOL070C	8	D	10		YKO_0808	D10	0.7032	+	+	+	
1763	YOL071W	8	D	11		YKO_0808	D11	0.6945	+	+	+	
1764	YOL072W	8	D	12		YKO_0808	D12	0.5748	+	+	+	
1766	YOL075C	8	E	1		YKO_0808	E01	1.0936	+	+	-	HIT
1767	YOL076W	8	E	2		YKO_0808	E02	0.9996	+	+	+	
1770	YOL079W	8	E	3		YKO_0808	E03	1.0337	+	+	+	
1771	YOL080C	8	E	4		YKO_0808	E04	1.1161	+	+	+	
1772	YOL081W	8	E	5		YKO_0808	E05	1.0472	slow	+	+	
1773	YOL082W	8	E	6		YKO_0808	E06	1.0766	+	+	+	
1774	YOL083W	8	E	7		YKO_0808	E07	1.0729	slow	+	+	
1775	YOL084W	8	E	8		YKO_0808	E08	1.0743	slow	+	+	
1776	YOL085C	8	E	9		YKO_0808	E09	1.0301	slow	+	+	
1018	YPL274W	8	E	10		YKO_0808	E10	1.0363	+	+	+	
1019	YPL273W	8	E	11		YKO_0808	E11	1.0383	+	+	+	
1020	YPL272C	8	E	12		YKO_0808	E12	1.0461	+	+	+	
1021	YPL271W	8	F	1		YKO_0808	F01	not grow n	-	-	-	Not grow n
1022	YPL270W	8	F	2		YKO_0808	F02	1.038	+	+	+	
1023	YPL269W	8	F	3		YKO_0808	F03	1.0431	+	+	+	
1025	YPL267W	8	F	4		YKO_0808	F04	1.0074	+	+	+	
1027	YPL265W	8	F	5		YKO_0808	F05	1.0079	+	+	+	
1028	YPL264C	8	F	6		YKO_0808	F06	1.0866	+	+	+	
1029	YPL263C	8	F	7		YKO_0808	F07	1.0563	+	+	+	
1030	YPL262W	8	F	8		YKO_0808	F08	1.0577	slow	+	+	
1031	YPL260W	8	F	9		YKO_0808	F09	1.0568	+	+	+	

	Euroscarf Information					Replica plate Information			Tau Toxicity Enhancer Primary Screen Results			
record no.	ORF name	Plate	Row	Col	Comment	Replica plate	Well	YPD (OD600nm)	Growth plate (SC+GAL comp.)	Transformation control plate (SC+GLU-Leu)	TEST Plate (SC+GAL-Leu)	Classification
1032	YPL261C	8	F	10		YKO_0808	F10	1.0281	+	-	+	Incongruence
1033	YPL259C	8	F	11		YKO_0808	F11	0.659	+	+	+	
1034	YPL258C	8	F	12		YKO_0808	F12	1.0236	+	+	+	
1035	YPL257W	8	G	1		YKO_0808	G01	1.0575	+	+	+	
1036	YPL256C	8	G	2		YKO_0808	G02	0.6579	+	+	+	
1038	YPL254W	8	G	3		YKO_0808	G03	not grow n	-	-	-	Not grow n
1039	YPL253C	8	G	4		YKO_0808	G04	1.0212	+	+	+	
1042	YPL250C	8	G	5		YKO_0808	G05	0.6471	+	+	+	
1043	YPL249C	8	G	6		YKO_0808	G06	1.0992	+	+	+	
1044	YPL248C	8	G	7		YKO_0808	G07	1.0433	slow	+	+	
1045	YPL247C	8	G	8		YKO_0808	G08	1.078	+	+	+	
1046	YPL246C	8	G	9		YKO_0808	G09	1.072	+	+	+	
1047	YPL245W	8	G	10		YKO_0808	G10	1.0236	+	+	+	
1048	YPL244C	8	G	11		YKO_0808	G11	1.1105	+	+	+	
1051	YPL241C	8	G	12		YKO_0808	G12	0.6621	+	+	+	
1052	YPL240C	8	H	1		YKO_0808	H01	1.0303	+	+	+	
--		8	H	2	empty	YKO_0808	H02	empty	empty	empty	empty	empty
1053	YPL239W	8	H	3		YKO_0808	H03	0.9725	+	+	-	HIT
1056	YPL236C	8	H	4		YKO_0808	H04	0.9759	+	+	+	
1058	YPL234C	8	H	5		YKO_0808	H05	1.0698	+	+	+	
1060	YPL232W	8	H	6		YKO_0808	H06	1.0612	+	+	+	
1062	YPL230W	8	H	7		YKO_0808	H07	1.0923	+	+	+	
1063	YPL229W	8	H	8		YKO_0808	H08	1.131	+	+	+	
1065	YPL227C	8	H	9		YKO_0808	H09	1.1016	+	+	+	
1066	YPL226W	8	H	10		YKO_0808	H10	1.1071	+	+	+	
1067	YPL225W	8	H	11		YKO_0808	H11	1.0541	+	+	+	
1069	YPL223C	8	H	12		YKO_0808	H12	0.6774	+	+	+	
1070	YPL222W	9	A	1		YKO_0809	A01	1.1924	+	+	+	
1071	YPL221W	9	A	2		YKO_0809	A02	1.2079	+	+	+	
1072	YPL220W	9	A	3		YKO_0809	A03	1.2112	+	+	+	
1073	YPL219W	9	A	4		YKO_0809	A04	1.2163	+	+	+	
1076	YPL216W	9	A	5		YKO_0809	A05	1.2105	+	+	+	
1077	YPL215W	9	A	6		YKO_0809	A06	1.1904	+	+	+	
1078	YPL214C	9	A	7		YKO_0809	A07	0.9603	+	+	+	
1079	YPL213W	9	A	8		YKO_0809	A08	1.1359	+	+	+	
--		9	A	9	empty	YKO_0809	A09	empty	empty	empty	empty	empty
1080	YPL212C	9	A	10		YKO_0809	A10	1.2019	+	+	+	
1084	YPL208W	9	A	11		YKO_0809	A11	1.1411	+	+	+	
1085	YPL207W	9	A	12		YKO_0809	A12	1.2257	+	+	-	HIT
1086	YPL206C	9	B	1		YKO_0809	B01	1.1438	+	+	+	
1087	YPL205C	9	B	2		YKO_0809	B02	1.1639	+	+	+	
1089	YPL203W	9	B	3		YKO_0809	B03	1.1346	+	+	+	
1090	YPL202C	9	B	4		YKO_0809	B04	1.0356	+	+	+	
1091	YPL201C	9	B	5		YKO_0809	B05	1.1559	+	+	+	
1092	YPL200W	9	B	6		YKO_0809	B06	1.1548	+	+	+	
1093	YPL199C	9	B	7		YKO_0809	B07	1.173	+	+	+	
1094	YPL198W	9	B	8		YKO_0809	B08	1.1618	+	+	-	HIT
1095	YPL197C	9	B	9		YKO_0809	B09	1.1507	+	+	+	
1096	YPL196W	9	B	10		YKO_0809	B10	1.1695	+	+	+	
1097	YPL195W	9	B	11		YKO_0809	B11	1.0589	+	+	+	
1098	YPL194W	9	B	12		YKO_0809	B12	1.0368	+	+	+	
1099	YPL193W	9	C	1		YKO_0809	C01	0.9252	slow	+	-	Doubt
1100	YPL192C	9	C	2		YKO_0809	C02	1.1326	+	+	+	
1101	YPL191C	9	C	3		YKO_0809	C03	1.1454	+	+	+	
1103	YPL189W	9	C	4		YKO_0809	C04	1.1674	+	+	+	
1104	YPL188W	9	C	5		YKO_0809	C05	1.1287	slow	-	-	Doubt
2065	YPL187W	9	C	6		YKO_0809	C06	1.1643	+	+	+	
2066	YPL185W	9	C	7		YKO_0809	C07	1.1805	+	+	+	
2067	YPL186C	9	C	8		YKO_0809	C08	1.1754	+	+	-	HIT
2068	YPL184C	9	C	9		YKO_0809	C09	1.1745	+	+	+	
2070	YPL181W	9	C	10		YKO_0809	C10	1.1816	+	+	+	
2071	YPL182C	9	C	11		YKO_0809	C11	0.851	+	-	-	Doubt
2072	YPL180W	9	C	12		YKO_0809	C12	1.0773	+	+	-	HIT
2073	YPL179W	9	D	1		YKO_0809	D01	1.1347	+	+	+	
2074	YPL178W	9	D	2		YKO_0809	D02	1.0973	+	+	+	
2075	YPL177C	9	D	3		YKO_0809	D03	1.1353	+	+	+	
2076	YPL176C	9	D	4		YKO_0809	D04	1.1448	+	+	+	
2078	YPL174C	9	D	5		YKO_0809	D05	0.9585	slow	+	-	Doubt
2079	YPL173W	9	D	6		YKO_0809	D06	1.1136	-	+	-	Doubt
2080	YPL172C	9	D	7		YKO_0809	D07	1.1545	+	+	+	
2081	YPL171C	9	D	8		YKO_0809	D08	1.174	+	+	-	HIT
2082	YPL170W	9	D	9		YKO_0809	D09	1.192	+	+	+	
2084	YPL168W	9	D	10		YKO_0809	D10	1.136	+	-	-	Doubt
2085	YPL167C	9	D	11		YKO_0809	D11	1.1541	+	+	+	
2086	YPL166W	9	D	12		YKO_0809	D12	1.1485	+	+	+	
2087	YPL165C	9	E	1		YKO_0809	E01	1.1776	+	+	+	
2088	YPL164C	9	E	2		YKO_0809	E02	1.1067	+	+	+	
2089	YPL163C	9	E	3		YKO_0809	E03	1.1365	+	+	+	
2090	YPL162C	9	E	4		YKO_0809	E04	1.1665	+	+	-	HIT
2091	YPL161C	9	E	5		YKO_0809	E05	0.9819	+	+	+	
2093	YPL159C	9	E	6		YKO_0809	E06	1.1341	+	+	-	HIT
2095	YPL157W	9	E	7		YKO_0809	E07	1.0434	+	+	+	
2096	YPL156C	9	E	8		YKO_0809	E08	1.1108	+	+	+	
2097	YPL155C	9	E	9		YKO_0809	E09	1.1311	+	-	+	Incongruence

	Euroscarf Information					Replica plate Information			Tau Toxicity Enhancer Primary Screen Results			
record no.	ORF name	Plate	Row	Col	Comment	Replica plate	Well	YPD (OD600nm)	Growth plate (SC+GAL comp.)	Transformation control plate (SC+GLU-Leu)	TEST Plate (SC+GAL-Leu)	Classification
2098	YPL154C	9	E	10		YKO_0809	E10	1.1618	+	+	+	
2100	YPL152W	9	E	11		YKO_0809	E11	0.8619	+	+	-	HIT
2102	YPL150W	9	E	12		YKO_0809	E12	1.1703	+	+	+	
2103	YPL149W	9	F	1		YKO_0809	F01	1.1718	+	+	+	
2105	YPL147W	9	F	2		YKO_0809	F02	1.1251	+	+	+	
2107	YPL145C	9	F	3		YKO_0809	F03	1.1129	+	+	+	
2108	YPL144W	9	F	4		YKO_0809	F04	1.1033	+	+	+	
2111	YPL141C	9	F	5		YKO_0809	F05	1.0932	+	+	+	
2112	YPL140C	9	F	6		YKO_0809	F06	1.1339	+	+	+	
2113	YPL139C	9	F	7		YKO_0809	F07	0.9933	+	+	-	HIT
2114	YPL138C	9	F	8		YKO_0809	F08	1.0962	+	+	+	
2115	YPL136W	9	F	9		YKO_0809	F09	1.1793	+	+	-	HIT
2117	YPL135W	9	F	10		YKO_0809	F10	1.1668	+	+	+	
2119	YPL133C	9	F	11		YKO_0809	F11	1.1743	+	+	-	HIT
2122	YPL130W	9	F	12		YKO_0809	F12	1.2003	+	+	-	HIT
2123	YPL129W	9	G	1		YKO_0809	G01	not grow n	-	-	-	Not grow n
2125	YPL127C	9	G	2		YKO_0809	G02	1.1262	+	+	+	
2127	YPL125W	9	G	3		YKO_0809	G03	1.1301	+	+	+	
2129	YPL123C	9	G	4		YKO_0809	G04	1.1581	+	+	+	
2131	YPL121C	9	G	5		YKO_0809	G05	1.1776	+	+	+	
2132	YPL120W	9	G	6		YKO_0809	G06	1.2083	+	+	+	
2133	YPL119C	9	G	7		YKO_0809	G07	1.161	+	-	+	Incongruence
2134	YPL118W	9	G	8		YKO_0809	G08	1.1691	-	+	-	Doubt
2136	YPL116W	9	G	9		YKO_0809	G09	1.165	+	+	+	
2137	YPL115C	9	G	10		YKO_0809	G10	1.1306	+	+	+	
2138	YPL114W	9	G	11		YKO_0809	G11	1.1928	+	+	-	HIT
2139	YPL113C	9	G	12		YKO_0809	G12	1.1406	+	+	-	HIT
2140	YPL112C	9	H	1		YKO_0809	H01	1.1951	+	+	+	
--		9	H	2	empty	YKO_0809	H02	empty	empty	empty	empty	empty
2141	YPL111W	9	H	3		YKO_0809	H03	1.1895	+	+	+	
2142	YPL110C	9	H	4		YKO_0809	H04	1.1791	+	+	+	
2143	YPL109C	9	H	5		YKO_0809	H05	1.1929	+	+	-	HIT
2144	YPL108W	9	H	6		YKO_0809	H06	1.1848	+	+	+	
2145	YPL107W	9	H	7		YKO_0809	H07	1.1616	+	+	+	
2146	YPL106C	9	H	8		YKO_0809	H08	0.8774	+	+	+	
2147	YPL105C	9	H	9		YKO_0809	H09	1.1265	+	+	+	
2148	YPL104W	9	H	10		YKO_0809	H10	1.1619	+	+	+	
2149	YPL103C	9	H	11		YKO_0809	H11	1.1876	+	-	-	Doubt
2150	YPL101W	9	H	12		YKO_0809	H12	1.1777	+	-	-	Doubt
2151	YPL102C	10	A	1		YKO_0810	A01	1.1488	+	+	+	
2152	YPL100W	10	A	2		YKO_0810	A02	0.8295	+	+	+	
2153	YPL099C	10	A	3		YKO_0810	A03	1.1791	+	+	+	
2154	YPL098C	10	A	4		YKO_0810	A04	1.1371	+	+	-	HIT
2155	YPL097W	10	A	5		YKO_0810	A05	0.8027	slow	+	-	Doubt
2156	YPL096W	10	A	6		YKO_0810	A06	1.1644	+	+	+	
2157	YPL095C	10	A	7		YKO_0810	A07	1.1652	+	+	+	
2160	YPL092W	10	A	8		YKO_0810	A08	0.8258	+	+	+	
3314	YBR174C	10	A	9		YKO_0810	A09	1.06	+	+	+	
--		10	A	10	empty	YKO_0810	A10	empty	empty	empty	empty	empty
3315	YBR175W	10	A	11		YKO_0810	A11	1.1287	+	+	+	
3316	YBR176W	10	A	12		YKO_0810	A12	1.1665	+	+	+	
3317	YBR177C	10	B	1		YKO_0810	B01	1.115	+	+	+	
3318	YBR178W	10	B	2		YKO_0810	B02	0.8101	+	+	+	
3319	YBR179C	10	B	3		YKO_0810	B03	1.0709	-	+	-	Doubt
3320	YBR180W	10	B	4		YKO_0810	B04	0.8334	+	+	+	
3321	YBR181C	10	B	5		YKO_0810	B05	0.724	+	+	+	
3322	YBR182C	10	B	6		YKO_0810	B06	1.1284	+	+	+	
3323	YBR183W	10	B	7		YKO_0810	B07	1.1665	+	+	+	
3324	YBR184W	10	B	8		YKO_0810	B08	1.0988	+	+	+	
3325	YBR185C	10	B	9		YKO_0810	B09	1.111	+	+	+	
3326	YBR186W	10	B	10		YKO_0810	B10	1.1243	+	+	+	
3327	YBR187W	10	B	11		YKO_0810	B11	1.1496	+	+	+	
3328	YBR188C	10	B	12		YKO_0810	B12	1.143	+	+	+	
3334	YBR194W	10	C	1		YKO_0810	C01	0.8684	+	+	+	
3335	YBR195C	10	C	2		YKO_0810	C02	0.8243	+	+	+	
3337	YBR197C	10	C	3		YKO_0810	C03	1.1143	+	+	+	
3339	YBR199W	10	C	4		YKO_0810	C04	1.1025	+	+	+	
3340	YBR200W	10	C	5		YKO_0810	C05	0.7404	+	+	+	
3341	YBR201W	10	C	6		YKO_0810	C06	1.1035	+	+	+	
3343	YBR203W	10	C	7		YKO_0810	C07	1.1262	+	+	+	
3344	YBR204C	10	C	8		YKO_0810	C08	1.0741	+	+	-	HIT
3345	YBR205W	10	C	9		YKO_0810	C09	1.1139	+	+	+	
3346	YBR206W	10	C	10		YKO_0810	C10	0.8591	+	+	+	
3347	YBR207W	10	C	11		YKO_0810	C11	1.086	+	+	+	
3348	YBR208C	10	C	12		YKO_0810	C12	1.1485	+	+	+	
3349	YBR209W	10	D	1	Hypothetical protein -- grow th on -met, no grow th on -lys, no grow th on drop-in media	YKO_0810	D01		+	+	+	
								1.0734				
3350	YBR210W	10	D	2		YKO_0810	D02	0.8102	+	+	+	
3352	YBR212W	10	D	3		YKO_0810	D03	1.1042	+	+	+	
3353	YBR213W	10	D	4		YKO_0810	D04	1.0923	+	+	+	

	Euroscarf Information					Replica plate Information			Tau Toxicity Enhancer Primary Screen Results			
record no.	ORF name	Plate	Row	Col	Comment	Replica plate	Well	YPD (OD600nm)	Growth plate (SC+GAL comp.)	Transformation control plate (SC+GLU-Leu)	TEST Plate (SC+GAL-Leu)	Classification
3354	YBR214W	10	D	5		YKO_0810	D05	1.1123	+	+	+	
3355	YBR215W	10	D	6		YKO_0810	D06	1.1199	slow	+	-	Doubt
3356	YBR216C	10	D	7		YKO_0810	D07	1.1492	slow	+	+	
3357	YBR217W	10	D	8		YKO_0810	D08	1.1115	slow	-	+	Incongruence
3358	YBR218C	10	D	9		YKO_0810	D09	1.0608	+	+	+	
3359	YBR219C	10	D	10		YKO_0810	D10	1.1127	+	+	+	
3360	YBR220C	10	D	11		YKO_0810	D11	1.072	+	+	+	
3361	YBR221C	10	D	12		YKO_0810	D12	1.0898	+	+	-	HIT
3362	YBR222C	10	E	1		YKO_0810	E01	0.8382	+	+	+	
3363	YBR223C	10	E	2		YKO_0810	E02	0.8375	+	+	+	
3364	YBR224W	10	E	3		YKO_0810	E03	0.7729	+	+	+	
3365	YBR225W	10	E	4		YKO_0810	E04	1.0825	+	+	+	
3366	YBR226C	10	E	5		YKO_0810	E05	1.1196	+	+	+	
3367	YBR227C	10	E	6		YKO_0810	E06	1.1405	+	+	+	
3368	YBR228W	10	E	7		YKO_0810	E07	1.1946	slow	+	-	Doubt
3369	YBR229C	10	E	8		YKO_0810	E08	1.0747	slow	+	-	Doubt
3370	YBR230C	10	E	9		YKO_0810	E09	1.1288	+	+	-	HIT
3371	YBR231C	10	E	10		YKO_0810	E10	1.0482	slow	+	-	Doubt
3373	YBR233W	10	E	11		YKO_0810	E11	1.0714	+	+	-	HIT
3375	YBR235W	10	E	12		YKO_0810	E12	1.1215	+	+	+	
3378	YBR238C	10	F	1		YKO_0810	F01	1.1436	+	+	+	
3379	YBR239C	10	F	2		YKO_0810	F02	0.8292	+	+	+	
3380	YBR240C	10	F	3		YKO_0810	F03	0.8397	+	+	+	
3381	YBR241C	10	F	4		YKO_0810	F04	0.8289	+	+	+	
3382	YBR242W	10	F	5		YKO_0810	F05	1.1016	+	+	+	
3384	YBR244W	10	F	6		YKO_0810	F06	1.0905	+	+	+	
3385	YBR245C	10	F	7		YKO_0810	F07	1.1771	+	+	-	HIT
3386	YBR246W	10	F	8		YKO_0810	F08	0.9947	slow	-	-	Doubt
3388	YBR248C	10	F	9		YKO_0810	F09	1.0484	slow	+	-	Doubt
3389	YBR249C	10	F	10		YKO_0810	F10	1.0922	+	+	+	
3390	YBR250W	10	F	11		YKO_0810	F11	1.1145	+	+	-	HIT
3391	YBR251W	10	F	12		YKO_0810	F12	1.1082	-	+	-	Doubt
3395	YBR255W	10	G	1		YKO_0810	G01	1.1213	+	+	+	
3398	YBR258C	10	G	2		YKO_0810	G02	0.8172	+	+	+	
3399	YBR259W	10	G	3		YKO_0810	G03	0.8061	+	+	+	
3400	YBR260C	10	G	4		YKO_0810	G04	1.1113	+	+	+	
3401	YBR261C	10	G	5		YKO_0810	G05	1.1067	+	+	+	
3402	YBR262C	10	G	6		YKO_0810	G06	1.1002	+	+	+	
3403	YBR263W	10	G	7		YKO_0810	G07	0.793	+	+	+	
3404	YBR264C	10	G	8		YKO_0810	G08	1.0534	+	-	+	Incongruence
3406	YBR266C	10	G	9		YKO_0810	G09	1.0307	slow	+	-	Doubt
3407	YBR267W	10	G	10	Incorrect -- PCR mating type A/Alpha	YKO_0810	G10	1.0035	+	+	-	HIT
3408	YBR268W	10	G	11		YKO_0810	G11	1.1142	-	+	-	Doubt
3985	YDR049W	10	G	12		YKO_0810	G12	1.1215	+	+	+	
3986	YDR050C	10	H	1		YKO_0810	H01	0.8343	+	+	+	
--		10	H	2	empty	YKO_0810	H02	empty	empty	empty	empty	empty
3987	YDR051C	10	H	3		YKO_0810	H03	1.1178	+	+	+	
3991	YDR055W	10	H	4		YKO_0810	H04	1.1199	+	+	+	
3992	YDR056C	10	H	5		YKO_0810	H05	1.1287	+	+	+	
3993	YDR057W	10	H	6		YKO_0810	H06	1.117	+	+	-	HIT
3994	YDR059C	10	H	7		YKO_0810	H07	0.8649	+	+	+	
3996	YDR061W	10	H	8		YKO_0810	H08	1.1022	+	+	-	HIT
3998	YDR063W	10	H	9		YKO_0810	H09	1.1134	+	+	+	
4000	YDR065W	10	H	10		YKO_0810	H10	1.0953	slow	+	-	Doubt
4001	YDR066C	10	H	11		YKO_0810	H11	1.1167	+	+	+	
4002	YDR067C	10	H	12		YKO_0810	H12	0.8106	+	+	+	
4003	YDR068W	11	A	1		YKO_0811	A01	1.0531	+	+	+	
4004	YDR069C	11	A	2		YKO_0811	A02	1.0958	+	+	+	
4005	YDR070C	11	A	3		YKO_0811	A03	1.1279	+	+	+	
4007	YDR072C	11	A	4		YKO_0811	A04	0.8601	+	+	+	
4008	YDR073W	11	A	5		YKO_0811	A05	0.8211	+	+	+	
4010	YDR075W	11	A	6		YKO_0811	A06	0.8734	+	+	+	
4011	YDR076W	11	A	7		YKO_0811	A07	1.0693	+	+	+	
4012	YDR077W	11	A	8		YKO_0811	A08	1.0968	+	+	+	
4013	YDR078C	11	A	9		YKO_0811	A09	0.8845	slow	+	-	Doubt
4014	YDR079W	11	A	10		YKO_0811	A10	1.1245	+	+	-	HIT
--		11	A	11	empty	YKO_0811	A11	empty	empty	empty	empty	empty
4015	YDR080W	11	A	12		YKO_0811	A12	1.0729	+	+	-	HIT
4018	YDR083W	11	B	1		YKO_0811	B01	1.0094	+	+	+	
4019	YDR084C	11	B	2		YKO_0811	B02	1.0915	+	+	+	
4020	YDR085C	11	B	3		YKO_0811	B03	0.892	+	+	+	
4024	YDR089W	11	B	4		YKO_0811	B04	1.1168	+	+	+	
4025	YDR090C	11	B	5		YKO_0811	B05	0.942	+	+	+	
4027	YDR092W	11	B	6		YKO_0811	B06	0.9922	+	+	+	
4028	YDR093W	11	B	7		YKO_0811	B07	1.0324	+	+	+	
4029	YDR094W	11	B	8		YKO_0811	B08	1.1225	+	+	+	
4030	YDR095C	11	B	9		YKO_0811	B09	0.8873	+	+	+	
4031	YDR096W	11	B	10		YKO_0811	B10	1.0834	+	+	+	
4032	YDR097C	11	B	11		YKO_0811	B11	0.9545	+	+	+	
4033	YDR098C	11	B	12		YKO_0811	B12	1.1302	+	+	+	
4034	YDR099W	11	C	1		YKO_0811	C01	0.9012	+	+	+	
4035	YDR100W	11	C	2		YKO_0811	C02	1.0734	+	+	+	

	Euroscarf Information					Replica plate Information			Tau Toxicity Enhancer Primary Screen Results			
record no.	ORF name	Plate	Row	Col	Comment	Replica plate	Well	YPD (OD600nm)	Growth plate (SC+GAL comp.)	Transformation control plate (SC+GLU-Leu)	TEST Plate (SC+GAL-Leu)	Classification
4036	YDR101C	11	C	3		YKO_0811	C03	0.8934	+	+	+	
4037	YDR102C	11	C	4		YKO_0811	C04	1.0819	+	+	+	
4038	YDR103W	11	C	5		YKO_0811	C05	0.8906	+	+	+	
4039	YDR104C	11	C	6		YKO_0811	C06	1.1481	+	+	+	
4040	YDR105C	11	C	7		YKO_0811	C07	1.1698	+	+	+	
4041	YDR107C	11	C	8		YKO_0811	C08	1.072	+	+	+	
4042	YDR108W	11	C	9		YKO_0811	C09	0.8928	+	+	+	
4043	YDR109C	11	C	10		YKO_0811	C10	1.1009	+	+	+	
4044	YDR110W	11	C	11		YKO_0811	C11	0.9536	+	+	+	
4045	YDR111C	11	C	12		YKO_0811	C12	1.1427	+	-	-	Doubt
4046	YDR112W	11	D	1		YKO_0811	D01	1.1192	+	+	+	
4048	YDR114C	11	D	2		YKO_0811	D02	1.0837	-	+	-	Doubt
4049	YDR115W	11	D	3		YKO_0811	D03	0.9788	+	+	+	
4050	YDR116C	11	D	4		YKO_0811	D04	1.0908	slow	+	+	
4051	YDR117C	11	D	5		YKO_0811	D05	1.1067	+	+	+	
4053	YDR119W	11	D	6		YKO_0811	D06	1.0714	+	+	+	
4054	YDR120C	11	D	7		YKO_0811	D07	0.8842	slow	+	+	
4055	YDR121W	11	D	8		YKO_0811	D08	1.0496	+	+	+	
4056	YDR122W	11	D	9		YKO_0811	D09	1.077	+	-	+	Incongruence
4057	YDR123C	11	D	10		YKO_0811	D10	1.0949	slow	+	+	
4058	YDR124W	11	D	11		YKO_0811	D11	0.8883	+	+	+	
4059	YDR125C	11	D	12		YKO_0811	D12	1.1147	+	+	+	
4060	YDR126W	11	E	1		YKO_0811	E01	1.1002	+	+	+	
4061	YDR127W	11	E	2		YKO_0811	E02	1.0556	+	+	+	
4062	YDR128W	11	E	3		YKO_0811	E03	0.8784	+	+	+	
4063	YDR129C	11	E	4		YKO_0811	E04	1.0892	+	+	+	
4064	YDR130C	11	E	5		YKO_0811	E05	1.0231	+	+	+	
4065	YDR131C	11	E	6		YKO_0811	E06	1.0747	+	+	+	
4066	YDR132C	11	E	7		YKO_0811	E07	1.0944	+	+	+	
4067	YDR133C	11	E	8		YKO_0811	E08	1.0271	+	+	+	
4068	YDR134C	11	E	9		YKO_0811	E09	1.0398	+	+	+	
4069	YDR135C	11	E	10		YKO_0811	E10	0.9359	+	+	+	
4070	YDR136C	11	E	11		YKO_0811	E11	0.8079	slow	+	+	
4071	YDR137W	11	E	12		YKO_0811	E12	1.0924	+	+	+	
7400	YPR021C	11	F	1	Hyperrecombination protein related to Top 1 p -- grow th on -met, grow th on -lys, mates poorly	YKO_0811	F01	1.0836	+	+	+	
4073	YDR139C	11	F	2		YKO_0811	F02	1.1014	+	+	+	
4074	YDR140W	11	F	3		YKO_0811	F03	0.8953	+	+	+	
4076	YDR142C	11	F	4		YKO_0811	F04	1.0938	+	+	+	
4077	YDR143C	11	F	5		YKO_0811	F05	1.0515	+	+	+	
4078	YDR144C	11	F	6		YKO_0811	F06	1.0596	+	+	+	
4080	YDR146C	11	F	7	Transcription factor -- grow th on -met, grow th on -lys, mates poorly	YKO_0811	F07	1.1132	+	+	+	
4177	YDR338C	11	F	8		YKO_0811	F08	1.0412	slow	+	+	
4179	YDR340W	11	F	9		YKO_0811	F09	1.0834	+	+	+	
4181	YDR344C	11	F	10		YKO_0811	F10	0.8854	+	+	+	
4182	YDR345C	11	F	11		YKO_0811	F11	0.9878	+	+	+	
4183	YDR346C	11	F	12		YKO_0811	F12	1.1259	+	+	+	
4184	YDR347W	11	G	1		YKO_0811	G01	1.0741	+	+	-	HIT
4185	YDR348C	11	G	2		YKO_0811	G02	1.099	+	+	+	
4186	YDR349C	11	G	3		YKO_0811	G03	1.0859	+	+	+	
4187	YDR350C	11	G	4		YKO_0811	G04	1.0552	-	+	-	Doubt
4188	YDR351W	11	G	5		YKO_0811	G05	1.036	+	+	+	
4189	YDR352W	11	G	6		YKO_0811	G06	1.0993	+	+	+	
4191	YDR354W	11	G	7		YKO_0811	G07	1.0958	slow	+	+	
4194	YDR357C	11	G	8		YKO_0811	G08	0.9892	+	+	+	
4195	YDR358W	11	G	9		YKO_0811	G09	1.0375	+	+	+	
4196	YDR359C	11	G	10		YKO_0811	G10	1.1545	+	+	+	
4197	YDR360W	11	G	11		YKO_0811	G11	1.0607	+	+	+	
4200	YDR363W	11	G	12		YKO_0811	G12	0.8365	+	+	+	
4201	YDR364C	11	H	1		YKO_0811	H01	not grow n	-	-	-	Not grow n
--		11	H	2	empty	YKO_0811	H02	empty	empty	empty	empty	empty
4204	YDR368W	11	H	3		YKO_0811	H03	0.895	+	+	+	
4205	YDR369C	11	H	4		YKO_0811	H04	1.081	+	-	+	Incongruence
4206	YDR370C	11	H	5		YKO_0811	H05	1.0629	+	+	+	
4207	YDR371W	11	H	6		YKO_0811	H06	1.0483	+	+	+	
4208	YDR372C	11	H	7		YKO_0811	H07	0.8572	+	+	+	
4210	YDR374C	11	H	8		YKO_0811	H08	1.0918	+	+	+	
4211	YDR375C	11	H	9		YKO_0811	H09	1.133	slow	+	-	Doubt
4213	YDR377W	11	H	10		YKO_0811	H10	0.8977	slow	+	-	Doubt
4214	YDR378C	11	H	11		YKO_0811	H11	0.8344	+	-	+	Incongruence
4215	YDR379W	11	H	12		YKO_0811	H12	0.9341	+	+	+	
4216	YDR380W	12	A	1		YKO_0812	A01	0.865	+	+	+	
4218	YDR382W	12	A	2		YKO_0812	A02	0.851	+	+	+	
4219	YDR383C	12	A	3		YKO_0812	A03	0.823	+	+	+	
4220	YDR384C	12	A	4		YKO_0812	A04	0.829	+	+	+	
4221	YDR385W	12	A	5		YKO_0812	A05	0.692	+	+	+	
4222	YDR386W	12	A	6		YKO_0812	A06	0.74	+	+	+	
4223	YDR387C	12	A	7		YKO_0812	A07	0.791	+	+	+	
4224	YDR388W	12	A	8		YKO_0812	A08	0.663	+	+	+	

Euroscarf Information						Replica plate Information			Tau Toxicity Enhancer Primary Screen Results			
record no.	ORF name	Plate	Row	Col	Comment	Replica plate	Well	YPD (OD600nm)	Growth plate (SC+GAL comp.)	Transformation control plate (SC+GLU-Leu)	TEST Plate (SC+GAL-Leu)	Classification
4225	YDR389W	12	A	9		YKO_0812	A09	1.04	+	+	+	
4227	YDR391C	12	A	10		YKO_0812	A10	0.894	+	+	-	HIT
4228	YDR392W	12	A	11		YKO_0812	A11	0.493	+	+	+	
--		12	A	12	empty	YKO_0812	A12	empty	empty	empty	empty	empty
4229	YDR393W	12	B	1		YKO_0812	B01	0.861	+	+	-	HIT
4231	YDR395W	12	B	2		YKO_0812	B02	0.879	+	+	+	
4235	YDR399W	12	B	3		YKO_0812	B03	0.856	+	+	+	
4236	YDR400W	12	B	4		YKO_0812	B04	0.867	+	+	+	
4237	YDR401W	12	B	5		YKO_0812	B05	0.81	+	+	+	
4238	YDR402C	12	B	6		YKO_0812	B06	0.815	+	+	-	HIT
4239	YDR403W	12	B	7		YKO_0812	B07	0.736	+	+	-	HIT
4241	YDR405W	12	B	8		YKO_0812	B08	0.844	-	+	-	Doubt
4242	YDR406W	12	B	9		YKO_0812	B09	0.795	+	+	+	
4244	YDR408C	12	B	10		YKO_0812	B10	0.681	slow	+	+	
4245	YDR409W	12	B	11		YKO_0812	B11	0.805	+	+	+	
4246	YDR410C	12	B	12	Sterile [expected phenotype]	YKO_0812	B12	0.866	+	+	+	
4247	YDR411C	12	C	1		YKO_0812	C01	0.869	+	+	+	
4250	YDR414C	12	C	2		YKO_0812	C02	0.909	+	+	+	
4251	YDR415C	12	C	3		YKO_0812	C03	0.872	+	+	+	
4254	YDR418W	12	C	4		YKO_0812	C04	0.595	slow	+	-	Doubt
4255	YDR419W	12	C	5		YKO_0812	C05	0.589	+	+	+	
4256	YDR420W	12	C	6		YKO_0812	C06	0.719	+	+	+	
4257	YDR421W	12	C	7		YKO_0812	C07	0.792	+	+	+	
4258	YDR422C	12	C	8		YKO_0812	C08	0.776	+	+	+	
4259	YDR423C	12	C	9		YKO_0812	C09	0.86	+	+	+	
4261	YDR425W	12	C	10		YKO_0812	C10	0.809	+	+	+	
4262	YDR426C	12	C	11		YKO_0812	C11	0.803	+	+	+	
4264	YDR428C	12	C	12		YKO_0812	C12	0.824	+	+	+	
4266	YDR430C	12	D	1		YKO_0812	D01	0.943	+	+	+	
4267	YDR431W	12	D	2		YKO_0812	D02	0.946	+	+	-	HIT
4268	YDR432W	12	D	3		YKO_0812	D03	0.851	slow	+	-	Doubt
4269	YDR433W	12	D	4		YKO_0812	D04	0.731	+	+	+	
4271	YDR435C	12	D	5		YKO_0812	D05	0.801	+	+	+	
4272	YDR436W	12	D	6		YKO_0812	D06	0.702	+	+	+	
241	YEL001C	12	D	7		YKO_0812	D07	0.86	+	+	+	
243	YEL003W	12	D	8		YKO_0812	D08	0.696	+	+	+	
244	YEL004W	12	D	9	Similar to K. lactis golgi uridine diphosphate-N-acetylglucosamine transporter -- growth on -met, no growth on -lys, no growth on drop-in media, confirmed alpha -- CORRECT STRAIN CAN BE FOUND IN PLATE 121 D6	YKO_0812	D09	0.799	+	+	+	
245	YEL005C	12	D	10		YKO_0812	D10	0.862	+	+	+	
246	YEL006W	12	D	11		YKO_0812	D11	0.76	+	+	+	
247	YEL007W	12	D	12		YKO_0812	D12	0.653	+	+	+	
248	YEL008W	12	E	1		YKO_0812	E01	0.969	+	+	+	
249	YEL009C	12	E	2		YKO_0812	E02	0.932	+	+	+	
250	YEL010W	12	E	3		YKO_0812	E03	0.889	+	+	+	
253	YEL013W	12	E	4		YKO_0812	E04	0.562	slow	+	+	
254	YEL014C	12	E	5		YKO_0812	E05	0.857	+	+	+	
255	YEL015W	12	E	6		YKO_0812	E06	0.738	+	+	+	
256	YEL016C	12	E	7		YKO_0812	E07	0.879	+	+	+	
257	YEL017C-A	12	E	8		YKO_0812	E08	0.764	+	+	+	
258	YEL017W	12	E	9		YKO_0812	E09	0.72	+	+	+	
7401	YPR083W	12	E	10		YKO_0812	E10	0.856	+	+	+	
261	YEL020C	12	E	11		YKO_0812	E11	0.847	+	+	+	
264	YEL023C	12	E	12		YKO_0812	E12	0.65	+	+	+	
265	YEL024W	12	F	1		YKO_0812	F01	0.903	slow	+	-	Doubt
266	YEL025C	12	F	2		YKO_0812	F02	0.911	+	+	+	
268	YEL027W	12	F	3		YKO_0812	F03	0.766	-	-	-	Doubt
269	YEL028W	12	F	4		YKO_0812	F04	0.899	+	+	+	
271	YEL030W	12	F	5		YKO_0812	F05	0.517	+	+	+	
272	YEL031W	12	F	6		YKO_0812	F06	0.633	slow	+	+	
274	YEL033W	12	F	7		YKO_0812	F07	0.892	slow	+	+	
7403	YPR091C	12	F	8		YKO_0812	F08	0.873	+	+	+	
278	YEL037C	12	F	9		YKO_0812	F09	0.886	+	+	+	
279	YEL038W	12	F	10		YKO_0812	F10	0.862	+	+	+	
280	YEL039C	12	F	11		YKO_0812	F11	0.868	+	+	+	
281	YEL040W	12	F	12		YKO_0812	F12	0.709	+	+	+	
282	YEL041W	12	G	1		YKO_0812	G01	0.928	+	+	+	
283	YEL042W	12	G	2		YKO_0812	G02	0.877	+	+	+	
284	YEL043W	12	G	3		YKO_0812	G03	0.912	+	-	-	Doubt
286	YEL045C	12	G	4	Similar to cytochrome c oxidase III of T. brucei kinetoplast -- no growth on -met, super slow growth on -lys, super slow growth on drop in media	YKO_0812	G04	0.831	slow	-	-	Doubt

	Euroscarf Information					Replica plate Information			Tau Toxicity Enhancer Primary Screen Results			
record no.	ORF name	Plate	Row	Col	Comment	Replica plate	Well	YPD (OD600nm)	Growth plate (SC+GAL comp.)	Transformation control plate (SC+GLU-Leu)	TEST Plate (SC+GAL-Leu)	Classification
287	YEL046C	12	G	5	L-threonine aldolase -- no growth on -met, super slow growth on -lys, super slow growth on drop in media	YKO_0812	G05	0.836	slow	-	-	Doubt
288	YEL047C	12	G	6		YKO_0812	G06	0.864	+	+	+	
289	YEL048C	12	G	7		YKO_0812	G07	0.966	+	+	+	
290	YEL049W	12	G	8		YKO_0812	G08	0.869	+	+	+	
291	YEL050C	12	G	9		YKO_0812	G09	0.803	-	+	-	Doubt
292	YEL051W	12	G	10		YKO_0812	G10	0.812	-	-	-	Doubt
293	YEL052W	12	G	11		YKO_0812	G11	0.854	+	+	+	
294	YEL053C	12	G	12		YKO_0812	G12	0.73	+	+	+	
295	YEL054C	12	H	1		YKO_0812	H01	0.969	+	+	+	
--		12	H	2	empty	YKO_0812	H02	empty	empty	empty	empty	empty
297	YEL056W	12	H	3		YKO_0812	H03	0.541	+	+	+	
298	YEL057C	12	H	4		YKO_0812	H04	0.601	+	+	+	
301	YEL059W	12	H	5		YKO_0812	H05	0.512	+	+	+	
302	YEL060C	12	H	6		YKO_0812	H06	0.64	+	+	+	
303	YEL061C	12	H	7		YKO_0812	H07	0.679	+	+	+	
304	YEL062W	12	H	8		YKO_0812	H08	0.976	+	+	+	
305	YEL063C	12	H	9		YKO_0812	H09	0.622	+	-	-	Doubt
306	YEL064C	12	H	10		YKO_0812	H10	0.881	+	+	+	
307	YEL065W	12	H	11		YKO_0812	H11	0.558	+	+	+	
308	YEL066W	12	H	12		YKO_0812	H12	0.643	+	+	+	
309	YEL067C	13	A	1		YKO_0813	A01	0.727	+	+	+	
310	YEL068C	13	A	2		YKO_0813	A02	0.755	+	+	+	
313	YEL071W	13	A	3		YKO_0813	A03	0.517	+	+	+	
314	YEL072W	13	A	4	Hypothetical protein -- mates like alpha PCR mating type alpha	YKO_0813	A04	0.738	+	+	+	
322	YER001W	13	A	5		YKO_0813	A05	0.709	+	+	+	
323	YER002W	13	A	6		YKO_0813	A06	0.801	+	+	+	
325	YER004W	13	A	7		YKO_0813	A07	0.824	+	+	+	
326	YER005W	13	A	8		YKO_0813	A08	0.605	+	+	+	
328	YER007C-A	13	A	9		YKO_0813	A09	0.955	+	+	+	
329	YER007W	13	A	10		YKO_0813	A10	0.912	+	+	+	
332	YER010C	13	A	11		YKO_0813	A11	0.645	+	+	+	
333	YER011W	13	A	12		YKO_0813	A12	0.979	+	-	-	Doubt
--		13	A	13	empty	YKO_0813	B01	empty	empty	empty	empty	empty
7399	YPR011C	13	B	2		YKO_0813	B02	0.833	+	+	+	
148	YER017C	13	B	3		YKO_0813	B03	0.591	-	-	-	Doubt
150	YER019W	13	B	4		YKO_0813	B04	0.925	+	+	+	
151	YER019C-A	13	B	5		YKO_0813	B05	0.838	+	+	+	
152	YER020W	13	B	6		YKO_0813	B06	0.764	+	+	+	
156	YER024W	13	B	7		YKO_0813	B07	0.695	+	+	+	
162	YER030W	13	B	8		YKO_0813	B08	0.588	+	+	+	
164	YER032W	13	B	9		YKO_0813	B09	0.9	+	+	+	
165	YER033C	13	B	10		YKO_0813	B10	0.814	+	+	+	
166	YER034W	13	B	11		YKO_0813	B11	0.945	+	+	+	
167	YER035W	13	B	12		YKO_0813	B12	0.937	+	+	+	
171	YER038W-A	13	C	1		YKO_0813	C01	0.898	+	+	+	
172	YER039C	13	C	2		YKO_0813	C02	0.876	+	+	+	
173	YER040W	13	C	3		YKO_0813	C03	0.66	+	+	+	
174	YER041W	13	C	4		YKO_0813	C04	0.79	+	+	+	
175	YER042W	13	C	5		YKO_0813	C05	0.879	+	+	+	
178	YER044C-A	13	C	6		YKO_0813	C06	0.806	+	+	+	
179	YER045C	13	C	7		YKO_0813	C07	0.515	+	+	+	
181	YER046W-A	13	C	8		YKO_0813	C08	0.69	+	+	+	
182	YER047C	13	C	9		YKO_0813	C09	0.735	+	+	+	
183	YER048C	13	C	10		YKO_0813	C10	0.773	+	+	+	
184	YER049W	13	C	11		YKO_0813	C11	0.895	+	+	+	
185	YER050C	13	C	12		YKO_0813	C12	0.891	-	-	-	Doubt
186	YER051W	13	D	1		YKO_0813	D01	0.873	+	+	+	
187	YER052C	13	D	2		YKO_0813	D02	0.861	+	+	+	
188	YER053C	13	D	3		YKO_0813	D03	0.915	+	+	+	
189	YER054C	13	D	4		YKO_0813	D04	0.88	+	+	+	
191	YER056C	13	D	5		YKO_0813	D05	0.85	+	+	+	
192	YER056C-A	13	D	6		YKO_0813	D06	0.619	+	+	+	
193	YER057C	13	D	7	Heat shock inducible inhibitor of cell growth -- growth on -met, super slow grow on -lys, super slow growth on drop in media -- APPEARS ALPHA	YKO_0813	D07	0.603	+	+	+	
194	YER058W	13	D	8		YKO_0813	D08	0.804	-	+	-	Doubt
195	YER059W	13	D	9		YKO_0813	D09	0.999	+	+	+	
196	YER060W	13	D	10		YKO_0813	D10	0.918	+	+	+	
197	YER060W-A	13	D	11	similar to Fcy2p -- growth on -met, no growth on -lys, no growth on drop-in media	YKO_0813	D11	0.905	+	+	+	

	Euroscarf Information					Replica plate Information			Tau Toxicity Enhancer Primary Screen Results			
record no.	ORF name	Plate	Row	Col	Comment	Replica plate	Well	YPD (OD600nm)	Growth plate (SC+GAL comp.)	Transformation control plate (SC+GLU-Leu)	TEST Plate (SC+GAL-Leu)	Classification
198	YER061C	13	D	12		YKO_0813	D12	0.661	+	-	-	Doubt
199	YER062C	13	E	1		YKO_0813	E01	0.822	+	+	+	
202	YER065C	13	E	2		YKO_0813	E02	0.883	+	+	+	
204	YER066C-A	13	E	3		YKO_0813	E03	0.896	+	+	+	
205	YER067W	13	E	4		YKO_0813	E04	0.82	+	+	+	
206	YER067C-A	13	E	5		YKO_0813	E05	0.894	+	+	+	
207	YER068W	13	E	6		YKO_0813	E06	not grown	-	-	-	Not grown
208	YER068C-A	13	E	7		YKO_0813	E07	0.772	+	+	+	
209	YER069W	13	E	8		YKO_0813	E08	0.592	+	+	+	
7405	YPR118W	13	E	9		YKO_0813	E09	0.846	+	+	+	
211	YER071C	13	E	10		YKO_0813	E10	0.608	+	+	+	
212	YER072W	13	E	11		YKO_0813	E11	0.991	+	+	+	
213	YER073W	13	E	12		YKO_0813	E12	0.966	+	+	+	
214	YER074W	13	F	1		YKO_0813	F01	0.712	+	+	+	
215	YER075C	13	F	2		YKO_0813	F02	0.884	+	+	+	
219	YER079W	13	F	3		YKO_0813	F03	0.822	+	+	+	
220	YER080W	13	F	4		YKO_0813	F04	0.882	+	+	+	
221	YER081W	13	F	5		YKO_0813	F05	0.887	+	+	+	
223	YER083C	13	F	6		YKO_0813	F06	0.657	+	+	+	
224	YER084W	13	F	7		YKO_0813	F07	0.736	+	+	+	
225	YER085C	13	F	8		YKO_0813	F08	0.744	+	+	+	
226	YER086W	13	F	9		YKO_0813	F09	0.961	slow	+	+	
228	YER087C-A	13	F	10		YKO_0813	F10	0.954	+	+	+	
4753	YGR123C	13	F	11		YKO_0813	F11	0.965	+	+	+	
4754	YGR124W	13	F	12		YKO_0813	F12	0.984	+	+	+	
4755	YGR125W	13	G	1		YKO_0813	G01	0.735	+	+	+	
4756	YGR126W	13	G	2		YKO_0813	G02	0.906	+	+	+	
4757	YGR127W	13	G	3		YKO_0813	G03	0.834	+	+	+	
4759	YGR129W	13	G	4		YKO_0813	G04	0.865	+	+	+	
4760	YGR130C	13	G	5		YKO_0813	G05	0.844	+	+	+	
4761	YGR131W	13	G	6		YKO_0813	G06	0.879	+	+	+	
4762	YGR132C	13	G	7		YKO_0813	G07	0.904	+	+	+	
4763	YGR133W	13	G	8		YKO_0813	G08	0.864	+	+	-	HIT
4765	YGR135W	13	G	9		YKO_0813	G09	0.583	+	+	+	
4766	YGR136W	13	G	10		YKO_0813	G10	0.933	+	+	+	
4767	YGR137W	13	G	11		YKO_0813	G11	0.972	+	+	+	
4768	YGR138C	13	G	12		YKO_0813	G12	0.924	+	+	+	
4769	YGR139W	13	H	1		YKO_0813	H01	0.559	+	+	+	
--		13	H	2	empty	YKO_0813	H02	empty	empty	empty	empty	empty
4771	YGR141W	13	H	3		YKO_0813	H03	0.986	+	+	+	
4772	YGR142W	13	H	4		YKO_0813	H04	0.935	+	+	+	
4773	YGR143W	13	H	5		YKO_0813	H05	0.605	+	+	+	
4774	YGR144W	13	H	6		YKO_0813	H06	0.944	+	+	+	
4776	YGR146C	13	H	7		YKO_0813	H07	0.876	+	+	+	
4778	YGR148C	13	H	8		YKO_0813	H08	1.005	+	+	+	
4779	YGR149W	13	H	9		YKO_0813	H09	0.822	+	+	+	
4780	YGR150C	13	H	10		YKO_0813	H10	0.973	slow	+	-	Doubt
4781	YGR151C	13	H	11		YKO_0813	H11	0.944	+	+	+	
4782	YGR152C	13	H	12		YKO_0813	H12	1.037	+	+	+	
4783	YGR153W	14	A	1		YKO_0814	A01	0.923	+	+	+	
4784	YGR154C	14	A	2		YKO_0814	A02	0.906	+	+	+	
4787	YGR157W	14	A	3		YKO_0814	A03	0.91	+	+	+	
4789	YGR159C	14	A	4		YKO_0814	A04	0.852	+	+	+	
4790	YGR160W	14	A	5		YKO_0814	A05	0.94	+	+	+	
4791	YGR161C	14	A	6		YKO_0814	A06	0.829	+	+	+	
4793	YGR163W	14	A	7		YKO_0814	A07	0.888	+	+	+	
4794	YGR164W	14	A	8		YKO_0814	A08	0.79	+	+	+	
4795	YGR165W	14	A	9		YKO_0814	A09	0.78	slow	+	-	Doubt
4796	YGR166W	14	A	10		YKO_0814	A10	0.839	+	+	+	
7133	YOL153C	14	A	11		YKO_0814	A11	0.885	+	+	+	
4798	YGR168C	14	A	12	Hypothetical protein -- growth on -met, no growth on -lys, no growth on drop-in media	YKO_0814	A12	0.947	+	+	-	HIT
4799	YGR169C	14	B	1		YKO_0814	B01	0.955	+	+	+	
--		14	B	2	empty	YKO_0814	B02	empty	empty	empty	empty	empty
4800	YGR170W	14	B	3		YKO_0814	B03	0.991	+	+	+	
4801	YGR171C	14	B	4		YKO_0814	B04	0.904	+	+	+	
4803	YGR173W	14	B	5		YKO_0814	B05	0.921	+	+	+	
4804	YGR174C	14	B	6		YKO_0814	B06	0.779	slow	+	-	Doubt
4806	YGR176W	14	B	7		YKO_0814	B07	0.868	+	+	+	
4807	YGR177C	14	B	8		YKO_0814	B08	0.987	+	+	+	
4808	YGR178C	14	B	9		YKO_0814	B09	0.947	+	+	-	HIT
4810	YGR180C	14	B	10		YKO_0814	B10	not grown	-	-	-	Not grown
4811	YGR181W	14	B	11		YKO_0814	B11	0.91	+	+	-	HIT
4812	YGR182C	14	B	12		YKO_0814	B12	0.855	+	+	+	
4813	YGR183C	14	C	1		YKO_0814	C01	0.958	+	+	-	HIT
4814	YGR184C	14	C	2		YKO_0814	C02	0.96	+	+	+	
4817	YGR187C	14	C	3		YKO_0814	C03	0.99	+	+	+	
4819	YGR189C	14	C	4		YKO_0814	C04	1.054	+	+	+	
4822	YGR192C	14	C	5		YKO_0814	C05	1.025	+	+	-	HIT

	Euroscarf Information					Replica plate Information			Tau Toxicity Enhancer Primary Screen Results			
record no.	ORF name	Plate	Row	Col	Comment	Replica plate	Well	YPD (OD600nm)	Growth plate (SC+GAL comp.)	Transformation control plate (SC+GLU-Leu)	TEST Plate (SC+GAL-Leu)	Classification
4823	YGR193C	14	C	6		YKO_0814	C06	1.017	+	+	-	HIT
4824	YGR194C	14	C	7		YKO_0814	C07	0.959	+	+	+	
4826	YGR196C	14	C	8		YKO_0814	C08	1	+	+	+	
4827	YGR197C	14	C	9		YKO_0814	C09	0.898	+	+	-	HIT
4829	YGR199W	14	C	10		YKO_0814	C10	0.882	+	+	+	
4830	YGR200C	14	C	11		YKO_0814	C11	0.881	+	+	-	HIT
4832	YGR202C	14	C	12		YKO_0814	C12	0.722	+	+	+	
4833	YGR203W	14	D	1		YKO_0814	D01	0.825	+	+	+	
4835	YGR205W	14	D	2		YKO_0814	D02	1.041	+	+	+	
4836	YGR206W	14	D	3		YKO_0814	D03	0.993	+	+	+	
4837	YGR207C	14	D	4		YKO_0814	D04	0.981	+	+	+	
4838	YGR208W	14	D	5		YKO_0814	D05	0.986	-	-	-	Doubt
4839	YGR209C	14	D	6		YKO_0814	D06	0.671	+	+	+	
4842	YGR212W	14	D	7		YKO_0814	D07	0.985	+	+	+	
4843	YGR213C	14	D	8		YKO_0814	D08	0.706	+	+	+	
4844	YGR214W	14	D	9		YKO_0814	D09	0.832	+	+	-	HIT
4845	YGR215W	14	D	10		YKO_0814	D10	0.814	-	-	-	Doubt
4847	YGR217W	14	D	11		YKO_0814	D11	0.83	+	+	-	HIT
916	YHL047C	14	D	12		YKO_0814	D12	0.825	+	+	+	
917	YHL046C	14	E	1		YKO_0814	E01	0.9	+	+	+	
918	YHL045W	14	E	2		YKO_0814	E02	1.036	+	+	+	
919	YHL044W	14	E	3		YKO_0814	E03	0.758	+	+	+	
920	YHL043W	14	E	4		YKO_0814	E04	0.888	+	+	+	
921	YHL042W	14	E	5		YKO_0814	E05	0.93	+	+	+	
922	YHL041W	14	E	6		YKO_0814	E06	0.957	+	+	+	
923	YHL040C	14	E	7		YKO_0814	E07	0.886	+	+	-	HIT
925	YHL038C	14	E	8		YKO_0814	E08	0.845	-	+	-	Doubt
926	YHL037C	14	E	9		YKO_0814	E09	0.862	+	+	-	HIT
927	YHL036W	14	E	10		YKO_0814	E10	0.88	+	+	-	HIT
928	YHL035C	14	E	11		YKO_0814	E11	0.834	+	+	-	HIT
929	YHL034C	14	E	12		YKO_0814	E12	0.725	+	+	-	HIT
930	YHL033C	14	F	1		YKO_0814	F01	0.84	+	+	+	
931	YHL032C	14	F	2		YKO_0814	F02	0.932	+	+	+	
932	YHL031C	14	F	3		YKO_0814	F03	0.866	+	+	+	
933	YHL030W	14	F	4	Cell wall biogenesis & architecture -- growth on -met, no growth on -lys, no growth on drop-in media -- APPEARS ALPHA	YKO_0814	F04	0.701	+	+	+	
934	YHL029C	14	F	5		YKO_0814	F05	0.947	+	+	+	
935	YHL028W	14	F	6		YKO_0814	F06	0.84	+	+	+	
936	YHL027W	14	F	7		YKO_0814	F07	0.989	+	+	+	
937	YHL026C	14	F	8		YKO_0814	F08	0.927	+	+	-	HIT
940	YHL023C	14	F	9		YKO_0814	F09	0.883	+	-	-	Doubt
941	YHL022C	14	F	10		YKO_0814	F10	0.732	+	+	-	HIT
942	YHL021C	14	F	11		YKO_0814	F11	0.852	+	+	-	HIT
943	YHL020C	14	F	12		YKO_0814	F12	0.905	+	+	+	
944	YHL019C	14	G	1		YKO_0814	G01	0.65	+	+	+	
946	YHL017W	14	G	2		YKO_0814	G02	0.988	+	+	+	
947	YHL016C	14	G	3		YKO_0814	G03	0.873	+	+	+	
949	YHL014C	14	G	4		YKO_0814	G04	0.943	+	+	+	
950	YHL013C	14	G	5		YKO_0814	G05	0.836	+	+	+	
951	YHL012W	14	G	6		YKO_0814	G06	0.691	+	+	+	
953	YHL010C	14	G	7		YKO_0814	G07	0.957	+	+	+	
954	YHL009C	14	G	8		YKO_0814	G08	0.915	+	+	+	
955	YHL008C	14	G	9		YKO_0814	G09	0.851	+	+	+	
956	YHL007C	14	G	10	Sterile [expected phenotype]	YKO_0814	G10	0.84	+	-	-	Doubt
957	YHL006C	14	G	11		YKO_0814	G11	0.89	+	+	+	
959	YHL005C	14	G	12	Hypothetical protein -- growth on -met, no growth on -lys, no growth on drop-in media, petite -- APPEARS ALPHA	YKO_0814	G12	0.795	slow	+	+	
960	YHL003C	14	H	1	Longevity assurance protein -- growth on -met, no growth on -lys, no growth on drop-in media -- APPEARS ALPHA	YKO_0814	H01	0.921	+	+	+	
--		14	H	2	empty	YKO_0814	H02	empty	empty	empty	empty	empty
964	YHR001W-A	14	H	3		YKO_0814	H03	0.98	+	+	+	
974	YHR011W	14	H	4		YKO_0814	H04	0.821	+	+	+	
975	YHR012W	14	H	5		YKO_0814	H05	0.94	+	+	+	
976	YHR013C	14	H	6		YKO_0814	H06	0.784	+	+	+	
977	YHR014W	14	H	7		YKO_0814	H07	0.936	+	+	+	
978	YHR015W	14	H	8		YKO_0814	H08	0.889	+	+	+	
981	YHR018C	14	H	9		YKO_0814	H09	0.856	+	+	+	
985	YHR022C	14	H	10		YKO_0814	H10	0.87	+	+	-	HIT

Euroscarf Information						Replica plate Information			Tau Toxicity Enhancer Primary Screen Results			
record no.	ORF name	Plate	Row	Col	Comment	Replica plate	Well	YPD (OD600nm)	Growth plate (SC+GAL comp.)	Transformation control plate (SC+GLU-Leu)	TEST Plate (SC+GAL-Leu)	Classification
992	YHR029C	14	H	11		YKO_0814	H11	0.81	+	+	+	
993	YHR030C	14	H	12		YKO_0814	H12	0.701	+	+	+	
994	YHR031C	15	A	1		YKO_0815	A01	0.834	+	+	+	
997	YHR034C	15	A	2		YKO_0815	A02	0.845	+	+	+	
998	YHR035W	15	A	3		YKO_0815	A03	0.99	+	+	+	
1000	YHR037W	15	A	4		YKO_0815	A04	0.914	+	+	+	
1001	YHR038W	15	A	5		YKO_0815	A05	0.949	+	+	+	
1002	YHR039C	15	A	6		YKO_0815	A06	0.874	+	+	+	
1006	YHR043C	15	A	7		YKO_0815	A07	0.926	+	+	+	
1007	YHR044C	15	A	8		YKO_0815	A08	0.911	+	+	+	
1873	YHR046C	15	A	9		YKO_0815	A09	0.641	+	+	+	
1874	YHR047C	15	A	10		YKO_0815	A10	0.94	+	+	+	
1875	YHR048W	15	A	11		YKO_0815	A11	0.857	+	+	+	
1876	YHR049W	15	A	12		YKO_0815	A12	0.829	+	+	-	HIT
1877	YHR049C-A	15	B	1		YKO_0815	B01	0.896	+	+	+	
1878	YHR050W	15	B	2		YKO_0815	B02	0.776	+	+	+	
--		15	B	3	empty	YKO_0815	B03	empty	empty	empty	empty	empty
1879	YHR051W	15	B	4	APPEARS TO BE ALPHA	YKO_0815	B04	0.892	slow	+	-	Doubt
1885	YHR057C	15	B	5		YKO_0815	B05	0.938	+	+	+	
1888	YHR060W	15	B	6		YKO_0815	B06	0.971	-	-	-	Doubt
1889	YHR061C	15	B	7		YKO_0815	B07	0.899	+	+	+	
1894	YHR066W	15	B	8		YKO_0815	B08	0.86	+	+	+	
1901	YHR073W	15	B	9		YKO_0815	B09	0.622	+	+	+	
1903	YHR075C	15	B	10		YKO_0815	B10	0.832	+	+	+	
1904	YHR076W	15	B	11		YKO_0815	B11	0.897	+	+	+	
1905	YHR077C	15	B	12		YKO_0815	B12	0.708	+	+	-	HIT
1906	YHR078W	15	C	1		YKO_0815	C01	0.905	+	+	+	
1907	YHR079C	15	C	2		YKO_0815	C02	0.836	+	+	+	
1908	YHR080C	15	C	3		YKO_0815	C03	1.019	+	+	+	
1909	YHR081W	15	C	4		YKO_0815	C04	0.883	+	+	+	
1910	YHR082C	15	C	5		YKO_0815	C05	0.974	+	+	+	
1914	YHR086W	15	C	6		YKO_0815	C06	0.98	+	+	+	
1915	YHR087W	15	C	7		YKO_0815	C07	0.852	+	+	+	
1919	YHR091C	15	C	8		YKO_0815	C08	0.873	-	+	-	Doubt
1920	YHR092C	15	C	9		YKO_0815	C09	0.956	+	+	+	
1921	YHR093W	15	C	10		YKO_0815	C10	0.855	+	+	+	
1922	YHR094C	15	C	11		YKO_0815	C11	0.809	+	+	+	
1923	YHR095W	15	C	12		YKO_0815	C12	0.765	+	+	+	
1924	YHR096C	15	D	1		YKO_0815	D01	0.966	+	+	+	
1925	YHR097C	15	D	2		YKO_0815	D02	1.006	+	+	+	
1928	YHR100C	15	D	3		YKO_0815	D03	0.878	+	+	+	
1931	YHR103W	15	D	4		YKO_0815	D04	1.014	+	+	+	
1932	YHR104W	15	D	5		YKO_0815	D05	0.91	+	-	+	Incongruence
1933	YHR105W	15	D	6		YKO_0815	D06	0.892	+	+	+	
1934	YHR106W	15	D	7		YKO_0815	D07	0.951	+	+	+	
1936	YHR108W	15	D	8		YKO_0815	D08	0.867	+	+	+	
1937	YHR109W	15	D	9		YKO_0815	D09	0.871	+	+	+	
1938	YHR110W	15	D	10		YKO_0815	D10	0.898	+	+	+	
1939	YHR111W	15	D	11		YKO_0815	D11	0.631	+	+	+	
1940	YHR112C	15	D	12		YKO_0815	D12	0.826	+	+	+	
1941	YHR113W	15	E	1		YKO_0815	E01	0.985	+	+	+	
1942	YHR114W	15	E	2		YKO_0815	E02	1.001	+	+	+	
1943	YHR115C	15	E	3		YKO_0815	E03	0.907	+	+	+	
1944	YHR116W	15	E	4		YKO_0815	E04	0.999	slow	+	-	Doubt
1945	YHR117W	15	E	5		YKO_0815	E05	0.955	+	+	+	
1948	YHR120W	15	E	6		YKO_0815	E06	0.872	-	+	-	Doubt
1949	YHR121W	15	E	7		YKO_0815	E07	0.901	+	+	+	
1951	YHR123W	15	E	8		YKO_0815	E08	0.88	+	+	+	
1952	YHR124W	15	E	9		YKO_0815	E09	0.563	+	+	+	
1953	YHR125W	15	E	10		YKO_0815	E10	0.777	+	+	+	
1954	YHR126C	15	E	11		YKO_0815	E11	0.785	+	+	+	
1957	YHR129C	15	E	12		YKO_0815	E12	0.655	+	+	+	
1958	YHR130C	15	F	1		YKO_0815	F01	0.967	+	+	+	
1960	YHR132C	15	F	2		YKO_0815	F02	1.058	+	+	+	
1961	YHR133C	15	F	3		YKO_0815	F03	0.944	+	+	+	
1962	YHR134W	15	F	4		YKO_0815	F04	0.692	+	+	+	
1963	YHR135C	15	F	5		YKO_0815	F05	0.991	+	+	+	
1964	YHR136C	15	F	6		YKO_0815	F06	0.854	+	+	+	
1965	YHR137W	15	F	7		YKO_0815	F07	0.926	+	+	+	
1966	YHR138C	15	F	8		YKO_0815	F08	0.814	+	+	+	
1967	YHR139C	15	F	9		YKO_0815	F09	0.914	+	+	+	
1968	YHR139C-A	15	F	10		YKO_0815	F10	0.822	+	+	+	
2835	YHR142W	15	F	11		YKO_0815	F11	0.847	+	+	+	
2836	YHR143W	15	F	12		YKO_0815	F12	0.706	+	+	+	
2841	YHR147C	15	G	1		YKO_0815	G01	0.988	slow	+	-	Doubt
2844	YHR150W	15	G	2		YKO_0815	G02	0.986	+	+	+	
2845	YHR151C	15	G	3		YKO_0815	G03	0.933	+	+	+	
2846	YHR152W	15	G	4		YKO_0815	G04	0.978	+	+	+	
2847	YHR153C	15	G	5		YKO_0815	G05	0.972	+	+	+	
2848	YHR154W	15	G	6		YKO_0815	G06	0.775	+	+	+	
2849	YHR155W	15	G	7		YKO_0815	G07	0.832	+	+	+	
2850	YHR156C	15	G	8		YKO_0815	G08	0.866	+	+	+	
2851	YHR157W	15	G	9		YKO_0815	G09	0.805	+	+	+	
2852	YHR158C	15	G	10		YKO_0815	G10	0.66	+	+	+	

	Euroscarf Information					Replica plate Information			Tau Toxicity Enhancer Primary Screen Results			
record no.	ORF name	Plate	Row	Col	Comment	Replica plate	Well	YPD (OD600nm)	Growth plate (SC+GAL comp.)	Transformation control plate (SC+GLU-Leu)	TEST Plate (SC+GAL-Leu)	Classification
2853	YHR159W	15	G	11		YKO_0815	G11	0.783	+	+	+	
2854	YHR160C	15	G	12		YKO_0815	G12	0.814	+	+	+	
2855	YHR161C	15	H	1		YKO_0815	H01	0.706	+	+	+	
--		15	H	2	empty	YKO_0815	H02	empty	empty	empty	empty	empty
2857	YHR163W	15	H	3		YKO_0815	H03	0.966	+	+	+	
2861	YHR167W	15	H	4		YKO_0815	H04	0.859	+	+	+	
2870	YHR176W	15	H	5		YKO_0815	H05	0.942	+	+	+	
2871	YHR177W	15	H	6	Similar to S. pombe pac2 protein -- growth on -met, super slow growth on -lys, super slow growth on drop in media, mates like alpha	YKO_0815	H06	0.907	+	+	+	
2872	YHR178W	15	H	7		YKO_0815	H07	0.953	+	-	-	Doubt
2873	YHR179W	15	H	8		YKO_0815	H08	0.897	+	+	+	
2876	YHR182W	15	H	9		YKO_0815	H09	0.886	+	+	+	
2877	YHR183W	15	H	10		YKO_0815	H10	0.761	+	+	+	
2878	YHR184W	15	H	11		YKO_0815	H11	0.858	+	+	+	
2883	YHR189W	15	H	12		YKO_0815	H12	0.883	+	+	+	
2889	YHR195W	16	A	1		YKO_0816	A01	0.883	+	+	-	HIT
2892	YHR198C	16	A	2		YKO_0816	A02	0.829	+	+	+	
2893	YHR199C	16	A	3		YKO_0816	A03	0.855	+	+	-	HIT
2894	YHR200W	16	A	4		YKO_0816	A04	0.823	+	+	+	
2896	YHR202W	16	A	5		YKO_0816	A05	0.871	+	+	+	
2897	YHR203C	16	A	6		YKO_0816	A06	0.731	+	+	+	
2898	YHR204W	16	A	7		YKO_0816	A07	0.853	+	+	-	HIT
2900	YHR206W	16	A	8		YKO_0816	A08	0.782	+	+	+	
2901	YHR207C	16	A	9		YKO_0816	A09	0.803	+	+	+	
2903	YHR209W	16	A	10		YKO_0816	A10	0.769	+	+	+	
2904	YHR210C	16	A	11		YKO_0816	A11	0.749	+	+	+	
3409	YCL001W	16	A	12		YKO_0816	A12	0.674	+	+	+	
3410	YCL002C	16	B	1		YKO_0816	B01	0.866	+	+	+	
3413	YCL005W	16	B	2		YKO_0816	B02	0.747	+	+	+	
7121	YMR118C	16	B	3		YKO_0816	B03	0.926	+	+	+	
--		16	B	4	empty	YKO_0816	B04	empty	empty	empty	empty	empty
3416	YCL008C	16	B	5		YKO_0816	B05	0.928	+	+	+	
3417	YCL009C	16	B	6		YKO_0816	B06	0.905	+	+	+	
3418	YCL010C	16	B	7		YKO_0816	B07	0.675	slow	+	-	Doubt
3419	YCL011C	16	B	8		YKO_0816	B08	0.811	+	+	+	
3420	YCL012W	16	B	9		YKO_0816	B09	0.846	+	+	+	
3421	YCL013W	16	B	10		YKO_0816	B10	0.818	+	+	+	
3422	YCL014W	16	B	11		YKO_0816	B11	0.787	+	+	+	
3423	YCL016C	16	B	12		YKO_0816	B12	0.621	+	+	+	
3430	YCL023C	16	C	1		YKO_0816	C01	0.888	+	+	+	
3431	YCL024W	16	C	2		YKO_0816	C02	0.816	+	+	+	
3432	YCL025C	16	C	3		YKO_0816	C03	0.891	+	+	-	HIT
3433	YCL026C	16	C	4		YKO_0816	C04	0.913	+	+	+	
3434	YCL027W	16	C	5		YKO_0816	C05	0.922	+	-	-	Doubt
3435	YCL028W	16	C	6		YKO_0816	C06	0.922	+	+	+	
3436	YCL029C	16	C	7		YKO_0816	C07	0.689	+	+	+	
3437	YCL030C	16	C	8		YKO_0816	C08	0.832	+	+	+	
3439	YCL032W	16	C	9		YKO_0816	C09	0.758	+	+	-	HIT
3440	YCL033C	16	C	10		YKO_0816	C10	0.732	+	+	+	
3441	YCL034W	16	C	11		YKO_0816	C11	0.746	+	+	+	
3443	YCL036W	16	C	12		YKO_0816	C12	0.722	+	+	-	HIT
3444	YCL037C	16	D	1		YKO_0816	D01	0.944	+	+	+	
3446	YCL039W	16	D	2		YKO_0816	D02	1.027	+	+	+	
3447	YCL040W	16	D	3		YKO_0816	D03	0.973	+	+	-	HIT
3449	YCL042W	16	D	4		YKO_0816	D04	1.055	+	+	+	
3451	YCL044C	16	D	5		YKO_0816	D05	0.942	+	+	+	
3452	YCL045C	16	D	6		YKO_0816	D06	0.932	+	+	+	
3453	YCL046W	16	D	7		YKO_0816	D07	0.89	+	+	+	
3454	YCL047C	16	D	8		YKO_0816	D08	0.811	+	+	+	
3455	YCL048W	16	D	9		YKO_0816	D09	0.779	+	+	+	
3456	YCL049C	16	D	10		YKO_0816	D10	0.901	+	+	+	
3457	YCL050C	16	D	11		YKO_0816	D11	0.778	+	+	-	HIT
3458	YCL051W	16	D	12		YKO_0816	D12	0.648	+	+	-	HIT
3462	YCL055W	16	E	1		YKO_0816	E01	0.979	+	+	+	
3463	YCL056C	16	E	2		YKO_0816	E02	1.025	+	+	+	
3464	YCL057W	16	E	3		YKO_0816	E03	0.964	+	+	+	
3467	YCL060C	16	E	4		YKO_0816	E04	0.777	+	+	+	
3468	YCL061C	16	E	5		YKO_0816	E05	0.879	+	+	+	
3469	YCL062W	16	E	6		YKO_0816	E06	0.899	+	+	+	
3470	YCL063W	16	E	7		YKO_0816	E07	0.721	+	+	+	
3471	YCL064C	16	E	8		YKO_0816	E08	0.888	+	+	+	
3476	YCL069W	16	E	9		YKO_0816	E09	0.802	+	+	+	
3481	YCR001W	16	E	10		YKO_0816	E10	0.727	+	+	+	
3482	YCR002C	16	E	11		YKO_0816	E11	0.729	+	+	+	
3483	YCR003W	16	E	12		YKO_0816	E12	0.612	slow	+	-	Doubt
3484	YCR004C	16	F	1		YKO_0816	F01	0.835	slow	+	-	Doubt
3485	YCR005C	16	F	2		YKO_0816	F02	0.988	+	+	+	
3486	YCR006C	16	F	3		YKO_0816	F03	0.974	+	+	+	
3487	YCR007C	16	F	4		YKO_0816	F04	0.962	+	+	+	
3488	YCR008W	16	F	5		YKO_0816	F05	0.703	+	+	+	

	Euroscarf Information					Replica plate Information			Tau Toxicity Enhancer Primary Screen Results			
record no.	ORF name	Plate	Row	Col	Comment	Replica plate	Well	YPD (OD600nm)	Growth plate (SC+GAL comp.)	Transformation control plate (SC+GLU-Leu)	TEST Plate (SC+GAL-Leu)	Classification
3489	YCR009C	16	F	6		YKO_0816	F06	0.562	slow	+	-	Doubt
3490	YCR010C	16	F	7		YKO_0816	F07	0.773	+	+	+	
3491	YCR011C	16	F	8		YKO_0816	F08	0.84	+	+	+	
3494	YCR014C	16	F	9		YKO_0816	F09	0.814	+	+	+	
3495	YCR015C	16	F	10		YKO_0816	F10	0.706	+	+	+	
3496	YCR016W	16	F	11		YKO_0816	F11	0.747	+	+	-	HIT
3497	YCR017C	16	F	12		YKO_0816	F12	0.588	+	+	+	
3499	YCR019W	16	G	1		YKO_0816	G01	1.002	+	+	+	
3500	YCR020C	16	G	2		YKO_0816	G02	0.973	+	+	+	
3501	YCR020C-A	16	G	3		YKO_0816	G03	0.943	+	+	+	
3502	YCR021C	16	G	4		YKO_0816	G04	0.891	+	+	+	
3503	YCR022C	16	G	5		YKO_0816	G05	0.811	+	+	+	
3504	YCR023C	16	G	6		YKO_0816	G06	0.929	+	+	+	
4081	YLR420W	16	G	7		YKO_0816	G07	0.878	+	+	+	
4082	YLR451W	16	G	8		YKO_0816	G08	0.734	+	+	+	
4083	YLR126C	16	G	9		YKO_0816	G09	0.764	+	+	+	
4085	YLR128W	16	G	10		YKO_0816	G10	0.757	+	+	+	
4087	YLR130C	16	G	11		YKO_0816	G11	0.824	+	+	+	
4088	YLR131C	16	G	12		YKO_0816	G12	0.491	+	+	+	
4090	YLR133W	16	H	1		YKO_0816	H01	0.892	+	+	+	
--		16	H	2	empty	YKO_0816	H02	empty	empty	empty	empty	empty
4091	YLR134W	16	H	3		YKO_0816	H03	0.921	+	+	+	
4092	YLR135W	16	H	4		YKO_0816	H04	0.871	+	+	+	
4093	YLR136C	16	H	5		YKO_0816	H05	0.959	+	+	+	
4094	YLR137W	16	H	6		YKO_0816	H06	0.881	+	+	+	
4095	YLR138W	16	H	7		YKO_0816	H07	0.739	+	+	+	
4096	YLR139C	16	H	8		YKO_0816	H08	0.645	slow	+	-	Doubt
4099	YLR142W	16	H	9		YKO_0816	H09	0.82	+	+	+	
4100	YLR143W	16	H	10		YKO_0816	H10	0.739	+	-	+	Incongruence
4101	YLR144C	16	H	11		YKO_0816	H11	0.705	+	+	-	HIT
7118	YMR074C	16	H	12		YKO_0816	H12	0.7	+	+	+	
4106	YLR149C	17	A	1		YKO_0817	A01	0.871	+	+	+	
4107	YLR150W	17	A	2		YKO_0817	A02	0.878	+	+	-	HIT
4108	YLR151C	17	A	3		YKO_0817	A03	0.906	+	+	+	
4109	YLR152C	17	A	4		YKO_0817	A04	0.903	+	+	+	
4111	YLR154C	17	A	5		YKO_0817	A05	0.915	+	+	+	
4113	YLR164W	17	A	6		YKO_0817	A06	0.919	+	+	+	
4114	YLR165C	17	A	7		YKO_0817	A07	0.934	+	+	+	
4117	YLR168C	17	A	8		YKO_0817	A08	0.837	+	+	+	
4118	YLR169W	17	A	9		YKO_0817	A09	0.897	+	+	+	
4119	YLR170C	17	A	10		YKO_0817	A10	0.915	+	+	+	
4120	YLR171W	17	A	11		YKO_0817	A11	0.857	+	+	+	
4121	YLR172C	17	A	12		YKO_0817	A12	0.862	+	+	-	HIT
4122	YLR173W	17	B	1		YKO_0817	B01	0.867	+	+	+	
4123	YLR174W	17	B	2		YKO_0817	B02	0.948	+	+	+	
4125	YLR176C	17	B	3		YKO_0817	B03	0.985	+	+	+	
4126	YLR177W	17	B	4		YKO_0817	B04	0.606	+	+	+	
--		17	B	5	empty	YKO_0817	B05	empty	empty	empty	empty	empty
4127	YLR178C	17	B	6		YKO_0817	B06	0.951	+	+	+	
4128	YLR179C	17	B	7		YKO_0817	B07	0.907	+	+	+	
4129	YLR180W	17	B	8		YKO_0817	B08	0.812	+	+	+	
4130	YLR181C	17	B	9		YKO_0817	B09	0.92	+	+	+	
4131	YLR182W	17	B	10		YKO_0817	B10	0.764	+	+	+	
4132	YLR183C	17	B	11		YKO_0817	B11	0.685	slow	+	+	
4133	YLR184W	17	B	12		YKO_0817	B12	0.895	slow	+	+	
4134	YLR185W	17	C	1		YKO_0817	C01	0.863	+	+	+	
4136	YLR187W	17	C	2		YKO_0817	C02	0.947	+	+	+	
4137	YLR188W	17	C	3		YKO_0817	C03	0.905	+	+	+	
4138	YLR189C	17	C	4		YKO_0817	C04	0.945	+	+	+	
4139	YLR190W	17	C	5		YKO_0817	C05	0.85	+	+	+	
4140	YLR191W	17	C	6		YKO_0817	C06	0.786	+	+	+	
4142	YLR193C	17	C	7		YKO_0817	C07	1.035	+	+	+	
4143	YLR194C	17	C	8		YKO_0817	C08	0.972	+	+	+	
4148	YLR199C	17	C	9		YKO_0817	C09	0.946	+	-	+	Incongruence
4149	YLR200W	17	C	10		YKO_0817	C10	0.785	+	+	-	HIT
4150	YLR201C	17	C	11		YKO_0817	C11	0.769	+	+	-	HIT
4151	YLR202C	17	C	12		YKO_0817	C12	0.881	slow	+	-	Doubt
4152	YLR203C	17	D	1		YKO_0817	D01	0.975	slow	+	-	Doubt
4153	YLR204W	17	D	2		YKO_0817	D02	0.815	slow	+	-	Doubt
4154	YLR205C	17	D	3		YKO_0817	D03	0.967	+	+	+	
4155	YLR206W	17	D	4		YKO_0817	D04	0.929	+	+	+	
4156	YLR207W	17	D	5		YKO_0817	D05	0.799	+	+	+	
4158	YLR209C	17	D	6		YKO_0817	D06	0.916	+	+	+	
4159	YLR210W	17	D	7		YKO_0817	D07	0.94	+	+	+	
4160	YLR211C	17	D	8		YKO_0817	D08	0.964	+	+	+	
4162	YLR213C	17	D	9		YKO_0817	D09	0.905	+	+	+	
4163	YLR214W	17	D	10		YKO_0817	D10	0.948	+	+	+	
4165	YLR216C	17	D	11		YKO_0817	D11	1.003	+	+	+	
4166	YLR217W	17	D	12		YKO_0817	D12	0.956	+	+	+	
4167	YLR218C	17	E	1		YKO_0817	E01	0.927	+	+	+	
4168	YLR219W	17	E	2		YKO_0817	E02	0.98	+	+	+	
4169	YLR220W	17	E	3		YKO_0817	E03	0.739	+	+	+	
4170	YLR221C	17	E	4		YKO_0817	E04	0.923	+	+	-	HIT
4173	YLR224W	17	E	5		YKO_0817	E05	0.944	+	+	+	

	Euroscarf Information					Replica plate Information			Tau Toxicity Enhancer Primary Screen Results			
record no.	ORF name	Plate	Row	Col	Comment	Replica plate	Well	YPD (OD600nm)	Growth plate (SC+GAL comp.)	Transformation control plate (SC+GLU-Leu)	TEST Plate (SC+GAL-Leu)	Classification
4174	YLR225C	17	E	6		YKO_0817	E06	0.997	+	+	+	
4176	YLR227C	17	E	7		YKO_0817	E07	0.958	+	+	+	
4849	YKL001C	17	E	8		YKO_0817	E08	0.988	+	+	+	
4850	YKL002W	17	E	9		YKO_0817	E09	0.676	slow	+	+	
4851	YKL003C	17	E	10		YKO_0817	E10	0.858	-	+	-	Doubt
4855	YKL006W	17	E	11		YKO_0817	E11	0.88	+	+	+	
4856	YKL007W	17	E	12		YKO_0817	E12	0.839	+	+	+	
4857	YKL008C	17	F	1		YKO_0817	F01	0.745	+	+	+	
4858	YKL009W	17	F	2		YKO_0817	F02	0.347	slow	+	+	
4859	YKL010C	17	F	3		YKO_0817	F03	0.961	+	+	+	
4860	YKL011C	17	F	4		YKO_0817	F04	0.945	+	+	+	
4864	YKL015W	17	F	5		YKO_0817	F05	0.895	+	+	+	
4865	YKL016C	17	F	6		YKO_0817	F06	0.857	-	+	-	Doubt
4866	YKL017C	17	F	7		YKO_0817	F07	0.893	+	+	+	
4869	YKL020C	17	F	8		YKO_0817	F08	0.951	+	+	+	
4872	YKL023W	17	F	9		YKO_0817	F09	0.891	+	+	+	
4874	YKL025C	17	F	10		YKO_0817	F10	0.973	+	+	+	
4875	YKL026C	17	F	11		YKO_0817	F11	0.959	+	+	+	
4876	YKL027W	17	F	12		YKO_0817	F12	0.888	+	-	-	Doubt
4878	YKL029C	17	G	1		YKO_0817	G01	0.929	+	-	+	Incongruence
4880	YKL031W	17	G	2		YKO_0817	G02	0.87	+	+	+	
4881	YKL032C	17	G	3		YKO_0817	G03	0.9	+	+	+	
4883	YKL034W	17	G	4		YKO_0817	G04	0.949	+	+	+	
4886	YKL037W	17	G	5		YKO_0817	G05	0.89	+	-	-	Doubt
4887	YKL038W	17	G	6		YKO_0817	G06	0.918	+	+	+	
4888	YKL039W	17	G	7		YKO_0817	G07	0.97	+	-	+	Incongruence
4889	YKL040C	17	G	8		YKO_0817	G08	0.945	+	+	+	
4890	YKL041W	17	G	9		YKO_0817	G09	0.909	+	+	+	
4892	YKL043W	17	G	10		YKO_0817	G10	0.901	+	+	+	
4893	YKL044W	17	G	11		YKO_0817	G11	0.952	+	+	+	
4895	YKL046C	17	G	12		YKO_0817	G12	0.973	+	+	+	
4896	YKL047W	17	H	1		YKO_0817	H01	0.958	+	+	+	
--		17	H	2	empty	YKO_0817	H02	empty	empty	empty	empty	empty
4897	YKL048C	17	H	3		YKO_0817	H03	1.062	+	+	+	
4899	YKL050C	17	H	4		YKO_0817	H04	0.858	+	+	+	
4900	YKL051W	17	H	5		YKO_0817	H05	0.638	+	+	-	HIT
4902	YKL053W	17	H	6		YKO_0817	H06	0.717	+	+	+	
4903	YKL054C	17	H	7		YKO_0817	H07	0.452	+	+	+	
4904	YKL055C	17	H	8		YKO_0817	H08	0.859	+	+	+	
4905	YKL056C	17	H	9		YKO_0817	H09	0.979	+	+	+	
4906	YKL057C	17	H	10		YKO_0817	H10	0.676	+	+	+	
4910	YKL061W	17	H	11		YKO_0817	H11	0.93	+	+	+	
4911	YKL062W	17	H	12		YKO_0817	H12	0.927	+	-	-	Doubt
4912	YKL063C	18	A	1		YKO_0818	A01	1.1446	+	+	+	
4913	YKL064W	18	A	2		YKO_0818	A02	0.9587	+	+	+	
4914	YKL065C	18	A	3		YKO_0818	A03	0.6845	+	+	+	
4915	YKL066W	18	A	4		YKO_0818	A04	1.1021	+	+	+	
4916	YKL067W	18	A	5		YKO_0818	A05	1.0887	+	+	+	
4917	YKL068W	18	A	6		YKO_0818	A06	1.0194	+	+	+	
4918	YKL069W	18	A	7		YKO_0818	A07	0.6958	+	+	+	
4919	YKL070W	18	A	8		YKO_0818	A08	1.191	+	+	+	
4920	YKL071W	18	A	9		YKO_0818	A09	1.1824	+	+	+	
4921	YKL072W	18	A	10		YKO_0818	A10	0.714	+	+	+	
4922	YKL073W	18	A	11		YKO_0818	A11	0.6741	+	+	+	
4923	YKL074C	18	A	12		YKO_0818	A12	0.7412	+	+	+	
4924	YKL075C	18	B	1		YKO_0818	B01	0.6384	+	+	+	
4925	YKL076C	18	B	2		YKO_0818	B02	1.0773	+	+	+	
4926	YKL077W	18	B	3		YKO_0818	B03	0.7226	+	+	+	
4928	YKL079W	18	B	4		YKO_0818	B04	1.1313	+	+	+	
4929	YKL080W	18	B	5		YKO_0818	B05	not grow n	-	-	-	Not grow n
--		18	B	6	empty	YKO_0818	B06	empty	empty	empty	empty	empty
4930	YKL081W	18	B	7		YKO_0818	B07	0.7358	+	+	+	
4933	YKL084W	18	B	8		YKO_0818	B08	1.1291	+	+	+	
4934	YKL085W	18	B	9		YKO_0818	B09	1.0643	+	+	+	
4935	YKL086W	18	B	10		YKO_0818	B10	1.0458	+	+	+	
4936	YKL087C	18	B	11		YKO_0818	B11	0.5262	slow	+	-	Doubt
4939	YKL090W	18	B	12		YKO_0818	B12	1.0087	+	+	+	
4940	YKL091C	18	C	1		YKO_0818	C01	0.6956	+	+	+	
4941	YKL092C	18	C	2		YKO_0818	C02	1.0252	+	+	+	
4942	YKL093W	18	C	3		YKO_0818	C03	0.691	+	+	+	
4943	YKL094W	18	C	4		YKO_0818	C04	1.1334	+	+	+	
4945	YKL096W	18	C	5		YKO_0818	C05	1.1094	+	+	+	
4946	YKL097C	18	C	6		YKO_0818	C06	1.1181	+	+	+	
4948	YKL098W	18	C	7		YKO_0818	C07	1.0132	+	+	+	
4950	YKL100C	18	C	8		YKO_0818	C08	1.1016	+	+	+	
4951	YKL101W	18	C	9		YKO_0818	C09	1.0871	+	+	+	
4952	YKL102C	18	C	10		YKO_0818	C10	0.724	+	+	+	
4953	YKL103C	18	C	11		YKO_0818	C11	1.0776	+	+	+	
4955	YKL105C	18	C	12		YKO_0818	C12	0.7395	+	+	+	
4956	YKL106W	18	D	1		YKO_0818	D01	0.7124	+	+	+	
4957	YKL107W	18	D	2		YKO_0818	D02	1.0512	+	+	+	
4959	YKL109W	18	D	3		YKO_0818	D03	1.0915	slow	+	-	Doubt
4960	YKL110C	18	D	4		YKO_0818	D04	1.1397	+	+	+	
4963	YKL113C	18	D	5		YKO_0818	D05	0.7647	+	+	+	

Euroscarf Information						Replica plate Information			Tau Toxicity Enhancer Primary Screen Results			
record no.	ORF name	Plate	Row	Col	Comment	Replica plate	Well	YPD (OD600nm)	Growth plate (SC+GAL comp.)	Transformation control plate (SC+GLU-Leu)	TEST Plate (SC+GAL-Leu)	Classification
4964	YKL114C	18	D	6		YKO_0818	D06	1.0427	+	+	+	
4966	YKL116C	18	D	7		YKO_0818	D07	0.7308	+	+	+	
4967	YKL117W	18	D	8		YKO_0818	D08	1.0823	+	+	+	
4968	YKL118W	18	D	9		YKO_0818	D09	1.1792	-	+	-	Doubt
4969	YKL119C	18	D	10		YKO_0818	D10	1.0909	-	-	-	Doubt
4970	YKL120W	18	D	11		YKO_0818	D11	1.0732	+	+	+	
4971	YKL121W	18	D	12		YKO_0818	D12	1.0773	+	+	+	
4973	YKL123W	18	E	1		YKO_0818	E01	1.0924	+	+	+	
4974	YKL124W	18	E	2		YKO_0818	E02	1.0444	+	+	+	
4976	YKL126W	18	E	3		YKO_0818	E03	1.0027	+	+	+	
4977	YKL127W	18	E	4		YKO_0818	E04	0.7079	+	+	+	
4978	YKL128C	18	E	5		YKO_0818	E05	1.0437	+	+	+	
4979	YKL129C	18	E	6		YKO_0818	E06	1.1373	+	+	+	
4980	YKL130C	18	E	7		YKO_0818	E07	1.0501	+	+	+	
4981	YKL131W	18	E	8		YKO_0818	E08	1.0792	+	+	+	
4982	YKL132C	18	E	9		YKO_0818	E09	1.1119	+	+	+	
4983	YKL133C	18	E	10		YKO_0818	E10	0.9094	+	+	+	
4984	YKL134C	18	E	11		YKO_0818	E11	0.7037	-	+	-	Doubt
4985	YKL135C	18	E	12	AP! complex subunit B 1 adaptin -- growth on -met, super slow growth on -lys, super slow growth on drop in media, mates like alpha. Confirmed Alpha -- CORRECT STRAIN CAN BE FOUND IN PLATE 121 F8	YKO_0818	E12	0.7273	+	+	+	
4986	YKL136W	18	F	1		YKO_0818	F01	0.6913	+	+	+	
4987	YKL137W	18	F	2		YKO_0818	F02	1.117	+	+	+	
4988	YKL138C	18	F	3		YKO_0818	F03	0.8264	+	+	+	
4990	YKL140W	18	F	4		YKO_0818	F04	1.1315	+	+	+	
4992	YKL142W	18	F	5		YKO_0818	F05	0.945	+	+	+	
4993	YKL143W	18	F	6		YKO_0818	F06	0.936	slow	+	+	
4996	YKL146W	18	F	7		YKO_0818	F07	0.7023	+	+	+	
4997	YKL147C	18	F	8		YKO_0818	F08	1.0943	+	+	+	
4998	YKL148C	18	F	9		YKO_0818	F09	1.0951	slow	+	+	
4999	YKL149C	18	F	10		YKO_0818	F10	1.0247	+	+	+	
5000	YKL150W	18	F	11		YKO_0818	F11	1.1341	+	+	+	
5001	YKL151C	18	F	12		YKO_0818	F12	1.0965	+	+	+	
7407	YPR151C	18	G	1		YKO_0818	G01	0.7059	+	+	+	
5006	YKL156W	18	G	2		YKO_0818	G02	1.1237	+	+	+	
5007	YKL157W	18	G	3		YKO_0818	G03	0.7365	+	+	+	
5008	YKL158W	18	G	4		YKO_0818	G04	0.7236	+	+	+	
5009	YKL159C	18	G	5		YKO_0818	G05	0.9936	+	+	+	
5010	YKL160W	18	G	6		YKO_0818	G06	1.1373	+	+	+	
5011	YKL161C	18	G	7		YKO_0818	G07	1.1429	+	+	+	
5012	YKL162C	18	G	8		YKO_0818	G08	1.1517	+	+	+	
5013	YKL163W	18	G	9		YKO_0818	G09	1.1189	+	+	+	
5014	YKL164C	18	G	10		YKO_0818	G10	0.7364	+	+	+	
5016	YKL166C	18	G	11		YKO_0818	G11	1.1245	+	+	+	
5017	YKL167C	18	G	12		YKO_0818	G12	1.1508	+	+	-	HIT
5018	YKL168C	18	H	1		YKO_0818	H01	0.6799	+	+	+	
--		18	H	1	empty	YKO_0818	H02	empty	empty	empty	empty	empty
5019	YKL169C	18	H	3		YKO_0818	H03	1.1459	slow	+	-	Doubt
5020	YKL170W	18	H	4		YKO_0818	H04	0.9174	slow	+	-	Doubt
5021	YKL171W	18	H	5		YKO_0818	H05	0.8905	+	-	+	Incongruence
5024	YKL174C	18	H	6		YKO_0818	H06	1.1146	+	+	+	
5025	YKL175W	18	H	7		YKO_0818	H07	0.6374	+	+	+	
5026	YKL176C	18	H	8		YKO_0818	H08	1.1792	+	+	+	
5027	YKL177W	18	H	9		YKO_0818	H09	1.1521	+	+	+	
5028	YKL178C	18	H	10		YKO_0818	H10	0.6484	+	+	+	
5029	YKL179C	18	H	11		YKO_0818	H11	1.0765	+	+	+	
5033	YKL183W	18	H	12		YKO_0818	H12	1.1539	+	+	+	
5034	YKL184W	19	A	1		YKO_0819	A01	1.1468	+	+	+	
5035	YKL185W	19	A	2		YKO_0819	A02	1.1094	+	+	+	
5037	YKL187C	19	A	3		YKO_0819	A03	1.016	+	+	+	
5038	YKL188C	19	A	4		YKO_0819	A04	1.0153	+	+	+	
5040	YKL190W	19	A	5		YKO_0819	A05	0.7094	+	+	+	
4657	YGR027C	19	A	6		YKO_0819	A06	1.1042	+	+	+	
4661	YGR031W	19	A	7		YKO_0819	A07	1.0818	+	+	+	
4663	YGR033C	19	A	8		YKO_0819	A08	0.669	+	+	+	
4664	YGR034W	19	A	9		YKO_0819	A09	1.0826	+	+	+	
4665	YGR035C	19	A	10		YKO_0819	A10	0.6513	+	+	+	
4666	YGR036C	19	A	11		YKO_0819	A11	1.1672	+	-	-	Doubt
4667	YGR037C	19	A	12		YKO_0819	A12	0.6732	+	+	+	
4669	YGR039W	19	B	1		YKO_0819	B01	1.0942	+	+	+	
4671	YGR041W	19	B	2		YKO_0819	B02	0.7778	+	+	+	
4672	YGR042W	19	B	3		YKO_0819	B03	0.7751	+	+	-	HIT
4673	YGR043C	19	B	4		YKO_0819	B04	1.0603	+	+	+	
4674	YGR044C	19	B	5		YKO_0819	B05	0.7333	+	+	+	
4675	YGR045C	19	B	6		YKO_0819	B06	1.0703	+	+	+	
--		19	B	7	empty	YKO_0819	B07	empty	empty	empty	empty	empty
4679	YGR049W	19	B	8		YKO_0819	B08	0.7865	+	+	+	
4681	YGR051C	19	B	9		YKO_0819	B09	1.0632	+	+	+	
4682	YGR052W	19	B	10		YKO_0819	B10	0.7768	+	+	+	

	Euroscarf Information					Replica plate Information			Tau Toxicity Enhancer Primary Screen Results			
record no.	ORF name	Plate	Row	Col	Comment	Replica plate	Well	YPD (OD600nm)	Growth plate (SC+GAL comp.)	Transformation control plate (SC+GLU-Leu)	TEST Plate (SC+GAL-Leu)	Classification
4684	YGR054W	19	B	11		YKO_0819	B11	1.0721	+	+	+	
4685	YGR055W	19	B	12		YKO_0819	B12	1.051	+	+	+	
4686	YGR056W	19	C	1		YKO_0819	C01	0.9424	+	+	+	
4687	YGR057C	19	C	2		YKO_0819	C02	1.0625	+	+	+	
4688	YGR058W	19	C	3		YKO_0819	C03	0.9987	+	+	+	
4689	YGR059W	19	C	4		YKO_0819	C04	1.0649	+	+	+	
4691	YGR061C	19	C	5		YKO_0819	C05	0.7369	slow	+	+	
4692	YGR062C	19	C	6		YKO_0819	C06	1.0551	slow	+	-	Doubt
4694	YGR064W	19	C	7		YKO_0819	C07	not grow n	-	-	-	Not grow n
4696	YGR066C	19	C	8		YKO_0819	C08	0.7776	+	+	+	
4697	YGR067C	19	C	9		YKO_0819	C09	0.7885	+	+	+	
4698	YGR068C	19	C	10		YKO_0819	C10	0.7813	+	+	+	
4699	YGR069W	19	C	11		YKO_0819	C11	1.0412	+	+	+	
4700	YGR070W	19	C	12		YKO_0819	C12	1.0939	+	+	-	HIT
4701	YGR071C	19	D	1		YKO_0819	D01	0.9647	+	+	+	
4702	YGR072W	19	D	2		YKO_0819	D02	0.7747	+	+	+	
4706	YGR076C	19	D	3		YKO_0819	D03	0.7452	+	+	-	HIT
4707	YGR077C	19	D	4		YKO_0819	D04	1.0497	+	+	+	
4708	YGR078C	19	D	5		YKO_0819	D05	0.7443	+	+	+	
4709	YGR079W	19	D	6		YKO_0819	D06	1.0844	+	-	+	Incongruence
4710	YGR080W	19	D	7		YKO_0819	D07	1.0359	+	+	+	
4711	YGR081C	19	D	8		YKO_0819	D08	0.7471	+	+	+	
4714	YGR084C	19	D	9		YKO_0819	D09	1.0392	+	+	-	HIT
4715	YGR085C	19	D	10		YKO_0819	D10	0.7427	+	+	+	
4717	YGR087C	19	D	11		YKO_0819	D11	1.1247	+	+	+	
4718	YGR088W	19	D	12		YKO_0819	D12	1.0764	+	-	+	Incongruence
4726	YGR096W	19	E	1		YKO_0819	E01	0.9909	+	+	+	
4727	YGR097W	19	E	2		YKO_0819	E02	1.0942	+	+	+	
4730	YGR100W	19	E	3		YKO_0819	E03	0.7666	+	+	+	
4731	YGR101W	19	E	4		YKO_0819	E04	0.6753	slow	+	-	Doubt
4732	YGR102C	19	E	5		YKO_0819	E05	0.7658	+	+	-	HIT
4734	YGR104C	19	E	6		YKO_0819	E06	not grow n	-	-	-	Not grow n
4735	YGR105W	19	E	7		YKO_0819	E07	1.1257	slow	+	+	
4737	YGR107W	19	E	8		YKO_0819	E08	0.7537	+	+	+	
4738	YGR108W	19	E	9		YKO_0819	E09	1.1246	+	+	+	
4739	YGR109C	19	E	10		YKO_0819	E10	0.7892	+	+	+	
4741	YGR111W	19	E	11		YKO_0819	E11	1.0817	+	+	+	
4742	YGR112W	19	E	12		YKO_0819	E12	0.7037	slow	+	-	Doubt
4748	YGR118W	19	F	1		YKO_0819	F01	0.7473	+	+	+	
4751	YGR121C	19	F	2		YKO_0819	F02	1.0463	+	+	+	
4752	YGR122W	19	F	3		YKO_0819	F03	0.85	+	+	+	
2353	YOR097C	19	F	4		YKO_0819	F04	1.0864	+	+	+	
2355	YOR099W	19	F	5		YKO_0819	F05	0.7833	+	+	+	
2356	YOR100C	19	F	6		YKO_0819	F06	1.073	+	+	+	
2357	YOR101W	19	F	7		YKO_0819	F07	1.0918	+	+	+	
2360	YOR104W	19	F	8		YKO_0819	F08	0.7646	+	+	+	
2361	YOR105W	19	F	9		YKO_0819	F09	0.9125	+	+	+	
2362	YOR106W	19	F	10		YKO_0819	F10	not grow n	-	-	-	Not grow n
2363	YOR107W	19	F	11		YKO_0819	F11	1.0914	+	+	+	
2364	YOR108W	19	F	12		YKO_0819	F12	1.1203	+	-	+	Incongruence
2365	YOR109W	19	G	1		YKO_0819	G01	0.7303	+	+	+	
2367	YOR111W	19	G	2		YKO_0819	G02	1.0531	+	+	+	
2368	YOR112W	19	G	3		YKO_0819	G03	1.0808	+	+	+	
2369	YOR113W	19	G	4		YKO_0819	G04	1.1306	+	+	+	
2370	YOR114W	19	G	5		YKO_0819	G05	0.7957	+	+	+	
2371	YOR115C	19	G	6		YKO_0819	G06	1.0758	+	+	+	
2374	YOR118W	19	G	7		YKO_0819	G07	1.0871	+	+	+	
2376	YOR120W	19	G	8		YKO_0819	G08	0.7976	+	-	-	Doubt
2377	YOR121C	19	G	9		YKO_0819	G09	1.1293	+	+	+	
2379	YOR123C	19	G	10		YKO_0819	G10	0.755	+	+	+	
2380	YOR124C	19	G	11		YKO_0819	G11	1.0868	+	-	+	Incongruence
2381	YOR125C	19	G	12		YKO_0819	G12	0.6032	slow	-	-	Doubt
2382	YOR126C	19	H	1		YKO_0819	H01	1.1253	+	+	+	
--		19	H	2	empty	YKO_0819	H02	empty	empty	empty	empty	empty
2383	YOR127W	19	H	3		YKO_0819	H03	0.6234	+	+	+	
2385	YOR129C	19	H	4		YKO_0819	H04	1.0808	+	+	+	
2386	YOR130C	19	H	5		YKO_0819	H05	1.1704	+	+	+	
2387	YOR131C	19	H	6		YKO_0819	H06	1.1477	+	+	+	
2388	YOR132W	19	H	7		YKO_0819	H07	1.165	+	+	+	
2389	YOR133W	19	H	8		YKO_0819	H08	0.6415	+	+	+	
2390	YOR134W	19	H	9		YKO_0819	H09	0.6078	+	+	+	
2391	YOR135C	19	H	10		YKO_0819	H10	0.5033	+	-	+	Incongruence
2392	YOR136W	19	H	11		YKO_0819	H11	1.078	+	-	-	Doubt
2393	YOR137C	19	H	12		YKO_0819	H12	0.7867	+	+	+	
2394	YOR138C	20	A	1		YKO_0820	A01	0.917	+	+	+	
2395	YOR139C	20	A	2		YKO_0820	A02	0.888	+	+	+	
2396	YOR140W	20	A	3		YKO_0820	A03	0.922	+	+	+	
2397	YOR141C	20	A	4		YKO_0820	A04	0.551	+	+	+	
2398	YOR142W	20	A	5		YKO_0820	A05	0.941	+	+	+	
2400	YOR144C	20	A	6		YKO_0820	A06	0.848	+	+	+	
2408	YOR152C	20	A	7		YKO_0820	A07	0.942	+	+	+	
2409	YOR153W	20	A	8		YKO_0820	A08	0.723	+	+	+	
2410	YOR154W	20	A	9		YKO_0820	A09	0.939	+	+	+	
2411	YOR155C	20	A	10		YKO_0820	A10	0.853	+	+	+	

	Euroscarf Information					Replica plate Information			Tau Toxicity Enhancer Primary Screen Results			
record no.	ORF name	Plate	Row	Col	Comment	Replica plate	Well	YPD (OD600nm)	Growth plate (SC+GAL comp.)	Transformation control plate (SC+GLU-Leu)	TEST Plate (SC+GAL-Leu)	Classification
2412	YOR156C	20	A	11		YKO_0820	A11	0.951	+	+	+	
2417	YOR161C	20	A	12		YKO_0820	A12	0.799	+	+	+	
2418	YOR162C	20	B	1		YKO_0820	B01	0.934	+	+	+	
2419	YOR163W	20	B	2		YKO_0820	B02	0.927	+	+	+	
2420	YOR164C	20	B	3		YKO_0820	B03	0.95	+	+	+	
2421	YOR165W	20	B	4		YKO_0820	B04	0.605	+	+	+	
2422	YOR166C	20	B	5		YKO_0820	B05	0.988	+	+	+	
2423	YOR167C	20	B	6		YKO_0820	B06	0.796	+	+	+	
2426	YOR170W	20	B	7		YKO_0820	B07	0.966	+	+	+	
--		20	B	8	empty	YKO_0820	B08	empty	empty	empty	empty	empty
2427	YOR171C	20	B	9		YKO_0820	B09	0.877	+	+	+	
2428	YOR172W	20	B	10		YKO_0820	B10	0.872	+	+	+	
2429	YOR173W	20	B	11		YKO_0820	B11	1.001	+	+	+	
2431	YOR175C	20	B	12		YKO_0820	B12	0.837	+	+	+	
2433	YOR177C	20	C	1		YKO_0820	C01	0.985	+	+	+	
2434	YOR178C	20	C	2		YKO_0820	C02	0.901	+	+	+	
2438	YOR182C	20	C	3		YKO_0820	C03	0.929	+	+	+	
2439	YOR183W	20	C	4		YKO_0820	C04	0.69	+	+	+	
2440	YOR184W	20	C	5		YKO_0820	C05	0.97	-	-	-	Doubt
2441	YOR185C	20	C	6		YKO_0820	C06	0.866	+	+	+	
2442	YOR186W	20	C	7		YKO_0820	C07	1.015	+	+	+	
2443	YOR187W	20	C	8		YKO_0820	C08	0.821	slow	+	-	Doubt
2444	YOR188W	20	C	9		YKO_0820	C09	0.935	+	+	+	
2445	YOR189W	20	C	10		YKO_0820	C10	0.794	+	+	+	
2446	YOR190W	20	C	11		YKO_0820	C11	0.912	+	+	+	
2447	YOR191W	20	C	12		YKO_0820	C12	0.879	+	+	+	
2448	YOR192C	20	D	1		YKO_0820	D01	0.985	+	+	+	
2449	YOR193W	20	D	2		YKO_0820	D02	0.979	+	+	+	
2451	YOR195W	20	D	3		YKO_0820	D03	0.999	+	+	+	
2452	YOR196C	20	D	4		YKO_0820	D04	1.021	+	+	+	
2453	YOR197W	20	D	5		YKO_0820	D05	0.918	+	+	+	
2454	YOR198C	20	D	6		YKO_0820	D06	0.676	+	+	+	
2455	YOR199W	20	D	7		YKO_0820	D07	0.96	slow	+	-	Doubt
2456	YOR200W	20	D	8		YKO_0820	D08	1.013	slow	-	-	Doubt
2457	YOR201C	20	D	9		YKO_0820	D09	0.858	slow	+	-	Doubt
2458	YOR202W	20	D	10		YKO_0820	D10	0.727	+	+	+	
2461	YOR205C	20	D	11		YKO_0820	D11	0.806	slow	+	-	Doubt
2464	YOR208W	20	D	12		YKO_0820	D12	0.889	+	+	+	
2465	YOR209C	20	E	1		YKO_0820	E01	0.688	+	+	+	
2467	YOR211C	20	E	2		YKO_0820	E02	0.983	slow	+	-	Doubt
2468	YOR212W	20	E	3	Sterile [expected phenotype]	YKO_0820	E03	0.973	+	+	+	
2469	YOR213C	20	E	4		YKO_0820	E04	1.008	+	+	+	
2470	YOR214C	20	E	5		YKO_0820	E05	0.991	+	+	-	HIT
2471	YOR215C	20	E	6		YKO_0820	E06	0.861	+	+	+	
2472	YOR216C	20	E	7		YKO_0820	E07	0.802	+	+	+	
2475	YOR219C	20	E	8		YKO_0820	E08	0.982	+	+	+	
2476	YOR220W	20	E	9		YKO_0820	E09	0.933	+	+	+	
2477	YOR221C	20	E	10		YKO_0820	E10	0.833	slow	-	-	Doubt
2478	YOR222W	20	E	11		YKO_0820	E11	0.906	+	+	+	
2479	YOR223W	20	E	12		YKO_0820	E12	0.781	+	+	+	
2481	YOR225W	20	F	1		YKO_0820	F01	0.923	+	+	+	
2482	YOR226C	20	F	2		YKO_0820	F02	0.951	+	+	+	
2483	YOR227W	20	F	3		YKO_0820	F03	0.947	+	+	+	
2484	YOR228C	20	F	4		YKO_0820	F04	0.905	+	+	+	
2485	YOR229W	20	F	5		YKO_0820	F05	1.018	+	+	+	
2486	YOR230W	20	F	6		YKO_0820	F06	1.026	+	+	+	
2487	YOR231W	20	F	7		YKO_0820	F07	0.9	+	+	+	
2489	YOR233W	20	F	8		YKO_0820	F08	1.013	+	+	-	HIT
2490	YOR234C	20	F	9		YKO_0820	F09	0.982	+	-	-	Doubt
2491	YOR235W	20	F	10		YKO_0820	F10	0.896	+	+	+	
2493	YOR237W	20	F	11		YKO_0820	F11	0.89	+	+	+	
2494	YOR238W	20	F	12		YKO_0820	F12	0.679	+	+	+	
2495	YOR239W	20	G	1		YKO_0820	G01	0.912	+	+	+	
2496	YOR240W	20	G	2		YKO_0820	G02	0.902	+	+	+	
2497	YOR241W	20	G	3		YKO_0820	G03	0.895	slow	+	-	Doubt
2498	YOR242C	20	G	4		YKO_0820	G04	0.885	+	+	+	
2499	YOR243C	20	G	5		YKO_0820	G05	0.958	+	+	+	
2501	YOR245C	20	G	6		YKO_0820	G06	0.912	+	+	+	
2502	YOR246C	20	G	7		YKO_0820	G07	0.808	+	+	+	
2503	YOR247W	20	G	8		YKO_0820	G08	0.727	+	+	+	
2504	YOR248W	20	G	9		YKO_0820	G09	0.893	+	+	+	
2507	YOR251C	20	G	10		YKO_0820	G10	not grow n	-	-	-	Not grow n
2508	YOR252W	20	G	11		YKO_0820	G11	0.894	+	+	+	
2509	YOR253W	20	G	12		YKO_0820	G12	0.848	+	+	+	
2511	YOR255W	20	H	1		YKO_0820	H01	0.906	+	+	+	
--		20	H	2	empty	YKO_0820	H02	empty	empty	empty	empty	empty
2514	YOR258W	20	H	3		YKO_0820	H03	0.7	+	+	+	
2519	YOR263C	20	H	4		YKO_0820	H04	0.968	+	+	+	
2520	YOR264W	20	H	5		YKO_0820	H05	1.026	+	+	+	
2533	YOR277C	20	H	6		YKO_0820	H06	0.924	+	+	+	
2535	YOR279C	20	H	7		YKO_0820	H07	0.814	+	+	+	
2536	YOR280C	20	H	8		YKO_0820	H08	1.002	+	+	+	
2539	YOR283W	20	H	9		YKO_0820	H09	0.955	+	+	+	

Euroscarf Information						Replica plate Information			Tau Toxicity Enhancer Primary Screen Results			
record no.	ORF name	Plate	Row	Col	Comment	Replica plate	Well	YPD (OD600nm)	Growth plate (SC+GAL comp.)	Transformation control plate (SC+GLU-Leu)	TEST Plate (SC+GAL-Leu)	Classification
2540	YOR284W	20	H	10		YKO_0820	H10	0.807	+	+	+	
2541	YOR285W	20	H	11		YKO_0820	H11	0.957	+	+	-	HIT
2542	YOR286W	20	H	12		YKO_0820	H12	0.923	+	+	+	
2544	YOR288C	21	A	1		YKO_0821	A01	0.887	+	+	+	
1207	YJL218W	21	A	2		YKO_0821	A02	0.888	+	+	+	
1208	YJL217W	21	A	3		YKO_0821	A03	0.95	+	+	+	
1209	YJL216C	21	A	4		YKO_0821	A04	0.891	+	+	+	
1210	YJL215C	21	A	5		YKO_0821	A05	0.87	+	+	+	
1211	YJL214W	21	A	6		YKO_0821	A06	0.887	+	+	+	
1213	YJL212C	21	A	7		YKO_0821	A07	0.901	+	+	+	
1214	YJL210W	21	A	8		YKO_0821	A08	0.801	+	+	-	HIT
1215	YJL211C	21	A	9		YKO_0821	A09	0.894	+	+	-	HIT
1216	YJL209W	21	A	10		YKO_0821	A10	0.867	slow	-	-	Doubt
1217	YJL208C	21	A	11		YKO_0821	A11	0.891	+	+	+	
1218	YJL207C	21	A	12		YKO_0821	A12	0.908	+	+	+	
1219	YJL206C	21	B	1		YKO_0821	B01	0.895	+	+	+	
1220	YJL206C-A	21	B	2		YKO_0821	B02	0.929	+	+	+	
1221	YJL204C	21	B	3		YKO_0821	B03	0.48	+	+	+	
1224	YJL201W	21	B	4		YKO_0821	B04	0.848	+	+	+	
1225	YJL200C	21	B	5		YKO_0821	B05	0.76	+	+	+	
1226	YJL199C	21	B	6		YKO_0821	B06	0.885	+	+	+	
1227	YJL198W	21	B	7		YKO_0821	B07	0.894	+	+	+	
1228	YJL197W	21	B	8		YKO_0821	B08	0.967	+	+	+	
--		21	B	9	empty	YKO_0821	B09	empty	empty	empty	empty	empty
1229	YJL196C	21	B	10		YKO_0821	B10	0.851	+	+	+	
1232	YJL193W	21	B	11		YKO_0821	B11	0.926	+	+	-	HIT
1233	YJL192C	21	B	12		YKO_0821	B12	0.948	+	+	-	HIT
1234	YJL191W	21	C	1		YKO_0821	C01	0.973	+	+	+	
1235	YJL190C	21	C	2		YKO_0821	C02	0.931	+	+	+	
1236	YJL189W	21	C	3		YKO_0821	C03	0.641	slow	+	+	
1237	YJL188C	21	C	4		YKO_0821	C04	0.659	slow	+	+	
1238	YJL187C	21	C	5		YKO_0821	C05	0.867	+	-	-	Doubt
1239	YJL186W	21	C	6		YKO_0821	C06	0.908	+	+	+	
1240	YJL185C	21	C	7		YKO_0821	C07	0.875	+	+	+	
1242	YJL183W	21	C	8		YKO_0821	C08	0.946	+	+	+	
1243	YJL181W	21	C	9		YKO_0821	C09	0.898	+	+	+	
1244	YJL182C	21	C	10		YKO_0821	C10	0.838	+	+	+	
1245	YJL180C	21	C	11		YKO_0821	C11	not grow n	-	-	-	Not grow n
1246	YJL179W	21	C	12		YKO_0821	C12	0.795	+	+	-	HIT
1247	YJL178C	21	D	1		YKO_0821	D01	1.008	+	+	+	
1250	YJL176C	21	D	2		YKO_0821	D02	not grow n	-	-	-	Not grow n
1253	YJL172W	21	D	3		YKO_0821	D03	0.989	+	+	+	
1254	YJL171C	21	D	4		YKO_0821	D04	0.903	+	+	+	
1255	YJL170C	21	D	5		YKO_0821	D05	0.942	+	+	+	
1256	YJL169W	21	D	6		YKO_0821	D06	0.982	+	+	+	
1257	YJL168C	21	D	7		YKO_0821	D07	0.937	+	+	+	
1259	YJL166W	21	D	8		YKO_0821	D08	0.887	slow	+	-	Doubt
1260	YJL165C	21	D	9		YKO_0821	D09	not grow n	-	-	-	Not grow n
1261	YJL164C	21	D	10		YKO_0821	D10	0.721	+	+	+	
1262	YJL163C	21	D	11		YKO_0821	D11	0.835	+	+	+	
1263	YJL162C	21	D	12		YKO_0821	D12	0.969	+	+	+	
1264	YJL161W	21	E	1		YKO_0821	E01	0.962	+	+	+	
1266	YJL159W	21	E	2		YKO_0821	E02	0.983	+	+	+	
1267	YJL158C	21	E	3		YKO_0821	E03	0.967	+	+	+	
1268	YJL157C	21	E	4		YKO_0821	E04	0.988	+	+	+	
1270	YJL155C	21	E	5		YKO_0821	E05	0.952	+	+	+	
1271	YJL154C	21	E	6		YKO_0821	E06	0.944	+	+	+	
1272	YJL153C	21	E	7		YKO_0821	E07	0.946	+	+	+	
1273	YJL152W	21	E	8		YKO_0821	E08	0.864	+	+	+	
1274	YJL151C	21	E	9		YKO_0821	E09	0.945	+	+	+	
1275	YJL150W	21	E	10		YKO_0821	E10	0.851	+	+	+	
1276	YJL149W	21	E	11		YKO_0821	E11	0.847	+	+	+	
1277	YJL148W	21	E	12		YKO_0821	E12	0.916	slow	+	-	Doubt
1278	YJL147C	21	F	1		YKO_0821	F01	0.922	+	+	+	
1279	YJL146W	21	F	2		YKO_0821	F02	0.96	+	+	+	
1280	YJL145W	21	F	3		YKO_0821	F03	0.946	+	+	+	
1281	YJL144W	21	F	4		YKO_0821	F04	0.902	+	+	+	
1283	YJL142C	21	F	5		YKO_0821	F05	0.94	+	+	+	
1285	YJL140W	21	F	6		YKO_0821	F06	0.77	-	+	-	Doubt
1286	YJL139C	21	F	7		YKO_0821	F07	0.954	+	+	+	
1287	YJL138C	21	F	8		YKO_0821	F08	0.79	+	+	+	
1290	YJL135W	21	F	9		YKO_0821	F09	0.901	+	+	+	
1291	YJL134W	21	F	10		YKO_0821	F10	0.851	+	+	+	
1292	YJL133W	21	F	11		YKO_0821	F11	0.839	+	+	+	
1293	YJL132W	21	F	12		YKO_0821	F12	0.846	+	+	-	HIT
1294	YJL131C	21	G	1		YKO_0821	G01	0.819	+	+	+	
1295	YJL130C	21	G	2		YKO_0821	G02	0.956	+	+	-	HIT
1296	YJL129C	21	G	3		YKO_0821	G03	0.939	+	+	+	
5233	YLR324W	21	G	4		YKO_0821	G04	0.913	+	+	-	HIT
5234	YLR325C	21	G	5		YKO_0821	G05	0.897	+	+	+	
5235	YLR326W	21	G	6		YKO_0821	G06	0.909	+	-	+	Incongruence
5236	YLR327C	21	G	7		YKO_0821	G07	0.92	+	+	-	HIT
5237	YLR328W	21	G	8		YKO_0821	G08	0.892	+	+	+	
5238	YLR329W	21	G	9		YKO_0821	G09	0.36	slow	+	+	

	Euroscarf Information					Replica plate Information			Tau Toxicity Enhancer Primary Screen Results			
record no.	ORF name	Plate	Row	Col	Comment	Replica plate	Well	YPD (OD600nm)	Growth plate (SC+GAL comp.)	Transformation control plate (SC+GLU-Leu)	TEST Plate (SC+GAL-Leu)	Classification
5239	YLR330W	21	G	10	slow growth, petite	YKO_0821	G10	0.884	+	-	+	Incongruence
5240	YLR331C	21	G	11	slow growth, petite	YKO_0821	G11	0.862	+	+	+	
5241	YLR332W	21	G	12		YKO_0821	G12	0.841	+	+	+	
5242	YLR333C	21	H	1		YKO_0821	H01	0.923	+	+	+	
--		21	H	2	empty	YKO_0821	H02	empty	empty	empty	empty	empty
5244	YLR335W	21	H	3		YKO_0821	H03	0.908	+	+	+	
5250	YLR341W	21	H	4		YKO_0821	H04	0.912	+	+	+	
5251	YLR342W	21	H	5		YKO_0821	H05	0.863	+	+	+	
5253	YLR344W	21	H	6		YKO_0821	H06	0.862	+	+	+	
5254	YLR345W	21	H	7		YKO_0821	H07	0.864	+	+	+	
5257	YLR348C	21	H	8		YKO_0821	H08	0.916	+	+	+	
5258	YLR349W	21	H	9		YKO_0821	H09	0.931	+	+	+	
5259	YLR350W	21	H	10		YKO_0821	H10	0.865	+	-	+	Incongruence
5260	YLR351C	21	H	11		YKO_0821	H11	0.819	+	+	-	HIT
5261	YLR352W	21	H	12		YKO_0821	H12	0.953	+	-	-	Doubt
5262	YLR353W	22	A	1		YKO_0822	A01	0.6999	+	+	+	
5263	YLR354C	22	A	2		YKO_0822	A02	0.7116	+	+	+	
5265	YLR356W	22	A	3		YKO_0822	A03	0.695	+	+	+	
5266	YLR357W	22	A	4	slow growth	YKO_0822	A04	0.6211	+	+	-	HIT
5269	YLR360W	22	A	5		YKO_0822	A05	0.6953	+	+	+	
5271	YLR362W	22	A	6	does not mate	YKO_0822	A06	0.6617	+	+	+	
5272	YLR363C	22	A	7		YKO_0822	A07	0.6431	+	+	+	
5273	YLR364W	22	A	8		YKO_0822	A08	0.6667	+	+	+	
5274	YLR365W	22	A	9		YKO_0822	A09	0.6565	+	-	+	Incongruence
5275	YLR366W	22	A	10		YKO_0822	A10	0.7576	+	+	+	
5276	YLR367W	22	A	11		YKO_0822	A11	0.6811	+	+	+	
5277	YLR368W	22	A	12		YKO_0822	A12	0.6696	+	+	+	
5280	YLR371W	22	B	1		YKO_0822	B01	0.737	+	+	+	
5281	YLR372W	22	B	2		YKO_0822	B02	0.6734	+	+	+	
5282	YLR373C	22	B	3		YKO_0822	B03	0.6503	+	+	+	
5283	YLR374C	22	B	4		YKO_0822	B04	0.6644	+	+	+	
5284	YLR375W	22	B	5		YKO_0822	B05	0.7068	+	+	+	
5285	YLR376C	22	B	6		YKO_0822	B06	0.9279	+	+	+	
5286	YLR377C	22	B	7	slow growth	YKO_0822	B07	0.781	+	+	+	
5289	YLR380W	22	B	8		YKO_0822	B08	0.7107	+	+	+	
5290	YLR381W	22	B	9		YKO_0822	B09	0.7049	+	+	-	HIT
--		22	B	10	empty	YKO_0822	B10	empty	empty	empty	empty	empty
5293	YLR384C	22	B	11		YKO_0822	B11	1.0017	+	+	-	HIT
5294	YLR385C	22	B	12		YKO_0822	B12	1.0347	+	+	+	
5295	YLR386W	22	C	1		YKO_0822	C01	0.7337	+	+	+	
5296	YLR387C	22	C	2		YKO_0822	C02	0.6737	+	+	+	
5297	YLR388W	22	C	3		YKO_0822	C03	1.0297	+	+	+	
5299	YLR390W	22	C	4		YKO_0822	C04	0.7155	+	+	+	
5301	YLR392C	22	C	5		YKO_0822	C05	1.0789	+	+	+	
5302	YLR393W	22	C	6	slow growth	YKO_0822	C06	0.9789	slow	+	+	
5304	YLR395C	22	C	7		YKO_0822	C07	0.9877	+	+	+	
5307	YLR398C	22	C	8		YKO_0822	C08	1.0138	+	+	+	
5309	YLR400W	22	C	9		YKO_0822	C09	1.0081	+	+	+	
5310	YLR401C	22	C	10		YKO_0822	C10	1.0256	+	+	+	
5311	YLR402W	22	C	11		YKO_0822	C11	1.0392	+	+	+	
5313	YLR404W	22	C	12		YKO_0822	C12	0.9854	+	+	+	
5314	YLR405W	22	D	1		YKO_0822	D01	0.6995	+	+	+	
5316	YLR407W	22	D	2		YKO_0822	D02	0.711	+	+	+	
5317	YLR408C	22	D	3		YKO_0822	D03	0.8529	+	+	+	
5319	YLR410W	22	D	4		YKO_0822	D04	0.9051	+	+	+	
5320	YLR412W	22	D	5		YKO_0822	D05	1.029	+	+	+	
5321	YLR413W	22	D	6		YKO_0822	D06	1.0124	+	+	+	
5322	YLR414C	22	D	7		YKO_0822	D07	0.5626	+	+	+	
5323	YLR415C	22	D	8		YKO_0822	D08	1.069	+	+	-	HIT
5324	YLR416C	22	D	9		YKO_0822	D09	0.9698	+	+	+	
5325	YLR417W	22	D	10		YKO_0822	D10	0.9988	+	+	+	
5326	YLR418C	22	D	11		YKO_0822	D11	0.8856	+	+	+	
5328	YLR421C	22	D	12		YKO_0822	D12	1.0623	+	+	+	
5137	YLR228C	22	E	1		YKO_0822	E01	0.6996	+	+	+	
5140	YLR231C	22	E	2		YKO_0822	E02	0.945	+	+	+	
5141	YLR232W	22	E	3		YKO_0822	E03	1.02	+	+	+	
5142	YLR233C	22	E	4		YKO_0822	E04	0.9627	+	+	+	
5143	YLR234W	22	E	5	grows well on -met, grows well on -lys	YKO_0822	E05	0.6352	+	+	+	
5144	YLR235C	22	E	6		YKO_0822	E06	1.0096	+	+	+	
5145	YLR236C	22	E	7		YKO_0822	E07	1.0267	+	+	+	
5147	YLR238W	22	E	8		YKO_0822	E08	0.7177	+	-	-	Doubt
5148	YLR239C	22	E	9		YKO_0822	E09	1.0086	slow	-	-	Doubt
5150	YLR241W	22	E	10		YKO_0822	E10	0.9945	+	+	+	
5151	YLR242C	22	E	11		YKO_0822	E11	0.9452	+	+	+	
5156	YLR247C	22	E	12		YKO_0822	E12	1.0464	+	+	+	
5157	YLR248W	22	F	1		YKO_0822	F01	0.6953	+	+	+	
5159	YLR250W	22	F	2		YKO_0822	F02	0.6938	+	+	+	
5160	YLR251W	22	F	3		YKO_0822	F03	1.0113	+	+	+	
5161	YLR252W	22	F	4		YKO_0822	F04	0.6736	+	+	+	
5162	YLR253W	22	F	5		YKO_0822	F05	1.0402	+	+	+	
5163	YLR254C	22	F	6		YKO_0822	F06	1.0158	+	+	+	
5164	YLR255C	22	F	7		YKO_0822	F07	0.9888	+	+	+	
5166	YLR257W	22	F	8		YKO_0822	F08	0.6538	+	+	+	

	Euroscarf Information					Replica plate Information			Tau Toxicity Enhancer Primary Screen Results			
record no.	ORF name	Plate	Row	Col	Comment	Replica plate	Well	YPD (OD600nm)	Growth plate (SC+GAL comp.)	Transformation control plate (SC+GLU-Leu)	TEST Plate (SC+GAL-Leu)	Classification
5167	YLR258W	22	F	9		YKO_0822	F09	0.6848	+	+	+	
5169	YLR260W	22	F	10	slow growth, petite	YKO_0822	F10	0.7257	+	+	+	
5170	YLR261C	22	F	11		YKO_0822	F11	0.6984	+	+	+	
5171	YLR262C	22	F	12		YKO_0822	F12	0.6989	+	+	-	HIT
5172	YLR263W	22	G	1		YKO_0822	G01	0.9039	+	+	+	
5173	YLR264W	22	G	2		YKO_0822	G02	0.9821	+	+	+	
5174	YLR265C	22	G	3		YKO_0822	G03	1.0316	+	+	+	
5175	YLR266C	22	G	4		YKO_0822	G04	0.9505	+	+	+	
5176	YLR267W	22	G	5		YKO_0822	G05	1.0344	+	+	+	
5177	YLR268W	22	G	6		YKO_0822	G06	1.0342	+	+	-	HIT
5178	YLR269C	22	G	7		YKO_0822	G07	1.0309	+	+	+	
5179	YLR270W	22	G	8	slow growth, petite	YKO_0822	G08	0.6358	-	-	-	Doubt
5180	YLR271W	22	G	9		YKO_0822	G09	1.0011	+	+	+	
5182	YLR273C	22	G	10		YKO_0822	G10	1.0202	+	+	-	HIT
5187	YLR278C	22	G	11		YKO_0822	G11	1.0489	+	-	+	Incongruence
5188	YLR279W	22	G	12		YKO_0822	G12	1.0396	+	+	+	
5189	YLR280C	22	H	1		YKO_0822	H01	1.0166	+	+	+	
--		22	H	2	empty	YKO_0822	H02	empty	empty	empty	empty	empty
5190	YLR281C	22	H	3		YKO_0822	H03	1.0158	+	+	+	
5191	YLR282C	22	H	4		YKO_0822	H04	1.0269	+	+	+	
5192	YLR283W	22	H	5		YKO_0822	H05	1.0363	+	+	+	
5193	YLR284C	22	H	6		YKO_0822	H06	1.0596	+	+	+	
5194	YLR285W	22	H	7		YKO_0822	H07	1.0593	+	+	+	
5196	YLR287C	22	H	8		YKO_0822	H08	1.0669	+	+	+	
5197	YLR287-A	22	H	9		YKO_0822	H09	0.9985	+	+	+	
5198	YLR288C	22	H	10	slow growth	YKO_0822	H10	0.6494	slow	+	-	Doubt
5199	YLR289W	22	H	11		YKO_0822	H11	1.0455	+	+	+	
5200	YLR290C	22	H	12		YKO_0822	H12	0.6975	+	+	+	
5202	YLR292C	23	A	1		YKO_0823	A01	0.854	+	+	+	
5204	YLR294C	23	A	2		YKO_0823	A02	0.996	+	+	+	
5205	YLR295C	23	A	3	slow growth	YKO_0823	A03	1.017	+	+	+	
5206	YLR296W	23	A	4		YKO_0823	A04	1.04	+	+	+	
5207	YLR297W	23	A	5		YKO_0823	A05	1.045	+	+	+	
5209	YLR299W	23	A	6		YKO_0823	A06	0.981	+	+	+	
5210	YLR300W	23	A	7		YKO_0823	A07	0.962	+	+	+	
5211	YLR303W	23	A	8		YKO_0823	A08	1.02	+	+	+	
5212	YLR304C	23	A	9	slow growth, petite	YKO_0823	A09	1.016	+	+	+	
5214	YLR306W	23	A	10		YKO_0823	A10	1.043	+	+	+	
5215	YLR307W	23	A	11		YKO_0823	A11	0.976	+	+	+	
5216	YLR308W	23	A	12	mates like alpha, no growth on -met, growth on -lys. Confirmed Alpha -- CORRECT STRAIN CAN BE FOUND IN PLATE 122 D4	YKO_0823	A12	0.867	+	+	+	
5217	YLR309C	23	B	1		YKO_0823	B01	0.913	+	+	+	
5219	YLR311C	23	B	2		YKO_0823	B02	0.851	+	+	+	
5220	YLR312C	23	B	3		YKO_0823	B03	1.037	+	+	+	
5221	YLR312W-A	23	B	4	slow growth, petite	YKO_0823	B04	0.996	slow	-	-	Doubt
5222	YLR313C	23	B	5		YKO_0823	B05	1.055	+	+	+	
5224	YLR315W	23	B	6		YKO_0823	B06	0.675	+	+	+	
5227	YLR318W	23	B	7	slow growth	YKO_0823	B07	0.983	+	+	+	
5228	YLR319C	23	B	8		YKO_0823	B08	0.954	+	+	+	
5229	YLR320W	23	B	9		YKO_0823	B09	0.602	+	+	+	
5231	YLR322W	23	B	10		YKO_0823	B10	0.821	+	+	+	
--		23	B	11	empty	YKO_0823	B11	empty	empty	empty	empty	empty
3505	YDR147W	23	B	12		YKO_0823	B12	0.942	+	+	+	
3506	YDR148C	23	C	1	slow growth, petite	YKO_0823	C01	1.021	+	+	+	
3507	YDR149C	23	C	2		YKO_0823	C02	0.661	+	+	+	
3508	YDR150W	23	C	3		YKO_0823	C03	0.758	+	+	-	HIT
3509	YDR151C	23	C	4		YKO_0823	C04	0.873	+	+	+	
3510	YDR152W	23	C	5		YKO_0823	C05	0.875	+	-	+	Incongruence
3511	YDR153C	23	C	6		YKO_0823	C06	0.884	+	+	+	
3512	YDR154C	23	C	7		YKO_0823	C07	1.017	+	+	+	
3513	YDR155C	23	C	8		YKO_0823	C08	0.963	+	+	+	
3514	YDR156W	23	C	9		YKO_0823	C09	0.925	+	+	+	
3515	YDR157W	23	C	10		YKO_0823	C10	0.987	+	-	+	Incongruence
3516	YDR158W	23	C	11	no growth on drop-in media	YKO_0823	C11	0.829	+	+	+	
3517	YDR159W	23	C	12	slow growth	YKO_0823	C12	0.579	+	+	+	
3519	YDR161W	23	D	1		YKO_0823	D01	0.973	+	+	-	HIT
3520	YDR162C	23	D	2		YKO_0823	D02	0.916	+	+	+	
3521	YDR163W	23	D	3		YKO_0823	D03	1.008	+	+	+	
3523	YDR165W	23	D	4		YKO_0823	D04	0.978	+	+	+	
3527	YDR169C	23	D	5		YKO_0823	D05	0.968	+	+	+	
3529	YDR171W	23	D	6		YKO_0823	D06	0.998	+	+	+	
3531	YDR173C	23	D	7		YKO_0823	D07	0.99	+	+	+	
3533	YDR175C	23	D	8	slow growth, petite	YKO_0823	D08	0.95	slow	+	-	Doubt
3534	YDR176W	23	D	9		YKO_0823	D09	0.398	+	+	-	HIT
3536	YDR178W	23	D	10		YKO_0823	D10	0.882	+	+	-	HIT
3537	YDR179C	23	D	11		YKO_0823	D11	0.984	+	+	+	
3538	YDR179W-A	23	D	12		YKO_0823	D12	1.023	+	+	+	
3540	YDR181C	23	E	1		YKO_0823	E01	0.941	+	+	+	
3542	YDR183W	23	E	2		YKO_0823	E02	0.754	+	+	-	HIT
3543	YDR184C	23	E	3		YKO_0823	E03	0.957	+	+	+	

	Euroscarf Information					Replica plate Information			Tau Toxicity Enhancer Primary Screen Results			
record no.	ORF name	Plate	Row	Col	Comment	Replica plate	Well	YPD (OD600nm)	Growth plate (SC+GAL comp.)	Transformation control plate (SC+GLU-Leu)	TEST Plate (SC+GAL-Leu)	Classification
3544	YDR185C	23	E	4		YKO_0823	E04	0.962	+	-	+	Incongruence
3545	YDR186C	23	E	5		YKO_0823	E05	0.91	+	+	+	
3550	YDR191W	23	E	6		YKO_0823	E06	0.972	+	+	+	
3551	YDR192C	23	E	7		YKO_0823	E07	0.892	+	+	+	
3552	YDR193W	23	E	8		YKO_0823	E08	0.948	+	-	+	Incongruence
3553	YDR194C	23	E	9	slow growth, petite	YKO_0823	E09	0.94	+	+	+	
3554	YDR195W	23	E	10	slow growth	YKO_0823	E10	0.96	+	-	+	Incongruence
3556	YDR197W	23	E	11	slow growth	YKO_0823	E11	0.929	+	+	+	
3557	YDR198C	23	E	12		YKO_0823	E12	0.797	+	+	+	
3558	YDR199W	23	F	1		YKO_0823	F01	0.878	+	+	+	
3559	YDR200C	23	F	2		YKO_0823	F02	0.805	+	+	+	
3562	YDR203W	23	F	3		YKO_0823	F03	0.994	+	+	+	
3563	YDR204W	23	F	4	slow growth, petite	YKO_0823	F04	1.039	-	+	-	Doubt
3565	YDR206W	23	F	5		YKO_0823	F05	1.001	+	+	+	
3566	YDR207C	23	F	6		YKO_0823	F06	0.607	+	+	+	
3568	YDR209C	23	F	7		YKO_0823	F07	0.942	+	+	+	
3569	YDR210W	23	F	8		YKO_0823	F08	0.916	+	+	+	
3572	YDR213W	23	F	9		YKO_0823	F09	0.959	+	+	+	
3573	YDR214W	23	F	10		YKO_0823	F10	0.937	+	+	+	
3574	YDR215C	23	F	11		YKO_0823	F11	0.945	+	+	+	
3575	YDR216W	23	F	12		YKO_0823	F12	0.979	+	+	+	
3576	YDR217C	23	G	1		YKO_0823	G01	0.929	+	+	-	HIT
3577	YDR218C	23	G	2		YKO_0823	G02	0.93	+	+	+	
3578	YDR219C	23	G	3		YKO_0823	G03	0.949	+	+	+	
3579	YDR220C	23	G	4		YKO_0823	G04	0.701	+	+	+	
3580	YDR221W	23	G	5		YKO_0823	G05	0.993	+	+	+	
3581	YDR222W	23	G	6		YKO_0823	G06	0.885	+	+	+	
3582	YDR223W	23	G	7		YKO_0823	G07	0.889	+	+	+	
3584	YDR225W	23	G	8		YKO_0823	G08	0.89	+	+	+	
3585	YDR226W	23	G	9	slow growth	YKO_0823	G09	0.714	+	+	+	
3586	YDR227W	23	G	10	does not mate, sterile	YKO_0823	G10	0.69	+	+	+	
3588	YDR229W	23	G	11		YKO_0823	G11	0.853	+	+	+	
3589	YDR230W	23	G	12	slow growth, petite	YKO_0823	G12	0.65	slow	+	-	Doubt
3590	YDR231C	23	H	1	slow growth, petite	YKO_0823	H01	0.983	+	+	-	HIT
--		23	H	2	empty	YKO_0823	H02	empty	empty	empty	empty	empty
3592	YDR233C	23	H	3		YKO_0823	H03	1.041	+	+	+	
3593	YDR234W	23	H	4	no growth on -lys, no growth on drop-in media	YKO_0823	H04	1.018	+	+	+	
3596	YDR237W	23	H	5	slow growth, petite	YKO_0823	H05	0.99	slow	-	-	Doubt
3598	YDR239C	23	H	6		YKO_0823	H06	0.972	+	+	+	
3600	YDR241W	23	H	7		YKO_0823	H07	0.838	+	+	+	
4561	YGL194C	23	H	8		YKO_0823	H08	0.972	+	+	+	
4562	YGL195W	23	H	9		YKO_0823	H09	0.959	+	-	-	Doubt
4563	YGL196W	23	H	10		YKO_0823	H10	0.774	+	+	+	
4564	YGL197W	23	H	11		YKO_0823	H11	0.895	+	+	+	
4565	YGL198W	23	H	12		YKO_0823	H12	1.006	+	+	+	
4566	YGL199C	24	A	1		YKO_0824	A01	0.847	+	+	+	
4567	YGL200C	24	A	2	super slow growth	YKO_0824	A02	not grown	-	-	-	Not grown
4569	YGL202W	24	A	3		YKO_0824	A03	0.857	+	+	+	
4570	YGL203C	24	A	4		YKO_0824	A04	0.793	+	+	+	
4571	YGL205W	24	A	5		YKO_0824	A05	0.869	+	+	+	
4574	YGL208W	24	A	6		YKO_0824	A06	0.75	+	+	+	
4575	YGL209W	24	A	7		YKO_0824	A07	0.825	+	+	+	
4576	YGL210W	24	A	8		YKO_0824	A08	0.921	+	+	+	
4577	YGL211W	24	A	9		YKO_0824	A09	0.917	+	+	+	
4578	YGL212W	24	A	10	slow growth	YKO_0824	A10	0.858	+	+	+	
4579	YGL213C	24	A	11		YKO_0824	A11	0.841	+	+	+	
4580	YGL214W	24	A	12		YKO_0824	A12	0.902	+	+	+	
4581	YGL215W	24	B	1		YKO_0824	B01	0.876	+	+	+	
4582	YGL216W	24	B	2		YKO_0824	B02	0.918	+	+	+	
4583	YGL217C	24	B	3		YKO_0824	B03	0.78	+	+	+	
4584	YGL218W	24	B	4		YKO_0824	B04	0.689	+	+	+	
4586	YGL220W	24	B	5	slow growth, petite	YKO_0824	B05	0.905	slow	-	-	Doubt
4587	YGL221C	24	B	6		YKO_0824	B06	0.909	+	-	+	Incongruence
4588	YGL222C	24	B	7		YKO_0824	B07	0.819	+	+	+	
4590	YGL224C	24	B	8		YKO_0824	B08	0.796	+	+	+	
4592	YGL226C-A	24	B	9		YKO_0824	B09	0.915	+	+	+	
4593	YGL226W	24	B	10		YKO_0824	B10	0.87	+	+	+	
4594	YGL227W	24	B	11		YKO_0824	B11	0.782	+	+	+	
--		24	B	12	empty	YKO_0824	B12	empty	empty	empty	empty	empty
4595	YGL228W	24	C	1		YKO_0824	C01	0.945	+	+	+	
4596	YGL229C	24	C	2		YKO_0824	C02	0.939	+	+	+	
4597	YGL230C	24	C	3		YKO_0824	C03	0.778	+	+	+	
4598	YGL231C	24	C	4		YKO_0824	C04	0.943	+	+	+	
4599	YGL232W	24	C	5		YKO_0824	C05	0.551	+	+	+	
4601	YGL234W	24	C	6	slow, no growth on drop-in media	YKO_0824	C06	0.696	slow	+	+	
4602	YGL235W	24	C	7		YKO_0824	C07	0.877	+	+	+	
4603	YGL236C	24	C	8		YKO_0824	C08	0.65	+	+	+	
4604	YGL237C	24	C	9	slow growth, petite	YKO_0824	C09	0.874	slow	+	+	
4608	YGL241W	24	C	10		YKO_0824	C10	0.92	+	+	+	
4609	YGL242C	24	C	11		YKO_0824	C11	0.899	+	+	+	
4610	YGL243W	24	C	12		YKO_0824	C12	0.958	+	-	+	Incongruence
4611	YGL244W	24	D	1		YKO_0824	D01	0.657	+	+	+	

	Euroscarf Information					Replica plate Information			Tau Toxicity Enhancer Primary Screen Results			
record no.	ORF name	Plate	Row	Col	Comment	Replica plate	Well	YPD (OD600nm)	Growth plate (SC+GAL comp.)	Transformation control plate (SC+GLU-Leu)	TEST Plate (SC+GAL-Leu)	Classification
4613	YGL246C	24	D	2	slow growth, petite	YKO_0824	D02	0.961	slow	+	+	
4615	YGL248W	24	D	3		YKO_0824	D03	0.871	+	+	+	
4616	YGL249W	24	D	4		YKO_0824	D04	0.812	+	+	+	
4617	YGL250W	24	D	5		YKO_0824	D05	0.929	+	+	+	
4618	YGL251C	24	D	6		YKO_0824	D06	0.828	+	+	+	
4619	YGL252C	24	D	7		YKO_0824	D07	0.914	+	-	+	Incongruence
4620	YGL253W	24	D	8		YKO_0824	D08	0.821	+	+	+	
4621	YGL254W	24	D	9		YKO_0824	D09	0.811	+	+	+	
4622	YGL255W	24	D	10		YKO_0824	D10	0.866	+	+	+	
4623	YGL256W	24	D	11		YKO_0824	D11	0.867	+	-	-	Doubt
4624	YGL257C	24	D	12		YKO_0824	D12	0.964	+	+	+	
4625	YGL258W	24	E	1		YKO_0824	E01	0.938	+	+	+	
4626	YGL259W	24	E	2		YKO_0824	E02	0.933	+	+	+	
4627	YGL260W	24	E	3		YKO_0824	E03	0.774	+	+	+	
4628	YGL261C	24	E	4		YKO_0824	E04	0.805	+	+	+	
4629	YGL262W	24	E	5		YKO_0824	E05	0.975	+	+	+	
4630	YGL263W	24	E	6		YKO_0824	E06	0.782	+	+	+	
4631	YGR001C	24	E	7	no growth on drop-in media	YKO_0824	E07	0.883	+	+	+	
4633	YGR003W	24	E	8		YKO_0824	E08	0.741	+	+	+	
4634	YGR004W	24	E	9		YKO_0824	E09	0.992	+	+	+	
4636	YGR006W	24	E	10	slow growth	YKO_0824	E10	not grown	-	-	-	Not grown
4637	YGR007W	24	E	11		YKO_0824	E11	0.882	+	+	+	
4638	YGR008C	24	E	12		YKO_0824	E12	0.931	+	+	+	
4640	YGR010W	24	F	1		YKO_0824	F01	0.925	+	+	+	
4641	YGR011W	24	F	2		YKO_0824	F02	0.905	+	+	+	
4642	YGR012W	24	F	3		YKO_0824	F03	0.905	+	+	+	
4644	YGR014W	24	F	4		YKO_0824	F04	0.729	+	+	+	
4645	YGR015C	24	F	5		YKO_0824	F05	0.919	+	+	+	
4646	YGR016W	24	F	6		YKO_0824	F06	0.901	+	+	+	
4647	YGR017W	24	F	7		YKO_0824	F07	0.837	+	+	-	HIT
4648	YGR018C	24	F	8		YKO_0824	F08	0.841	+	+	+	
4649	YGR019W	24	F	9		YKO_0824	F09	0.868	+	+	+	
4650	YGR020C	24	F	10	slow growth, petite	YKO_0824	F10	0.943	-	-	-	Doubt
4651	YGR021W	24	F	11		YKO_0824	F11	0.871	+	+	+	
4652	YGR022C	24	F	12		YKO_0824	F12	0.938	+	+	+	
4653	YGR023W	24	G	1		YKO_0824	G01	0.867	+	+	+	
4655	YGR025W	24	G	2		YKO_0824	G02	0.954	+	+	+	
4656	YGR026W	24	G	3		YKO_0824	G03	0.89	+	+	+	
2737	YPL091W	24	G	4		YKO_0824	G04	0.921	+	+	+	
2738	YPL090C	24	G	5		YKO_0824	G05	0.774	+	+	+	
2739	YPL089C	24	G	6		YKO_0824	G06	0.908	+	+	+	
2740	YPL088W	24	G	7		YKO_0824	G07	0.844	+	+	+	
2741	YPL087W	24	G	8		YKO_0824	G08	0.674	+	+	+	
2742	YPL086C	24	G	9		YKO_0824	G09	0.876	+	+	+	
2744	YPL084W	24	G	10		YKO_0824	G10	0.841	+	+	+	
2747	YPL081W	24	G	11		YKO_0824	G11	0.899	+	+	+	
2748	YPL080C	24	G	12		YKO_0824	G12	0.935	+	+	+	
2749	YPL079W	24	H	1		YKO_0824	H01	0.875	+	+	+	
--		24	H	2	empty	YKO_0824	H02	empty	empty	empty	empty	empty
2750	YPL078C	24	H	3	slow growth	YKO_0824	H03	0.918	+	+	+	
2751	YPL077C	24	H	4		YKO_0824	H04	0.894	+	+	+	
2754	YPL074W	24	H	5		YKO_0824	H05	0.931	+	+	+	
2755	YPL072W	24	H	6		YKO_0824	H06	0.896	+	+	+	
2756	YPL073C	24	H	7		YKO_0824	H07	0.86	+	+	+	
2757	YPL071C	24	H	8		YKO_0824	H08	0.938	+	+	+	
2758	YPL070W	24	H	9		YKO_0824	H09	0.921	+	+	+	
2759	YPL069C	24	H	10		YKO_0824	H10	0.512	+	+	+	
2760	YPL068C	24	H	11		YKO_0824	H11	0.893	+	+	+	
2761	YPL067C	24	H	12		YKO_0824	H12	0.958	+	+	+	
2762	YPL066W	25	A	1		YKO_0825	A01	0.864	+	+	+	
2763	YPL065W	25	A	2		YKO_0825	A02	0.694	+	+	+	
2764	YPL064C	25	A	3		YKO_0825	A03	0.991	+	+	+	
2766	YPL062W	25	A	4		YKO_0825	A04	0.648	+	+	+	
2767	YPL061W	25	A	5		YKO_0825	A05	0.61	+	+	+	
2768	YPL060W	25	A	6		YKO_0825	A06	0.905	slow	+	-	Doubt
2770	YPL058C	25	A	7		YKO_0825	A07	0.957	+	+	+	
2771	YPL057C	25	A	8		YKO_0825	A08	0.834	+	+	+	
2772	YPL056C	25	A	9		YKO_0825	A09	0.874	+	+	+	
2773	YPL055C	25	A	10		YKO_0825	A10	0.741	+	+	+	
2774	YPL054W	25	A	11		YKO_0825	A11	0.962	+	+	+	
2775	YPL053C	25	A	12		YKO_0825	A12	0.77	+	+	-	HIT
2776	YPL052W	25	B	1		YKO_0825	B01	0.979	+	+	+	
2777	YPL051W	25	B	2		YKO_0825	B02	1.011	+	+	+	
2779	YPL049C	25	B	3		YKO_0825	B03	1.04	+	+	+	
2780	YPL048W	25	B	4		YKO_0825	B04	0.72	+	+	+	
2781	YPL047W	25	B	5		YKO_0825	B05	0.675	+	+	+	
2782	YPL046C	25	B	6		YKO_0825	B06	0.953	+	+	+	
2786	YPL042C	25	B	7		YKO_0825	B07	0.969	+	+	+	
2787	YPL041C	25	B	8		YKO_0825	B08	0.875	+	+	-	HIT
2788	YPL040C	25	B	9		YKO_0825	B09	0.963	+	+	+	
2789	YPL039W	25	B	10		YKO_0825	B10	0.972	+	+	+	
2790	YPL038W	25	B	11		YKO_0825	B11	0.976	+	+	+	
2791	YPL037C	25	B	12		YKO_0825	B12	1.023	+	+	+	
--		25	C	1	empty	YKO_0825	C01	empty	empty	empty	empty	empty

	Euroscarf Information					Replica plate Information			Tau Toxicity Enhancer Primary Screen Results			
record no.	ORF name	Plate	Row	Col	Comment	Replica plate	Well	YPD (OD600nm)	Growth plate (SC+GAL comp.)	Transformation control plate (SC+GLU-Leu)	TEST Plate (SC+GAL-Leu)	Classification
2794	YPL035C	25	C	2		YKO_0825	C02	1.009	+	+	+	
2795	YPL033C	25	C	3		YKO_0825	C03	0.959	+	+	+	
2796	YPL032C	25	C	4		YKO_0825	C04	0.933	+	+	+	
2798	YPL030W	25	C	5		YKO_0825	C05	1.018	+	+	+	
2799	YPL029W	25	C	6		YKO_0825	C06	0.915	-	+	-	Doubt
2802	YPL026C	25	C	7		YKO_0825	C07	0.958	+	+	+	
2803	YPL025C	25	C	8		YKO_0825	C08	0.947	+	+	+	
2805	YPL023C	25	C	9		YKO_0825	C09	1.003	+	+	+	
2806	YPL022W	25	C	10		YKO_0825	C10	0.933	+	+	+	
2807	YPL021W	25	C	11		YKO_0825	C11	0.992	+	+	-	HIT
2809	YPL019C	25	C	12		YKO_0825	C12	0.871	+	+	+	
2810	YPL018W	25	D	1		YKO_0825	D01	0.862	+	+	+	
2813	YPL015C	25	D	2		YKO_0825	D02	1	+	+	+	
2814	YPL014W	25	D	3		YKO_0825	D03	0.942	+	+	+	
2815	YPL013C	25	D	4	slow growth, petite	YKO_0825	D04	0.901	-	+	-	Doubt
2819	YPL009C	25	D	5		YKO_0825	D05	1.013	+	+	+	
2820	YPL008W	25	D	6		YKO_0825	D06	0.861	+	+	+	
2822	YPL006W	25	D	7	mates like alpha. Confirmed Alpha -- CORRECT STRAIN CAN BE FOUND IN PLATE 123 H11	YKO_0825	D07	0.896	+	+	+	
2823	YPL005W	25	D	8		YKO_0825	D08	0.987	-	+	-	Doubt
2825	YPL003W	25	D	9		YKO_0825	D09	0.992	+	-	+	Incongruence
2826	YPL002C	25	D	10		YKO_0825	D10	0.813	+	+	+	
2827	YPL001W	25	D	11		YKO_0825	D11	0.834	+	+	+	
2828	YPR001W	25	D	12	slow growth, bi-mater	YKO_0825	D12	0.864	+	+	+	
2829	YPR002W	25	E	1		YKO_0825	E01	0.946	+	+	+	
2830	YPR003C	25	E	2		YKO_0825	E02	0.972	+	+	+	
2831	YPR004C	25	E	3		YKO_0825	E03	0.985	+	+	+	
2832	YPR005C	25	E	4		YKO_0825	E04	0.973	+	+	+	
5522	YPR106W	25	E	5		YKO_0825	E05	1.056	+	+	+	
5525	YPR109W	25	E	6		YKO_0825	E06	0.966	+	+	+	
5527	YPR111W	25	E	7		YKO_0825	E07	0.993	+	+	+	
5530	YPR114W	25	E	8	grows on -met, grows on -lys	YKO_0825	E08	0.703	+	+	-	HIT
5531	YPR115W	25	E	9		YKO_0825	E09	0.718	+	+	+	
5532	YPR116W	25	E	10	slow growth, petite	YKO_0825	E10	0.892	-	-	-	Doubt
5533	YPR117W	25	E	11		YKO_0825	E11	0.954	+	+	+	
5534	YPR119W	25	E	12		YKO_0825	E12	0.875	+	+	+	
5535	YPR120C	25	F	1		YKO_0825	F01	0.776	+	+	+	
5536	YPR121W	25	F	2		YKO_0825	F02	0.985	+	+	+	
5537	YPR122W	25	F	3		YKO_0825	F03	0.999	+	+	+	
5538	YPR123C	25	F	4	petite	YKO_0825	F04	0.971	+	+	+	
5539	YPR124W	25	F	5	slow growth, petite	YKO_0825	F05	0.679	slow	+	+	
5540	YPR125W	25	F	6		YKO_0825	F06	0.985	+	+	+	
5541	YPR126C	25	F	7		YKO_0825	F07	0.841	+	+	+	
5542	YPR127W	25	F	8		YKO_0825	F08	0.908	+	+	+	
5543	YPR128C	25	F	9		YKO_0825	F09	0.975	+	+	+	
5544	YPR129W	25	F	10		YKO_0825	F10	0.532	+	-	+	Incongruence
5545	YPR130C	25	F	11		YKO_0825	F11	0.866	+	+	+	
7391	YOL151W	25	F	12		YKO_0825	F12	0.995	+	+	+	
5547	YPR132W	25	G	1		YKO_0825	G01	0.882	+	+	+	
5549	YPR134W	25	G	2	slow growth	YKO_0825	G02	0.964	slow	+	-	Doubt
5550	YPR135W	25	G	3		YKO_0825	G03	0.793	slow	+	+	
5553	YPR138C	25	G	4		YKO_0825	G04	0.894	+	+	+	
5554	YPR139C	25	G	5		YKO_0825	G05	0.828	+	+	+	
5555	YPR140W	25	G	6		YKO_0825	G06	0.889	+	+	+	
5556	YPR141C	25	G	7		YKO_0825	G07	0.977	+	+	+	
5560	YPR145W	25	G	8		YKO_0825	G08	0.97	+	+	+	
5561	YPR146C	25	G	9		YKO_0825	G09	0.958	+	+	+	
5562	YPR147C	25	G	10		YKO_0825	G10	0.972	+	+	+	
5563	YPR148C	25	G	11		YKO_0825	G11	0.922	+	+	+	
5564	YPR149W	25	G	12		YKO_0825	G12	0.953	+	+	+	
5565	YPR150W	25	H	1		YKO_0825	H01	1.023	+	+	+	
--		25	H	2	empty	YKO_0825	H02	empty	empty	empty	empty	empty
5567	YPR152C	25	H	3		YKO_0825	H03	1.008	+	+	+	
5568	YPR153W	25	H	4	bi-mater	YKO_0825	H04	0.929	+	+	+	
5569	YPR154W	25	H	5		YKO_0825	H05	1.005	+	+	+	
5570	YPR155C	25	H	6		YKO_0825	H06	0.849	+	+	+	
5571	YPR156C	25	H	7		YKO_0825	H07	0.932	+	+	+	
5572	YPR157W	25	H	8		YKO_0825	H08	1.027	+	-	+	Incongruence
5573	YPR158W	25	H	9		YKO_0825	H09	0.987	+	-	+	Incongruence
5574	YPR159W	25	H	10		YKO_0825	H10	0.908	+	+	+	
5575	YPR160W	25	H	11	slow growth	YKO_0825	H11	0.922	+	+	+	
5578	YPR163C	25	H	12		YKO_0825	H12	1.012	+	-	+	Incongruence
5579	YPR164W	26	A	1		YKO_0826	A01	0.773	+	+	+	
5581	YPR166C	26	A	2	slow growth, petite	YKO_0826	A02	0.944	+	+	+	
5582	YPR167C	26	A	3		YKO_0826	A03	0.96	+	+	+	
5585	YPR170C	26	A	4		YKO_0826	A04	0.876	+	+	+	
5586	YPR171W	26	A	5		YKO_0826	A05	0.931	+	+	+	
5587	YPR172W	26	A	6		YKO_0826	A06	0.923	+	+	+	
5588	YPR173C	26	A	7		YKO_0826	A07	0.966	+	+	+	
5589	YPR174C	26	A	8		YKO_0826	A08	0.982	+	+	+	
5594	YPR179C	26	A	9		YKO_0826	A09	0.817	+	+	+	

	Euroscarf Information					Replica plate Information			Tau Toxicity Enhancer Primary Screen Results			
record no.	ORF name	Plate	Row	Col	Comment	Replica plate	Well	YPD (OD600nm)	Growth plate (SC+GAL comp.)	Transformation control plate (SC+GLU-Leu)	TEST Plate (SC+GAL-Leu)	Classification
5599	YPR184W	26	A	10		YKO_0826	A10	0.987	+	+	+	
5600	YPR185W	26	A	11		YKO_0826	A11	0.917	+	+	+	
5603	YPR188C	26	A	12		YKO_0826	A12	0.907	+	+	+	
5604	YPR189W	26	B	1		YKO_0826	B01	0.942	+	+	+	
5606	YPR191W	26	B	2	slow growth, petite	YKO_0826	B02	0.764	+	+	+	
5607	YPR192W	26	B	3		YKO_0826	B03	0.898	+	+	+	
5608	YPR193C	26	B	4		YKO_0826	B04	0.788	+	+	+	
5609	YPR194C	26	B	5		YKO_0826	B05	0.625	+	+	+	
5610	YPR195C	26	B	6		YKO_0826	B06	0.926	+	+	+	
5611	YPR196W	26	B	7		YKO_0826	B07	0.854	+	+	+	
5612	YPR197C	26	B	8		YKO_0826	B08	0.898	+	+	+	
5613	YPR198W	26	B	9		YKO_0826	B09	0.966	+	+	+	
5614	YPR199C	26	B	10		YKO_0826	B10	0.958	+	+	+	
5615	YPR200C	26	B	11		YKO_0826	B11	0.88	+	+	+	
5616	YPR201W	26	B	12		YKO_0826	B12	1.006	+	+	-	HIT
5809	YCR090C	26	C	1		YKO_0826	C01	1.025	+	+	+	
--		26	C	2	empty	YKO_0826	C02	empty	empty	empty	empty	empty
5810	YCR091W	26	C	3		YKO_0826	C03	0.985	+	+	+	
5811	YCR092C	26	C	4		YKO_0826	C04	1.034	+	+	+	
5813	YCR094W	26	C	5		YKO_0826	C05	0.934	+	+	-	HIT
5815	YCR098C	26	C	6		YKO_0826	C06	0.999	+	+	+	
5816	YCR099C	26	C	7		YKO_0826	C07	0.994	+	+	-	HIT
5817	YCR100C	26	C	8		YKO_0826	C08	0.979	+	+	+	
5818	YCR101C	26	C	9		YKO_0826	C09	1.016	+	+	+	
5819	YCR102C	26	C	10		YKO_0826	C10	0.985	+	+	+	
5821	YCR105W	26	C	11		YKO_0826	C11	0.948	+	+	+	
5822	YCR106W	26	C	12		YKO_0826	C12	0.967	+	+	+	
5823	YDL130W-A	26	D	1		YKO_0826	D01	1.035	+	+	+	
5828	YDR363W-A	26	D	2		YKO_0826	D02	0.763	+	+	+	
5829	YDR525W-A	26	D	3		YKO_0826	D03	0.95	+	+	+	
5830	YDR535C	26	D	4		YKO_0826	D04	0.979	+	+	+	
5831	YDR536W	26	D	5		YKO_0826	D05	0.955	+	+	+	
5833	YDR538W	26	D	6		YKO_0826	D06	0.978	+	+	+	
5834	YDR539W	26	D	7		YKO_0826	D07	0.914	+	+	+	
5835	YDR540C	26	D	8		YKO_0826	D08	0.989	+	+	+	
5836	YDR541C	26	D	9		YKO_0826	D09	0.996	+	+	+	
5838	YER039C-A	26	D	10		YKO_0826	D10	0.983	+	+	+	
5841	YER091C-A	26	D	11		YKO_0826	D11	0.919	+	+	+	
5842	YER144C	26	D	12		YKO_0826	D12	0.913	+	+	+	
5843	YER188W	26	E	1		YKO_0826	E01	1.017	+	+	+	
5844	YFL034C-A	26	E	2		YKO_0826	E02	0.975	+	+	+	
5845	YFR032C	26	E	3		YKO_0826	E03	0.975	+	+	+	
5846	YFR032C-A	26	E	4		YKO_0826	E04	0.903	slow	-	+	Incongruence
5847	YFR033C	26	E	5		YKO_0826	E05	1.014	+	+	+	
5848	YFR034C	26	E	6		YKO_0826	E06	0.904	+	+	+	
5849	YFR035C	26	E	7		YKO_0826	E07	0.964	+	+	+	
5850	YFR036W	26	E	8		YKO_0826	E08	0.615	+	+	+	
5852	YFR038W	26	E	9	Incorrect.	YKO_0826	E09	0.984	+	+	+	
5854	YFR040W	26	E	10		YKO_0826	E10	0.981	+	+	+	
5855	YFR041C	26	E	11		YKO_0826	E11	0.96	+	+	+	
5857	YFR043C	26	E	12		YKO_0826	E12	0.888	+	-	+	Incongruence
5858	YFR044C	26	F	1		YKO_0826	F01	0.706	+	+	+	
5859	YFR045W	26	F	2		YKO_0826	F02	0.974	+	+	+	
5860	YFR046C	26	F	3		YKO_0826	F03	0.964	+	+	+	
5861	YFR047C	26	F	4		YKO_0826	F04	0.983	+	+	+	
5862	YFR048W	26	F	5		YKO_0826	F05	1.051	-	-	-	Doubt
5863	YFR049W	26	F	6		YKO_0826	F06	0.96	+	-	+	Incongruence
5867	YFR053C	26	F	7		YKO_0826	F07	0.988	+	+	+	
5868	YFR054C	26	F	8		YKO_0826	F08	0.897	+	+	+	
5869	YFR055W	26	F	9		YKO_0826	F09	0.914	+	+	+	
5870	YFR056C	26	F	10		YKO_0826	F10	0.854	+	-	+	Incongruence
5871	YFR057W	26	F	11		YKO_0826	F11	0.971	+	+	+	
5873	YGR220C	26	F	12	slow growth	YKO_0826	F12	0.881	-	-	-	Doubt
5874	YGR221C	26	G	1		YKO_0826	G01	0.998	+	+	+	
5876	YGR223C	26	G	2		YKO_0826	G02	0.913	+	+	+	
5877	YGR224W	26	G	3		YKO_0826	G03	0.907	+	+	+	
5878	YGR225W	26	G	4		YKO_0826	G04	0.786	+	+	+	
5879	YGR226C	26	G	5		YKO_0826	G05	0.965	+	+	+	
5880	YGR227W	26	G	6		YKO_0826	G06	0.926	+	+	+	
5881	YGR228W	26	G	7		YKO_0826	G07	0.905	+	-	+	Incongruence
5883	YGR230W	26	G	8		YKO_0826	G08	0.986	+	+	+	
5884	YGR231C	26	G	9		YKO_0826	G09	0.962	+	+	-	HIT
5885	YGR232W	26	G	10		YKO_0826	G10	0.908	+	+	+	
5886	YGR233C	26	G	11		YKO_0826	G11	0.93	+	+	+	
5887	YGR234W	26	G	12		YKO_0826	G12	0.852	+	+	+	
5888	YGR235C	26	H	1		YKO_0826	H01	0.966	+	+	+	
--		26	H	2	empty	YKO_0826	H02	empty	empty	empty	empty	empty
5889	YGR236C	26	H	3		YKO_0826	H03	0.951	+	+	+	
5890	YGR237C	26	H	4		YKO_0826	H04	0.968	+	-	+	Incongruence
5893	YGR240C	26	H	5		YKO_0826	H05	0.981	+	-	+	Incongruence
5894	YGR241C	26	H	6		YKO_0826	H06	0.997	+	+	+	
5895	YGR242W	26	H	7		YKO_0826	H07	1.028	+	+	+	
5896	YGR243W	26	H	8		YKO_0826	H08	1.012	+	+	+	
5897	YGR244C	26	H	9		YKO_0826	H09	1.028	+	+	+	

	Euroscarf Information					Replica plate Information			Tau Toxicity Enhancer Primary Screen Results			
record no.	ORF name	Plate	Row	Col	Comment	Replica plate	Well	YPD (OD600nm)	Growth plate (SC+GAL comp.)	Transformation control plate (SC+GLU-Leu)	TEST Plate (SC+GAL-Leu)	Classification
5900	YGR247W	26	H	10		YKO_0826	H10	1.013	+	+	+	
5902	YGR249W	26	H	11		YKO_0826	H11	0.951	+	+	+	
3025	YBL001C	26	H	12		YKO_0826	H12	1.018	+	+	+	
7392	YOL152W	27	A	1		YKO_0827	A01	1.0769	+	+	+	
3027	YBL003C	27	A	2		YKO_0827	A02	1.0534	+	+	+	
3029	YBL005W	27	A	3		YKO_0827	A03	0.8221	+	+	+	
3032	YBL006C	27	A	4		YKO_0827	A04	0.6544	+	+	+	
3033	YBL007C	27	A	5		YKO_0827	A05	0.7209	+	+	+	
3034	YBL008W	27	A	6		YKO_0827	A06	0.7009	+	+	+	
3035	YBL009W	27	A	7		YKO_0827	A07	0.7012	+	+	+	
3036	YBL010C	27	A	8		YKO_0827	A08	1.1105	+	+	+	
3037	YBL011W	27	A	9		YKO_0827	A09	0.6986	+	+	+	
3038	YBL012C	27	A	10	slow growth, petite	YKO_0827	A10	0.6198	slow	+	-	Doubt
3039	YBL013W	27	A	11		YKO_0827	A11	0.7213	+	+	-	HIT
3041	YBL015W	27	A	12		YKO_0827	A12	0.7451	+	+	+	
3042	YBL016W	27	B	1		YKO_0827	B01	1.0323	+	+	+	
3043	YBL017C	27	B	2		YKO_0827	B02	0.9824	+	+	+	
3045	YBL019W	27	B	3		YKO_0827	B03	1.0278	+	+	+	
3047	YBL021C	27	B	4	slow growth, petite	YKO_0827	B04	1.0351	slow	+	+	
3048	YBL022C	27	B	5	slow growth, petite	YKO_0827	B05	0.9862	-	+	-	Doubt
3050	YBL024W	27	B	6		YKO_0827	B06	1.0654	+	+	+	
3053	YBL027W	27	B	7		YKO_0827	B07	1.067	+	-	+	Incongruence
3054	YBL028C	27	B	8		YKO_0827	B08	0.8897	+	+	-	HIT
3055	YBL029W	27	B	9		YKO_0827	B09	1.0357	+	+	+	
3057	YBL031W	27	B	10		YKO_0827	B10	0.7411	+	+	+	
3058	YBL032W	27	B	11		YKO_0827	B11	0.7241	+	+	+	
3062	YBL036C	27	B	12		YKO_0827	B12	0.7381	+	+	+	
3063	YBL037W	27	C	1		YKO_0827	C01	1.032	+	+	+	
3064	YBL038W	27	C	2	slow growth, petite	YKO_0827	C02	0.9912	slow	+	-	Doubt
--		27	C	3	empty	YKO_0827	C03	empty	empty	empty	empty	empty
3065	YBL039C	27	C	4		YKO_0827	C04	0.9988	+	+	+	
3068	YBL042C	27	C	5		YKO_0827	C05	1.024	+	+	+	
3069	YBL043W	27	C	6		YKO_0827	C06	1.0783	+	+	+	
3070	YBL044W	27	C	7	slow growth, petite	YKO_0827	C07	1.0144	slow	+	-	Doubt
3071	YBL045C	27	C	8	slow growth, petite	YKO_0827	C08	0.6831	slow	+	-	Doubt
3072	YBL046W	27	C	9		YKO_0827	C09	0.7201	+	+	+	
3073	YBL047C	27	C	10		YKO_0827	C10	0.7611	+	+	+	
3074	YBL048W	27	C	11		YKO_0827	C11	0.7407	+	+	+	
3075	YBL049W	27	C	12		YKO_0827	C12	0.7417	+	+	+	
3077	YBL051C	27	D	1		YKO_0827	D01	1.0123	+	+	+	
3078	YBL052C	27	D	2		YKO_0827	D02	0.9883	+	+	+	
3079	YBL053W	27	D	3		YKO_0827	D03	0.9996	+	+	+	
3080	YBL054W	27	D	4		YKO_0827	D04	1.0308	+	+	+	
3081	YBL055C	27	D	5		YKO_0827	D05	1.0449	+	+	+	
3082	YBL056W	27	D	6		YKO_0827	D06	1.0432	+	+	+	
3083	YBL057C	27	D	7		YKO_0827	D07	1.0101	+	+	+	
3084	YBL058W	27	D	8		YKO_0827	D08	not grown	-	-	-	Not grown
3085	YBL059W	27	D	9		YKO_0827	D09	1.0018	+	+	+	
3086	YBL060W	27	D	10		YKO_0827	D10	0.9982	+	+	+	
3087	YBL061C	27	D	11		YKO_0827	D11	0.694	+	+	+	
3088	YBL062W	27	D	12		YKO_0827	D12	1.0675	+	+	+	
3089	YBL063W	27	E	1		YKO_0827	E01	1.0691	+	+	+	
3090	YBL064C	27	E	2		YKO_0827	E02	0.9988	+	+	+	
3091	YBL065W	27	E	3		YKO_0827	E03	0.9852	+	+	+	
3092	YBL066C	27	E	4		YKO_0827	E04	1.0541	+	+	+	
3093	YBL067C	27	E	5		YKO_0827	E05	0.5781	+	+	+	
3094	YBL068W	27	E	6		YKO_0827	E06	1.1195	+	+	+	
3095	YBL069W	27	E	7		YKO_0827	E07	1.06	+	-	+	Incongruence
3096	YBL070C	27	E	8		YKO_0827	E08	1.0827	+	+	+	
3097	YBL071C	27	E	9		YKO_0827	E09	1.0546	+	-	-	Doubt
3098	YBL072C	27	E	10		YKO_0827	E10	0.8911	+	+	+	
3101	YBL075C	27	E	11		YKO_0827	E11	1.0873	+	+	+	
3104	YBL078C	27	E	12		YKO_0827	E12	1.0119	+	+	+	
3105	YBL079W	27	F	1		YKO_0827	F01	0.9972	+	+	+	
3106	YBL080C	27	F	2	slow growth, petite	YKO_0827	F02	0.9905	+	+	+	
3107	YBL081W	27	F	3		YKO_0827	F03	0.9653	+	+	+	
3108	YBL082C	27	F	4		YKO_0827	F04	1.0098	+	+	+	
3109	YBL083C	27	F	5		YKO_0827	F05	0.9908	+	+	+	
3111	YBL085W	27	F	6		YKO_0827	F06	1.0639	+	+	+	
3112	YBL086C	27	F	7		YKO_0827	F07	1.0304	+	+	+	
3113	YBL087C	27	F	8		YKO_0827	F08	1.0658	+	+	+	
3114	YBL088C	27	F	9		YKO_0827	F09	1.0389	+	-	+	Incongruence
3115	YBL089W	27	F	10		YKO_0827	F10	1.048	+	+	+	
3116	YBL090W	27	F	11	slow growth, petite	YKO_0827	F11	0.6541	-	+	-	Doubt
3117	YBL091C	27	F	12		YKO_0827	F12	0.9413	+	+	+	
7394	YPL158C	27	G	1		YKO_0827	G01	1.0434	+	+	+	
3120	YBL094C	27	G	2		YKO_0827	G02	1.0206	+	+	+	
4370	YGL002W	27	G	3		YKO_0827	G03	0.9838	+	+	+	
4371	YGL003C	27	G	4		YKO_0827	G04	1.0867	+	+	+	
4372	YGL004C	27	G	5		YKO_0827	G05	1.0165	+	+	+	
4373	YGL005C	27	G	6		YKO_0827	G06	1.0648	+	+	+	
4374	YGL006W	27	G	7		YKO_0827	G07	1.0465	+	+	+	
4375	YGL007W	27	G	8		YKO_0827	G08	1.0731	+	+	+	
4378	YGL010W	27	G	9		YKO_0827	G09	0.7248	+	-	-	Doubt

	Euroscarf Information					Replica plate Information			Tau Toxicity Enhancer Primary Screen Results			
record no.	ORF name	Plate	Row	Col	Comment	Replica plate	Well	YPD (OD600nm)	Growth plate (SC+GAL comp.)	Transformation control plate (SC+GLU-Leu)	TEST Plate (SC+GAL-Leu)	Classification
4380	YGL012W	27	G	10	growth on -met, no growth on -lys, mates like alpha, no growth on drop-in media. PCR mating type alpha	YKO_0827	G10	1.0634	+	+	+	
4381	YGL013C	27	G	11		YKO_0827	G11	1.0438	+	+	+	
4382	YGL014W	27	G	12		YKO_0827	G12	0.7679	+	+	+	
4383	YGL015C	27	H	1		YKO_0827	H01	1.0084	+	-	+	Incongruence
--		27	H	2	empty	YKO_0827	H02	empty	empty	empty	empty	empty
4384	YGL016W	27	H	3		YKO_0827	H03	0.7326	+	+	+	
4385	YGL017W	27	H	4		YKO_0827	H04	0.6995	+	+	+	
4387	YGL019W	27	H	5		YKO_0827	H05	0.7519	+	+	-	HIT
4389	YGL021W	27	H	6		YKO_0827	H06	0.7335	+	+	+	
4391	YGL023C	27	H	7		YKO_0827	H07	0.5972	+	+	+	
4392	YGL024W	27	H	8		YKO_0827	H08	0.6964	+	+	+	
4393	YGL025C	27	H	9		YKO_0827	H09	0.7169	+	+	+	
4394	YGL026C	27	H	10	no growth on drop-in media	YKO_0827	H10	0.719	+	+	+	
4395	YGL027C	27	H	11		YKO_0827	H11	0.7649	+	+	+	
4396	YGL028C	27	H	12		YKO_0827	H12	0.7507	+	+	+	
7396	YPL194W	28	A	1		YKO_0828	A01	0.857	+	+	+	
4399	YGL031C	28	A	2		YKO_0828	A02	0.901	+	-	+	Incongruence
4400	YGL032C	28	A	3		YKO_0828	A03	0.99	+	+	+	
4401	YGL033W	28	A	4		YKO_0828	A04	0.893	+	+	+	
4402	YGL034C	28	A	5		YKO_0828	A05	0.987	+	+	+	
4403	YGL035C	28	A	6		YKO_0828	A06	0.97	+	+	+	
4404	YGL036W	28	A	7		YKO_0828	A07	0.964	+	+	+	
4405	YGL037C	28	A	8		YKO_0828	A08	0.983	+	+	+	
4407	YGL039W	28	A	9		YKO_0828	A09	0.992	+	+	+	
4409	YGL041C	28	A	10		YKO_0828	A10	0.976	+	+	+	
4410	YGL042C	28	A	11		YKO_0828	A11	0.954	+	+	+	
4411	YGL043W	28	A	12		YKO_0828	A12	0.951	+	+	+	
4413	YGL045W	28	B	1		YKO_0828	B01	0.981	+	+	+	
4414	YGL046W	28	B	2		YKO_0828	B02	0.952	+	+	+	
4417	YGL049C	28	B	3		YKO_0828	B03	0.944	+	+	+	
4418	YGL050W	28	B	4		YKO_0828	B04	0.986	+	+	+	
4419	YGL051W	28	B	5		YKO_0828	B05	0.975	+	+	+	
4420	YGL053W	28	B	6		YKO_0828	B06	1.003	+	+	+	
4421	YGL054C	28	B	7		YKO_0828	B07	0.968	+	+	+	
4423	YGL056C	28	B	8		YKO_0828	B08	0.991	+	+	+	
4424	YGL057C	28	B	9		YKO_0828	B09	0.994	+	+	+	
4425	YGL058W	28	B	10		YKO_0828	B10	0.712	slow	+	+	
4426	YGL059W	28	B	11		YKO_0828	B11	0.976	+	+	+	
4427	YGL060W	28	B	12		YKO_0828	B12	1.03	+	+	+	
4429	YGL062W	28	C	1		YKO_0828	C01	0.991	+	+	+	
4430	YGL063W	28	C	2		YKO_0828	C02	0.968	+	+	+	
4431	YGL064C	28	C	3	slow growth, petite	YKO_0828	C03	0.957	slow	+	-	Doubt
--		28	C	4	empty	YKO_0828	C04	empty	empty	empty	empty	empty
4433	YGL066W	28	C	5		YKO_0828	C05	0.761	+	+	+	
4434	YGL067W	28	C	6		YKO_0828	C06	1.008	+	+	+	
4438	YGL071W	28	C	7	petite	YKO_0828	C07	0.728	+	+	-	HIT
4439	YGL072C	28	C	8		YKO_0828	C08	0.671	slow	+	-	Doubt
4443	YGL076C	28	C	9		YKO_0828	C09	1.041	slow	-	-	Doubt
4444	YGL077C	28	C	10		YKO_0828	C10	0.926	+	+	+	
4445	YGL078C	28	C	11		YKO_0828	C11	0.935	+	+	+	
4446	YGL079W	28	C	12		YKO_0828	C12	0.995	+	+	+	
4447	YGL080W	28	D	1		YKO_0828	D01	1.052	+	-	-	Doubt
4448	YGL081W	28	D	2		YKO_0828	D02	not grown	-	-	-	Not grown
4449	YGL082W	28	D	3		YKO_0828	D03	0.823	+	+	+	
4450	YGL083W	28	D	4		YKO_0828	D04	0.992	+	+	+	
4451	YGL084C	28	D	5		YKO_0828	D05	1.054	+	+	+	
4452	YGL085W	28	D	6		YKO_0828	D06	1.027	+	+	+	
4453	YGL086W	28	D	7		YKO_0828	D07	0.935	+	-	+	Incongruence
4454	YGL087C	28	D	8		YKO_0828	D08	0.862	+	+	+	
4456	YGL089C	28	D	9		YKO_0828	D09	1.032	+	+	+	
4457	YGL090W	28	D	10		YKO_0828	D10	0.975	+	+	+	
4461	YGL094C	28	D	11		YKO_0828	D11	0.917	+	+	+	
4463	YGL096W	28	D	12		YKO_0828	D12	0.991	+	+	+	
1970	YNL242W	28	E	1		YKO_0828	E01	0.974	+	+	+	
1971	YNL241C	28	E	2		YKO_0828	E02	0.938	+	+	+	
1973	YNL239W	28	E	3		YKO_0828	E03	0.988	+	+	+	
1974	YNL238W	28	E	4		YKO_0828	E04	0.938	+	+	+	
1975	YNL237W	28	E	5		YKO_0828	E05	0.88	+	+	+	
1976	YNL236W	28	E	6		YKO_0828	E06	1.004	+	+	+	
1977	YNL235C	28	E	7		YKO_0828	E07	1.015	+	+	+	
1978	YNL234W	28	E	8		YKO_0828	E08	0.979	+	+	+	
1979	YNL233W	28	E	9		YKO_0828	E09	0.788	+	+	+	
1981	YNL231C	28	E	10		YKO_0828	E10	0.91	+	+	+	
1982	YNL230C	28	E	11		YKO_0828	E11	0.921	+	+	+	
1983	YNL229C	28	E	12		YKO_0828	E12	0.832	+	+	+	
1984	YNL228W	28	F	1		YKO_0828	F01	0.969	+	-	+	Incongruence
1985	YNL226W	28	F	2		YKO_0828	F02	0.935	+	+	+	
1986	YNL227C	28	F	3		YKO_0828	F03	0.954	+	-	+	Incongruence
1988	YNL224C	28	F	4		YKO_0828	F04	0.951	+	+	+	

Euroscarf Information						Replica plate Information			Tau Toxicity Enhancer Primary Screen Results			
record no.	ORF name	Plate	Row	Col	Comment	Replica plate	Well	YPD (OD600nm)	Growth plate (SC+GAL comp.)	Transformation control plate (SC+GLU-Leu)	TEST Plate (SC+GAL-Leu)	Classification
1989	YNL223W	28	F	5		YKO_0828	F05	1.006	+	+	+	
1993	YNL219C	28	F	6		YKO_0828	F06	0.846	+	+	+	
1994	YNL218W	28	F	7	grows well on -met, no growth on -lys	YKO_0828	F07	0.846	+	+	+	
1995	YNL217W	28	F	8		YKO_0828	F08	0.997	+	+	+	
1997	YNL215W	28	F	9		YKO_0828	F09	0.727	+	+	+	
1998	YNL214W	28	F	10		YKO_0828	F10	0.887	+	+	+	
1999	YNL213C	28	F	11	slow growth, petite	YKO_0828	F11	0.928	-	+	-	Doubt
2000	YNL212W	28	F	12		YKO_0828	F12	0.975	+	+	+	
2001	YNL211C	28	G	1		YKO_0828	G01	0.929	+	+	+	
2004	YNL208W	28	G	2		YKO_0828	G02	0.992	+	+	+	
2006	YNL206C	28	G	3		YKO_0828	G03	0.945	+	-	+	Incongruence
2007	YNL205C	28	G	4		YKO_0828	G04	0.878	+	+	+	
2008	YNL204C	28	G	5		YKO_0828	G05	1.013	+	+	+	
2009	YNL202W	28	G	6		YKO_0828	G06	0.854	+	+	+	
2010	YNL203C	28	G	7		YKO_0828	G07	0.941	+	+	+	
2011	YNL201C	28	G	8		YKO_0828	G08	0.821	+	+	+	
2012	YNL200C	28	G	9		YKO_0828	G09	0.998	+	+	+	
2013	YNL199C	28	G	10		YKO_0828	G10	0.786	+	+	+	
2014	YNL198C	28	G	11		YKO_0828	G11	0.839	+	+	+	
2015	YNL197C	28	G	12		YKO_0828	G12	0.929	+	+	+	
2016	YNL196C	28	H	1		YKO_0828	H01	0.979	+	+	+	
--		28	H	2	empty	YKO_0828	H02	empty	empty	empty	empty	empty
2017	YNL195C	28	H	3		YKO_0828	H03	0.942	+	+	+	
2018	YNL194C	28	H	4		YKO_0828	H04	0.914	+	+	+	
2019	YNL193W	28	H	5		YKO_0828	H05	1.022	+	+	+	
2020	YNL192W	28	H	6		YKO_0828	H06	0.992	+	+	+	
2021	YNL191W	28	H	7		YKO_0828	H07	0.97	+	+	+	
2022	YNL190W	28	H	8		YKO_0828	H08	1.038	+	+	+	
2025	YNL187W	28	H	9		YKO_0828	H09	0.952	+	+	+	
2028	YNL184C	28	H	10	slow growth, petite	YKO_0828	H10	0.945	slow	-	-	Doubt
2029	YNL183C	28	H	11		YKO_0828	H11	0.913	+	+	+	
2033	YNL179C	28	H	12		YKO_0828	H12	1.013	+	+	+	
2035	YNL177C	29	A	1	slow growth, petite	YKO_0829	A01	0.817	slow	+	-	Doubt
2036	YNL176C	29	A	2		YKO_0829	A02	0.872	+	+	+	
2038	YNL175C	29	A	3		YKO_0829	A03	0.958	+	+	+	
2039	YNL173C	29	A	4		YKO_0829	A04	0.989	+	+	+	
2041	YNL170W	29	A	5	slow growth, petite	YKO_0829	A05	0.887	slow	+	-	Doubt
2042	YNL171C	29	A	6		YKO_0829	A06	0.745	+	+	-	HIT
2043	YNL169C	29	A	7		YKO_0829	A07	0.948	+	+	+	
2044	YNL168C	29	A	8		YKO_0829	A08	0.963	+	+	+	
2045	YNL167C	29	A	9		YKO_0829	A09	0.997	+	+	+	
2046	YNL166C	29	A	10		YKO_0829	A10	0.992	+	+	+	
2047	YNL165W	29	A	11		YKO_0829	A11	1.002	+	+	+	
2048	YNL164C	29	A	12		YKO_0829	A12	1.007	+	+	+	
2050	YNL162W	29	B	1		YKO_0829	B01	0.922	+	+	+	
2052	YNL160W	29	B	2	slow growth, petite	YKO_0829	B02	0.864	slow	+	-	Doubt
2053	YNL159C	29	B	3		YKO_0829	B03	0.945	+	+	+	
2055	YNL157W	29	B	4		YKO_0829	B04	0.944	+	+	+	
2056	YNL156C	29	B	5		YKO_0829	B05	0.986	+	+	+	
2057	YNL155W	29	B	6		YKO_0829	B06	0.664	+	+	+	
2058	YNL154C	29	B	7		YKO_0829	B07	0.944	+	+	+	
2064	YNL148C	29	B	8		YKO_0829	B08	0.749	+	+	+	
5041	YKL191W	29	B	9		YKO_0829	B09	0.975	+	+	+	
5047	YKL197C	29	B	10		YKO_0829	B10	0.872	+	+	+	
5048	YKL198C	29	B	11		YKO_0829	B11	0.96	+	+	+	
5049	YKL199C	29	B	12		YKO_0829	B12	0.952	+	+	+	
5050	YKL200C	29	C	1		YKO_0829	C01	0.975	+	+	+	
5055	YKL205W	29	C	2		YKO_0829	C02	0.936	+	+	+	
5056	YKL206C	29	C	3		YKO_0829	C03	0.993	+	+	+	
5057	YKL207W	29	C	4		YKO_0829	C04	1.023	+	+	+	
--		29	C	5	empty	YKO_0829	C05	empty	empty	empty	empty	empty
5058	YKL208W	29	C	6	petite	YKO_0829	C06	0.888	slow	+	-	Doubt
5061	YKL211C	29	C	7	no growth on drop-in media	YKO_0829	C07	0.746	+	+	-	HIT
5062	YKL212W	29	C	8		YKO_0829	C08	0.914	+	-	-	Doubt
5063	YKL213C	29	C	9		YKO_0829	C09	0.682	+	+	+	
5064	YKL214C	29	C	10		YKO_0829	C10	0.975	+	+	+	
5066	YKL216W	29	C	11		YKO_0829	C11	0.94	+	+	+	
5067	YKL217W	29	C	12		YKO_0829	C12	0.989	+	+	+	
5068	YKL218C	29	D	1		YKO_0829	D01	1.021	+	+	+	
5070	YKL221W	29	D	2		YKO_0829	D02	0.96	+	+	+	
5071	YKL222C	29	D	3		YKO_0829	D03	0.934	+	+	+	
5072	YKR001C	29	D	4		YKO_0829	D04	0.655	slow	-	+	Incongruence
5074	YKR003W	29	D	5		YKO_0829	D05	0.834	+	+	+	
5076	YKR005C	29	D	6		YKO_0829	D06	0.985	+	+	+	
5078	YKR007W	29	D	7		YKO_0829	D07	0.32	+	-	-	Doubt
5080	YKR009C	29	D	8		YKO_0829	D08	0.943	+	+	+	
5082	YKR011C	29	D	9		YKO_0829	D09	0.931	+	+	+	
5083	YKR012C	29	D	10		YKO_0829	D10	0.944	+	+	+	
5084	YKR013W	29	D	11		YKO_0829	D11	0.896	+	+	+	
5085	YKR014C	29	D	12		YKO_0829	D12	1.026	+	+	+	
5086	YKR015C	29	E	1		YKO_0829	E01	0.939	+	+	+	
5087	YKR016W	29	E	2		YKO_0829	E02	0.921	+	+	+	

	Euroscarf Information					Replica plate Information			Tau Toxicity Enhancer Primary Screen Results			
record no.	ORF name	Plate	Row	Col	Comment	Replica plate	Well	YPD (OD600nm)	Growth plate (SC+GAL comp.)	Transformation control plate (SC+GLU-Leu)	TEST Plate (SC+GAL-Leu)	Classification
5088	YKR017C	29	E	3		YKO_0829	E03	0.951	+	+	+	
5089	YKR018C	29	E	4		YKO_0829	E04	0.959	+	+	+	
5091	YKR020W	29	E	5		YKO_0829	E05	0.835	+	+	+	
5092	YKR021W	29	E	6		YKO_0829	E06	0.91	+	+	+	
5095	YKR024C	29	E	7	slow growth	YKO_0829	E07	0.925	slow	-	-	Doubt
5097	YKR026C	29	E	8		YKO_0829	E08	0.842	+	+	+	
5101	YKR030W	29	E	9		YKO_0829	E09	0.923	+	+	+	
5102	YKR031C	29	E	10		YKO_0829	E10	0.789	+	+	+	
5103	YKR032W	29	E	11		YKO_0829	E11	0.949	+	+	+	
5104	YKR033C	29	E	12		YKO_0829	E12	0.911	+	+	+	
5106	YKR035C	29	F	1		YKO_0829	F01	0.785	+	+	+	
5113	YKR042W	29	F	2		YKO_0829	F02	0.978	+	+	+	
5114	YKR043C	29	F	3	slow growth	YKO_0829	F03	0.878	+	+	+	
5115	YKR044W	29	F	4		YKO_0829	F04	0.941	+	+	+	
5116	YKR045C	29	F	5		YKO_0829	F05	0.894	+	+	+	
5118	YKR047W	29	F	6		YKO_0829	F06	0.8	+	+	+	
5119	YKR048C	29	F	7		YKO_0829	F07	0.903	+	+	+	
5120	YKR049C	29	F	8		YKO_0829	F08	0.939	+	+	+	
5121	YKR050W	29	F	9		YKO_0829	F09	0.956	+	+	+	
5122	YKR051W	29	F	10		YKO_0829	F10	0.839	+	+	+	
5123	YKR052C	29	F	11		YKO_0829	F11	0.878	+	+	+	
5125	YKR054C	29	F	12		YKO_0829	F12	0.721	+	+	+	
5126	YKR055W	29	G	1	petite	YKO_0829	G01	0.824	+	+	-	HIT
5127	YKR056W	29	G	2		YKO_0829	G02	0.92	+	+	+	
5128	YKR057W	29	G	3		YKO_0829	G03	0.832	+	+	+	
5129	YKR058W	29	G	4	slow growth	YKO_0829	G04	0.886	+	+	-	HIT
5130	YKR059W	29	G	5		YKO_0829	G05	0.869	+	+	+	
5131	YKR060W	29	G	6		YKO_0829	G06	0.705	+	-	+	Incongruence
5132	YKR061W	29	G	7		YKO_0829	G07	0.92	+	+	+	
5135	YKR064W	29	G	8		YKO_0829	G08	0.91	+	+	+	
5136	YKR065C	29	G	9		YKO_0829	G09	0.789	slow	+	+	
3603	YDR244W	29	G	10		YKO_0829	G10	0.794	slow	+	-	Doubt
3606	YDR247W	29	G	11		YKO_0829	G11	0.942	+	-	+	Incongruence
3607	YDR248C	29	G	12		YKO_0829	G12	0.892	+	+	+	
3608	YDR249C	29	H	1		YKO_0829	H01	0.883	+	+	+	
--		29	H	2	empty	YKO_0829	H02	empty	empty	empty	empty	empty
3609	YDR250C	29	H	3		YKO_0829	H03	0.978	+	+	+	
3610	YDR251W	29	H	4		YKO_0829	H04	0.865	+	+	+	
3611	YDR252W	29	H	5		YKO_0829	H05	0.971	+	-	+	Incongruence
3612	YDR253C	29	H	6	slow growth	YKO_0829	H06	0.819	+	+	+	
3613	YDR254W	29	H	7		YKO_0829	H07	0.899	+	+	+	
3614	YDR255C	29	H	8		YKO_0829	H08	0.877	+	+	+	
3615	YDR256C	29	H	9		YKO_0829	H09	0.941	+	+	+	
3616	YDR257C	29	H	10		YKO_0829	H10	0.939	+	+	+	
3617	YDR258C	29	H	11		YKO_0829	H11	0.84	+	-	+	Incongruence
3618	YDR259C	29	H	12		YKO_0829	H12	0.966	+	+	+	
3619	YDR260C	30	A	1		YKO_0830	A01	0.755	+	-	+	Incongruence
3620	YDR261C	30	A	2		YKO_0830	A02	0.947	+	+	+	
3621	YDR262W	30	A	3		YKO_0830	A03	0.942	+	+	+	
3622	YDR263C	30	A	4		YKO_0830	A04	0.938	+	+	+	
3623	YDR264C	30	A	5		YKO_0830	A05	0.903	+	-	+	Incongruence
3624	YDR265W	30	A	6		YKO_0830	A06	0.723	+	+	-	HIT
3625	YDR266C	30	A	7		YKO_0830	A07	0.83	+	+	+	
3628	YDR269C	30	A	8		YKO_0830	A08	0.98	+	+	+	
3629	YDR270W	30	A	9		YKO_0830	A09	0.904	+	+	+	
3630	YDR271C	30	A	10		YKO_0830	A10	0.829	+	+	+	
3631	YDR272W	30	A	11		YKO_0830	A11	0.969	+	+	+	
3632	YDR273W	30	A	12		YKO_0830	A12	0.948	+	+	+	
3633	YDR274C	30	B	1		YKO_0830	B01	0.963	+	+	+	
3634	YDR275W	30	B	2		YKO_0830	B02	0.959	+	+	+	
3635	YDR276C	30	B	3	slow growth	YKO_0830	B03	0.914	slow	+	+	
3636	YDR277C	30	B	4		YKO_0830	B04	0.888	slow	+	+	
3637	YDR278C	30	B	5		YKO_0830	B05	1.027	+	+	+	
3638	YDR279W	30	B	6		YKO_0830	B06	1.017	+	+	+	
3640	YDR281C	30	B	7		YKO_0830	B07	1.01	+	+	+	
3641	YDR282C	30	B	8		YKO_0830	B08	1.015	+	+	+	
3643	YDR284C	30	B	9		YKO_0830	B09	1	+	+	+	
3644	YDR285W	30	B	10		YKO_0830	B10	0.957	+	+	+	
3645	YDR286C	30	B	11		YKO_0830	B11	0.787	+	+	+	
3646	YDR287W	30	B	12		YKO_0830	B12	0.985	+	+	+	
3648	YDR289C	30	C	1		YKO_0830	C01	0.949	+	-	-	Doubt
3649	YDR290W	30	C	2		YKO_0830	C02	0.886	slow	-	-	Doubt
3650	YDR291W	30	C	3		YKO_0830	C03	0.981	+	+	+	
3652	YDR293C	30	C	4		YKO_0830	C04	0.841	+	+	+	
3653	YDR294C	30	C	5		YKO_0830	C05	0.935	+	+	+	
--		30	C	6	empty	YKO_0830	C06	empty	empty	empty	empty	empty
3654	YDR295C	30	C	7	slow growth, petite	YKO_0830	C07	0.761	slow	+	-	Doubt
3656	YDR297W	30	C	8		YKO_0830	C08	0.896	+	-	-	Doubt
3657	YDR298C	30	C	9	super slow growth, petite	YKO_0830	C09	0.693	-	-	-	Doubt
3663	YDR304C	30	C	10		YKO_0830	C10	0.678	+	+	+	
3664	YDR305C	30	C	11		YKO_0830	C11	0.828	+	+	+	
3665	YDR306C	30	C	12		YKO_0830	C12	0.932	+	+	+	
3666	YDR307W	30	D	1		YKO_0830	D01	1.021	+	+	+	
3668	YDR309C	30	D	2		YKO_0830	D02	1.016	+	+	+	

Euroscarf Information						Replica plate Information			Tau Toxicity Enhancer Primary Screen Results			
record no.	ORF name	Plate	Row	Col	Comment	Replica plate	Well	YPD (OD600nm)	Growth plate (SC+GAL comp.)	Transformation control plate (SC+GLU-Leu)	TEST Plate (SC+GAL-Leu)	Classification
3669	YDR310C	30	D	3		YKO_0830	D03	0.825	+	+	+	
3671	YDR312W	30	D	4		YKO_0830	D04	1.013	+	+	+	
3672	YDR313C	30	D	5		YKO_0830	D05	1.045	+	+	+	
3673	YDR314C	30	D	6		YKO_0830	D06	1.02	+	-	-	Doubt
3674	YDR315C	30	D	7		YKO_0830	D07	1.004	+	+	-	HIT
3675	YDR316W	30	D	8		YKO_0830	D08	1.014	slow	+	+	
3676	YDR317W	30	D	9		YKO_0830	D09	1.011	+	+	+	
3677	YDR318W	30	D	10		YKO_0830	D10	0.91	+	+	+	
3678	YDR319C	30	D	11		YKO_0830	D11	0.672	+	+	+	
3679	YDR320C	30	D	12		YKO_0830	D12	0.765	+	+	+	
3680	YDR321W	30	E	1		YKO_0830	E01	0.998	+	+	+	
3681	YDR322W	30	E	2	super slow, petite	YKO_0830	E02	1.027	-	-	-	Doubt
3682	YDR323C	30	E	3	super slow on YPGE	YKO_0830	E03	0.952	+	+	+	
3688	YDR329C	30	E	4		YKO_0830	E04	0.866	slow	+	+	
3689	YDR330W	30	E	5		YKO_0830	E05	1.044	+	+	+	
3691	YDR332W	30	E	6	super slow on YPGE	YKO_0830	E06	1.006	+	+	+	
3692	YDR333C	30	E	7		YKO_0830	E07	1.015	+	+	+	
3693	YDR334W	30	E	8		YKO_0830	E08	0.908	+	+	+	
3694	YDR335W	30	E	9		YKO_0830	E09	not grown	-	-	-	Not grown
3695	YDR336W	30	E	10		YKO_0830	E10	0.98	+	+	+	
3696	YDR337W	30	E	11		YKO_0830	E11	0.891	+	+	+	
1393	YIL001W	30	E	12		YKO_0830	E12	0.889	+	+	+	
1394	YIL002C	30	F	1		YKO_0830	F01	0.929	+	+	+	
1397	YIL005W	30	F	2	met pap	YKO_0830	F02	0.778	+	+	-	HIT
1403	YIL011W	30	F	3	grows well on -met, grows well on -lys	YKO_0830	F03	0.942	+	+	+	
1404	YIL012W	30	F	4	grows well on -met, grows well on -lys	YKO_0830	F04	0.996	+	+	+	
1405	YIL013C	30	F	5		YKO_0830	F05	0.753	+	+	+	
1406	YIL014W	30	F	6	grows well on -met, grows well on -lys	YKO_0830	F06	0.994	+	+	-	HIT
1408	YIL015W	30	F	7	grows well on -met, grows well on -lys	YKO_0830	F07	0.983	+	+	+	
1409	YIL016W	30	F	8		YKO_0830	F08	0.956	+	+	+	
1410	YIL017C	30	F	9		YKO_0830	F09	0.737	slow	+	-	Doubt
1413	YIL020C	30	F	10		YKO_0830	F10	0.887	+	+	+	
1416	YIL023C	30	F	11		YKO_0830	F11	0.742	+	+	+	
1417	YIL024C	30	F	12		YKO_0830	F12	0.864	+	+	+	
1418	YIL025C	30	G	1	grows well on -met, grows well on -lys	YKO_0830	G01	0.923	+	+	+	
1420	YIL027C	30	G	2		YKO_0830	G02	0.982	+	+	+	
1421	YIL028W	30	G	3		YKO_0830	G03	0.775	slow	+	-	Doubt
1422	YIL029C	30	G	4		YKO_0830	G04	0.792	slow	+	-	Doubt
1425	YIL032C	30	G	5	grows slow on -met, grows well on -lys	YKO_0830	G05	0.892	slow	+	+	
1427	YIL034C	30	G	6	grows slow on -met, grows well on -lys	YKO_0830	G06	0.95	+	+	+	
1428	YIL035C	30	G	7		YKO_0830	G07	0.996	slow	+	+	
1429	YIL036W	30	G	8	slow growth, petite	YKO_0830	G08	0.842	slow	+	+	
1430	YIL037C	30	G	9	papillation on -met	YKO_0830	G09	1.011	+	+	+	
1432	YIL039W	30	G	10		YKO_0830	G10	0.903	+	+	+	
1433	YIL040W	30	G	11		YKO_0830	G11	0.78	slow	+	+	
1434	YIL041W	30	G	12		YKO_0830	G12	0.707	+	+	-	HIT
1436	YIL043C	30	H	1		YKO_0830	H01	0.889	+	+	-	HIT
--		30	H	2	empty	YKO_0830	H02	empty	empty	empty	empty	empty
1437	YIL044C	30	H	3	slow growth	YKO_0830	H03	1.004	+	+	+	
1438	YIL045W	30	H	4		YKO_0830	H04	1.003	+	+	+	
1442	YIL049W	30	H	5	grows slow on -met, grows well on -lys	YKO_0830	H05	0.951	+	+	+	
1443	YIL050W	30	H	6	grows well on -met, grows well on -lys	YKO_0830	H06	0.845	+	+	+	
1446	YIL053W	30	H	7		YKO_0830	H07	0.582	+	+	-	HIT
1450	YIL057C	30	H	8	papillation on -met	YKO_0830	H08	0.824	+	+	+	
1457	YIL064W	30	H	9		YKO_0830	H09	0.857	+	+	+	
1458	YIL065C	30	H	10		YKO_0830	H10	0.805	+	+	-	HIT
1465	YIL072W	30	H	11		YKO_0830	H11	0.89	+	+	+	
1466	YIL073C	30	H	12		YKO_0830	H12	0.552	+	+	-	HIT
1469	YIL076W	31	A	1		YKO_0831	A01	0.8145	+	+	+	
1470	YIL077C	31	A	2		YKO_0831	A02	0.7671	+	+	+	
1472	YIL079C	31	A	3		YKO_0831	A03	0.8042	+	+	+	
1475	YIL084C	31	A	4		YKO_0831	A04	0.7815	+	+	+	
1477	YIL086C	31	A	5		YKO_0831	A05	0.7956	+	+	+	
1478	YIL087C	31	A	6		YKO_0831	A06	0.8213	+	+	+	
1479	YIL088C	31	A	7	grows slow on -met, grows well on -lys	YKO_0831	A07	0.8041	+	+	+	
1481	YIL090W	31	A	8		YKO_0831	A08	0.7807	+	+	+	
1484	YIL093C	31	A	9	grows well on -met, grows well on -lys	YKO_0831	A09	0.7427	+	+	-	HIT
1486	YIL095W	31	A	10	papillation on -met	YKO_0831	A10	0.7509	+	+	+	
1487	YIL096C	31	A	11		YKO_0831	A11	0.8026	+	+	+	
1488	YIL097W	31	A	12	grows well on -met, grows well on -lys	YKO_0831	A12	0.7804	+	+	+	
1398	YIL006W	31	B	1		YKO_0831	B01	0.7701	+	+	+	
1399	YIL007C	31	B	2		YKO_0831	B02	0.7615	+	+	+	
1400	YIL008W	31	B	3	grows on -met	YKO_0831	B03	0.8019	+	+	+	

	Euroscarf Information					Replica plate Information			Tau Toxicity Enhancer Primary Screen Results			
record no.	ORF name	Plate	Row	Col	Comment	Replica plate	Well	YPD (OD600nm)	Growth plate (SC+GAL comp.)	Transformation control plate (SC+GLU-Leu)	TEST Plate (SC+GAL-Leu)	Classification
1401	YIL009W	31	B	4	grows well on -met, grows well on -lys	YKO_0831	B04	0.7672	+	+	+	
1402	YIL010W	31	B	5		YKO_0831	B05	0.8211	+	+	+	
1407	YIL015C-A	31	B	6		YKO_0831	B06	0.7928	+	+	+	
1431	YIL038C	31	B	7		YKO_0831	B07	0.7453	+	+	+	
1435	YIL042C	31	B	8		YKO_0831	B08	0.7606	+	+	+	
1440	YIL047C	31	B	9	grows well on -met, grows well on -lys	YKO_0831	B09	0.7789	+	+	+	
1445	YIL052C	31	B	10		YKO_0831	B10	0.7459	+	+	+	
1447	YIL054W	31	B	11	grows well on -met, grows well on -lys	YKO_0831	B11	0.7944	+	+	+	
1448	YIL055C	31	B	12		YKO_0831	B12	0.7778	+	+	+	
1452	YIL059C	31	C	1		YKO_0831	C01	0.8438	+	+	+	
1453	YIL060W	31	C	2		YKO_0831	C02	0.7956	+	+	-	HIT
1460	YIL067C	31	C	3		YKO_0831	C03	0.9979	+	-	+	Incongruence
1462	YIL069C	31	C	4	grows well on -met, no growth on -lys no growth on drop-in media mates like alpha. Confirmed Alpha -- CORRECT STRAIN CAN BE FOUND IN PLATE 139 G4	YKO_0831	C04	0.7709	+	+	+	
1463	YIL070C	31	C	5		YKO_0831	C05	1.0195	+	-	+	Incongruence
1464	YIL071C	31	C	6		YKO_0831	C06	0.7884	+	+	+	
--		31	C	7	empty	YKO_0831	C07	empty	empty	empty	empty	empty
1467	YIL074C	31	C	8		YKO_0831	C08	0.7644	+	+	+	
1480	YIL089W	31	C	9		YKO_0831	C09	0.7294	+	+	+	
1483	YIL092W	31	C	10		YKO_0831	C10	0.7222	slow	+	+	
5622	YFL006W	31	C	11		YKO_0831	C11	0.7539	+	+	-	HIT
5627	YFL011W	31	C	12		YKO_0831	C12	0.7739	+	+	-	HIT
5633	YFL015C	31	D	1		YKO_0831	D01	0.8037	+	+	-	HIT
5639	YFL020C	31	D	2		YKO_0831	D02	0.8029	+	+	+	
5640	YFL021W	31	D	3		YKO_0831	D03	0.7903	+	+	+	
5642	YFL023W	31	D	4		YKO_0831	D04	0.7244	+	+	+	
5644	YFL025C	31	D	5	grows well on -met, no growth on -lys, no growth on drop-in media, mates like alpha	YKO_0831	D05	0.7988	+	+	+	
5645	YFL026W	31	D	6		YKO_0831	D06	0.806	+	+	+	
5646	YFL027C	31	D	7		YKO_0831	D07	0.8046	+	+	+	
5647	YFL028C	31	D	8		YKO_0831	D08	0.825	+	+	-	HIT
5649	YFL030W	31	D	9		YKO_0831	D09	0.7945	+	+	+	
5650	YFL031W	31	D	10		YKO_0831	D10	0.8498	+	+	-	HIT
5651	YFL032W	31	D	11		YKO_0831	D11	0.7644	+	+	-	HIT
5653	YFL034W	31	D	12		YKO_0831	D12	0.7716	+	+	+	
5656	YFL035C-B	31	E	1		YKO_0831	E01	0.9396	+	+	-	HIT
5657	YFL036W	31	E	2	slow growth, petite	YKO_0831	E02	0.911	-	+	-	Doubt
5661	YFL040W	31	E	3		YKO_0831	E03	1.002	+	+	-	HIT
5662	YFL041W	31	E	4		YKO_0831	E04	1.0231	+	+	+	
5664	YFL043C	31	E	5		YKO_0831	E05	1.0325	+	+	+	
5665	YFL044C	31	E	6		YKO_0831	E06	0.7712	+	-	-	Doubt
5667	YFL046W	31	E	7		YKO_0831	E07	0.8786	+	+	+	
5668	YFL047W	31	E	8		YKO_0831	E08	0.7727	+	+	+	
5669	YFL048C	31	E	9		YKO_0831	E09	0.8266	+	+	-	HIT
5670	YFL049W	31	E	10		YKO_0831	E10	0.8065	+	+	+	
5671	YFL050C	31	E	11		YKO_0831	E11	0.8028	+	+	+	
5672	YFL051C	31	E	12		YKO_0831	E12	0.7486	+	-	-	Doubt
5673	YFL052W	31	F	1		YKO_0831	F01	1.0215	+	+	+	
5674	YFL053W	31	F	2		YKO_0831	F02	1.015	+	+	+	
5675	YFL054C	31	F	3		YKO_0831	F03	0.9805	+	+	+	
5676	YFL055W	31	F	4		YKO_0831	F04	1.0064	+	+	-	HIT
5677	YFL056C	31	F	5		YKO_0831	F05	1.0324	+	+	+	
5680	YFR001W	31	F	6		YKO_0831	F06	0.6803	+	+	+	
5685	YFR006W	31	F	7		YKO_0831	F07	0.7775	+	+	+	
5686	YFR007W	31	F	8		YKO_0831	F08	0.8118	+	+	+	
5687	YFR008W	31	F	9		YKO_0831	F09	0.8058	+	-	-	Doubt
5688	YFR009W	31	F	10		YKO_0831	F10	0.8219	+	+	+	
5689	YFR010W	31	F	11		YKO_0831	F11	0.8299	+	+	+	
5691	YFR012W	31	F	12		YKO_0831	F12	0.7465	+	-	+	Incongruence
5693	YFR014C	31	G	1		YKO_0831	G01	0.9982	+	+	+	
5694	YFR015C	31	G	2		YKO_0831	G02	1.0145	+	+	+	
5695	YFR016C	31	G	3		YKO_0831	G03	0.9855	+	+	+	
5696	YFR017C	31	G	4		YKO_0831	G04	0.9967	+	+	-	HIT
5697	YFR018C	31	G	5		YKO_0831	G05	1.0009	+	-	-	Doubt
5699	YFR020W	31	G	6		YKO_0831	G06	0.9202	+	+	+	
5700	YFR021W	31	G	7		YKO_0831	G07	0.7482	+	+	+	
5701	YFR022W	31	G	8		YKO_0831	G08	0.7912	+	-	+	Incongruence
5702	YFR023W	31	G	9		YKO_0831	G09	0.7653	+	+	-	HIT
5704	YFR024C-A	31	G	10		YKO_0831	G10	0.7603	+	-	-	Doubt
5706	YFR026C	31	G	11		YKO_0831	G11	0.7592	+	+	+	
5712	YFR031C-A	31	G	12		YKO_0831	G12	0.7346	+	-	-	Doubt
5908	YGR256W	31	H	1		YKO_0831	H01	0.7938	+	+	+	
--		31	H	2	empty	YKO_0831	H02	empty	empty	empty	empty	empty
5911	YGR259C	31	H	3		YKO_0831	H03	0.9736	+	+	+	

Euroscarf Information						Replica plate Information			Tau Toxicity Enhancer Primary Screen Results			
record no.	ORF name	Plate	Row	Col	Comment	Replica plate	Well	YPD (OD600nm)	Growth plate (SC+GAL comp.)	Transformation control plate (SC+GLU-Leu)	TEST Plate (SC+GAL-Leu)	Classification
5912	YGR260W	31	H	4		YKO_0831	H04	0.987	+	+	+	
5913	YGR261C	31	H	5		YKO_0831	H05	1.0463	+	-	+	Incongruence
5915	YGR263C	31	H	6		YKO_0831	H06	0.7667	+	-	-	Doubt
5918	YGR266W	31	H	7		YKO_0831	H07	0.8168	+	+	+	
5920	YGR268C	31	H	8		YKO_0831	H08	0.7548	+	+	+	
5921	YGR269W	31	H	9		YKO_0831	H09	0.7691	+	+	-	HIT
5922	YGR270W	31	H	10		YKO_0831	H10	0.7321	+	+	+	
5927	YGR275W	31	H	11		YKO_0831	H11	0.7209	+	+	+	
5931	YGR279C	31	H	12		YKO_0831	H12	0.7332	+	+	-	HIT
5933	YGR281W	32	A	1		YKO_0832	A01	0.965	+	+	+	
5934	YGR282C	32	A	2		YKO_0832	A02	0.965	+	+	+	
5935	YGR283C	32	A	3		YKO_0832	A03	0.956	+	+	+	
5936	YGR284C	32	A	4		YKO_0832	A04	0.936	+	-	+	Incongruence
5937	YGR285C	32	A	5		YKO_0832	A05	not grow n	-	-	-	Not grow n
5938	YGR286C	32	A	6		YKO_0832	A06	0.957	+	+	+	
5939	YGR287C	32	A	7		YKO_0832	A07	0.958	+	+	+	
5940	YGR288W	32	A	8		YKO_0832	A08	1.004	+	+	+	
5942	YGR290W	32	A	9		YKO_0832	A09	1	+	+	+	
5947	YHR021W-A	32	A	10		YKO_0832	A10	0.985	+	-	+	Incongruence
5948	YHR039C-B	32	A	11	petite	YKO_0832	A11	not grow n	-	-	-	Not grow n
5949	YHR079C-B	32	A	12		YKO_0832	A12	0.782	+	+	+	
5950	YIL009C-A	32	B	1		YKO_0832	B01	0.952	+	+	+	
5951	YIR017C	32	B	2		YKO_0832	B02	1.042	+	+	+	
5952	YIR018W	32	B	3		YKO_0832	B03	1.016	+	+	+	
5953	YIR019C	32	B	4		YKO_0832	B04	0.963	+	+	+	
5954	YIR020C	32	B	5		YKO_0832	B05	0.986	+	+	+	
5955	YIR020W-B	32	B	6	petite	YKO_0832	B06	1.013	+	+	+	
5956	YIR021W	32	B	7		YKO_0832	B07	1.036	+	+	+	
5959	YIR024C	32	B	8		YKO_0832	B08	0.978	+	+	+	
5960	YIR025W	32	B	9		YKO_0832	B09	0.942	+	-	+	Incongruence
5961	YIR026C	32	B	10		YKO_0832	B10	1.025	+	+	+	
5962	YIR027C	32	B	11		YKO_0832	B11	0.938	+	+	+	
5963	YIR028W	32	B	12		YKO_0832	B12	0.935	+	-	-	Doubt
5964	YIR029W	32	C	1		YKO_0832	C01	1.002	+	+	+	
5966	YIR031C	32	C	2		YKO_0832	C02	1.061	+	+	+	
5968	YIR033W	32	C	3		YKO_0832	C03	1.034	+	+	+	
5969	YIR034C	32	C	4	no grow th on drop-in media	YKO_0832	C04	1.014	+	+	+	
5970	YIR035C	32	C	5		YKO_0832	C05	1.05	+	+	+	
5971	YIR036C	32	C	6		YKO_0832	C06	1.013	+	+	+	
5972	YIR037W	32	C	7		YKO_0832	C07	1.035	+	+	+	
--		32	C	8	empty	YKO_0832	C08	empty	empty	empty	empty	empty
5973	YIR038C	32	C	9		YKO_0832	C09	1.048	+	-	+	Incongruence
5974	YIR039C	32	C	10		YKO_0832	C10	0.816	+	+	+	
5975	YIR042C	32	C	11		YKO_0832	C11	0.827	+	+	+	
5978	YKL033W-A	32	C	12		YKO_0832	C12	0.694	+	+	+	
5980	YKL162C-A	32	D	1		YKO_0832	D01	1.057	+	+	+	
5981	YKR035W-A	32	D	2		YKO_0832	D02	0.903	+	+	+	
5982	YKR066C	32	D	3		YKO_0832	D03	1.051	+	+	+	
5983	YKR067W	32	D	4		YKO_0832	D04	0.955	+	+	+	
5985	YKR069W	32	D	5		YKO_0832	D05	1.017	+	+	+	
5986	YKR070W	32	D	6		YKO_0832	D06	0.99	+	+	+	
5988	YKR072C	32	D	7		YKO_0832	D07	1.025	+	+	+	
5989	YKR073C	32	D	8		YKO_0832	D08	0.919	+	+	+	
5990	YKR074W	32	D	9		YKO_0832	D09	0.929	+	-	+	Incongruence
5991	YKR075C	32	D	10		YKO_0832	D10	0.978	+	+	+	
5992	YKR076W	32	D	11		YKO_0832	D11	0.802	+	+	+	
5993	YKR077W	32	D	12		YKO_0832	D12	0.914	+	+	+	
5994	YKR078W	32	E	1		YKO_0832	E01	1.012	+	+	+	
5996	YKR080W	32	E	2		YKO_0832	E02	1.047	+	+	+	
5998	YKR082W	32	E	3		YKO_0832	E03	0.964	+	+	+	
6000	YKR084C	32	E	4		YKO_0832	E04	0.936	+	+	+	
6195	YMR062C	32	E	5		YKO_0832	E05	1.053	+	+	+	
6196	YMR063W	32	E	6		YKO_0832	E06	1.058	+	+	+	
6198	YMR065W	32	E	7		YKO_0832	E07	0.912	+	-	+	Incongruence
6200	YMR067C	32	E	8		YKO_0832	E08	0.935	slow	+	-	Doubt
6201	YMR068W	32	E	9		YKO_0832	E09	0.919	+	+	-	HIT
6202	YMR069W	32	E	10		YKO_0832	E10	0.902	+	+	-	HIT
6203	YMR070W	32	E	11		YKO_0832	E11	0.974	+	+	+	
6204	YMR071C	32	E	12	slow grow th, petite	YKO_0832	E12	0.917	slow	-	-	Doubt
6205	YMR072W	32	F	1	slow grow th, petite	YKO_0832	F01	0.804	slow	+	-	Doubt
6206	YMR073C	32	F	2		YKO_0832	F02	0.927	+	+	+	
6208	YMR075C-A	32	F	3		YKO_0832	F03	1.032	+	+	+	
6209	YMR075W	32	F	4		YKO_0832	F04	0.949	+	+	+	
6211	YMR077C	32	F	5		YKO_0832	F05	0.975	+	+	+	
6212	YMR078C	32	F	6		YKO_0832	F06	0.83	+	+	+	
6214	YMR080C	32	F	7		YKO_0832	F07	0.954	+	+	+	
6215	YMR081C	32	F	8		YKO_0832	F08	0.896	+	+	+	
6216	YMR082C	32	F	9		YKO_0832	F09	0.885	+	+	+	
6217	YMR083W	32	F	10	slow grow th, petite	YKO_0832	F10	0.847	+	+	-	HIT
6218	YMR084W	32	F	11	slow grow th, petite	YKO_0832	F11	0.894	-	+	-	Doubt
6219	YMR085W	32	F	12		YKO_0832	F12	0.941	+	+	+	
6220	YMR086C-A	32	G	1		YKO_0832	G01	0.965	+	+	+	

	Euroscarf Information					Replica plate Information			Tau Toxicity Enhancer Primary Screen Results			
record no.	ORF name	Plate	Row	Col	Comment	Replica plate	Well	YPD (OD600nm)	Growth plate (SC+GAL comp.)	Transformation control plate (SC+GLU-Leu)	TEST Plate (SC+GAL-Leu)	Classification
6221	YMR086W	32	G	2		YKO_0832	G02	1.002	+	+	+	
6222	YMR087W	32	G	3		YKO_0832	G03	0.977	+	+	+	
6223	YMR088C	32	G	4		YKO_0832	G04	0.927	+	+	+	
6224	YMR089C	32	G	5	slow growth, petite	YKO_0832	G05	0.927	-	+	-	Doubt
6225	YMR090W	32	G	6		YKO_0832	G06	0.938	+	+	+	
6226	YMR091C	32	G	7	slow growth	YKO_0832	G07	0.683	+	+	+	
6227	YMR092C	32	G	8		YKO_0832	G08	0.877	+	+	+	
6229	YNR070W	32	G	9		YKO_0832	G09	0.853	+	+	+	
6230	YNR071C	32	G	10		YKO_0832	G10	0.767	+	+	+	
6231	YNR072W	32	G	11		YKO_0832	G11	0.855	+	+	+	
6232	YNR073C	32	G	12		YKO_0832	G12	0.844	+	+	+	
6233	YNR074C	32	H	1		YKO_0832	H01	0.993	+	+	+	
--		32	H	2	empty	YKO_0832	H02	empty	empty	empty	empty	empty
6234	YNR075W	32	H	3		YKO_0832	H03	0.919	+	+	+	
6235	YOL013W-A	32	H	4		YKO_0832	H04	1.017	+	+	+	
6236	YOL086C	32	H	5	slow growth, petite, mates like alpha. Confirmed Alpha -- CORRECT STRAIN CAN BE FOUND IN PLATE 131 A9	YKO_0832	H05	0.922	+	+	+	
6237	YOL087C	32	H	6		YKO_0832	H06	0.871	+	+	+	
6238	YOL088C	32	H	7		YKO_0832	H07	0.949	+	+	+	
6239	YOL089C	32	H	8		YKO_0832	H08	0.914	+	+	+	
6240	YOL090W	32	H	9		YKO_0832	H09	0.82	+	+	+	
6241	YOL091W	32	H	10		YKO_0832	H10	0.919	+	+	+	
6242	YOL092W	32	H	11		YKO_0832	H11	0.749	+	+	+	
6243	YOL093W	32	H	12	slow growth, petite	YKO_0832	H12	0.794	+	+	+	
6245	YOL095C	33	A	1	slow growth, petite	YKO_0833	A01	0.769	+	+	+	
6246	YOL096C	33	A	2		YKO_0833	A02	0.938	slow	+	-	Doubt
6248	YOL098C	33	A	3		YKO_0833	A03	0.916	+	+	+	
6249	YOL099C	33	A	4		YKO_0833	A04	1.019	+	+	+	
6250	YOL100W	33	A	5	slow growth, petite	YKO_0833	A05	0.958	slow	+	-	Doubt
6251	YOL101C	33	A	6		YKO_0833	A06	0.688	+	+	+	
6253	YOL103W	33	A	7		YKO_0833	A07	0.984	+	+	+	
6254	YOL104C	33	A	8		YKO_0833	A08	0.913	+	+	+	
6255	YOL105C	33	A	9		YKO_0833	A09	0.965	+	+	+	
6256	YOL106W	33	A	10		YKO_0833	A10	0.996	+	+	+	
6257	YOL107W	33	A	11		YKO_0833	A11	1.009	+	+	+	
6258	YOL108C	33	A	12		YKO_0833	A12	0.917	+	+	+	
6259	YOL109W	33	B	1		YKO_0833	B01	0.879	+	+	+	
6260	YOL110W	33	B	2		YKO_0833	B02	0.986	+	+	+	
6261	YOL111C	33	B	3		YKO_0833	B03	1.017	+	+	+	
6262	YOL112W	33	B	4		YKO_0833	B04	1.06	+	+	-	HIT
6263	YOL113W	33	B	5		YKO_0833	B05	1.007	+	+	+	
6264	YOL114C	33	B	6		YKO_0833	B06	0.994	+	+	+	
6265	YOL115W	33	B	7		YKO_0833	B07	1.01	+	+	+	
6266	YOL116W	33	B	8		YKO_0833	B08	0.955	+	+	+	
6267	YOL117W	33	B	9		YKO_0833	B09	1.011	+	+	-	HIT
6268	YOL118C	33	B	10		YKO_0833	B10	0.991	+	+	+	
6269	YOL119C	33	B	11		YKO_0833	B11	0.975	+	+	+	
6271	YOL121C	33	B	12		YKO_0833	B12	0.738	+	+	+	
6272	YOL122C	33	C	1		YKO_0833	C01	1.051	+	+	+	
6274	YOL124C	33	C	2		YKO_0833	C02	1.029	+	+	+	
6276	YOL126C	33	C	3		YKO_0833	C03	1.062	+	+	+	
6278	YOL128C	33	C	4		YKO_0833	C04	0.989	+	+	+	
6279	YOL129W	33	C	5		YKO_0833	C05	0.993	+	+	+	
6281	YOL131W	33	C	6		YKO_0833	C06	1.001	+	+	+	
6282	YOL132W	33	C	7		YKO_0833	C07	1.003	+	+	+	
6286	YOL136C	33	C	8		YKO_0833	C08	0.762	+	+	+	
--		33	C	9	empty	YKO_0833	C09	empty	empty	empty	empty	empty
6287	YOL137W	33	C	10		YKO_0833	C10	0.974	+	+	-	HIT
6288	YOL138C	33	C	11		YKO_0833	C11	0.906	+	+	-	HIT
6385	YBR232C	33	C	12		YKO_0833	C12	1.028	+	+	+	
6387	YDR424C	33	D	1		YKO_0833	D01	0.911	+	+	+	
6388	YEL011W	33	D	2		YKO_0833	D02	1.079	+	+	+	
6390	YER064C	33	D	3		YKO_0833	D03	1.08	+	+	+	
6391	YER077C	33	D	4		YKO_0833	D04	1.013	+	+	+	
6392	YER078C	33	D	5		YKO_0833	D05	1.012	+	+	+	
6393	YER088C	33	D	6		YKO_0833	D06	0.935	+	+	+	
6395	YER090W	33	D	7		YKO_0833	D07	0.93	+	+	-	HIT
6396	YER091C	33	D	8		YKO_0833	D08	1.019	+	+	+	
6397	YER092W	33	D	9		YKO_0833	D09	0.899	+	+	+	
6399	YER093C-A	33	D	10		YKO_0833	D10	0.935	+	+	+	
6401	YER095W	33	D	11		YKO_0833	D11	0.855	+	+	+	
6402	YER096W	33	D	12		YKO_0833	D12	0.998	+	+	+	
6403	YER097W	33	E	1		YKO_0833	E01	0.992	+	+	+	
6404	YER098W	33	E	2		YKO_0833	E02	1.008	+	+	+	
6405	YGR134W	33	E	3		YKO_0833	E03	1.017	+	+	+	
6407	YGR210C	33	E	4		YKO_0833	E04	1.012	+	-	+	Incongruence
6408	YHL024W	33	E	5		YKO_0833	E05	0.98	+	+	+	
6409	YHL025W	33	E	6	petite	YKO_0833	E06	0.592	slow	+	-	Doubt
6410	YHR016C	33	E	7		YKO_0833	E07	0.971	+	+	+	

	Euroscarf Information					Replica plate Information			Tau Toxicity Enhancer Primary Screen Results			
record no.	ORF name	Plate	Row	Col	Comment	Replica plate	Well	YPD (OD600nm)	Growth plate (SC+GAL comp.)	Transformation control plate (SC+GLU-Leu)	TEST Plate (SC+GAL-Leu)	Classification
6411	YHR017W	33	E	8		YKO_0833	E08	0.943	+	+	+	
6412	YHR032W	33	E	9		YKO_0833	E09	0.936	+	+	-	HIT
6413	YHR045W	33	E	10		YKO_0833	E10	0.945	+	+	+	
6414	YHR064C	33	E	11		YKO_0833	E11	0.826	+	+	+	
6415	YHR140W	33	E	12		YKO_0833	E12	0.981	+	+	+	
6416	YHR162W	33	F	1		YKO_0833	F01	1.008	+	+	+	
6417	YHR168W	33	F	2	no growth on -met, no growth on -lys, no growth on drop-in media s petite	YKO_0833	F02	0.965	slow	+	-	Doubt
6420	YHR181W	33	F	3		YKO_0833	F03	1.046	+	+	+	
6421	YHR191C	33	F	4	grows well on -met, grows well on -lys, mates like alpha. Confirmed Het Diploid 10/15/01	YKO_0833	F04	0.75	+	+	+	
6422	YHR193C	33	F	5	grows well on -met, grows well on -lys, mates like alpha. Confirmed Het Diploid 10/15/01	YKO_0833	F05	0.857	+	+	+	
6423	YLL030C	33	F	6	grows well on -met, grows well on -lys, mates like alpha. Confirmed Het Diploid 10/15/01	YKO_0833	F06	0.877	+	+	+	
6424	YLL044W	33	F	7	grows well on -met, grows well on -lys, mates like alpha. Confirmed Het Diploid 10/15/01	YKO_0833	F07	0.957	+	+	+	
6425	YLL048C	33	F	8		YKO_0833	F08	0.99	+	+	+	
6426	YLL049W	33	F	9	grows well on -met, grows well on -lys, mates like alpha. Confirmed Het Diploid 10/15/01	YKO_0833	F09	0.629	+	+	+	
6427	YLL059C	33	F	10		YKO_0833	F10	0.997	+	+	+	
6428	YLR030W	33	F	11		YKO_0833	F11	0.896	+	+	+	
6429	YLR031W	33	F	12		YKO_0833	F12	0.958	+	+	+	
6430	YLR032W	33	G	1		YKO_0833	G01	0.989	+	+	+	
6432	YLR034C	33	G	2		YKO_0833	G02	0.973	+	+	+	
6433	YLR035C	33	G	3		YKO_0833	G03	0.934	+	+	+	
6434	YLR036C	33	G	4		YKO_0833	G04	0.941	+	+	+	
6435	YLR037C	33	G	5		YKO_0833	G05	1.008	+	+	+	
6436	YLR038C	33	G	6		YKO_0833	G06	0.975	slow	+	-	Doubt
6437	YLR039C	33	G	7		YKO_0833	G07	0.781	+	+	+	
6438	YLR040C	33	G	8	slow growth, petite	YKO_0833	G08	0.952	+	+	+	
6439	YLR041W	33	G	9		YKO_0833	G09	0.991	+	+	+	
6440	YLR050C	33	G	10		YKO_0833	G10	0.962	+	+	+	
6441	YLR052W	33	G	11		YKO_0833	G11	0.9	+	+	+	
6443	YMR142C	33	G	12		YKO_0833	G12	0.676	+	+	+	
6444	YMR158W	33	H	1	slow growth, petite	YKO_0833	H01	0.904	slow	+	-	Doubt
--		33	H	2	empty	YKO_0833	H02	empty	empty	empty	empty	empty
6445	YMR171C	33	H	3		YKO_0833	H03	1.052	+	+	+	
6446	YMR181C	33	H	4		YKO_0833	H04	0.793	+	+	+	
6447	YMR209C	33	H	5		YKO_0833	H05	0.994	+	+	+	
6448	YMR271C	33	H	6		YKO_0833	H06	1.002	+	+	+	
6449	YMR279C	33	H	7		YKO_0833	H07	1.008	+	+	+	
6450	YMR306W	33	H	8		YKO_0833	H08	0.972	+	+	+	
6451	YMR311C	33	H	9		YKO_0833	H09	0.984	+	-	+	Incongruence
6452	YMR312W	33	H	10		YKO_0833	H10	0.98	+	+	+	
6453	YMR313C	33	H	11		YKO_0833	H11	0.942	+	+	+	
6455	YMR315W	33	H	12		YKO_0833	H12	0.944	+	+	+	
6456	YMR316C-A	34	A	1		YKO_0834	A01	0.911	+	+	+	
6457	YMR316C-B	34	A	2		YKO_0834	A02	0.978	+	+	+	
6458	YMR316W	34	A	3		YKO_0834	A03	1.046	+	+	+	
6459	YMR317W	34	A	4		YKO_0834	A04	1.044	+	+	+	
6460	YMR318C	34	A	5		YKO_0834	A05	1.032	+	+	-	HIT
6461	YMR319C	34	A	6		YKO_0834	A06	1.012	+	+	+	
6462	YMR320W	34	A	7		YKO_0834	A07	1.004	+	+	-	HIT
6464	YNL250W	34	A	8		YKO_0834	A08	0.591	+	+	+	
6465	YNL252C	34	A	9		YKO_0834	A09	0.986	slow	-	-	Doubt
6468	YNL279W	34	A	10		YKO_0834	A10	1.019	+	+	+	
6470	YNL300W	34	A	11		YKO_0834	A11	0.893	+	-	-	Doubt
6472	YNL316C	34	A	12		YKO_0834	A12	1.016	+	+	-	HIT
6473	YOL016C	34	B	1		YKO_0834	B01	0.965	+	+	+	
6475	YOR096W	34	B	2		YKO_0834	B02	0.676	+	+	+	
6476	YOR306C	34	B	3		YKO_0834	B03	0.473	+	+	+	
6477	YOR317W	34	B	4		YKO_0834	B04	0.992	+	+	+	
6479	YPL132W	34	B	5	petite	YKO_0834	B05	1.014	slow	+	-	Doubt
6480	YPL134C	34	B	6		YKO_0834	B06	0.99	+	-	+	Incongruence
6483	YML070W	34	B	7		YKO_0834	B07	0.892	+	+	-	HIT
6484	YML071C	34	B	8		YKO_0834	B08	0.958	+	-	-	Doubt
6486	YML074C	34	B	9		YKO_0834	B09	0.997	+	+	-	HIT
6487	YML090W	34	B	10		YKO_0834	B10	1.028	+	+	+	

	Euroscarf Information					Replica plate Information			Tau Toxicity Enhancer Primary Screen Results			
record no.	ORF name	Plate	Row	Col	Comment	Replica plate	Well	YPD (OD600nm)	Growth plate (SC+GAL comp.)	Transformation control plate (SC+GLU-Leu)	TEST Plate (SC+GAL-Leu)	Classification
6491	YML094W	34	B	11	petite	YKO_0834	B11	0.667	+	+	+	
6492	YML095C	34	B	12		YKO_0834	B12	1.005	+	+	-	HIT
6493	YML095C-A	34	C	1		YKO_0834	C01	0.697	+	+	+	
6494	YML096W	34	C	2		YKO_0834	C02	0.913	+	+	+	
6495	YML097C	34	C	3		YKO_0834	C03	0.924	+	+	+	
6497	YML099C	34	C	4		YKO_0834	C04	1.063	+	+	-	HIT
6498	YML100W	34	C	5		YKO_0834	C05	1.018	+	+	+	
6499	YML100W-A	34	C	6		YKO_0834	C06	0.979	+	+	-	HIT
6500	YML101C	34	C	7		YKO_0834	C07	1.013	+	+	+	
6501	YML102C-A	34	C	8		YKO_0834	C08	0.886	+	+	-	HIT
6502	YML102W	34	C	9		YKO_0834	C09	0.843	+	+	+	
--		34	C	10	empty	YKO_0834	C10	empty	empty	empty	empty	empty
6503	YML103C	34	C	11		YKO_0834	C11	0.902	+	+	+	
6504	YML104C	34	C	12		YKO_0834	C12	1.064	+	-	-	Doubt
6506	YML106W	34	D	1		YKO_0834	D01	1.06	+	+	+	
6507	YML107C	34	D	2		YKO_0834	D02	0.966	+	+	+	
6508	YML108W	34	D	3		YKO_0834	D03	1.051	+	+	+	
6509	YML109W	34	D	4		YKO_0834	D04	1.044	+	+	+	
6513	YML113W	34	D	5		YKO_0834	D05	1.053	+	+	+	
6516	YML116W	34	D	6		YKO_0834	D06	1.026	+	-	-	Doubt
6517	YML117W	34	D	7		YKO_0834	D07	1.02	+	+	+	
6518	YML117W-A	34	D	8		YKO_0834	D08	1.013	+	+	-	HIT
6519	YML118W	34	D	9		YKO_0834	D09	0.969	+	+	+	
6520	YML119W	34	D	10		YKO_0834	D10	0.964	+	+	+	
6521	YML120C	34	D	11		YKO_0834	D11	0.961	+	+	+	
6522	YML121W	34	D	12		YKO_0834	D12	not grow n	-	-	-	Not grow n
6523	YML122C	34	E	1		YKO_0834	E01	0.959	+	+	+	
6524	YML123C	34	E	2		YKO_0834	E02	0.923	+	+	+	
6525	YML124C	34	E	3		YKO_0834	E03	0.906	+	+	+	
6529	YML128C	34	E	4		YKO_0834	E04	0.83	+	+	+	
6532	YML131W	34	E	5		YKO_0834	E05	1.035	+	+	+	
6533	YMR004W	34	E	6		YKO_0834	E06	0.862	+	-	+	Incongruence
6535	YMR095C	34	E	7		YKO_0834	E07	1.022	+	+	+	
6536	YMR096W	34	E	8		YKO_0834	E08	0.971	+	+	+	
6539	YMR099C	34	E	9		YKO_0834	E09	0.934	+	+	+	
6540	YMR100W	34	E	10		YKO_0834	E10	0.815	+	+	+	
6541	YMR101C	34	E	11		YKO_0834	E11	1.007	+	+	+	
6542	YMR102C	34	E	12		YKO_0834	E12	0.906	+	+	+	
6543	YMR103C	34	F	1		YKO_0834	F01	1.035	+	+	+	
6545	YMR105C	34	F	2		YKO_0834	F02	1.03	slow	+	-	Doubt
6546	YMR106C	34	F	3		YKO_0834	F03	0.996	+	+	+	
6547	YMR107W	34	F	4		YKO_0834	F04	1.013	+	+	+	
6549	YMR109W	34	F	5		YKO_0834	F05	0.968	+	-	+	Incongruence
6550	YMR110C	34	F	6		YKO_0834	F06	0.95	+	+	+	
6551	YMR111C	34	F	7		YKO_0834	F07	0.984	+	+	+	
6554	YMR114C	34	F	8		YKO_0834	F08	0.989	+	+	+	
6555	YMR115W	34	F	9		YKO_0834	F09	1.021	+	+	+	
6556	YMR116C	34	F	10		YKO_0834	F10	0.267	slow	+	-	Doubt
6560	YMR119W-A	34	F	11		YKO_0834	F11	0.896	+	-	-	Doubt
6561	YMR120C	34	F	12		YKO_0834	F12	0.887	+	+	-	HIT
6562	YMR121C	34	G	1		YKO_0834	G01	1.015	+	+	+	
6563	YMR122C	34	G	2		YKO_0834	G02	0.847	+	+	+	
6564	YMR123W	34	G	3		YKO_0834	G03	0.595	slow	+	+	
6565	YMR124W	34	G	4		YKO_0834	G04	0.992	+	+	+	
6566	YMR125W	34	G	5		YKO_0834	G05	0.905	+	-	+	Incongruence
6567	YMR126C	34	G	6		YKO_0834	G06	0.825	+	-	+	Incongruence
6568	YMR127C	34	G	7	slow growth	YKO_0834	G07	0.933	+	+	+	
6570	YMR129W	34	G	8		YKO_0834	G08	0.921	+	+	+	
6571	YMR130W	34	G	9		YKO_0834	G09	0.989	+	+	+	
6573	YMR132C	34	G	10		YKO_0834	G10	0.933	+	+	+	
6574	YMR133W	34	G	11		YKO_0834	G11	0.986	+	+	+	
6576	YMR135C	34	G	12		YKO_0834	G12	0.902	+	+	+	
5425	YPR006C	34	H	1		YKO_0834	H01	1.054	+	+	+	
--		34	H	2	empty	YKO_0834	H02	empty	empty	empty	empty	empty
5428	YPR009W	34	H	3		YKO_0834	H03	1.013	+	+	+	
5431	YPR012W	34	H	4		YKO_0834	H04	1.003	+	+	+	
5433	YPR014C	34	H	5		YKO_0834	H05	1.036	+	+	+	
5434	YPR015C	34	H	6		YKO_0834	H06	0.851	+	+	+	
5436	YPR017C	34	H	7		YKO_0834	H07	0.966	+	+	+	
5437	YPR018W	34	H	8		YKO_0834	H08	0.846	+	+	+	
5439	YPR020W	34	H	9		YKO_0834	H09	0.996	+	-	-	Doubt
5446	YPR027C	34	H	10		YKO_0834	H10	0.971	+	-	+	Incongruence
5447	YPR028W	34	H	11		YKO_0834	H11	0.94	+	+	+	
5448	YPR029C	34	H	12		YKO_0834	H12	0.859	+	+	+	
5449	YPR030W	35	A	1		YKO_0835	A01	0.763	+	+	+	
5451	YPR032W	35	A	2		YKO_0835	A02	0.738	+	+	+	
5455	YPR036W	35	A	3	slow growth, petite	YKO_0835	A03	not grow n	-	-	-	Not grow n
5457	YPR038W	35	A	4		YKO_0835	A04	0.93	+	+	+	
5458	YPR039W	35	A	5		YKO_0835	A05	0.932	+	+	+	
5459	YPR040W	35	A	6		YKO_0835	A06	0.872	+	+	+	
5461	YPR042C	35	A	7		YKO_0835	A07	0.899	+	-	+	Incongruence
5463	YPR044C	35	A	8		YKO_0835	A08	0.741	+	+	+	
5464	YPR045C	35	A	9		YKO_0835	A09	0.736	+	+	+	
5465	YPR046W	35	A	10		YKO_0835	A10	0.88	+	+	+	

	Euroscarf Information					Replica plate Information			Tau Toxicity Enhancer Primary Screen Results			
record no.	ORF name	Plate	Row	Col	Comment	Replica plate	Well	YPD (OD600nm)	Growth plate (SC+GAL comp.)	Transformation control plate (SC+GLU-Leu)	TEST Plate (SC+GAL-Leu)	Classification
5466	YPR047W	35	A	11	slow growth, petite	YKO_0835	A11	0.936	slow	+	-	Doubt
5468	YPR049C	35	A	12		YKO_0835	A12	0.565	+	+	+	
5470	YPR051W	35	B	1		YKO_0835	B01	0.914	+	+	+	
5471	YPR052C	35	B	2		YKO_0835	B02	0.993	+	+	+	
5472	YPR053C	35	B	3		YKO_0835	B03	0.986	+	+	+	
5473	YPR054W	35	B	4		YKO_0835	B04	0.988	+	+	+	
5476	YPR057W	35	B	5		YKO_0835	B05	0.882	slow	+	+	
5477	YPR058W	35	B	6		YKO_0835	B06	0.922	+	+	+	
5478	YPR059C	35	B	7		YKO_0835	B07	0.993	+	+	+	
5479	YPR060C	35	B	8		YKO_0835	B08	0.827	+	+	+	
5480	YPR061C	35	B	9		YKO_0835	B09	1.026	+	+	+	
5481	YPR062W	35	B	10		YKO_0835	B10	1	+	+	+	
5482	YPR063C	35	B	11		YKO_0835	B11	0.966	+	+	+	
5484	YPR065W	35	B	12		YKO_0835	B12	0.646	+	+	+	
5485	YPR066W	35	C	1	red colony on YPD: ade mutant?	YKO_0835	C01	1.081	+	+	+	
5487	YPR068C	35	C	2		YKO_0835	C02	0.897	+	+	+	
5488	YPR069C	35	C	3		YKO_0835	C03	0.997	+	+	+	
5489	YPR070W	35	C	4		YKO_0835	C04	0.958	+	+	+	
5490	YPR071W	35	C	5		YKO_0835	C05	1.053	+	+	+	
5492	YPR073C	35	C	6		YKO_0835	C06	0.95	+	+	+	
5493	YPR074C	35	C	7		YKO_0835	C07	0.97	+	+	+	
5494	YPR075C	35	C	8		YKO_0835	C08	0.97	+	+	+	
5495	YPR076W	35	C	9		YKO_0835	C09	1.053	+	+	+	
5496	YPR077C	35	C	10		YKO_0835	C10	1.025	+	+	+	
--		35	C	11	empty	YKO_0835	C11	empty	empty	empty	empty	empty
5498	YPR079W	35	C	12		YKO_0835	C12	1.068	+	+	+	
5501	YPR084W	35	D	1		YKO_0835	D01	0.877	+	+	+	
5504	YPR087W	35	D	2		YKO_0835	D02	0.841	+	+	+	
5506	YPR089W	35	D	3		YKO_0835	D03	1.034	+	+	+	
5507	YPR090W	35	D	4		YKO_0835	D04	0.791	+	+	+	
5509	YPR092W	35	D	5		YKO_0835	D05	1.058	+	+	+	
5510	YPR093C	35	D	6		YKO_0835	D06	1.058	+	+	+	
5512	YPR095C	35	D	7		YKO_0835	D07	1.065	+	+	+	
5513	YPR096C	35	D	8		YKO_0835	D08	1.066	+	+	+	
5514	YPR097W	35	D	9		YKO_0835	D09	1.041	+	+	+	
5515	YPR098C	35	D	10		YKO_0835	D10	1.02	+	+	+	
5516	YPR099C	35	D	11	slow growth, petite	YKO_0835	D11	0.831	-	-	-	Doubt
5517	YPR100W	35	D	12	slow growth, petite	YKO_0835	D12	1.017	slow	-	-	Doubt
5518	YPR101W	35	E	1		YKO_0835	E01	0.581	+	+	+	
1298	YJL127C	35	E	2		YKO_0835	E02	not grown	-	-	-	Not grown
1299	YJL126W	35	E	3		YKO_0835	E03	0.979	+	+	+	
1301	YJL124C	35	E	4		YKO_0835	E04	0.961	+	+	+	
1302	YJL123C	35	E	5		YKO_0835	E05	1.052	+	+	+	
1303	YJL122W	35	E	6		YKO_0835	E06	1.06	+	+	+	
1304	YJL120W	35	E	7		YKO_0835	E07	1.022	+	-	+	Incongruence
1305	YJL121C	35	E	8		YKO_0835	E08	1.028	+	+	+	
1306	YJL118W	35	E	9		YKO_0835	E09	0.917	+	+	+	
1307	YJL119C	35	E	10		YKO_0835	E10	1.063	+	+	+	
1308	YJL117W	35	E	11		YKO_0835	E11	1.069	+	+	+	
1309	YJL116C	35	E	12		YKO_0835	E12	1.013	+	+	+	
1310	YJL115W	35	F	1		YKO_0835	F01	0.845	+	+	+	
1311	YJL112W	35	F	2		YKO_0835	F02	1.01	+	+	+	
1313	YJL110C	35	F	3		YKO_0835	F03	1.063	+	+	+	
1315	YJL108C	35	F	4		YKO_0835	F04	1.1	+	+	+	
1316	YJL107C	35	F	5		YKO_0835	F05	1.079	+	+	+	
1317	YJL106W	35	F	6		YKO_0835	F06	1.1	+	+	+	
1321	YJL102W	35	F	7	slow growth	YKO_0835	F07	0.972	-	-	-	Doubt
1323	YJL100W	35	F	8		YKO_0835	F08	1.067	+	+	+	
1324	YJL099W	35	F	9		YKO_0835	F09	0.923	+	+	+	
1325	YJL098W	35	F	10		YKO_0835	F10	0.983	+	+	+	
1327	YJL096W	35	F	11	slow growth	YKO_0835	F11	1.009	-	+	-	Doubt
1328	YJL095W	35	F	12		YKO_0835	F12	0.852	+	+	+	
1330	YJL093C	35	G	1		YKO_0835	G01	0.658	+	+	+	
1331	YJL092W	35	G	2		YKO_0835	G02	1.049	+	+	+	
1334	YJL089W	35	G	3		YKO_0835	G03	1.079	+	+	+	
1335	YJL088W	35	G	4		YKO_0835	G04	1.089	+	+	+	
1339	YJL084C	35	G	5		YKO_0835	G05	1.069	+	+	+	
1340	YJL083W	35	G	6		YKO_0835	G06	0.986	+	+	+	
1341	YJL082W	35	G	7		YKO_0835	G07	1.05	+	+	+	
1343	YJL080C	35	G	8		YKO_0835	G08	0.831	+	+	+	
1344	YJL079C	35	G	9		YKO_0835	G09	0.979	+	+	+	
1346	YJL077C	35	G	10		YKO_0835	G10	0.97	+	+	+	
1350	YJL073W	35	G	11		YKO_0835	G11	1.032	+	+	+	
1352	YJL071W	35	G	12		YKO_0835	G12	1.065	+	+	+	
1355	YJL068C	35	H	1		YKO_0835	H01	1.043	+	+	+	
--		35	H	2	empty	YKO_0835	H02	empty	empty	empty	empty	empty
1356	YJL067W	35	H	3		YKO_0835	H03	1.084	+	+	+	
1357	YJL066C	35	H	4		YKO_0835	H04	1.047	+	+	+	
1358	YJL064W	35	H	5		YKO_0835	H05	0.762	+	-	+	Incongruence
1359	YJL065C	35	H	6		YKO_0835	H06	1.028	+	-	+	Incongruence
1360	YJL063C	35	H	7	slow growth, petite	YKO_0835	H07	0.936	slow	-	-	Doubt
1361	YJL062W	35	H	8		YKO_0835	H08	0.965	+	+	+	
1363	YJL060W	35	H	9		YKO_0835	H09	0.947	+	+	+	

Euroscarf Information						Replica plate Information			Tau Toxicity Enhancer Primary Screen Results			
record no.	ORF name	Plate	Row	Col	Comment	Replica plate	Well	YPD (OD600nm)	Growth plate (SC+GAL comp.)	Transformation control plate (SC+GLU-Leu)	TEST Plate (SC+GAL-Leu)	Classification
1364	YJL059W	35	H	10		YKO_0835	H10	0.93	+	+	+	
1365	YJL058C	35	H	11		YKO_0835	H11	0.987	+	+	+	
1366	YJL057C	35	H	12		YKO_0835	H12	1.048	+	+	+	
1367	YJL056C	36	A	1		YKO_0836	A01	0.821	+	+	-	HIT
1368	YJL055W	36	A	2		YKO_0836	A02	0.861	+	+	+	
1370	YJL053W	36	A	3		YKO_0836	A03	0.876	+	+	+	
1371	YJL052W	36	A	4	slow growth, petite	YKO_0836	A04	0.933	+	+	+	
1372	YJL051W	36	A	5		YKO_0836	A05	0.962	+	+	+	
1374	YJL049W	36	A	6		YKO_0836	A06	1.043	+	+	+	
1375	YJL048C	36	A	7		YKO_0836	A07	1.028	+	+	+	
1376	YJL047C	36	A	8		YKO_0836	A08	0.847	+	+	+	
1377	YJL046W	36	A	9	slow growth, petite	YKO_0836	A09	0.954	+	+	+	
1378	YJL045W	36	A	10		YKO_0836	A10	1.034	+	+	+	
1379	YJL044C	36	A	11		YKO_0836	A11	0.952	+	+	+	
1380	YJL043W	36	A	12		YKO_0836	A12	1.046	+	+	+	
1384	YJL038C	36	B	1		YKO_0836	B01	0.973	+	+	+	
1385	YJL037W	36	B	2		YKO_0836	B02	1.059	+	+	+	
1386	YJL036W	36	B	3		YKO_0836	B03	0.674	+	+	+	
1392	YJL030W	36	B	4		YKO_0836	B04	1.036	+	+	+	
6577	YEL012W	36	B	5		YKO_0836	B05	1.037	+	+	+	
6583	YER031C	36	B	6		YKO_0836	B06	1.048	+	+	-	HIT
6584	YER046W	36	B	7		YKO_0836	B07	1.069	+	+	+	
6585	YER063W	36	B	8		YKO_0836	B08	1.036	+	+	+	
6586	YER066W	36	B	9		YKO_0836	B09	1.029	+	+	+	
6589	YGR188C	36	B	10		YKO_0836	B10	0.745	+	+	+	
6590	YGR201C	36	B	11		YKO_0836	B11	1.008	+	+	+	
6591	YGR204W	36	B	12		YKO_0836	B12	1.02	+	+	+	
6593	YHL002W	36	C	1		YKO_0836	C01	1.077	+	+	+	
6595	YHL011C	36	C	2		YKO_0836	C02	0.879	+	+	+	
6597	YHL039W	36	C	3		YKO_0836	C03	1.031	+	+	+	
6600	YHR003C	36	C	4		YKO_0836	C04	1.079	+	+	+	
6601	YHR004C	36	C	5		YKO_0836	C05	0.978	+	+	-	HIT
6603	YHR006W	36	C	6		YKO_0836	C06	1.044	+	+	+	
6605	YHR008C	36	C	7		YKO_0836	C07	1.008	+	+	+	
6606	YHR009C	36	C	8		YKO_0836	C08	0.944	+	+	+	
6608	YHR025W	36	C	9	no growth on drop-in media	YKO_0836	C09	0.779	+	+	+	
6609	YHR026W	36	C	10	petite	YKO_0836	C10	0.897	-	-	-	Doubt
6611	YHR041C	36	C	11	slow growth	YKO_0836	C11	0.777	+	+	+	
--		36	C	12	empty	YKO_0836	C12	empty	empty	empty	empty	empty
6613	YHR059W	36	D	1		YKO_0836	D01	1.105	+	+	+	
6615	YHR067W	36	D	2	slow growth	YKO_0836	D02	1.013	slow	-	-	Doubt
6623	YHR127W	36	D	3		YKO_0836	D03	1.104	+	+	+	
6625	YHR131C	36	D	4		YKO_0836	D04	1.077	+	+	+	
6633	YHR180W	36	D	5		YKO_0836	D05	1.05	+	+	+	
6634	YHR185C	36	D	6		YKO_0836	D06	1.054	+	+	+	
6637	YHR194W	36	D	7		YKO_0836	D07	0.997	+	+	+	
6641	YLL007C	36	D	8		YKO_0836	D08	1.063	+	+	+	
6643	YMR154C	36	D	9		YKO_0836	D09	1.03	+	+	+	
6645	YNL274C	36	D	10		YKO_0836	D10	1.056	+	+	+	
6650	YOL141W	36	D	11		YKO_0836	D11	0.953	+	+	+	
6659	YOL150C	36	D	12		YKO_0836	D12	1.065	+	-	+	Incongruence
6664	YOL158C	36	E	1		YKO_0836	E01	1.068	+	+	+	
6665	YOL159C	36	E	2		YKO_0836	E02	1.065	+	+	+	
6666	YOL160W	36	E	3		YKO_0836	E03	1.077	+	+	+	
6667	YOL162W	36	E	4		YKO_0836	E04	1.034	+	+	+	
6668	YOL163W	36	E	5		YKO_0836	E05	1.083	+	+	+	
2551	YJR073C	36	E	6		YKO_0836	E06	1.011	+	-	+	Incongruence
2553	YJR075W	36	E	7		YKO_0836	E07	0.962	+	+	+	
2556	YJR078W	36	E	8		YKO_0836	E08	0.959	+	-	+	Incongruence
2557	YJR079W	36	E	9		YKO_0836	E09	1.02	+	+	+	
2559	YJR082C	36	E	10		YKO_0836	E10	0.89	+	+	+	
2560	YJR083C	36	E	11		YKO_0836	E11	0.929	+	+	+	
2565	YJR088C	36	E	12		YKO_0836	E12	0.934	+	+	+	
2569	YJR092W	36	F	1		YKO_0836	F01	1.052	+	+	+	
2580	YJR102C	36	F	2		YKO_0836	F02	0.963	+	+	+	
2581	YJR103W	36	F	3		YKO_0836	F03	1.007	+	+	+	
2583	YJR105W	36	F	4		YKO_0836	F04	0.98	+	+	+	
2586	YJR108W	36	F	5		YKO_0836	F05	1.003	+	+	+	
2588	YJR110W	36	F	6		YKO_0836	F06	1.012	+	+	+	
2589	YJR111C	36	F	7		YKO_0836	F07	0.976	+	+	+	
2593	YJR115W	36	F	8		YKO_0836	F08	0.964	+	+	+	
2605	YJR127C	36	F	9		YKO_0836	F09	1.038	+	-	+	Incongruence
2606	YJR128W	36	F	10		YKO_0836	F10	0.926	+	+	+	
2607	YJR129C	36	F	11		YKO_0836	F11	0.673	+	+	+	
2608	YJR130C	36	F	12		YKO_0836	F12	0.973	+	+	+	
2613	YJR135C	36	G	1		YKO_0836	G01	1.07	+	+	+	
2615	YJR137C	36	G	2	grows well on -met, grows slow on -lys	YKO_0836	G02	0.906	+	+	+	
2624	YJR146W	36	G	3		YKO_0836	G03	1	+	+	+	
2625	YJR147W	36	G	4		YKO_0836	G04	0.992	+	+	+	
2627	YJR149W	36	G	5		YKO_0836	G05	0.97	+	+	+	
2630	YJR152W	36	G	6		YKO_0836	G06	1.027	+	-	-	Doubt
2632	YJR154W	36	G	7		YKO_0836	G07	1	+	+	+	
6003	YKR087C	36	G	8		YKO_0836	G08	0.977	+	+	+	

	Euroscarf Information					Replica plate Information			Tau Toxicity Enhancer Primary Screen Results			
record no.	ORF name	Plate	Row	Col	Comment	Replica plate	Well	YPD (OD600nm)	Growth plate (SC+GAL comp.)	Transformation control plate (SC+GLU-Leu)	TEST Plate (SC+GAL-Leu)	Classification
6004	YKR088C	36	G	9		YKO_0836	G09	1.01	+	+	+	
6005	YKR089C	36	G	10		YKO_0836	G10	0.954	+	-	+	Incongruence
6006	YKR090W	36	G	11		YKO_0836	G11	0.963	+	-	-	Doubt
6007	YKR091W	36	G	12		YKO_0836	G12	0.978	+	+	+	
6008	YKR092C	36	H	1		YKO_0836	H01	1.049	+	+	+	
--		36	H	2	empty	YKO_0836	H02	empty	empty	empty	empty	empty
6009	YKR093W	36	H	3		YKO_0836	H03	0.876	+	+	+	
6013	YKR097W	36	H	4		YKO_0836	H04	0.731	+	+	+	
6014	YKR098C	36	H	5		YKO_0836	H05	0.956	+	+	+	
6015	YKR099W	36	H	6		YKO_0836	H06	0.774	+	+	+	
6016	YKR100C	36	H	7		YKO_0836	H07	0.988	+	+	+	
6017	YKR101W	36	H	8		YKO_0836	H08	0.886	+	+	+	
6019	YKR103W	36	H	9		YKO_0836	H09	0.902	+	+	+	
6020	YKR104W	36	H	10		YKO_0836	H10	0.659	+	+	+	
6021	YKR105C	36	H	11		YKO_0836	H11	0.986	+	-	+	Incongruence
6022	YLL018C-A	36	H	12	slow growth, petite	YKO_0836	H12	0.956	+	-	-	Doubt
6023	YLR262C-A	37	A	1		YKO_0837	A01	0.7397	+	+	+	
6025	YLR422W	37	A	2		YKO_0837	A02	0.692	+	+	+	
6026	YLR423C	37	A	3		YKO_0837	A03	0.9347	+	+	+	
6028	YLR425W	37	A	4		YKO_0837	A04	0.7525	+	+	+	
6029	YLR426W	37	A	5		YKO_0837	A05	0.649	+	+	+	
6030	YLR427W	37	A	6		YKO_0837	A06	0.6303	+	+	+	
6031	YLR428C	37	A	7		YKO_0837	A07	0.6258	+	+	+	
6032	YLR429W	37	A	8		YKO_0837	A08	0.608	+	+	+	
6034	YLR431C	37	A	9		YKO_0837	A09	0.5924	+	+	+	
6035	YLR432W	37	A	10		YKO_0837	A10	0.6026	+	+	+	
6036	YLR433C	37	A	11		YKO_0837	A11	0.6164	+	+	+	
6037	YLR434C	37	A	12		YKO_0837	A12	0.7377	+	+	+	
6038	YLR435W	37	B	1		YKO_0837	B01	0.7366	+	+	+	
6039	YLR436C	37	B	2		YKO_0837	B02	0.7126	+	+	+	
6040	YLR437C	37	B	3		YKO_0837	B03	0.7272	+	+	+	
6042	YLR438W	37	B	4		YKO_0837	B04	0.7228	+	+	+	
6045	YLR441C	37	B	5		YKO_0837	B05	0.6625	+	+	+	
6047	YLR443W	37	B	6		YKO_0837	B06	0.7215	+	+	+	
6048	YLR444C	37	B	7		YKO_0837	B07	0.7248	+	+	+	
6049	YLR445W	37	B	8		YKO_0837	B08	0.7302	+	+	+	
6050	YLR446W	37	B	9		YKO_0837	B09	0.6902	+	+	+	
6051	YLR447C	37	B	10	petite	YKO_0837	B10	0.7246	-	-	-	Doubt
6052	YLR448W	37	B	11		YKO_0837	B11	0.7141	+	+	+	
6053	YLR449W	37	B	12		YKO_0837	B12	0.7301	+	+	+	
6054	YLR450W	37	C	1		YKO_0837	C01	0.7451	+	+	+	
6055	YLR452C	37	C	2		YKO_0837	C02	0.6873	+	+	+	
6056	YLR453C	37	C	3		YKO_0837	C03	0.759	+	+	+	
6057	YLR454W	37	C	4		YKO_0837	C04	0.9535	+	+	+	
6059	YLR456W	37	C	5		YKO_0837	C05	0.7115	+	+	+	
6063	YLR460C	37	C	6		YKO_0837	C06	0.7078	+	+	+	
6064	YLR461W	37	C	7		YKO_0837	C07	0.6973	+	+	+	
6065	YML009C	37	C	8		YKO_0837	C08	0.7192	+	+	+	
6066	YML010C-B	37	C	9		YKO_0837	C09	0.7183	+	+	+	
6067	YML021C	37	C	10		YKO_0837	C10	0.7076	+	+	+	
6068	YML081C-A	37	C	11	slow growth	YKO_0837	C11	0.7097	+	+	+	
6069	YMR060C	37	C	12	slow growth	YKO_0837	C12	0.6319	+	+	+	
--		37	D	1	empty	YKO_0837	D01	empty	empty	empty	empty	empty
6070	YMR158C-B	37	D	2		YKO_0837	D02	0.7489	+	+	+	
6071	YMR169C	37	D	3		YKO_0837	D03	0.7333	+	+	+	
6072	YMR174C	37	D	4		YKO_0837	D04	0.7025	+	+	+	
6073	YMR175W	37	D	5		YKO_0837	D05	0.7012	+	+	+	
6074	YMR194C-A	37	D	6		YKO_0837	D06	0.7284	+	+	+	
6075	YMR326C	37	D	7		YKO_0837	D07	0.7236	+	+	+	
6076	YNR032C-A	37	D	8		YKO_0837	D08	0.7224	+	+	+	
6077	YNR050C	37	D	9	super slow growth, no growth on -met, no growth on -lys ,no growth on drop-in media, mates like a	YKO_0837	D09	0.7368	+	+	+	
6078	YNR051C	37	D	10		YKO_0837	D10	0.3328	slow	+	+	
6083	YNR056C	37	D	11		YKO_0837	D11	0.7442	+	+	+	
6084	YNR057C	37	D	12		YKO_0837	D12	0.7335	+	+	+	
6085	YNR058W	37	E	1		YKO_0837	E01	0.7192	+	+	+	
6086	YNR059W	37	E	2		YKO_0837	E02	0.7053	+	+	+	
6087	YNR060W	37	E	3		YKO_0837	E03	0.7161	+	+	+	
6088	YNR061C	37	E	4		YKO_0837	E04	0.698	+	+	+	
6089	YNR062C	37	E	5		YKO_0837	E05	0.6984	+	+	+	
6090	YNR063W	37	E	6		YKO_0837	E06	0.7456	+	+	+	
6091	YNR064C	37	E	7		YKO_0837	E07	0.733	+	+	+	
6092	YNR065C	37	E	8		YKO_0837	E08	0.7345	+	+	+	
6093	YNR066C	37	E	9		YKO_0837	E09	0.7726	+	+	+	
6094	YNR067C	37	E	10		YKO_0837	E10	0.7379	+	+	+	
6095	YNR068C	37	E	11	petite, mates like alpha, no growth on -met, growth on -lys. PCR mating type alpha	YKO_0837	E11	0.7637	+	+	+	
6865	YAL012W	37	E	12	slow growth	YKO_0837	E12	0.6859	slow	-	-	Doubt

	Euroscarf Information					Replica plate Information			Tau Toxicity Enhancer Primary Screen Results			
record no.	ORF name	Plate	Row	Col	Comment	Replica plate	Well	YPD (OD600nm)	Growth plate (SC+GAL comp.)	Transformation control plate (SC+GLU-Leu)	TEST Plate (SC+GAL-Leu)	Classification
6867	YAL047C	37	F	1	slow growth	YKO_0837	F01	0.6176	+	+	+	
6868	YAL054C	37	F	2		YKO_0837	F02	0.7336	+	+	+	
6869	YAL058C-A	37	F	3		YKO_0837	F03	0.7262	+	+	+	
6870	YAR050W	37	F	4		YKO_0837	F04	0.7235	+	+	+	
6871	YCL006C	37	F	5		YKO_0837	F05	0.7077	+	+	+	
6874	YCL022C	37	F	6		YKO_0837	F06	0.7005	+	+	+	
6875	YCL023C	37	F	7		YKO_0837	F07	0.6978	+	+	+	
6876	YCL038C	37	F	8		YKO_0837	F08	0.7236	+	+	+	
6877	YCL058C	37	F	9		YKO_0837	F09	0.5137	+	+	+	
6878	YCL074W	37	F	10		YKO_0837	F10	0.7669	+	+	+	
6879	YCL075W	37	F	11		YKO_0837	F11	0.7541	+	+	+	
6880	YCL076W	37	F	12		YKO_0837	F12	0.717	+	+	+	
6881	YGL199C	37	G	1		YKO_0837	G01	0.7461	+	+	+	
6882	YGL214W	37	G	2		YKO_0837	G02	0.7553	+	+	+	
6883	YGL217C	37	G	3		YKO_0837	G03	0.7031	+	+	+	
6885	YGL235W	37	G	4		YKO_0837	G04	0.7183	+	+	+	
6887	YGR011W	37	G	5		YKO_0837	G05	0.7133	+	+	+	
6888	YGR018C	37	G	6		YKO_0837	G06	0.6628	+	+	+	
6889	YGR022C	37	G	7		YKO_0837	G07	0.6647	+	+	+	
6890	YGR025W	37	G	8		YKO_0837	G08	0.7097	+	+	+	
6893	YJR069C	37	G	9		YKO_0837	G09	0.711	+	+	+	
6894	YJR070C	37	G	10		YKO_0837	G10	0.7286	+	+	+	
6896	YJR074W	37	G	11		YKO_0837	G11	0.5896	+	+	+	
6897	YJR077C	37	G	12	slow growth, petite	YKO_0837	G12	0.6843	+	+	-	HIT
6898	YJR080C	37	H	1		YKO_0837	H01	0.7255	+	+	+	
--		37	H	2	empty	YKO_0837	H02	empty	empty	empty	empty	empty
6899	YJR084W	37	H	3		YKO_0837	H03	0.5997	+	+	+	
6901	YJR087W	37	H	4		YKO_0837	H04	0.6596	+	+	+	
6903	YJR091C	37	H	5		YKO_0837	H05	0.6964	+	+	+	
6905	YJR094C	37	H	6		YKO_0837	H06	0.6013	+	+	+	
6906	YJR094W-A	37	H	7		YKO_0837	H07	0.6586	+	+	+	
6907	YJR095W	37	H	8		YKO_0837	H08	0.7506	+	+	+	
6908	YJR096W	37	H	9		YKO_0837	H09	0.7379	+	+	+	
6909	YJR097W	37	H	10		YKO_0837	H10	0.7237	+	+	+	
6910	YJR098C	37	H	11		YKO_0837	H11	0.7085	+	+	+	
6911	YJR099W	37	H	12		YKO_0837	H12	0.7334	+	+	+	
6912	YJR100C	38	A	1		YKO_0838	A01	0.732	+	+	+	
6913	YJR104C	38	A	2	no growth on drop-in media	YKO_0838	A02	0.863	+	+	+	
6914	YJR106W	38	A	3		YKO_0838	A03	0.971	+	+	+	
6915	YJR107W	38	A	4		YKO_0838	A04	0.917	+	+	+	
6916	YJR109C	38	A	5	no growth on drop-in media	YKO_0838	A05	0.897	+	+	+	
6918	YJR113C	38	A	6	slow growth, petite	YKO_0838	A06	0.826	slow	+	-	Doubt
6919	YJR116W	38	A	7		YKO_0838	A07	0.932	+	+	+	
6920	YJR117W	38	A	8		YKO_0838	A08	0.753	+	+	+	
6921	YJR118C	38	A	9		YKO_0838	A09	0.71	+	+	+	
6922	YJR119C	38	A	10		YKO_0838	A10	0.93	+	+	+	
6923	YJR120W	38	A	11	slow growth, petite	YKO_0838	A11	0.806	+	+	-	HIT
6924	YJR121W	38	A	12	slow growth, petite	YKO_0838	A12	0.837	+	+	+	
6925	YJR122W	38	B	1	slow growth, petite, no growth on -lys, no growth on drop-in media	YKO_0838	B01	0.555	slow	-	-	Doubt
6927	YJR124C	38	B	2		YKO_0838	B02	0.966	+	+	+	
6928	YJR125C	38	B	3		YKO_0838	B03	0.961	+	+	+	
6929	YJR126C	38	B	4		YKO_0838	B04	0.922	+	+	+	
6930	YJR131W	38	B	5		YKO_0838	B05	0.951	+	+	+	
6931	YJR133W	38	B	6		YKO_0838	B06	0.962	+	+	+	
6932	YJR134C	38	B	7		YKO_0838	B07	0.99	+	+	+	
6933	YJR139C	38	B	8	no growth on drop-in media	YKO_0838	B08	0.865	+	+	+	
6934	YJR140C	38	B	9		YKO_0838	B09	0.998	+	+	+	
6936	YJR142W	38	B	10		YKO_0838	B10	0.806	+	+	+	
6937	YJR144W	38	B	11	slow growth	YKO_0838	B11	0.925	-	+	-	Doubt
6938	YJR145C	38	B	12		YKO_0838	B12	0.835	+	+	+	
6939	YJR148W	38	C	1		YKO_0838	C01	0.785	+	+	+	
6940	YJR150C	38	C	2		YKO_0838	C02	0.976	+	+	+	
6941	YJR153W	38	C	3		YKO_0838	C03	0.965	+	+	+	
6942	YKL005C	38	C	4		YKO_0838	C04	0.985	+	+	+	
6943	YKL030W	38	C	5		YKO_0838	C05	0.873	+	+	+	
6945	YLR146C	38	C	6		YKO_0838	C06	0.96	+	+	+	
6948	YLR343W	38	C	7		YKO_0838	C07	0.939	+	+	+	
6952	YML067C	38	C	8		YKO_0838	C08	0.91	+	+	+	
6953	YML068W	38	C	9		YKO_0838	C09	0.772	+	+	+	
6954	YML072C	38	C	10		YKO_0838	C10	0.802	+	+	+	
6956	YMR136W	38	C	11		YKO_0838	C11	0.801	+	+	+	
6957	YMR172W	38	C	12		YKO_0838	C12	0.757	+	+	+	
6959	YOR300W	38	D	1		YKO_0838	D01	0.872	+	+	+	
--		38	D	2	empty	YKO_0838	D02	empty	empty	empty	empty	empty
6960	YOR309C	38	D	3		YKO_0838	D03	0.874	+	+	+	
3889	YDL191W	38	D	4		YKO_0838	D04	0.896	+	+	+	
3890	YDL192W	38	D	5		YKO_0838	D05	0.845	+	+	+	
3895	YDL197C	38	D	6		YKO_0838	D06	0.987	+	+	+	

Euroscarf Information						Replica plate Information			Tau Toxicity Enhancer Primary Screen Results			
record no.	ORF name	Plate	Row	Col	Comment	Replica plate	Well	YPD (OD600nm)	Growth plate (SC+GAL comp.)	Transformation control plate (SC+GLU-Leu)	TEST Plate (SC+GAL-Leu)	Classification
3896	YDL198C	38	D	7		YKO_0838	D07	0.81	-	+	-	Doubt
3897	YDL199C	38	D	8		YKO_0838	D08	1.019	+	+	+	
3898	YDL200C	38	D	9		YKO_0838	D09	0.972	+	+	+	
3899	YDL201W	38	D	10		YKO_0838	D10	0.851	+	+	+	
3901	YDL203C	38	D	11		YKO_0838	D11	0.859	+	+	+	
3902	YDL204W	38	D	12		YKO_0838	D12	0.828	+	+	+	
3904	YDL206W	38	E	1		YKO_0838	E01	not grown	-	-	-	Not grown
3908	YDL210W	38	E	2		YKO_0838	E02	0.985	+	+	+	
3909	YDL211C	38	E	3		YKO_0838	E03	0.73	+	+	+	
3911	YDL213C	38	E	4		YKO_0838	E04	0.92	+	+	+	
3912	YDL214C	38	E	5		YKO_0838	E05	1.028	+	+	+	
3913	YDL215C	38	E	6		YKO_0838	E06	0.976	+	+	+	
3914	YDL216C	38	E	7		YKO_0838	E07	1	+	+	+	
3916	YDL218W	38	E	8		YKO_0838	E08	0.956	+	+	+	
3917	YDL219W	38	E	9		YKO_0838	E09	0.993	+	+	+	
3920	YDL222C	38	E	10		YKO_0838	E10	1.016	+	+	+	
3921	YDL223C	38	E	11		YKO_0838	E11	0.815	+	+	+	
3922	YDL224C	38	E	12		YKO_0838	E12	0.832	+	+	+	
3923	YDL225W	38	F	1		YKO_0838	F01	0.845	+	+	+	
3924	YDL226C	38	F	2		YKO_0838	F02	0.895	+	+	+	
3925	YDL227C	38	F	3		YKO_0838	F03	0.718	+	+	+	
3926	YDL229W	38	F	4		YKO_0838	F04	0.975	+	+	+	
3927	YDL230W	38	F	5		YKO_0838	F05	0.966	+	+	+	
3928	YDL231C	38	F	6		YKO_0838	F06	0.968	+	+	+	
3929	YDL232W	38	F	7	slow growth	YKO_0838	F07	0.974	+	+	+	
3930	YDL233W	38	F	8		YKO_0838	F08	0.886	+	+	+	
3931	YDL234C	38	F	9		YKO_0838	F09	0.866	+	+	+	
3933	YDL236W	38	F	10		YKO_0838	F10	0.801	+	+	+	
3934	YDL237W	38	F	11		YKO_0838	F11	0.874	+	+	+	
3935	YDL238C	38	F	12		YKO_0838	F12	0.813	+	+	+	
3936	YDL239C	38	G	1		YKO_0838	G01	1.009	+	+	+	
3937	YDL240W	38	G	2		YKO_0838	G02	1.011	+	+	+	
3938	YDL241W	38	G	3		YKO_0838	G03	0.94	+	+	+	
3939	YDL242W	38	G	4		YKO_0838	G04	1.005	+	+	+	
3940	YDL243C	38	G	5		YKO_0838	G05	0.405	+	+	-	HIT
3941	YDR001C	38	G	6		YKO_0838	G06	0.845	+	+	+	
3943	YDR003W	38	G	7		YKO_0838	G07	0.966	+	+	+	
3944	YDR004W	38	G	8		YKO_0838	G08	0.939	+	+	+	
3945	YDR005C	38	G	9		YKO_0838	G09	0.924	+	+	+	
3946	YDR006C	38	G	10		YKO_0838	G10	0.941	+	+	+	
3948	YDR008C	38	G	11	no growth on drop-in media	YKO_0838	G11	0.857	+	+	+	
3949	YDR009W	38	G	12		YKO_0838	G12	0.766	slow	+	-	Doubt
3950	YDR010C	38	H	1		YKO_0838	H01	0.883	+	+	+	
--		38	H	2	empty	YKO_0838	H02	empty	empty	empty	empty	empty
3951	YDR011W	38	H	3		YKO_0838	H03	1.024	+	+	+	
3953	YDR014W	38	H	4		YKO_0838	H04	0.974	+	+	+	
3954	YDR015C	38	H	5		YKO_0838	H05	1.041	+	+	+	
3956	YDR017C	38	H	6		YKO_0838	H06	not grown	-	-	-	Not grown
3957	YDR018C	38	H	7		YKO_0838	H07	1.059	+	-	+	Incongruence
3958	YDR019C	38	H	8		YKO_0838	H08	1.035	+	+	+	
3959	YDR020C	38	H	9		YKO_0838	H09	0.937	+	+	+	
3961	YDR022C	38	H	10		YKO_0838	H10	0.877	+	+	+	
3963	YDR024W	38	H	11		YKO_0838	H11	0.914	+	+	+	
3964	YDR025W	38	H	12		YKO_0838	H12	0.998	+	-	+	Incongruence
3965	YDR026C	39	A	1		YKO_0839	A01	0.835	+	+	+	
3966	YDR027C	39	A	2	slow growth	YKO_0839	A02	0.588	+	+	+	
3967	YDR028C	39	A	3	slow growth	YKO_0839	A03	not grown	-	-	-	Not grown
3968	YDR029W	39	A	4		YKO_0839	A04	0.882	+	+	+	
3969	YDR030C	39	A	5		YKO_0839	A05	0.895	+	+	+	
3970	YDR031W	39	A	6		YKO_0839	A06	0.924	+	+	+	
3971	YDR032C	39	A	7		YKO_0839	A07	0.934	+	+	+	
3972	YDR033W	39	A	8		YKO_0839	A08	0.923	+	+	+	
3973	YDR034C	39	A	9		YKO_0839	A09	0.889	+	+	+	
3974	YDR035W	39	A	10		YKO_0839	A10	0.947	+	-	-	Doubt
3975	YDR036C	39	A	11		YKO_0839	A11	0.91	+	-	-	Doubt
3978	YDR042C	39	A	12	slow growth, petite	YKO_0839	A12	0.742	slow	+	-	Doubt
3979	YDR043C	39	B	1		YKO_0839	B01	0.902	+	+	+	
3982	YDR046C	39	B	2		YKO_0839	B02	0.972	+	+	+	
5714	YAL064C-A	39	B	3		YKO_0839	B03	0.943	+	+	+	
5716	YBL091C-A	39	B	4		YKO_0839	B04	0.924	+	+	+	
5717	YBR269C	39	B	5		YKO_0839	B05	0.88	+	+	+	
5719	YBR271W	39	B	6		YKO_0839	B06	0.95	+	+	+	
5721	YBR273C	39	B	7		YKO_0839	B07	0.921	+	+	+	
5722	YBR274W	39	B	8		YKO_0839	B08	0.946	+	+	+	
5725	YBR277C	39	B	9		YKO_0839	B09	0.929	+	-	+	Incongruence
5726	YBR278W	39	B	10		YKO_0839	B10	0.958	+	-	+	Incongruence
5729	YBR281C	39	B	11		YKO_0839	B11	0.865	+	+	-	HIT
5730	YBR282W	39	B	12		YKO_0839	B12	0.849	slow	+	-	Doubt
5731	YBR283C	39	C	1		YKO_0839	C01	0.927	+	+	+	
5732	YBR284W	39	C	2		YKO_0839	C02	0.87	+	+	+	
5733	YBR285W	39	C	3		YKO_0839	C03	0.995	+	+	+	
5734	YBR286W	39	C	4	slow growth	YKO_0839	C04	0.922	+	+	+	

Euroscarf Information						Replica plate Information			Tau Toxicity Enhancer Primary Screen Results			
record no.	ORF name	Plate	Row	Col	Comment	Replica plate	Well	YPD (OD600nm)	Growth plate (SC+GAL comp.)	Transformation control plate (SC+GLU-Leu)	TEST Plate (SC+GAL-Leu)	Classification
5738	YBR290W	39	C	5		YKO_0839	C05	0.91	+	+	+	
5739	YBR291C	39	C	6		YKO_0839	C06	1.011	+	+	-	HIT
5740	YBR292C	39	C	7		YKO_0839	C07	1.061	+	+	+	
5741	YBR293W	39	C	8		YKO_0839	C08	1.036	+	+	+	
5743	YBR295W	39	C	9		YKO_0839	C09	1.024	+	+	+	
5744	YBR296C	39	C	10	slow growth	YKO_0839	C10	1.007	+	+	+	
5745	YBR297W	39	C	11		YKO_0839	C11	0.949	+	+	-	HIT
5746	YBR298C	39	C	12		YKO_0839	C12	1.025	+	+	+	
5747	YBR300C	39	D	1		YKO_0839	D01	1.025	+	+	+	
5749	YCL001W-A	39	D	2		YKO_0839	D02	1.061	+	+	+	
--		39	D	3	empty	YKO_0839	D03	empty	empty	empty	empty	empty
5751	YCR020W-B	39	D	4	slow growth	YKO_0839	D04	not grown	-	-	-	Not grown
5752	YCR024C	39	D	5	slow growth, petite	YKO_0839	D05	0.961	slow	-	-	Doubt
5753	YCR024C-A	39	D	6		YKO_0839	D06	1.009	+	+	+	
5754	YCR025C	39	D	7		YKO_0839	D07	0.998	+	+	+	
5755	YCR026C	39	D	8		YKO_0839	D08	0.983	+	+	+	
5756	YCR027C	39	D	9		YKO_0839	D09	1.021	+	-	+	Incongruence
5757	YCR028C	39	D	10		YKO_0839	D10	0.463	slow	-	-	Doubt
5760	YCR031C	39	D	11		YKO_0839	D11	0.854	+	+	+	
5763	YCR034W	39	D	12		YKO_0839	D12	0.922	+	+	+	
5765	YCR036W	39	E	1		YKO_0839	E01	1.005	+	+	+	
5766	YCR037C	39	E	2		YKO_0839	E02	0.994	+	+	+	
5767	YCR043C	39	E	3		YKO_0839	E03	0.983	+	+	+	
5769	YCR045C	39	E	4		YKO_0839	E04	1.01	+	+	+	
5773	YCR049C	39	E	5		YKO_0839	E05	1.053	+	+	+	
5774	YCR050C	39	E	6		YKO_0839	E06	0.926	+	+	+	
5775	YCR051W	39	E	7		YKO_0839	E07	1.035	+	+	+	
5780	YCR059C	39	E	8		YKO_0839	E08	0.994	+	-	+	Incongruence
5782	YCR061W	39	E	9		YKO_0839	E09	0.996	+	+	+	
5786	YCR065W	39	E	10		YKO_0839	E10	0.923	+	+	-	HIT
5787	YCR066W	39	E	11		YKO_0839	E11	0.958	+	+	+	
5789	YCR068W	39	E	12		YKO_0839	E12	0.985	+	+	+	
5791	YCR071C	39	F	1	slow growth, petite	YKO_0839	F01	0.887	-	+	-	Doubt
5794	YCR073W-A	39	F	2	slow growth, petite	YKO_0839	F02	0.997	+	+	+	
5796	YCR076C	39	F	3		YKO_0839	F03	0.979	+	+	+	
5797	YCR077C	39	F	4		YKO_0839	F04	1.016	-	+	-	Doubt
5798	YCR079W	39	F	5		YKO_0839	F05	1.001	+	+	+	
5799	YCR081W	39	F	6		YKO_0839	F06	0.926	-	-	-	Doubt
5800	YCR082W	39	F	7		YKO_0839	F07	0.989	+	+	+	
5803	YCR085W	39	F	8		YKO_0839	F08	0.918	+	+	+	
5804	YCR086W	39	F	9		YKO_0839	F09	0.984	+	+	+	
5805	YCR087C-A	39	F	10		YKO_0839	F10	0.879	+	+	+	
5806	YCR087W	39	F	11		YKO_0839	F11	0.893	+	+	+	
6775	YJL007C	39	F	12		YKO_0839	F12	0.979	+	+	-	HIT
6784	YJL016W	39	G	1		YKO_0839	G01	1.048	+	+	+	
6785	YJL017W	39	G	2		YKO_0839	G02	1.043	+	+	+	
6788	YJL020C	39	G	3		YKO_0839	G03	0.991	+	+	+	
6789	YJL021C	39	G	4		YKO_0839	G04	0.982	+	+	+	
6790	YJL022W	39	G	5	slow growth	YKO_0839	G05	1.017	+	+	+	
6791	YJL023C	39	G	6	slow growth, petite	YKO_0839	G06	0.908	slow	+	-	Doubt
6792	YJL024C	39	G	7		YKO_0839	G07	1.044	+	+	-	HIT
6797	YJL029C	39	G	8	Confirmed Het Diploid 10/15/01	YKO_0839	G08	0.75	slow	+	-	Doubt
6798	YJR001W	39	G	9		YKO_0839	G09	0.822	+	+	+	
6802	YJR005W	39	G	10		YKO_0839	G10	0.938	+	+	+	
6805	YJR008W	39	G	11		YKO_0839	G11	0.971	+	-	+	Incongruence
6806	YJR009C	39	G	12		YKO_0839	G12	0.986	+	+	-	HIT
6807	YJR010C-A	39	H	1		YKO_0839	H01	0.997	+	+	+	
--		39	H	2	empty	YKO_0839	H02	empty	empty	empty	empty	empty
6808	YJR010W	39	H	3		YKO_0839	H03	1.019	+	+	+	
6809	YJR011C	39	H	4		YKO_0839	H04	0.984	+	+	+	
6812	YJR014W	39	H	5		YKO_0839	H05	1.013	+	+	+	
6813	YJR015W	39	H	6		YKO_0839	H06	0.994	+	+	-	HIT
6816	YJR018W	39	H	7	slow on ypg	YKO_0839	H07	not grown	-	-	-	Not grown
6817	YJR019C	39	H	8		YKO_0839	H08	0.952	+	+	+	
6818	YJR020W	39	H	9		YKO_0839	H09	1.018	+	+	+	
6819	YJR021C	39	H	10		YKO_0839	H10	1.021	+	+	+	
6822	YJR024C	39	H	11		YKO_0839	H11	0.955	+	-	+	Incongruence
6823	YJR025C	39	H	12		YKO_0839	H12	0.988	+	+	-	HIT
6824	YJR026W	40	A	1		YKO_0840	A01	0.899	+	+	+	
6828	YJR030C	40	A	2		YKO_0840	A02	0.607	+	+	-	HIT
6829	YJR031C	40	A	3		YKO_0840	A03	1.078	+	+	+	
6831	YJR033C	40	A	4		YKO_0840	A04	0.897	+	+	+	
6833	YJR035W	40	A	5		YKO_0840	A05	0.94	+	+	+	
6834	YJR036C	40	A	6		YKO_0840	A06	1	+	+	+	
6841	YJR043C	40	A	7		YKO_0840	A07	1.005	+	+	+	
6846	YJR048W	40	A	8		YKO_0840	A08	1.032	+	+	-	HIT
6847	YJR049C	40	A	9	grows well on -met, grows well on -lys	YKO_0840	A09	0.967	+	+	-	HIT
6848	YJR050W	40	A	10		YKO_0840	A10	0.776	+	+	+	
6849	YJR051W	40	A	11		YKO_0840	A11	0.921	+	+	+	
6850	YJR052W	40	A	12		YKO_0840	A12	0.962	+	-	+	Incongruence
6851	YJR053W	40	B	1		YKO_0840	B01	0.91	+	+	-	HIT
6852	YJR054W	40	B	2	grows well on -met, grows well on -lys	YKO_0840	B02	0.977	+	+	+	
6853	YJR055W	40	B	3		YKO_0840	B03	not grown	-	-	-	Not grown

	Euroscarf Information					Replica plate Information			Tau Toxicity Enhancer Primary Screen Results			
record no.	ORF name	Plate	Row	Col	Comment	Replica plate	Well	YPD (OD600nm)	Growth plate (SC+GAL comp.)	Transformation control plate (SC+GLU-Leu)	TEST Plate (SC+GAL-Leu)	Classification
6854	YJR056C	40	B	4	grows well on -met, grows well on -lys	YKO_0840	B04	0.879	+	+	+	
6856	YJR058C	40	B	5		YKO_0840	B05	0.974	+	+	-	HIT
6857	YJR059W	40	B	6		YKO_0840	B06	1.027	+	+	-	HIT
6858	YJR060W	40	B	7		YKO_0840	B07	1.038	+	+	+	
6859	YJR061W	40	B	8		YKO_0840	B08	0.831	+	+	+	
6860	YJR062C	40	B	9		YKO_0840	B09	0.948	+	+	-	HIT
6861	YJR063W	40	B	10	slow growth. Confirmed Het Diploid 10/15/01	YKO_0840	B10	0.916	+	+	+	
3793	YDL096C	40	B	11		YKO_0840	B11	0.817	+	+	+	
3796	YDL099W	40	B	12		YKO_0840	B12	0.843	+	+	-	HIT
3797	YDL100C	40	C	1		YKO_0840	C01	0.977	+	+	+	
3798	YDL101C	40	C	2	slow growth	YKO_0840	C02	0.966	+	+	+	
3801	YDL104C	40	C	3	slow growth, petite	YKO_0840	C03	0.977	+	+	-	HIT
3803	YDL106C	40	C	4		YKO_0840	C04	1.007	+	+	+	
3804	YDL107W	40	C	5	slow growth, petite	YKO_0840	C05	0.8	slow	+	-	Doubt
3806	YDL109C	40	C	6		YKO_0840	C06	1.006	+	+	+	
3807	YDL110C	40	C	7	slow growth	YKO_0840	C07	0.973	+	+	+	
3809	YDL112W	40	C	8		YKO_0840	C08	0.903	+	+	+	
3810	YDL113C	40	C	9	slow growth, petite	YKO_0840	C09	0.828	+	+	+	
3811	YDL114W	40	C	10		YKO_0840	C10	0.854	+	+	+	
3813	YDL116W	40	C	11		YKO_0840	C11	0.739	+	+	+	
3814	YDL117W	40	C	12		YKO_0840	C12	0.834	+	+	+	
3815	YDL118W	40	D	1		YKO_0840	D01	0.932	+	+	-	HIT
3816	YDL119C	40	D	2		YKO_0840	D02	0.713	+	+	+	
3818	YDL121C	40	D	3		YKO_0840	D03	0.965	+	+	+	
--		40	D	4	empty	YKO_0840	D04	empty	empty	empty	empty	empty
3819	YDL122W	40	D	5		YKO_0840	D05	0.879	+	+	+	
3820	YDL123W	40	D	6		YKO_0840	D06	0.831	+	+	+	
3821	YDL124W	40	D	7		YKO_0840	D07	0.896	+	+	+	
3822	YDL125C	40	D	8		YKO_0840	D08	0.871	+	+	+	
3824	YDL127W	40	D	9		YKO_0840	D09	0.822	+	+	+	
3825	YDL128W	40	D	10		YKO_0840	D10	0.847	+	+	+	
3826	YDL129W	40	D	11		YKO_0840	D11	0.75	+	+	+	
3827	YDL130W	40	D	12		YKO_0840	D12	0.747	+	+	+	
3828	YDL131W	40	E	1		YKO_0840	E01	1.003	+	+	+	
3830	YDL133W	40	E	2		YKO_0840	E02	0.924	+	+	+	
3831	YDL134C	40	E	3		YKO_0840	E03	0.873	+	+	+	
3832	YDL134C-A	40	E	4		YKO_0840	E04	0.807	+	+	+	
3833	YDL135C	40	E	5		YKO_0840	E05	0.941	+	+	+	
3834	YDL136W	40	E	6		YKO_0840	E06	0.843	+	+	-	HIT
3835	YDL137W	40	E	7		YKO_0840	E07	1.012	+	+	-	HIT
3836	YDL138W	40	E	8		YKO_0840	E08	0.858	+	+	+	
3840	YDL142C	40	E	9		YKO_0840	E09	0.934	+	+	+	
3842	YDL144C	40	E	10		YKO_0840	E10	0.814	+	+	+	
3844	YDL146W	40	E	11	slow growth, petite	YKO_0840	E11	0.592	slow	+	-	Doubt
3847	YDL149W	40	E	12		YKO_0840	E12	0.89	+	+	+	
3849	YDL151C	40	F	1		YKO_0840	F01	0.395	+	+	-	HIT
3852	YDL154W	40	F	2		YKO_0840	F02	0.945	+	+	+	
3853	YDL155W	40	F	3		YKO_0840	F03	0.262	+	+	+	
3854	YDL156W	40	F	4		YKO_0840	F04	0.938	+	+	+	
3855	YDL157C	40	F	5		YKO_0840	F05	0.922	+	+	+	
3857	YDL159W	40	F	6	does not mate, sterile	YKO_0840	F06	0.93	+	+	+	
3859	YDL161W	40	F	7	super slow growth	YKO_0840	F07	0.783	+	+	+	
3860	YDL162C	40	F	8		YKO_0840	F08	0.757	+	+	+	
3866	YDL168W	40	F	9		YKO_0840	F09	0.759	+	+	+	
3867	YDL169C	40	F	10		YKO_0840	F10	0.692	+	+	+	
3868	YDL170W	40	F	11		YKO_0840	F11	0.695	+	+	+	
3869	YDL171C	40	F	12		YKO_0840	F12	0.818	+	+	+	
3870	YDL172C	40	G	1		YKO_0840	G01	1.005	+	+	+	
3871	YDL173W	40	G	2		YKO_0840	G02	0.87	+	+	+	
3872	YDL174C	40	G	3		YKO_0840	G03	0.832	+	+	+	
3873	YDL175C	40	G	4		YKO_0840	G04	0.917	+	+	+	
3874	YDL176W	40	G	5		YKO_0840	G05	0.808	+	+	+	
3875	YDL177C	40	G	6		YKO_0840	G06	0.842	+	+	+	
3876	YDL178W	40	G	7		YKO_0840	G07	0.975	+	+	+	
3877	YDL179W	40	G	8		YKO_0840	G08	0.791	+	+	+	
3878	YDL180W	40	G	9		YKO_0840	G09	0.855	+	+	+	
3879	YDL181W	40	G	10		YKO_0840	G10	0.668	slow	+	-	Doubt
3880	YDL182W	40	G	11		YKO_0840	G11	0.626	+	+	+	
3881	YDL183C	40	G	12		YKO_0840	G12	0.911	+	+	+	
3882	YDL184C	40	H	1		YKO_0840	H01	0.996	+	+	-	HIT
--		40	H	2	empty	YKO_0840	H02	empty	empty	empty	empty	empty
3884	YDL186W	40	H	3		YKO_0840	H03	1.016	+	+	+	
3885	YDL187C	40	H	4		YKO_0840	H04	0.992	+	+	+	
3886	YDL188C	40	H	5		YKO_0840	H05	0.979	+	+	+	
3887	YDL189W	40	H	6		YKO_0840	H06	0.894	+	+	+	
3888	YDL190C	40	H	7		YKO_0840	H07	0.992	+	+	+	
1596	YOR300W	40	H	8		YKO_0840	H08	0.927	+	+	+	
1603	YOR306C	40	H	9		YKO_0840	H09	0.923	+	+	+	
1606	YOR309C	40	H	10		YKO_0840	H10	0.726	+	+	+	
1622	YOR325W	40	H	11		YKO_0840	H11	0.751	+	+	+	
1630	YOR333C	40	H	12		YKO_0840	H12	0.8	+	+	-	HIT

	Euroscarf Information					Replica plate Information			Tau Toxicity Enhancer Primary Screen Results			
record no.	ORF name	Plate	Row	Col	Comment	Replica plate	Well	YPD (OD600nm)	Growth plate (SC+GAL comp.)	Transformation control plate (SC+GLU-Leu)	TEST Plate (SC+GAL-Leu)	Classification
1642	YOR345C	41	A	1		YKO_0841	A01	0.6948	+	+	+	
1663	YOR366W	41	A	2		YKO_0841	A02	0.6375	+	+	-	HIT
1676	YOR379C	41	A	3		YKO_0841	A03	0.6367	+	+	+	
5329	YNL001W	41	A	4		YKO_0841	A04	0.6466	+	+	+	
5332	YNL004W	41	A	5		YKO_0841	A05	0.6382	+	+	+	
5333	YNL005C	41	A	6	slow growth, petite	YKO_0841	A06	0.5732	slow	+	-	Doubt
5336	YNL008C	41	A	7		YKO_0841	A07	0.6217	+	+	+	
5337	YNL009W	41	A	8		YKO_0841	A08	0.6313	+	+	+	
5338	YNL010W	41	A	9		YKO_0841	A09	0.6324	+	+	+	
5340	YNL012W	41	A	10		YKO_0841	A10	0.6314	+	+	+	
5341	YNL013C	41	A	11		YKO_0841	A11	0.6193	+	+	+	
5343	YNL015W	41	A	12		YKO_0841	A12	0.6057	+	+	-	HIT
5344	YNL016W	41	B	1		YKO_0841	B01	0.7173	+	-	-	Doubt
5346	YNL020C	41	B	2		YKO_0841	B02	0.7308	+	+	+	
5347	YNL021W	41	B	3		YKO_0841	B03	0.6832	+	+	+	
5348	YNL022C	41	B	4		YKO_0841	B04	0.708	+	+	+	
5349	YNL023C	41	B	5		YKO_0841	B05	0.6885	+	+	+	
5350	YNL024C	41	B	6		YKO_0841	B06	0.7119	+	+	+	
5351	YNL025C	41	B	7		YKO_0841	B07	0.8976	+	+	+	
5353	YNL027W	41	B	8		YKO_0841	B08	0.7132	+	+	+	
5354	YNL028W	41	B	9		YKO_0841	B09	0.6803	+	+	+	
5355	YNL029C	41	B	10		YKO_0841	B10	0.6894	+	+	+	
5356	YNL030W	41	B	11		YKO_0841	B11	0.697	+	+	+	
5357	YNL031C	41	B	12		YKO_0841	B12	0.7221	+	+	+	
5358	YNL032W	41	C	1		YKO_0841	C01	0.7402	+	+	+	
5359	YNL034W	41	C	2		YKO_0841	C02	0.7369	+	+	+	
5360	YNL035C	41	C	3		YKO_0841	C03	0.7265	+	+	+	
5362	YNL037C	41	C	4		YKO_0841	C04	0.6386	+	+	+	
5365	YNL040W	41	C	5		YKO_0841	C05	0.7027	+	+	+	
5366	YNL041C	41	C	6		YKO_0841	C06	0.6832	+	+	+	
5368	YNL043C	41	C	7		YKO_0841	C07	0.7175	+	+	+	
5369	YNL044W	41	C	8		YKO_0841	C08	0.7212	+	+	+	
5370	YNL045W	41	C	9		YKO_0841	C09	0.7206	+	+	+	
5371	YNL046W	41	C	10		YKO_0841	C10	0.7188	+	+	+	
5374	YNL049C	41	C	11		YKO_0841	C11	0.7144	+	+	+	
5375	YNL050C	41	C	12		YKO_0841	C12	0.7164	+	+	+	
5376	YNR001C	41	D	1		YKO_0841	D01	0.7187	+	+	+	
5377	YNR002C	41	D	2		YKO_0841	D02	0.7312	+	+	+	
5379	YNR004W	41	D	3		YKO_0841	D03	0.6955	+	+	+	
5380	YNR005C	41	D	4		YKO_0841	D04	0.7605	+	+	+	
--		41	D	5	empty	YKO_0841	D05	empty	empty	empty	empty	empty
5381	YNR006W	41	D	6		YKO_0841	D06	0.7243	+	+	+	
5382	YNR007C	41	D	7		YKO_0841	D07	0.71	+	+	+	
5383	YNR008W	41	D	8		YKO_0841	D08	0.7186	+	+	+	
5384	YNR009W	41	D	9		YKO_0841	D09	0.7187	+	+	+	
5385	YNR010W	41	D	10		YKO_0841	D10	0.5904	+	+	+	
5387	YNR012W	41	D	11		YKO_0841	D11	0.7019	+	+	+	
5388	YNR013C	41	D	12		YKO_0841	D12	0.6706	+	+	+	
5389	YNR014W	41	E	1		YKO_0841	E01	0.7031	+	+	+	
5390	YNR015W	41	E	2		YKO_0841	E02	0.7073	+	+	+	
5393	YNR018W	41	E	3		YKO_0841	E03	0.7063	+	+	+	
5394	YNR019W	41	E	4		YKO_0841	E04	0.6979	+	+	+	
5395	YNR020C	41	E	5		YKO_0841	E05	0.6471	+	+	-	HIT
5396	YNR021W	41	E	6		YKO_0841	E06	0.8328	+	+	+	
5397	YNR022C	41	E	7		YKO_0841	E07	0.6915	+	+	+	
5399	YNR024W	41	E	8		YKO_0841	E08	0.7042	+	+	+	
5400	YNR025C	41	E	9		YKO_0841	E09	0.6822	+	+	+	
5402	YNR027W	41	E	10		YKO_0841	E10	0.7319	+	+	+	
5403	YNR028W	41	E	11		YKO_0841	E11	0.7079	+	+	+	
5404	YNR029C	41	E	12		YKO_0841	E12	0.6707	+	+	+	
5405	YNR030W	41	F	1		YKO_0841	F01	0.7103	+	+	+	
5406	YNR031C	41	F	2		YKO_0841	F02	0.7186	+	+	+	
5407	YNR032W	41	F	3		YKO_0841	F03	0.7192	+	+	+	
5409	YNR034W	41	F	4		YKO_0841	F04	0.7108	+	+	-	HIT
5411	YNR036C	41	F	5	slow growth, petite	YKO_0841	F05	0.6202	slow	+	-	Doubt
5412	YNR037C	41	F	6	slow growth, petite	YKO_0841	F06	0.653	slow	+	-	Doubt
5414	YNR039C	41	F	7		YKO_0841	F07	0.7218	+	+	+	
5415	YNR040W	41	F	8		YKO_0841	F08	0.7234	+	+	+	
5416	YNR041C	41	F	9	slow growth, petite	YKO_0841	F09	0.6659	-	+	-	Doubt
5417	YNR042W	41	F	10		YKO_0841	F10	0.7268	+	+	+	
5420	YNR045W	41	F	11		YKO_0841	F11	0.6365	-	+	-	Doubt
5422	YNR047W	41	F	12		YKO_0841	F12	0.6753	+	+	+	
5423	YNR048W	41	G	1		YKO_0841	G01	0.7059	+	+	+	
5424	YNR049C	41	G	2		YKO_0841	G02	0.7365	+	+	+	
3121	YBL095W	41	G	3		YKO_0841	G03	0.791	+	+	+	
3122	YBL096C	41	G	4		YKO_0841	G04	0.7419	+	+	+	
3124	YBL098W	41	G	5		YKO_0841	G05	0.7021	+	+	+	
3125	YBL099W	41	G	6	slow growth, petite	YKO_0841	G06	0.3818	slow	+	-	Doubt
3126	YBL100C	41	G	7	slow growth, petite	YKO_0841	G07	0.7196	+	+	+	
3127	YBL101C	41	G	8		YKO_0841	G08	0.7218	+	+	+	
3130	YBL102W	41	G	9		YKO_0841	G09	0.7167	+	+	+	
3131	YBL103C	41	G	10		YKO_0841	G10	0.7456	+	+	+	
3132	YBL104C	41	G	11		YKO_0841	G11	0.7193	+	+	+	
3134	YBL106C	41	G	12		YKO_0841	G12	0.6846	+	+	+	

	Euroscarf Information					Replica plate Information			Tau Toxicity Enhancer Primary Screen Results			
record no.	ORF name	Plate	Row	Col	Comment	Replica plate	Well	YPD (OD600nm)	Growth plate (SC+GAL comp.)	Transformation control plate (SC+GLU-Leu)	TEST Plate (SC+GAL-Leu)	Classification
3135	YBL107C	41	H	1		YKO_0841	H01	0.6267	+	+	+	
--		41	H	2	empty	YKO_0841	H02	empty	empty	empty	empty	empty
3136	YBR001C	41	H	3		YKO_0841	H03	0.6274	+	+	+	
3138	YBR003W	41	H	4	slow growth, petite	YKO_0841	H04	0.5742	slow	+	-	Doubt
3140	YBR005W	41	H	5		YKO_0841	H05	0.6295	+	+	+	
3141	YBR006W	41	H	6		YKO_0841	H06	0.6178	+	+	+	
3142	YBR007C	41	H	7		YKO_0841	H07	0.6142	+	+	+	
3143	YBR008C	41	H	8		YKO_0841	H08	0.69	+	+	+	
3144	YBR009C	41	H	9		YKO_0841	H09	0.6848	+	+	+	
3145	YBR010W	41	H	10		YKO_0841	H10	0.6884	+	+	+	
3147	YBR012C	41	H	11		YKO_0841	H11	0.7233	+	+	+	
3150	YBR013C	41	H	12		YKO_0841	H12	0.6886	+	+	+	
3151	YBR014C	42	A	1		YKO_0842	A01	0.838	+	+	+	
3152	YBR015C	42	A	2		YKO_0842	A02	0.918	+	+	+	
3153	YBR016W	42	A	3		YKO_0842	A03	0.906	+	+	-	HIT
3155	YBR018C	42	A	4		YKO_0842	A04	0.842	slow	+	-	Doubt
3156	YBR019C	42	A	5		YKO_0842	A05	0.582	-	+	-	Doubt
3157	YBR020W	42	A	6		YKO_0842	A06	0.797	-	+	-	Doubt
3158	YBR021W	42	A	7		YKO_0842	A07	0.701	+	-	-	Doubt
3159	YBR022W	42	A	8		YKO_0842	A08	0.818	+	+	+	
3160	YBR023C	42	A	9		YKO_0842	A09	0.772	+	+	+	
3161	YBR024W	42	A	10		YKO_0842	A10	0.882	+	+	-	HIT
3162	YBR025C	42	A	11		YKO_0842	A11	0.878	+	+	+	
3163	YBR026C	42	A	12	slow growth, petite	YKO_0842	A12	0.793	+	+	-	HIT
3164	YBR027C	42	B	1		YKO_0842	B01	0.731	+	+	+	
3165	YBR028C	42	B	2		YKO_0842	B02	0.619	+	+	-	HIT
3167	YBR030W	42	B	3		YKO_0842	B03	0.923	+	+	+	
3168	YBR031W	42	B	4		YKO_0842	B04	0.829	+	+	+	
3169	YBR032W	42	B	5		YKO_0842	B05	0.898	+	+	+	
3170	YBR033W	42	B	6		YKO_0842	B06	0.877	+	+	-	HIT
3171	YBR034C	42	B	7		YKO_0842	B07	0.611	+	+	+	
3173	YBR036C	42	B	8		YKO_0842	B08	0.855	+	+	-	HIT
3174	YBR037C	42	B	9	slow growth, petite	YKO_0842	B09	0.783	-	+	-	Doubt
3177	YBR040W	42	B	10		YKO_0842	B10	0.924	+	+	-	HIT
3178	YBR041W	42	B	11		YKO_0842	B11	0.877	+	+	+	
3179	YBR042C	42	B	12		YKO_0842	B12	0.982	+	+	+	
3180	YBR043C	42	C	1		YKO_0842	C01	0.843	+	-	+	Incongruence
3181	YBR044C	42	C	2		YKO_0842	C02	0.808	+	+	+	
3182	YBR045C	42	C	3		YKO_0842	C03	0.959	+	+	+	
3183	YBR046C	42	C	4		YKO_0842	C04	0.911	+	-	-	Doubt
3184	YBR047W	42	C	5		YKO_0842	C05	0.947	+	+	+	
3185	YBR048W	42	C	6		YKO_0842	C06	0.857	+	+	+	
3187	YBR050C	42	C	7		YKO_0842	C07	0.809	+	+	+	
3188	YBR051W	42	C	8		YKO_0842	C08	0.711	+	+	+	
3189	YBR052C	42	C	9		YKO_0842	C09	0.932	+	+	-	HIT
3190	YBR053C	42	C	10		YKO_0842	C10	0.944	+	+	+	
3191	YBR054W	42	C	11		YKO_0842	C11	1.016	+	+	+	
3193	YBR056W	42	C	12		YKO_0842	C12	0.865	+	+	-	HIT
3194	YBR057C	42	D	1		YKO_0842	D01	0.881	+	+	+	
3195	YBR058C	42	D	2		YKO_0842	D02	0.912	+	+	+	
3196	YBR059C	42	D	3		YKO_0842	D03	0.921	+	+	-	HIT
3198	YBR061C	42	D	4		YKO_0842	D04	0.921	+	+	-	HIT
3199	YBR062C	42	D	5		YKO_0842	D05	0.942	+	+	+	
--		42	D	6	empty	YKO_0842	D06	empty	empty	empty	empty	empty
3200	YBR063C	42	D	7		YKO_0842	D07	0.924	+	-	-	Doubt
3201	YBR064W	42	D	8		YKO_0842	D08	0.915	+	+	+	
3202	YBR065C	42	D	9		YKO_0842	D09	0.994	+	+	-	HIT
3203	YBR066C	42	D	10		YKO_0842	D10	0.935	+	+	+	
3204	YBR067C	42	D	11		YKO_0842	D11	0.946	+	-	-	Doubt
3205	YBR068C	42	D	12		YKO_0842	D12	0.937	+	+	-	HIT
3206	YBR069C	42	E	1		YKO_0842	E01	0.833	+	+	+	
3208	YBR071W	42	E	2		YKO_0842	E02	0.947	+	+	-	HIT
3209	YBR072W	42	E	3		YKO_0842	E03	0.872	+	+	+	
3210	YBR073W	42	E	4		YKO_0842	E04	0.86	+	+	+	
3211	YBR074W	42	E	5		YKO_0842	E05	0.93	+	-	-	Doubt
3212	YBR075W	42	E	6		YKO_0842	E06	0.941	+	+	+	
3213	YBR076W	42	E	7		YKO_0842	E07	1.013	+	+	+	
3214	YBR077C	42	E	8		YKO_0842	E08	0.304	slow	+	-	Doubt
2930	YNL146W	42	E	9		YKO_0842	E09	0.965	+	+	+	
2931	YNL145W	42	E	10		YKO_0842	E10	0.916	+	+	+	
2932	YNL144C	42	E	11		YKO_0842	E11	0.954	+	+	+	
2933	YNL143C	42	E	12		YKO_0842	E12	0.83	+	+	-	HIT
2935	YNL141W	42	F	1		YKO_0842	F01	0.848	+	+	-	HIT
2937	YNL139C	42	F	2		YKO_0842	F02	0.91	+	+	+	
2940	YNL136W	42	F	3		YKO_0842	F03	0.633	+	+	-	HIT
2941	YNL135C	42	F	4		YKO_0842	F04	0.883	+	+	+	
2942	YNL134C	42	F	5		YKO_0842	F05	0.878	+	-	-	Doubt
2943	YNL133C	42	F	6		YKO_0842	F06	0.154	slow	+	-	Doubt
2947	YNL129W	42	F	7		YKO_0842	F07	0.969	+	+	+	
2948	YNL128W	42	F	8		YKO_0842	F08	0.694	+	+	+	
2949	YNL127W	42	F	9		YKO_0842	F09	0.715	+	+	+	
2953	YNL123W	42	F	10		YKO_0842	F10	0.686	+	+	+	
2954	YNL122C	42	F	11		YKO_0842	F11	0.774	+	-	-	Doubt
2959	YNL117W	42	F	12		YKO_0842	F12	0.85	slow	+	-	Doubt

	Euroscarf Information					Replica plate Information			Tau Toxicity Enhancer Primary Screen Results			
record no.	ORF name	Plate	Row	Col	Comment	Replica plate	Well	YPD (OD600nm)	Growth plate (SC+GAL comp.)	Transformation control plate (SC+GLU-Leu)	TEST Plate (SC+GAL-Leu)	Classification
2960	YNL116W	42	G	1		YKO_0842	G01	0.824	+	+	+	
2968	YNL108C	42	G	2		YKO_0842	G02	0.923	+	+	+	
2975	YNL101W	42	G	3		YKO_0842	G03	0.932	+	+	+	
2978	YNL098C	42	G	4		YKO_0842	G04	0.804	+	+	+	
2982	YNL094W	42	G	5		YKO_0842	G05	0.833	+	+	-	HIT
2984	YNL092W	42	G	6		YKO_0842	G06	0.925	+	+	+	
2987	YNL089C	42	G	7		YKO_0842	G07	0.794	+	+	+	
2995	YNL081C	42	G	8	slow growth, petite	YKO_0842	G08	0.829	slow	+	-	Doubt
2999	YNL077W	42	G	9		YKO_0842	G09	0.911	+	+	+	
3007	YNL069C	42	G	10	no growth on "drop-in" media	YKO_0842	G10	0.793	+	+	+	
3012	YNL064C	42	G	11		YKO_0842	G11	not grown	-	-	-	Not grown
3013	YNL063W	42	G	12		YKO_0842	G12	0.907	+	+	+	
3017	YNL057W	42	H	1		YKO_0842	H01	0.974	+	+	+	
--		42	H	2	empty	YKO_0842	H02	empty	empty	empty	empty	empty
3018	YNL058C	42	H	3		YKO_0842	H03	0.998	+	+	+	
3021	YNL054W	42	H	4		YKO_0842	H04	0.914	+	+	-	HIT
2258	YIL099W	42	H	5		YKO_0842	H05	0.943	+	+	-	HIT
2259	YIL100W	42	H	6		YKO_0842	H06	0.977	+	+	-	HIT
2260	YIL101C	42	H	7		YKO_0842	H07	0.837	+	+	+	
2262	YIL103W	42	H	8		YKO_0842	H08	0.911	+	+	+	
2264	YIL105C	42	H	9		YKO_0842	H09	0.999	+	+	-	HIT
2266	YIL107C	42	H	10		YKO_0842	H10	0.805	+	+	+	
2267	YIL108W	42	H	11		YKO_0842	H11	0.969	+	+	+	
2269	YIL110W	42	H	12		YKO_0842	H12	not grown	-	-	-	Not grown
2271	YIL112W	43	A	1		YKO_0843	A01	0.823	+	+	+	
2272	YIL113W	43	A	2	slow growth on -met, growth on -lys	YKO_0843	A02	0.869	+	-	-	Doubt
2273	YIL114C	43	A	3		YKO_0843	A03	0.919	+	+	+	
2275	YIL116W	43	A	4		YKO_0843	A04	0.698	+	+	-	HIT
2276	YIL117C	43	A	5		YKO_0843	A05	0.852	+	+	+	
2278	YIL119C	43	A	6		YKO_0843	A06	0.913	+	+	+	
2279	YIL120W	43	A	7		YKO_0843	A07	0.843	+	+	-	HIT
2280	YIL121W	43	A	8	growth on -met, growth on -lys	YKO_0843	A08	0.797	+	+	+	
2282	YIL123W	43	A	9		YKO_0843	A09	0.709	+	+	-	HIT
2283	YIL124W	43	A	10		YKO_0843	A10	0.674	+	+	-	HIT
2284	YIL125W	43	A	11	growth on -met,slow growth on -lys	YKO_0843	A11	0.784	+	+	-	HIT
2287	YIL128W	43	A	12		YKO_0843	A12	0.823	+	+	-	HIT
2289	YIL130W	43	B	1		YKO_0843	B01	0.949	+	+	-	HIT
2291	YIL132C	43	B	2	papillation on -met	YKO_0843	B02	0.534	slow	+	-	Doubt
2292	YIL133C	43	B	3	slow growth on -met, growth on -lys	YKO_0843	B03	0.905	+	+	+	
2293	YIL134W	43	B	4	super slow growth	YKO_0843	B04	0.831	+	+	-	HIT
2294	YIL135C	43	B	5		YKO_0843	B05	0.895	+	+	+	
2296	YIL137C	43	B	6		YKO_0843	B06	0.774	+	+	+	
2297	YIL138C	43	B	7		YKO_0843	B07	0.909	+	+	+	
2298	YIL139C	43	B	8		YKO_0843	B08	0.837	+	-	-	Doubt
2299	YIL140W	43	B	9	super slow growth	YKO_0843	B09	0.798	+	+	+	
2300	YIL141W	43	B	10	growth on -met, growth on -lys	YKO_0843	B10	0.588	+	+	+	
2304	YIL145C	43	B	11	slow growth on -met, growth on -lys	YKO_0843	B11	0.759	+	+	-	HIT
2305	YIL146C	43	B	12		YKO_0843	B12	0.854	+	+	+	
2307	YIL148W	43	C	1		YKO_0843	C01	0.894	+	+	-	HIT
2308	YIL149C	43	C	2		YKO_0843	C02	0.913	+	+	-	HIT
2311	YIL152W	43	C	3		YKO_0843	C03	0.869	+	+	+	
2312	YIL153W	43	C	4		YKO_0843	C04	0.798	+	+	-	HIT
2313	YIL154C	43	C	5	slow growth on -met, growth on -lys, no growth on drop-in media	YKO_0843	C05	0.764	+	+	+	
2314	YIL155C	43	C	6		YKO_0843	C06	0.909	+	+	+	
2315	YIL156W	43	C	7		YKO_0843	C07	0.907	+	-	-	Doubt
2316	YIL157C	43	C	8	slow growth, growth on -met, growth on -lys	YKO_0843	C08	0.967	+	+	-	HIT
2318	YIL159W	43	C	9	growth on -met, growth on -lys	YKO_0843	C09	0.786	+	+	-	HIT
2319	YIL160C	43	C	10		YKO_0843	C10	0.78	+	-	-	Doubt
2320	YIL161W	43	C	11		YKO_0843	C11	0.84	+	-	-	Doubt
2321	YIL162W	43	C	12		YKO_0843	C12	0.905	+	+	-	HIT
2322	YIL163C	43	D	1		YKO_0843	D01	0.962	+	+	+	
2323	YIL164C	43	D	2		YKO_0843	D02	1.031	+	+	-	HIT
2324	YIL165C	43	D	3	slow growth on -met, growth on -lys	YKO_0843	D03	0.947	+	+	+	
2325	YIL166C	43	D	4	slow growth on -met, growth on -lys	YKO_0843	D04	0.952	+	+	+	
2326	YIL167W	43	D	5	growth on -met, growth on -lys	YKO_0843	D05	0.866	+	+	+	
2327	YIL168W	43	D	6		YKO_0843	D06	0.971	+	+	-	HIT
--		43	D	7	empty	YKO_0843	D07	empty	empty	empty	empty	empty
2329	YIL170W	43	D	8		YKO_0843	D08	0.996	+	+	-	HIT
2332	YIL173W	43	D	9	slow growth on -met, growth on -lys	YKO_0843	D09	0.808	+	+	+	

	Euroscarf Information					Replica plate Information			Tau Toxicity Enhancer Primary Screen Results			
record no.	ORF name	Plate	Row	Col	Comment	Replica plate	Well	YPD (OD600nm)	Growth plate (SC+GAL comp.)	Transformation control plate (SC+GLU-Leu)	TEST Plate (SC+GAL-Leu)	Classification
2337	YIR001C	43	D	10		YKO_0843	D10	0.75	+	+	+	
2338	YIR002C	43	D	11		YKO_0843	D11	0.92	+	+	+	
2339	YIR003W	43	D	12		YKO_0843	D12	0.869	+	+	-	HIT
2341	YIR005W	43	E	1		YKO_0843	E01	0.639	+	+	+	
2343	YIR007W	43	E	2	papillation on -met	YKO_0843	E02	0.646	+	+	+	
2345	YIR009W	43	E	3	growth on -met, growth on -lys	YKO_0843	E03	0.892	+	+	+	
2349	YIR013C	43	E	4		YKO_0843	E04	0.897	+	+	-	HIT
2350	YIR014W	43	E	5	slow growth on -met, growth on -lys	YKO_0843	E05	0.929	+	+	+	
2352	YIR016W	43	E	6		YKO_0843	E06	0.82	+	+	+	
7201	YDL194W	43	E	7		YKO_0843	E07	0.637	+	+	+	
7202	YDR007W	43	E	8	no growth on drop-in media	YKO_0843	E08	0.859	+	+	+	
7204	YDR048C	43	E	9		YKO_0843	E09	0.862	+	+	+	
7206	YFR011C	43	E	10		YKO_0843	E10	0.832	+	+	-	HIT
7207	YFR013W	43	E	11		YKO_0843	E11	0.895	+	+	+	
7209	YNL051W	43	E	12		YKO_0843	E12	0.801	+	+	+	
7210	YNL052W	43	F	1	petite	YKO_0843	F01	0.864	+	+	+	
7211	YNL056W	43	F	2		YKO_0843	F02	0.901	+	+	+	
7213	YNL065W	43	F	3		YKO_0843	F03	0.913	+	+	+	
7214	YNL066W	43	F	4		YKO_0843	F04	0.964	+	+	+	
7215	YNL067W	43	F	5		YKO_0843	F05	0.849	+	+	+	
7216	YNL068C	43	F	6		YKO_0843	F06	0.84	+	+	-	HIT
7217	YNL070W	43	F	7		YKO_0843	F07	0.889	+	+	-	HIT
7218	YNL071W	43	F	8		YKO_0843	F08	0.83	slow	-	-	Doubt
7219	YNL072W	43	F	9		YKO_0843	F09	0.951	+	+	-	HIT
7220	YNL073W	43	F	10	super slow growth	YKO_0843	F10	0.783	slow	+	-	Doubt
7221	YNL074C	43	F	11		YKO_0843	F11	0.871	+	+	-	HIT
7222	YNL076W	43	F	12		YKO_0843	F12	0.727	+	-	-	Doubt
7223	YNL078W	43	G	1		YKO_0843	G01	0.967	+	+	+	
7224	YNL079C	43	G	2		YKO_0843	G02	0.68	+	+	-	HIT
7225	YNL080C	43	G	3		YKO_0843	G03	0.758	+	+	+	
7226	YNL082W	43	G	4		YKO_0843	G04	0.771	+	+	+	
7227	YNL083W	43	G	5		YKO_0843	G05	0.799	+	+	-	HIT
7228	YNL085W	43	G	6		YKO_0843	G06	0.768	+	+	+	
7229	YNL087W	43	G	7		YKO_0843	G07	1.012	+	+	-	HIT
7230	YNL090W	43	G	8		YKO_0843	G08	0.858	+	+	+	
7231	YNL091W	43	G	9		YKO_0843	G09	0.886	+	+	+	
7232	YNL093W	43	G	10		YKO_0843	G10	0.829	+	+	-	HIT
7233	YNL095C	43	G	11		YKO_0843	G11	0.829	+	+	-	HIT
7234	YNL097C	43	G	12		YKO_0843	G12	0.818	+	+	+	
7235	YNL099C	43	H	1		YKO_0843	H01	0.975	+	+	+	
--		43	H	2	empty	YKO_0843	H02	empty	empty	empty	empty	empty
7236	YNL100W	43	H	3		YKO_0843	H03	0.982	+	+	-	HIT
7237	YNL104C	43	H	4		YKO_0843	H04	0.956	+	+	-	HIT
7238	YNL105W	43	H	5		YKO_0843	H05	0.744	+	+	+	
7239	YNL106C	43	H	6		YKO_0843	H06	0.844	+	+	+	
7240	YNL107W	43	H	7		YKO_0843	H07	0.816	+	+	+	
7241	YNL115C	43	H	8		YKO_0843	H08	0.921	+	+	-	HIT
7242	YNL119W	43	H	9		YKO_0843	H09	0.772	+	+	+	
7243	YNL120C	43	H	10		YKO_0843	H10	0.814	+	+	-	HIT
7244	YNL121C	43	H	11		YKO_0843	H11	0.705	+	+	-	HIT
7245	YNL125C	43	H	12		YKO_0843	H12	0.924	+	+	-	HIT
7247	YNL130C	44	A	1		YKO_0844	A01	0.863	+	+	+	
6961	YBR189W	44	A	2		YKO_0844	A02	0.773	+	+	+	
6962	YCR095C	44	A	3		YKO_0844	A03	0.705	+	+	+	
6963	YCR102W-A	44	A	4		YKO_0844	A04	0.821	+	+	-	HIT
6964	YDL133C-A	44	A	5		YKO_0844	A05	0.838	+	+	-	HIT
6967	YDR058C	44	A	6		YKO_0844	A06	0.707	+	+	-	HIT
6969	YDR174W	44	A	7		YKO_0844	A07	0.683	+	+	+	
6970	YDR202C	44	A	8		YKO_0844	A08	0.954	+	+	-	HIT
6971	YDR205W	44	A	9		YKO_0844	A09	0.881	+	+	+	
6972	YDR445C	44	A	10		YKO_0844	A10	0.901	+	+	-	HIT
6973	YDR537C	44	A	11		YKO_0844	A11	0.797	+	+	-	HIT
6975	YFR039C	44	A	12		YKO_0844	A12	0.857	+	+	+	
6976	YGL219C	44	B	1		YKO_0844	B01	0.81	+	+	+	
6978	YGR028W	44	B	2		YKO_0844	B02	0.933	+	+	+	
6979	YGR032W	44	B	3		YKO_0844	B03	0.925	+	+	-	HIT
6980	YGR038W	44	B	4		YKO_0844	B04	0.696	+	+	-	HIT
6981	YGR040W	44	B	5		YKO_0844	B05	0.849	+	+	+	
6984	YGR050C	44	B	6		YKO_0844	B06	0.748	+	+	-	HIT
6985	YGR053C	44	B	7		YKO_0844	B07	0.926	+	+	+	
6986	YGR063C	44	B	8		YKO_0844	B08	0.837	+	+	+	
6988	YGR086C	44	B	9		YKO_0844	B09	0.955	+	+	+	
6989	YGR089W	44	B	10		YKO_0844	B10	0.925	+	-	-	Doubt
6990	YGR092W	44	B	11		YKO_0844	B11	0.804	+	+	+	
6991	YGR093W	44	B	12		YKO_0844	B12	0.895	+	+	-	HIT
6992	YGR106C	44	C	1		YKO_0844	C01	0.908	+	+	+	
6993	YGR110W	44	C	2		YKO_0844	C02	0.978	+	+	+	
6995	YGR117C	44	C	3		YKO_0844	C03	0.974	+	+	+	
6996	YGR238C	44	C	4		YKO_0844	C04	0.869	+	+	-	HIT
6997	YGR239C	44	C	5	slow growth, petite	YKO_0844	C05	0.933	+	+	+	
6998	YGR248W	44	C	6		YKO_0844	C06	0.911	+	+	+	
6999	YGR250C	44	C	7		YKO_0844	C07	0.845	+	+	-	HIT

	Euroscarf Information					Replica plate Information			Tau Toxicity Enhancer Primary Screen Results			
record no.	ORF name	Plate	Row	Col	Comment	Replica plate	Well	YPD (OD600nm)	Growth plate (SC+GAL comp.)	Transformation control plate (SC+GLU-Leu)	TEST Plate (SC+GAL-Leu)	Classification
7000	YJL129C	44	C	8	growth on-met, slow growth on -lys	YKO_0844	C08	0.783	+	-	-	Doubt
7001	YJL132W	44	C	9		YKO_0844	C09	0.898	+	+	-	HIT
7002	YJL136C	44	C	10		YKO_0844	C10	0.834	+	+	+	
7003	YJL137C	44	C	11		YKO_0844	C11	0.809	+	+	+	
7004	YJL139C	44	C	12		YKO_0844	C12	0.757	+	+	+	
7126	YOL125W	44	D	1	Incorrect	YKO_0844	D01	0.82	+	+	+	
7006	YJL141C	44	D	2		YKO_0844	D02	0.927	+	+	+	
7007	YJL151C	44	D	3		YKO_0844	D03	0.74	+	+	+	
7009	YJL160C	44	D	4		YKO_0844	D04	0.881	+	+	-	HIT
7010	YJL161W	44	D	5		YKO_0844	D05	0.873	+	+	-	HIT
7011	YJL163C	44	D	6		YKO_0844	D06	0.91	+	+	+	
7012	YJL165C	44	D	7		YKO_0844	D07	0.659	+	+	-	HIT
--		44	D	8	empty	YKO_0844	D08	empty	empty	empty	empty	empty
7013	YJL172W	44	D	9		YKO_0844	D09	0.928	+	+	+	
7015	YJL175W	44	D	10		YKO_0844	D10	0.715	slow	+	-	Doubt
7016	YJL177W	44	D	11		YKO_0844	D11	0.954	+	+	+	
7018	YJL189W	44	D	12	slow growth	YKO_0844	D12	0.223	slow	+	-	Doubt
7019	YJL191W	44	E	1	slow growth	YKO_0844	E01	0.897	+	+	+	
7021	YJL196C	44	E	2	slow growth	YKO_0844	E02	1.003	+	+	+	
7022	YJL200C	44	E	3	super slow, petite	YKO_0844	E03	0.919	+	+	-	HIT
7024	YJL206C	44	E	4	slow growth	YKO_0844	E04	0.794	+	+	-	HIT
7025	YJL213W	44	E	5		YKO_0844	E05	0.641	+	+	+	
7026	YKL096W-A	44	E	6		YKO_0844	E06	0.917	+	+	+	
7027	YKL115C	44	E	7		YKO_0844	E07	0.983	+	+	-	HIT
7028	YKL139W	44	E	8	slow growth	YKO_0844	E08	0.326	slow	+	+	
7032	YKL194C	44	E	9	slow growth	YKO_0844	E09	0.874	slow	+	-	Doubt
7034	YKL201C	44	E	10		YKO_0844	E10	0.875	+	+	+	
7035	YKL202W	44	E	11		YKO_0844	E11	0.896	+	+	-	HIT
7036	YKL204W	44	E	12		YKO_0844	E12	0.542	+	+	+	
7038	YKL215C	44	F	1		YKO_0844	F01	0.933	+	+	+	
7039	YKL220C	44	F	2		YKO_0844	F02	0.96	+	+	+	
7041	YKR010C	44	F	3		YKO_0844	F03	0.843	+	+	+	
7042	YKR019C	44	F	4	super slow, petite	YKO_0844	F04	1.05	+	+	-	HIT
7043	YKR023W	44	F	5		YKO_0844	F05	0.926	+	+	-	HIT
7044	YKR027W	44	F	6		YKO_0844	F06	0.819	+	+	+	
7045	YKR028W	44	F	7		YKO_0844	F07	1.031	+	+	-	HIT
7046	YKR029C	44	F	8		YKO_0844	F08	0.783	+	+	-	HIT
7047	YKR034W	44	F	9	slow growth	YKO_0844	F09	0.878	+	+	-	HIT
7048	YKR036C	44	F	10		YKO_0844	F10	0.829	+	+	-	HIT
7050	YKR039W	44	F	11		YKO_0844	F11	0.922	+	+	-	HIT
7051	YKR040C	44	F	12		YKO_0844	F12	0.871	+	+	+	
7052	YKR041W	44	G	1		YKO_0844	G01	0.924	+	+	+	
7053	YKR046C	44	G	2		YKO_0844	G02	0.942	+	-	+	Incongruence
7054	YKR053C	44	G	3		YKO_0844	G03	0.926	+	+	+	
7055	YML035C	44	G	4		YKO_0844	G04	0.908	slow	+	-	Doubt
7153	YAR002C-A	44	G	5		YKO_0844	G05	0.928	+	+	+	
7155	YBR083W	44	G	6		YKO_0844	G06	0.868	+	+	-	HIT
7156	YBR084C-A	44	G	7		YKO_0844	G07	0.998	+	+	+	
7159	YBR090C	44	G	8		YKO_0844	G08	0.912	+	+	+	
7160	YBR100W	44	G	9		YKO_0844	G09	0.906	+	+	+	
7122	YMR119W	44	G	10		YKO_0844	G10	0.801	+	+	+	
7163	YBR125C	44	G	11		YKO_0844	G11	0.878	+	+	-	HIT
7164	YBR131W	44	G	12		YKO_0844	G12	0.875	+	+	+	
7165	YBR150C	44	H	1		YKO_0844	H01	0.918	+	+	+	
--		44	H	2	empty	YKO_0844	H02	empty	empty	empty	empty	empty
7166	YBR168W	44	H	3		YKO_0844	H03	0.894	+	+	+	
7167	YBR169C	44	H	4		YKO_0844	H04	0.67	+	+	+	
7168	YBR270C	44	H	5		YKO_0844	H05	0.828	+	+	+	
7169	YBR272C	44	H	6		YKO_0844	H06	0.801	+	+	+	
7170	YBR275C	44	H	7		YKO_0844	H07	0.866	+	+	+	
7171	YBR276C	44	H	8		YKO_0844	H08	0.843	+	+	+	
7172	YBR280C	44	H	9		YKO_0844	H09	0.875	+	+	+	
7173	YBR287W	44	H	10		YKO_0844	H10	0.922	+	+	+	
7174	YBR288C	44	H	11		YKO_0844	H11	0.953	+	+	+	
7175	YBR289W	44	H	12	slow growth	YKO_0844	H12	0.546	+	+	-	HIT
7176	YBR294W	45	A	1		YKO_0845	A01	0.871	+	+	-	HIT
7177	YBR301W	45	A	2		YKO_0845	A02	0.841	+	+	+	
7178	YCL026C-A	45	A	3		YKO_0845	A03	0.932	+	+	-	HIT
7179	YCR028C-A	45	A	4	slow growth	YKO_0845	A04	0.828	slow	+	-	Doubt
7180	YCR030C	45	A	5		YKO_0845	A05	0.894	+	+	-	HIT
7181	YCR032W	45	A	6		YKO_0845	A06	0.953	+	+	-	HIT
7182	YCR033W	45	A	7		YKO_0845	A07	0.797	+	+	+	
7183	YCR046C	45	A	8	super slow growth	YKO_0845	A08	0.788	slow	+	-	Doubt
7184	YCR047C	45	A	9	super slow growth	YKO_0845	A09	0.567	+	+	+	
7185	YCR048W	45	A	10		YKO_0845	A10	0.893	+	+	+	
7186	YCR053W	45	A	11	slow growth	YKO_0845	A11	0.737	+	-	-	Doubt
7189	YCR060W	45	A	12		YKO_0845	A12	0.878	+	+	+	
7190	YCR062W	45	B	1		YKO_0845	B01	0.901	+	+	+	
7192	YCR067C	45	B	2		YKO_0845	B02	0.96	+	+	+	
7193	YCR069W	45	B	3		YKO_0845	B03	0.926	+	+	+	
7195	YCR073C	45	B	4		YKO_0845	B04	0.913	+	+	+	
7196	YCR075C	45	B	5		YKO_0845	B05	0.943	+	+	+	
7197	YCR083W	45	B	6		YKO_0845	B06	0.902	+	+	+	

Euroscarf Information						Replica plate Information			Tau Toxicity Enhancer Primary Screen Results			
record no.	ORF name	Plate	Row	Col	Comment	Replica plate	Well	YPD (OD600nm)	Growth plate (SC+GAL comp.)	Transformation control plate (SC+GLU-Leu)	TEST Plate (SC+GAL-Leu)	Classification
7198	YCR084C	45	B	7	super slow growth	YKO_0845	B07	not grown	-	-	-	Not grown
7199	YCR088W	45	B	8		YKO_0845	B08	0.869	+	+	+	
7200	YCR089W	45	B	9		YKO_0845	B09	0.814	+	+	+	
6679	YBR191W	45	B	10		YKO_0845	B10	0.709	slow	+	+	
6681	YCL035C	45	B	11		YKO_0845	B11	0.797	+	+	+	
6691	YDR071C	45	B	12		YKO_0845	B12	0.81	+	+	+	
6692	YDR074W	45	C	1	growth on -met, growth on -lys	YKO_0845	C01	0.582	+	+	-	HIT
6694	YER027C	45	C	2		YKO_0845	C02	0.683	+	+	+	
6695	YER037W	45	C	3	does not mate with alpha, mat a pap. Confirmed Het Diploid 10/15/01	YKO_0845	C03	0.926	+	+	+	
6696	YGR155W	45	C	4	slow growth, slow growth on -lys, slow growth on drop-in media, no growth on -met	YKO_0845	C04	1.034	+	+	+	
6704	YLR192C	45	C	5		YKO_0845	C05	0.927	+	+	+	
6706	YLR237W	45	C	6		YKO_0845	C06	0.975	+	+	-	HIT
6707	YLR246W	45	C	7		YKO_0845	C07	0.911	+	+	+	
6709	YLR334C	45	C	8		YKO_0845	C08	0.818	+	+	-	HIT
6711	YLR346C	45	C	9		YKO_0845	C09	0.909	+	-	+	Incongruence
6712	YLR358C	45	C	10	slow growth	YKO_0845	C10	0.679	+	+	+	
6713	YLR361C	45	C	11		YKO_0845	C11	0.821	+	+	+	
6714	YLR370C	45	C	12		YKO_0845	C12	0.726	+	+	+	
6715	YLR382C	45	D	1	slow growth	YKO_0845	D01	0.495	slow	+	-	Doubt
6716	YLR394W	45	D	2		YKO_0845	D02	0.956	+	+	+	
6717	YLR406C	45	D	3		YKO_0845	D03	0.988	+	+	+	
6719	YML022W	45	D	4	no growth on -met, no growth on -lys, no growth on drop-in media	YKO_0845	D04	0.824	+	+	+	
6721	YML027W	45	D	5		YKO_0845	D05	0.91	+	+	+	
6725	YML036W	45	D	6	slow growth	YKO_0845	D06	0.839	+	+	+	
6726	YML038C	45	D	7		YKO_0845	D07	0.948	+	+	+	
6727	YML041C	45	D	8		YKO_0845	D08	0.906	+	+	+	
--		45	D	9	empty	YKO_0845	D09	empty	empty	empty	empty	empty
6728	YML042W	45	D	10		YKO_0845	D10	0.888	+	+	+	
6729	YML047C	45	D	11		YKO_0845	D11	0.841	+	+	+	
6733	YML075C	45	D	12		YKO_0845	D12	0.597	+	+	+	
6734	YML076C	45	E	1		YKO_0845	E01	0.892	+	+	+	
6736	YML086C	45	E	2		YKO_0845	E02	0.923	+	+	+	
6740	YMR048W	45	E	3		YKO_0845	E03	0.698	+	+	+	
6741	YMR135W-A	45	E	4		YKO_0845	E04	0.81	+	+	-	HIT
6743	YMR137C	45	E	5		YKO_0845	E05	0.91	+	+	+	
6744	YMR138W	45	E	6		YKO_0845	E06	0.871	+	+	+	
6745	YMR139W	45	E	7		YKO_0845	E07	0.83	+	+	+	
6746	YMR160W	45	E	8		YKO_0845	E08	0.807	+	+	+	
6748	YMR173W	45	E	9		YKO_0845	E09	0.857	+	+	+	
6751	YMR198W	45	E	10		YKO_0845	E10	0.753	+	+	-	HIT
6753	YOR298C-A	45	E	11		YKO_0845	E11	0.822	+	+	+	
6757	YOR364W	45	E	12		YKO_0845	E12	0.822	+	+	+	
6762	YPL183C	45	F	1		YKO_0845	F01	0.904	+	+	-	HIT
6763	YPL183W-A	45	F	2		YKO_0845	F02	not grown	slow	-	-	Not grown
6764	YPL189W	45	F	3		YKO_0845	F03	0.969	+	+	+	
6767	YPL224C	45	F	4		YKO_0845	F04	0.925	+	+	+	
7297	YGR295C	45	F	5		YKO_0845	F05	0.977	+	+	+	
7298	YHR132W-A	45	F	6		YKO_0845	F06	0.87	+	+	+	
7299	YIL030C	45	F	7		YKO_0845	F07	0.908	+	+	+	
7301	YIL058W	45	F	8		YKO_0845	F08	0.883	+	+	+	
7302	YIL092W	45	F	9		YKO_0845	F09	0.847	+	+	-	HIT
7303	YIR023W	45	F	10		YKO_0845	F10	0.811	+	+	+	
7304	YIR030C	45	F	11		YKO_0845	F11	0.787	+	+	+	
7305	YIR032C	45	F	12		YKO_0845	F12	0.85	+	+	+	
7306	YIR043C	45	G	1		YKO_0845	G01	0.941	+	+	+	
7307	YIR044C	45	G	2		YKO_0845	G02	0.87	+	+	+	
7308	YJR003C	45	G	3		YKO_0845	G03	0.909	+	+	+	
7310	YJR055W	45	G	4		YKO_0845	G04	not grown	-	-	-	Not grown
7311	YKL053C-A	45	G	5		YKO_0845	G05	0.901	+	+	+	
7312	YKR106W	45	G	6		YKO_0845	G06	0.903	+	+	+	
7314	YMR191W	45	G	7		YKO_0845	G07	0.904	+	+	+	
7315	YMR322C	45	G	8		YKO_0845	G08	0.892	+	+	+	
7316	YNL138W	45	G	9	grows on -met, grows on -lys, does not mate, sterile. Confirmed Het Diploid 10/15/01	YKO_0845	G09	0.834	+	+	+	
7317	YNL140C	45	G	10		YKO_0845	G10	0.818	+	+	+	
7318	YNL142W	45	G	11		YKO_0845	G11	0.887	+	+	-	HIT
7319	YNL315C	45	G	12	slow growth, petite	YKO_0845	G12	0.567	slow	+	-	Doubt
7320	YOL151W	45	H	1		YKO_0845	H01	0.909	+	+	+	
--		45	H	2	empty	YKO_0845	H02	empty	empty	empty	empty	empty
7321	YOL152W	45	H	3		YKO_0845	H03	0.764	+	+	+	
7322	YOL155C	45	H	4		YKO_0845	H04	0.866	+	+	+	
7323	YOR265W	45	H	5		YKO_0845	H05	0.886	+	+	-	HIT

	Euroscarf Information					Replica plate Information			Tau Toxicity Enhancer Primary Screen Results			
record no.	ORF name	Plate	Row	Col	Comment	Replica plate	Well	YPD (OD600nm)	Growth plate (SC+GAL comp.)	Transformation control plate (SC+GLU-Leu)	TEST Plate (SC+GAL-Leu)	Classification
7324	YOR266W	45	H	6		YKO_0845	H06	0.911	+	+	+	
7325	YOR267C	45	H	7		YKO_0845	H07	0.905	+	+	-	HIT
7326	YOR268C	45	H	8		YKO_0845	H08	0.951	+	+	+	
7327	YOR269W	45	H	9		YKO_0845	H09	0.712	+	+	+	
7328	YOR270C	45	H	10		YKO_0845	H10	not grown	-	-	-	Not grown
7329	YOR271C	45	H	11		YKO_0845	H11	0.848	+	+	-	HIT
7331	YOR273C	45	H	12		YKO_0845	H12	0.904	+	+	+	
7332	YOR274W	46	A	1		YKO_0846	A01	0.7368	+	+	-	HIT
7333	YOR275C	46	A	2		YKO_0846	A02	0.6907	+	+	+	
7334	YOR276W	46	A	3		YKO_0846	A03	0.6522	+	+	+	
7335	YOR298C-A	46	A	4		YKO_0846	A04	0.6327	+	+	+	
7336	YOR302W	46	A	5	no growth on drop-in media	YKO_0846	A05	0.6816	+	+	+	
7337	YOR303W	46	A	6	no growth on drop-in media	YKO_0846	A06	0.6613	+	+	+	
7338	YPL004C	46	A	7		YKO_0846	A07	0.6734	+	+	+	
7339	YPL017C	46	A	8		YKO_0846	A08	0.6631	+	+	+	
7340	YPL027W	46	A	9		YKO_0846	A09	0.6628	+	+	+	
7341	YPL034W	46	A	10		YKO_0846	A10	0.6718	+	+	+	
7342	YPL036W	46	A	11		YKO_0846	A11	0.648	+	+	+	
7343	YPL078C	46	A	12	slow growth, petite	YKO_0846	A12	0.4893	+	+	-	HIT
7344	YPL137C	46	B	1		YKO_0846	B01	0.7143	+	+	-	HIT
6602	YHR005C	46	B	2		YKO_0846	B02	0.6867	+	+	+	
7379	YNL096C	46	B	3		YKO_0846	B03	0.7259	+	+	+	
2435	YOR179C	46	B	4		YKO_0846	B04	0.8456	+	+	+	
2436	YOR180C	46	B	5		YKO_0846	B05	0.9457	+	+	+	
3812	YDL115C	46	B	6		YKO_0846	B06	0.7518	+	+	+	
7069	YFL013W-A	46	B	7		YKO_0846	B07	0.7212	+	+	+	
7070	YFL014W	46	B	8		YKO_0846	B08	0.6941	+	+	+	
7072	YFL019C	46	B	9		YKO_0846	B09	0.706	+	+	+	
7076	YFL042C	46	B	10		YKO_0846	B10	0.7329	+	+	+	
7080	YFR019W	46	B	11		YKO_0846	B11	0.5443	+	+	+	
7081	YFR024C	46	B	12		YKO_0846	B12	0.7006	+	+	+	
7082	YFR025C	46	C	1		YKO_0846	C01	0.7349	+	+	+	
7085	YFR030W	46	C	2		YKO_0846	C02	0.7389	+	+	+	
7089	YHR146W	46	C	3		YKO_0846	C03	0.8476	+	+	+	
7090	YHR171W	46	C	4		YKO_0846	C04	0.7328	+	+	+	
7092	YJL042W	46	C	5		YKO_0846	C05	0.9215	+	+	+	
7093	YJL070C	46	C	6		YKO_0846	C06	1.0166	+	+	+	
7094	YJL078C	46	C	7		YKO_0846	C07	0.9234	+	+	+	
7095	YJL094C	46	C	8		YKO_0846	C08	0.7065	+	+	+	
7097	YJL101C	46	C	9		YKO_0846	C09	0.7375	+	+	-	HIT
7099	YJL105W	46	C	10		YKO_0846	C10	0.7177	+	+	+	
7101	YJL128C	46	C	11		YKO_0846	C11	0.7136	+	+	+	
7111	YLR455W	46	C	12	slow growth	YKO_0846	C12	0.692	+	+	+	
7103	YKR094C	46	D	1		YKO_0846	D01	0.71	+	+	+	
7104	YKR095W	46	D	2		YKO_0846	D02	0.755	+	+	+	
7105	YKR096W	46	D	3		YKO_0846	D03	0.7437	+	+	+	
7106	YKR102W	46	D	4		YKO_0846	D04	0.9093	+	+	+	
7107	YLR110C	46	D	5		YKO_0846	D05	0.901	+	+	+	
7108	YLR390W-A	46	D	6	super slow, petite	YKO_0846	D06	0.728	+	+	+	
7109	YLR439W	46	D	7		YKO_0846	D07	0.918	+	+	+	
7110	YLR442C	46	D	8		YKO_0846	D08	0.8804	+	+	+	
7385	YNL268W	46	D	9		YKO_0846	D09	0.7285	+	+	+	
--		46	D	10	empty	YKO_0846	D10	empty	empty	empty	empty	empty
7113	YML066C	46	D	11	slow growth	YKO_0846	D11	0.7174	+	+	+	
7116	YML115C	46	D	12		YKO_0846	D12	0.7156	+	+	+	
7117	YMR037C	46	E	1		YKO_0846	E01	0.6735	+	+	+	
7119	YMR104C	46	E	2		YKO_0846	E02	0.722	+	+	+	
7381	YNL109W	46	E	3	slow growth	YKO_0846	E03	0.7275	+	+	+	
7123	YNR052C	46	E	4		YKO_0846	E04	0.7324	+	+	+	
7124	YNR055C	46	E	5		YKO_0846	E05	0.7283	+	+	+	
7125	YNR069C	46	E	6		YKO_0846	E06	0.7116	+	+	+	
7382	YNL111C	46	E	7		YKO_0846	E07	0.6883	+	+	+	
7129	YOL147C	46	E	8		YKO_0846	E08	0.7073	+	+	+	
7136	YPR007C	46	E	9		YKO_0846	E09	0.7059	+	+	+	
7137	YPR008W	46	E	10		YKO_0846	E10	0.7249	+	+	+	
7140	YPR013C	46	E	11		YKO_0846	E11	0.7354	+	+	+	
7142	YPR022C	46	E	12		YKO_0846	E12	0.7176	+	+	+	
7143	YPR023C	46	F	1		YKO_0846	F01	0.7026	+	+	+	
7144	YPR024W	46	F	2	slow growth	YKO_0846	F02	0.7004	slow	+	+	
7145	YPR026W	46	F	3		YKO_0846	F03	0.7541	+	+	+	
7146	YPR031W	46	F	4		YKO_0846	F04	0.7787	+	+	+	
7147	YPR037C	46	F	5		YKO_0846	F05	0.9435	+	+	+	
7148	YPR043W	46	F	6	slow growth	YKO_0846	F06	0.6273	slow	+	+	
7149	YPR050C	46	F	7		YKO_0846	F07	0.9655	+	+	+	
7150	YPR064W	46	F	8		YKO_0846	F08	0.9353	+	+	+	
7152	YPR078C	46	F	9		YKO_0846	F09	0.7462	+	+	+	
3218	YBR081C	46	F	10	super slow growth	YKO_0846	F10	not grown	-	-	-	Not grown
3219	YBR082C	46	F	11		YKO_0846	F11	0.7363	+	+	+	
3222	YBR084W	46	F	12		YKO_0846	F12	0.6943	+	+	+	
3223	YBR085W	46	G	1	Confirmed Het Diploid 10/15/01	YKO_0846	G01	0.6425	+	+	+	
3229	YBR090C-A	46	G	2		YKO_0846	G02	0.7261	+	+	+	

	Euroscarf Information					Replica plate Information			Tau Toxicity Enhancer Primary Screen Results			
record no.	ORF name	Plate	Row	Col	Comment	Replica plate	Well	YPD (OD600nm)	Growth plate (SC+GAL comp.)	Transformation control plate (SC+GLU-Leu)	TEST Plate (SC+GAL-Leu)	Classification
3231	YBR092C	46	G	3		YKO_0846	G03	0.9011	+	+	+	
3232	YBR093C	46	G	4		YKO_0846	G04	0.9319	+	+	+	
3233	YBR094W	46	G	5		YKO_0846	G05	0.9645	+	+	+	
3234	YBR095C	46	G	6		YKO_0846	G06	0.8134	+	+	+	
3237	YBR098W	46	G	7		YKO_0846	G07	0.9445	+	+	+	
3238	YBR099C	46	G	8		YKO_0846	G08	0.7324	+	+	+	
3239	YBR100W	46	G	9		YKO_0846	G09	0.7311	+	+	+	
3242	YBR103W	46	G	10		YKO_0846	G10	0.7493	+	+	+	
3243	YBR104W	46	G	11		YKO_0846	G11	0.6901	+	+	+	
3244	YBR105C	46	G	12		YKO_0846	G12	0.6704	+	+	+	
3245	YBR106W	46	H	1		YKO_0846	H01	0.6177	+	+	-	HIT
--		46	H	2	empty	YKO_0846	H02	empty	empty	empty	empty	empty
3246	YBR107C	46	H	3		YKO_0846	H03	0.9131	+	+	+	
3247	YBR108W	46	H	4		YKO_0846	H04	0.8206	+	+	+	
3250	YBR111C	46	H	5		YKO_0846	H05	0.6404	+	+	+	
3252	YBR113W	46	H	6		YKO_0846	H06	0.6341	+	+	+	
3253	YBR114W	46	H	7		YKO_0846	H07	0.6276	+	+	+	
3254	YBR115C	46	H	8		YKO_0846	H08	0.6695	+	+	+	
3255	YBR116C	46	H	9		YKO_0846	H09	0.6629	+	+	+	
3258	YBR119W	46	H	10		YKO_0846	H10	0.6675	+	+	+	
3259	YBR120C	46	H	11	slow growth, petite	YKO_0846	H11	0.5416	slow	+	-	Doubt
3260	YBR121C	46	H	12	QC Failure	YKO_0846	H12	0.6934	+	+	-	HIT
3265	YBR126C	47	A	1		YKO_0847	A01	0.83	+	+	+	
3266	YBR127C	47	A	2	petite	YKO_0847	A02	0.2	slow	+	+	
3267	YBR128C	47	A	3		YKO_0847	A03	0.895	+	+	+	
3268	YBR129C	47	A	4		YKO_0847	A04	0.87	+	+	+	
3269	YBR130C	47	A	5		YKO_0847	A05	0.951	+	+	+	
3271	YBR132C	47	A	6		YKO_0847	A06	0.866	slow	+	-	Doubt
3272	YBR133C	47	A	7		YKO_0847	A07	0.918	+	+	+	
3273	YBR134W	47	A	8		YKO_0847	A08	0.923	+	+	+	
3276	YBR137W	47	A	9		YKO_0847	A09	0.948	+	+	+	
3277	YBR138C	47	A	10		YKO_0847	A10	1.007	+	+	+	
3278	YBR139W	47	A	11		YKO_0847	A11	0.691	+	+	+	
3280	YBR141C	47	A	12		YKO_0847	A12	0.939	+	+	+	
3283	YBR144C	47	B	1		YKO_0847	B01	0.912	+	+	+	
3284	YBR145W	47	B	2		YKO_0847	B02	0.882	+	+	+	
3285	YBR146W	47	B	3		YKO_0847	B03	0.942	+	+	+	
3286	YBR147W	47	B	4		YKO_0847	B04	0.945	+	+	+	
3287	YBR148W	47	B	5		YKO_0847	B05	0.896	+	+	+	
3288	YBR149W	47	B	6		YKO_0847	B06	1	+	+	+	
3290	YBR151W	47	B	7		YKO_0847	B07	0.941	+	+	+	
3295	YBR156C	47	B	8		YKO_0847	B08	0.933	+	+	+	
3296	YBR157C	47	B	9		YKO_0847	B09	0.982	+	+	+	
3297	YBR158W	47	B	10		YKO_0847	B10	0.911	+	+	+	
3298	YBR159W	47	B	11		YKO_0847	B11	0.924	+	+	+	
3300	YBR161W	47	B	12		YKO_0847	B12	0.903	+	+	+	
3301	YBR162C	47	C	1		YKO_0847	C01	0.972	+	+	+	
3302	YBR162W-A	47	C	2		YKO_0847	C02	0.918	+	+	+	
3303	YBR163W	47	C	3	slow growth	YKO_0847	C03	0.846	slow	+	-	Doubt
3304	YBR164C	47	C	4		YKO_0847	C04	0.999	+	+	+	
3305	YBR165W	47	C	5		YKO_0847	C05	0.962	+	+	+	
3306	YBR166C	47	C	6		YKO_0847	C06	0.983	+	+	+	
3310	YBR170C	47	C	7		YKO_0847	C07	0.985	+	+	+	
3311	YBR171W	47	C	8		YKO_0847	C08	0.977	+	+	+	
3312	YBR172C	47	C	9		YKO_0847	C09	0.993	+	+	+	
3697	YDL001W	47	C	10		YKO_0847	C10	not grown	-	-	-	Not grown
3698	YDL002C	47	C	11		YKO_0847	C11	0.868	+	+	+	
3702	YDL006W	47	C	12		YKO_0847	C12	0.733	+	+	+	
3705	YDL009C	47	D	1		YKO_0847	D01	1.04	+	+	+	
3706	YDL010W	47	D	2		YKO_0847	D02	0.939	+	+	+	
3707	YDL011C	47	D	3		YKO_0847	D03	1.08	+	+	+	
3708	YDL012C	47	D	4		YKO_0847	D04	0.94	+	+	+	
3709	YDL013W	47	D	5		YKO_0847	D05	0.918	+	+	+	
3714	YDL018C	47	D	6		YKO_0847	D06	0.752	+	+	+	
3715	YDL019C	47	D	7		YKO_0847	D07	0.99	+	+	+	
3716	YDL020C	47	D	8		YKO_0847	D08	0.881	+	+	+	
3717	YDL021W	47	D	9		YKO_0847	D09	0.942	+	+	+	
3718	YDL022W	47	D	10		YKO_0847	D10	0.923	+	+	+	
--		47	D	11	empty	YKO_0847	D11	empty	empty	empty	empty	empty
3719	YDL023C	47	D	12		YKO_0847	D12	0.98	+	+	+	
3720	YDL024C	47	E	1		YKO_0847	E01	0.956	+	+	+	
3721	YDL025C	47	E	2		YKO_0847	E02	0.955	+	+	+	
3722	YDL026W	47	E	3		YKO_0847	E03	0.852	+	+	+	
3723	YDL027C	47	E	4		YKO_0847	E04	0.907	+	+	+	
3728	YDL032W	47	E	5		YKO_0847	E05	0.961	slow	-	-	Doubt
3729	YDL033C	47	E	6		YKO_0847	E06	0.976	+	+	+	
3730	YDL034W	47	E	7		YKO_0847	E07	0.983	+	+	+	
3731	YDL035C	47	E	8		YKO_0847	E08	0.9	+	+	+	
3732	YDL036C	47	E	9		YKO_0847	E09	0.936	+	+	+	
3733	YDL037C	47	E	10		YKO_0847	E10	0.901	+	+	+	
3734	YDL038C	47	E	11		YKO_0847	E11	0.976	+	+	+	
3735	YDL039C	47	E	12		YKO_0847	E12	0.976	+	+	+	
3737	YDL041W	47	F	1	does not mate, sterile	YKO_0847	F01	0.864	+	+	+	
3738	YDL042C	47	F	2	does not mate, sterile	YKO_0847	F02	0.959	+	+	+	

Euroscarf Information						Replica plate Information			Tau Toxicity Enhancer Primary Screen Results			
record no.	ORF name	Plate	Row	Col	Comment	Replica plate	Well	YPD (OD600nm)	Growth plate (SC+GAL comp.)	Transformation control plate (SC+GLU-Leu)	TEST Plate (SC+GAL-Leu)	Classification
3740	YDL044C	47	F	3	slow growth, petite	YKO_0847	F03	0.829	slow	+	-	Doubt
3742	YDL045W-A	47	F	4	slow growth	YKO_0847	F04	0.686	slow	+	-	Doubt
3743	YDL046W	47	F	5		YKO_0847	F05	0.939	+	+	+	
3745	YDL048C	47	F	6		YKO_0847	F06	0.929	+	+	+	
3746	YDL049C	47	F	7	slow growth, petite	YKO_0847	F07	0.908	+	+	+	
3747	YDL050C	47	F	8		YKO_0847	F08	0.914	+	+	+	
3748	YDL051W	47	F	9		YKO_0847	F09	0.855	+	+	+	
3749	YDL052C	47	F	10		YKO_0847	F10	0.927	+	+	-	HIT
3750	YDL053C	47	F	11		YKO_0847	F11	0.987	+	+	+	
3751	YDL054C	47	F	12		YKO_0847	F12	0.784	+	+	+	
3753	YDL056W	47	G	1		YKO_0847	G01	0.795	+	+	+	
3754	YDL057W	47	G	2	slow growth, petite	YKO_0847	G02	0.743	slow	+	-	Doubt
3756	YDL059C	47	G	3		YKO_0847	G03	0.924	+	+	+	
3758	YDL061C	47	G	4		YKO_0847	G04	0.881	+	+	+	
3759	YDL062W	47	G	5	slow growth, petite	YKO_0847	G05	0.704	slow	+	-	Doubt
3760	YDL063C	47	G	6	super slow growth	YKO_0847	G06	0.824	slow	+	-	Doubt
3762	YDL065C	47	G	7		YKO_0847	G07	0.876	+	+	+	
3763	YDL066W	47	G	8		YKO_0847	G08	0.903	+	+	+	
3765	YDL068W	47	G	9	slow growth, petite	YKO_0847	G09	0.923	slow	+	-	Doubt
3766	YDL069C	47	G	10	petite	YKO_0847	G10	0.884	slow	+	-	Doubt
3767	YDL070W	47	G	11		YKO_0847	G11	0.941	+	+	+	
3768	YDL071C	47	G	12		YKO_0847	G12	0.657	+	+	+	
3770	YDL073W	47	H	1	slow growth, petite, sterile	YKO_0847	H01	0.858	+	+	+	
--		47	H	2	empty	YKO_0847	H02	empty	empty	empty	empty	empty
3773	YDL076C	47	H	3	super slow, petite	YKO_0847	H03	0.925	+	+	+	
3774	YDL077C	47	H	4	petite	YKO_0847	H04	0.884	+	+	+	
3775	YDL078C	47	H	5	super slow, petite	YKO_0847	H05	0.859	+	+	+	
3776	YDL079C	47	H	6		YKO_0847	H06	0.833	+	+	+	
3777	YDL080C	47	H	7		YKO_0847	H07	0.855	+	+	+	
3778	YDL081C	47	H	8		YKO_0847	H08	0.89	+	+	+	
3779	YDL082W	47	H	9		YKO_0847	H09	0.876	+	+	+	
3780	YDL083C	47	H	10		YKO_0847	H10	0.818	+	+	+	
3782	YDL085W	47	H	11		YKO_0847	H11	0.963	+	+	+	
3783	YDL086W	47	H	12		YKO_0847	H12	0.993	+	+	+	
3785	YDL088C	48	A	1		YKO_0848	A01	0.63	+	+	+	
3786	YDL089W	48	A	2		YKO_0848	A02	0.805	+	+	+	
3787	YDL090C	48	A	3	petite, does not mate, sterile	YKO_0848	A03	0.654	+	+	+	
3788	YDL091C	48	A	4		YKO_0848	A04	0.815	+	+	+	
3790	YDL093W	48	A	5		YKO_0848	A05	0.767	+	+	+	
3791	YDL094C	48	A	6		YKO_0848	A06	0.793	+	+	+	
3792	YDL095W	48	A	7		YKO_0848	A07	0.83	+	+	+	
4274	YDR438W	48	A	8		YKO_0848	A08	0.816	+	+	+	
4275	YDR439W	48	A	9		YKO_0848	A09	0.797	+	+	+	
4276	YDR440W	48	A	10	slow growth	YKO_0848	A10	0.2	slow	+	-	Doubt
4277	YDR441C	48	A	11		YKO_0848	A11	0.837	+	+	+	
4278	YDR442W	48	A	12	slow growth	YKO_0848	A12	0.911	+	+	+	
4279	YDR443C	48	B	1		YKO_0848	B01	0.815	+	+	+	
4280	YDR446W	48	B	2		YKO_0848	B02	0.832	+	+	+	
4281	YDR447C	48	B	3		YKO_0848	B03	0.849	+	+	+	
4282	YDR448W	48	B	4	slow on ypge	YKO_0848	B04	0.612	slow	+	+	
4284	YDR450W	48	B	5		YKO_0848	B05	0.79	+	+	+	
4285	YDR451C	48	B	6		YKO_0848	B06	0.733	+	+	+	
4286	YDR452W	48	B	7		YKO_0848	B07	0.771	+	+	+	
4287	YDR453C	48	B	8		YKO_0848	B08	0.715	+	+	+	
4289	YDR455C	48	B	9		YKO_0848	B09	0.825	+	+	+	
4290	YDR456W	48	B	10		YKO_0848	B10	0.907	+	+	+	
4291	YDR457W	48	B	11		YKO_0848	B11	not grown	-	-	-	Not grown
4292	YDR458C	48	B	12		YKO_0848	B12	0.775	+	+	+	
4293	YDR459C	48	C	1		YKO_0848	C01	0.866	+	+	+	
4296	YDR462W	48	C	2		YKO_0848	C02	0.961	+	+	+	
4297	YDR463W	48	C	3		YKO_0848	C03	0.803	+	+	+	
4299	YDR465C	48	C	4		YKO_0848	C04	0.886	+	+	+	
4300	YDR466W	48	C	5		YKO_0848	C05	0.757	+	+	+	
4301	YDR467C	48	C	6		YKO_0848	C06	0.681	+	+	+	
4303	YDR469W	48	C	7		YKO_0848	C07	0.649	+	+	+	
4304	YDR470C	48	C	8	slow growth, petite	YKO_0848	C08	0.661	slow	+	-	Doubt
4305	YDR471W	48	C	9		YKO_0848	C09	0.936	+	+	+	
4308	YDR474C	48	C	10		YKO_0848	C10	0.774	+	+	+	
4309	YDR475C	48	C	11		YKO_0848	C11	0.862	+	+	+	
4310	YDR476C	48	C	12		YKO_0848	C12	0.811	+	+	+	
4313	YDR479C	48	D	1		YKO_0848	D01	0.884	+	+	+	
4314	YDR480W	48	D	2		YKO_0848	D02	0.895	+	+	+	
4315	YDR481C	48	D	3		YKO_0848	D03	0.848	+	+	+	
4316	YDR482C	48	D	4		YKO_0848	D04	0.894	+	+	+	
4318	YDR484W	48	D	5		YKO_0848	D05	0.847	slow	+	-	Doubt
4319	YDR485C	48	D	6		YKO_0848	D06	0.794	+	+	+	
4320	YDR486C	48	D	7	slow growth	YKO_0848	D07	0.889	+	+	+	
4322	YDR488C	48	D	8		YKO_0848	D08	0.646	+	+	+	
4324	YDR490C	48	D	9		YKO_0848	D09	0.699	+	+	+	
4325	YDR491C	48	D	10		YKO_0848	D10	0.775	+	+	+	
4326	YDR492W	48	D	11		YKO_0848	D11	0.742	+	+	-	HIT

Euroscarf Information						Replica plate Information			Tau Toxicity Enhancer Primary Screen Results			
record no.	ORF name	Plate	Row	Col	Comment	Replica plate	Well	YPD (OD600nm)	Growth plate (SC+GAL comp.)	Transformation control plate (SC+GLU-Leu)	TEST Plate (SC+GAL-Leu)	Classification
--		48	D	12	empty	YKO_0848	D12	empty	empty	empty	empty	empty
4328	YDR494W	48	E	1		YKO_0848	E01	0.928	+	+	+	
4329	YDR495C	48	E	2		YKO_0848	E02	0.778	+	+	+	
4330	YDR496C	48	E	3		YKO_0848	E03	0.892	+	+	+	
4331	YDR497C	48	E	4		YKO_0848	E04	0.84	+	+	+	
4334	YDR500C	48	E	5		YKO_0848	E05	0.799	+	+	+	
4335	YDR501W	48	E	6		YKO_0848	E06	0.757	+	+	+	
4337	YDR503C	48	E	7		YKO_0848	E07	0.836	+	+	+	
4338	YDR504C	48	E	8		YKO_0848	E08	0.814	+	+	+	
4339	YDR505C	48	E	9		YKO_0848	E09	0.855	+	+	+	
4340	YDR506C	48	E	10		YKO_0848	E10	0.78	+	+	+	
4341	YDR507C	48	E	11	petite	YKO_0848	E11	0.304	slow	+	-	Doubt
4342	YDR508C	48	E	12		YKO_0848	E12	0.893	+	+	+	
4343	YDR509W	48	F	1		YKO_0848	F01	0.48	+	+	+	
4345	YDR511W	48	F	2		YKO_0848	F02	0.732	+	+	+	
4346	YDR512C	48	F	3		YKO_0848	F03	0.804	slow	+	-	Doubt
4347	YDR513W	48	F	4		YKO_0848	F04	0.845	+	+	+	
4348	YDR514C	48	F	5		YKO_0848	F05	0.764	+	+	+	
4350	YDR516C	48	F	6		YKO_0848	F06	0.844	+	+	+	
4351	YDR517W	48	F	7		YKO_0848	F07	0.834	+	+	+	
4352	YDR518W	48	F	8	slow growth, petite	YKO_0848	F08	0.537	slow	+	-	Doubt
4353	YDR519W	48	F	9		YKO_0848	F09	0.843	+	+	+	
4354	YDR520C	48	F	10		YKO_0848	F10	0.688	+	+	+	
4356	YDR522C	48	F	11		YKO_0848	F11	0.932	+	+	+	
4358	YDR524C	48	F	12		YKO_0848	F12	0.789	+	+	+	
4359	YDR525W	48	G	1		YKO_0848	G01	0.854	+	+	+	
4362	YDR528W	48	G	2		YKO_0848	G02	0.798	+	+	+	
4363	YDR529C	48	G	3	slow growth, petite	YKO_0848	G03	0.813	slow	+	-	Doubt
4364	YDR530C	48	G	4		YKO_0848	G04	0.694	+	+	+	
4366	YDR532C	48	G	5	slow growth, petite	YKO_0848	G05	0.539	slow	+	+	
4367	YDR533C	48	G	6		YKO_0848	G06	0.732	+	+	+	
4368	YDR534C	48	G	7		YKO_0848	G07	0.754	+	+	+	
4468	YGL101W	48	G	8		YKO_0848	G08	0.79	+	+	+	
4471	YGL104C	48	G	9		YKO_0848	G09	0.844	+	+	+	
4472	YGL105W	48	G	10	slow growth	YKO_0848	G10	0.733	+	+	+	
4474	YGL107C	48	G	11	slow growth, petite	YKO_0848	G11	0.467	slow	+	-	Doubt
4475	YGL108C	48	G	12		YKO_0848	G12	0.937	+	+	+	
4476	YGL109W	48	H	1		YKO_0848	H01	0.979	+	+	+	
--		48	H	2	empty	YKO_0848	H02	empty	empty	empty	empty	empty
4477	YGL110C	48	H	3	slow growth, petite	YKO_0848	H03	not grown	-	-	-	Not grown
4481	YGL114W	48	H	4		YKO_0848	H04	0.872	+	+	+	
4482	YGL115W	48	H	5	slow growth, petite	YKO_0848	H05	0.606	+	+	+	
4484	YGL117W	48	H	6		YKO_0848	H06	0.857	+	+	+	
4485	YGL118C	48	H	7		YKO_0848	H07	0.954	+	+	+	
4488	YGL121C	48	H	8		YKO_0848	H08	0.87	+	+	+	
4491	YGL124C	48	H	9		YKO_0848	H09	0.91	+	+	+	
4492	YGL125W	48	H	10		YKO_0848	H10	0.925	+	+	+	
4493	YGL126W	48	H	11		YKO_0848	H11	0.842	+	+	+	
4494	YGL127C	48	H	12		YKO_0848	H12	0.667	+	+	+	
4496	YGL129C	49	A	1	slow growth, petite	YKO_0849	A01	0.649	slow	+	-	Doubt
4498	YGL131C	49	A	2		YKO_0849	A02	0.879	+	+	+	
4499	YGL132W	49	A	3		YKO_0849	A03	0.872	+	+	+	
4500	YGL133W	49	A	4		YKO_0849	A04	0.742	+	+	+	
4502	YGL135W	49	A	5	slow growth, petite	YKO_0849	A05	0.768	+	+	+	
4503	YGL136C	49	A	6		YKO_0849	A06	0.821	+	+	+	
4505	YGL138C	49	A	7		YKO_0849	A07	0.885	+	+	+	
4506	YGL139W	49	A	8		YKO_0849	A08	0.909	+	+	+	
4507	YGL140C	49	A	9		YKO_0849	A09	0.871	+	+	+	
4508	YGL141W	49	A	10		YKO_0849	A10	0.82	+	+	+	
4510	YGL143C	49	A	11	slow growth, petite	YKO_0849	A11	0.938	slow	+	-	Doubt
4511	YGL144C	49	A	12		YKO_0849	A12	0.954	+	+	+	
4513	YGL146C	49	B	1	slow growth	YKO_0849	B01	0.837	+	+	+	
4514	YGL147C	49	B	2	slow growth	YKO_0849	B02	0.869	+	+	+	
4515	YGL148W	49	B	3	no growth on "drop-in" media	YKO_0849	B03	0.903	+	+	+	
4516	YGL149W	49	B	4		YKO_0849	B04	0.746	+	+	+	
4518	YGL151W	49	B	5		YKO_0849	B05	0.954	+	+	+	
4519	YGL152C	49	B	6		YKO_0849	B06	0.909	+	+	+	
4520	YGL153W	49	B	7		YKO_0849	B07	0.979	+	+	+	
4521	YGL154C	49	B	8	no growth on drop-in media, slow growth on -lys	YKO_0849	B08	0.95	+	+	+	
4523	YGL156W	49	B	9		YKO_0849	B09	0.951	+	+	+	
4524	YGL157W	49	B	10		YKO_0849	B10	0.956	+	+	+	
4525	YGL158W	49	B	11		YKO_0849	B11	0.908	+	+	+	
4526	YGL159W	49	B	12		YKO_0849	B12	0.932	+	+	+	
4527	YGL160W	49	C	1		YKO_0849	C01	0.943	+	+	+	
4528	YGL161C	49	C	2		YKO_0849	C02	0.943	+	+	+	
4529	YGL162W	49	C	3		YKO_0849	C03	0.913	+	+	+	
4530	YGL163C	49	C	4		YKO_0849	C04	0.788	+	+	+	
4531	YGL164C	49	C	5		YKO_0849	C05	1.018	+	+	+	
4532	YGL165C	49	C	6		YKO_0849	C06	1.017	+	+	+	
4533	YGL166W	49	C	7		YKO_0849	C07	0.937	+	+	+	

	Euroscarf Information					Replica plate Information			Tau Toxicity Enhancer Primary Screen Results			
record no.	ORF name	Plate	Row	Col	Comment	Replica plate	Well	YPD (OD600nm)	Growth plate (SC+GAL comp.)	Transformation control plate (SC+GLU-Leu)	TEST Plate (SC+GAL-Leu)	Classification
4534	YGL167C	49	C	8	petite	YKO_0849	C08	0.886	slow	+	+	
4535	YGL168W	49	C	9	petite	YKO_0849	C09	0.929	slow	+	+	
4537	YGL170C	49	C	10		YKO_0849	C10	0.893	+	+	+	
4540	YGL173C	49	C	11	slow growth	YKO_0849	C11	0.767	slow	+	+	
4541	YGL174W	49	C	12		YKO_0849	C12	0.877	+	+	+	
4542	YGL175C	49	D	1		YKO_0849	D01	0.729	+	+	+	
4543	YGL176C	49	D	2		YKO_0849	D02	0.927	+	+	+	
4544	YGL177W	49	D	3		YKO_0849	D03	0.92	+	+	+	
4546	YGL179C	49	D	4		YKO_0849	D04	0.956	+	+	+	
4547	YGL180W	49	D	5		YKO_0849	D05	0.931	+	+	+	
4548	YGL181W	49	D	6		YKO_0849	D06	0.933	+	+	+	
6099	YER101C	49	D	7		YKO_0849	D07	0.973	+	+	+	
6101	YER103W	49	D	8	petite	YKO_0849	D08	0.799	slow	+	-	Doubt
6104	YER106W	49	D	9		YKO_0849	D09	0.974	+	+	+	
6106	YER108C	49	D	10		YKO_0849	D10	0.818	+	+	+	
6107	YER109C	49	D	11		YKO_0849	D11	0.884	+	+	+	
6108	YER110C	49	D	12	slow growth, petite	YKO_0849	D12	0.429	slow	+	-	Doubt
--		49	E	1	empty	YKO_0849	E01	empty	empty	empty	empty	empty
6109	YER111C	49	E	2		YKO_0849	E02	0.648	+	+	+	
6111	YER113C	49	E	3		YKO_0849	E03	0.908	+	+	+	
6112	YER114C	49	E	4		YKO_0849	E04	0.908	+	+	+	
6113	YER115C	49	E	5		YKO_0849	E05	0.978	+	+	+	
6114	YER116C	49	E	6		YKO_0849	E06	0.949	+	+	+	
6115	YER117W	49	E	7		YKO_0849	E07	0.948	+	+	+	
6116	YER118C	49	E	8		YKO_0849	E08	0.971	+	+	+	
6117	YER119C	49	E	9		YKO_0849	E09	0.892	+	+	+	
6118	YER119C-A	49	E	10		YKO_0849	E10	0.855	+	+	+	
6119	YER120W	49	E	11		YKO_0849	E11	0.876	+	+	+	
6120	YER121W	49	E	12		YKO_0849	E12	0.967	+	+	+	
6122	YER123W	49	F	1		YKO_0849	F01	0.932	+	+	+	
6123	YER124C	49	F	2		YKO_0849	F02	0.887	+	+	+	
6127	YER128W	49	F	3		YKO_0849	F03	0.885	+	+	+	
6128	YER129W	49	F	4		YKO_0849	F04	0.8	+	+	+	
6129	YER130C	49	F	5		YKO_0849	F05	0.799	+	+	+	
6130	YER131W	49	F	6		YKO_0849	F06	0.717	+	+	+	
6131	YER132C	49	F	7		YKO_0849	F07	0.889	+	+	+	
6133	YER134C	49	F	8		YKO_0849	F08	0.914	+	+	+	
6134	YER135C	49	F	9		YKO_0849	F09	0.829	+	+	+	
6136	YER137C	49	F	10		YKO_0849	F10	0.825	+	+	+	
6137	YER139C	49	F	11		YKO_0849	F11	0.882	+	+	+	
6138	YER140W	49	F	12		YKO_0849	F12	0.971	+	+	+	
6139	YER141W	49	G	1	slow growth, petite	YKO_0849	G01	0.679	+	+	+	
6140	YER142C	49	G	2		YKO_0849	G02	0.731	+	+	+	
6141	YER143W	49	G	3		YKO_0849	G03	0.892	+	+	+	
6142	YER145C	49	G	4		YKO_0849	G04	0.762	+	+	+	
6146	YER149C	49	G	5		YKO_0849	G05	0.891	+	-	+	Incongruence
6147	YER150W	49	G	6		YKO_0849	G06	0.867	+	+	+	
6148	YER151C	49	G	7		YKO_0849	G07	0.453	slow	+	-	Doubt
6149	YER152C	49	G	8		YKO_0849	G08	0.945	+	+	+	
6150	YER153C	49	G	9	slow growth, petite	YKO_0849	G09	0.828	slow	+	-	Doubt
6151	YER154W	49	G	10	slow growth, petite	YKO_0849	G10	0.645	slow	+	-	Doubt
6152	YER155C	49	G	11		YKO_0849	G11	0.676	+	+	+	
6153	YER156C	49	G	12		YKO_0849	G12	0.82	+	+	+	
6155	YER158C	49	H	1		YKO_0849	H01	0.947	+	+	+	
--		49	H	2	empty	YKO_0849	H02	empty	empty	empty	empty	empty
6157	YER161C	49	H	3		YKO_0849	H03	0.567	+	+	+	
6158	YER162C	49	H	4		YKO_0849	H04	0.717	+	+	+	
6159	YER163C	49	H	5		YKO_0849	H05	0.938	+	+	+	
6160	YER164W	49	H	6		YKO_0849	H06	0.728	+	+	+	
6162	YER166W	49	H	7		YKO_0849	H07	0.837	+	+	+	
6163	YER167W	49	H	8		YKO_0849	H08	0.835	+	+	+	
6165	YER169W	49	H	9	slow growth, petite	YKO_0849	H09	0.652	slow	+	-	Doubt
6166	YER170W	49	H	10		YKO_0849	H10	0.909	+	+	+	
6169	YER173W	49	H	11		YKO_0849	H11	0.828	+	+	+	
6170	YER174C	49	H	12		YKO_0849	H12	0.997	+	+	+	
6171	YER175C	50	A	1		YKO_0850	A01	0.845	+	+	+	
6172	YER176W	50	A	2		YKO_0850	A02	0.863	+	+	+	
6173	YER177W	50	A	3		YKO_0850	A03	0.793	+	+	+	
6174	YER178W	50	A	4		YKO_0850	A04	0.916	+	+	+	
6175	YER179W	50	A	5		YKO_0850	A05	0.911	+	+	+	
6176	YER180C	50	A	6		YKO_0850	A06	0.889	+	+	+	
6177	YER181C	50	A	7		YKO_0850	A07	0.877	+	+	+	
6178	YER182W	50	A	8		YKO_0850	A08	0.853	+	+	+	
6179	YER183C	50	A	9		YKO_0850	A09	0.869	+	+	+	
6180	YER184C	50	A	10		YKO_0850	A10	0.866	+	+	+	
6181	YER185W	50	A	11		YKO_0850	A11	0.908	+	+	+	
6182	YER186C	50	A	12		YKO_0850	A12	0.85	+	+	+	
6183	YER187W	50	B	1		YKO_0850	B01	0.982	+	+	+	
6185	YMR052C-A	50	B	2		YKO_0850	B02	0.784	+	+	+	
6186	YMR052W	50	B	3		YKO_0850	B03	0.933	+	+	+	
6187	YMR053C	50	B	4		YKO_0850	B04	0.944	+	+	+	
6188	YMR054W	50	B	5		YKO_0850	B05	0.997	+	+	+	
6189	YMR055C	50	B	6		YKO_0850	B06	0.937	+	+	+	
6190	YMR056C	50	B	7		YKO_0850	B07	0.935	+	+	+	

Euroscarf Information						Replica plate Information			Tau Toxicity Enhancer Primary Screen Results			
record no.	ORF name	Plate	Row	Col	Comment	Replica plate	Well	YPD (OD600nm)	Growth plate (SC+GAL comp.)	Transformation control plate (SC+GLU-Leu)	TEST Plate (SC+GAL-Leu)	Classification
6191	YMR057C	50	B	8		YKO_0850	B08	1.008	+	+	+	
6192	YMR058W	50	B	9		YKO_0850	B09	0.911	+	+	+	
6832	YJR034W	50	B	10		YKO_0850	B10	0.911	+	+	+	
6837	YJR039W	50	B	11		YKO_0850	B11	0.777	+	+	+	
6842	YJR044C	50	B	12		YKO_0850	B12	0.893	+	+	+	
6853	YJR055W	50	C	1	papillation on -met	YKO_0850	C01	0.933	+	+	+	
6864	YJR066W	50	C	2		YKO_0850	C02	0.886	+	+	+	
2261	YIL102C	50	C	3	papillation on -met, growth on - lys	YKO_0850	C03	0.88	+	+	+	
2270	YIL111W	50	C	4		YKO_0850	C04	0.763	+	+	+	
2281	YIL122W	50	C	5		YKO_0850	C05	0.878	+	+	+	
2290	YIL131C	50	C	6		YKO_0850	C06	0.979	+	+	+	
2295	YIL136W	50	C	7		YKO_0850	C07	0.976	+	+	+	
2317	YIL158W	50	C	8		YKO_0850	C08	0.997	+	+	+	
2340	YIR004W	50	C	9		YKO_0850	C09	0.854	slow	+	+	
1449	YIL056W	50	C	10		YKO_0850	C10	0.92	+	+	+	
1476	YIL085C	50	C	11		YKO_0850	C11	0.821	+	+	+	
1485	YIL094C	50	C	12	no growth on drop-in media	YKO_0850	C12	0.988	+	+	+	
3744	YDL047W	50	D	1		YKO_0850	D01	0.344	slow	-	-	Doubt
3764	YDL067C	50	D	2	petite	YKO_0850	D02	1.046	slow	+	-	Doubt
3771	YDL074C	50	D	3		YKO_0850	D03	0.923	+	+	+	
3772	YDL075W	50	D	4	slow growth	YKO_0850	D04	0.626	slow	+	+	
4311	YDR477W	50	D	5		YKO_0850	D05	0.836	slow	+	+	
4317	YDR483W	50	D	6		YKO_0850	D06	0.845	+	+	+	
4355	YDR521W	50	D	7	slow growth, petite	YKO_0850	D07	not grown	-	-	-	Not grown
4357	YDR523C	50	D	8		YKO_0850	D08	0.856	slow	+	-	Doubt
1561	YLR006C	50	D	9		YKO_0850	D09	0.921	+	+	+	
565	YML010W-A	50	D	10		YKO_0850	D10	0.919	slow	+	+	
614	YMR038C	50	D	11	slow growth on drop-in media, slow growth on - lys, growth on -met	YKO_0850	D11	0.29	slow	-	-	Doubt
1661	YOR364W	50	D	12		YKO_0850	D12	0.961	+	+	+	
3313	YBR173C	50	E	1		YKO_0850	E01	0.577	+	+	+	
--		50	E	2	empty	YKO_0850	E02	empty	empty	empty	empty	empty
336	YER014W	50	E	3	slow growth, petite,slow growth on drop-in media	YKO_0850	E03	0.899	slow	+	-	Doubt
147	YER016W	50	E	4		YKO_0850	E04	0.646	+	+	+	
160	YER028C	50	E	5		YKO_0850	E05	0.926	+	+	+	
177	YER044C	50	E	6	slow growth, no growth on drop-in media	YKO_0850	E06	0.89	+	+	+	
190	YER055C	50	E	7		YKO_0850	E07	not grown	-	-	-	Not grown
991	YHR028C	50	E	8		YKO_0850	E08	0.773	+	+	+	
996	YHR033W	50	E	9		YKO_0850	E09	0.881	+	+	+	
3414	YCL006C	50	E	10		YKO_0850	E10	0.868	+	+	+	
3445	YCL038C	50	E	11	Failure: Tag Duplicated in ORF YDR074W. For correct deletion go to 6876	YKO_0850	E11	0.94	+	+	+	
7249	YAL024C	50	E	12		YKO_0850	E12	0.671	+	+	+	
7250	YBR299W	50	F	1		YKO_0850	F01	0.921	+	+	+	
7253	YCR107W	50	F	2		YKO_0850	F02	1.001	+	+	+	
7256	YDR242W	50	F	3		YKO_0850	F03	0.959	+	+	+	
7257	YDR326C	50	F	4		YKO_0850	F04	0.883	+	+	+	
7258	YDR417C	50	F	5		YKO_0850	F05	0.945	+	+	+	
7259	YDR444W	50	F	6		YKO_0850	F06	0.854	+	+	+	
7260	YDR461W	50	F	7	mates with a, papillation with alpha. Confirmed Het Diploid 10/15/01	YKO_0850	F07	0.937	+	+	+	
7261	YDR493W	50	F	8		YKO_0850	F08	0.957	+	+	+	
7264	YDR502C	50	F	9		YKO_0850	F09	0.873	+	+	+	
7265	YDR506C	50	F	10		YKO_0850	F10	1.021	+	+	+	
7267	YDR515W	50	F	11		YKO_0850	F11	0.931	+	+	+	
7269	YER089C	50	F	12		YKO_0850	F12	0.97	+	+	+	
7270	YFL001W	50	G	1		YKO_0850	G01	0.512	+	+	+	
7272	YFL003C	50	G	2		YKO_0850	G02	0.961	+	+	+	
7273	YFL004W	50	G	3		YKO_0850	G03	0.878	+	+	+	
7275	YFL007W	50	G	4		YKO_0850	G04	0.974	+	+	+	
7276	YFL010C	50	G	5		YKO_0850	G05	0.938	+	+	+	
7277	YFL010W-A	50	G	6		YKO_0850	G06	1.001	+	+	+	
7278	YFL012W	50	G	7		YKO_0850	G07	0.95	+	+	+	
7279	YFL013C	50	G	8		YKO_0850	G08	0.854	+	+	+	
7281	YFL033C	50	G	9		YKO_0850	G09	0.964	+	+	+	
7283	YGR122C-A	50	G	10		YKO_0850	G10	0.94	+	+	+	
7390	YOL148C	50	G	11	super slow growth	YKO_0850	G11	not grown	-	-	-	Not grown
7286	YGR254W	50	G	12		YKO_0850	G12	0.962	+	+	+	
7289	YGR258C	50	H	1		YKO_0850	H01	0.913	+	+	+	
--		50	H	2	empty	YKO_0850	H02	empty	empty	empty	empty	empty
7290	YGR271W	50	H	3		YKO_0850	H03	0.898	+	+	+	
7389	YNR033W	50	H	4		YKO_0850	H04	0.783	+	+	+	
7292	YGR273C	50	H	5		YKO_0850	H05	0.948	+	+	+	
7293	YGR276C	50	H	6		YKO_0850	H06	0.898	+	+	+	
7294	YGR289C	50	H	7		YKO_0850	H07	0.97	+	+	+	

	Euroscarf Information					Replica plate Information			Tau Toxicity Enhancer Primary Screen Results			
record no.	ORF name	Plate	Row	Col	Comment	Replica plate	Well	YPD (OD600nm)	Growth plate (SC+GAL comp.)	Transformation control plate (SC+GLU-Leu)	TEST Plate (SC+GAL-Leu)	Classification
7295	YGR291C	50	H	8		YKO_0850	H08	0.935	+	+	+	
7296	YGR292W	50	H	9		YKO_0850	H09	0.606	+	+	+	
7345	YBR020W	50	H	10		YKO_0850	H10	0.931	-	+	-	Doubt
7346	YBR075W	50	H	11		YKO_0850	H11	0.935	+	+	+	
7362	YFL033C	50	H	12		YKO_0850	H12	0.959	+	+	+	
7364	YFL063W	51	A	1		YKO_0851	A01	0.785	+	+	+	
7367	YJL103C	51	A	2		YKO_0851	A02	0.783	+	+	+	
7368	YML073C	51	A	3		YKO_0851	A03	0.886	slow	+	-	Doubt
7369	YNL011C	51	A	4		YKO_0851	A04	0.755	+	+	+	
7370	YNL014W	51	A	5		YKO_0851	A05	0.79	+	+	+	
7825		51	A	6		YKO_0851	A06	0.928	slow	+	-	Doubt
7826		51	A	7		YKO_0851	A07	0.763	+	+	+	
2406	YOR150W	70	A	1		YKO_0852	A01	0.862	slow	+	-	Doubt
2414	YOR158W	70	A	2	petite	YKO_0852	A02	0.906	slow	+	-	Doubt
5246	YLR337C	70	A	3	petite	YKO_0852	A03	0.891	+	+	+	
5247	YLR338W	70	A	4		YKO_0852	A04	0.754	+	+	+	
5278	YLR369W	70	A	5	slow growth, petite, slow growth on -lys, no growth on drop-in media	YKO_0852	A05	0.921	slow	+	-	Doubt
5298	YLR389C	70	A	6		YKO_0852	A06	0.966	+	+	+	
5300	YLR391W	70	A	7		YKO_0852	A07	0.952	+	+	+	
5149	YLR240W	70	A	8	extremly slow growth, petite	YKO_0852	A08	not grown	-	-	-	Not grown
5153	YLR244C	70	A	9	slow growth no growth on drop-in media	YKO_0852	A09	0.69	+	+	+	
4572	YGL206C	70	A	10	slow growth, petite	YKO_0852	A10	not grown	-	-	-	Not grown
4589	YGL223C	70	A	11	slow growth, petite,slow growth on -lys,no growth on -met, no growth on drop-in media	YKO_0852	A11	not grown	-	-	-	Not grown
5308	YLR399C	70	A	12		YKO_0852	A12	not grown	-	-	-	Not grown
5312	YLR403W	70	B	1	slow growth	YKO_0852	B01	0.442	+	+	+	
5305	YLR396C	70	B	2	petite	YKO_0852	B02	0.937	slow	+	-	Doubt
4607	YGL240W	70	B	3	slow growth, petite	YKO_0852	B03	0.998	slow	+	-	Doubt
2769	YPL059W	70	B	4	slow growth petite lys-no growth on drop-in media	YKO_0852	B04	0.534	slow	+	-	Doubt
2778	YPL050C	70	B	5		YKO_0852	B05	0.954	+	+	+	
2783	YPL045W	70	B	6	petite	YKO_0852	B06	not grown	-	-	-	Not grown
2797	YPL031C	70	B	7	slow growth, petite	YKO_0852	B07	0.369	-	+	-	Doubt
2804	YPL024W	70	B	8		YKO_0852	B08	0.762	+	+	+	
5872	YGR219W	70	B	9	petite	YKO_0852	B09	0.843	slow	+	-	Doubt
5875	YGR222W	70	B	10	petite	YKO_0852	B10	0.924	slow	+	-	Doubt
5882	YGR229C	70	B	11		YKO_0852	B11	0.867	+	+	+	
3051	YBL025W	70	B	12	slow growth	YKO_0852	B12	not grown	-	-	-	Not grown
3059	YBL033C	70	C	1	slow growth, petite, papillation on mat a, slow grow drop in media, slow grow on -lys -- Riboflavin auxotroph-grow with 50um riboflavin	YKO_0852	C01	0.859	+	+	+	
4388	YGL020C	70	C	2		YKO_0852	C02	0.975	+	+	+	
4406	YGL038C	70	C	3	slow growth, petite	YKO_0852	C03	not grown	-	-	-	Not grown
4437	YGL070C	70	C	4	slow growth	YKO_0852	C04	0.758	+	+	+	
4462	YGL095C	70	C	5	slow growth, petite	YKO_0852	C05	0.693	slow	+	-	Doubt
4455	YGL088W	70	C	6		YKO_0852	C06	0.859	+	+	+	
2059	YNL153C	70	C	7		YKO_0852	C07	0.589	+	+	+	
1987	YNL225C	70	C	8	slow growth, petite	YKO_0852	C08	0.472	slow	+	-	Doubt
5077	YKR006C	70	C	9	slow growth	YKO_0852	C09	0.883	slow	+	-	Doubt
3604	YDR245W	70	C	10		YKO_0852	C10	0.783	+	+	+	
3627	YDR268W	70	C	11	petite	YKO_0852	C11	0.818	slow	+	-	Doubt
3642	YDR283C	70	C	12		YKO_0852	C12	0.926	+	+	+	
3655	YDR296W	70	D	1	petite	YKO_0852	D01	0.921	slow	+	-	Doubt
3659	YDR300C	70	D	2	slow growth petite no growth on drop-in media	YKO_0852	D02	0.958	slow	+	-	Doubt
1411	YIL018W	70	D	3		YKO_0852	D03	0.977	+	+	+	
1459	YIL066C	70	D	4	grows well on -met, grows well on -lys	YKO_0852	D04	0.92	+	+	+	
5636	YFL018C	70	D	5	slow growth	YKO_0852	D05	0.928	+	+	-	HIT
5914	YGR262C	70	D	6	slow growth	YKO_0852	D06	not grown	-	-	-	Not grown
6197	YMR064W	70	D	7	petite	YKO_0852	D07	0.776	slow	+	-	Doubt
6199	YMR066W	70	D	8		YKO_0852	D08	0.949	slow	+	-	Doubt
6510	YML110C	70	D	9		YKO_0852	D09	0.948	slow	+	-	Doubt
6511	YML111W	70	D	10		YKO_0852	D10	0.924	+	+	+	
6512	YML112W	70	D	11	slow growth	YKO_0852	D11	not grown	-	-	-	Not grown
6530	YML129C	70	D	12	petite	YKO_0852	D12	0.971	+	+	+	
6537	YMR097C	70	E	1	super slow growth	YKO_0852	E01	0.834	slow	+	-	Doubt
6538	YMR098C	70	E	2	petite	YKO_0852	E02	0.893	slow	+	-	Doubt

Euroscarf Information						Replica plate Information			Tau Toxicity Enhancer Primary Screen Results			
record no.	ORF name	Plate	Row	Col	Comment	Replica plate	Well	YPD (OD600nm)	Growth plate (SC+GAL comp.)	Transformation control plate (SC+GLU-Leu)	TEST Plate (SC+GAL-Leu)	Classification
6652	YOL143C	70	E	3	slow growth, petite ,no growth on drop-in media, slow grow on -lys	YKO_0852	E03	not grown	-	-	-	Not grown
6866	YAL016W	70	E	4	slow growth	YKO_0852	E04	not grown	-	-	-	Not grown
6884	YGL218W	70	E	5	super slow, petite	YKO_0852	E05	0.917	+	+	+	
6902	YJR090C	70	E	6	super slow growth	YKO_0852	E06	0.728	+	+	+	
6947	YLR286C	70	E	7		YKO_0852	E07	0.761	+	+	+	
3900	YDL202W	70	E	8	grows on -met, grows on -lys, mates with alpha, papillation on mat a	YKO_0852	E08	0.833	-	+	-	Doubt
5727	YBR279W	70	E	9	grows on -met, grows on -lys, papillation on mat a & mat alpha	YKO_0852	E09	0.697	+	+	+	
5768	YCR044C	70	E	10	slow growth	YKO_0852	E10	0.622	+	+	+	
5784	YCR063W	70	E	11		YKO_0852	E11	0.301	slow	-	-	Doubt
6771	YJL003W	70	E	12	petite	YKO_0852	E12	0.85	+	+	+	
6772	YJL004C	70	F	1		YKO_0852	F01	0.883	+	+	+	
6774	YJL006C	70	F	2		YKO_0852	F02	0.372	slow	-	-	Doubt
6780	YJL012C	70	F	3		YKO_0852	F03	0.998	+	+	+	
6781	YJL013C	70	F	4		YKO_0852	F04	0.909	+	+	+	
6795	YJL027C	70	F	5	slow growth, petite	YKO_0852	F05	0.848	slow	+	-	Doubt
6796	YJL028W	70	F	6		YKO_0852	F06	0.783	+	+	+	
6801	YJR004C	70	F	7	petite	YKO_0852	F07	0.867	-	+	-	Doubt
6830	YJR032W	70	F	8		YKO_0852	F08	0.734	+	+	+	
6835	YJR037W	70	F	9	papillation on -met	YKO_0852	F09	0.883	+	+	+	
--		70	F	10	empty	YKO_0852	F10	empty	empty	empty	empty	empty
6845	YJR047C	70	F	11		YKO_0852	F11	0.92	+	+	+	
6838	YJR040W	70	F	12		YKO_0852	F12	0.904	+	+	+	
6836	YJR038C	70	G	1		YKO_0852	G01	0.644	+	+	+	
3858	YDL160C	70	G	2	slow growth	YKO_0852	G02	0.896	slow	+	-	Doubt
3865	YDL167C	70	G	3		YKO_0852	G03	0.853	slow	+	-	Doubt
3883	YDL185W	70	G	4	petite	YKO_0852	G04	1.004	-	-	-	Doubt
1628	YOR331C	70	G	5		YKO_0852	G05	0.823	-	-	-	Doubt
5331	YNL003C	70	G	6	Incorrect	YKO_0852	G06	0.879	+	+	+	
3215	YBR078W	70	G	7		YKO_0852	G07	0.838	+	+	+	
2992	YNL084C	70	G	8	slow growth, petite	YKO_0852	G08	0.846	+	+	+	
2257	YIL098C	70	G	9		YKO_0852	G09	0.603	+	+	+	
7017	YJL184W	70	G	10	slow growth	YKO_0852	G10	not grown	-	-	-	Not grown
6760	YPL148C	70	G	11	petite	YKO_0852	G11	0.979	+	+	+	
7135	YPL268W	70	G	12	slow growth	YKO_0852	G12	0.906	+	+	+	
7151	YPR067W	70	H	1	slow growth, petite , no grow on -lys, no growth on drop-in media	YKO_0852	H01	0.777	+	+	-	HIT
--		70	H	2	empty	YKO_0852	H02	empty	empty	empty	empty	empty
3236	YBR097W	70	H	3	super slow growth	YKO_0852	H03	0.72	+	+	-	HIT
3240	YBR101C	70	H	4	slow growth	YKO_0852	H04	0.816	+	+	+	
3261	YBR122C	70	H	5	petite	YKO_0852	H05	0.914	slow	+	-	Doubt
3736	YDL040C	70	H	6	super slow, petite	YKO_0852	H06	0.783	slow	+	-	Doubt
3769	YDL072C	70	H	7		YKO_0852	H07	0.759	+	+	+	
6121	YER122C	70	H	8	petite	YKO_0852	H08	0.869	slow	+	-	Doubt
1348	YJL075C	70	H	9		YKO_0852	H09	0.912	+	+	+	
3172	YBR035C	70	H	10	super slow growth	YKO_0852	H10	0.839	+	+	+	
5491	YPR072W	70	H	11	slow growth, petite	YKO_0852	H11	0.907	+	+	+	
6672	YOR008C-A	70	H	12	grew without riboflavin! Should not.	YKO_0852	H12	0.915	+	+	+	
2384	YOR128C	71	A	1	no growth on drop-in media,no growth on -met,growth on -lys, colony is pink- ade mutant?? OK	YKO_0853	A01	0.996	+	+	+	
285	YEL044W	71	A	2	super slow growth, grows slow on -lys, no growth on -met OK	YKO_0853	A02	0.53	+	+	+	
227	YER087W	71	A	3	slow growth, petite, no growth on -met, slow growth on -lys OK	YKO_0853	A03	0.923	+	+	-	HIT
270	YEL029C	71	A	4	Similar to YNR027W -- slow grow, petite,no growth on drop-in media, super slow growth on -met, no growth on -lys, mates like alpha, not like mat a. Confirmed Alpha 10/15/01 -- CORRECT STRAIN CAN BE FOUND IN PLATE 121 D7	YKO_0853	A04	0.878	+	+	+	

	Euroscarf Information					Replica plate Information			Tau Toxicity Enhancer Primary Screen Results			
record no.	ORF name	Plate	Row	Col	Comment	Replica plate	Well	YPD (OD600nm)	Growth plate (SC+GAL comp.)	Transformation control plate (SC+GLU-Leu)	TEST Plate (SC+GAL-Leu)	Classification
973	YHR010W	71	A	5	60S large subunit of ribosomal protein L27.e -- slow grow, petite,no growth on drop-in media, super slow growth on -met, no growth on -lys, mates like alpha, not like mat a	YKO_0853	A05	0.842	+	+	+	
984	YHR021C	71	A	6	ribosomal protein S27.e -- growth on -met, growth on -lys	YKO_0853	A06	0.748	+	+	+	
1515	YLL027W	71	A	7	Similar to H. influenzae & E. coli hypothetical proteins. Mutant is a new lysine auxotroph. -- slow grow, petite, no growth on drop-in media,grows on -met, no growth on -lys	YKO_0853	A07	0.846	slow	-	-	Doubt
4175	YLR226W	71	A	8	Hypothetical protein -- slow growth	YKO_0853	A08	0.512	+	+	-	HIT
1666	YOR369C	71	A	9	40S small subunit of ribosomal protein S12 -- grows on -met, grows on -lys, mates with alpha, papillation on mat a	YKO_0853	A09	0.847	+	+	+	
7280	YFL016C	71	A	10	slow, petite	YKO_0853	A10	0.694	slow	+	-	Doubt
7288	YGR257C	71	A	11	petite	YKO_0853	A11	0.802	slow	+	-	Doubt
7374	YNL055C	71	A	12		YKO_0853	A12	0.65	+	+	+	
7347	YDR417C	71	B	1		YKO_0853	B01	0.68	+	+	+	
4797	YGR167W	71	B	2	slow grow	YKO_0853	B02	0.426	slow	-	-	Doubt
3415	YCL007C	71	B	3	slow grow	YKO_0853	B03	0.43	slow	-	-	Doubt
4105	YLR148W	71	B	4	slow grow	YKO_0853	B04	0.73	+	+	-	HIT
5005	YKL155C	71	B	5	slow grow	YKO_0853	B05	0.881	slow	+	-	Doubt
145	YER014C-A	71	B	6	super slow growth	YKO_0853	B06	not grown	-	-	-	Not grown
210	YER070W	71	B	7	slow grow	YKO_0853	B07	0.917	+	+	+	
277	YEL036C	71	B	8	slow grow	YKO_0853	B08	0.843	slow	+	-	Doubt
1147	YNL296W	71	B	9	slow grow	YKO_0853	B09	0.876	+	+	+	
4072	YDR138W	71	B	10	Hyperrecombination protein related to Top1p -- grows -met, grows -lys, mates poorly	YKO_0853	B10	0.908	+	+	+	
7406	YPR133W-A	71	B	11	slow grow	YKO_0853	B11	0.786	+	+	+	
4397	YGL029W	71	B	12	slow grow	YKO_0853	B12	1.049	+	+	+	
3119	YBL093C	71	C	1	slow growth	YKO_0853	C01	not grown	-	-	-	Not grown
3026	YBL002W	71	C	2	slow growth	YKO_0853	C02	0.843	+	+	-	HIT
5546	YPR131C	71	C	3	slow grow	YKO_0853	C03	0.424	+	+	+	
7005	YJL140W	71	C	4	super slow growth	YKO_0853	C04	not grown	-	-	-	Not grown
7161	YBR112C	71	C	5	super slow growth	YKO_0853	C05	not grown	-	-	-	Not grown
7102	YKR085C	71	C	6	slow growth, petite	YKO_0853	C06	0.892	+	+	+	
7284	YGR162W	71	C	7	slow growth	YKO_0853	C07	0.869	+	+	+	
7291	YGR272C	71	C	8	super slow growth,slow growth on drop-in media, slow growth on -lys OK	YKO_0853	C08	0.619	slow	+	+	
7263	YDR500C	71	C	9	slow grow	YKO_0853	C09	0.939	+	+	+	
7266	YDR512C	71	C	10	slow grow	YKO_0853	C10	0.972	slow	+	-	Doubt
7285	YGR252W	71	C	11	slow grow	YKO_0853	C11	0.557	slow	+	+	
7287	YGR255C	71	C	12	slow grow	YKO_0853	C12	1.014	slow	+	-	Doubt
7375	YNL059C	71	D	1	super slow growth	YKO_0853	D01	0.583	+	+	+	
7376	YNL069C	71	D	2	slow grow	YKO_0853	D02	0.902	+	+	+	
7383	YNL147W	71	D	3	slow grow	YKO_0853	D03	0.785	+	+	+	
7384	YNL220W	71	D	4	super slow growth, no growth on drop-in media, ade mutant?? Colony is red	YKO_0853	D04	0.685	+	-	-	Doubt
7386	YNL284C	71	D	5	slow growth, petite	YKO_0853	D05	0.955	+	+	-	HIT
7387	YNL315C	71	D	6	slow growth, petite	YKO_0853	D06	0.855	+	+	-	HIT
7395	YPL183W	71	D	7	grows -met, grows -lys, mates with alpha, papillation with mat a	YKO_0853	D07	0.946	+	+	+	
2403	YOR147W	71	D	8	slow growth	YKO_0853	D08	0.989	+	+	+	
1152	YNL292W	71	D	9		YKO_0853	D09	0.959	+	+	+	
849	YMR263W	71	D	10		YKO_0853	D10	0.957	+	+	+	
1137	YNL307C	71	D	11		YKO_0853	D11	0.934	+	+	+	
1167	YNL277W	71	D	12		YKO_0853	D12	1.011	+	+	+	
7441	YAL016C-B	72	A	1		YKO_0854	A01	0.921	+	+	+	
7442	YAL037C-A	72	A	2		YKO_0854	A02	0.996	+	+	+	
7443	YAL067W-A	72	A	3		YKO_0854	A03	1.015	+	+	+	
7444	YAR035C-A	72	A	4		YKO_0854	A04	1.026	+	+	+	
7445	YBL008W-A	72	A	5		YKO_0854	A05	0.993	+	+	+	
7446	YBL029C-A	72	A	6		YKO_0854	A06	0.998	+	+	+	
7447	YBL039W-A	72	A	7		YKO_0854	A07	0.909	+	+	+	
7448	YBL071C-B	72	A	8		YKO_0854	A08	0.82	+	+	+	

Euroscarf Information						Replica plate Information			Tau Toxicity Enhancer Primary Screen Results			
record no.	ORF name	Plate	Row	Col	Comment	Replica plate	Well	YPD (OD600nm)	Growth plate (SC+GAL comp.)	Transformation control plate (SC+GLU-Leu)	TEST Plate (SC+GAL-Leu)	Classification
7449	YBL071W-A	72	A	9		YKO_0854	A09	0.747	+	+	+	
7450	YBL101W-C	72	A	10		YKO_0854	A10	1.019	+	+	+	
7451	YBR056W-A	72	A	11		YKO_0854	A11	0.984	+	+	+	
7452	YBR058C-A	72	A	12		YKO_0854	A12	0.88	+	+	+	
7453	YBR072C-A	72	B	1		YKO_0854	B01	0.941	+	+	+	
7454	YBR085C-A	72	B	2		YKO_0854	B02	1.037	+	+	+	
7455	YBR111W-A	72	B	3		YKO_0854	B03	0.409	slow	+	+	
7456	YBR182C-A	72	B	4		YKO_0854	B04	1.009	+	+	+	
7457	YBR196C-A	72	B	5		YKO_0854	B05	0.692	slow	+	+	
7458	YBR196C-B	72	B	6		YKO_0854	B06	0.963	slow	+	+	
7459	YBR200W-A	72	B	7		YKO_0854	B07	0.995	+	+	+	
7460	YBR221W-A	72	B	8		YKO_0854	B08	0.944	+	+	+	
--		72	B	9	empty	YKO_0854	B09	empty	empty	empty	empty	empty
7462	YBR296C-A	72	B	10		YKO_0854	B10	0.914	+	+	+	
7463	YCL001W-B	72	B	11		YKO_0854	B11	0.92	+	+	+	
7464	YCL057C-A	72	B	12		YKO_0854	B12	0.997	+	+	+	
--		72	C	1	empty	YKO_0854	C01	empty	empty	empty	empty	empty
7466	YCR075W-A	72	C	2		YKO_0854	C02	0.559	+	+	+	
7467	YDL085C-A	72	C	3		YKO_0854	C03	1.049	+	+	+	
7468	YDL159W-A	72	C	4		YKO_0854	C04	1.074	+	+	+	
7469	YDL160C-A	72	C	5		YKO_0854	C05	1.007	+	+	+	
7470	YDR003W-A	72	C	6		YKO_0854	C06	1.033	+	+	+	
--		72	C	7	empty	YKO_0854	C07	empty	empty	empty	empty	empty
7472	YDR034W-B	72	C	8		YKO_0854	C08	0.88	+	+	+	
7473	YDR079C-A	72	C	9		YKO_0854	C09	not grow n	-	-	-	Not grow n
7474	YDR169C-A	72	C	10		YKO_0854	C10	0.976	+	+	+	
7475	YDR182W-A	72	C	11		YKO_0854	C11	0.931	+	+	+	
7476	YDR194W-A	72	C	12		YKO_0854	C12	1.031	+	+	+	
7477	YDR246W-A	72	D	1		YKO_0854	D01	1.055	+	+	+	
--		72	D	2	empty	YKO_0854	D02	empty	empty	empty	empty	empty
7479	YDR322C-A	72	D	3		YKO_0854	D03	1.014	+	+	+	
7480	YDR379C-A	72	D	4		YKO_0854	D04	1.025	+	+	+	
7481	YDR524C-B	72	D	5		YKO_0854	D05	1.034	+	+	+	
7482	YDR524W-A	72	D	6		YKO_0854	D06	0.961	+	+	+	
--		72	D	7	empty	YKO_0854	D07	empty	empty	empty	empty	empty
7484	YEL059C-A	72	D	8		YKO_0854	D08	0.929	slow	+	-	Doubt
7485	YER053C-A	72	D	9		YKO_0854	D09	0.897	+	+	+	
--		72	D	10	empty	YKO_0854	D10	empty	empty	empty	empty	empty
--		72	D	11	empty	YKO_0854	D11	empty	empty	empty	empty	empty
7488	YER087C-B	72	D	12		YKO_0854	D12	0.994	+	+	+	
7489	YER175W-A	72	E	1		YKO_0854	E01	1.016	+	+	+	
7490	YER180C-A	72	E	2		YKO_0854	E02	1.002	+	+	+	
--		72	E	3	empty	YKO_0854	E03	empty	empty	empty	empty	empty
7492	YFL041W-A	72	E	4		YKO_0854	E04	0.968	+	+	+	
7493	YFR012W-A	72	E	5		YKO_0854	E05	1.039	+	+	+	
7494	YFR032C-B	72	E	6		YKO_0854	E06	0.953	+	+	+	
7495	YGL006W-A	72	E	7		YKO_0854	E07	0.983	+	+	+	
7496	YGL007C-A	72	E	8		YKO_0854	E08	0.99	+	+	+	
7497	YGL041C-B	72	E	9		YKO_0854	E09	0.922	slow	+	+	
7498	YGL188C-A	72	E	10		YKO_0854	E10	0.9	slow	+	+	
--		72	E	11	empty	YKO_0854	E11	empty	empty	empty	empty	empty
7500	YGR035W-A	72	E	12		YKO_0854	E12	0.983	+	+	+	
7501	YGR121W-A	72	F	1		YKO_0854	F01	1.01	+	+	+	
7502	YGR146C-A	72	F	2		YKO_0854	F02	1.004	+	+	+	
7503	YGR169C-A	72	F	3		YKO_0854	F03	0.905	+	+	+	
7504	YGR174W-A	72	F	4		YKO_0854	F04	1.001	+	+	+	
7505	YGR204C-A	72	F	5		YKO_0854	F05	1.003	+	+	+	
--		72	F	6	empty	YKO_0854	F06	empty	empty	empty	empty	empty
7507	YGR271C-A	72	F	7		YKO_0854	F07	0.56	+	+	+	
7508	YHL015W-A	72	F	8		YKO_0854	F08	0.959	+	+	+	
7509	YHR007C-A	72	F	9		YKO_0854	F09	0.95	+	+	+	
7510	YHR022C-A	72	F	10		YKO_0854	F10	0.836	+	+	+	
7511	YHR050W-A	72	F	11		YKO_0854	F11	0.907	+	+	+	
--		72	F	12	empty	YKO_0854	F12	empty	empty	empty	empty	empty
7513	YHR086W-A	72	G	1		YKO_0854	G01	1.051	+	+	+	
7514	YHR175W-A	72	G	2		YKO_0854	G02	0.887	slow	+	-	Doubt
7515	YIL002W-A	72	G	3		YKO_0854	G03	1.006	+	+	+	
7516	YIL046W-A	72	G	4		YKO_0854	G04	0.979	+	+	+	
7517	YIL134C-A	72	G	5		YKO_0854	G05	0.999	+	+	+	
7518	YIR018C-A	72	G	6		YKO_0854	G06	0.976	+	+	+	
7519	YIR021W-A	72	G	7		YKO_0854	G07	0.968	+	+	+	
7520	YJL012C-A	72	G	8		YKO_0854	G08	1.024	+	+	+	
7521	YJL047C-A	72	G	9		YKO_0854	G09	0.982	+	+	+	
7522	YJL062W-A	72	G	10		YKO_0854	G10	0.843	slow	+	-	Doubt
7523	YJL077W-B	72	G	11		YKO_0854	G11	0.966	+	+	+	
7524	YJL127C-B	72	G	12		YKO_0854	G12	0.943	+	+	+	
--		72	H	1	empty	YKO_0854	H01	empty	empty	empty	empty	empty
7526	YJL136W-A	72	H	2		YKO_0854	H02	1.025	+	+	+	
--		72	H	3	empty	YKO_0854	H03	empty	empty	empty	empty	empty
7528	YJR005C-A	72	H	4		YKO_0854	H04	0.977	+	+	+	
7529	YJR135W-A	72	H	5		YKO_0854	H05	1.009	+	+	+	
7530	YJR151W-A	72	H	6		YKO_0854	H06	0.874	+	+	+	
7531	YKL018C-A	72	H	7		YKO_0854	H07	0.971	+	+	+	
7532	YKL068W-A	72	H	8		YKO_0854	H08	0.947	+	+	+	

	Euroscarf Information					Replica plate Information			Tau Toxicity Enhancer Primary Screen Results			
record no.	ORF name	Plate	Row	Col	Comment	Replica plate	Well	YPD (OD600nm)	Growth plate (SC+GAL comp.)	Transformation control plate (SC+GLU-Leu)	TEST Plate (SC+GAL-Leu)	Classification
7533	YKL096C-B	72	H	9		YKO_0854	H09	0.606	+	+	+	
7534	YKL106C-A	72	H	10		YKO_0854	H10	0.955	+	+	+	
--		72	H	11	empty	YKO_0854	H11	empty	empty	empty	empty	empty
--		72	H	12	empty	YKO_0854	H12	empty	empty	empty	empty	empty
7537	YAL021C	73	A	1		YKO_0855	A01	0.436	+	+	+	
7538	YAL044W-A	73	A	2		YKO_0855	A02	0.83	+	+	+	
7539	YBR133C	73	A	3		YKO_0855	A03	0.894	+	+	+	
7541	YCL021W-A	73	A	4		YKO_0855	A04	0.945	+	+	+	
7542	YCL026C-B	73	A	5		YKO_0855	A05	0.994	+	+	+	
7544	YER007W	73	A	6		YKO_0855	A06	0.995	+	+	+	
7545	YER016W	73	A	7		YKO_0855	A07	0.86	+	+	+	
7546	YER099C	73	A	8		YKO_0855	A08	1.027	+	+	+	
7547	YER105C	73	A	9		YKO_0855	A09	0.996	+	+	+	
7548	YER155C	73	A	10		YKO_0855	A10	0.893	+	+	+	
7549	YER186W-A	73	A	11		YKO_0855	A11	0.983	+	+	+	
7551	YGL100W	73	A	12		YKO_0855	A12	1.009	+	+	+	
7552	YGL119W	73	B	1		YKO_0855	B01	0.777	slow	+	-	Doubt
7553	YGL134W	73	B	2		YKO_0855	B02	1.004	+	+	+	
7554	YGL178W	73	B	3		YKO_0855	B03	0.879	+	+	+	
7556	YGL184C	73	B	4		YKO_0855	B04	0.837	+	+	+	
7557	YGL185C	73	B	5		YKO_0855	B05	1.035	+	+	+	
7558	YGL190C	73	B	6		YKO_0855	B06	0.914	+	+	+	
7559	YGL191W	73	B	7		YKO_0855	B07	1.015	+	+	+	
7560	YGL192W	73	B	8		YKO_0855	B08	0.977	+	+	+	
7561	YGL216W	73	B	9		YKO_0855	B09	0.849	+	+	+	
7562	YGR180C	73	B	10		YKO_0855	B10	not grow n	-	-	-	Not grow n
7563	YHR091C	73	B	11		YKO_0855	B11	0.926	+	+	+	
7565	YKR004C-A	73	B	12		YKO_0855	B12	0.863	+	+	+	
7567	YKR099C-A	73	C	1		YKO_0855	C01	0.962	+	+	+	
7568	YLL006W-A	73	C	2		YKO_0855	C02	1.035	+	+	+	
7570	YLR264C-A	73	C	3		YKO_0855	C03	1.012	+	+	+	
--		73	C	4	empty	YKO_0855	C04	empty	empty	empty	empty	empty
7571	YLR285C-A	73	C	5		YKO_0855	C05	0.939	+	+	+	
7572	YLR307C-A	73	C	6		YKO_0855	C06	1.003	+	+	+	
7573	YLR312C-B	73	C	7		YKO_0855	C07	0.993	+	+	+	
7574	YLR342W-A	73	C	8		YKO_0855	C08	1.002	+	+	+	
7575	YLR361C-A	73	C	9		YKO_0855	C09	1.051	+	+	+	
7576	YLR363W-A	73	C	10		YKO_0855	C10	0.895	+	+	+	
7577	YLR406C-A	73	C	11		YKO_0855	C11	0.959	+	+	+	
7578	YLR412C-A	73	C	12		YKO_0855	C12	0.994	+	+	+	
7579	YML007C-A	73	D	1		YKO_0855	D01	0.616	+	+	+	
7580	YML054C-A	73	D	2		YKO_0855	D02	0.968	+	+	+	
7581	YML058W-A	73	D	3		YKO_0855	D03	0.999	+	+	+	
7582	YMR001C-A	73	D	4		YKO_0855	D04	1.008	+	+	+	
7583	YMR013W-A	73	D	5		YKO_0855	D05	1.009	+	+	+	
7585	YMR105W-A	73	D	6		YKO_0855	D06	0.99	+	+	+	
7587	YMR175W-A	73	D	7		YKO_0855	D07	1.002	+	+	+	
7588	YMR182W-A	73	D	8		YKO_0855	D08	0.994	+	+	+	
7589	YMR194C-B	73	D	9		YKO_0855	D09	1.021	+	+	+	
7590	YMR230W-A	73	D	10		YKO_0855	D10	0.902	+	+	+	
7591	YMR242W-A	73	D	11		YKO_0855	D11	0.951	+	+	+	
7592	YMR247W-A	73	D	12		YKO_0855	D12	0.925	+	+	+	
7593	YMR272W-B	73	E	1		YKO_0855	E01	1.014	+	+	+	
7594	YMR315W-A	73	E	2		YKO_0855	E02	0.999	+	+	+	
7596	YNL042W-B	73	E	3		YKO_0855	E03	0.973	+	+	+	
7597	YNL067W-B	73	E	4		YKO_0855	E04	1.031	+	+	+	
7598	YNL097C-A	73	E	5		YKO_0855	E05	1.08	+	+	+	
7599	YNL130C-A	73	E	6		YKO_0855	E06	1.003	+	+	+	
7601	YNL146C-A	73	E	7		YKO_0855	E07	0.949	+	+	+	
7602	YNL162W-A	73	E	8		YKO_0855	E08	1.014	+	+	+	
7603	YNL277W-A	73	E	9		YKO_0855	E09	0.929	+	+	+	
7605	YOL013W-B	73	E	10		YKO_0855	E10	0.952	+	+	+	
7606	YOL019W-A	73	E	11		YKO_0855	E11	0.926	+	+	+	
7607	YOL038C-A	73	E	12		YKO_0855	E12	0.964	+	+	+	
7608	YOL052C-A	73	F	1		YKO_0855	F01	0.891	+	+	+	
7609	YOL077W-A	73	F	2		YKO_0855	F02	0.936	+	+	+	
7610	YOL086W-A	73	F	3		YKO_0855	F03	0.988	+	+	+	
7611	YOL097W-A	73	F	4		YKO_0855	F04	0.953	+	+	+	
7612	YOL159C-A	73	F	5		YKO_0855	F05	1.019	+	+	+	
7613	YOL164W-A	73	F	6		YKO_0855	F06	0.951	+	+	+	
7616	YOR020W-A	73	F	7		YKO_0855	F07	0.964	+	+	+	
7618	YOR034C-A	73	F	8		YKO_0855	F08	0.783	+	+	+	
7620	YOR161C-C	73	F	9		YKO_0855	F09	0.92	+	+	+	
7621	YOR293C-A	73	F	10		YKO_0855	F10	0.866	+	+	+	
7622	YOR316C-A	73	F	11		YKO_0855	F11	0.9	+	+	+	
7623	YOR376W-A	73	F	12		YKO_0855	F12	0.911	+	+	+	
7625	YPL038W-A	73	G	1		YKO_0855	G01	0.922	+	+	+	
7626	YPL096C-A	73	G	2		YKO_0855	G02	0.935	+	+	+	
7627	YPL119C-A	73	G	3		YKO_0855	G03	0.938	+	+	+	
7628	YPL152W-A	73	G	4		YKO_0855	G04	0.93	+	+	+	
7629	YPL189C-A	73	G	5		YKO_0855	G05	0.953	+	+	+	
7631	YPR108W-A	73	G	6		YKO_0855	G06	0.959	+	+	+	
7632	YPR159C-A	73	G	7		YKO_0855	G07	0.928	+	+	+	
7633	YAR042W	74	A	1		YKO_0856	A01	0.858	+	+	+	

	Euroscarf Information					Replica plate Information			Tau Toxicity Enhancer Primary Screen Results			
record no.	ORF name	Plate	Row	Col	Comment	Replica plate	Well	YPD (OD600nm)	Growth plate (SC+GAL comp.)	Transformation control plate (SC+GLU-Leu)	TEST Plate (SC+GAL-Leu)	Classification
7634	YBL091C-A	74	A	2		YKO_0856	A02	0.943	+	+	+	
7635	YBL104C	74	A	3		YKO_0856	A03	0.909	+	+	+	
7636	YBR074W	74	A	4		YKO_0856	A04	0.93	+	+	+	
7637	YBR098W	74	A	5		YKO_0856	A05	0.915	+	+	+	
7638	YBR122C	74	A	6		YKO_0856	A06	0.568	slow	+	-	Doubt
7639	YBR157C	74	A	7		YKO_0856	A07	0.941	+	+	+	
7640	YBR201W	74	A	8		YKO_0856	A08	0.942	+	+	+	
7641	YBR230W-A	74	A	9		YKO_0856	A09	1.021	+	+	+	
7642	YCL002C	74	A	10		YKO_0856	A10	0.92	+	+	+	
--		74	A	11	empty	YKO_0856	A11	empty	empty	empty	empty	empty
7644	YCL012C	74	A	12		YKO_0856	A12	0.951	+	+	+	
7645	YCL014W	74	B	1		YKO_0856	B01	0.833	+	+	+	
7646	YCL061C	74	B	2		YKO_0856	B02	0.851	+	+	+	
7647	YCR061W	74	B	3		YKO_0856	B03	0.987	+	+	+	
7648	YDR318W	74	B	4		YKO_0856	B04	0.881	+	+	+	
7649	YDR475C	74	B	5		YKO_0856	B05	0.419	+	-	-	Doubt
7650	YER109C	74	B	6		YKO_0856	B06	0.951	+	+	+	
--		74	B	7	empty	YKO_0856	B07	empty	empty	empty	empty	empty
7652	YFL031W	74	B	8		YKO_0856	B08	0.968	+	+	+	
7653	YFL042C	74	B	9		YKO_0856	B09	0.925	+	+	+	
7654	YFR045W	74	B	10		YKO_0856	B10	0.993	+	+	+	
7655	YGL033W	74	B	11		YKO_0856	B11	1.001	+	+	+	
7656	YGL045W	74	B	12		YKO_0856	B12	1.028	+	+	+	
7657	YGL186C	74	C	1		YKO_0856	C01	0.698	+	+	+	
--		74	C	2	empty	YKO_0856	C02	empty	empty	empty	empty	empty
7659	YGR225W	74	C	3		YKO_0856	C03	1.029	+	+	+	
--		74	C	4	empty	YKO_0856	C04	empty	empty	empty	empty	empty
--		74	C	5	empty	YKO_0856	C05	empty	empty	empty	empty	empty
--		74	C	6	empty	YKO_0856	C06	empty	empty	empty	empty	empty
--		74	C	7	empty	YKO_0856	C07	empty	empty	empty	empty	empty
7664	YJL012C	74	C	8		YKO_0856	C08	1.028	+	+	+	
7665	YJL016W	74	C	9		YKO_0856	C09	0.907	+	+	+	
--		74	C	10	empty	YKO_0856	C10	empty	empty	empty	empty	empty
7667	YJL020C	74	C	11		YKO_0856	C11	0.944	+	+	+	
7668	YJL088W	74	C	12		YKO_0856	C12	1.019	+	+	+	
7669	YJL096W	74	D	1		YKO_0856	D01	1	slow	+	-	Doubt
7670	YJL160C	74	D	2		YKO_0856	D02	0.994	+	+	+	
7671	YJR060W	74	D	3		YKO_0856	D03	0.875	slow	+	-	Doubt
7672	YJR085C	74	D	4		YKO_0856	D04	1.018	+	+	+	
7673	YJR086W	74	D	5		YKO_0856	D05	0.997	+	+	+	
--		74	D	6	empty	YKO_0856	D06	empty	empty	empty	empty	empty
7675	YJR101W	74	D	7		YKO_0856	D07	0.928	+	+	-	HIT
7676	YJR112W-A	74	D	8		YKO_0856	D08	0.961	+	+	+	
7677	YJR114W	74	D	9		YKO_0856	D09	0.663	slow	+	-	Doubt
7678	YJR143C	74	D	10		YKO_0856	D10	0.925	+	+	+	
7679	YJR151C	74	D	11		YKO_0856	D11	0.979	+	+	+	
7680	YKL002W	74	D	12		YKO_0856	D12	0.617	+	+	+	
7681	YKL033W-A	74	E	1		YKO_0856	E01	0.955	+	+	+	
--		74	E	2	empty	YKO_0856	E02	empty	empty	empty	empty	empty
7683	YKL157W	74	E	3		YKO_0856	E03	0.988	+	+	+	
7684	YKL198C	74	E	4		YKO_0856	E04	0.972	+	+	+	
7685	YKL201C	74	E	5		YKO_0856	E05	1.01	+	+	+	
--		74	E	6	empty	YKO_0856	E06	empty	empty	empty	empty	empty
7687	YKR054C	74	E	7		YKO_0856	E07	0.756	+	+	+	
7688	YKR100C	74	E	8		YKO_0856	E08	0.957	+	+	+	
7689	YLR054C	74	E	9		YKO_0856	E09	0.964	+	+	+	
7690	YLR194C	74	E	10		YKO_0856	E10	0.876	slow	+	-	Doubt
7691	YLR211C	74	E	11		YKO_0856	E11	0.957	+	+	+	
--		74	E	12	empty	YKO_0856	E12	empty	empty	empty	empty	empty
7693	YLR371W	74	F	1		YKO_0856	F01	0.726	+	+	+	
--		74	F	2	empty	YKO_0856	F02	empty	empty	empty	empty	empty
7695	YLR419W	74	F	3		YKO_0856	F03	0.965	+	+	+	
7696	YLR445W	74	F	4		YKO_0856	F04	0.991	+	+	+	
7697	YML034W	74	F	5		YKO_0856	F05	1.018	+	+	+	
7698	YML104C	74	F	6		YKO_0856	F06	0.882	+	+	+	
7699	YMR143W	74	F	7		YKO_0856	F07	0.797	slow	+	+	
7700	YMR202W	74	F	8		YKO_0856	F08	not grow n	-	-	-	Not grow n
--		74	F	9	empty	YKO_0856	F09	empty	empty	empty	empty	empty
7702	YMR269W	74	F	10		YKO_0856	F10	0.944	+	+	+	
--		74	F	11	empty	YKO_0856	F11	empty	empty	empty	empty	empty
7704	YNL090W	74	F	12		YKO_0856	F12	0.957	+	+	+	
7705	YNL147W	74	G	1		YKO_0856	G01	0.741	+	+	+	
7706	YNL209W	74	G	2		YKO_0856	G02	0.947	+	+	+	
7707	YNL280C	74	G	3		YKO_0856	G03	not grow n	-	-	-	Not grow n
--		74	G	4	empty	YKO_0856	G04	empty	empty	empty	empty	empty
7709	YNR052C	74	G	5		YKO_0856	G05	0.533	+	+	+	
7710	YOL048C	74	G	6		YKO_0856	G06	0.58	+	+	+	
7711	YOL140W	74	G	7		YKO_0856	G07	0.921	+	+	+	
--		74	G	8	empty	YKO_0856	G08	empty	empty	empty	empty	empty
7713	YOL145C	74	G	9		YKO_0856	G09	not grow n	-	-	-	Not grow n
7714	YOL154W	74	G	10		YKO_0856	G10	0.934	+	+	+	
7715	YOL164W	74	G	11		YKO_0856	G11	0.897	+	+	+	
7716	YOR026W	74	G	12		YKO_0856	G12	0.818	+	+	+	
7717	YOR069W	74	H	1		YKO_0856	H01	0.741	+	+	+	

	Euroscarf Information					Replica plate Information			Tau Toxicity Enhancer Primary Screen Results			
record no.	ORF name	Plate	Row	Col	Comment	Replica plate	Well	YPD (OD600nm)	Growth plate (SC+GAL comp.)	Transformation control plate (SC+GLU-Leu)	TEST Plate (SC+GAL-Leu)	Classification
7718	YOR087W	74	H	2		YKO_0856	H02	0.986	+	+	+	
7719	YOR239W	74	H	3		YKO_0856	H03	0.921	+	+	+	
--		74	H	4	empty	YKO_0856	H04	empty	empty	empty	empty	empty
7721	YOR298C-A	74	H	5		YKO_0856	H05	1.037	+	+	+	
7722	YPL075W	74	H	6		YKO_0856	H06	not grow n	-	-	-	Not grow n
7723	YPL165C	74	H	7		YKO_0856	H07	0.953	+	+	+	
7724	YPL249C-A	74	H	8		YKO_0856	H08	0.875	slow	+	+	
7725	YPL277C	74	H	9		YKO_0856	H09	0.923	+	+	+	
7726	YPR089W	74	H	10		YKO_0856	H10	0.959	+	+	+	
7727	YPR098C	74	H	11		YKO_0856	H11	0.88	+	+	+	
7728	YPR141C	74	H	12		YKO_0856	H12	0.903	+	+	+	
7729	YAL049C	75	A	1		YKO_0857	A01	0.927	+	+	+	
7730	YBR062C	75	A	2		YKO_0857	A02	0.954	+	+	+	
7731	YBR105C	75	A	3		YKO_0857	A03	0.935	+	+	+	
--		75	A	4	empty	YKO_0857	A04	empty	empty	empty	empty	empty
--		75	A	5	empty	YKO_0857	A05	empty	empty	empty	empty	empty
7734	YBR274W	75	A	6		YKO_0857	A06	0.972	+	+	+	
7735	YCL005W-A	75	A	7		YKO_0857	A07	not grow n	-	-	-	Not grow n
--		75	A	8	empty	YKO_0857	A08	empty	empty	empty	empty	empty
7737	YCR061W	75	A	9		YKO_0857	A09	1.004	+	+	+	
7738	YCR095W-A	75	A	10		YKO_0857	A10	0.93	+	+	+	
7739	YDL026W	75	A	11		YKO_0857	A11	0.945	+	+	+	
7740	YDL036C	75	A	12		YKO_0857	A12	0.959	+	+	+	
7741	YDL069C	75	B	1		YKO_0857	B01	0.917	slow	+	-	Doubt
7742	YDL077C	75	B	2		YKO_0857	B02	0.751	+	+	+	
7743	YDR090C	75	B	3		YKO_0857	B03	0.948	+	+	+	
7744	YDR092W	75	B	4		YKO_0857	B04	0.88	+	+	+	
7745	YDR147W	75	B	5		YKO_0857	B05	0.81	+	+	+	
7746	YDR179W-A	75	B	6		YKO_0857	B06	0.902	+	+	+	
7747	YDR315C	75	B	7		YKO_0857	B07	0.834	+	+	+	
7748	YDR433W	75	B	8		YKO_0857	B08	0.575	slow	+	-	Doubt
7749	YDR448W	75	B	9		YKO_0857	B09	0.917	+	+	+	
7750	YDR485C	75	B	10		YKO_0857	B10	0.868	+	+	+	
7751	YDR501W	75	B	11		YKO_0857	B11	0.947	+	+	+	
7752	YDR518W	75	B	12		YKO_0857	B12	0.949	+	+	+	
7753	YEL022W	75	C	1		YKO_0857	C01	0.991	+	+	+	
7754	YEL041W	75	C	2		YKO_0857	C02	1.025	+	+	+	
7755	YER015W	75	C	3		YKO_0857	C03	0.987	+	+	+	
7756	YER026C	75	C	4		YKO_0857	C04	1.055	slow	-	-	Doubt
--		75	C	5	empty	YKO_0857	C05	empty	empty	empty	empty	empty
7758	YER076C	75	C	6		YKO_0857	C06	0.936	+	+	+	
7759	YFL010W-A	75	C	7		YKO_0857	C07	0.969	+	+	+	
7760	YFR038W	75	C	8		YKO_0857	C08	0.98	+	+	+	
7761	YGL023C	75	C	9		YKO_0857	C09	0.677	+	+	+	
7762	YGL032C	75	C	10		YKO_0857	C10	1.002	+	+	+	
--		75	C	11	empty	YKO_0857	C11	empty	empty	empty	empty	empty
7764	YGL081W	75	C	12		YKO_0857	C12	0.974	+	+	+	
7765	YGL101W	75	D	1		YKO_0857	D01	0.862	+	+	+	
7766	YGL104C	75	D	2		YKO_0857	D02	0.939	+	+	+	
--		75	D	3	empty	YKO_0857	D03	empty	empty	empty	empty	empty
7768	YGL196W	75	D	4		YKO_0857	D04	0.968	+	+	+	
7769	YGL202W	75	D	5		YKO_0857	D05	0.97	+	+	+	
7770	YGL211W	75	D	6		YKO_0857	D06	0.945	+	+	+	
7771	YGL224C	75	D	7		YKO_0857	D07	0.949	+	+	+	
--		75	D	8	empty	YKO_0857	D08	empty	empty	empty	empty	empty
7773	YGL237C	75	D	9		YKO_0857	D09	0.899	+	+	+	
7774	YGR037C	75	D	10		YKO_0857	D10	0.881	+	+	+	
7775	YGR062C	75	D	11		YKO_0857	D11	0.932	+	+	+	
7776	YGR161W-C	75	D	12		YKO_0857	D12	0.915	+	+	+	
7777	YGR244C	75	E	1		YKO_0857	E01	0.99	+	+	+	
7778	YHL001W	75	E	2		YKO_0857	E02	0.996	+	+	+	
7779	YHL004W	75	E	3		YKO_0857	E03	0.771	+	+	-	HIT
7780	YHR001W	75	E	4		YKO_0857	E04	0.942	+	+	+	
--		75	E	5	empty	YKO_0857	E05	empty	empty	empty	empty	empty
7782	YHR063C	75	E	6		YKO_0857	E06	0.929	+	+	+	
7783	YHR071W	75	E	7		YKO_0857	E07	0.977	+	+	+	
--		75	E	8	empty	YKO_0857	E08	empty	empty	empty	empty	empty
--		75	E	9	empty	YKO_0857	E09	empty	empty	empty	empty	empty
7786	YHR090C	75	E	10		YKO_0857	E10	0.846	+	+	+	
7787	YHR098C	75	E	11		YKO_0857	E11	0.967	+	+	+	
--		75	E	12	empty	YKO_0857	E12	empty	empty	empty	empty	empty
7789	YHR141C	75	F	1		YKO_0857	F01	0.607	+	+	+	
7790	YHR149C	75	F	2		YKO_0857	F02	0.919	+	+	+	
--		75	F	3	empty	YKO_0857	F03	empty	empty	empty	empty	empty
--		75	F	4	empty	YKO_0857	F04	empty	empty	empty	empty	empty
7793	YHR187W	75	F	5		YKO_0857	F05	0.854	+	+	+	
7794	YHR192W	75	F	6		YKO_0857	F06	0.871	+	+	+	
--		75	F	7	empty	YKO_0857	F07	empty	empty	empty	empty	empty
--		75	F	8	empty	YKO_0857	F08	empty	empty	empty	empty	empty
7797	YHR205W	75	F	9		YKO_0857	F09	0.615	+	+	+	
--		75	F	10	empty	YKO_0857	F10	empty	empty	empty	empty	empty
7799	YIL041W	75	F	11		YKO_0857	F11	0.888	+	+	+	
7800	YIL127C	75	F	12		YKO_0857	F12	0.906	+	+	+	
--		75	G	1	empty	YKO_0857	G01	empty	empty	empty	empty	empty

Euroscarf Information						Replica plate Information			Tau Toxicity Enhancer Primary Screen Results			
record no.	ORF name	Plate	Row	Col	Comment	Replica plate	Well	YPD (OD600nm)	Growth plate (SC+GAL comp.)	Transformation control plate (SC+GLU-Leu)	TEST Plate (SC+GAL-Leu)	Classification
7802	YJL059W	75	G	2		YKO_0857	G02	0.995	+	+	+	
--		75	G	3	empty	YKO_0857	G03	empty	empty	empty	empty	empty
7804	YKL065C	75	G	4		YKO_0857	G04	0.964	+	+	+	
7805	YKL137W	75	G	5		YKO_0857	G05	0.995	+	+	+	
--		75	G	6	empty	YKO_0857	G06	empty	empty	empty	empty	empty
7807	YKR091W	75	G	7		YKO_0857	G07	0.931	+	+	+	
7808	YLR084C	75	G	8		YKO_0857	G08	0.885	+	+	+	
7809	YLR118C	75	G	9		YKO_0857	G09	0.941	+	+	+	
7810	YLR125W	75	G	10		YKO_0857	G10	0.816	+	+	+	
--		75	G	11	empty	YKO_0857	G11	empty	empty	empty	empty	empty
7812	YLR251W	75	G	12		YKO_0857	G12	0.871	+	+	+	
7813	YLR329W	75	H	1		YKO_0857	H01	0.969	+	+	+	
7814	YLR332W	75	H	2		YKO_0857	H02	0.926	+	+	+	
--		75	H	3	empty	YKO_0857	H03	empty	empty	empty	empty	empty
--		75	H	4	empty	YKO_0857	H04	empty	empty	empty	empty	empty
7817	YMR032W	75	H	5		YKO_0857	H05	0.983	+	+	+	
--		75	H	6	empty	YKO_0857	H06	empty	empty	empty	empty	empty
--		75	H	7	empty	YKO_0857	H07	empty	empty	empty	empty	empty
--		75	H	8	empty	YKO_0857	H08	empty	empty	empty	empty	empty
--		75	H	9	empty	YKO_0857	H09	empty	empty	empty	empty	empty
--		75	H	10	empty	YKO_0857	H10	empty	empty	empty	empty	empty
7823	YNL162W	75	H	11		YKO_0857	H11	0.859	+	+	+	
7824	YOL073C	75	H	12		YKO_0857	H12	0.823	+	+	+	

Appendix II

Table II.1. Statistical analysis of *mir1*Δ-tau40 growth inoculated at 0.05 OD_{600} by 2-way ANOVA followed by Tukey's multicomparison test

		mir1Δ-pESC vs. mir1Δ-tau40					mir1Δ-pESC DMSO vs. mir1Δ-tau40 DMSO				
	Time (h)	**Mean Diff.**	**95% CI of diff.**	**Significant?**	**Summary**	**Adjusted P Value**	**Mean Diff.**	**95% CI of diff.**	**Significant?**	**Summary**	**Adjusted P Value**
starting OD600 = 0.05	**0**	-0.002967	-0.05413 to 0.04819	No	ns	0.9988	-0.01273	-0.06389 to 0.03843	No	ns	0.9179
	2.5	-0.00245	-0.05361 to 0.04871	No	ns	0.9993	-0.0067	-0.05786 to 0.04446	No	ns	0.9866
	6	-0.003917	-0.05508 to 0.04724	No	ns	0.9973	-0.008216	-0.05938 to 0.04294	No	ns	0.9759
	21	0.0206	-0.03056 to 0.07176	No	ns	0.7259	0.002684	-0.04848 to 0.05384	No	ns	0.9991
	23	-0.004667	-0.05583 to 0.04649	No	ns	0.9954	0.01423	-0.03693 to 0.06539	No	ns	0.8896
	25	0.02368	-0.02748 to 0.07484	No	ns	0.6299	0.02338	-0.02778 to 0.07454	No	ns	0.6394
	27	-0.01803	-0.06919 to 0.03313	No	ns	0.7992	0.04155	-0.009609 to 0.09271	No	ns	0.156
	29	-0.01443	-0.06559 to 0.03673	No	ns	0.8855	0.005783	-0.04538 to 0.05694	No	ns	0.9913
	31	-0.02563	-0.07679 to 0.02553	No	ns	0.5672	-0.01187	-0.06303 to 0.03929	No	ns	0.9322
	45.5	0.08773	0.03657 to 0.1389	Yes	****	< 0.0001	0.0602	0.009041 to 0.1114	Yes	*	0.0136
	47.5	0.09512	0.04396 to 0.1463	Yes	****	< 0.0001	0.06102	0.009857 to 0.1122	Yes	*	0.012
	49.5	0.1278	0.07666 to 0.1790	Yes	****	< 0.0001	0.07875	0.02759 to 0.1299	Yes	***	0.0005
	51.5	0.1562	0.1050 to 0.2073	Yes	****	< 0.0001	0.08947	0.03831 to 0.1406	Yes	****	< 0.0001
	53.5	0.2263	0.1752 to 0.2775	Yes	****	< 0.0001	0.1111	0.05991 to 0.1622	Yes	****	< 0.0001
	69.5	0.5528	0.5016 to 0.6039	Yes	****	< 0.0001	0.4888	0.4377 to 0.5400	Yes	****	< 0.0001

Table II.2. Statistical analysis of mir1Δ-tau40 growth inoculated at 0.1 OD600 by 2-way ANOVA followed by Tukey's multicomparison test

		mir1Δ-pESC vs. mir1Δ-tau40					mir1Δ-pESC DMSO vs. mir1Δ-tau40 DMSO				
	Time (h)	**Mean Diff.**	**95% CI of diff.**	**Significant?**	**Summary**	**Adjusted P Value**	**Mean Diff.**	**95% CI of diff.**	**Significant?**	**Summary**	**Adjusted P Value**
starting OD600 = 0.1	**0**	0.008833	-0.04664 to 0.06430	No	ns	0.9765	0.004484	-0.05099 to 0.05995	No	ns	0.9968
	2.5	-0.03207	-0.08754 to 0.02340	No	ns	0.4427	-0.02832	-0.08379 to 0.02715	No	ns	0.5516
	6	-0.04257	-0.09804 to 0.01290	No	ns	0.1969	-0.03425	-0.08972 to 0.02122	No	ns	0.3829
	21	0.1194	0.06395 to 0.1749	Yes	****	< 0.0001	0.1253	0.06978 to 0.1807	Yes	****	< 0.0001
	23	0.1538	0.09835 to 0.2093	Yes	****	< 0.0001	0.1581	0.1027 to 0.2136	Yes	****	< 0.0001
	25	0.05913	0.003664 to 0.1146	Yes	*	0.0316	0.05857	0.003097 to 0.1140	Yes	*	0.034
	27	0.1358	0.08035 to 0.1913	Yes	****	< 0.0001	0.1181	0.06261 to 0.1736	Yes	****	< 0.0001
	29	-0.02058	-0.07605 to 0.03489	No	ns	0.773	-0.007383	-0.06285 to 0.04809	No	ns	0.986
	31	0.004567	-0.05090 to 0.06004	No	ns	0.9966	0.02737	-0.02810 to 0.08284	No	ns	0.5798
	45.5	0.2033	0.1479 to 0.2588	Yes	****	< 0.0001	0.1926	0.1371 to 0.2480	Yes	****	< 0.0001
	47.5	0.1042	0.04875 to 0.1597	Yes	****	< 0.0001	0.1115	0.05606 to 0.1670	Yes	****	< 0.0001
	49.5	0.1399	0.08438 to 0.1953	Yes	****	< 0.0001	0.1339	0.07838 to 0.1893	Yes	****	< 0.0001
	51.5	0.1536	0.09813 to 0.2091	Yes	****	< 0.0001	0.164	0.1085 to 0.2194	Yes	****	< 0.0001
	53.5	0.2491	0.1936 to 0.3045	Yes	****	< 0.0001	0.2289	0.1734 to 0.2844	Yes	****	< 0.0001
	69.5	0.4712	0.4157 to 0.5267	Yes	****	< 0.0001	0.5529	0.4974 to 0.6084	Yes	****	< 0.0001

Table II.3. Statistical analysis of mir1Δ-tau40 growth inoculated at 0.2 OD600 by 2-way ANOVA followed by Tukey's multicomparison test

		mir1Δ-pESC vs. mir1Δ-tau40					mir1Δ-pESC DMSO vs. mir1Δ-tau40 DMSO				
	Time (h)	**Mean Diff.**	**95% CI of diff.**	**Significant?**	**Summary**	**Adjusted P Value**	**Mean Diff.**	**95% CI of diff.**	**Significant?**	**Summary**	**Adjusted P Value**
starting OD600 = 0.2	**0**	0.0057	-0.05208 to 0.06348	No	ns	0.9942	0.00305	-0.05473 to 0.06083	No	ns	0.99910
	2.5	-0.0236	-0.08140 to 0.03416	No	ns	0.7165	-0.01945	-0.07723 to 0.03833	No	ns	0.82050
	6	-0.0376	-0.09540 to 0.02016	No	ns	0.335	-0.02708	-0.08486 to 0.03070	No	ns	0.62030
	21	0.1156	0.05780 to 0.1734	Yes	****	< 0.0001	0.1182	0.06045 to 0.1760	Yes	****	< 0.0001
	23	0.1678	0.1100 to 0.2255	Yes	****	< 0.0001	0.1654	0.1076 to 0.2232	Yes	****	< 0.0001
	25	0.0402	-0.01761 to 0.09795	No	ns	0.2773	0.03228	-0.02550 to 0.09006	No	ns	0.47320
	27	0.1361	0.07834 to 0.1939	Yes	****	< 0.0001	0.1051	0.04730 to 0.1629	Yes	****	< 0.0001
	29	-0.0124	-0.07021 to 0.04535	No	ns	0.9449	-0.01002	-0.06780 to 0.04776	No	ns	0.97000
	31	0.0403	-0.01746 to 0.09810	No	ns	0.2741	0.04617	-0.01161 to 0.1039	No	ns	0.16730
	45.5	0.2570	0.1992 to 0.3148	Yes	****	< 0.0001	0.2014	0.1436 to 0.2592	Yes	****	< 0.0001
	47.5	0.1840	0.1262 to 0.2417	Yes	****	< 0.0001	0.1523	0.09449 to 0.2100	Yes	****	< 0.0001
	49.5	0.2086	0.1509 to 0.2664	Yes	****	< 0.0001	0.1774	0.1196 to 0.2352	Yes	****	< 0.0001
	51.5	0.3555	0.2977 to 0.4133	Yes	****	< 0.0001	0.2229	0.1651 to 0.2806	Yes	****	< 0.0001
	53.5	0.4409	0.3831 to 0.4986	Yes	****	< 0.0001	0.3503	0.2925 to 0.4081	Yes	****	< 0.0001
	69.5	0.5908	0.5302 to 0.6514	Yes	****	< 0.0001	0.5956	0.5310 to 0.6602	Yes	****	< 0.0001